University of Alberta

Risk estimation for railways exposed to landslides

by

©

Christopher Martin Bunce

A thesis submitted to the Faculty of Graduate Studies and Research
in partial fulfillment of the requirements for the degree of

Doctor of Philosophy

Geotechnical Engineering
Department of Civil and Environmental Engineering

Edmonton, Alberta

Fall 2008

Your file Votre référence
ISBN: 978-0-494-46286-7
Our file Notre référence
ISBN: 978-0-494-46286-7

"Everyone complains about the weather but no one does anything about it"

Charles Dudley Warner (1829 - 1900)

Abstract

Railways have three basic options for managing their exposure to geotechnical hazards: reduce the source of the hazards, spatially avoid the hazards, or reduce the temporal exposure to the hazards. Although railway tracks and the supporting infrastructure are exposed to geotechnical hazards all the time, the most vulnerable components of the railway, the trains and the railway personnel, are only exposed as they pass the hazards. As a result, provided that the occurrence of geotechnical hazards can be reliably predicted, reduction of the temporal exposure of trains and personnel to hazards, during high hazard periods, requires the least capital expense, and is therefore the most economic option. This thesis demonstrates a means of using precipitation indices to identify periods of higher potential landslide hazard for a site in Maple Ridge, BC. Over 100 years of landslide records compiled by the Canadian Pacific railway and others for this site are correlated with daily precipitation data from the Maple Ridge, BC area. Two methods are used to predict the occurrence of landslides using precipitation data. One method consists of using the three parameter Generalized Extreme Value (GEV) frequency distribution analysis of various duration of antecedent precipitation to develop reliable estimates of the return period of each duration antecedent precipitation. Durations of up to a year were considered. The rarest antecedent duration concurrent with the landslide event is assumed to have triggered the landslide. The other method uses the coincidence of up to three elevated antecedent precipitation conditions correlated with the landslide records to identify indices that, when combined, provide reliable prediction of precipitation induced landslide events. An event tree risk analysis for the probability of both train accidents and the probability of death of individual (PDI) railway employees due to a geotechnical

hazard is developed. The risk analysis is used to quantify the benefits of using a precipitation induced landslide warning system and to measure the effectiveness of other risk reduction strategies for geotechnical hazards. Risk can be used to evaluate the merits of various mitigative options and their net costs and benefits. It is shown that the PDI of railway personnel as a result of geotechnical hazards on CP is within tolerable limits when compared to published tolerable employee risk. It is shown for the Maple Ridge site that a precipitation induce landslide warning system and a hazard detection system would reduce the probability of a fatality by 39% and 80% respectively. With this information the cost and delays introduced by each system can be compared.

Dedication

This thesis is dedicated to all those who have died or been injured as the result of the impact of natural hazards on Canadian Pacific. Let their passing, their loss and their families loss not be in vain. We have a duty to learn from the tragic accidents that befell these individuals and improve management of the risks attributed to natural hazards that have the potential to place others at risk.

Acknowledgements

I would not have completed this thesis without the encouragement and dedication of Nancy Jacklin, my best friend, wife, and the love of my life. Her commitment to this project has been unwavering and complete. Nance has taken on countless family responsibilities on my behalf so that I could complete this thesis. I would have given up several years ago had it not been for her. Thanks goes to my kids Louise and Owen, who partially gave up their father for the last several years, my parents Jill and Hubert, my mother in-law Lilian and my friends who have all supported my goal for higher education.

I also thank Mario Ruel, Dr. Tim Keegan, Dr. Jean Hutchinson, Paul Lemay, and Cindy Hicks all members of the Railway Ground Hazard Research Project - Technical committee who have commented and contributed to many of the ideas captured here. I especially thank key committee members Dr. Derek Martin and Clive MacKay who mentored me through this thesis and during my initial years at Canadian Pacific respectively. Derek and Clive's thought provoking discussions led to the exploration of the this thesis. Thanks to Dr Norbert Morgenstern the concept of risk became an overarching theme of the thesis.

I would like to thank several others who have supported my quest for this degree, past and present, at CP including Eddie Choi, Tony Morris, Brent Szafron, Brent Laing, Gerry Ewenson, Vern Graham and Gord Pozzobon.

Table of contents

List of Tables

List of Figures

List of Photos

List of Abbreviations and Terms

AAR - American Association of Railroads

AD - Anderson Darling is a quantitative "goodness of fit" test that can be used to evaluate the ability of some extreme value statistical analysis to match the data.

Antecedent - (noun) A preceding event, condition or cause, something coming before. (adjective) Prior in time or order, occurring earlier in time. (Merriam-Webster 2005)

Antecedent duration - The length of time that a parameter is summed. To reduce confusion "period" is limited to use with "return" and "duration" with "antecedent".

APEGBC - Association of Professional Engineers and Geoscientists of British Columbia

ASCE - American Society of Civil Engineers

ARPET- Antecedent Rainfall Percent Exceedance Time (Chowdhury and Flentje 1998)

BC - British Columbia

BNSF - Burlington Northern Santa Fe Railway

CASC - CP chop code for the Cascade Subdivision in the Vancouver Service Area running from North Bend to Vancouver Harbour, BC.

Canadian Cordillera - The mountainous and plateau region of Western Canada. This document uses the term to describe the southern portion of the mountainous areas of BC and Alberta traversed by CP track.

Class 1 railway - In the US, the Association of American Railroads (2006) defines a "Class 1 railroad" as one that had revenue of at least $319.3 million in 2005. The US components of both CN and CP qualify as class 1 railroads based on their US operations. As a result, the AAR categorizes seven rail companies as Class 1 railroads in the US. In Canada, the Canadian Transportation Authority (2003) defines a Class 1 railway or Class 1 rail carrier as a company that has earned gross revenues exceeding $250 million for each of the previous two years. CN & CP qualify as Class 1 railways in Canada.

Clearance envelope - The clearance envelope of a train is the area within the plane perpendicular to the tracks required for a train to pass any point without interference. The height of the clearance envelope is based on highest head-on profile of a train. The width of the clearance envelope also considers the extra width needed to account for longer cars becoming tangent to curved track. There is an additional 150 mm (6 inch) buffer included in the clearance envelope to allow air flow in tunnels and some sway of the cars. The term clearance envelop is used when working within tunnels or restricted openings but applies everywhere within a railway network. Anything that comes within the clearance envelope of a train when provisions are not taken to halt train traffic is considered to be "foul" of the rails or clearance envelope.

CN - Canadian National Railway - CN is Canada's largest railway and the fourth largest railway in North America.

CP - Canadian Pacific (previously Canadian Pacific Railway and previous to that CP Rail) is Canada's oldest transcontinental railway and the seventh largest Class 1 railway in North America.

CP NHID - The Canadian Pacific - Natural Hazard Incident Database

Chop code - A unique four letter abbreviation for CP subdivision name

CS - Campbell Scientific is a supplier of automated weather station instrumentation and general use digital computer data-loggers.

CTA - Canadian Transportation Agency

CTC - Central Traffic Control is a system of communication and infrastructure whereby personnel in a central location can control the switches and signals along the track. They also have radio communication with the trains and other track vehicles to direct their movement and limit those vehicles that can occupy the track at any given time. CTC commonly communicates using a low voltage electrical "track circuit" that uses the rails as conductors. The CTC system is effectively an HDS. If the track circuit is broken the adjacent signals will direct trains to proceed at restricted speed. CTC is vulnerable to falling hazards provided they are energetic enough to break the rail. However, experience demonstrates that a CTC track circuit is not vulnerable to erosion or earth and debris slide hazards from below the track, as they seldom have sufficient energy to break a rail. When an erosion event, earth slide or debris flow do not result in a broken rail the train crossing unsupported (skeleton) track or miss aligned track, but still continuous rails, can break the rails and track circuit and result in a train accident. This research considers a CTC system to be secondary HDS.

DMR - District of Maple Ridge

Duration - (noun) The time that something lasts or exists. To reduce confusion duration is used with antecedent.

EC - Environment Canada

ENSO - El Niño Southern Oscillation

FRA - The Federal Railroad Authority is the US Government Department of Transportation agency with the responsibility to "promulgate and enforce rail safety regulations" (Federal Railroad Authority 2007). The Office of Safety within the FRA is responsible for the analysis of rail related accidents and the issuance of recommendations, notices, and requirements to change and improve safety practices within the US Railway industry.

FOTS - A Fibre Optic Transmission System is a bundle of multiple glass fibres used for the transmission of data. FOTS are normally installed at burial depths of 0.3 to 1.8 m along most mainline rail corridors in North America within a 75 to 100 mm diameter PVC conduit. The railways commonly utilize one or more fibres for their own communications and therefore FOTS is also effectively an HDS. If the FOTS system is broken, the railways are immediately aware that there is a problem within a specific section of the system. There are several limitations of using the FOTS as an HDS and therefore does not provide notification of hazardous rock falls. First, the FOTS is buried and therefore is not vulnerable to most falling hazards. Second, experience has demonstrated that the FOTS and the PVC conduit it is installed within usually remain intact during erosion and debris flow events that inundate or erode beneath the track. Therefore, it is only sub-grade landslides with sufficient movement to break the FOTS that would be detected by a FOTS HDS. Thirdly, FOTS is not linked directly to the CTC system and therefore requires human intervention to provide positive communications with approaching trains. This cannot be relied upon in a real time train control system.

GBO - General Bulletin Order are "instructions regarding the track condition restrictions and other information, which affect the safety of the movement of a train or engine" (AREMA 2003)

GEV - Generalized Extreme Value frequency distribution analysis

GEV APIL RPA - Generalized Extreme Value Antecedent Precipitation Induced Landslide Return Period Assessment

GIS - Geographic Information System

GOI - General Operating Instructions is a set of instructions or rules that governs the movement of all rail traffic.

GSC - The Geological Survey of Canada is a branch of the Earth Sciences Sector of the Canadian Federal Government, Natural Resources Canada.

HDS - A Hazard Detection System is any system that senses the possible occurrence of a hazard that may affect the safe passage of trains and is connected to the railway signal system such that it is able to notify oncoming trains that it has detected a possible hazard. Within CP the most common HDS is referred to as a signal fence or slide fence (AREMA 2003). These are called signal fences because they are connected to the signal system and the horizontally strung wires effectively form a fence.

A signal fence is a trip-wire hazard detection system TW-HDS. A TW-HDS is normally composed of 8 to 10 m tall vertical timber poles, spaced 8 to 12 m along-side the up-slope side of the track from which ductile wire is strung at 300 mm spacing. They may also include overhead wires strung at 150 to 300 mm spacing from horizontal cantilevered beams attached to the top of the timber poles. The wires are connected to the signal system such that if a wire breaks, the signals direct approaching trains to proceed at restricted speed. TW-HDS are used primarily to detect when rock fall debris reaches the track. If the rock fall debris is large enough and moving fast enough to break one or more of the copper wires, the electrical circuit will be broken.

There are TW-HDS versions where the wire is strung from 1.5 to 2 m tall vertical timber posts along the up-slope side of the track. These are used in areas where the rock fall is known to only have a limited bounce height or where the earth and debris slides and flows are constrained to moving along the ground. Similarly, when earth or debris encroaches on the fence it will break one or more wires and set the signals to restricted speed.

There is currently an initiative to develop a seismically triggered rock fall detection system (S-RFDS).

Hi-rail (vehicle) - Any road vehicle that is equipped with railway wheels and road wheels. The track wheels can be raised and lowered allowing it to travel on a railway track (when down) and a roadway (when up). Prior to the introduction of hi-rail vehicles, maintenance-of-way personnel traveled along the track in track "motor cars".

ID - Intensity Duration is the relationship between the intensity of a period of precipitation and the duration of the precipitation. Generally, the longer the duration is the lower the intensity. For this research, the precipitation does not have to be continuous.

IDF - Hydrologist and meteorologists use Intensity Duration Frequency data and plots to summarize and present the return period of precipitation events.

Index - In this document, an index will indicate a scale that expresses the level of one parameter on a continuum in relation to another, usually a threshold. They refer to the any number of potential precipitation indices in this research.

ME - Moment Estimate

MEI - Multivariate El Nino Southern Oscillation (ENSO) Index

MLE - Maximum Likelihood Estimate

MOW or Maintenance-of-way - This is the effort required to maintain all the components of the railways to achieve safe passage or trains. Maintenance-of-way employees include the TMF, Track Programs crews, Structures employees, Signals and Communications employees and contractors.

NIST - National Institute of Standards and Technology is an agency of the United States Commerce Department that develops and promotes measurement, standards, and technology.

NMC - The Network Management Centre is the office where all the RTC at CP control the movement of trains and switches and interact with each other. The NMC is equivalent to a control tower at an airport and the RTC are equivalent to the air traffic controllers.

NOAA - National Oceanic and Atmospheric Administration - see NWS

NWS - The National Weather Service is the Branch of the US Government National Oceanic and Atmospheric Administration (NOAA) that provides weather, hydrologic, and climate forecasts and warnings for the United States, its territories, adjacent waters and ocean areas.

Operator - The individual responsible for the operation of a track vehicle. This includes the locomotive operator and those that operate hi-rail vehicles and on-track equipment.

PDI - Probability of Death of an Individual usually expressed as a probability per year.

PIL - Precipitation Induced Landslide

Q-Q - Q-Q plot is a plot of the actual and the predicted value resulting from the fitting of a data set to a distribution. It provides a qualitative visual assessment of the goodness of fit of a distribution. The better the distribution fits the data the closer the plot will approximate a straight line with a slope of unity passing through the origin. Q stands for quartile.

RAC - Railway Association of Canada

Railway or **Railroad** - Within the US and Canada rail companies are known as railroads and railways respectively. In this document, these companies will be referred to as railways.

Railway Ground Hazard Research Project (RGHRP) - This project is a cooperative research effort between the two Canadian Class 1 railways, CN and CP, Transport Canada and the University of Alberta and the Queens University.

RailWIS - A RailWIS is proprietary weather information system developed and provided by RadHyPS Inc. and accessed under a license agreement by CP.

Restricted speed - The speed of the train or track vehicle that will permit stopping within one-half the sight distance of the operator (AREMA 2003). It also directs that the train or equipment operator to prepared to stop short of a switch not properly lined. In no case shall the equipment speed exceed the "slow speed" (15 mph). At restricted speed the operator should be watching for a hazard such as broken rail, misaligned track, or debris or equipment foul of the track.

Return period - The reoccurrence interval between event equaling or exceeding a specific magnitude (Chow et al. 1988). To reduce confusion "period" is limited to use with 'return" and "duration" with "antecedent".

RFDS - Rock Fall Detection System - see HDS.

RTC - Rail Traffic Controller

Running trades - Railway employees who operate and travel on the trains as part of their job function.

S&C or Signals and Communications - The group of employees who build and maintain the signals and communications systems. These systems make it possible to control the movement of trains and allow communication between personnel working at disparate locations within the rail network. It can also refer to the infrastructure for which this group is responsible.

Siding - A location where there are two tracks for a distance of 1.6 to 3 km (1 to 2 miles). The second track allows trains traveling one direction to pass a second train (temporarily stopped in the siding) traveling in the opposite direction. An system of sidings along with a centrally controlled signal system allows two way rail traffic without having one track dedicated to rail traffic in each direction. The distance between sidings, length of trains, and train speed influence the density of rail traffic accommodated by this technique. As the frequency of trains increases, the number of sidings required to allow un-restricted train movement increases.

Signal fence - See HDS

Slide detector fence - See HDS

SPC or Standard Practice Circular - At CP a Standard Practice Circulars summarizes and provides the TMS and the employees under their direction with a general education and advice on how to identify and manage a wide variety of conditions that may arise that are their responsibility to resolve. As indicated in the SPC if the TMS and their crew are not able to resolve the issue, additional resources are available within the company and from third parties.

STB or Surface Transportation Board - The STB is a regulatory agency of the U.S. Department of Transportation. It reviews proposed railroad mergers and resolves railroad rate and service disputes.

SWE - Snow Water Equivalent

TSB - Transportation Safety Board is an independent agency Government of Canada created to improve transportation safety by investigating accidents

TC - Transport Canada is the Canadian federal government agency responsible for the development and administration of policies, regulations, and service for Canadian transportation systems.

Tip-over-post - A landslide detection system used by the railways to detect landslide movement greater than a decimetres. It usually consists of 2 m long fence-posts driven up to 1 metre into the ground. Level switches are attached to the fence posts and connected to the signal system. If a fence post rotates due to ground movement (or other causes) the liquid level switch will open and cause an open circuit similar to trip-wire signal fence. Commonly, multiple tip-over-posts are connected in series to increase the potential that at least one tip-over-post is rotated sufficiently to be tripped by the landslide.

TMF - The Track Maintenance Forces are the crews of CP personnel who maintain and repair the track and its associated infrastructure excluding bridges and larger culverts.

TMS - Track Maintenance Supervisor - The front line supervisor (staff, non-union employee who direct union employees) responsible for inspecting the track and directing the day-to-day maintenance of the track, sub-grade, and ditches. The TMS has a counterpart, the structures supervisor, who is responsible for the maintenance of structures including culverts and bridges, and who generally looks after slope stability issues outside the 6 m wide top of the railway embankment.

Track vehicle - Any vehicle that can travel along the track that is not a train. This includes track maintenance and hi-rail vehicles commonly limited to MOW activities.

Track unit - A general term for any vehicle that can travel on the rails. It includes hi-rail vehicles, locomotives, rolling stock, rail mounted work equipment, etc.

Threshold - A specific value of an index over or under which the potential for an event changes.

UBC RF - University of British Columbia Research Forest located near Maple Ridge, BC

WMO - The World Meteorological Organization is an agency of the United Nations that provides standards and guidance on the state and behaviour of the Earth's climate.

WIS or Weather Information Service - CP subscribes to RailWIS a system specifically developed for CP by RadHyPS Inc. of Gatineau, Quebec.

List of Variables

Chapter 2, 3 and 4 and Appendix C - List of variables after Guzzetti et al. (2007)

Variable	Description	Units
$A(d)$ & $A(c\text{-}d)$	Antecedent precipitation. The cumulative precipitation prior to the landslide. d indicates the duration and is measured in days. Where d is a single value, the cumulative precipitation is summed for the d days prior to the landside. Where c - d is two values separated by a hyphen the cumulative precipitation is summed over the c to d interval of days prior to the landslide. $A_{(d)}$ differ from E where c is set to the start of the period of continuous precipitation prior to a landslide.	mm
A_{MAP}	Normalized antecedent rainfall. Antecedent rainfall divided by MAP (A_{MAP}=A/MAP).	–
$A_{(y)}$	Antecedent yearly precipitation up to the date of the event. The cumulative yearly precipitation measured before the landslide triggering rainfall event.	mm
API	Antecedent Precipitation Index, or antecedent soil moisture.	–
$A_{(y)MAP}$	Normalized antecedent yearly precipitation up to the date of the event. Antecedent yearly precipitation divided by MAP. ($A_{(y)MAP}$=$A_{(y)}/MAP$).	–
C	Critical rainfall. The total amount of rainfall from the time of a distinct increase in rainfall intensity (t_0) to the time of the triggering of the first landslide (t_f).	mm
C_{MAP}	Normalized critical rainfall. Critical rainfall divided by MAP. (C_{MAP}=C/MAP).	–
D	Rainfall duration. The duration of the rainfall event or antecedent duration.	hours, or days
D_C	Duration of the critical rainfall event.	hours
$E_{(h)\ or\ (d)}$	Cumulative event rainfall. The total rainfall measured from the beginning of the rainfall event to the time of the landslide. Also known as storm rainfall. h indicates the considered period in hours;	mm

Variable	Description	Units
	"d indicates the considered period in days.	
E_{MAP}	Normalized cumulative event rainfall. Cumulative event rainfall divided by MAP ($E_{MAP}=E/MAP$). Also known as normalized storm rainfall.	–
F_c	Sum of normalized antecedent yearly precipitation and normalized event rainfall. ($F_C=A_{(y)MAP} + E_{MAP}$)	–
I	Rainfall intensity. The amount of precipitation in a period divided by the duration. This is the rate of precipitation over the considered duration. Depending on the duration of the measuring period, rainfall intensity measures peak or average precipitation rates.	mm/h
I_{MAP}	Normalized rainfall intensity. Rainfall intensity divided by *MAP*. ($I_{MAP}=I/MAP$)	Hours^{-1}
I_{max}	Maximum hourly rainfall intensity	mm/h
I_p	Peak rainfall intensity. The highest rainfall intensity (rainfall rate) during a rainfall event.	mm/h
$\hat{I}_{(h)}$	Mean rainfall intensity for final storm period. h indicates the considered period, in hours, most commonly from 3 to 24 hours.	mm/h
I_c	Critical hourly rainfall intensity	mm/h
I_f	Rainfall intensity at the time of the landslide	mm/h
I_{fMAP}	Normalized rainfall intensity at the time of the landslide. Rainfall intensity at the time of the landslide divided by MAP. ($I_{fMAP}=I_f/MAP$)	1/h
MAP	Mean Annual Precipitation. The long term yearly average precipitation obtained from historical rainfall records. This is a proxy for local climatic conditions.	mm
N	Ratio between the MAP of two different distant areas	–
R	Daily rainfall. The total amount of rainfall for the day of the landslide event.	mm
RDs	Rainy Days. This is the average number of rainy days in a year. The long term yearly average of rainy (or wet) days, obtained from historical rainfall records. A proxy for local climatic conditions.	#

Variable	Description	Units
RDN	Rainy-day normal. The ratio between the *MAP* and the average number of rainy-days in a year. (*RDN=MAP/RDs*)	Mm/#
R_{MAP}	Normalized daily rainfall. Daily rainfall divided by *MAP*. (R_{MAP}=*R/MAP*)	–
$T_{(d)}$	Return period of antecedent duration *d* consistent with the definition in antecedent precipitation	Years

Chapter 5 - List of variables for risk estimation

D_{Si} = Sight distance of the locomotive operator

D_{St} = Stopping distance of the locomotive operator

$E[F_I{:}Accident]$ = The expected value of the $p[F_I{:}Accident]$ probability function

F_H = The frequency of a hazard in events per year

L_H = The length of a hazard

L_R = The length of the section of track of interest

L_S = The length of a signal block

$L_{S\text{-}East}$ = The length of a signal block for east bound rail traffic

$L_{S\text{-}West}$ = The length of a signal block for west bound rail traffic

L_T = The length of a train

$N_{Freight}$ = The number of freight trains in a specific time

$N_{MOW\text{-}TV}$ = The number of MOW track vehicles in a specific time

$N_{Passenger}$ = The number of passenger trains in a specific time

N_T = The number of trains in a specific time

PDI = The probability of death of an individual

$P[Accident_\tau]$ = The probability of a train accident (derailment or train damage) due to a Type τ incident, where τ is either I, II or III

$P[Accident_\tau(V_i)]$ = The probability of a train accident due to a Type τ incident, where τ is either I, II or III where the probability is dependent on V_i

$P[Derail._{\tau}]$ = The probability of a derailment at a specific location considering all volume classes of landslides at that site due to a Type τ incident, where τ is either I or III

$P[Derail._{\tau}:Accident(V_i)]$ = The conditional probability of a derailment given an accident caused by a landslide of volume V_i due to a Type τ incident, where τ is either I, II, or III

$P[Derail._{\tau}:H]$ = The conditional probability of a derailment given a landslide occurs for all volumes of landslides due to a Type τ incident, where τ is either I, II, or III

$P[Derail._{\tau}:H(V_i)]$ = The conditional probability of a derailment given a landslide occurs for a specific volume class of landslide due to a Type τ incident, where τ is either I, II, or III

$P[Derail._{\tau}(V_i)]$ = The probability of a derailment at a specific location considering a specific volume class of landslide at that site due to a Type τ incident, where τ is either I, II or III

$P[Derail._{\tau}(V_i):Accident]$ = The conditional probability of a derailment for each volume of landslide given that an accident has occurred due to a Type τ incident, where τ is either I, II, or III

$P[F]$ = The probability of a fatality due to all scenarios

$P[F_{\tau}]$ = The probability of a fatality due to a Type τ incident, where τ is either I, II or III

$P[F_{\tau}:Accident]$ = The conditional probability of a fatality given an accident occurs due to a Type τ incident, where τ is either I, II or III

$p[F_I:Accident]$ = The conditional probability function of a fatality given a Type I accident

$P[F_{\tau}:Derail.]$ = The conditional probability of a fatality given a Type τ derailment, where τ is either I, II or III

$P[F_{\tau}:Train\ damage]$ = The conditional probability of a fatality given a train damage Type τ incident where τ is either I, II or III

$P[F_\tau(V_i){:}Accident]$ = The conditional probability of a fatality for each volume of landside given an accident due to a Type τ incident, where τ is either I, II or III

$P[Freight]$ = The probability that the next track vehicle will be a freight train

$P[H]$ = The probability of the hazard

$P[H(V_i)]$ = The probability of the hazard of a specific volume range, V_i

$P[HDS]$ = The probability that a hazard detection system is present or not. $P[HDS]$ is usually either 1 or 0. If the HDS is not functioning or has not been reset, trains will proceed at restricted speed under the assumption that a hazard may be influencing the track for a Type III incident.

$P[HDS\ trig.{:}H]$ = The conditional probability that the HDS is triggered given the hazard has occurred

$P[HDS\ trig.{:}NH]$ = The conditional probability that the HDS will be triggered when no hazard has occurred

$P[Individual\ fatality{:}Crew\ fatality]$ = The conditional probability of death given at least one train crew member fatality as a result of a geotechnical train accident

$P[MOW\text{-}TV_\tau]$ = The probability that the next track vehicle will be a MOW track vehicle where τ is either I or III

$P[Impass.{:}H(V_i)]$ = The conditional probability that the track is impassable given the hazard of volume, V_i, has occurred for a Type III incident. $P[Impass.{:}H(V_i)] = 0$ for passable track and 1 for impassable track.

$P[Passenger]$ = The probability that the next track vehicle will be a passenger train

$P[S_I{:}H]$ = The probability that a train will be in the path of the hazard when it occurs for a Type I incident

$P[S_I{:}H(V_i)]$ = The probability that a train will be in the path of the hazard when it occurs for a specific volume of the landslide for a Type I incident

$P[Train\ damage_\tau]$ = The probability of train damage given a hazard has affected the track for a Type τ incident, where τ is either I, II or III

$P[TC]$ = The probability that a track circuit is present and working for a Type III incident. This is assumed to be very close to one and is to 0.997 to represent the failure of the track circuit system of 1 day per year. This assumes that the trains operate at track speed under the direction of the NMC despite the lack of indication by the signal system.

$P[TC\ trig.:H\&TC]$ = The conditional probability that the track circuit is broken by the landslide provided a track circuit is present

$P[Train]$ = The probability that the next track vehicle along the track will be a train rather than an MOW track vehicle for a Type III incident

$P[Train\ inside\ signal]$ = The probability that a track vehicle is temporally within the signal and therefore will not receive information from the signal system and will therefore encounter a hazard along the track without having slowed to restricted speed.

$P[Train\ stops]$ = The probability that a train stops before encountering a hazard that has rendered the track impassable for a Type III incident.

SD = Sight distance

t = time

t_s = The time a train is stopped for Type II incident

t_{SI} = The duration of a service interruption

V_i = The volume of landslide class, i, normally subdivided into classes by order of magnitude

v_T = The speed of the train

δ_D = The residual probability that a derailment can occur even though the train operator is able to see the obstruction within the sight distance

δ_{Ts} = The residual probability that train damage can occur even though the train operator is able to see the obstruction within the sight distance

μ_D = The expected value of D_{Si}/D_{St} at $P[Derail.]$ = 0.5

σ_D = The standard deviation or steepness of the probability derailment function

Risk estimation for railways exposed to landslides

Chapter 1 Railways, precipitation induced landslides and risk

The safety and efficiency of North American railways are reduced by exposure to numerous geotechnical hazards. These hazards include surficial erosion, subsurface piping erosion, earth slides, rock slides, track settlement, debris flows, snow avalanches, and earthquakes. The occurrence of several of these hazards is primarily or partially controlled by the preceding weather conditions. Current communication capabilities provide the means to supply field railway personnel with representative, timely information about the weather conditions provided appropriate warnings are available. However, at present, railways do not utilize weather information to identify conditions that could induce geotechnical hazards of concern to railways. Similarly, a methodology for the quantification of geotechnical risks and the variation of these risks due to the weather or other affects has not previously been developed within the railway industry. This thesis develops a methodology to identify precipitation conditions that result in periods of increased landslide activity. It also provides a means of quantifying the risk of these hazards and the risk reduction realized by various operational railway strategies. This will allow the railway industry to quantify the risk reduction resulting from specific actions and reduce its exposure to geotechnical hazards by implementing the most beneficial actions.

To minimize the likelihood of service interruptions due to weather conditions, Canadian Pacific (CP) railway has developed a weather information system, RailWIS, that provides warning and notification of severe weather conditions. However, this system lacks appropriate indices and thresholds capable of identifying and predicting periods of increased exposure to landslide hazards. The intent of the research, undertaken as part of this Ph.D., is to develop a methodology to identify weather criteria so that warnings can be issued for several classes of geotechnical hazards.

For several decades Japanese railways have utilized a weather information system to notify trains when geotechnical hazards are more likely to occur. Similar systems are also in use on a smaller geographic scale in urban areas such as Hong Kong and Rio de Janeiro. These systems are intended to notify key personnel within various organizations, or the public within the area affected, that severe weather conditions are occurring and that risk management measures should be considered or implemented to reduce the consequences of the hazard. To be effective, the weather information systems must be able to differentiate between severe and non-severe weather that induces geotechnical hazards.

The research, completed as partial fulfillment of this Ph.D., demonstrates that it is possible to establish weather indices with the ability to identify periods when earth slides, large rock slides, and debris flows within the areas covered by CP rail network, are more likely to occur.

1.1 Description of the influence of geotechnical hazards on railways

As with any outdoor industry, railways are influenced by the weather and have suffered significant losses due to these varied influences. Leeper and Smith (1998), Rossetti (2006), Bunce et al. (2003), and Changnon (2006) have each described the significance of weather on railways. The limited ability of railways to climb and descend grades of more than 2% has forced railway engineers to select routes more exposed to geotechnical hazards than other transportation modes such as highways, pipelines and electrical and fibre optics transmission systems. Due to the distributed nature and size of the rail network in North America, most railways cross various types of geologic terrain and are exposed to numerous and varied geotechnical hazards. As a result, railways are more exposed to geotechnical hazards than other linear corridors and avoiding these hazards is prohibitively expensive.

The severity and distribution of weather and hydrologic conditions often influences the severity and distribution of geotechnical hazards. Previously, it has been difficult to correlate hazardous events with weather events for two primary reasons:

1. The record of hazardous events in most areas was incomplete.
2. The distribution and duration of climatic data have not always been sufficient to provide an accurate spatial distribution or frequency analysis of the

climatic conditions inducing or contributing to the occurrence of the hazard at a specific location.

These short comings are gradually being overcome by two factors.

1. The railway industry in Canada has records of the most significant geotechnical hazards over the past 125 years. In addition, since 1973, CP has compiled records of the majority of geotechnical hazard events. These are contained within the CP Natural Hazard Incident Database (CP NHID). These records include both those events that resulted in train accidents and those that influenced the safety of the track but did not cause an accident. This research utilizes these records.
2. The analysis of hazardous events, where representative climatic data is available, avoids the issue of insufficient spatial data. Climate data is available and a sufficient period of record has been established for reliable analysis of weather data. The development and distribution of a greater number of weather monitoring systems with the ability to provide accurate information from a larger area, such as weather radar, are beginning to provide representative data in more areas.

1.2 Description of the potential for an improved system of managing weather induced geotechnical hazards

1.2.1 Previous systems

In the past, railways have relied, to a large degree, on the experience and local knowledge of the regional personnel to determine when and how to respond to severe weather. Within CP this was the responsibility of the Track Maintenance Supervisor (TMS). The railway relied upon the TMS to slow or stop trains in response to weather conditions that were or could be detrimental to the safety of trains. However, for various reasons discussed further in Appendices A and C, CP and other railways have diminished the effectiveness of personnel, in this position, to assess the changes in the exposure of the track to weather sensitive geotechnical hazards.

1.2.2 Identification of weather information systems and needs

More than 35 years ago the geotechnical engineer at CN asked "are [train] speed restrictions warranted after a certain amount of rain has fallen?" (Peckover 1972). Leeper and Smith (1998), Ryerson (1998), Bunce et al. (2003), Rossetti (2006) and Bunce et al. (2006), discuss the need for and benefit of providing weather information to railways. Plotkin (2003) indicated that railways need an improved understanding of landslide triggers to provide greater protection from landslides. Plotkin notes that warning systems must provide sufficient advance notice of a hazard due to the inability of trains to stop within a distance of less than 1.6 to 3.2 km (1 to 2 miles). He also notes that trains are unable to avoid obstacles on the track. For these reasons, operational limitations (such as restricted speed slow orders and more inspections) are an effective way to respond to hazard notifications. Plotkin also indicates that the US Federal Railroad Authority (FRA) has been involved in initiatives with railway organizations in the US and the Canadian Railway Ground Hazard Research Project (RGHRP) investigating the influence of the weather and other natural hazards on railways including the efforts of this research.

The FRA (1997) issued Safety Advisory 97-1 requiring that each railway with trains on a specific class of track and higher, and all passenger trains within the warning area, and the employees controlling the movement of these trains, receive all US National Weather Service (NWS) notifications of flash flood warnings within 15 minutes of issuance by the NWS. The FRA indicates that the use of weather information service (WIS) providers was an acceptable means of meeting this requirement.

In the Weather Information for Surface Transportation, National needs Assessment Report, by the Office of the Federal Coordinator for Meteorological Service and Supporting Research (2002) it is identified that rain could cause erosion "washouts" and landslides. They also note the following regarding railways and landslide hazards.

> "Safety risks to personnel and equipment (accidents are likely with possible injury or death); railway roadbed scoured, buried, damaged or destroyed; rail damage from line stretch and foreign debris impact likely; rail sensor failure likely; increased monitoring of crews and equipment; increased risk of

hazardous material spill (increased monitoring, mitigation, reclamation, reporting); public relations effects."

Spiker and Gori (2003) identify 9 elements of a national landslide hazard mitigation strategy. Within this strategy they identify the following elements relating to the development of precipitation indices.

1. Research landslide thresholds and triggers to develop the ability to predict landslide behaviour
2. Develop landslide prediction systems capable of displaying changing landslide hazards in both time and space
3. Incorporate rainfall monitoring and integrate real-time monitoring utilizing NEXRAD weather radar information

Some parts of the Japanese railway network have utilized a system to notify train operators of weather related hazards, including landslides, since the mid 1980's (Katayose 1987). Baum et al. (2005), studied landslides affecting the operation of the Burlington Northern Santa Fe (BNSF) railway track along the shore of Puget Sound near Seattle, Washington. They suggested that a landslide early warning system could be developed to allow the railway to reduce the exposure of trains to derailments caused by landslides. Attributes of these two examples are used in the development of the proposed system.

A description of existing weather information systems used at CP and other North American railways is included in Appendix A and C. Each of these researchers, agencies and policy makers have identified the need and benefit of developing landslide warning systems including those based on precipitation indices.

1.3 Goals of the current research

To comply with FRA 97-1 all North American Class 1 railways subscribe to weather information services (WIS) to provide warnings of severe weather conditions and to provide access to location-specific weather information. This information allows the railways to modify operations to reduce the potential for severe weather to cause service delays and reduce the severity of any potential derailments. RadHyPS Inc. maintains RailWIS to provide warning and notification of severe weather conditions to CP. However, WIS need criteria upon which to issue warnings but these criteria are not available for landslide hazards. To provide an effective warning system with limited false-positives, specific landslide/weather criteria need to be developed for use by the railway industry. For geotechnical hazards the weather criteria may need to utilize several different parameters and combinations of parameters to provide reliable warnings.

The hazard scenario of precipitation inducing a landslide is longer and more complex than other weather hazard indicators like low temperature causing broken rails or wind blowing over empty double stack container rail cars. For example, landslides are often attributed to prolonged rainfall or a combination of short high intensity and antecedent rainfall conditions (Caine 1980, Rahardjo et al. 2001b, Jakob and Weatherly 2003, Guzzetti et al. 2007 and others). However, determining what intensity and duration of long-term (antecedent) rainfall condition will cause a landslide to mobilize requires a relatively detailed assessment of the landslide characteristics, external forces on the landslide, and the influence of the weather conditions.

The research completed as partial fulfillment of this Ph.D. provides a method of determining the precipitation indices and thresholds appropriate for earth slides and debris flows. It also determines the indices and thresholds for a case study site traversed by the CP tracks in Maple Ridge, BC. The research identifies indices that result in a tolerable number of false-positive warnings and no false-negative outcomes. This type of precipitation induced landslide warning criteria will make all WIS more valuable tools in reducing losses and service interruptions due to severe weather conditions.

There are two primary achievements of this research:

1. The first is the demonstration of a relationship between antecedent precipitation conditions and landslide activity. The demonstrated relationship provides a methodology for the determination of precipitation warning criteria needed to predict periods of higher hazard due to landslides and provides for the development of several criteria for use within a weather information system. Control measures that utilize these relationships are shown to be sufficiently reliable to benefit the railway industry without causing undue delays.

2. The second goal is to develop a means of quantifying the future risk due to landslides based on the historical performance recorded in the CP NHID. This also allows the quantification of the variation in future risk due to precipitation and various operating conditions. The variation in risk of train accidents and loss of life, from geotechnical hazards within the railway industry are the primary focus of the risk estimation.

1.4 Scope of current research

Previously the scope of this area of research was limited by the constraints identified in Section 1.1. However, as discussed these limitations are gradually being overcome. As a result, it is now possible to analyze precipitation induced landslides.

The type of geotechnical hazards considered is limited to those most directly caused by weather such as hazards induced by severe and/or prolonged rainfall and snow melting. These hazards are limited to debris slides, debris flows, earth slides, earth flows, and rock slides (Cruden and Varnes 1996, and Keegan 2007). This research does not investigate events directly triggered by stream and river flood conditions.

The scope of the current research is further limited by the following:

1. The volume of the landslides considered are larger than 100 m^3.
2. The landslides investigated is limited to those documented in the CP natural hazard incident database (CP NHID).
3. Representative weather station data must be available for the landslide location. The weather station data must include a representative historical data set.

Once the appropriate indices are identified and thresholds developed, the data from a weather station is used to warn of hazards over the length of track for which it is representative.

1.5 Method of completing research

The research has been completed using the following steps. The geotechnical hazards were compiled into the CP-NHID. A literature review was completed. Sources of climatic data are described, assessed and utilized. A case study is undertaken on a site with both valid precipitation information and an extensive history of landslide activity. Two different precipitation analysis techniques are applied to the landslide and precipitation data to investigate correlations between the two data sets. A quantitative risk assessment methodology is developed to evaluate the benefit of a precipitation induced landslide warning system and other risk mitigation techniques. This methodology is applied to the case study.

1.5.1 Literature review

A review of the geotechnical, hydrotechnical and risk literature on the following five areas has been completed and summarized in Chapters 2 and 3.

1. The development of indices for precipitation induced landslides.
2. The use of weather indices for warning of geotechnical hazards.
3. The analysis of precipitation data to determine the reoccurrence interval of extreme events.
4. The management of geotechnical hazards in the operation of railways.
5. The application of risk management within the geotechnical and railway industry.

1.5.2 Methodology to establish precipitation indices

The date of the landslide activity is compared to the precipitation records, drainage basin area, and the magnitude of the landslide activity to identify the most significant precipitation indices that are correlated to the landslide movement. Numerous indices including antecedent and intensity duration indices are considered. In some cases there may not be a correlation between a landslide and the weather conditions due to insufficient spatial distribution of climate data or other processes influencing the stability of the slope. Provided there is sufficient climate data the method is useful for testing the sensitivity of slopes to extreme precipitation conditions.

With respect to goal 1 in Section 1.3, the objective of the research is to identify a relationship between several types of landslides and the specific weather that has induced them. In general the spatial distribution of geotechnical hazards is denser than the spatial distribution of weather stations. Therefore a set of precipitation indices would be developed for each weather station and for each relevant class of geotechnical hazard in the area represented by the weather station. This research develops a set of precipitation indices and thresholds for multiple types of landslide railway hazards for a specific weather station. When the precipitation index thresholds are exceeded, a landslide warning with multiple levels is issued, depending on the severity of the previous and forecast precipitation. The indices are based on currently available daily precipitation data currently used by railways to monitor operating conditions.

1.5.3 Case study of precipitation conditions, landslide and train accidents

CP and other railways in North America have been in operation for more than 125 years. During this time CP has compiled records of the influence of natural hazards on their operation in the CP NHID. The CP NHID has been updated to 2007 September as part of this research and the ongoing CP geotechnical hazard management strategy and the Railway Ground Hazard Research project.

For the purpose of this research a case study area with a long landslide history was selected on the southern limit of the District of Maple Ridge, approximately 30 km (20 miles) east of Vancouver, BC. Due to the proximity of this site to the transportation corridor afforded by the Fraser River and the populated area of Vancouver, landslides are documented in this area from before the railway was constructed in 1881. The area typifies the type of sites that are sensitive to precipitation. This area was selected because landslides have occurred or have been reactivated numerous times, are in close proximity to each other in the same geotechnical setting and there is a continuous precipitation record over the period of complete landslide records.

The research demonstrates that it is possible to establish a relationship between landslides that cause train accidents, delays and damage to the track structure and the precipitation conditions that preceded these events.

1.5.4 Development of risk assessment methodology

Currently, risk analysis within geotechnical engineering at CP is limited to the incomplete qualitative methods described later in Section 5.1.1.

To address the second research topic (identified in Section 1.3, Bullet 2) a methodology for quantifying the risk, and the variation in risk as the result of precipitation and other operating conditions, is developed. The methodology developed follows the risk assessment process outlined in Canadian Standards Association (1997) and Canadian Standards Association (1991).

Risk estimation is the most detailed component of the risk management process developed as part of this research. The risk estimation is accomplished with an event tree analysis and quantifies the probability of fatalities and train accidents.

With the development of the risk estimation, it is now possible to quantify the advantages and disadvantages resulting from a change in the operating conditions, especially those that reduce the hazard such as stabilization efforts, reduced train operations, and warning systems. An overall risk estimation of the probability of death of an individual due to landslides on the CP has been calculated. This risk level is within accepted levels for work places in developed countries. The risk estimation and variation has been completed for a number of operating scenarios relevant to the case study site.

1.6 Application of research in railway industry

Application of the research completed for this PhD has the potential to improve the current system of identifying and managing precipitation induced geotechnical hazards. The combination of risk analysis and precipitation criteria can be used to reduce the exposure of personnel and equipment to landslide hazards. The ability of railway industry to manage the exposure of trains to the risks associated with precipitation induced landslides provides an opportunity for the development of a practical application. The precipitation indices and thresholds developed as part of this research, for the Maple Ridge BC site, have been integrated into the RailWIS system since 2008 January. These warning criteria are effectively reducing the exposure of trains, personnel and passengers to landslide hazards periodically experienced in this area.

Implementation of the results of this research will augment the weather information services currently utilized by both Canadian and most US Class 1 railways. Either the weather service providers or the railways would use presently available raw and processed meteorological data to compile the appropriate indices for a specific site or region. These precipitation indices would be compared to the appropriate thresholds for the site or regions. The research establishes a methodology for determining which indices and thresholds are appropriate for a specific region. A railway can then use the risk estimation process to identify the appropriate response warranted for each threshold exceeded. The risk estimation process also provides railways a means of evaluating the relative benefit of engineering and monitoring measures to reduce and identify the temporal variation of the hazard respectively.

This research should make WIS systems more valuable tools in reducing losses and service interruption due to severe weather conditions. It also reduces the need for currently issued heavy rainfall warnings which have no influence on rail operations.

Ultimately, a tool such as RailWIS could rank current weather conditions against previous weather events, and provide a rating of the severity of the present condition versus previous landslide inducing conditions.

Chapter 2 Review of precipitation-induced landslide literature

This chapter opens with information on the terminology used in the railway industry and this research. Second, it discusses the influence of geotechnical hazards on the railway. Third, is an explanation of the physical processes that result in precipitation influencing the stability of landslides. Fourth, is a summary of the research of the relationship between precipitation and landslides completed by others. The fifth section of the chapter summarises the risk approaches developed for application with geotechnical hazards. A summary of the topics reviewed concludes the chapter.

2.1 Terminology

The railway industry utilizes extensive jargon and terminology to describe infrastructure and operations of the railway. A brief description of the terminology used at CP is included in Appendix A, Section 2.2 and in the List of abbreviations and terms. Additional railway terminology is defined in the AREMA (2003) railway engineering guide.

The four warning conditions false-positive, false negative, true-positive and true negative are defined relative to the landslide warning system developed in this research in Appendix A, Section 2.1.

2.1.1 List of variables

A set of consistent variables has been adopted for use in this thesis. There are three sub-sets of variables.

1. **Variables used in the analysis of precipitation induced landslides**
   Where possible, this thesis utilizes nomenclature adopted by previous researchers. Guzzetti et al. (2007) compiled a table of rainfall and climate variables previously used in the literature for the definition of rainfall thresholds for precipitation induced landslides. An adapted version of the Guzzetti et al. (2007) variables is used.
2. **Rainfall analysis**
   The variables based on those used by Chleborad (2000) are included in

Appendix H. Those used by G. Chen (University of Calgary, personal communication 2007) for the frequency distribution analysis are included in Appendices I, J and K.

3. **Risk estimation**

The variables used within the risk estimation in Chapter 5 follow the structure used by previous geotechnical risk estimation practitioners including Fell (1994), Roberts (2005), and others. The nomenclature of the risk estimation variables is described in Section 5.5.1.2.

With the exception of those used in Appendices F to J, each set of variables is included in the List of variables following the Table of contents.

2.2 Influence of geotechnical hazards during the history of CP

CP has suffered losses as the result of numerous landslides during its history. An internal review of damage and train accidents in 1997 revealed that CP incurred a loss of $75 million between 1960 and 1995 as the result of rock falls, debris slides, earth slides, sub-grade failures, and erosion events. This is more than $2 million per year adjusted to 2005 Canadian dollars.

The following three sub-sections provide background information needed to understand the hazards and available data with which this research is completed.

2.2.1 Description of the CP Natural Hazard Incident Database - CP NHID

In the early 1970's Peckover (1972) and the Railway Transportation Committee (1973) identified the benefit and need to document the influence of geotechnical events on the railways in Western Canada. Subsequently, Transport Canada required that both CP and CN collect and maintain records of these events. As a result, over the last 35 years, valuable records of geotechnical incidents have been compiled. This is now the state-of-practice in Canadian railways. The collection of geotechnical hazard data motivated by the Railway Transportation Committee (1973) was known as the Rock fall database at CP until the mid 1990's when it was realized that other geotechnical hazards were being captured in the data base. In 1997, CP compiled a database of all train accidents caused by hazards in the physical environment. The previous rock fall database and the CP train accident and loss records related to natural hazards from 1960 to 1995 were combined. As part of this thesis, this expanded database has been supplemented by data collected by Peckover (1972), the Railway Transportation Commission (1973) publication, and other internal CP correspondence. In 2007 the database was also updated with the train accident records from 1995 to September 2007. The geotechnical group within CP retains the primary responsibility for collecting and verifying the data and periodically supplementing this with complementary information collected by the Train Accident prevention group within CP. Keegan (2007) described a similar process at CN.

In the case of the CP NHID the quantity and quality of information varies from region to region, and from decade to decade. However, the regional distribution of the data and the period over which it has been recorded is rivalled by few other data sets in Canada. The CP NHID contains 3,700 records of geotechnical hazards that have affected the CP right-of-way, a nominally 500 m (1600 ft) wide 22,400 km (14,000 mile) strip of land across North America. This works out to a hazard density of 0.3 landslides/per km^2. In comparison, the Geologic Survey of Canada landslide database (Natural Resources Canada 2007) contains 5,200 records of landslides during the history of the railway (1881 to 2007) distributed across the 9 million km^2 of Canada. This works out to 0.0006 landslides per km^2, 2.7 orders of magnitude lower density than the CP NHID. No national landslide database appears to exist in the US. The spatial distribution of the GSC and CP NHID databases are shown in Figures 3.8 and 3.9 respectively.

There are several reasons for the difference in the CP NHID and GSC databases. The two most significant are that CP records events down to a volume of as little as 0.03 m^3. The GSC database does not indicate a volume for all the records but is likely limited to events larger than a few m^3 at the smallest. The second reason is that CP records are from a narrow corridor occupied daily for more than 125 years where most potentially hazardous events are recorded. Conversely, the GSC data comes from all over Canada's scarcely populated regions and therefore many events are not recorded because no one observed them.

The database of geotechnical events has and continues to allow Canadian railways and the geotechnical research community to understand the processes and nature of these hazards to an extent unachievable had these events not been recorded and compiled in a single location. The CN and CP databases have been used by Shi (2006), Keegan (2007), Keegan et al. (2007), Lan et al. (2007), Eshraghian et al. (2005 and 2007) and others as part of the Railway Ground Hazard Research Project (Transport Canada 2007).

Guzzetti et al. (2008) discusses the incompleteness of the world wide dataset of Precipitation Induced Landslides (PIL) from regions of Italy and around the world.

2.2.2 Characterization of geotechnical hazards affecting railways

Maertens (1990), Selig and Waters (2002), AREMA (2003), Keegan (2007), and Keegan et al. (2007) all discuss the various types of ground hazards that influence railways. Maertens described the influence of climate and terrain on the Norfolk Southern railway in Virginia and Ohio. He limited his discussion to railway engineering and geographic considerations and does not consider geotechnical engineering issues. Selig and Waters (2002) discussed the geotechnical and mechanical consideration of railway track from the rails to the base of the track sub-grade but do not consider landslide hazards. Cruden and Varnes (1996) classify landslide hazards without consideration of railways. Keegan (2007) extended Cruden and Varnes specifically for railway ground hazards.

Keegan (2007) has successfully modified the classification of Cruden and Varnes (1996) to include all ground hazards experienced on the CN rail network. This classification has been adopted by CP. Keegan (2007) provides a detailed scenario describing each of the processes and combination of processes that result in losses within the Canadian railway industry. Consistent with Cruden and Varnes (1996), this work has provided a technical language upon which the railway industry and supporting engineering consultant community in North America and around the world can communicate without ambiguity. The classification of Keegan (2007) is used throughout this thesis and is recommended for adoption by others. Figure 2.1 shows an overview of the railway ground hazard classification developed by Keegan (2007).

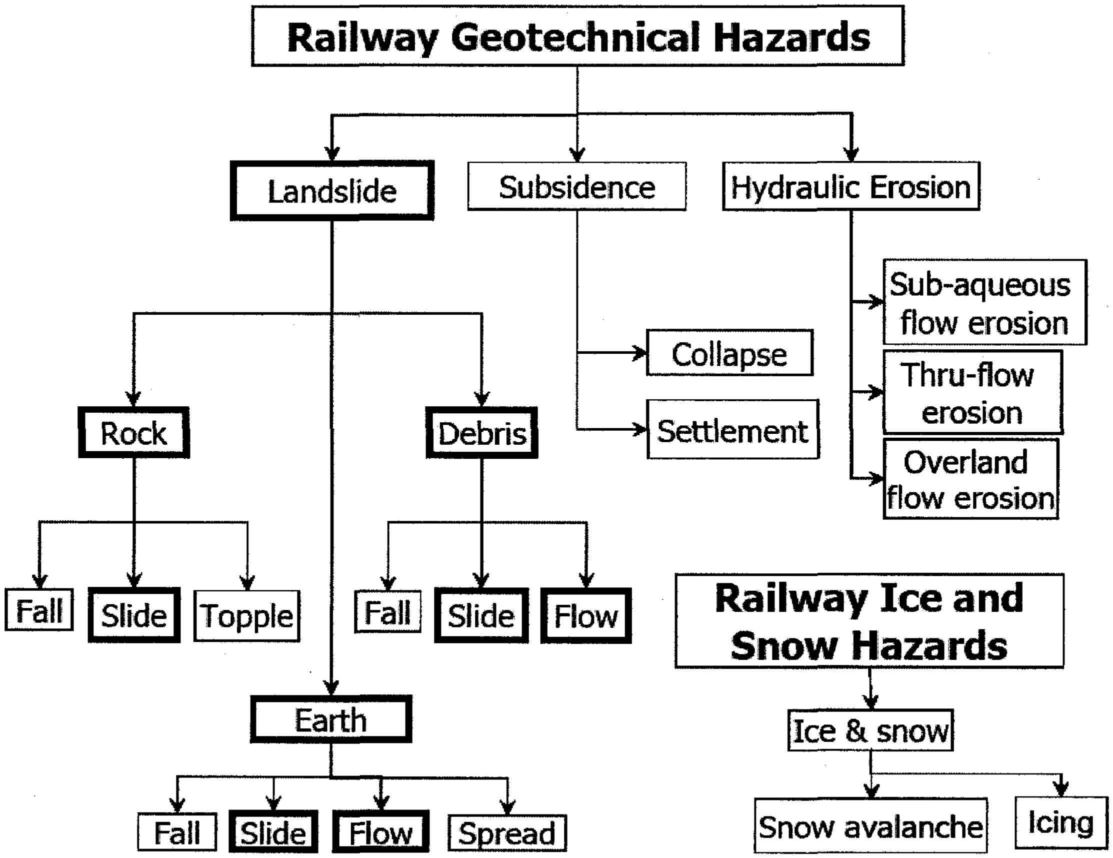

Figure 2.1 Overview of railway ground hazards (after Keegan 2007). The bold boxes are the landslide hazards most influenced by precipitation and the primary focus of this research.

A list of loss outcomes due to geotechnical hazards is included in Section 5.4.2 and some example scenarios are provided in Section 5.4.2.1.

2.2.3 Spatial distribution of geotechnical hazards

Geotechnical hazards are distributed throughout the CP network, however, groupings can be made by hazard type, soil conditions, climatic region and amount of topographic relief. The dominant hazards for 5 regions of similar geotechnical characteristics are identified in Table 2.1. The spatial distribution of landslides by type, subdivision and region is illustrated in Figure 2.2.

There are 823 earth slides and debris flow slides within the CP NHID. Of these hazards 570 (69%) are within the 1,820 km (1,130 miles) of track within the mountainous region of BC and Alberta or the Canadian Cordillera. The remaining

Table 2.1 – Region and most common geotechnical hazards

Number	Service Area	Hazard
1	Vancouver and B.C. Interior	Debris flows, rock slides, erosion (washouts) and landslides
2	Alberta, Saskatchewan, Western and Southern Manitoba, and St Paul	Landslides and track subsidence
3	Northern Ontario and Eastern Manitoba	Erosion (predominantly sand fills) and landslides
4	Northeast US	Landslides and erosion
5	Chicago	Landslides, karst sink-holes and erosion

15,200 km (9,430 miles) of mainline track in the rest of the network account for 257 other hazards. Therefore, the frequency of landslides along CP track inside and outside the Canadian Cordillera is one landslide every 3.2 km (2 miles) and one landslide every 60 km (37 miles), respectively. Therefore, the density of hazards along CP track in the Canadian Cordillera is almost 20 times that of the rest of the CP network. Based on this simple analysis it would be expected that CP should spend about 20 times more resources within the Canadian Cordillera than the rest of its network. The ratio of current expenditures is 5.7 to 1, inside to outside the Canadian Cordillera because non-safety, service reliability considerations also influence the allocation of resources.

2.3 Weather and landslides

Numerous researchers have successfully investigated the relationship between precipitation and landslide activity. The mechanisms and physical process that cause landslides to be influenced by precipitation are described in Appendix B. In summary, the hydrologic cycle controls the flow of water through the atmosphere, soil, groundwater, lakes and other components. The land surface water partitioning determines how much water infiltrates into the ground. Infiltration is controlled by the Richards equation (Appendix B, Section 1.2, Equation B1) and several formulations have been derived to estimate infiltration into the groundwater system. Snow and ice accumulation and melt also intercept and influence water storage and the temporal

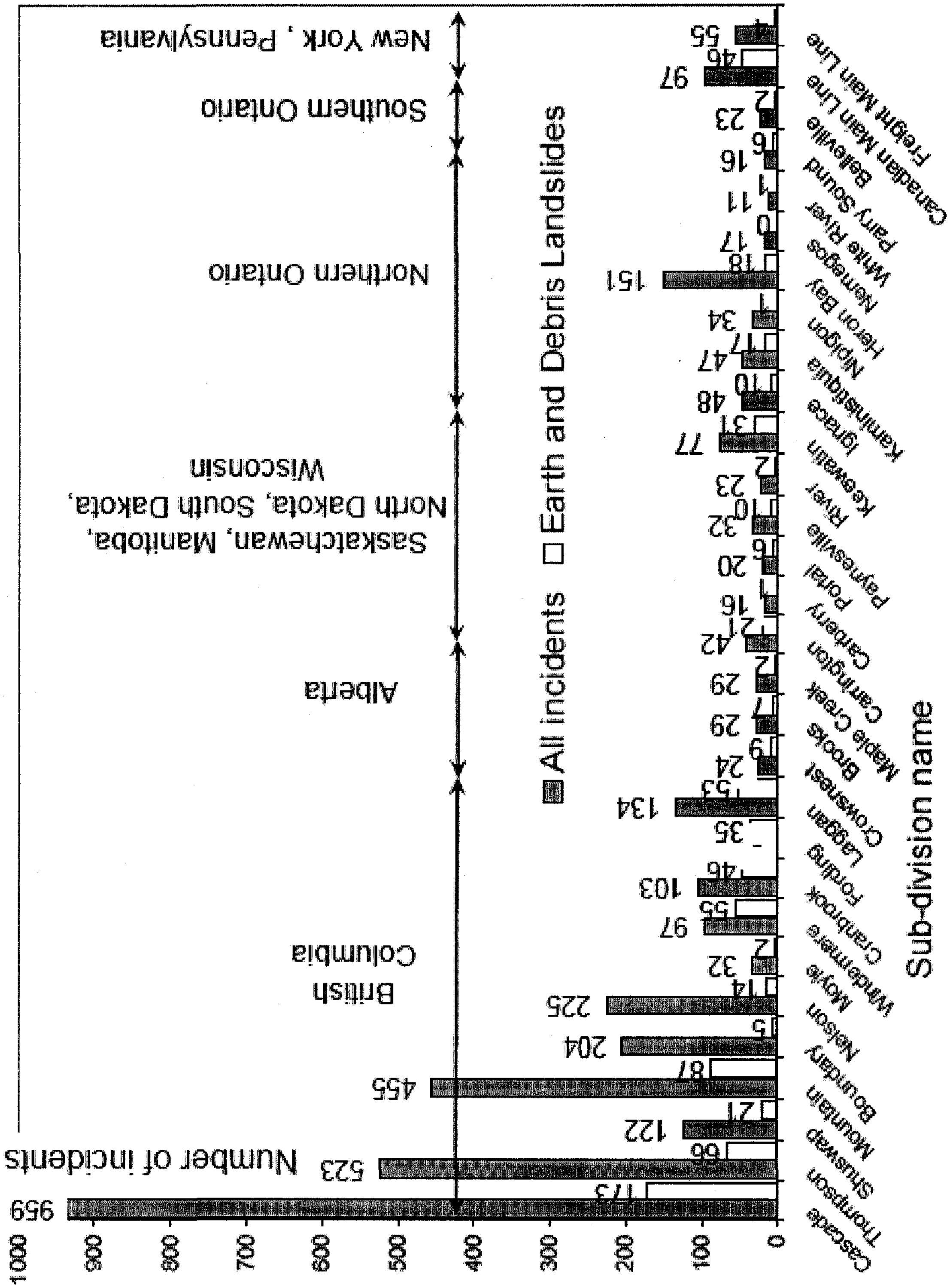

Figure 2.2 The number and distribution of all incidence and earth and debris slides and flows across the CP rail network for the 30 sub-divisions with the most incidents

variability of infiltration. Evaporation and transpiration reduce the water available for infiltration into the soil and groundwater. Groundwater migration is governed by Darcy's law. The groundwater condition influences the stability of the slope commonly assessed using limit equilibrium analysis. Debris flow are a type of landslide dependent on high water content and therefore strongly influenced by precipitation and weather conditions. Of the parameters that change in time, precipitation is one of the most variable and therefore influences the temporal aspect of landslide activity.

As discussed in Appendix B, there are numerous processes influencing the amount and rate at which water reaches the saturated and unsaturated soil all of which can be modelled to some degree depending on the available information. Despite understanding the physical processes controlling infiltration and slope stability, the complexity and number of parameters required to monitor, model and predict the influence of these processes on the Factor of Safety (FOS) of all the potential hazardous sites to which a railway is exposed, would not be feasible for a railway operator. Since precipitation is the primary source of inflow to these processes it is reasonable to use precipitation as an indicator of the condition of the slope, especially the change in the condition of the soil moisture properties. In many cases the antecedent precipitation provides an index representing the initial conditions and high intensity precipitation provides an index for the shorter time frame processes. As is demonstrated in Section 2.3.1 the complexity and enormous variety of the unstable conditions can be forecast to some extent by developing empirical relationships between precipitation and known landslide occurrences.

2.3.1 Weather indices for the prediction of landslides

Section 2.3 identified precipitation as the largest source of water to the soil and groundwater systems. Numerous researchers have proposed and demonstrated the connection between precipitation and geotechnical hazards. Appendix C provides a review of the extensive body of literature describing the development of various weather indices for the prediction of geotechnical hazards. A summary of this work is provided in this section.

To provide a consistent jargon the following definitions of program, system, index and threshold are used in this research. From the most general to the most specific a warning system consist of a weather monitoring and hazard notification **program**. Within a program a **system** of weather **indices** would be employed and each index would have a **threshold** that when exceed would prompt some action by the program.

The research reviewed in Appendix C demonstrates that weather can significantly influence the stability of slopes and embankments. It is also clear that due to the range of precipitation conditions, it is one of the most widely and rapidly varying of the parameters influencing the stability of a given slope. Table 2.2 provides a summary of the types of relationships and plots that are used to distinguish which precipitation conditions induce landslides.

Table 2.2 indicates that researchers have taken a wide variety of approaches to assess how to establish which duration of antecedent precipitation a landslide is most sensitive. For those not considering the influence of antecedent conditions beyond a few days this is relatively simple because of the coincidence of the precipitation and the landslide. In most cases, these researchers are investigating landslides with primarily permeable soils such that antecedent conditions are not significant (Rahardjo et al. 2000 and Aleotti 2004) but this is not true for all landslides.

Ko Ko et al. (2003), Chowdhury and Flentje (2002), Floris et al. (2004), Tommasi et al. (2006), and Terlien (1998) identify various means of discriminating which of the infinite number of possible antecedent precipitation indices and relationship available is the most critical indices for a specific location. Each of these provides some insight into the determination of the most important indices. The method proposed by Petrucci and Polemio (2003), Floris et al. (2004) and Floris and Bozzano (2007) that selects the most critical precipitation index based on the antecedent precipitation duration, coincident with the landslide, that has the highest return period, appears the most promising. These authors use of the Generalized Extreme Value (GEV) distribution to determine the return period of the antecedent precipitation provides a robust estimate of the return period for multiple antecedent precipitation durations.

2.3.2 Use of weather indices for warning of geotechnical hazards

Weather information systems are used in numerous urban areas such as Hong

Table 2.2 Summary of precipitation-induced landslide relationships for the literature

Relationship	Plot type	Attributes and limitations	Authors
Intensity versus duration and intensity duration frequency	ID and IDF	- Unlimited accounting of antecedent conditions - Limited resolution - Widely adopted - Critical rainfall determine by inspection of data	Caine 1980, Guzzetti et al. 2005 and 2007, and others
		Critical antecedent duration determined using maximum return period	Zézere et al. 1999, Fiorillo et al. 2001, Petrucci and Polemio 2003, Floris et al. 2004, Tommasi et al. 2006, Floris Bozzano 2007, Walker 2007, and others
Intensity versus cumulative event rainfall	IE plots	- Limited accounting of antecedent conditions - I and E are not independent	Okada et al. 1994, Ortigao et al. 2001, and others
Daily rainfall versus decay type antecedent precipitation index (API)	Decay API	- Depending on the formulation may introduce discontinuous annual function - temperature data may be required - R and decay type API map not independent	Crozier 1999, Crozier and Elyes 1980, Godt et al. 2006, Inagaki and Sadohara 2005, and Sirangelo et al. 2003, and others
Short cumulative event versus long cumulative event	$A_{(c-d)}/A_{(d+1)-f)}$ plots where $c<d<e$	- Empirical determination of c, d, and e required	Chleborad 2000
Multi factor indices combining I, $\hat{I}_{(6h)}$, $A_{(28)}$, stream flow data and storm classification		- Requires hourly rainfall and stream flow data additional weather forecast information	Jakob et al. 2003 and Jakob et al. 2006

Kong (Dai and Lee 2001, Hong Kong Observatory 2005, and others), Rio de Janeiro (Ortigao and Justi, 2004) and San Francisco (Cannon and Ellen 1985 and others). These systems are intended to notify key personnel within an organization and the public, that severe weather conditions are occurring and that risk management measures should be assessed or implemented. To be effective the weather information systems must be able to differentiate between severe weather and non-severe weather and result in a minimal number of false alarms. Appendix C includes citations and a description of various existing and proposed precipitation-induced landslide-warning systems.

It is clear from the review of the available literature that the Japanese railway systems have the most highly developed precipitation-induced landslide warning system for railways. Consistent with Japanese railway practice the use of specific criteria for each relevant weather station is recommended for adoption in the development of a precipitation induce landslide warning system. Additional justification for this approach is provided in Section 3.4. The remainder of this research focuses on this approach.

2.3.2 Vision for application of geotechnical weather indices

Once a methodology of identifying which precipitation index is most critical, and what threshold is appropriate for each indices, each railway or weather information service provider can identify a system of indices and thresholds for each Class 1 railway. The WIS would notify the railway when a threshold for a specific weather station was exceeded and over what area of tracks the warning was applicable. The railway would then respond based on the risk level and tolerance they deem appropriate. The existing literature on assessing risk is reviewed in Section 2.4 and the variation in risk due to a threshold being exceeded is developed in Chapter 5.

2.4 Risk Management

Risk management is the process of understanding risk, quantifying it, comparing one set of risks to another set of risks, reducing risks to acceptable levels by selecting various actions, and then re-evaluating the risks to determine if additional actions are warranted. In some cases, risks may be accepted because either they are tolerable or the cost of pursuing other options is prohibitive. The Canadian Standards Association (1997) Q850-97 Risk management: Guidelines for decision-makers document provides a consistent framework and terminology in which all risk management processes can be completed. This guideline can be consulted for the definition of the numerous terms. This framework is used in this research and is shown in Figure 2.3.

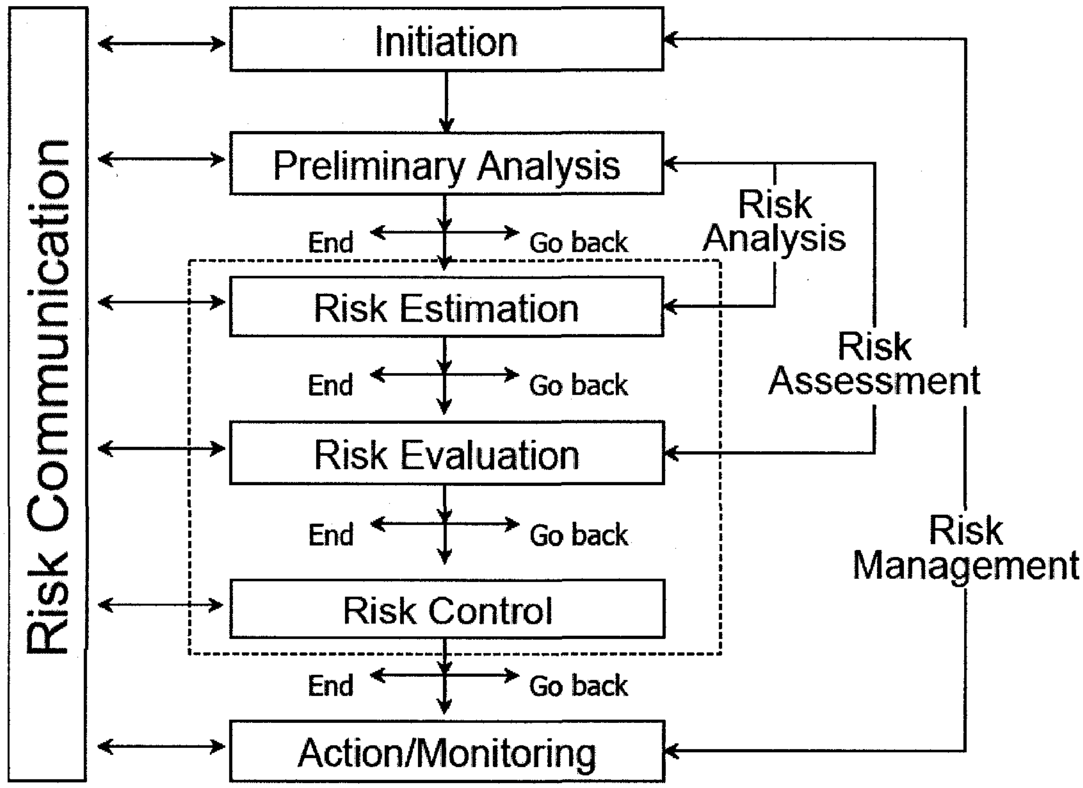

Figure 2.3 Canadian Safety Association risk management process flow chart (after Canadian Standards Association Q850 (1997). The dashed box indicates the focus of this research.

The Proceedings of the International Conference on Landslide Risk Management in Vancouver, Canada (Hungr et al. 2005) provides a diverse and thorough review of risk management applied to landslide hazards. Most of the concepts developed in Chapter 5 of this research come from the 8 state-of-the-art papers in those proceedings. Additional discussion of risk management research, its application in geotechnical and non- geotechnical fields and is limited application to the geotechnical engineering within of the North American railway industry is included in Appendix D

Based the work summarized in Appendix D and the application of quantitative risk estimation techniques by others for linear corridors (Roberds 2005, Walker et al.

2000, Bunce et al. 1997, and McClung 1999) a risk estimation process is developed in Chapter 5 of this thesis.

The use of quantitative risk estimation allows comparison of specific sites with the entire system and one site versus a second. It also allows the calculation of the annual cost or risk liability of a site given different levels of investment or intervention consistent with Tatone (2007). Quantitative risk estimation can be used to compare the safety record of regions, departments and groups of employee of a railway. It can also be used to compare one railway to a second, and railway and non-railway risks to assess a railway's safety record.

2.5 Conclusion

In this chapter the relationship between precipitation and landslides has been reviewed. Previous studies have indicated that of all the weather conditions measured, several different rainfall based criteria have the highest correlation with landslide hazards. Numerous means of analyzing precipitation and landslide data have been assessed and numerous antecedent precipitation indices identified. The Caine (1980) presentation of the criteria has become the most widespread system and the RISK AWARE initiative (2005) and Guzzetti et al. (2007 and 2008) have adopted this approach. The use of the maximum return period antecedent precipitation to identify the critical precipitation duration that induces a landslide has been reviewed. The evaluation of risk, and specifically quantitative risk estimation in geotechnical engineering, has also been reviewed.

Chapter 3 Development of precipitation indices for predicting landslides on railways

It is proposed that a methodology for identifying which precipitation-induced landslide indices are the most appropriate be developed by adopting and applying the science and techniques reviewed in Chapter 2. The proposed system will function much as the Japanese railway system (Katayose 1987 and Rimm-Kaufman 1996) does with specific criteria developed for each available weather station or group of weather stations. This provides the greatest resolution of the most spatially relevant data. There are two challenges to this effort. Identification of:

1. the critical index type for each location, and
2. the critical threshold of the index at which risk mitigation should be undertaken.

The identification of the most critical precipitation indices will be undertaken using a combination of methods, depending on the amount of landslide data. The methods are based on modified versions of the methods presented by Fiorillo (2001), Floris and Bozzano (2007), Walker (2007), and Chleborad (2000). Where CP landslide data is insufficient the widely accepted Intensity Duration (ID) criteria utilized most recently by Guzzetti et al. (2007 and 2008) can be applied. The use of ID relationships will allow for the adoption of existing criteria where CP landslide event data is limited or unreliable. Provided longer antecedent indices can be appropriately analyzed and compared to shorter duration indices there should not be a need for measures that integrate decay functions into antecedent precipitation indices.

The need for normalization of indices should not be required because indices and thresholds will be weather station specific. They would only be considered where there are no CP landslide data available and the use of indices and thresholds developed for similar hazards, climates, and geotechnical conditions must be used.

3.1 Distribution and quality of climatic information

There are a wide array of types, sources, and qualities of weather information. The most relevant ones to this study are discussed in the subsequent subsections.

3.1.1 Sources of information

There are several sources of precipitation and other weather data. These include the national weather services of Canada and the US and provincial and municipal agencies. The use and access to weather radar and satellite data capable of detecting moisture conditions on the ground will also be reviewed.

3.1.1.1 Conventional national weather services data

Climatic information is available from a broadly distributed network of weather stations throughout North America. Since the inception of CP in 1881, the density and distribution of weather stations and the quality and frequency of the data has changed drastically. Until the 1960's weather data was collected and recorded manually or mechanically. In the past 40 to 50 years, automated digital weather stations, most with real time or near real time communications, with a central data collection and distribution centre, have become ubiquitous (Environment Canada 2004).

There are over 250 active weather stations operated by the national weather services of Canada and the US near CP rail lines. These stations have the ability to provide near real-time data on a current and ongoing basis. The national weather services also provide weather predictions for the majority of these stations.

Due to the historical nature of the CP Natural Hazard Incident Database (CP NHID) it is also necessary to access historical climatic records. General access to historical data is provided through the internet for free, or for a minimal charge from Environment Canada (2005) and the US National Climate Data Center (2007).

3.1.1.2 Weather radar

As with conventional precipitation data, each of the national weather services operates weather radar systems. This information can be obtained for a fee from these services (D. Jobin, personal communications 2007). Weather radars are typically located at major airports so information is available for many urban and surrounding rural areas (Hoblit et al. 1999).

Weather radar provides an estimate of the reflectivity of the precipitation in the atmosphere at a set time interval (Gekat et al. 2004). Doppler radar is also available in most areas and provides an indication of the radial velocity of the atmosphere around the radar station.

Weather radar does not yet provide useful precipitation information in mountainous terrain for two reasons. Severe orographic effects cause highly spatially variable micro-climatic conditions due to the air mass being differentially lifted, channelled, heated, cooled, and supplied with moisture by variably exposed and vegetated slopes and lakes present in mountainous terrain. Also the radar beam is obstructed by topography and therefore shielded from some areas (Germann and Joss 2004). Although efforts have been made to overcome these deficiencies (Gabella et al. 2001, Li et al. 1995) weather radar data for topographically variable areas are not generally available. As a result, weather radar information is available throughout the topographically flatter and more densely populated regions of North America.

3.1.1.3 Other terrestrial weather data sources – province, state and private data suppliers

Additional weather stations are operated by provincial, state, county and regional government agencies, and private companies. These include stations owned and operated by railways. Union Pacific (UP) railway maintains a system of 264 weather stations along its rail network (Rossetti 2006). In British Columbia the two Canadian railways are known to have at least two weather stations each. The Canadian railways share the data from their weather stations with other provincial agencies in exchange for access to the provincial government weather station data.

Similar data sharing initiatives including the MADIS system (NOAA 2007c), the Clarus Initiative (2007 and Pisano et al. 2005) and the CP RailWIS system are successfully drawing data together from disparate sources throughout North America. The MADIS system ingests precipitation data from over 30 different agencies. Challenges of using data from a variety of suppliers include accounting for the variability in collection standards, the quality of the data, and the reduced availability of historical data. The two national weather services attempt to follow World Meteorological Organization (WMO) standards in the collection and documentation of weather data. Other agencies do not adhere to such standards and therefore may not provide consistent information that can be directly compared to federal government data.

Numerous researchers have investigated means of testing and correlating precipitation data to improve its reliability, however usually, if there is a significant period of record this may not provide significant benefit.

In summary, there are several times more conventional ground weather data sources than are available through either of the national weather services. Like the MADIS, the Clarus Initiative (Pisano et al. 2005), and the RailWIS systems (RadHyPS Inc. 2007) arrangements with each data collector must be undertaken to obtain this data to provide the greatest resolution of weather conditions possible.

3.1.1.4 Other data sources

There are other sources of precipitation data including space based systems. Two of these are:

1. The National Aeronautics and Space Administration (NASA) MODIS or Moderate Resolution Imaging Spectroradiometer system (National Aeronautics and Space Administration 2008b), and
2. The NASA Tropical Rainfall Measuring Mission (TRMM), Multi-satellite Precipitation Analysis (TMPA) systems. This satellite based system provides means for quantifying land surface characteristics such as land cover type and extent, cryosphere (snow and sea ice) cover, surface temperature, leaf area index, and fire occurrence. This system does not provide direct measurement of precipitation.

NASA is proposing the deployment of additional Global Precipitation measuring systems (National Aeronautics and Space Administration 2008a) in 2013. The use of the TMPA global rainfall map to predict landslides world wide is explored by Hong and Alder (2007), Hong et al. (2007a) and Hong et al. (2007b). All these systems require reliable precipitation induced landslide indices and thresholds.

3.1.2 Standard observation

A number of weather observations are undertaken at different locations. The current standard Environment Canada daily observations include temperature (maximum, minimum and mean temperature), heat degree days, cool degree days, total rain, total snow, total precipitation, snow-on-the-ground, direction of maximum wind gust and speed of maximum wind gust. Precipitation is the sum of the rainfall and the snow water equivalent (SWE) depth of water. All observations are not available all the time, at all stations. However, precipitation data is often one of the few fields available throughout the historical records.

3.1.2.1 Access to precipitation data

Access to historical Environment Canada weather data was realized via the EC website (Environment Canada 2005). The web site provides access to historical and current weather as recent as the previous day. Hourly precipitation data in not available.

Even though it is a standard field on the EC website, snow-on-the-ground measurements are only provided at a limited number of stations and historical data is very limited. Available snow-on-the-ground data is reviewed in Section 3.1.2.3.

3.1.2.2 Precipitation

Evaluation of the data quality and period of record has to be determined on a case by case basis. In many cases the climate record at a specific station is discontinuous. However, Environment Canada has established, replaced, and modified the location and instrumentation such that statistical analysis of climatic conditions and return period calculations can usually be undertaken by merging or combining nearby weather stations such that a continuous and representative record can be compiled.

An isohyetal map is a contour map where the contours join points of equal rainfall during a specified period. Provided there is a high density of rainfall gauge data, the maps can be an effective means of determining the precipitation at a given point and they provide a means of determining the rainfall distribution over a watershed. Froehlich (1995) shows how isopluvial maps (maps with contours identifying regions of equal precipitation) of the National weather service (Miller 1964) can be used to estimate the intensity duration relationship for rainfalls of 1 to 10 days for various return periods. However, this method does not lend itself to automated calculation because the first step is dependent on the acquisition of data from paper maps. Furthermore, it is limited to 10 day antecedent duration by the nature of the NWS maps.

Isohyetal maps can be used to correlate orographic influences and assist in the prediction of precipitation at un-gauged locations at variable elevations. Previously, isohyetal maps were not available in real time and were therefore used to analyze specific precipitation periods. Near real-time isohyetal maps are becoming more common. By processing real-time precipitation data, NOAA (2007a) distributes isohyetal maps of grid-data via the internet.

NOAA (2007a) produces isohyetal maps for numerous periods that can be used to identify and assist in the prediction of various hazards. Some of these maps are produced every week and can be used to aid in identifying areas where increased antecedent rainfall is occurring on a near real-time basis. The Climate Prediction Center (NOAA 2007b) compiles numerous maps using 30, 60, 180 and 365 day accumulated and forecast rainfall information to assess the potential for wild fires, droughts, floods, and other hazards. This information is available on a daily basis for the 30 day accumulated precipitation (NOAA 2006). These can be used to identify areas where increased antecedent rainfall is occurring on a near real-time basis.

Daily and 24 hour precipitation are not necessarily equivalent. As noted by Walker (2007), Crozier (1999), and others, daily rainfall is reported over a given 24 hour period. At Environment Canada the period is between 00:00 and 23:59 but this not the practice in every country. Twenty-four hour precipitation is summed over the previous 24 hour period, each hour of the day. A rainfall event extending from before to after midnight will be divided between two days of daily rainfall but may fall in the same 24 hour rainfall period. As a result, the daily rainfall will not necessarily equal the 24 hour rainfall because the periods can be different, especially if the peak 24 hour rainfall is being compared to the daily rainfall. As a result, a landslide reported in the morning may have been only partially impacted by the daily rainfall. Unfortunately the time of day of most landslides is not recorded in the CP NHID.

3.1.2.3 Snow

Two types of snow data are generally available:

1. Weather stations with snow-pillow data. These stations are normally located in drainage basins, at higher elevations, and with snow accumulations of several metres annually.

2. Weather stations with snow-on-the-ground information. These are usually major airports.

Snow-on-the-ground and snow-pillow information are point measurements consistent with rainfall point data. As with rainfall data there can be significant variation of snow accumulation due to orographic, melting, and wind drifting effects that influence snow deposition within a drainage basin. However, the point information from a snow-pillow or snow-on-the-ground station is the best estimate of the stored precipitation within a drainage basin.

Snow-on-the-ground information is reportedly available for 826 locations in Canada within areas covered by CP and active in 2007. However, it is the author's experience that this data is not always available. Table 3.1 provides an indication of the snow-on-the-ground sites near CP track in each province.

Table 3.1 Environment Canada (M. Petrou, Environment Canada, Personal communications 2007) snow-on-the-ground stations near CP track

Province	Number of stations with snow-on-the-ground measurements
BC	90
Alberta	307
Saskatchewan	136
Manitoba	84
Ontario	150
Quebec	59

Snow-pillow information is available from the British Columbia Ministry of Environment (2006), River Forecast Centre. About 9 locations in southern British Columbia are in relatively close proximity to CP tracks.

3.1.2.4 Data quality and quantity

Data quality and quantity are always an issue. Weather station data is chronically incomplete due to several factors. First, the instrumentation is expected to function 24 hours a day, every day of the year in all types of weather. Second, the precipitation instruments must be able to accurately measure rainfall over 4 orders of magnitude from 0.1 mm/hr to over 100 mm/hr. However, maintaining mechanical components sensitive enough to achieve this level of accuracy over this range of conditions is challenging. As a result, precipitation measuring instruments are not reliable 100% of the time. However, provided there is data from 30 years or more the absence of some data is this overshadowed by the available data.

3.1.2.5 Historical availability of climatic data

The availability of historical climate data is highly variable. Generally, in larger sites the climate record is continuous or can be assembled from multiple weather stations with sufficient temporal overlap to account for changes in the orographic effects between stations. In the hinterland the weather stations are located at airports but the data is often less continuous depending on individuals who collect and maintain the weather station.

3.1.2.6 Spatial distribution of weather stations relevant to the railway

This section discusses criteria for deciding if data is relevant when multiple stations are available near the landslide site.

In most cases there will not be a weather station in close proximity to the landslide site. As a result, precipitation data has to be extracted from nearby stations. This is a common problem in hydrology and numerous methods have been developed to approximate the precipitation at a given location from nearby weather stations.

Specifically for railway hazards, Muraishi and Okada (1988) utilized the inverse weighted distance method (Equation 3.1) and found the best fit for the power relationship to be with $j = k = 0.98$ for the cumulonimbus dominated weather systems typical of southern Japan. Muraishi and Okada used this relationship to empirically fit available data so the units are not respected.

$$P_E = \frac{\sum_{i=1}^{a} P_i^j / D_i^k}{\sum_{i=1}^{a} 1 / D_i^k}$$

Equation 3.1

Where P_E is the estimated hourly precipitation at a specific point (landslide location), P_i is the measured hourly precipitation at a rain gauge, D_i is the distance between the location of P_i and the landslide, k is the power coefficient and a is the number of nearby rainfall gauges.

The inverse distance (American Society of Civil Engineers 1996) or specifically the reciprocal distance squared method, where j is set to 1 and k is set to 2 consistent with Dean and Snyder (1977), and Scire et al. (2000) is used in this thesis.

To decide whether there is value in including the next nearest station some guidance is provided. Assuming the precipitation at the nearest two rain gauges for a given storm record are within an order of magnitude of each other and given that precipitation is measured to the nearest 0.1 mm. To be significant the farther gauge must contribute more than 0.1 mm despite the distance weighting. Figure 3.1 indicates the asymptotic nature of Equation 3.1 with k = 2 for increasing distance from the landslide. It is evident from Figure 3.1 that the estimated precipitation for two and three precipitation gauges does not change more than 1/100th of the estimated precipitation once the 2nd and 3rd precipitation gauges are more than 7 and 10 times, respectively from the nearer precipitation gauges. The curves of Figure 3.1 are developed by setting P_1/P_2 in Equation 3.1 to 10 and varying the ratio of D_1/D_2.

As would be expected Muraishi and Okada (1988) found that Equation 3.1 is inapplicable when the precipitation was influenced by either orographic effects or local convective storms. As a result, the selection of anything but the closest precipitation gauge data must include the assessment of whether the next nearest gauges will have recorded representative data or not.

It should be noted that the use of Equation 3.1, to merge data from multiple locations, in order to estimate the precipitation at an intermediate location averages the data, and therefore results in an estimate less than the daily precipitation of the wettest of the two or more nearby stations. Simultaneous precipitation data from the winter of 1960/61 from the N Vancouver 2nd Narrows and Burnaby Capital Hill, Environment Canada weather stations are used to demonstrate this effect. These stations are on either side of Mile 123.40 on the Cascade Subdivision (CASC 124.30) east of Vancouver, BC. The North Vancouver and Capital Hill weather stations are 5.3 km northwest and

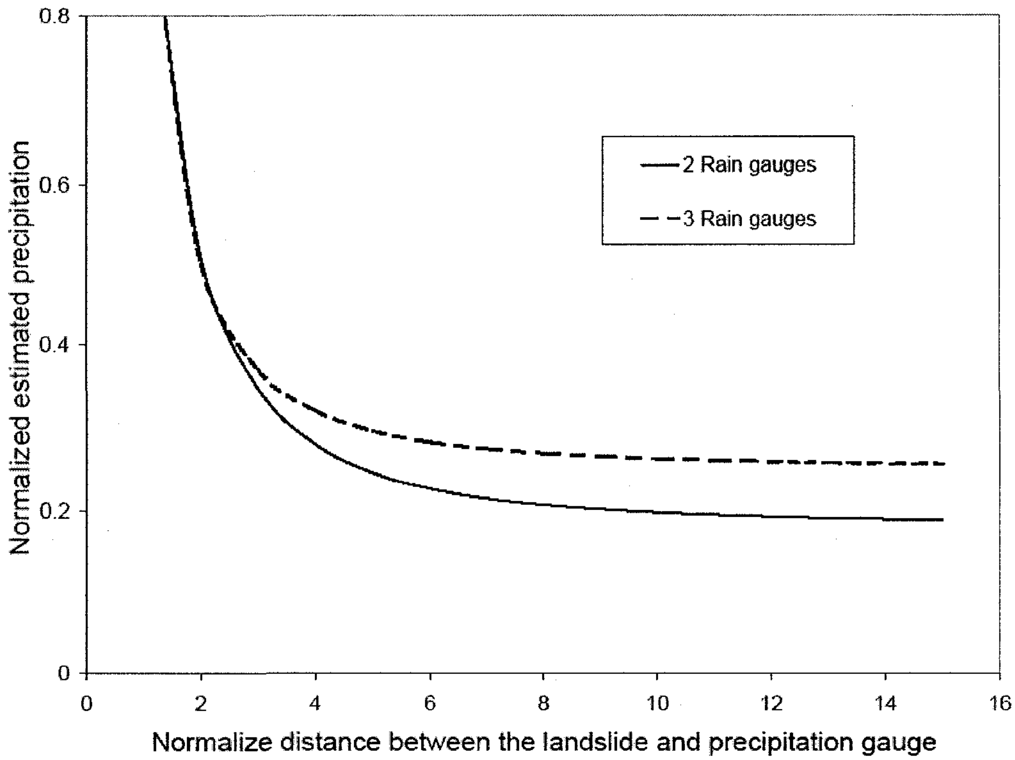

Figure 3.1 Sensitivity to proximity of rain gauges. The influence of the distance between two and three rain gauges on the estimated precipitation at a third site with no precipitation gauge.

3.1 km southeast, respectively, of the CASC 123.40 landslide location. As can be seen in Figure 3.2 the calculated precipitation at CASC 123.40 is always less than the peak precipitation at either station. Only when the two stations record the same precipitation (usually small accumulations) does the calculated precipitation at CASC 124.30 equal the peak precipitation at either station. On average, for 12 months starting 1960 September the calculated precipitation at CASC 123.40 is only 84% of the peak precipitation at either station. However, for longer antecedent durations this condition becomes less severe. For instance the average of the 14 day antecedent precipitation at CASC 123.4 is 93% of the maximum precipitation at either of the two weather stations for the same 12 months. Similarly, the $A_{(30)}$ is 96% and the $A_{(365)}$ is 99% of the maximum precipitation at either of the two weather stations. This also demonstrates that time averaging results in a higher correlation between weather stations.

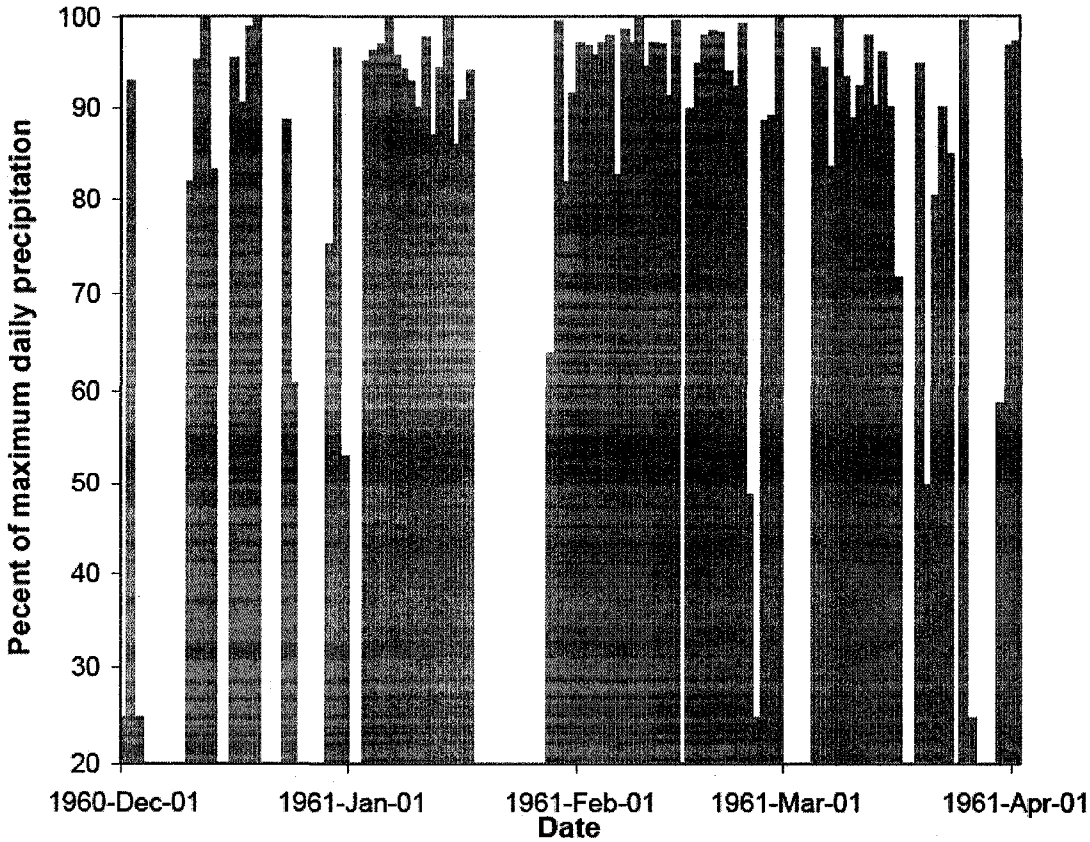

Figure 3.2 Percent of maximum daily precipitation at North Vancouver, 2nd Narrow and Burnaby Capital Hill weather stations predicted for a landslide at CASC 123.40 between the two weather stations for the month of 1961 October using Equation 3.1 with k = 2.

As a result, calculating the precipitation at a landslide location based on two or more nearby stations reduces the extremes in the precipitation data. It also introduces precipitation with a different, less severe return period when antecedent distribution fitting of the precipitation data is utilized. As a result, application of the reciprocal distance method is only appropriate when a weather station is not available for significant distance and the climate is expected to be between the extremes of the two or more nearest weather stations. If data from multiple stations are available the station that is most representative of the landslide location should be used for the precipitation analysis of the site.

3.1.3 Weather radar

The American Society of Civil Engineers (1996) provides a description of how weather radar is used to estimate precipitation. Weather radar provides a measurement of the radar reflectivity of the precipitation in a volume of atmosphere (Stull 2000). The reflectively is a proportional to the size measure and number of rain drops in a volume of air. Therefore, weather radar is capable of determining the severity of rainfall in the atmosphere.

3.1.3.1 Uses of weather radar

After some recent landslides, CP used weather radar to determine the spatial distribution of rainfall on an approximately 2 by 2 km grid (Gekat et al. 2004). To achieve the representative results the radar reflection intensity must be correlated with recorded rainfall at specific locations within the area covered by the weather radar. CP has used weather radar data to investigate the conditions resulting in landslides and overland flow erosion failures. Shi (2006) investigated one of these cases for her masters thesis. Similarly, weather radar data has been used to interrogate the temporal and spatial variation in precipitation at a specific location and within drainage basins (Collier and Hardaker 2004; Shi 2006). Hoblit et al. (1999) describe how weather radar can be used to increase the reliability of flash flood forecasts. Misumi et al. (2005) describes the use of X-band weather radar to estimate rainfall over complex terrain without the normal effects of beam attenuation or shadowing. Ryerson (1998) describes how weather radar is used by a railway weather service information provider to improve warnings and forecasts of severe rainfall and snow fall conditions.

3.1.3.2 Limitations of weather radar

There are a number of limitations to weather radar (Stull 2000). Due to convection of air masses and evaporation the amount of rain drops in the air is not directly related to the amount of water that reaches the ground. As a result, radar data has to be calibrated to rain gauge data to provide a reliable estimate of how much rain reached the ground. Once this calibration step is undertaken estimates of the rainfall at a specific location can be made.

Weather data has not been used in this study for the following reasons:

1. A large volume of data would have to be acquired, calibrated and processed.
2. The period of record of weather radar data is only now approaching 30 years and the data from the first years is of significantly lower quality from that available today. As a result, sufficient weather radar data is not available for reliable statistical return period frequency analysis.

Provided calibrated weather radar data was available for the area of the case study it should be possible to use the radar rainfall time series in place of a conventional rain gauge and produce consistent results.

3.1.4 Data required for statistical analysis of precipitation return periods

The length of data required to complete a return period analysis is dependent on the length and accuracy of the return period prediction desired. The longer the return period estimate and the more accurate the prediction desired the longer the period of record required (Sevruk and Geiger 1981). Statistical analysis can be completed to assess the reliability of return period estimates. However this is a statistical exercise beyond the scope of this thesis. Miller (1964) used 50 years of data for his analysis of 2 to 10 day precipitation return periods for primary data set. However, he used 20 years (and as little as 18 years) of data for his secondary data set. The primary and secondary data sets were defined as those as being more and less reliable, respectively, due to the longer and shorter period of record. The Rainfall Frequency Atlas of Canada (Hogg and Carr 1985) was based on a little as 7 years of data at some locations. However, more confidence was placed in results based on periods of record of 20 years or more. Based on these and the work of Miller (1964) and Hogg and Carr (1985) this research recommends the use of at least 30 years of daily precipitation data to predict return periods of up to 100 years.

3.1.5 Definition of antecedent precipitation and consideration when using antecedent precipitation data

As with many temporally variable conditions precipitation is a process that can be represented by an infinite number of measurements depending on the term over which the precipitation is measured or sampled. For example weather radar measures the amount of precipitation in the atmosphere on a time frame of seconds, while a tipping bucket rain gauge measures the time taken to accumulate the equivalent of a few tenths of a millimetre of precipitation. As a result, the temporal sampling frequency of a tipping bucket could be seconds, hours, or days; depending on the precipitation intensity and the sensitivity (volume of the bucket) of the instrument.

As demonstrated by Guzzetti et al. (2007) the number of variables used by researchers to describe precipitation is already large and therefore there is the potential for mixing data of different types. To reduce this, specific definitions are introduced and utilized in this thesis as per the List of variables. The variables used are consistent with Guzzetti et al. (2007) wherever possible.

To provide clarity the definition of antecedent precipitation, $A_{(c\text{-}d)}$ is the precipitation within a specific period as described by the subscript values c and d contained within brackets. The values of c and d are relative to the date of the landslide or current date depending on the use. This definition is consistent with that used by Chleborad (2000) and others. In this way the antecedent precipitation is independent of periods without precipitation. This definition avoids any confusion about when an antecedent duration starts and ends and what the period it is relative to. Figure 3.3 demonstrates the definition of these terms.

As can be seen in Figure 3.3, neither of the antecedent durations nor the period over which the intensity is measured are required to have continuous precipitation. All periods are defined with respect to the landslide. As per Govi and Sorzana, (Guzzetti et al. 2007) the term "Critical intensity" is reserved for the case where continuous precipitation is recorded prior to the landslide. However, where the critical intensity is based on daily precipitation it is possible that it is discontinuous in the hourly precipitation domain. In Figure 3.3 the critical intensity would be the average slope of the cumulative precipitation on the 25th, 26th, and 27th dates.

The definition of Cannon and Ellen (1985) suggests that antecedent rainfall is the cumulative precipitation measured before the "landslide triggering rainfall event". The Govi and Sorzana definition is the sum of the rainfall from some date c days before the landslide to a second date $c + d$ days before the landslide where d is the number of days of the "landslide triggering rainfall". The difference in the two definitions is whether the period of antecedent rainfall is defined with respect to the landslide

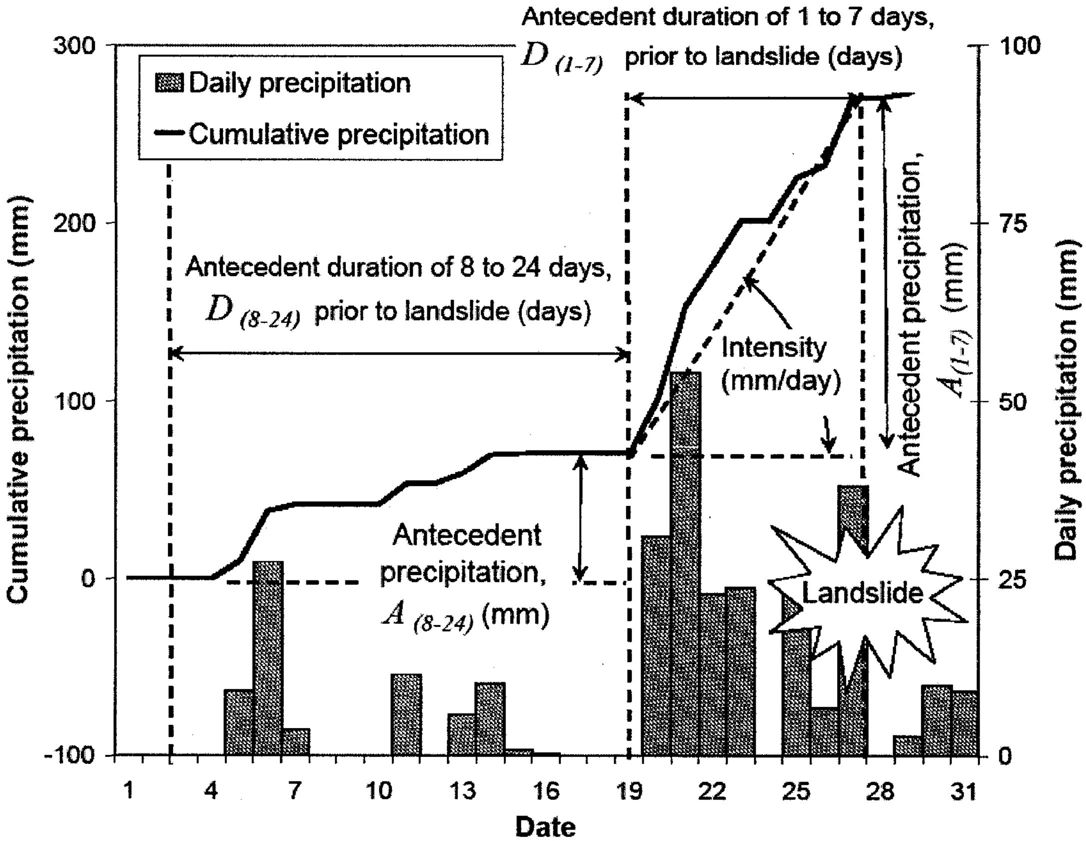

Figure 3.3 Definition of precipitation parameters after Aleotti (2004)

(Chowdhury and Flentje 2002, and Caine 1980) or the "landslide triggering rainfall event" (Guzzetti et al. 2007). It is the general contention of this study that landslides are induced by the combination of prior precipitation over different time frames and that these periods should be assessed independently.

The ID plots used by Guzzetti et al. (2007 and 2008) and others effectively use the definition of $I = A_{(c-d)}/D$ with c = 0 and $d = D$ used for this study. This is because the rainfall intensity, I, is defined as the amount of rainfall in a period divided by the duration of the measuring period without regard to when the measuring period starts, d days before the landside. Therefore, as noted by Guzzetti et al. (2007), I is not limited to being traditional, continuous rainfall intensity but is an average precipitation rate over a specific time period. Caine (1980) and subsequent researchers have effectively used I as a continuum from the traditional intensity of a rainfall as per the meteorological definition, to the average precipitation rate definition. A similar practice will be followed in this thesis.

Chowdhury and Flentje (1998) definition of antecedent rainfall is equivalent to the one used here with c set to zero for all periods. The disadvantage of this approach is that each antecedent index is not independent of the next shorter one. Therefore, plotting for example the $A_{(1-7)}$ versus the $A_{(1-15)}$ results in a large portion of the plot being void of data because $A_{(1-7)}$ is always less than $A_{(1-15)}$. This is also true of, and very evident in the Ortigao et al. (2001) type plot in Figure C2 where the upper left area contains no data. Plotting for example the $A_{(1-7)}$ versus the $A_{(8-15)}$, as per the Chleborad (2000) method, results in the correlation of two independent variables with no limitation on their distribution within the plot and no loss of information.

The goal of analyzing historical precipitation data is to determine what precipitation conditions or combination of conditions triggered or contributed to landslide activity. Researchers have proposed numerous methods of identifying the most significant precipitation event that triggered or contributed to a landslide event. For precipitation events shorter then several days investigators have little difficulty distinguishing the beginning and end of a storm event and therefore they can identify the intensity, I and duration D that induced the landslide. However, when a landslide is caused by an antecedent precipitation conditions longer than a few days (Cannon and Ellen 1985) where the rainfall may been light, heavy or zero for some portions of the antecedent duration the length of the most significant antecedent duration is not obvious.

The following section compares three periods with different precipitation conditions at the same location near Maple Ridge, BC that did and did not result in landslides.

Case 1 - On March 24, 2007 the depth of precipitation on the day of the landslide was normal but the antecedent precipitation prior to the landslide was high.

Case 2 - March 11, 2007 the daily precipitation was the second highest on record the antecedent precipitation was high and a landslide occurred.

Case 3 - 2003 October 16 the highest one day precipitation in more than 50 years occurred but no landslide resulted.

3.1.5.1 Case 1 - Landslides at Cascade Subdivision Mile 103.4 on March 24, 2007

Precipitation for the 15 and 365 days prior to March 24, 2007 are shown in Figures 3.4 and 3.5 respectively. As can be seen, the rainfall on the day, day prior and two days prior to the March 24, 2007 landslides were each less than 50 mm. A Gumbel analysis of the data indicates this depth of rainfall has a return period of less than 2

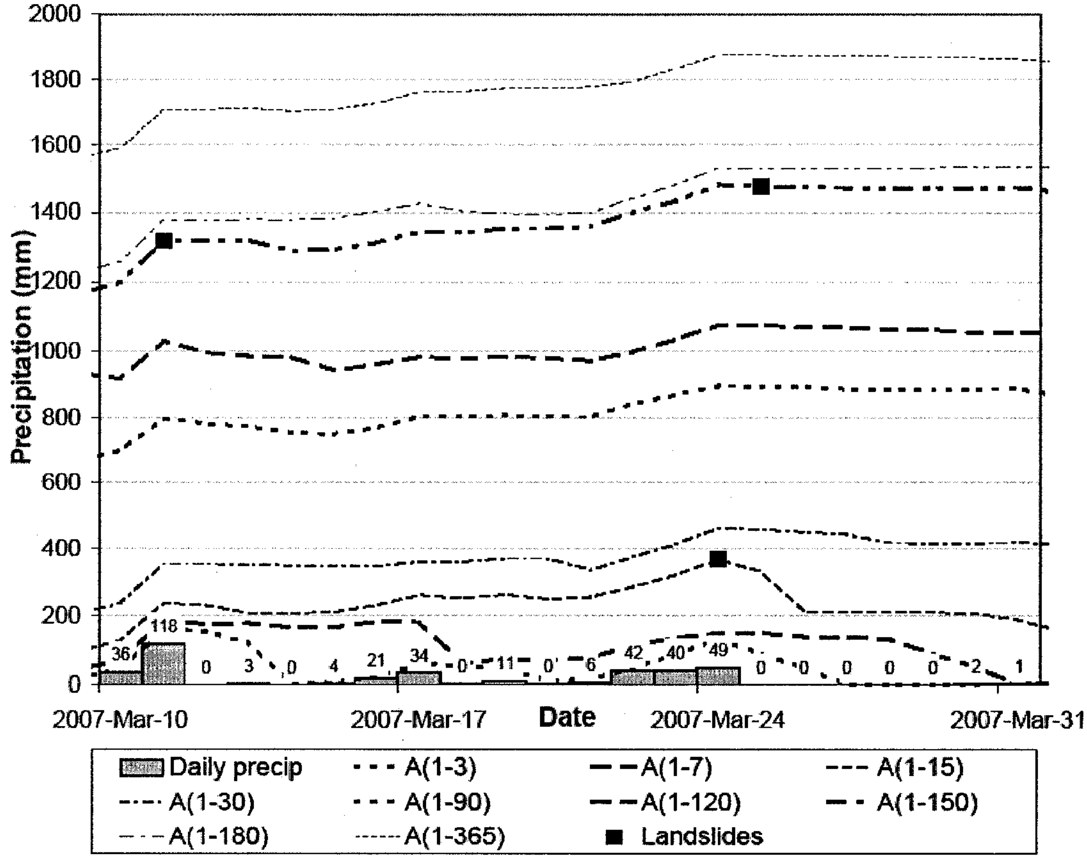

Figure 3.4 Daily and antecedent precipitation for the combined Haney and Pit Meadows CS weather stations with landslide data from Cascade Subdivision between miles 103.4 and 104.70 for March 2007. The landslides are shown on the line of the antecedent duration with the highest return period for the date of the landslide using a Gumbel frequency analysis of the precipitation data.

years. To evaluate the most critical antecedent condition the cumulative precipitation prior to the landslide has been summed for the durations shown in Figure 3.4. As can be seen from Figure 3.4 with the exception of the 3 and 7 day antecedent precipitation all the other durations of antecedent precipitations reach their highest level in the period of the graph (March 10 to 31, 2007) on March 24, 2007. This is due to the previous precipitation and the 49 mm of rain on the day of the landslide.

Based on this incident precipitation indices could be set as shown in Table 3.2. A landslide would be considered more likely when any one of these individual criteria was approached or exceeded. This would result in relatively frequent warnings given the relatively low return period of some of the precipitation events and the number of different criteria.

Table 3.2 Return period for the antecedent precipitation of March 24, 2007 when 15 landslides occurred between miles 103.20 and 104.20 occurred at Maple Ridge, BC

Antecedent duration (days)	Antecedent precipitation (mm)	Return period[1] (years)
3	131.2	3.1
7	149.6	1.4
9	204.8	3.7
15	365.8	50.6
30	461.6	16.7
90	895.0	7.6
120	1,076.6	6.6
150	1,480.8	27.8
180	1,531.4	18.0
365	1,876.6	3.35

[1] In this example the Gumbel return periods are shown

Study of Figure 3.5 reveals that some of the same or higher antecedent precipitation conditions at the time of the March 24, 2007 landslide had occurred within the previous year and no landslides had occurred. For instance the 30 day antecedent rainfall reached similar levels to those of March 25th in 2006 November but no landslides occurred. Due to the nature of the Gumbel distributions (see Chapter 4) the 7 day rainfall return period less than 2 years are not related to their reoccurrence interval

(Hogg and Carr 1985). For instance, in this case, a return period of 1.4 years for the $A_{(1\text{-}7)}$ indicates this antecedent rainfall of 149.6 mm in 7 days will be exceeded about 4 times per year.

3.1.5.2 Case 2 - Landslide at Cascade Subdivision Mile 103.41 on March 11, 2007

As can be seen in Figures 3.4 the rainfall on the day of the March 11, 2007 landslide was 118 mm. This is the second highest one day rainfall in more than 50 years. Using the criteria in Table 3.2 would result in warning of the March 11, 2007 landslide but these criteria would result in numerous warnings when no landslide occurred. To provide a warning of this hazard a criterion that for the one day rainfall exceeding 118 mm (or some lower threshold) should be added as an "or" condition.

3.1.5.3 Case 3 - No landslide at Cascade Subdivision miles 102.50 to 104.9 on 2003 October 16

On 2003 October 16, 136.4 mm of rain was recorded at the Pitt Meadows CS weather station. This is the highest rainfall in the 52 year period of record for this weather station. This event occurred early in the fall before any significant antecedent precipitation had occurred. No landslides were recorded for more than 6 weeks following this unusual precipitation event. However, a rainfall on 2003 November 28 of 87.8 mm did cause a landslide at CASC 104.50. As a result, warnings issued on the basis of one day rainfall would also result in false alarms.

3.1.5.4 Discussion

As a result of the cases described above the rainfall conditions for each recorded landslide need to be considered in the development of a multiple indices and threshold warning system. If all the antecedent conditions are included this will produce a lower bound limit for landslides above which landslides are possible. However, given the desire to limit false-negative warnings an upper bound threshold above which landslides are assured is desired.

To develop an upper bound precipitation criterion only the most severe antecedent precipitation conditions at the time of the landslide should be considered as having induced a landslide. A consistent approach of selecting the most unusual or rarest rainfall event as being the most likely to have triggered the landslide has been proposed by Fiorillo et al. (2001), Chowdhury and Flentje (2002) and Ibsen and Casagli (2004), and Floris and Bozzano (2007). Floris et al. (2004) suggests that landslides are caused by rare events and therefore investigates the highest return period event for a given rainfall duration.

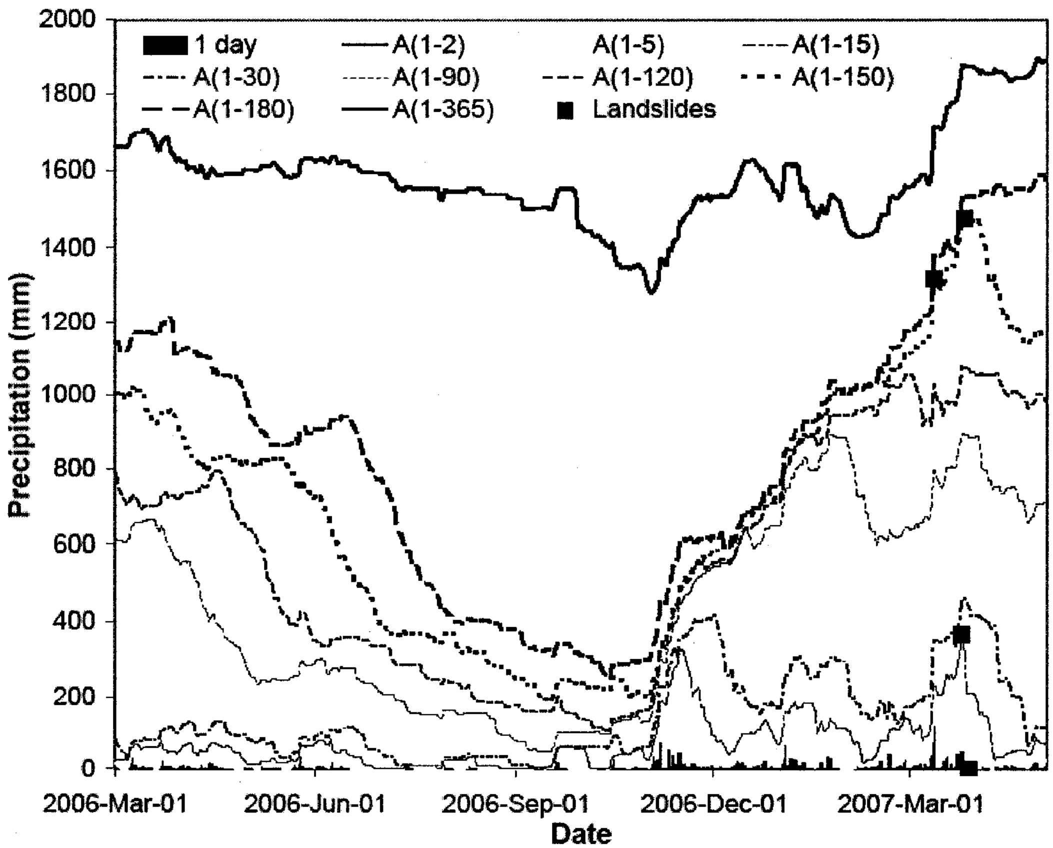

Figure 3.5 Daily and antecedent precipitation for the Haney and Pit Meadows CS weather stations with landslide data from Cascade Subdivision between miles 103.4 and 104.70 for 2006 March 1 to 2007 May 1.

Chowdhury and Flentje (1998) introduce the antecedent rainfall percentage exceedance time (ARPET) concept. They compute the percentage exceedance time of each rainfall which provides an indication of how rare the precipitation event is but it does not provide an indication of how rare the depth of precipitation is because only the rank of the antecedent rainfall is considered not the magnitude. Therefore, a precipitation event that exceeded the next highest event by 50% is assigned the same percentage exceedance as the event which exceeds the next highest event by 1%. This does not allow for the discrimination of severe events versus non-severe events when the percentage exceedance is compared for two different antecedent durations. In addition, expressing the rarity of the precipitation conditions as a "probability of exceedance" has little meaning in the physical or railway world.

The conventionally Gumbel extreme value frequency distribution used by Hogg and Carr (1985) can be used to compute the return period of rainfall as used in most precipitation intensity Duration Frequency (IDF) curves (World Meteorological Organization 1973 and 1983). However, the Gumbel distribution is neither upper nor lower bound limited and therefore only suited to the analysis of a limited set of antecedent duration precipitation conditions general less than 10 days duration as shown in Section 4.2.4 and suggested by Miller (1964). The Generalized Extreme Value (GEV) frequency distribution analysis of Jenkinson (1955) is better suited to the analysis of antecedent precipitation data of durations more than 10 days. Fiorillo et al. (2001), Petrucci and Polemio (2003) and Floris and Bozzano (2007) use the GEV frequency distribution to compute the return period for antecedent durations up to 180 days.

To determine which frequency distribution provides the best representation of the data or test the "goodness of fit" a means of assessing which frequency distribution provides the most reliable result must be identified. A methodology for assessing the goodness of fit is provided in Section 4.2.4.

3.2 Climatic regions within North America

Grouping of similar climatic indices by climatic regions using the classification of the Köppen/ Trewartha (Trewartha 1981) system is proposed by Guzzetti et al. (2005). To be consistent with Guzzetti et al. the CP rail network is classified by climatic region. This system is largely based on the natural vegetation of the region. The system results in the classification of North America covered by CP network into the following six climatic regions.

1. The west coast of BC is classified at a Do indicating temperate mid-latitude climate with a strong temperate oceanic influence.
2. The interior of BC is classified as H for highland climate. In this region altitude plays a dominant role influencing temperature and orographic precipitation.
3. The south-western prairies of Alberta and Saskatchewan and the western portions of South and North Dakota are classified BSk. This indicates that these areas have a climate that is dry in the summer, with more than 70% of the annual precipitation in the winter months, but at least one winter month below 0° C.
4. Regions classified at Dcb include a small portion of eastern central Alberta, a band across the south central quarter of Saskatchewan, the south-western third to the south-eastern corner of Manitoba, the southern limit of western Ontario between Manitoba and Thunder Bay, North Dakota, northern Minnesota and Wisconsin, southern Ontario, and New York state. Dcb indicates the regions have a temperate mid-latitude continental climate, with less than 4 months over 10° C, and the average temperature of the warmest month is below 22° C.
5. Eastern South Dakota, southern Minnesota and Wisconsin, Iowa, and Illinois are considered Dca indicating they have a temperate mid-latitude continental climate, with the warmest month above or equal to 22° C.
6. The south-eastern portion of Manitoba and the western two-thirds of Ontario are considered Boreal or type E.

It should be possible to group precipitation indices and thresholds by these areas using these climatic regions. However, the role of geology and groundwater will also have a significant role in the selection of indices and thresholds. A map of North American climate zones (Trewartha 1981) is available at http://fp.arizona.edu/kkh/dendro/climate_links.htm.

3.3 Other studies on the influence of precipitation on landslide hazards

A number of studies on the influence of precipitation on geotechnical hazards were reviewed in Appendix C, Section 1.0 and there are numerous others. Guzzetti et al. (2005 and 2007) provide a summary of several papers and many others have demonstrated a link between precipitation and landslides including, Aleotti (2004), Aleotti and Chowdhury (1999), Baum et al. (2002), Floris and Bozzano (2007), Findlay et al. (1997), Franks (1999), Godt et al. (2006), Grivas et al. (1996), Vu et al. (2005), Ibsen and Casagli (2004), Jacob et al. (2006 and 2007), Kawamoto et al. (2000), Ko Ko et al. (2003, 2004, and 2005), Leventhal et al. (2000), Matsushi and Matsukura (2007), Muraishi et al. (1992), Okada et al. (1994), Ortigao and Justi (2004), Shi (2006), Sidle (2006a and 2006b), Toll (2001), Toll et al. (2001), Tommasi et al. (2006), Towhata et al. (2005), Walker (2007) and others. Most of these papers present one or more types or formulations of indices that are most representative of the hazards in their area of study but few provide a means of determining which index is the most appropriate for a given site.

3.3.1 Correlation of precipitation with geotechnical hazards from other regions

As discussed in Appendix C, numerous authors and researchers have provided correlations between precipitation and the activation of landslides. The following subsections discuss various groupings of these studies and the results.

3.3.1.1 Previous studies relating precipitation and geotechnical hazards – relevance to geotechnical conditions in North America

There are four regions within North America for which analysis of precipitation-induced landslides has been investigated. These are the San Francisco Bay area, California, the Seattle area of Washington State, the Blue Ridge Mountains of Virginia and specific regions of British Columbia, Canada.

Research in the San Francisco Bay area has been completed and summarized by Cannon and Ellen (1985), Wilson et al. (1993), Wilson (1997), Wieczorek (1996), Keefer et al. (1987) and others. They use a combination of three factors: the rainy season antecedent rainfall, $A_{(c-d)}$ and the average intensity for a storm, I as it relates to the duration of the storm, D. The antecedent precipitation in the rainy season must exceed a threshold of 250 to 400 mm, depending on the soil thickness, before the landslide hazard is elevated no matter what the storm rainfall intensity. They also require that an intensity duration storm rainfall threshold be exceeded before landslides are predicted. Within the ID plot they limit duration to generally less than 24 hours. This method appears to be applicable anywhere. The use of short and long term indices appears reliable provided local thresholds are adopted. As a result, provided the antecedent rainy season threshold is exceeded, they predict that a landslide could occur during a high intensity short duration storm or a longer (up to 24 hour) storm with a lower average intensity over the duration of the storm.

Research in the Puget Sound region of Washington has been documented by Baum et al. (1998), Chleborad (2000), Baum et al. (2005) and Godt et al. (2006) among others. This group has recommended the use of a decay type API combined with dual independent antecedent indices of $A_{(1-3)}$ and $A_{(4-15)}$. They propose fixed and variable thresholds dependent on a combination of both antecedent indices as depicted in Figure C3.

Others have published efforts to decipher precipitation-induced landslides in the Blue Ridge Mountains of Virginia as per Guzzetti et al. (2007). Choi and Wong (1998) showed that rain infiltration reduced the FOS of a railway embankment in Northern Ontario between 2.1% and 3.2% with and without the train load respectively. Boundary County (2007) identified a train derailment caused by a debris slide in 1959. They indicate the debris slide was likely caused by a combination of precipitation and human activity.

The final region is British Columbia. These investigations have been documented by Jacob and Weatherly (2006), and Jacob et al. (2005 and 2006). They used combined multiple indices and thresholds based on rainfall intensity, 24 day antecedent precipitation ($A_{(1-24)}$), and stream flow and combined them into a single index.

3.3.1.2 Influence of antecedent precipitation

Since Cannon and Ellen (1985) introduced the requirement that the seasonal rainfall exceed a specific threshold before precipitation-induced landslides are likely in the San Francisco Bay area, it has been recognized in the literature that antecedent precipitation has a significant influence on slope stability. Antecedent indices and thresholds have been applied successfully in the San Francisco Bay area by Keefer et al. (1987), Wilson et al. (1993) and others to develop warning systems. Other researchers have reinforced the importance of antecedent rainfall by including similar thresholds for longer term precipitation.

Wieczorek and Glade (2004) reviewed the work of others that demonstrates the significance of antecedent precipitation in some regions of Korea, Italy, New Zealand and the US. They note that many researchers identify the influence of antecedent precipitation on landslides, however, there in no consistent time period over which the antecedent precipitation accumulates that is most likely to influence landslides stability. Depending on the location, antecedent durations of 2 to 45 days with high precipitation before a high intensity event have been correlated to landslide activity. They suggest that the influence of antecedent precipitation is both geologic and climatic. In warmer areas evaporation will reduce the influence of antecedent precipitation. In contrast, in cooler area and in areas of sub-zero temperatures, the influence of antecedent precipitation can be increased due to storage of precipitation as ice and snow. They describe the 1,900 mm antecedent conditions that developed over the 6 months prior to Hurricane Mitch in 1998 November that caused the 1.8 million m^3 catastrophic debris flow from the inactive Casita volcano in Nicaragua. Similarly, earlier hurricane rainfalls preceded by less severe antecedent conditions did not cause debris flows.

Zêzere et al. (1999) documented that the most relevant antecedent duration for a 1.3 million m^3 Calhandriz landslide near Lisbon, Portugal was up to 75 days. Porter et el. (2002) concluded that artesian groundwater pressures, possibly induced by increasing precipitation levels were one of five factors controlling the stability of the numerous multi-million cubic metre Thompson River Landslides of South central British Columbia, Canada. Palynchuk et al. (2007) suggests that antecedent precipitation contributes to the formation of sink holes in loose sand fill railway embankments in Southern Ontario, Canada. The sink holes were formed by the loose fill migrating into voids formed after buried timber decays. Tatone (2007) analyzed factors influencing the fatal 1995 January rock fall fatality at Mile 111.00 of the Nelson Subdivision in southwestern, BC (Transportation Safety Board 1995). He considers the influence and frequency of the combination of the 15 day antecedent precipitation, the mean temperature of the previous 10 days and the average mean temperature of the previous 10 days to assess the potential for freeze thaw to have influenced the rock slope and induce failure.

Toll (2001), Terlien (1998) and Zêzere et al. (1999) all demonstrate that deeper (and larger) landslides are more influenced by groundwater conditions than shallow landslides. As a result, larger landslides are more sensitive to longer term antecedent events and less sensitive to shorter term precipitation conditions. They therefore conclude that the larger the volume of the landslide the greater the reliance on longer indices. This is consistent with the unsaturated and saturated groundwater flow and landslide stability theories whereby more time is required for water to reach deeper soil horizons involved in larger landslides. However, large or small landslides that are influenced by groundwater can be dependent on antecedent conditions despite their volume. Therefore larger landslides are more likely to be predicted by longer antecedent indices but smaller landslide may be predicted by either long or short antecedent duration indices.

Leventhal et al. (2000) assessed the 650,000 m^3 landslide at Coal Cliff south of Sydney, Australia and found that 600 mm of rain in 90 days was required before this landslide and others in the region would move. Wooten et al. (2006) document a landslide in North Carolina that damaged a mobile home and a water treatment facility that was triggered by less then 125 mm in 24 hours but had been preceded by 10 days of rainfall. They also found that greater than 125 mm in 24 hours induced landslides regardless of the antecedent rainfall. Wieczorek and Glade (2004) cite an earlier co-authored work of Wieczorek that identified a requirement for at least 280 mm of antecedent rainfall before a landslide occurred in La Honda, California regardless of the storm rainfall.

These studies and many others demonstrate the connection of antecedent precipitation and landslide activity. Some studies have determined that rainfall intensity at the time of the landslide is also required and some have found that little or no rainfall is required during the landslide.

3.3.1.3 Influence of rainfall intensity

Within the CP network it is uncommon to experience torrential rains capable of inducing a landslide without some antecedent precipitation having occurred. Unlike Hong Kong (Findlay et al. 1997, Franks 1999, and others) or Singapore (Rahardjo et al. 2000, Toll et al. 2001 and others) the CP network does not experience prolonged heavy Monsoon type rains, nor does it have rapidly weathering residual soils typical of these two areas. As a result, there are relatively limited areas where rainfall intensity has an influence on landslide activity independent of antecedent conditions. The exceptions to this generality are the Kamloops and Northern Ontario areas.

West of Kamloops, British Columbia, arid conditions are intermittently interrupted by severe convective storms during the spring and summer months. This results in high run-off events that are able to mobilize the loose, dry, eolian, silt rich surficial soils in relatively steep, small drainage basins of 0.5 km^2. Initially the silt is entrained in the stream flow. The density of the stream flow is increased. The higher density flow is able to entrain additional larger grain size material. Typically the rail-bed is built on fills across gullies occupied by these streams with a culvert to convey the stream beneath the track. When a stream flow encounters the lower gradient produced by the rail-bed fill the stream deposits some of the entrained sediment. If sufficient material accumulates upstream and within the flatter gradient of the culvert, the culvert can become blocked. The debris and water then impound on the up stream side of the track until the water or debris level exceeds the elevation of the track. In many cases the top of the up-hill rail is the highest elevation the water must flow over. Once it does this the water is trapped between the rails and it has flowed several hundred metres along the track before flowing down the downhill slope. In severe cases the flow across and along the track has eroded the down-slope shoulder of the track and undermined the track. These events are Debris flow - avulsions and Debris flow - avulsion - gully erosions (Keegan 2007) depending on whether they deposit on the rail bed or deposit and erode the down-slope shoulder of the track bed.

A scenario dependent on the influence of precipitation intensity and snowmelt run-off is included for North Ontario in Section 3.3.4.3.1.

Based on the limitation of infiltration and permeability, it appears unlikely that landslides (of any significant volume), cited by Caine (1980), could be triggered by high intensity rainfalls shorter than a few minutes. Caine cites two different landslides as being triggered by a 0.02 hour (1.2 minutes) rainfall of only 2.3 mm and 1.0 mm each. It is suggested that 1.2 minute rainfall could not reduce the FOS from more than one to less than one without the slope being saturated by some recent prior precipitation event or groundwater discharge condition. As a result it would be overly conservative to issue a warning based solely on a single index related to short duration high intensity rainfalls. There is no information available in CP records that supports this failure scenario within CP.

3.3.1.3.1 Intense precipitation without antecedent precipitation

Wieczorek and Glade (2004) also review the influence of rainfall intensity on landslide activity. They cite numerous authors who found that landslides in Hong Kong and Korea were dominantly controlled by rainfall intensity regardless of the antecedent precipitation. It is important to note that due to the monsoon climate Hong Kong receives up to between 8 and 37% of its annual average rainfall of 2,000 to 2,400 mm in a single day and it is these days to which high intensity landslide activity is attributed (Franks 1999). Brand et al. (1984) and Findley et al. (1997), while studying precipitation-induced landslides in Hong Kong, concluded that although the 4 to 30 day antecedent rainfalls were associated with landslides the use of this index only provided a marginal improvement in the ability to predict landslides. They show that the 1 hour rainfall was the best predictor of landslides. This is similar to the high intensity rainfall induced landslides in Singapore (Rahardjo et al. 2000). In comparison, the most intense rainfall recorded within the CP network is 173 mm per day at Hope, BC. This accounts for no more than 9% of the average annual rainfall of 2,010 mm.

Based on the review of several studies within North Carolina and their own experience Wooten et al. (2006) concluded that 125 mm within a 24 hour period was a reasonable lower threshold, above which rainfall induced landslides were possible.

3.3.1.3.2 Intense and antecedent precipitation

In many cases researchers identify that a minimum intensity rainfall is required to trigger a landslide but that an antecedent precipitation threshold must also be exceeded before the landslide can occur. Cannon and Ellen (1985), Keefer et al. (1987), and Wilson et al. (1993) all identify that intense rains induce landslides in the San Francisco Bay area provided an antecedent threshold is exceeded. Keefer et al. (1987) provided an expression which relates the relationships previously determined by others to the physical conditions. They express the intensity duration relationship such that:

$$I_r = \frac{Q_c}{D} + I_o \qquad \text{Equation 3.2}$$

Where I_r is the rainfall intensity, Q_c is the critical volume of water that can be retained in the soil before a landslide occurs, D is the duration of the rainfall intensity I_r. I_o is the rate at which rain drains from the slope. Keefer et al. (1987) approximate the relationships developed by others as shown in Table 3.3.

Table 3.3 Thresholds for precipitation-induced landslides using the intensity duration method proposed by Keefer et al. (1987)

Location	Q_c (mm)	I_o (mm/hr)	Researcher
World	13.65	4.49	Caine (1980)
San Francisco Bay Area, California	38.1	6.86	Ellen and Cannon (1985)
La Honda, California	9	1.52	Wieczorek (1996)

Glade et al. (2000) and Glade (1998) also investigate a large number of landslides in New Zealand. They found that the antecedent daily rainfall index was useful for accounting for both intense recent rainfall and longer term antecedent rainfall by using a decay function to model the run-off and evaporation of the precipitation.

Guzzetti et al. (2008) update their findings on the influence of intensity and duration of precipitation on landslides and debris flows in their identification of global minimum rainfall induced landslides.

3.3.1.3.3 Influence of precipitation event return period and landslide volume

Since the frequency-magnitude studies of Hungr et al. (1999), Evans et al. (2004) and others demonstrate that the larger the volume of a landslide the lower its likelihood of occurrence, it is reasonable to assume that the longer the return period of a precipitation event the larger the landslide it may induce. No investigation of this relationship has been found in the literature.

3.3.1.3.4 Conclusion

Within the railway industry the correlation of landslide and hourly or fraction of an hour rainfall-intensity data at the time of a landslide is questionable for several reasons.

1. The rainfall information must be from the landslide location because high intensity convective rain is very localized and variable in time. The rainfall intensity at two locations a few miles apart during a convective rain storm may vary by one order of magnitude or more at the same time and over short periods.
2. Unless the landslide damages some occupied building or equipment the recorded time of the landslide is not reliable enough to compare to hourly rainfall. This is especially true of the railway landslide data where the time of the landslide is recorded as the time it was first observed rather than when it occurred. Even on busy tracks, observations are only made approximately once ever hour by train crews.

Due to the inaccessibility of hourly rainfall data on a real-time basis and bullets 1 and 2 above, hourly precipitation data is not analyzed in this thesis.

3.3.1.4 Summary of weather correlations

At a minimum, authors utilize the available rainfall data. As a result, the daily rainfall is the most common index. However, there is no reason that landslides should be sensitive to the daily rainfall any more or less than to any other duration of antecedent precipitation. As a result all antecedent rainfall durations should be tested and the one with the best correlation with the landslide record selected to be used as an index to warn of future landslide activity.

3.3.2 Influence of other weather conditions on antecedent precipitation and correlation with geotechnical hazards

3.3.2.1 Temperature

Only a few authors (Chleborad 2000 and Jacob et al. 2005) have identified a connection between temperature and landslide activity. In both cases the correlation is due to the weather conditions that accompany the heavy precipitation raising the temperature. As a result, temperature is an indicator of the type of weather system responsible for the rainfall. By itself temperature has not been demonstrated to have a significant physical influence on landslides.

The influence of temperature on snowmelt conditions is cited and discussed in Appendix B, Section 1.3 and is considered further in Section 3.3.2.2.

3.3.2.2 Snowmelt – high storage conditions

Snow accumulation during the winter months can result in a large volume of water being stored. When melting occurs, the water is released for infiltration and run-off. Numerous authors (Chleborad 1997, Jakob and Weatherly 2003, Toews 1991, Gray et al. 2001 and Guzzetti et al. 2005) have recognized this effect. CP has experienced several debris flows as a result of this condition. Two of the most recent occurrences within CP are the March 2007 debris flows caused by the melting of heavy snow accumulations in the Lytton area of Southern BC. Immediately prior to the debris flows the snow thawed rapidly and caused high flows and bed-load such that debris plugged culverts and flowed over the track. Similar conditions occurred on the Fording River Subdivision in southeast BC during 1995 June.

Chleborad (1997) discusses the prediction of landslides based on snowmelt in the Central Rock Mountains of Washington State, USA. He found that starting annually in March the six day moving average of daily temperatures could be used to determine the first occurrence of snowmelt induced landslides. He used temperature data recorded at a lower elevation than the drainage basins and undertook an approximate accounting for the lapse-rate (the change in temperature with change in elevation) between the elevation of the drainage basin and the elevation of the weather recording location. As a result, the temperature is an index of the snowmelt conditions that induce landsliding. It is not a prediction of when snowmelt occurs at a given elevation.

Antecedent indexes can be used to assess the influence of snowmelt on landslides. The relationship between snow accumulation, snowmelt, and various antecedent durations is captured by the four cases below and depicted in Figure 3.6.

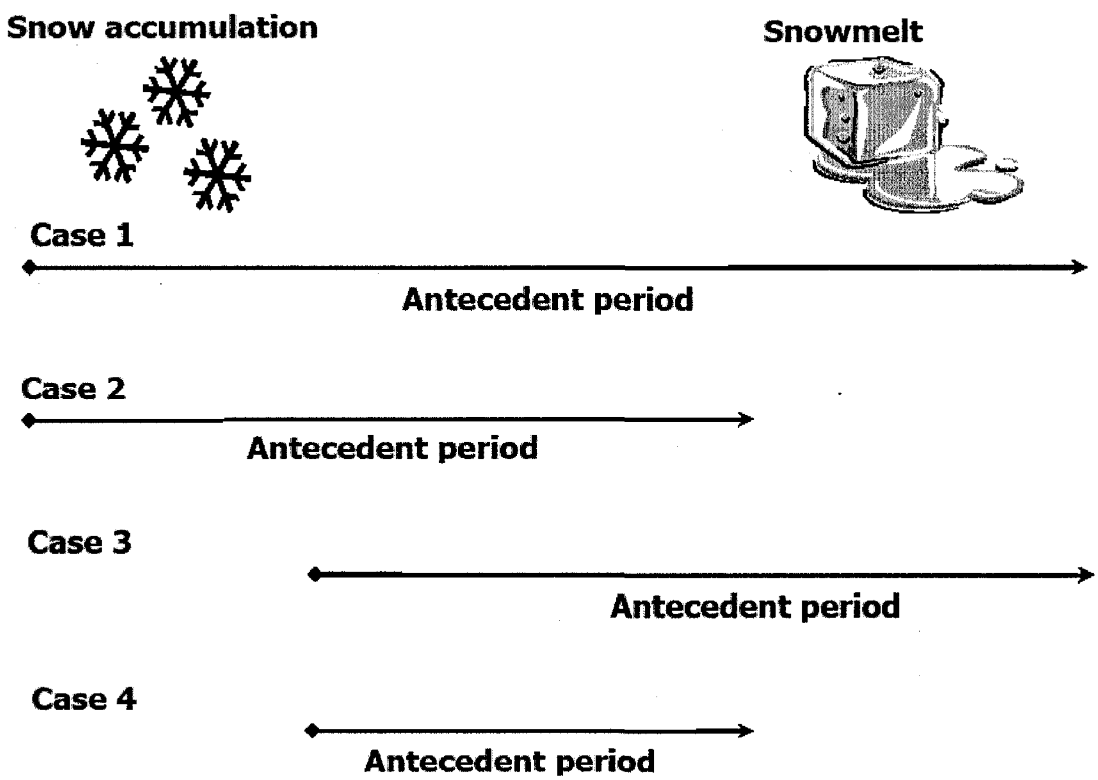

Figure 3.6 Temporal relationship between snow accumulation and snowmelt

Case 1 - Snowfall during the antecedent duration that melts before the end of the antecedent duration:

In this case the precipitation has all reached the soil and is available for infiltration within the antecedent duration. The antecedent index does not change if the precipitation occurred during the beginning or the end of the antecedent duration so the index is independent of whether the precipitation falls as snow or rain. By using multiple antecedent durations with non-overlapping durations, this effect is captured. This is a common scenario in temperate areas like the BC Lower Mainland and when early and late season snowfalls occur during warmer weather in the fall and spring across North America. An example of this scenario is documented by Vu et al. (2005). As a result, snowmelt in relatively warm conditions is effectively accounted for by the use of antecedent precipitation indices.

Case 2 - Snowfall during the antecedent duration that does not melt during the antecedent duration:

In this case the precipitation is not available for infiltration within the antecedent duration in which it fell. Where this is common a means of accounting for snow on the ground at the end of the antecedent duration is needed to discount the antecedent duration precipitation. However, it is unusual to have landslide activity under these conditions because snow is accumulating and therefore not available for infiltration.

Case 3 - Snowfall prior to one antecedent duration that melts during the antecedent duration:

In this case, precipitation available for infiltration may be greater than that accounted for by the antecedent duration. This can be avoided by assuring that one of the antecedent durations extends longer than the snow accumulation season. Where snowmelt is a factor this is usually the case. If the highest correlation landslide and antecedent duration does not include the entire snow accumulation period, accounting of the earlier snowfall may be required.

Case 4 - Snowfall prior to an antecedent duration that does not melt during the antecedent duration:

In this case, no precipitation or melt will be accounted for by the antecedent duration. Similar to Cases 2 and 3 this can be avoided by assuring that at least one of the antecedent durations extends longer than the snow accumulation season. Where snowmelt influences landslides this is usually the case.

In summary, provided the appropriate antecedent durations are selected it should be possible to capture the influence of most combinations of snow accumulation, melting, and antecedent duration. The selection of antecedent duration such that Case 1 occurs is preferable.

If it is found that landslides are insensitive to antecedent durations such that Case 1 is not satisfied two other options are available. The most reliable method is to use data derived from snow-on-the-ground or snow-pillow measurements. The second, less reliable option is accounting for the snow water equivalent for the duration of the snow accumulation and melting period.

In North America snow-on-the-ground data is generally available for weather stations at major airports and at snow-pillow weather sites used for avalanche forecasting and dam reservoir capacity and river flow prediction studies. This data can be used to derive the snowmelt by the difference in snow height from one day to the next multiplied by a factor to account for the snow water equivalence (*SWE*).

In the absence of snow-on-the-ground information the United States Army Corp of Engineers (1998) publication provides guidance in the direct accounting of the *SWE* and snowmelt. They indicate that the accumulation of snow is dependent on the melting level and this is a function of temperature, wind, precipitable water, atmospheric circulation patterns, frontal activity, lapse-rate, and the stability of the air mass, elevation, slope, aspect, exposure, vegetation, and ground temperature. They document that the form of precipitation changes at various temperatures noting that snow accumulation can occur as warm as 4° C and rain can fall as cold as -1° C.

In the absence of snow-on-the-ground data an estimate of the *SWE* of the snow can be derived by accumulating the precipitation that falls near and below 0° C and allowing the *SWE* to thaw at temperatures above 0° C.

$$SA_i = P_i \quad for \quad T_i < Ts$$ Equation 3.3

$$SA_i = 0 \quad for \quad T_i > Ts$$ Equation 3.4

$$SM_i = 0 \quad for \quad T_i < 0$$ Equation 3.5

$$SM_i = (Cd + 0.177P_i)T_i \quad for \quad T_i > 0 \quad and \quad ST_i > (Cd + 0.177P_i)T_i$$

Equation 3.6

$$SM_i = ST_{i-1} \quad for \quad ST_{i-1} < (Cd + 0.177P_i)T_i$$ Equation 3.7

$$ST_i = ST_{i-1}Ca + SA_i - SM_i$$ Equation 3.8

Where *SA* is the net *SWE* accumulation due to daily precipitation, P_i. *SM* is the snowmelt, and *ST* is the total *SWE* depth. *Cd* is the degree day melting coefficient. This is determined from the average snow pack melting and air temperature relationship at the nearest representative station. *i* is a specific day and *i-1* is the previous day. *Ca* is a constant to account for the ablation of the snow from day to day and is slightly less than unity. *T* is the mean daily temperature, *Ts* is the temperature at which snow accumulates and *Tm* is the temperature at which snowmelts. The product of the coefficient 0.177 and the precipitation is included to account for the melting effect of rain on snow above 0° C. As discussed in Appendix B, Section 1.3 when the appropriate weather data is available, the United States Army Corp of Engineers (1998) provides several additional factors to account for wind speed, short and low wave radiation, snow-albedo and other factors.

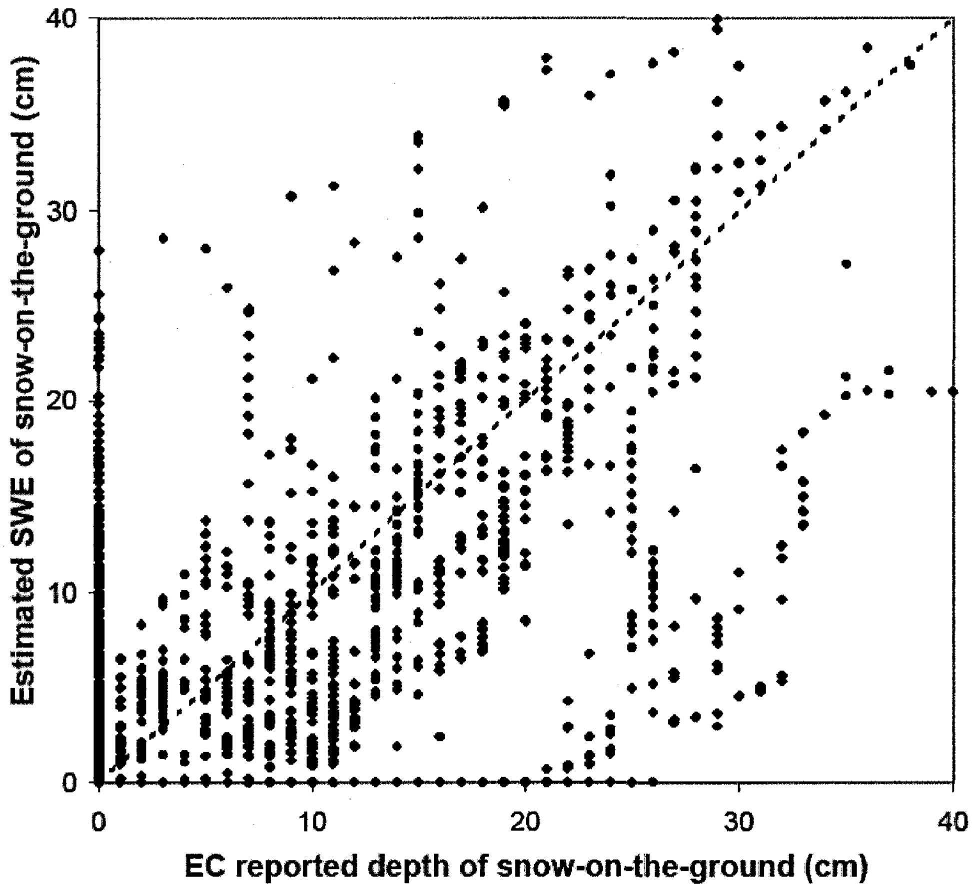

Figure 3.7 Reported snow-on-the-ground versus calculated SWE of snow for Banff, Alberta 1995 to 2006.

As an example the formulation above is used to back estimate the snow depth compared to the recorded snow-on-the-ground data from Banff, Alberta between 1995 to 2006. As indicated by the formula wind and solar radiation are not considered. Using the method of the United States Army Corp of Engineers (1998) *Cd* and *Ca* equal 1.9 and 0.95 respectively. Figure 3.7 shows a relatively poor correlation (Correlation coefficient = 0.69) of the measures and calculated accumulated snow. This is due to highly variable conditions that influence snow accumulation and melting that are not considered in this basic model and includes reporting effects where the precipitation during sub-zero temperatures is reported one day but the snow accumulation is not recorded until the following day. Similarly, the use of average temperature does not reflect the melting conditions for the entire day. This method is relatively crude and should only be used in the absence of appropriate Case 1 antecedent durations or snow-on-the ground data.

3.3.3 Relationship of precipitation type, soil type and hazard potential, frequency magnitude and infiltration

There are a large number of combinations of precipitation, soil type and infiltration and run-off characteristics. The following is a description of some of the scenarios and relationships that have been investigated.

3.3.3.1 High precipitation storage – high infiltration conditions

There are two conditions where high precipitation storage and high infiltration conditions contribute to precipitation-induced landslides. The first is the storage of moisture in snow that subsequently melts slowly. The second is storage of moisture in the soil.

The snowmelt aspects of the first scenario are discussed in Sections 3.3.2.1 and 3.3.4.2. The temperature of the ground during the slow melting, and the soil type also influence the potential for slope instability. If the ground is unfrozen (often due to a thick snow pack insulating the ground from the air temperature) a higher percent of the snowmelt will infiltrate. Redding and Devito (2005) discuss some of the factors influencing this process. If the melt rate is lower than the permeability the soils will drain faster than infiltration occurs. Therefore, provided the melt rate is higher than the soil permeability, low permeability soils will increase in pore pressure and there will be an increased potential for landslides. No literature has been identified that deals with these scenarios and landslides.

The second but less common scenario is where high silt and clay content soils and weak bedrock are exposed to a prolonged infiltration and the low permeability and resulting poor drainage of the soil/rock results in increased pore pressure. These conditions occur when repeated seasons and or years of higher than average precipitation raise groundwater levels that then contribute to the instability of slope. These are poorly represented in the precipitation-induced landslide literature and are difficult to assess because of the temporal disconnection between precipitation and landslide activity. Geertsema et al. (2007) discuss a number of landslides in northern British Columbia that are apparently induced by longer term climate conditions and perhaps multi-decadal temperature and precipitation trends. Studies (Floris and Bozzano 2007, Floris et al. 2004) have identified long antecedent durations upwards of 135 days. Studies of large landslides in impermeable soils and rock may also represent this scenario (Leventhal et al. 2000).

Precipitation-induced landslide indices developed for these types of scenarios would have two applications within the railway industry.

1. Operations - Within the railway operations environment precipitation-induced landslide indices that exceed a threshold for periods of months or seasons is of limited use to the day to day operation of the railway. However, in severe cases an on-going "slow order" to reduce train speed could be imposed to reduce the consequences of derailment, on sections of track with known vulnerability.
2. Planning - During periods of long term high antecedent precipitation it may be justified to provide additional capital, allocated specifically for the mitigation of known or potential precipitation induced landslides. Conversely, during prolonged droughts capital expenditures on known precipitation induced landslides may be reduced.

3.3.3.2 Seasonal precipitation storage – high infiltration

There are three scenarios where seasonal precipitation storage results in high run-off:

1. Infiltration from snowmelt,
2. Thawing of infiltrated moisture, and

3. Prolonged rainfall.

1. Infiltration from snowmelt

The most common scenario where seasonal precipitation storage results in high run-off and infiltration, occurs as a result of snow accumulation during the winter, rapid snowmelt, and high run-off during the spring and early summer. Some literature on this topic has been reviewed in Sections 2.2.2.1.2 and 3.3.2.1.

2. Thawing of infiltrated moisture

The thawing of infiltrated moisture is common in silt rich soils exposed to periodic snow or rain combined with periodic freeze-thaw cycles over the course of winter. The permeability profile in silt soils decreases downward due to desiccation and freeze-thaw jointing at the surface and undisturbed consolidation at depth. Moisture infiltrates into the shallow soil during periods of above 0° C temperatures but does not drain deeper into the soil due to its permeability profile. This results in soils near or above their liquid limit when the phase of the moisture in the frozen soil changes from solid to liquid during the spring thaw.

CP suffers this condition during the spring in arid areas where silt soils are present such as the Salmon Arm and the Columbia Valley areas of south-central and south-eastern British Columbia. Shallow earth-slides and debris flows, limited to the depth of frost penetration (1 to 2 m deep), occur when the saturated soils thaw. These landslides can block the track making it impassable to trains. These slides are similar to the shallow, high mobility slides in permeable soils of Singapore and Hong Kong except that the soil saturation is dependent on the phase transformation from soil to liquid rather than from rapidly infiltrated precipitation.

3. Infiltration due to prolonged rainfall

Prolonged rainfall will result in continued infiltration, saturation of surface soils, and an increase in the groundwater level. In areas where prolonged rainfall is common the shallow soils have reached slope angles during previous events such that they are stable. As a result, prolonged rainfall usually only influences large landslides by raising the groundwater level.

3.3.3.3 Limited precipitation storage and high run-off conditions - Thin soils over bedrock

Limited precipitation storage and high run-off conditions are common where thin, higher permeability soils overly less permeable soil or rock. This situation is typical of the Hong Kong conditions previously discussed in Section 3.3.1.3.1. This condition is also present in the Cordevole River Basin in the Dolomites of northeast Italy (Pasuto and Silvano 1997) and other areas. In this area precipitation-induced landslides were triggered by a combination of at least 250 mm in the 15 days prior to the landslide and not less than 70 mm in the final 24 to 48 hours of the landslide. Depending on the level of storage this situation results in precipitation-induced landslide indices insensitive to antecedent conditions longer than 10 to 15 days.

As discussed in Section 3.3.1.3 areas of Western Ontario with thin soil over impermeable bedrock are sensitive to high run-off events due to high intensity rainfall. A description of this scenario is included below but this is not a landslide or debris flow type hazard and therefore will not be pursued further in this thesis.

At several locations in Western Ontario thin soil over impermeable bedrock and frozen ground in the spring combined with intense convective rain can result in high run-off events. The result of these events can be similar to those of the Kamloops area (Section 3.3.1.3) however, there is less topography so gradients are shallower and less material is available for entrainment. As a result, limited culvert capacity due to damage and or ice blockage is usually a contributing factor. For whatever reason if insufficient culvert capacity is not available run-off impounds upstream of the rail embankment. If it over-tops the track it can flow across the track and erode the down-stream side of the embankment. This type of event is classified as Overland Flow Erosion although the Through-flow - earth slides scenario may also contribute to the failure of the embankment (Keegan 2007)

3.3.3.4 Influence of run-off gradient

The gradient of a slope influences the apportionment of land surface water between run-off and infiltration. Generally, the steeper the slope is the greater the run-off, and the lower the infiltration. The Rational method for run-off calculation (Chow et al. 1988) includes run-off coefficients dependent on the steepness of the ground. These coefficients increase (therefore the infiltration decreases) by up to 8% for slopes between 0 and 7 degrees (Chow et al. 1988) and are expected to decrease more for steeper slopes. This effect was demonstrated by Lee et al. (2001) in their experiment using artificial rain on a steep slope. As a result, it is expected that steeper slopes are less sensitive to longer antecedent rainfalls because more of the precipitation that falls prior to a landslide has flowed from the area. This does not preclude steeper slopes from being sensitive to shorter term antecedent rainfalls. The requirement that steeper slopes consist of soils with higher shear strength also needs to be considered.

1. Debris flows

Several authors have identified that debris flows are more common where the average gradient of the land surface is steeper. However, due to the mobility and drainage area effects some debris flows will occur in drainage with initiating gradient as low as 20 degrees. Deposition angles are lower than initiating gradient and therefore extend into the high single digits (VanDine 1985).

2. Overland and stream flow erosion

Consistent with the scenario described in Section 3.3.1.3, Shi (2005) demonstrated that high stream flow conditions constrained by culverts under the railway could result in the impoundment of water upstream of the rail embankment where they cross stream gullies and valleys. The impounded water can either trigger embankment failure or overtop the embankment and cause erosion of the down-slope side of the embankment. Shi modeled the flow conditions in the drainage basin to determine the peak flows consistent with standard hydrologic analysis. This could be used to estimate the time delay between rainfall event and the peak flow condition. The gradient of the flow path would be considered in this analysis.

3.3.4 Geographic distribution of climatic and geotechnical conditions

The Geologic Survey of Canada (GSC) as part of the Earth Sciences Sector of Natural Resources Canada has initiated the "Reducing Risks from Natural Hazards Program" to improve Canada's understanding of landslides and minimize the losses incurred from landslides (Natural Resources Canada 2007). They collect and

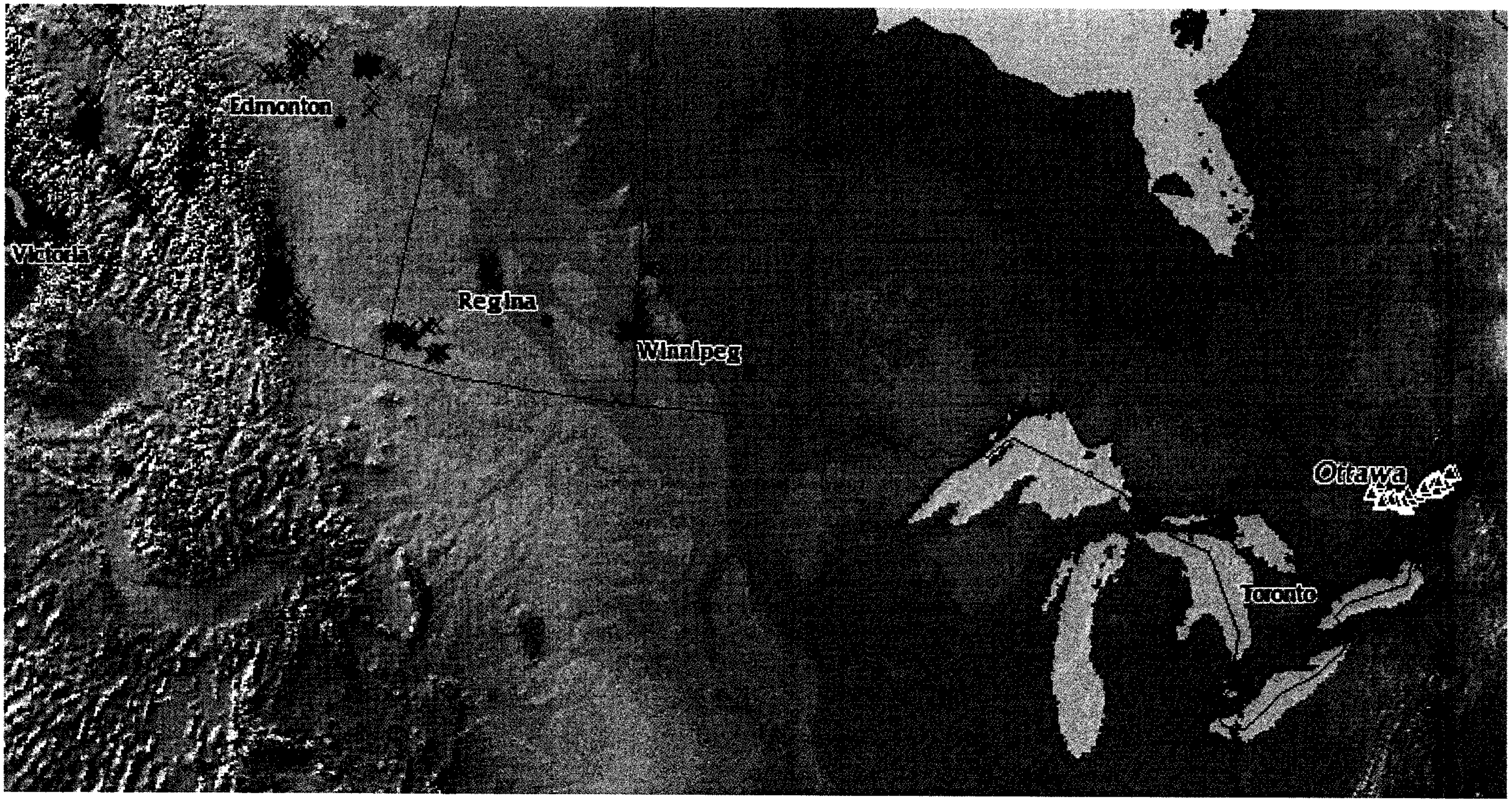

Figure 3.8 Map of landslides in Canada documented by National Resources Canada (2007) reproduced with permission from P. Bobrowsky of the GSC (personal communication - 2007 December 13).

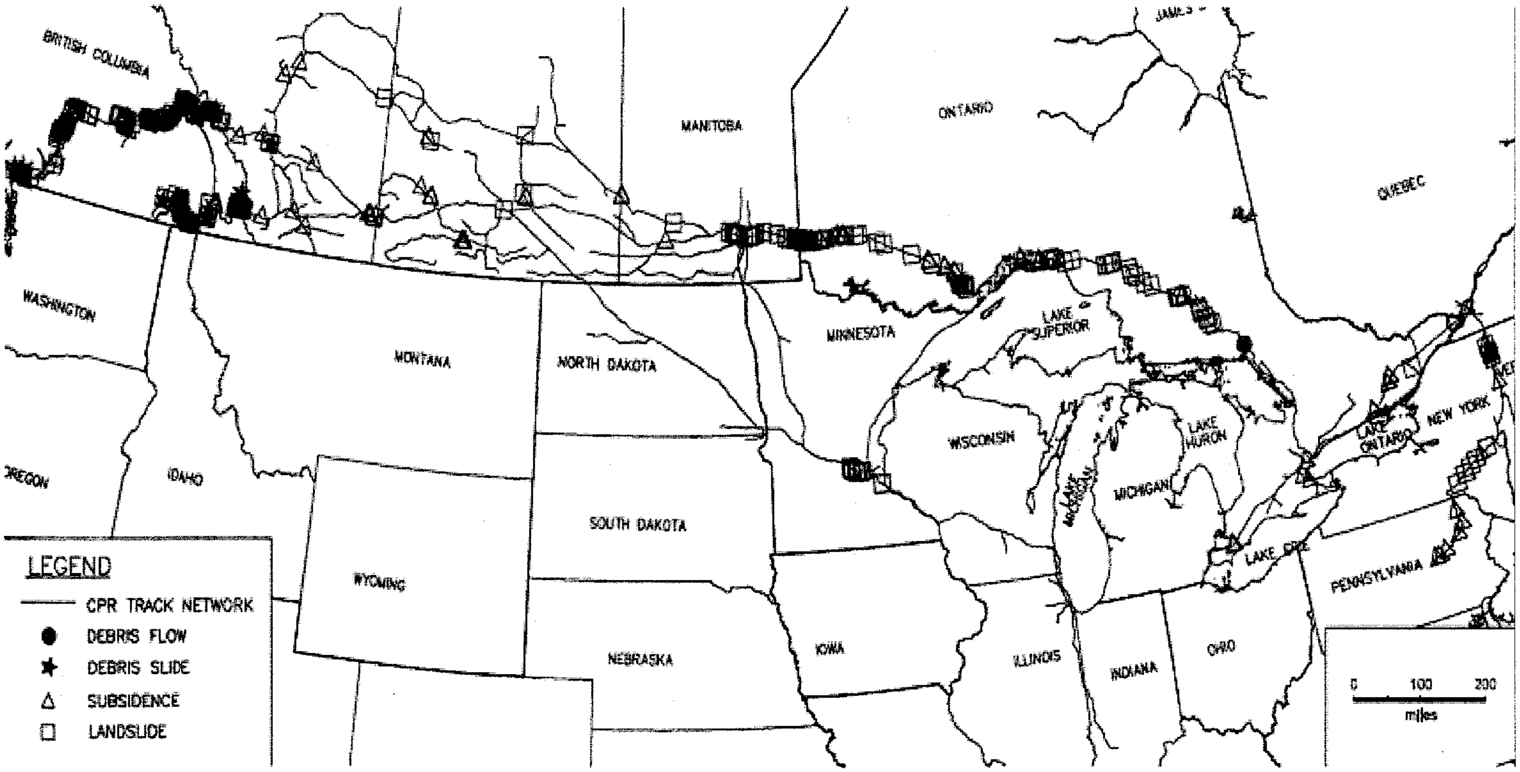

Figure 3.9 Map of CP network and recorded precipitation sensitive hazard locations as of 2003.

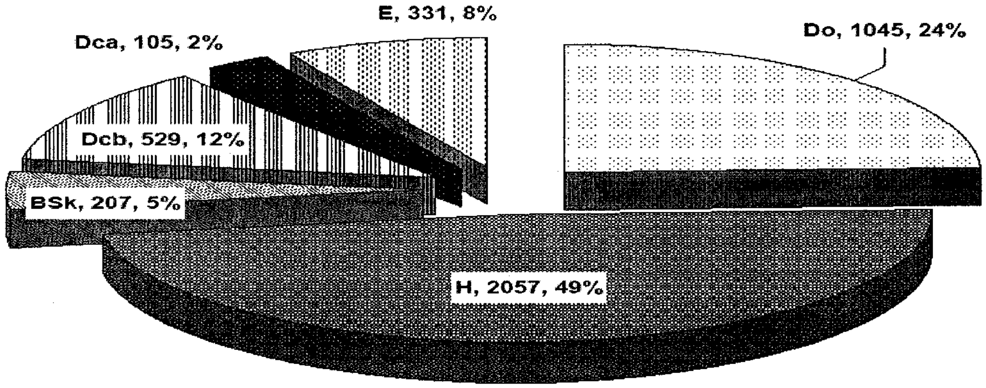

Figure 3.10 Distribution of hazard by geography including rock falls and all geotechnical hazards

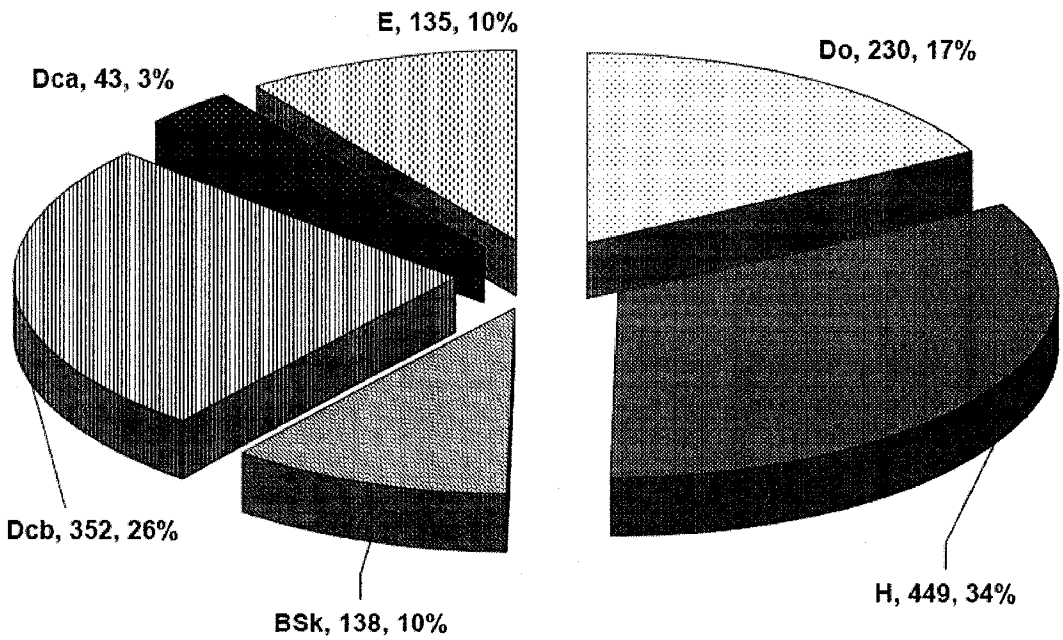

Figure 3.11 Distribution of precipitation-induced geotechnical hazards by climate region. Do - Temperate oceanic, H - Highland, BSk - Dry, semi arid with dry summer and one sub zero month, Dcb - Temperate continental with the warmest below 22° C, Dca - Temperate continental with the warmest month above 22° C, E - Boreal

disseminate information about landslides across Canada and present it via an internet hosted map as shown in Figure 3.8. However, the distribution of the landslide incident data is spatially filtered or selected based on where the GSC has acquired data and therefore does not fully represent distribution of hazards across Canada. The filtering is generally related to higher population densities, recreational users (National Park and Provincial Parks) and GSC study areas.

In the absence of a uniformly filtered national landslide database the CP NHID is relied upon to represent the diverse distribution and extent of geotechnical hazards on or adjacent to the CP right-of-way across North America. The filtering of the CP is such that only those natural hazards that influence CP are recorded. As a result a landslide only a few hundred meters away from the right-of-way that is not a hazard to railway safety and operations is not included in the database.

As can be seen from the map in Figure 3.9 of the CP network and related hazard locations the hazards are concentrated in the mountainous areas of British Columbia and Alberta but a number occur in other locations as well.

Table 3.4 Climate zones and geotechnical hazards

Climate zone	All geotechnical hazards		PIL hazards		Track length		PIL hazards	
	Number	%	Number	%	(km)	(miles)	(per km)	(per mile)
Do	1,044	24	230	17	345	215	0.67	1.07
H	2,056	49	449	34	1,337	831	0.34	0.54
BSk	206	5	138	10	2,640	1,641	0.05	0.08
Dcb	524	12	352	26	9,273	5,763	0.04	0.06
Dca	104	2	43	3	1,236	768	0.03	0.06
E	330	8	135	10	2,156	1,340	0.06	0.10
Total	4,264	100	1,347	100	16,986	10,557	0.08	0.13

To investigate the relationship between precipitation-induced landslides and climate type the climate type of each of the approximately 4,000 hazards was added to the CP NHID. Figure 3.10 and 3.11 illustrate the climate zone as per section 3.2, the number of incidents and the percent of landslides in each zone. Figure 3.10 includes all hazards in the data base. Figure 3.11 includes only those considered to be induced by precipitation conditions.

Overall, the number of hazards that are considered sensitive to daily precipitation is about 30% of the total. By far the largest group of hazards considered insensitive to daily precipitation is rock falls less than 100 m^3. This does not indicate that rock falls are insensitive to precipitation, but it indicates that the temporal resolution of daily precipitation records is insufficient to establish a correlation with rock falls smaller than 100 m^3.

The greatest number of hazards exist in the CP, Vancouver, and BC Interior Service Areas classified at $_{Do}$ and $_{H}$ regions respectively. This is due to the steeper slopes, higher relief that increases the influence of gravity, geologic complexity and orographic-induced precipitation. The additional moisture in the $_{Do}$ region is likely responsible for the order of magnitude higher, hazards per track-km in this climatic zone. The 0.34 hazards/track km (0.54 hazard/track mile) in the $_{H}$ climatic zone is due to the greater relief and higher snow accumulation in the mountainous region compared to the flatter remainder of the CP system.

The density of hazards per track km of 0.05 (0.08 hazards/track mile) or less is relatively consistent over the remainder of the CP network. The slightly higher percent of hazards per track km in climatic zone $_{E}$ is due to the preponderance of weak, organic soils in this climatic zone. The accumulation of organic soils is partially caused by the reduced rate of decay of organic soils due to sub-zero temperatures for much of the year.

3.4 Discussion of proposed analysis method

The proposed precipitation analysis combines several components from the work completed by others. Two methods are used with adaptations that provide improvement:

1. **Modified Chleborad (2000) method**

   The method of multiple independent antecedent duration precipitation indices consistent with Chleborad (2000) can be used to define thresholds where sufficient landslide data is present. A preliminary step for identifying the most critical antecedent duration or index is introduced in Chapter 4 and

Appendix H. The introduction of more than two independent antecedent precipitation indices will be also be demonstrated.

2. **Generalized Extreme Value Antecedent Precipitation Induced Landslide Return Period Analysis (GEV-APIL-RPA)**

   For locations where the landslide data is limited the GEV-APIL-RPA procedure is recommended because significant guidance is available in the literature to set thresholds when only a few landslide records are available. Return period calculations will be used to identify the most critical antecedent precipitation duration influencing the landslide provided an adequate frequency distribution can be fit to the data. The GEV frequency distribution is fit to the antecedent precipitation as per Floris and Bozzano (2007), and Petrucci and Polemio (2003).

In areas where there is insufficient landslide incident data to develop a unique set of indices and thresholds it is possible to draw on the experience of others by selecting an appropriate ID curve for the types of landslide hazards and geology of the area. The MAP and/or RDN normalization techniques can be used to modify ID curves to suite the climatic conditions of the area.

3.4.1 Justification for selection of method

Other methods are not pursued for the reasons provided below:

1. **Decay type antecedent precipitation index (API) methods**

   Decay type API methods introduce an additional variable intended to assist in modeling the physical reality of the hydrology of the slope. However, unless the K factor in Equation C4 or C5 is based on the influence of temperature, evaporation and run-off conditions (frozen ground, snow accumulation or vegetation) the application of the K factor does not add any additional information. The K factor is a calibration factor derived by trial and error. This is also true if the duration of summation is fixed as per Glade et al. (2000) and Glade (1998). If K is varied throughout the time of year to account for variations in the conditions above a step function (and related discontinuity) is introduced into the decay type API function. This produces a discontinuous decay type API and inhibits the comparison of conditions across the step. Petrucci and Polemia (2003) indicate that based on the work of others the use of decay factors is complex due to the interactions of various lithologies and permeability contrasts when considering the influence of antecedent precipitation on landslides.

2. **Gumbel antecedent precipitation induced landslide return period analysis**

   It is demonstrated in Section 4.2.4 that the Gumbel frequency distribution does not provide reliable return period estimates for the longer duration antecedent precipitation data. The more robust GEV frequency distributions are shown to fit the longer duration antecedent precipitation and provide a meaningful comparison of the return period estimates of one antecedent duration to those of a second antecedent duration. The fitting of historical data to a distribution introduces a smoothing of the results. Provided the distribution fits the data adequately this should be an advantage. However, if the fit is not appropriate the data is smeared and the resolution of the basic data is reduced.

3. **Multiple data type regression**

   The methods of Jakob and Weatherly (2003) may be applicable where multiple data types need to be combined. Unless multiple data sources are available and a single index is required multiple regression analysis is not warranted.

4. **ARPET analysis**

   The ARPET (Chowdhury and Flentje 1998 and Flentje and Chowdhury 2001) method uses antecedent durations but does not provide an equitable means of comparing the ARPET of one antecedent duration to a second antecedent duration. Ko Ko et al. (2003) demonstrate a method for the selecting one or more of the most sensitive precipitation inducing landslide indices. However, this method appears best suited to landslides when the date of the landslide is not accurately known.

5. **The Caine (1980) type intensity duration plot**

   The ID relationships developed by others are prone to inconsistent data analysis. However in the absence of an extensive landside history the wealth of experience summarized in this body of work cannot be dismissed. The use global ID threshold curves proposed by Caine (1980) and Guzzetti et al. (2007 and 2008) will result in excessive false-positive warnings. As a result, ID PIL thresholds for sites with similar geotechnical conditions should be used as guidance for setting the slope and y-intercept of the threshold in the log intensity, log duration plot.

6. **Existing urban and railway PIL warning systems**

   The Japanese railway, Hong Kong, Rio de Janeiro warning systems do not allow for the consideration of the influence of antecedent precipitation. Where antecedent precipitation is not significant the modified Chleborad and GEV-APIL-RPA methods simplify to methods effectively the same as those used in the locations identified.

All the methods use the same data and attempt to identify an index or set of indices to which a set of landslides are most sensitive. When dealing with non-uniform conditions it is advantageous to maintain as few limitations as possible on the number of indices and period of the indices. This should provide the most opportunity to find the best ones. The methods that restrict the number of indices have been developed and demonstrated to be applicable for specific climatic and geotechnical conditions for which they were developed. A more general method is needed where this experience does not pre-exist. The variation of antecedent durations between 1 and 365 days, and the ability to use delayed indices consistent with Chleborad increase the number of indices available for use. The more indices that are tested the higher the probability of finding an index that fits the geologic and hydrologic conditions of the site. The proposed methods provide a means of assessing an infinite number of indices and selecting the ones that are best correlated to the landslide activity.

3.4.2 Justification for the use of daily rainfall data

Consistent with Glade et al. (2000) this research will utilize daily rainfall data for several reasons:

1. Daily rainfall is readily available for weather stations for numerous locations throughout North America near CP rail network.

2. Any warning system that uses the results of this research requires that data be readily available.
3. Sufficient period of record of daily rainfall data is available for historical landslide studies and frequency analysis of precipitation intensity.
4. This research and that of others demonstrates that daily data is adequate for the prediction of precipitation-induced landslides.
5. Daily rainfall is available throughout the world should others compare the findings of this research to the research of others.
6. The railway industry can accommodate daily notification of increased landslide hazard.

3.4.3 General summary of procedure

The numerous studies demonstrated in the literature demonstrated that a single threshold is unlikely to provide warning of all landslide periods. As a result, systems that provide a relationship between two or more indices are more likely of providing warning of landslide activity.

1. Identify the locations and times of the landslide hazards for which indices are to be developed.
2. Select the most representative weather station.
3. Complete the statistical analysis of the weather station data. To reduce the computational demand the Gumbel distribution can be used provided the antecedent precipitation data can adequately modeled. Once the Gumbel distribution is unable to adequately match the data the GEV distribution can be used.
4. Identify which one or more antecedent duration produced was the rarest (highest return period) on the day of the landslide.
5. Select the antecedent precipitations associated with the rarest events and plot these on an IDF type plot.
6. Identify the climatic region of the landslide and compare the rarest events with the IDF from Guzzetti et al. (2007). Provided the general GEV criteria and analyzed event data are consistent the criteria can be computed.

7. If more than one geotechnical hazard exist for a given rainfall station repeat *steps 1 to 6 plotting the second set of data of the same IDF.*

When no correlation between a landslide and the weather conditions can be found several conditions may be present. These include:

1. Insufficient spatial distribution of climate data to provide representative information at remote landslide locations. This situation will likely arise during the application of the methodology developed by this study. When it does, the railway will have to assess the costs and benefits of acquiring more climate data. The requirement for proximity of weather stations to a landslide will likely require a site evaluation of the topographic, orographic effects, and climatic effects at the landslide site.
2. Other processes influencing the stability of the slope including river erosion and anthropogenic modification of the topography and groundwater conditons.

Undoubtedly, these situations will arise during the implementation of the methodology developed. Some of these limitations are evaluated and can be accommodated by the risk assessment component of the research.

3.5 Conclusions

In Chapter 3 the following topics are presented. The sources of precipitation data are identified. Other studies on precipitation induced landslides are reviewed. The types of landslides that are sensitive to different patterns of precipitation and infiltration including snow accumulation and melting are discussed. The various climatic regions within North America traversed by the CP network are described. The geographic distribution of landslides in the CP network relative to the climatic regions is also reviewed. Finally, the proposed analysis is summarized.

Chapter 4 Case study correlating antecedent precipitation and CP geotechnical hazard records

4.1 Selection of events from the CP Natural Hazard Incident Database

An area of landsliding in Maple Ridge, BC has been selected from CP NHID and CP geotechnical files for this thesis. This area was selected based on the current level of influence it has on safety and service of rail operations. It is not the most active landslide area covered by the network. Additional criteria for the selection of these events are included in Sections 1.4 and 4.1.1.

The CP and other railways in Canada and the United States have been in operation for more than 100 years. During this time, they have compiled records of the influence of natural hazards on their operation. Although the quantity and quality of information varies greatly from railway to railway, region-to-region and decade to decade the regional distribution of the data is larger, and the period over which it has been records is longer, than those considered by Guzzetti et al. (2007).

4.1.1 Criteria for case study selection

The following criteria were used for the selection of the Maple Ridge, BC case study and are recommended for the selection of other landslide precipitation studies.

1. Nominally, the volume of the landslides considered will be at least 100 m^3. Where multiple landslides smaller than 100 m^3 of the same type have occurred in the same area they will be considered. This volume threshold has been selected for three reasons:
   a) Smaller slides are sensitive to local changes in drainage conditions and highly localized weather conditions. As a result, some landslides may be excluded as being too small to be reliably predicted by daily precipitation information. For example, in an extreme case, small rock fall (often less than 0.1 m^3) often occur at the first wetting of a previously dry slope due to the loss of cohesion as the soil moisture of the fine soils within the joints increases. It is not expected that a reliable correlation can be established between events less than 100

m^3 and precipitation events since small rock falls and slides can be triggered by any magnitude of precipitation event.

b) There are 250 weather stations in Canada and the US distributed along CP track over about 22,400 km (14,000 miles) of mainline track (or on average one per 90 km of track). As a result, weather conditions that influence landslides need to be large enough that they are represented by the nearest weather stations. Landslides that are triggered by intense convective type storms tend to be smaller because the total rainfall during a convective event is small. Convective rainfalls are more commonly associated with high run-off events not large landslides, unless there is a severe antecedent condition, which should be indicated by the nearest weather station.

d) There is less documentation for smaller events. Larger volume landslides result in more investigative and event documentation.

2. The landslide location must be within 25 km of a weather station with reliable data recorded at the time of the landslide. Weather conditions are more spatially uniform the longer the duration of the event. This is due to temporal averaging. The five-minute rainfall at two sites 1 km apart might vary by an order of magnitude during a low-pressure storm but the 1-day rainfall is more likely to be within a few millimetres.

3. It must be possible to compile a reliable climate record representative of the landslide location that extends at least 30 years. This is consistent with most hydrologic and precipitation frequency studies (Hogg and Carr 1985).

4.2 Precipitation data

4.2.1 Consideration for use of point precipitation data

As with any hydrologic process the surface water and groundwater that influence a landslide are derived from a drainage area or basin. The surface and groundwater drainage areas of a given landslide, whether known, or unknown, are constant over time provided two conditions exist. First, if the drainage area is changed by a geomorphic process or more commonly anthropogenic activity, the drainage area would change and any Precipitation Induced Landslide (PIL) indices based on the old drainage area would have to be modified. Second, the groundwater drainage area of a landslide may vary over time due to a groundwater divide being overtopped during high groundwater conditions, compared to lower ones. However, it would be expected that the same degree of groundwater flow between groundwater divides would occur given the same pattern of depth of precipitation in a given period. Provided these two conditions are met or accounted for, a given landslide can be assumed to have a constant surface and groundwater drainage area.

The World Meteorological Organization (1973 and 1983) indicates that point precipitation is an adequate estimate of catchment precipitation for a small drainage area. It also states that there is a reduction in the depth of precipitation accumulating over an area compared to that recorded at a point, but that the reduction is insignificant unless the drainage area is greater then 25 km^2.

As a result, an empirical index developed from comparing coincident precipitation and landslide activity to historical precipitation data need not account for the area of the drainage recharging the landslide unless the drainage area exceeds 25 km^2. For landslides with larger drainage areas, the estimation of applicable area precipitation reduction factors is well developed (World Meteorological Organization 1973 and 1983, ASCE 1996, Chow et al. 1988).

The area of the drainage basin directing water to the each landslide site should be evaluated and documented for comparison to other sites. It is expected that a relationship between drainage basin size and weather conditions may exist.

4.2.2 Analysis of precipitation data

As discussed in Appendix B, Section 1.4 and 3.4 two types of analysis will be completed for each case study: A modified Chleborad (2000) type analysis and a return period type analysis. Both are explained in more detail below.

4.2.2.1 Modified Chleborad method

As discussed in Appendix C, Section 1.1, Chleborad (2000) provides a method of identifying when precipitation induced landslides are likely to occur in response to short and longer duration antecedent precipitation. He plots the $A_{(3)}$ against the $A_{(4\text{-}15)}$ and shows that landslides only occur in the high $A_{(3)}$ and high $A_{(4\text{-}15)}$ half of the plot (Figure C3). However, Chleborad does not provide a means of determining which antecedent durations are most likely to be correlated with landslide activity. Appendix H provides a methodology that can be used to identify the most relevant indices.

Chleborad (2000) identified two antecedent precipitation indices to which landslides are sensitive in the Seattle Washington area. He presents these in an x versus y plot of one index versus the other. However, there are no reasons that additional indices cannot be identified that correlate the precipitation conditions and landslides induced by precipitation. Multiple indices would define a volume within an x, y, z plot or multi-index system. Provided a reliable third (or more) index can be identified, fewer non-landslide inducing precipitation events should exceed all three (or more) thresholds. Therefore fewer false-positive warnings would be issued.

Based on the work of Cannon and Ellen (1985), Keefer et al. (1987), Wilson et al. (1993), and others it is reasonable to make the $A_{(c\text{-}d)}$ and $A_{((d+1)\text{-}e)}$ graphs (where $c < d < e$) asymptotic to the y axis provided the it can be shown that the shorter $A_{(c\text{-}d)}$ index does not result in landslides at low values of $A_{((d+1)\text{-}e)}$.

The modified Chleborad method is applied in the Maple Ridge, BC case study that follows in Section 4.5.13.1.

4.2.2.2 Antecedent precipitation data analysis and return period calculations

The assumption that landslides are induced by rare antecedent precipitation conditions is adopted consistent with Floris et al. (2004), Floris and Bozzano (2007), Ibsen and Casagli (2004), Walker (2007), and Zézere et al. (1999), Ko Ko et al. (2003) and others. Adoption of this assumption requires a means of identifying which conditions are the rarest. Real time data evaluation requires that the current condition be compared to frequency distribution of previous events to establish how rare they are. Although the *ARPET* system of Chowdhury and Flentje (2002) provides a means of ranking antecedent precipitation, it results in a ranking regardless of the magnitude of the precipitation condition relative to the next most severe event. All the antecedent durations have the same likelihood of occurrence. For example, using an *ARPET* analysis, the third largest 15 day antecedent precipitation is expected to occur as often as the third largest 60 day antecedent precipitation event. Since these two data sets are independent samples from a much larger population, there is no reason that the probability of these two events should be equal. By fitting historical antecedent precipitation data to a frequency distribution, the precipitation record can be represented by two or three variables (depending on the distribution selected) per antecedent duration for each weather station. More importantly, using this method, the probability (or return period) of an antecedent duration event is independent of the other antecedent duration events. The ability to distinguish unusual and extreme events from frequent and low intensity events can be achieved provided a frequency distribution with a good fit to the data can be identified.

Klemes (2000) identified the dilemma of relying on extreme event statistics to determine hydrologic parameters (flood flows in his case) used to design water conveying structures. Klemes notes that the actual design flow used widely in the most applications including the railway industry is the 1 in 100 or 1 in 200 year flood. However, the method and statistics used to derive this design flow can be significantly influenced by the flow of non-flood years. He suggests contrary to common practice, and the procedures used for this research, there is no reason to believe that "the probability of a severe storm hitting this basin should depend on the accumulation of snow in the few driest winters ...". In other words, why is the precipitation during dry years considered when determining the precipitation of the wettest years? However, despite this perplexing situation, provided a frequency distribution that fits the data can be found, hydrologist and meteorologist have used the extreme annual series, including data from drought years, to successfully predict the precipitation or stream flow in the wettest years.

Precipitation and hydrologic analysis of rainfall up to 1 to 2 days is undertaken using an Intensity-Duration-Frequency (IDF) analysis and requires the fitting of the history of recorded precipitations and the frequency at which they have occurred to a frequency distribution. One of the most common frequency distributions used for up to two day duration rainfalls is the Gumbel (Hogg and Carr 1985, Sevruk and Geiger 1981, Islam and Kumar 2003, and others). Similar techniques should be applicable to longer antecedent durations provided appropriate distributions can be identified that will adequately model the antecedent precipitation data. This is justified below.

The accepted frequency analysis of hydrologic parameters, including precipitation, has four basic steps:

1. Aggregate the antecedent precipitation, $A_{(d)}$ over a duration, d,
2. Extract the highest aggregated precipitation in a given period, T, from the population,
3. Fit the a distribution to the extracted maximum $A_{(d)}$ from each period, T, and
4. Use the distribution to predict the frequency of various precipitation conditions reoccurring per period, T.

Normally d varies from 5 minutes to 24 hours and sometimes 48 hours and T is one year. This results in frequency of reoccurrence expressed as the return period of an event in years. Return period is the reciprocal of the probability of the event. However, there is no physical reason why these parameters cannot be varied provided d does not exceed T, as this would result in the $A_{(d)}$ of a period not being independent of the $A_{(d)}$ from the previous or subsequent period. As shown in Section 2.3 and Appendices B and C precipitation and infiltration processes are not limited to a one or two day period. Precipitation is influenced by:

1. Convective process with periods of minutes to hours,
2. Cyclonic weather systems with periods of hours to several days,
3. Temperature and atmospheric circulation patterns controlled by the annual weather cycle (including the accumulation and melting of snow), and
4. The disruption of the ocean-atmosphere system like El Niño in the Pacific. These longer duration processes have been connected with seasonal and multi-year droughts and wet cycles.

In some precipitation analysis the requirement that the precipitation be continuous is invoked. However, this is usually required to achieve stream hydrographs with a single idealized pulse of flow rather than the complication of analyzing multiple overlapping surges of flow. When considering the infiltration of precipitation into the soil, the requirement for continuous precipitation is diminished due to low infiltration rates (due to the hydraulic conductivity of the soil) compared to precipitation and surface water flow rates. For example the instantaneous flow in a small creek is highly dependent on the precipitation within the last 24 hours, the groundwater condition in an aquifer is dependent on the precipitation over a longer period as function of the permeability of the soil. This is consistent with the groundwater time delay effects identified by Hvorslev (1951) and Iverson (2000). This suggests that infiltration is not significantly influenced by whether precipitation is continuous, or discontinuous; provided the hydraulic conductivity of the soil is lower than the precipitation intensity. As a result, the extension of accepted intensity frequency duration analysis of precipitation to longer durations is appropriate when considering the influence of precipitation on soil moisture in the unsaturated zone, groundwater and associated landslide activity.

As indicated, d must be shorter than T. As a result, analysis of d approaching 365 days requires T be extended to several years or possibly a decade. However, this reduces the quantity of data available for analysis and results in distribution fitting to ten points for a century of precipitation data. For this reason the antecedent precipitation frequency analysis in this thesis has been limited to 365 days. In summary, to achieve adequate sampling of the variability of the precipitation that could induce landslides it is necessary to aggregate precipitation over days and months to identify indices that represent the influence of precipitation on shallow and deep groundwater conditions or the snow accumulation and melting processes.

The importance of an adequately fit distribution is critical to the accurate identification of which precipitation events are the rarest. A poorly fit frequency distribution could result in the selection of precipitation indices that are not reflective of the most severe antecedent precipitation condition at the time of the landslide. As a result, the incorrect antecedent indices and threshold will be identified as inducing the landslide.

An example, using a poorly fit distribution, is reviewed to demonstrate the importance of this issue. The method of completing a Gumbel distribution analysis of antecedent precipitation data is provided in Appendix G. As can be seen from Figure 4.1, the calculated Gumbel return periods for antecedent durations longer than a month are not representative of the expected return period of the antecedent precipitation because the antecedent precipitation durations longer than 15 days are not well matched by the Gumbel distribution.

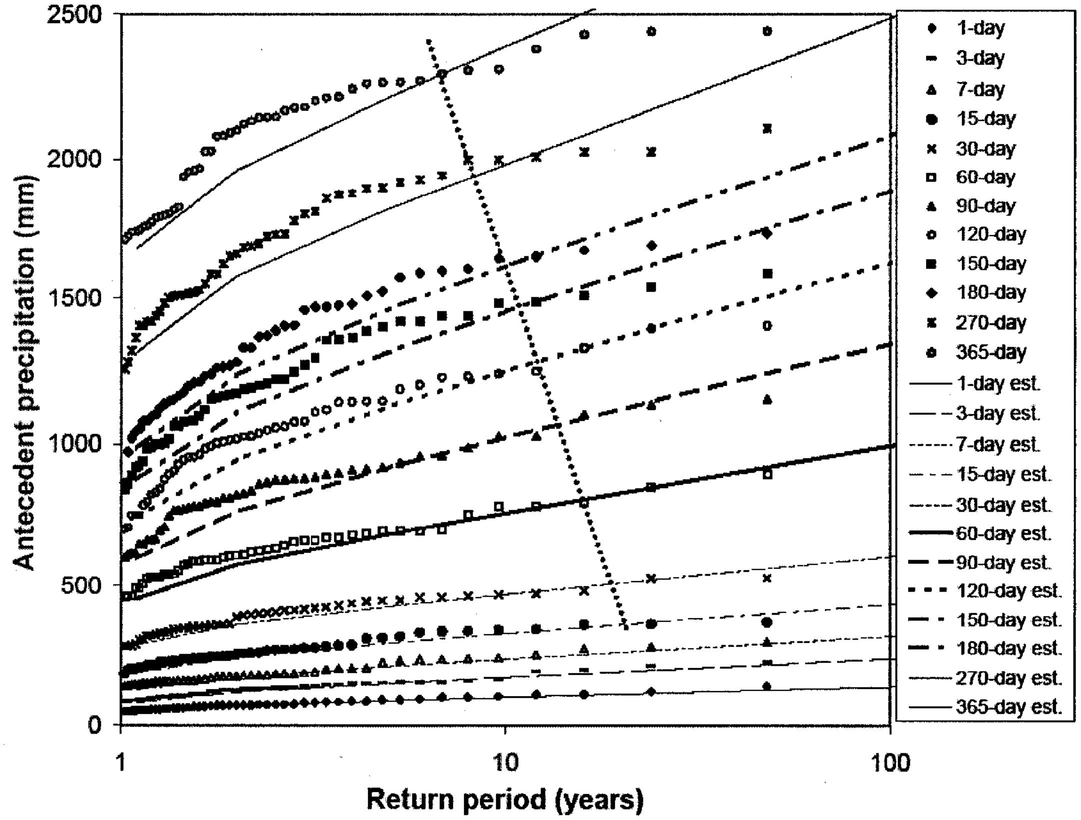

Figure 4.1 Precipitation return period plot for the Gumbel distribution analysis of Maple Ridge, BC data between 1953 and 2007. The markers are the recorded antecedent precipitations. The lines are the Gumbel distribution prediction of the antecedent precipitation.

If the Gumbel distribution is used where the antecedent precipitation data is not well matched to the data the following scenario can develop. For the 15 landslides that occurred on March 24, 2007 between miles 102.50 and 104.50 of the Cascade Subdivision in Maple Ridge, BC the antecedent precipitation conditions are summarized in Table 4.1.

In this case it is clear that the Gumbel distribution overestimates the return periods shorter than 10 years (those for d = 30, 60, 90, 120, 180, 270 and 365) and underestimates the ones longer that 10 years (d = 15 days). It is only reliable for the 150 day antecedent duration where the antecedent precipitation happens to fall on the

Table 4.1 Example of Gumbel frequency precipitation analysis for 1953 to 2007 Maple Ridge, BC precipitation data

Gumbel results		Antecedent precipitation on March 24, 2007 (mm)	Gumbel return period (years)	Return period based on nearest neighbour (years)
Antecedent period (days)	1	49	1.1	1.1
	3	131	3.1	2.4
	7	149	1.5	1.2
	15	365	23.8	42
	30	461	9.1	7.5
	60	588	2.2	1.5
	90	895	4.3	3.4
	120	1076.6	3.8	3.0
	150	1480.8	11.6	11.6
	180	1531.4	6.8	4.9
	270	1635.4	2.4	1.8
	365	1876.6	1.6	1.4

dividing line between over and under estimated return periods included in Figure 4.1. The dividing line crosses each antecedent series between 10 to 30 years for the 270 and 15 day antecedent durations, respectively. The concern is that return periods for antecedent precipitations for the longer antecedent durations (greater than 15 days) could be underestimated or overestimated depending on which side of the dotted line the antecedent precipitation plots in Figure 4.1. This could result in an overestimated return period being selected as the critical index, when an underestimated return period was the landslide inducing condition. Furthermore, the difficulty with any distribution that does not fit the higher return periods is that if the predicted precipitation return period curve is above actual precipitation data at the higher return periods the range of return periods will be condensed. Alternately, if the predicted precipitation return period curve is below the actual precipitation data at the higher return periods the range of return periods will be increased. This is less of a concern. The analysis completed by Walker (2007) appears to have suffered because of a poorly fit Gumbel distribution for the lower return periods.

In summary, the fit of the frequency distribution to the whole data set is important, but the fit of the distribution to the maximum tail, the most extreme of the extreme events, is the most critical. A specific example using the Maple Ridge, BC data follows.

The highest Maple Ridge, BC 180-day antecedent precipitation ($A_{(1-180)}$) was 1,730.4 on March 29, 1999. Given that the data record is 52 years long one would expect the predicted return period for this precipitation to be no less than 52 years given that this is the maximum $A_{(1-180)}$. However, Gumbel analysis predicts 1,730 mm of precipitation over 180 days to have a return period of only 17.8 years. Although the calculated return period may not approximate the expected return period event for cases where the Gumbel distribution does fit the antecedent precipitation data, the return period calculation does provide a representation of the relative severity of each event relative to the other events in that antecedent duration similar to the *ARPET* analysis. As a result, all $A_{(1-180)}$ predicted return periods between 1,680 and 1,730 mm would have shorter return periods than would be expected. Thus, like *ARPET* the "Gumbel return period" is an index not a reliable return period calculation. As with *ARPET* the Gumbel return period from one antecedent duration, that does not fit the Gumbel distribution, and a second antecedent duration, that does fit the Gumbel distribution, cannot be meaningfully compared because they will not reliably distinguish which event is the rarer, and therefore which is most likely to have induced a landslide.

Several tests are available to determine the "goodness-of-fit" (Reliability Analysis Center 2003) or "test of fit" (Bury 1999) which are discussed in Section 4.2.4. As is discussed in Section 4.2.4 the visual inspection of the Q-Q type plot is one of the best means of assuring that a distribution fits a data set including the maximum tail of the data.

In conclusion, the analysis of antecedent precipitation data is critical to the identification of the most severe antecedent precipitation. This depends on a good fit between the data and the frequency distribution being achieved. The representation of the data, in as few parameters as possible, aids in the timely analysis of real time data.

As will be shown in Section 4.2.4 other frequency distribution are available that fit the antecedent precipitation better than the Gumbel distribution.

4.2.3 Reliability of past precipitation to predict future precipitation with consideration of climate change

It is important that the historical precipitation record be representative of the future precipitation conditions to be of use. Zhang et al. (2001) assessed the spatial and temporal characteristics of heavy precipitation events in Canada and found that, there appears to be no change in the either the frequency or intensity of extreme precipitation for the country as a whole during the last century. The upward trend in annual precipitation was caused by an increase in the number of small to moderate precipitation events. Small to moderate precipitation events would not significantly influence short duration antecedent conditions but could influence longer duration antecedent conditions.

One concern is that warmer temperatures, because of global warming, will cause coastal regions to become wetter, and arid regions hotter. Global warming should also increase the snow accumulation in cold areas, influenced by oceanic storms, such as the west coast of North America. This is consistent with the findings of Scheiner et al. (1997) that indicate that 16 of 21 regions within the US have longer term trend of increasing precipitation.

Potter and Savonis (2003) have identified several potential influences of climate change on transportation. However, longer period antecedent precipitation is considered a second order effect. This is because climate change is expected to influence intense rainfall more than average annual rainfall.

Miles (2001) presents data that indicates annual precipitation within the Georgia Basin of southwestern British Columbia will increase by 5 to 13% by the middle of the 21st century compared to the 1960 to 1991 period. Some of these prediction suggest that winter months will experience most of the increase and summer months will be drier. If realized these changes would have an influence on the short and long term antecedent precipitation conditions. As these changes occur an increase in the frequency of landsliding would be expected due the increased frequency of PIL thresholds being exceeded. During the initial period of increased precipitation the threshold based on the previous data should be appropriate. However, if the annual depth and distribution of precipitation throughout the year changes significantly it will alter surface and groundwater flow patterns and may alter the precipitation conditions required to induce landslides. As a result, of these conditions, if climate change is realized, PIL thresholds will likely have to be periodically re-evaluated. However, because the year to year changes in precipitation due to climate change are smaller than the variability in the average annual precipitation it should sufficient to re-evaluate the PIL indices once every decade. The updated thresholds would be based on the most recent 20 to 30 years of landslide and climate data.

4.2.3.1 Potential influence of climate change on the correlation of precipitation indices with landslide activity

If climate change does influence precipitation over the next decades it is important to have a base-line from which to compare. This thesis should contribute to the establishment of base-line thresholds, which may or may not require updating in the event of changes in precipitation patterns.

As more accurate predictions regarding the influence of climate change on antecedent precipitation become, available the analysis methodology developed in this thesis should be reapplied to the data. The return period of the antecedent precipitation at which a landslide is induced by precipitation may change. However, the antecedent precipitation thresholds should not change as they are controlled by the physical geometric and geotechnical conditions at a potential landslide site.

4.2.4 Selection of frequency distribution

As discussed in Section 4.2.2 it is important to fit the historical antecedent precipitation data to a representative frequency distribution. This section discusses the application and merits of several distributions. The World Meteorological Organization (Sevruk and Geiger 1981) discusses the use of various means of completing frequency analysis of extreme precipitation data. They conclude that there is no theoretical basis for the selection of one distribution over any other. They discuss the merits of various distributions but conclude that there is little benefit to the application of any one of several distributions. They recognize that various jurisdictions have adopted different distributions as standard and this has set a precedent for future analysis in that jurisdiction. Environment Canada adopted the Gumbel distribution (Hogg and Carr 1985). The US National Weather Service (Miller 1964) use Gumbel but they also use the log-normal distribution. However, these papers were written about the time of some of the first publications on the Generalized Extreme Value frequency distribution (GEV) and therefore GEV is not specifically considered.

Analysis of extreme antecedent precipitation events in excess of 10 days is not generally considered but Loucks et al. (2005) did analyze longer duration rainfall events up to 25 days using the GEV. They found that the GEV distribution could be useful for modeling these antecedent precipitation conditions. The GEV frequency distribution is expressed as

$$P(Z \leq z) = F(z;\mu,\sigma,k) = \exp\left\{-\left(1-\frac{k(z-\mu)}{\sigma}\right)^{1/k}\right\} \qquad \text{Equation 4.1}$$

Where μ, σ, k are the location, scale and shape parameter respectively.

However, Loucks et al. notes that if the k value is positive, the GEV is bounded from above. This means that at for long return periods the depth of precipitation reaches a maximum value equal to $\mu + \sigma / k$. This is consistent with the antecedent data analyzed for this thesis and is appropriate for precipitation data because there the maximum amount of precipitation in any period is limited, not unlimited. In other words, there is a physical maximum volume of water that can be transported by the atmosphere within a given temperature range (determined by the climate and latitude) and time period. As will be shown in the data analysed antecedent precipitation for the longer durations is bounded above. The Gumbel and GEV frequency distributions equations are included in Appendix G and I respectively.

Walker (2007), Ibsen and Casagli (2004) and Zêzere (1999) use the Gumbel extreme value analysis to predict the return period of precipitation for various antecedent durations. Floris et al. (2004), Floris and Bozzano (2007) use the GEV distribution for analyzing return period of antecedent precipitation before landslides. Petrucci and Polemio (2003) used historical rainfall data to characterize multiple damaging hydrological events. They indicate the General Extreme Value function can be used to analyze each antecedent rainfall duration, $A_{(c\text{-}d)}$ where c=0 and d=1, 5, 10, 20, 30, 60, 90, 120 and 180 days. However, none of this research discusses the goodness-of-fit of this distribution to the antecedent data.

Two tests can be undertaken to assess the ability of different distributions to represent the data. The first is the sample correlation coefficient (Devore 1982), r.

$$r = \frac{n\left(\sum_{i=1}^{n} u_i v_i\right) - \left(\sum_{i=1}^{n} u_i\right)\left(\sum_{i=1}^{n} v_i\right)}{\sqrt{n\left(\sum_{i=1}^{n} u_i^2\right) - \left(\sum_{i=1}^{n} u_i\right)^2}\sqrt{\left(\sum_{i=1}^{n} v_i^2\right) - \left(\sum_{i=1}^{n} v_i\right)^2}}$$

Equation 4.2

Where u_i is the antecedent precipitation annual maximum series and v_i is the predicted antecedent precipitation for the same return periods using

$$T_i = \frac{(n+1)}{i}$$

Equation 4.3

where T_i is the return period for the ith ranked antecedent precipitation and n is the number of years of data. A complete description of the application of the sample correlation coefficient is provided in Appendix J.

Since v_i approximates u_i the two should have the same values for all i such that plotting v_i versus u_i should yield a straight, diagonal line across an equally dimensioned plot. This is referred to as a Quantile-Quantile (Q-Q) plot (NIST/ SEMATECH 2006). The closer r is to unity and the straighter the line of the Q-Q plot of the actual and modeled data the better the distribution fits the data. Since the highest return period events are often of most interest it is also important the maximum tail be close to the diagonal. The proximity of the minimum tail is not so critical for this application. Figure 4.2 is a Q-Q plot for the 180 day antecedent precipitation data shown in Figure 4.1. The correlation coefficient r of 0.9557 is relatively high given the over and under-estimation of the Gumbel distribution at the high and low tails. In this case, the numerous points in the mid and low range, just below the diagonal, balance the few points in the high tail, that are well above the diagonal. This results in an r close to unity, but the Q-Q plot clearly demonstrates the inability of the Gumbel distribution to fit the data to the diagonal, especially in the area of greatest interest. Consequently, the Gumbel analysis results are not acceptable because of the concern discussed in Section 4.2.2.

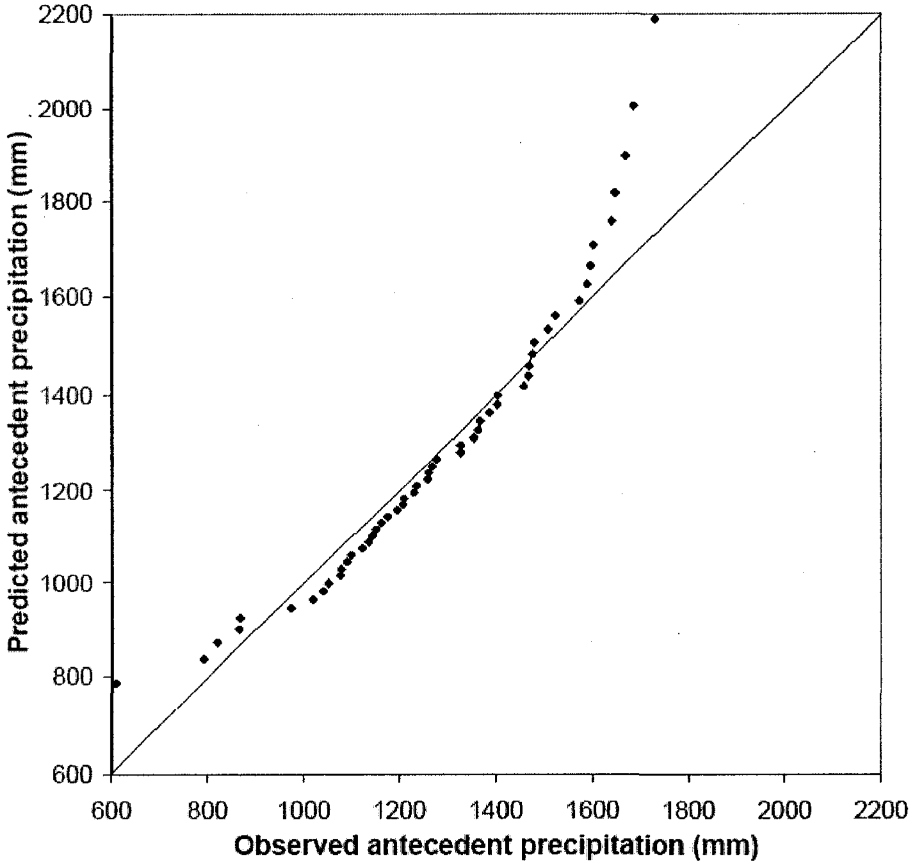

Figure 4.2 The Q-Q plot for the 180 day antecedent precipitation for 1953 to 2007 Maple Ridge, BC data. r = 0.9557 for this example

The second goodness-of-fit test is the Anderson-Darling (AD) statistic *p-value* (Bury 1999). This test is a distribution dependant test that can be used with the Gumbel and Weibull distributions. However, this test cannot be used to assess the goodness-of-fit of the Generalized Extreme Value (GEV) Distribution (G. Chen, personal communication 2007).

The Anderson-Darling statistic *p-value* is calculated using the formulation

$$A^2 = -n - \frac{1}{n}\sum_{i=1}^{n}\{(2i-1)\ln(u_i) + (2n+1-2i)\ln(1-u_i)\}$$ Equation 4.4

$$v = A^2\left(1 + \frac{1}{5\sqrt{n}}\right)$$ Equation 4.5

$$p-value = \exp\left(0.8506277v - 14.0358032v^2 + 8.8154537v^{2.5}\right)$$ Equation 4.6

If the *p-value* is less than the significance level of 0.05 then the distribution does not fit the data. The *p-value* for the Gumbel distribution of the 180 day antecedent precipitation data for 1953 to 2007 for Maple Ridge, BC is 0.0107. This is less than 0.05 so the hypothesis that the 180 day antecedent precipitation can be represented by a Gumbel distribution is not valid. This is consistent with the visual assessment of the Q-Q plot (Figures 4.2) indicating that the Gumbel distribution does not fit the data well despite the high r value. A complete description of the application of the Anderson-Darling statistic *p-value* is provided in Appendix J.

For this thesis three distributions were considered: the Gumbel, Weibull, and Generalized Extreme Value. In addition, there are two ways to calculate the Gumbel distribution parameters: the Moment Estimate (ME) method (Hogg and Carr 1985), and the Maximum Likelihood Estimate (MLE) method (Bury 1999 and Chow et al. 1988). For a selected data set from Maple Ridge, BC, G. Chen (personal communication 2007) demonstrated that the Gumbel distribution using Moment Estimate method can be used for antecedent durations up to 7 days. He further showed that there was no benefit in using the Gumbel distribution using MLE method despite the added computational effort. For antecedent durations greater than 7 days, Chen demonstrated that the Weibull distribution provides a good fit to the data, but its ability to fit the 1, 3, 7, 60, 180, 270, 365 day antecedent durations was inferior to the GEV. The Weibull and GEV produced indistinguishable results for the 15, 30, 90, 120 day antecedent precipitations. Although it is computationally intensive to compute the parameters governing the GEV distribution, Chen found that it provides the best fit to all the antecedent durations. In addition to the GEV providing the lowest *r* values (see Table 4.2) and Figure 4.3 the GEV distribution also provides as good or better fit than the Weibull distribution based on the Q-Q plot and the fit of the maximum tail. Table 4.2 summaries the results of Chen supplemented with additional analysis of the same Maple Ridge, BC data by the author. Figures 4.3 and 4.4 compare the values included in Table 4.2 and demonstrate the benefits of each distribution.

Figure 4.3 shows the following about the 1953 to 2007 Maple Ridge, BC precipitation data:

1. The Gumbel ME and Gumbel MLE are equivalent and the Q-Q plots indicate that there is no advantage to undertaking the extra effort to calculate the two

Gumbel parameters by the MLE method.

2. The Gumbel distribution is not able to model the precipitation data for antecedent durations greater than 10 days.
3. The Weibull distribution is inferior to the Gumbel and GEV for antecedent durations shorter than 10 days.

Table 4.2 Summary of the analysis by G. Chen (personal communication 2007) and additional analysis of the Maple Ridge, BC 1953 to 2007 precipitation data

Antecedent duration (days):	Gumbel (ME)	Gumbel (MLE)		Weibull (MLE)		GEV
Variable	*r*	*p-value*	*r*	*p-value*	*r*	*r*
1	0.9952	0.6002	0.9952	0.0058	0.9605	0.9973
3	0.9921	0.5608	0.9921	0.0369	0.9718	0.9917
7	0.9906	0.2438	0.9906	0.0026	0.9577	0.9895
15	0.9766	0.0688	0.9766	0.1164	0.9878	0.9911
30	0.9715	0.0528	0.9715	0.4944	0.9920	0.9938
60	0.9652	0.0026	0.9652	0.4145	0.9897	0.9878
90	0.9489	0.0039	0.9489	0.5053	0.9887	0.9866
120	0.9687	0.0124	0.9687	0.8367	0.9957	0.9957
180	0.9557	0.0107	0.9557	0.6806	0.9955	0.9954
270	0.9487	0.0052	0.9487	0.3769	0.9922	0.9922
365	0.8939	0.0000	0.8939	0.0724	0.9662	0.9691

4. It also indicates that the GEV is equivalent to or better than the Gumbel and Weibull distributions for all antecedent durations. This is not surprising because as its name suggests the GEV distribution simplifies to the Gumbel (k=1) and Weibull if these are the best fitting distributions.
5. It suggests that the fit of the Weibull distribution is equivalent to the fit of the GEV for antecedent durations between 10 and 365 days. However, it will be shown on inspection of the Q-Q plots (Figure 4.3) for several cases the GEV is

better than the Weibull at fitting the maximum tail of specific antecedent duration data sets.

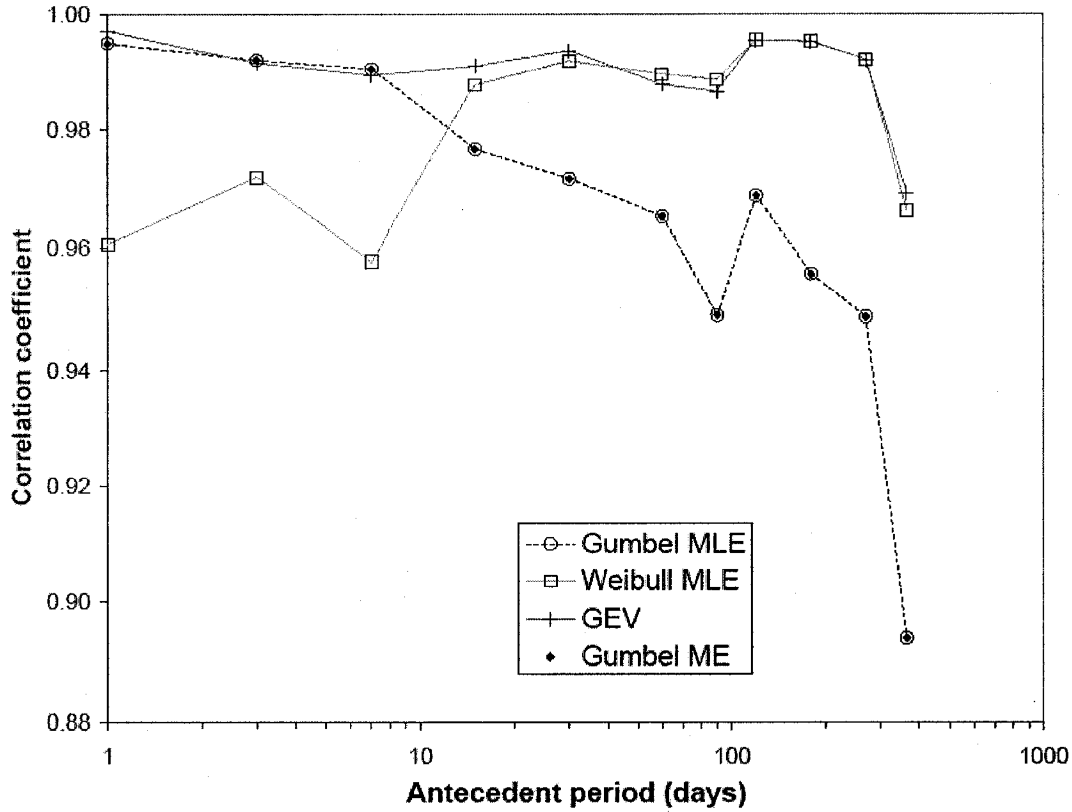

Figure 4.3 The correlation coefficient for Gumbel, Weibull and GEV distributions for 1953 to 2007 Maple Ridge, BC precipitation data for several antecedent durations

Figure 4.4 indicates the following about the 1953 to 2007 Maple Ridge, BC precipitation data:

1 The Gumbel distribution fits the data for antecedent durations less than 10 days but its ability to provide reliable analysis of longer periods decreases rapidly for antecedent durations greater than 10 days.

2. The Weibull distribution fits the data for antecedent durations greater than 10 days but does not fit the data as well as the Gumbel for periods less than 10 days.

3. The ability of the Weibull distribution to fit antecedent duration data greater than 180 days decreases rapidly as the period increases.

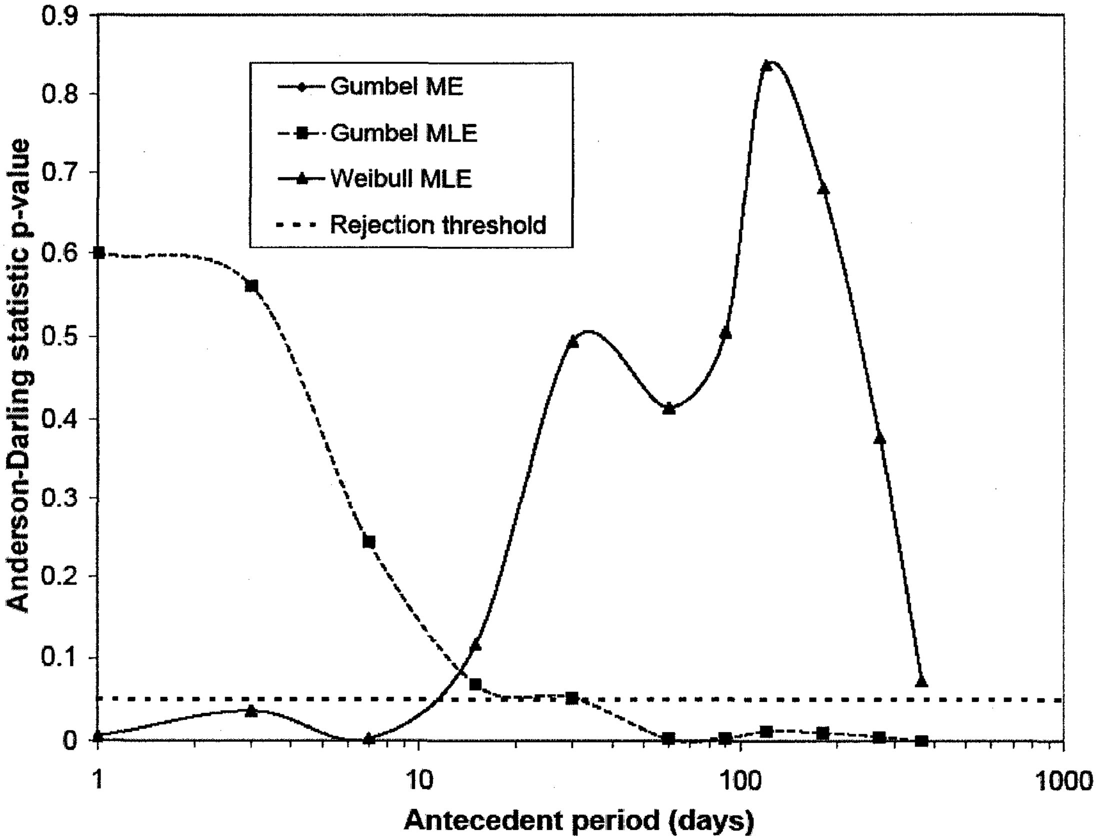

Figure 4.4 The Anderson-Darling Statistic *p-values* for Gumbel and Weibull distributions for 1953 to 2007 Maple Ridge, BC precipitation data for several antecedent durations

Due to the derivation of the GEV distribution it is not appropriate to apply the Anderson-Darling Statistic to the GEV. No other suitable test statistic was identified by G. Chen (personal communication 2007) or by the author.

It should be noted that Chow et al. (1988) suggests that antecedent precipitation of 365 days, or annual precipitation, is typically normally distributed. However, this conclusion was based on a sample population of annual precipitation data not the annual maximum series of the running sum of the 365 day precipitation for each day of each year. This second population may have an extreme value distribution as suggested by the reasonably good fit of the GEV analysis to the 365 day antecedent duration data.

The combined interpretation of Figures 4.3 and 4.4 suggest that an r of 0.98 and higher is required to achieve a tolerable AD *p-value* above 0.05.

It must be recalled that these plots are only for the Maple Ridge, BC data and, due to differences in the type of precipitation patterns that Maple Ridge, BC receives compared to other areas of the CP network, these conclusions cannot be applied everywhere. Similar analysis will be required within each climatic zone and possibly each weather station. As a result, the antecedent precipitation data from each weather station will have to be analyzed with multiple distributions and the distributions goodness-of-fit assessed until reliable patterns emerge.

The benefit of the GEV distribution is most clearly identified in the Q-Q plots. Figures 4.5 to 4.16 show the Gumbel and GEV Q-Q plots for the 1, 3, 7, 15, 30, 60, 90, 120, 150, 180, 270 and 365 day antecedent durations for the 1953 to 2007 Maple Ridge, BC precipitation data. Consistent with the correlation coefficient results, it is clear that the Gumbel distribution provides a relatively good fit for the daily precipitation, and a good fit for the 3 and 7 day antecedent precipitations durations when compared to the GEV distribution. However, for the antecedent durations longer than 7 days the Gumbel is inferior to the GEV, especially for the higher antecedent precipitation durations, which are often of most interest to this study and most meteorological investigations. Figure 4.16 shows the slight deterioration in the ability of the GEV to fit the annual precipitation data. This suggests that the other distributions such as the normal distribution, suggested by Chow et al. (1988) may fit the 365 day and longer antecedent durations better than the GEV. Fitting of antecedent precipitation durations longer then one year has not been completed as part of this research.

It can be concluded from the Maple Ridge, BC data that the GEV distribution is equivalent to, or superior to the Gumbel distribution for antecedent durations of up to one year. Similarly, G. Chen (personal communication 2007) concluded that the GEV was superior to the Weibull distribution at fitting the Maple Ridge, BC data.

The GEV frequency distribution analysis was also completed for precipitation data from Lytton, BC and Kenora Ontario. The results are included in Appendix K. These two stations were chosen because they represent different climatic conditions compared to the climate of the Maple Ridge site and each other. Lytton is a semi arid highland climate. Kenora is a temperate mid-latitude continental climate. The results demonstrate the ability of the GEV to fit the antecedent precipitation at these locations

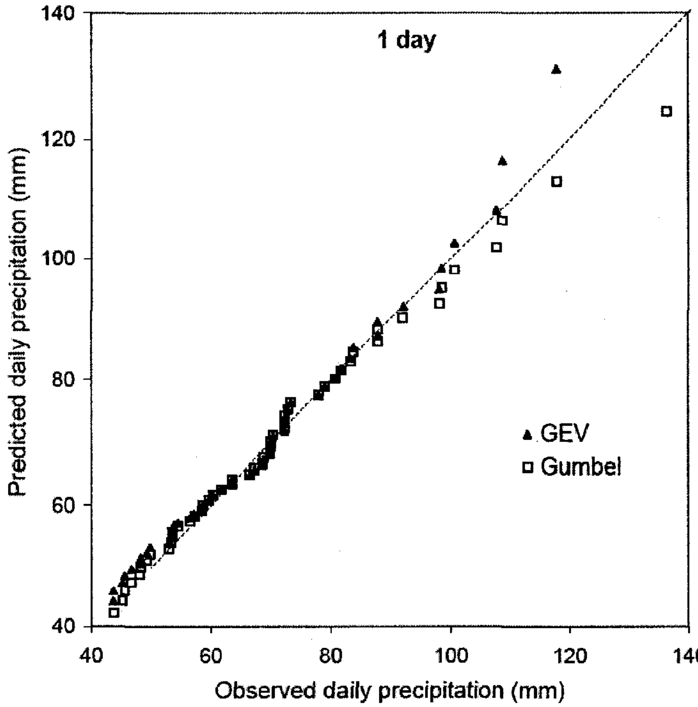

Figure 4.5 The Q-Q plot for the GEV and Gumbel distributions for the daily precipitation at Maple Ridge, BC between 1953 and 2007

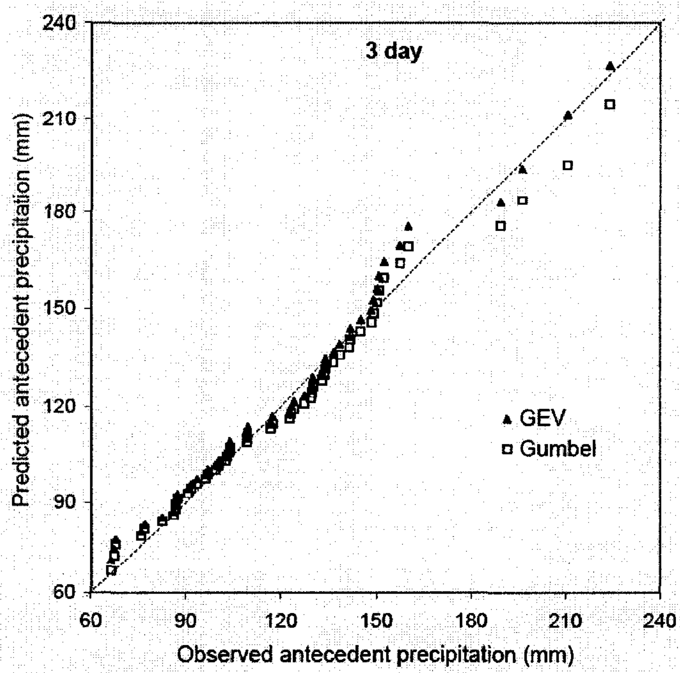

Figure 4.6 The Q-Q plot for the GEV and Gumbel distributions for the 3 day antecedent precipitation at Maple Ridge, BC between 1953 and 2007

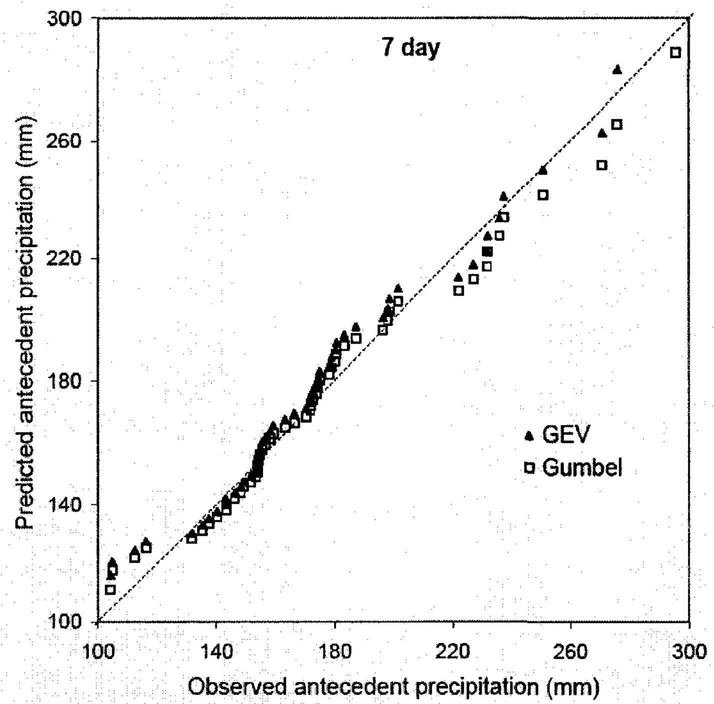

Figure 4.7 The Q-Q plot for the GEV and Gumbel distributions for the 7 day antecedent precipitation at Maple Ridge, BC between 1953 and 2007

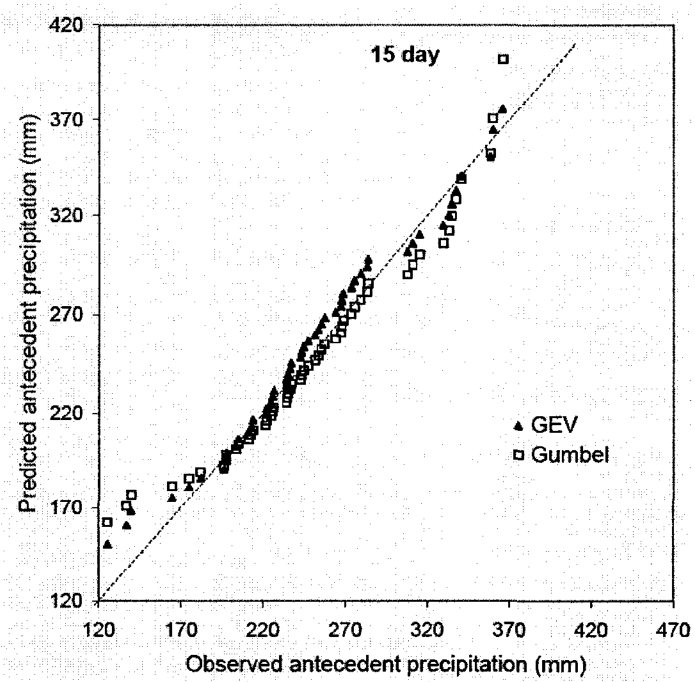

Figure 4.8 The Q-Q plot for the GEV and Gumbel distributions for the 15 day antecedent precipitation at Maple Ridge, BC between 1953 and 2007

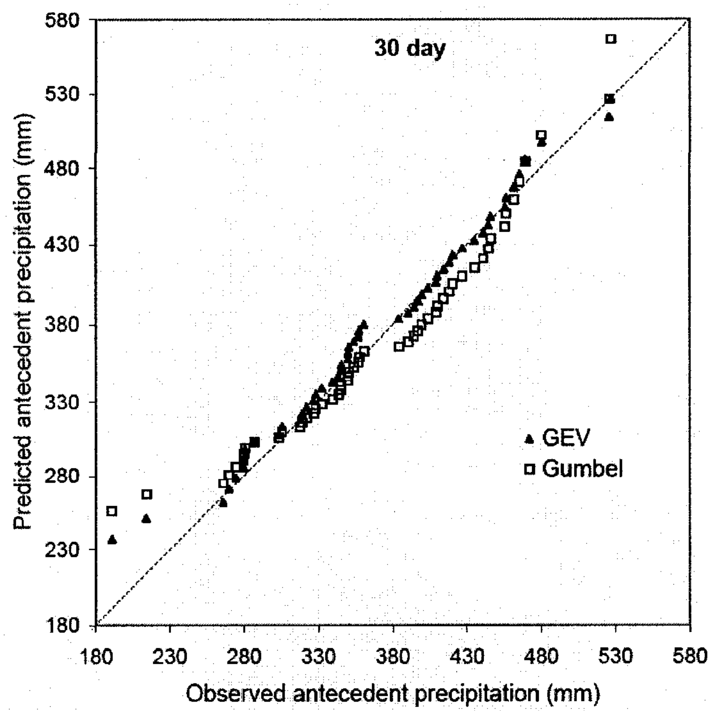

Figure 4.9 The Q-Q plot for the GEV and Gumbel distributions for the 30 day antecedent precipitation at Maple Ridge, BC between 1953 and 2007

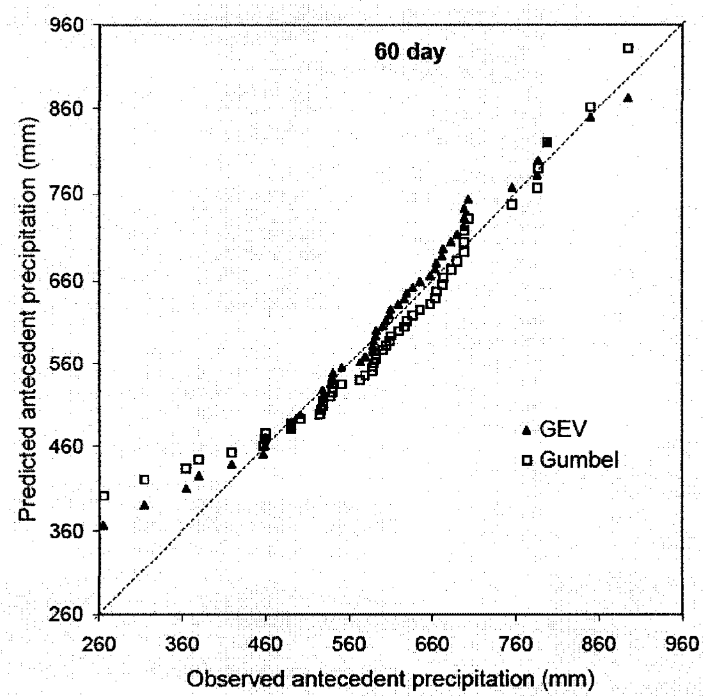

Figure 4.10 The Q-Q plot for the GEV and Gumbel distributions for the 60 day antecedent precipitation at Maple Ridge, BC between 1953 and 2007

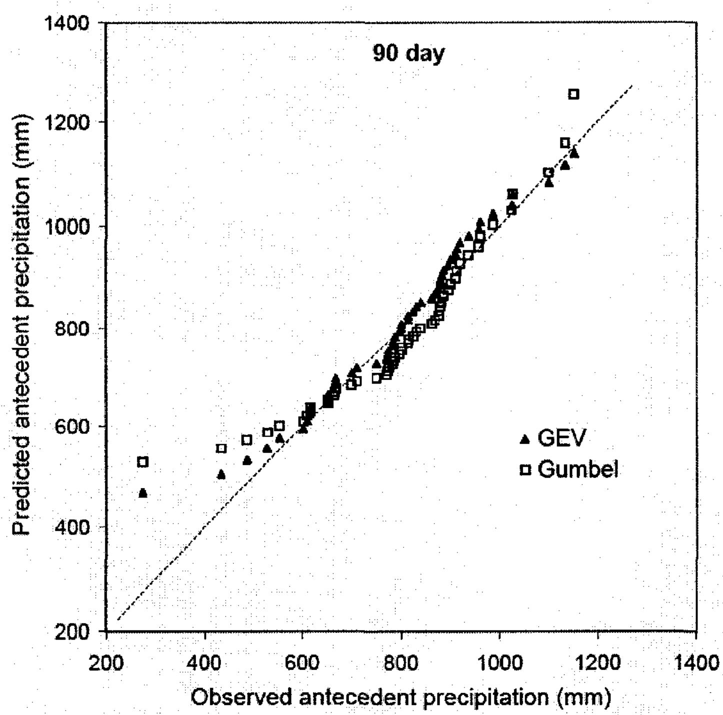

Figure 4.11 The Q-Q plot for the GEV and Gumbel distributions for the 90 day antecedent precipitation at Maple Ridge, BC between 1953 and 2007

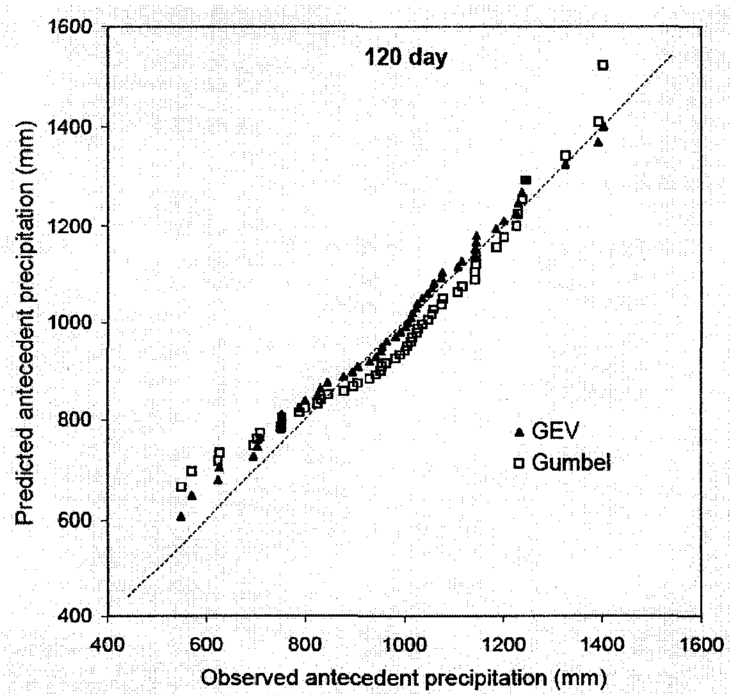

Figure 4.12 The Q-Q plot for the GEV and Gumbel distributions for the 120 day antecedent precipitation at Maple Ridge, BC between 1953 and 2007

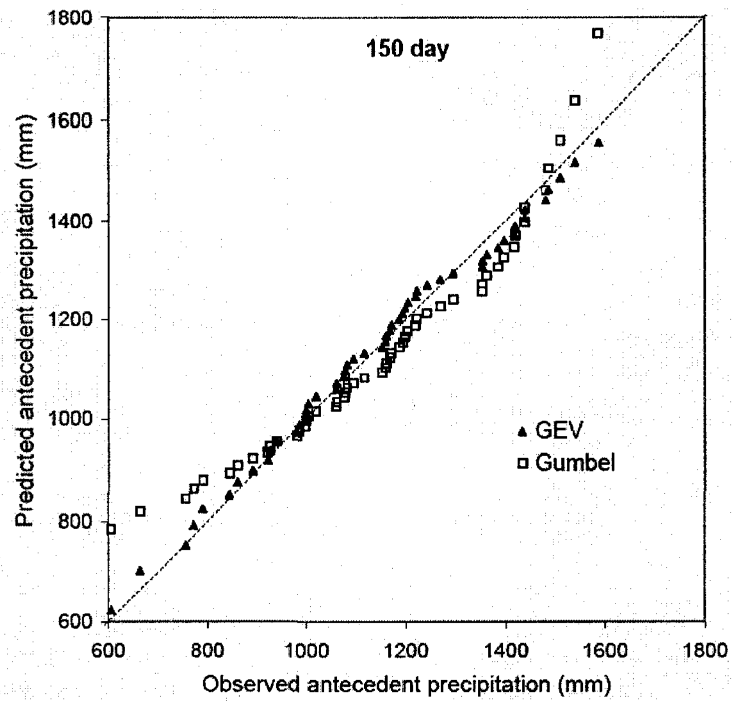

Figure 4.13 The Q-Q plot for the GEV and Gumbel distributions for the 150 day antecedent precipitation at Maple Ridge, BC between 1953 and 2007

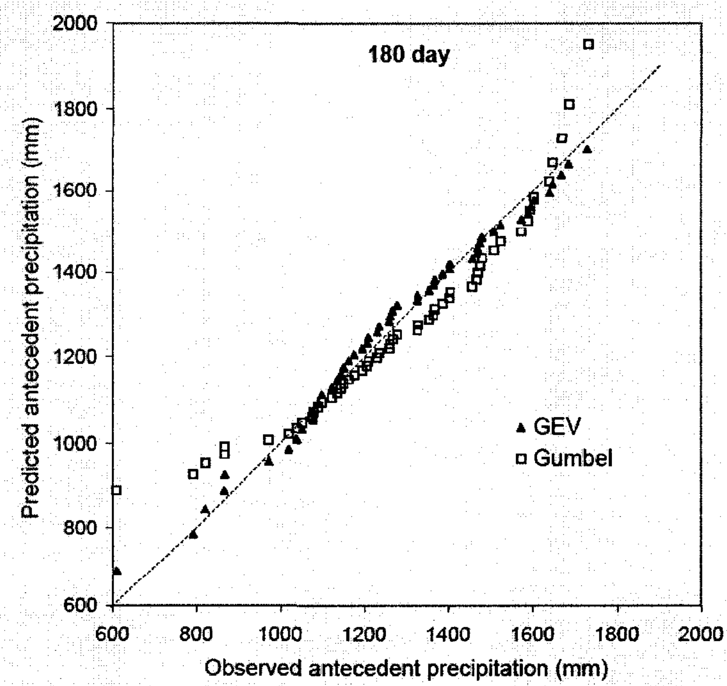

Figure 4.14 The Q-Q plot for the GEV and Gumbel distributions for the 180 day antecedent precipitation at Maple Ridge, BC between 1953 and 2007

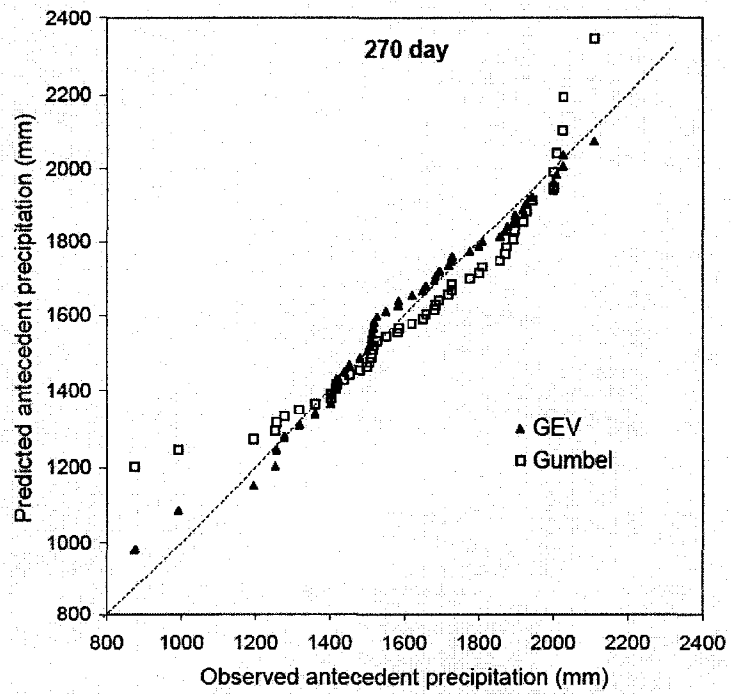

Figure 4.15 The Q-Q plot for the GEV and Gumbel distributions for the 270 day antecedent precipitation at Maple Ridge, BC between 1953 and 2007

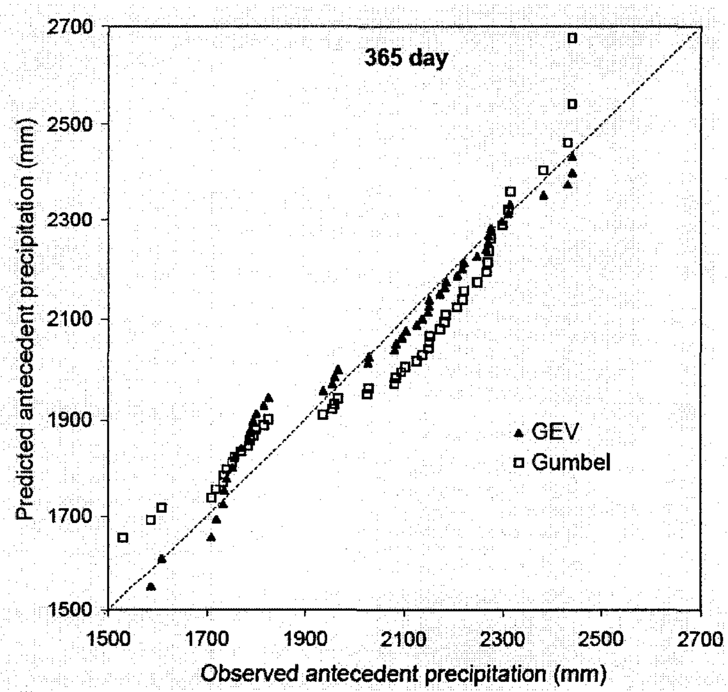

Figure 4.16 The Q-Q plot for the GEV and Gumbel distributions for the 365 day antecedent precipitation at Maple Ridge, BC between 1953 and 2007

equal to or better than the Gumbel distribution, especially for the longer antecedent durations, where the distribution tends to be upper bound limited.

As described later in Section 4.8.1.14 the Maple Ridge, BC precipitation record was compiled by using information from several weather stations to fill missing data and extend the duration of the continuous record. It may not always be possible to do this without introducing incompatible data. The stations at Maple Ridge, BC were within 10 km of each other, close to the same elevation, and had similar orographic influences on the precipitation received. The data from each weather station should be assessed separately and consideration given to if they can be combined based on the similarity of the frequency distributions of each data set.

4.2.5 Snow melt data analysis

Snowmelt plays a significant role in a number of landslides experienced by the railway and in one of the case studies in Appendix K. The snow accumulation and melt analysis will depend on snow-on-the-ground and snow-pillow information where it is available. The algorithms discussed in Section 3.3.2.2 can be used where necessary but will generally be avoided because of its dependence on data that is not commonly available. Wherever possible, antecedent durations will be adjusted to achieve the conditions of Case 1 of Section 3.3.2.2.

4.3 Other issues

4.3.1 Hydrologic modeling and surface flow erosion

Shi (2006) demonstrated the value of considering the drainage basin size in the assessment of hydrologic hazards and the influence of hydrologic hazards combined with high infiltration rates and their influence on slope stability conditions. This thesis takes an empirical approach to the relationship between precipitation and landslide hazard. As a result, basin analysis will be limited to the approximate assessments outlined in Section 4.3.2.

4.3.2 Determination of the drainage basin size

Drainage basin size can be assessed from available topographic maps and in many cases digital elevation models are available that can be analyzed within geographic information systems (GIS). The three dimensional visualization within Google Earth Pro (Google 2007) can be used to develop an assessment of the drainage basin size for use in this analysis.

4.3.3 Consideration of evaporation and transpiration

As discussed in Appendix B, Section 1.4 evaporation and transpiration are the two primary means be which moisture is returned to the atmosphere. However, the rate at which this process removes moisture from the ground is influenced by numerous factors including temperature, humidity, vegetation and others. The average loss of water due to evaporation and transpiration is assumed to be relatively constant over the longer antecedent durations considered. However, it could have a significant influence on short antecedent durations. For example the same antecedent precipitation occurring during (a) cool humid conditions, during a low pressure storm, over a few winter days winter, when vegetation is dormant, would be expected to result in more infiltration than (b) warm low humidity conditions, interrupted by a series of convective storms, over the same number of late spring days, when vegetation transpiration is at its greatest. As a result, the potential for precipitation induced landslides would be greater in scenario (a).

In most cases temperature, humidity and vegetation data are not available in the historic record or the available real time data to make it practical to incorporate this data into the assessment of the water balance. As a result, evaporation and transpiration are not considered in this thesis because the focus is on developing a functional system within the railway industry.

4.4 Description of case study

A case study should include the components listed below. Case studies should be selected based on the influence of a landslide or series of landslides and the impact on the railway. Once a landslide site has been selected, the existence and proximity of weather stations, with data representative of the time of the landslide(s) and meeting the conditions of Section 4.1.1, should be determined. Provided data from one or more weather station is available, the most representative weather stations should be selected. Then the Natural Hazard Incident Database (CP NHID) should be reviewed and all the possible precipitation induced landslides are extracted. The spatial limits of the landslides considered are determined by the proximity of the next nearest currently active representative weather station. This methodology is employed because, in a real time application, only those weather stations that are active will produce warnings based on the exceedance of index thresholds. There is usually no value in developing a threshold for a historic weather station that will not produce weather information in the future. However, there may be cases, where the absence of weather data will justify the re-deployment of a weather station. In this case the historic data could be used to determine the frequency of historic precipitation conditions. The frequency analysis would be used to evaluate the return period of current conditions.

Most of the following sections should be included in a case study:

1. Name of case study
2. General description and location
3. Railway operations
4. Topography
5. Local geology
6 Hydrology
7. General geotechnical conditions
8. Landslide characteristics
9. Landslide history
10. Stabilization efforts
11. Climate conditions
12. Weather data
13. Weather data analysis
14. Comparison of landslide history and antecedent precipitation
15. Safety margin and warning thresholds
16. Case study conclusions

It is suggested that consistent information be compiled for further case studies.

4.4.1 Name of case study

Landslides and derailments are almost always given a name based on the location (mileage) and the track subdivision (sub). The landslide name may also include the name of people involved in the landslide, or a nearby location.

4.4.2 General description and location

A general description of the landslide hazards and the location of the hazards will be provided. This will include the track mileage of the landslide(s).

It is important to understand a few subtleties of track mileage. When the railway was built more than 100 years ago track mileage markers were placed at one mile intervals. Over the course of time these markers have been moved and replaced either accidentally or on purpose. In some areas the track has been realigned but the mileage markers have not been shifted to account for these changes (except when major reroutes were undertaken such as the first Rogers Pass relocation in South Western British Columbia). Consequently, there are many long and short miles on the railway. Therefore, track mileage markers should be considered landmarks or reference point and not as an absolute distance scale.

In addition to the non-uniform spacing of mileage markers, additional errors are introduced during the reporting of landslide locations. Generally, a TMS will know their track well enough to identify a landslide location within about two tenths of a mile. As a result, there can be up to 320 m (0.2 miles) error in the location of a landslide. In addition, if a landslide is near a mile marker, or other feature with an assigned mileage, the TMS often assign the landslide the same mileage as the feature, despite the fact that the two are separated by hundreds of metres (several tenths of a mile). These errors were more prevalent in the past but still occur today. Since the mid 1990's accurate reporting and documentation of landslide locations has been emphasized both with the track maintenance personnel and with geotechnical engineers working for the railway.

As a result, the location of a landslide provided in the CP NHID is reliable to within a few hundred metres. Adjustments to some landslide locations have been made based on surveying, mapping, photographic documentation, references to nearby landmarks and aerial imagery, especially that available via Google Earth Pro (Google

2007). The latitudes and longitudes of most landslides are included in the CP NHID, an excerpt of which is included in Appendix E.

For brevity, CP has adopted a "Chop code" abbreviation for each subdivision name. Chop codes consist of the first four letters of the subdivision names consisting of one word, or the first two letters of the first two words for subdivision names consisting of more than one word. Mileage is also documented employing a standard format. Leading and trailing zeros (to the nearest 100^{th} of a km or mile) are used to ensure consistent alphabetic sorting. For example, a location at Mile 14.1 on the Cascade Subdivision in British Columbia is known as CASC 014.10. Similarly, a location at Mile 625.3 on the Freight Main Line in Pennsylvania is known as FRMA 625.30. This Chop code nomenclature is used throughout this thesis.

It is normal practice within the railway industry to refer to directions with respect to the orientation and running direction of the track. For a subdivision with the low mile in the east and the high mile in the west (as most are), "track north" would indicate the direction perpendicular to the track, to the right, when looking west, toward the higher mileages. If the track happens to be traveling north around a mountain range, track north would be geographic east. For clarity, directions will be differentiated by "geographic direction", relative to the compass directions and "track direction", relative to the running direction of the track.

4.4.3 Railway operations

The basic structure, number of tracks and the maximum operating track speed will be identified. The track speed is used in the risk evaluation of Section 5.0.

4.4.4 Topography

A description of the topography of each landslide and the surrounding area will be included. Copyright restrictions limit the re-publication of maps in this type of document, but generally, they should be included in a case study.

4.4.5 Local geology

The relevant local geology of each case study will be included. A discussion of how the geology pertains to the landslide activity and the influence of precipitation will be included.

4.4.6 Hydrology

A general description of the surface and subsurface drainage being directed to the landslides will be provided. The groundwater drainage area assessment will be based on an interpretation of known geologic and hydro-geologic conditions such as surface drainage density, soil type, and seepage points. The watershed or drainage area of each case study could be assessed using GIS techniques (Browning 2003) on available topographic data.

4.4.7 General geotechnical conditions

The general geotechnical conditions for each case study will be reviewed. References will be provided to publicly available geotechnical documentation of these landslides where available. Where it is relevant or unusual a description of the track structure will be included. This is of more significance where settlement due to bearing capacity failure contributes to the geotechnical hazard.

4.4.8 Landslide characteristics

Commentary on the causes and contributing factors influencing the landslide activity will be provided. Where available, information on landslide movement rates will be indicated.

4.4.9 Landslide history

The historic and active landslides will be extracted from the CP NHID and summarized for each case study. The CP database only includes those landslide episodes that resulted in one or more landslides reaching the track and being reported. Where landslides do not cause an accident or delay in rail traffic, the local TMS forces remove landslide debris and may or may not report the incident. As a result, the database is not entirely complete. The omission of these landslides does not influence the analysis because landslides that do not reach the track are not a hazard to the trains. However, this deficiency may result in an under representation of smaller landslides in the CP NHID.

4.4.10 Stabilization efforts

A description of stabilization methods and their success and service life will be included.

4.4.11 Climate conditions

The climatic zone of the landslide site and the precipitation conditions will be included in this section. The seasonal variation of precipitation and snow accumulation will be reviewed. The start and end of the annual precipitation cycle will be identified. Any larger scale climatic conditions that relate to this location will be discussed in this section. A description of the dominant vegetation will be included.

4.4.12 Weather data

The location, elevation, and period of weather station records will be included in a table in this section. The proximity of the weather stations to the landslides is calculated using the relationship:

$$d = \frac{2\pi r}{360}\cos^{-1}\left\{\begin{array}{l}\cos(a_1)\cos(b_1)\cos(a_2)\cos(b_2)+\\ \cos(a_1)\sin(b_1)\cos(a_2)\sin(b_2)+\\ \sin(a_1)\sin(a_2)\end{array}\right\}$$

Equation 4.7 (Math Forum 2007)

Where r is the radius of the earth (6371 km), a_1, and b_1 are the latitude and longitude the weather station and a_2 and b_2 are the latitude and longitude of the landslide location.

To distinguish which weather stations will provide the best record for the landslides the stations are ranked using an index calculated by dividing the length of record by the distance from the landsides. The weather station records with the higher ranks should be more applicable to the analysis of the precipitation at the landslide location than those with lower ranks because they are closer and or have longer periods of record.

4.4.13 Weather data analysis

A discussion of the results of the precipitation analysis will be included in each case study. This will include a review of the goodness-of-fit of the GEV distribution.

To improve the clarity of subsequent sections the following terminology and definitions will be used consistently throughout the discussion. Each term will be considered to define a domain with some type of transformation required to shift from one domain to the next. The "precipitation" domain is the combined rain and snow accumulating in a day. The "antecedent precipitation" domain indicates the precipitation has been summed over durations of two of more days. Therefore, summation is the transformation from the precipitation domain to the antecedent precipitation domain. The "probability" domain is the probability that a specific antecedent precipitation will be exceeded. As demonstrated in Section 4.2.4, once the appropriate parameters have been derived, the GEV distribution (Equation D.1) can be used to transform the various antecedent precipitation events into the probability domain. The "return period" domain is the expected time between or frequency of antecedent precipitation events of a specific magnitude. Return period is used because it provides an temporal representation of the probability of an event. Return period is the inverse of probability. The "intensity duration" domain (ID) is the precipitation or antecedent precipitation divided by the antecedent duration and plotted against the duration. Consistent with hydrologic practice (Chow et al. 1988), Caine (1980) and subsequent authors (Guzzetti et al. 2007) investigated precipitation induced landslides using intensity duration plots where intensity is expressed as the depth of precipitation occurring in a unit of time (usually mm per hour) and the duration in plotted in hours. This domain is commonly depicted on a log-log plot referred to as an intensity duration frequency (IDF) plot when the return period (frequency) of the precipitation is also provided. Within the hydrologic sciences, precipitation events plotted on an IDF plot are, or are treated as, continuous events of uninterrupted precipitation (although often they are discontinuous when sampled on an hourly frequency). As discussed in Section 4.2.2.2, the use of ID and IDF plots for the analysis of precipitation induced landslides does not assume or require a continuous or uninterrupted precipitation event and is the precipitation over any duration defined on the abscissa of an IDF or ID plot.

4.4.14 Comparison of landslide history and antecedent precipitation

For each landslide the rarest precipitation event, or the antecedent duration with the highest return period, is selected as the condition that induced the landslide. This is similar to the approach employed by Ko Ko et al. (2003). In cases where the rarest precipitation event is relatively common (has a low return period) the second rarest precipitation event is also selected and the combination of these events is considered to have induced the landslide.

The amount of landslide data available for the modified Chleborad method will also be discussed and if sufficient this will be applied.

4.4.15 Safety margin and warning thresholds

Safety margins need to be applied to each threshold to address uncertainty in the timing of the event, missing precipitation data, and response time of the railway. This will also ensure that a warning will be provided if similar, but not quite as severe conditions, occur that could induce landslides. Once a safety margin is applied to the determined antecedent precipitation threshold or determined return period threshold it will be referred to as an antecedent precipitation warning threshold, or return period warning threshold (or simply as a warning threshold where the threshold domain is implied).

Safety margins are best applied in the probability domain rather than the antecedent precipitation domain. This is because shifting the probability of the warning threshold value relative to the determined threshold in the probability domain will result in an equivalent probability shift being applied to each threshold. If the safety margin is applied in the precipitation domain, warning antecedent precipitation thresholds could result in a more or less severe return period decrease (or probability increase) being applied in one antecedent index versus another antecedent index. For example, if the determined threshold is to be reduced by 5% to derive the warning threshold this might result in a return period threshold dropping from 5 to 4 years (probability increase from 0.20 to 0.25). The same 5% reduction in the antecedent precipitation domain of a second index might result in the return period dropping from 5 to 4.5 years (probability increase from 0.2 to 0.22). By applying the safety margin in the probability domain a uniform increase in probability of the warning threshold can be assured for all indices. Using:

$$T_{(d)} = \frac{1}{P_{(d)}} \qquad \text{Equation 4.8}$$

and defining $T'_{(d)})$ as the warning return period

$$T'_{(d)} = \frac{1}{k_{sm}P} \qquad \text{Equation 4.9}$$

$$T'_{(d)} = \frac{T_{(d)}}{k_{sm}} \qquad \text{Equation 4.10}$$

The use of return period warning thresholds will introduce additional false-positive results but these should not be onerous provided they are infrequent. The inclusion of thresholds for the non-sensitive indices is also recommended to provide warning of rare events and the combination of rare events. Furthermore, it is considered prudent to include additional criteria based on the continuous threshold in the intensity duration domain, as per Caine (1980), to account for conditions that have not been experienced but have a high likelihood of causing a landslide.

4.4.16 Case study conclusions

Conclusions on the applicability of the GEV analysis, the sensitivity of the landslides to various antecedent precipitation durations, and appropriate thresholds is provided. The reliability of the combined indices is also reviewed.

4.5 Case study

The remainder of the section is a case study of the Maple Ridge area of BC. This area has relatively frequent precipitation induced landslides, has been studied by others, and has one of the highest densities of freight and passenger rail traffic within the CP network. Within the case study a description of the items listed in Section 4.4 is provided.

4.5.1 Cascade 102.50 to 104.90 Maple Ridge, BC - Landslides from 1780 to 2007

The landslides that occur along the CP track within the District of Maple Ridge in the Vancouver Lower Mainland of British Columbia are used as an example case study. These hazards affect several miles of track along the north side of the Fraser River.

The following section contains a description and analysis of these landslides using the reporting structure provided in Section 4.4.

4.5.2 General description and location

The Cascade Subdivision between miles 102.50 to 104.90 is a 5.4 km (3.4 miles) length of track located between the silt and clay bluffs of Maple Ridge, BC to the north and Fraser River to the south (Photos 4.1 and 4.2). A residential area of the District of Maple Ridge (DMR) is located on the top of the bluff. There are several streets and dozens of houses along the crest of the slope. River Road parallels the crest of the slope and several short streets, including Fir Street run perpendicular to the crest of the slope from River Road south towards the crest of the slope. These perpendicular streets are present towards the west end of the area.

This area is similar in land-use, geography, geology, climate, landslide activity, and railway hazards to three other areas. These other areas include those (a) studied by Chleborad (2000), Baum et al. (2005), Godt et al. (2006) and others near Seattle, Washington; (b) the south bank of the Fraser River traversed by CN below the Mount Lemon bluffs, 19 km (12 track miles) upstream of the CASC 102.50 to 104.90 location (Keegan 2007); and (c) a slope traversed by the BNSF on the west side of Surrey, BC. The limits of the CASC 102.50 to 104.90 area are the 1880 Haney Earth slide to the east and the Little Port Hammond Earth slide to the west. Due to concerns about the stability of the area and the hazard exposure of rail transportation and urban development, this area has been studied by numerous authors and groups on behalf of CP, the BC Ministry of Environment, and the District of Maple Ridge as referenced by Golder Associates Ltd. (2004).

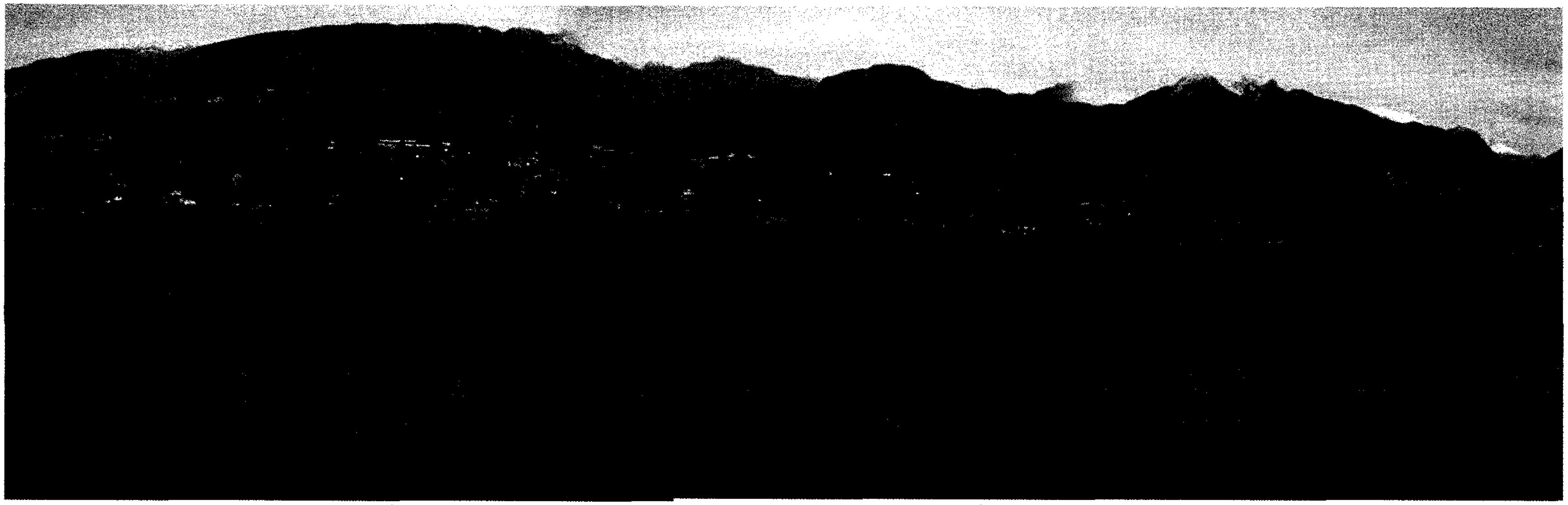

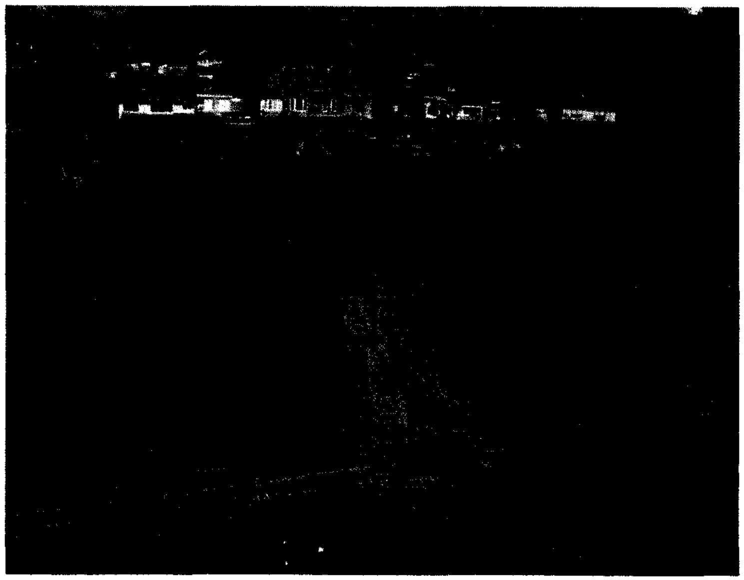

Photo 4.1 (above) Oblique aerial panorama of the Maple Ridge, BC bluffs between Mile 103.35 on the right and 104.1 on the left taken on March 25, 2007. Residential development occupies the top of the bluffs. The source of the March 24, 2007, CASC 103.30 above-track earth slide can be seen on the far right. A yellow excavator is clearing debris from the March 24, 2007 CASC 103.75 landslide on the far left.

Photo 4.2 (left). Oblique aerial view shows the March 24, 2007 CASC 103.35 earth slide in the middle right and the CASC 103.39 debris flow in the left of the photo. An intact island of soil and horizontal stratigraphy in the back-scarp can be seen in the CASC 103.35 earth slide. The narrow flow path of the CASC 103.39 debris flow from the crest of the slope to the track elevation is also visible.

Photos by Alastair Grogan

4.5.3 Railway operations

The track bed supports two tracks mounted on timber ties with a total width of 10 to 15 m depending on the curvature of the track. The track alignment is dominated by several long tangents with gentle curves. There are double tracks, to accommodate the unimpeded flow of east and west rail traffic.

Maximum track speed is 48 kmph (30 mph) for freight and 80 kmph (50 mph) for passenger rail service (Canadian Pacific Railway 2005). CP operates between 20 and 25 freight trains per day along this length of track. The West Coast Express (2008c) commuter transit rail service operates 10 trains per day on this track five days per week between Mission to the east and downtown Vancouver to the west.

4.5.4 Topography

The CASC 102.50 to 104.90 area is typified by a 10 to 30 m high bluff located on the north side of the Fraser River which flows west (Photos 4.1 and 4.2). The track is located 5 to 7 m above the high water mark of the river. Below the track, the slope down to the river is predominantly 30° with some 10 to 15 m long 45° sections. The track bed is on a 10 to 15 m wide bench developed from cuts and low fills. The original track profile indicates the cuts were up to 18 m high above base of rail and the fills extended up to 7 m below base of rail. The slope above the track is at slope angles up to 37° overall, with local 5 to 10 m high area with slopes of 45°. At the top of the steep slope next to the track the land slopes upwards at 1 to 2 degrees to the north.

4.5.5 Local geology

The local geology consists of horizontally interbedded Pleistocene glacio-marine silty clay and fine sand layers extending from below river level to within 5 to 10 m of the top of the slope above the track. Pleistocene glacial drift of gravel and sand are exposed along the top of the slope (Armstrong 1980). The silty clay and fine sand layers are thought to extend northward for 2 km or more until they lap onto colluvium, till, or bedrock along the toe of the mountains north of DMR.

4.5.6 Hydrology

The hydrology of the area is dominated by the Fraser River flowing west along the toe of the slope. Infiltration and runoff from within the urban development of the District of Maple Ridge to the north flow south to discharge into the Fraser River. The Alouette River flowing from East to West sub-parallel to the Fraser River forms the northern boundary of the hydraulic regime.

The river bank has been increasingly protected with angular boulders and cobbles (rip-rap) over the history of the railway in response to river erosion and below-track bank-erosion earth slides. Northwest Hydraulics (1979) completed a study for the BC Ministry of Environment documenting the placement of rip-rap protection in at least 5 locations. CP has subsequently placed additional rip-rap erosion protection at CASC 104.23 in 1999 and CASC 102.95 in 2007.

4.5.6.1 Surface drainage

The surface drainage from some areas of the terrace above and to the north of the track drain down three short (100 to 300 m long), well defined gullies from the top of the slope to the track. The flow from each defined gully is conveyed under the track in several culverts.

There is also a DMR storm sewer that conveys runoff from the urban development north of River Road under Fir Street and then down the slope. This storm sewer then goes under the track at CASC 103.99, and into the Fraser River. Despite the storm sewer at CASC 103.99 the capacity and network of urban storm water drainage is poorly developed and considered inadequate by CP. Most of the residential properties along the top of the slope have no means of conveying surface water off their property other than to discharge it into the ground or over the crest of the slope onto CP property. As with most urban development the residential development has reduced the vegetation and increased the peak surface water runoff flow rates, especially during intense rainfall and prolonged periods of precipitation. It is further possible that disturbance of the natural conditions within the DMR has increased infiltration into the Haney Clays.

4.5.6.2 Subsurface drainage

Following some of the landslides the back scarp of the landslides (Photo 4.3) demonstrates that horizontal flow within the fine sand conveys high pore pressures towards the slope and contributes to causing some of the landslides. These sand seams typically continue to discharge for several days following a landslide.

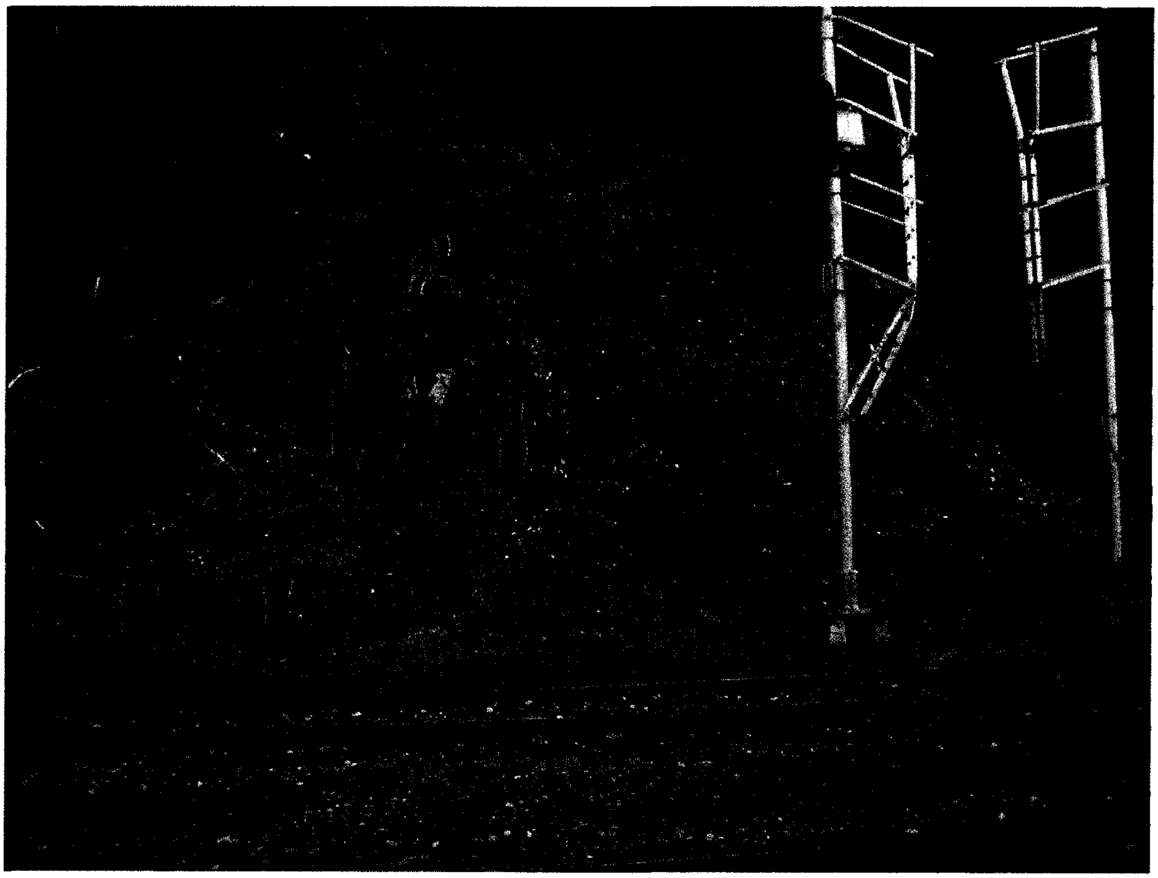

Photo 4.3 Photo is of CASC 103.41 following the March 24, 2007 earth slide at this location. The debris has been removed from the track. The flow from the interbedded silty clay and fine sand layers is illustrated by piping points at, below, and above the elevation of the black signal-light housing. The miniature alluvial fans of non-cohesive sand in the ditch to the left of the signal post are evidence of piping of the sand seams. Photo by Alastair Grogan

Drilling data has not been reviewed to assess the spatial extent of the groundwater basin, but based on the geomorphology of the area and the proximity of the Alouette River to the north, the total recharge area is 2 to 3 km^2. The recharge area of any one landslide would be a small portion of the total. It is possible that drainage from the mountain slopes above Maple Ridge, BC discharges into the aquifers discussed above.

4.5.7 General geotechnical conditions

Under dry conditions the slopes above and below the track are stable. However, during prolonged precipitation there have been 79 earth slides, debris slides, or earth flows recorded from the crest of the slope, mid slope above the track, and the slope below the track. Airphoto interpretation by Thurber Engineering Ltd. (Unpublished report by Cullum-Kenyon, C. and Gerath, R. F. 1998. Cascade sub, Mile 103 to 104.7, Maple Ridge Slope instability, Report to Canadian Pacific Railway File. No. 17-6-251, Thurber Engineering Ltd.) demonstrates that additional unrecorded landslides have occurred since 1938.

4.5.8 Landslide characteristics

There are four types of landslides in this area: (a) earth slide, (b) earth slide - earth flow, (c) debris slide - debris flow; and (d) bank erosion- earth slide events as classified by Keegan (2007).

Preparatory causes of the first three (a), (b) and (c) include the Quaternary glacial materials, contrast in permeability causing piping at the exposed face, and significant antecedent precipitation resulting in excess pore pressures often combined with intense precipitation. Over steepening, vegetation removal, and blocked and re-routed drainage by neighbouring property owners are additional anthropogenic preparatory processes that contribute to these earth slides. As will be demonstrated, the landslide activity is dependent on antecedent precipitation. Consistent with the experience in San Francisco (Cannon and Ellen 1985) and Seattle (Chleborad 2000, Baum et al. 2005, Godt et al. 2006), landslides are induced in the late fall and winter months by multi-day heavy precipitation that occurs after the soil has been saturated by the fall and winter rains. High-intensity, short-duration convective precipitation in the spring and fall months does not result in landslides, demonstrating the requirement for saturation of the soil prior to the landslides being induced. I hypothesize that pore pressures within the thinly bedded silt and sand layers increase to levels that reduce the effective stress on the failure surface, where the intact silts and sands contact the disturbed colluvium (Photo 4.3). The requirement for long term antecedent precipitation preceding the landslides suggests that groundwater recharge from a significant distance or through the low permeability silts clay soils contributes to causing the landslides.

Preparatory causes of the type (d) bank erosion - earth slides include the weak glacial soils, contrast in permeability resulting in subsurface drainage from a long distance, significant antecedent precipitation resulting in excess pore pressure and over steepening of the toe of the slope by river erosion.

4.5.9 Landslide history

The landslide history of this site is included in Table 4.3. There are a total of 79 landslides identified between CASC 102.50 and 104.90 over a period of 227 years. In the 32 years between 1975, when CP started maintaining more reliable records, to 2007 September, there have been at least 50 landslides in 20 episodes. On average, there is one landslide episode every 1.6 years. Multiple landslide episodes have occurred in the same winter such that in the last 32 years there have been 13 winters with landsides (one landslide-prone winter every 2.5 years).

The CP NHID only includes those landslide episodes that were recorded. In this area landslides below the track may go unreported because they do not immediately influence the safety of the track where the shoulder of the track bed is wide. Above-track earth and debris slides that do not reach the track and or ditch may also go unrecorded. If one landslide influences the track safety a geotechnical engineer is commonly dispatched and they will often identify additional landslides not observed or reported by the TMF. As a result, the CP NHID for the CASC 102.50 to 104.90 area should not be considered complete. However, the major incidents should all be represented in the period 1975 to 2007.

In the 1975 to 2007 period there have been two train accidents where a moving train has impacted and/or been derailed after impacting debris across the track. There has been one derailment due to a sub-grade earth slide in the same period. Therefore, there has been one train accident every 10.6 years or one accident per 4 wet winters.

It is clear from the geotechnical assessments of the landslides that the grading and surface water management practices of the residential properties at the crest of the slope has significantly influenced the earth slide - earth flow, debris slide - debris flow preparatory causes. In numerous cases the landslides have originated in fill material at the crest of the slope (Photo 4.2). Yard waste and garbage have been found in the landslide debris. The removal of vegetation to improve the view from the residences may also increase the amount of organic debris on the slope, decrease uptake of surface water, and reduce the stabilization of the shallow soils by the vegetation root mat. In several cases subsurface drainage pipes have been identified in the back-scarps of the landslides, discharging water into the soil mass before, during, and after the landslide was induced. CP continues to work with the DMR and individual landowners to improve drainage and slope stability conditions in this area.

4.5.10 Stabilization efforts

Stabilization efforts undertaken by CP in this area have been numerous. Prior to 1960 a timber pile and lagging wall had been installed along the up-slope side of the ditch to support the slope immediately above the ditch.

In the late 1960's a 2 to 4 m deep trench drain was developed along the up-slope ditch of the track between CASC 103.60 and 104.00 to improve drainage and attempt to reduce suspected artesian pore pressure in the slope above a below-track bank erosion - earth slide (Cook, P.M. 1968. Haney Slides near Mile 103.5 Cascade sub March 29, 1968. Paul M. Cook P. Eng. Vancouver, BC.). Rip-rap erosion protection was also placed along the river shore. These two measures have been effective.

In 1997 shallow inclined sub-horizontal drains were drilled into the slope between CASC 103.30 and 103.50 to attempt to drain the slope internally by intersecting the more permeable sediments and to reduce pore pressures. These drains have been effective in draining groundwater from the subsurface and flow year round. However, subsequent shallow landslides above the drains demonstrate the limited utility of this measure. It is assumed that the drains do not provide adequate drainage or do not intersect all the confined aquifers in the sand layers.

Numerous areas of the shoreline (within the tidal zone) have been armoured with erosion protection in response to erosion and landsliding (Northwest Hydraulic Consultant 1987). This appears to be relatively successful with remobilization of previous slides being unusual.

Table 4.3 Landslides on the between CASC 102.50 and 104.90, Maple Ridge, BC. Train accidents and derailments are emphasized by **bold** text.

Ref. No.	Mileage	Date	Volume	Name/comments
1	104.35	1790's	1.3 million m^3 earth slide above and below the current level of the track	Port Hammond Earth slide
2	103.0	1880-Jan-30	1.5 million m^3 earth slide above and below the track	Haney Earth slide
3	104.60	1904 to 1929	300,000 m^3 earth slide above the track	Minor Port Hammond Earth slide
4	103.92	1904 to 1929	80,000 m^3 earth slide above the track	Fir Street earth slide
5	103.31 to 103.91	1937 and 1938	22,000 m^3 in eighteen landslides from above the track	Based on air photo interpretation[1]
6	103.31 to 103.57	1952 and 1953	1,800 m^3 in six landslides from above the track	Based on air photo interpretation[1]
7	103.5 and 103.9	1975-Dec to 1976-Mar	7600 m^3 in two landslides above the track and one 7000 m3 bank erosion - earth slide below the track	Maple Ridge landslides
8	104.27	1977-Jan-19	1,200 m^3 bank erosion - earth slide below the track	Fraser River bank erosion - earth slide
9	103.51 104.25	1980-Dec to 1981-Mar	2,100 m^3 in six landslides above the track	Maple Ridge landslides
10	102.95	1981-May-3	1,000 m^3 bank erosion - earth slide below the track	Port Haney Station bank erosion - earth slide and **derailment**
11	102.95	1985-Mar-1	1,000 m^3 reactivation of bank erosion - earth slide below the track	Port Haney Station bank erosion - earth slide
12	104.57	1995-Nov	600 m^3 bank erosion - earth slide below the track	Fraser River bank erosion - earth slide
13	104.50	1996-Jan-16	70 m^3 debris slide above the track	Maple Ridge landslides

Table 4.3 Landslides on the between CASC 102.50 and 104.90, Maple Ridge, BC.
Train accidents and derailments are emphasized by **bold** text.

Ref. No.	Mileage	Date	Volume	Name/comments
14	103.32 to 103.80	1997-Jan-29	450 m^3 in four landslides above the track	Maple Ridge landslides
15	103.39 to 104.30	1997-Mar-18 and 19	2,600 m^3 in six landslides above the track	Maple Ridge landslides and **train accident**
16	102.95	1999-Jan	1,000 m^3 reactivation of bank erosion - earth slide below the track	Port Haney Station bank erosion - earth slide
17	104.23	1999-Jan-14	4,000 m^3 bank erosion - earth slide below the track	Fraser River erosion bank erosion - earth slide
18	103.75	1999-Dec-21	50 m^3 debris slide from above the track	Maple Ridge landslides
19	103.80	2000-Jan	20 m^3 debris slide from above the track	Maple Ridge landslides
20	102.95	2001-May	500 m^3 reactivation of landslide below the track	Port Haney Station bank erosion - earth slide
21	104.50	2003-Nov-28	100 m^3 debris slide from above the track	Maple Ridge landslides
22	103.39 to 104.3	2005-Jan-20	300 m^3 in six landslides from above the track	Maple Ridge landslides
23	103.41	2007-Mar-11	80 m^3 debris slide from above the track	Maple Ridge landslides
24	103.20 to 104.20	2007-March-24	2,850 m^3 in fifteen landslides from above and one 2,000 m^3 bank erosion - earth slide below the track	Maple Ridge landslides and Fraser River erosion landslides
25	103.81	2007-Mar-25	500 m^3 debris slide from above the track	Maple Ridge landslides and **derailment**
26	102.95	2007-May	400 m^3 reactivation of bank erosion - earth slide	Port Haney Station bank erosion - earth slide

[1] - Unpublished report - Thurber Engineering Ltd 1998. Cascade sub, Mile 103 to 104.7, Maple Ridge Slope instability. Report to Canadian Pacific Railway File. No. 17-6-251

4.5.11 Climate conditions

This case study area is within the temperate oceanic climatic zone. Harry and Wright (1957), Bruce (1961) and Schaefer (1973) describe the climate and rainfall of nearby Vancouver and the surrounding Fraser Valley. The precipitation in this area is dominated by coastal low-pressure systems that bring repetitive and prolonged precipitation to the area through the winter months. Annual precipitation averages 1,855 mm. Snowfall is limited to one to two events per year, accounting for 38 mm (about 2%) of the annual precipitation. Typically, the snow has a high water content and the temperate conditions result in rapid melting. Due to the heavy rainfall and moderate average monthly temperatures of 0° to 20° C the area has a positive moisture balance and therefore surface runoff is present.

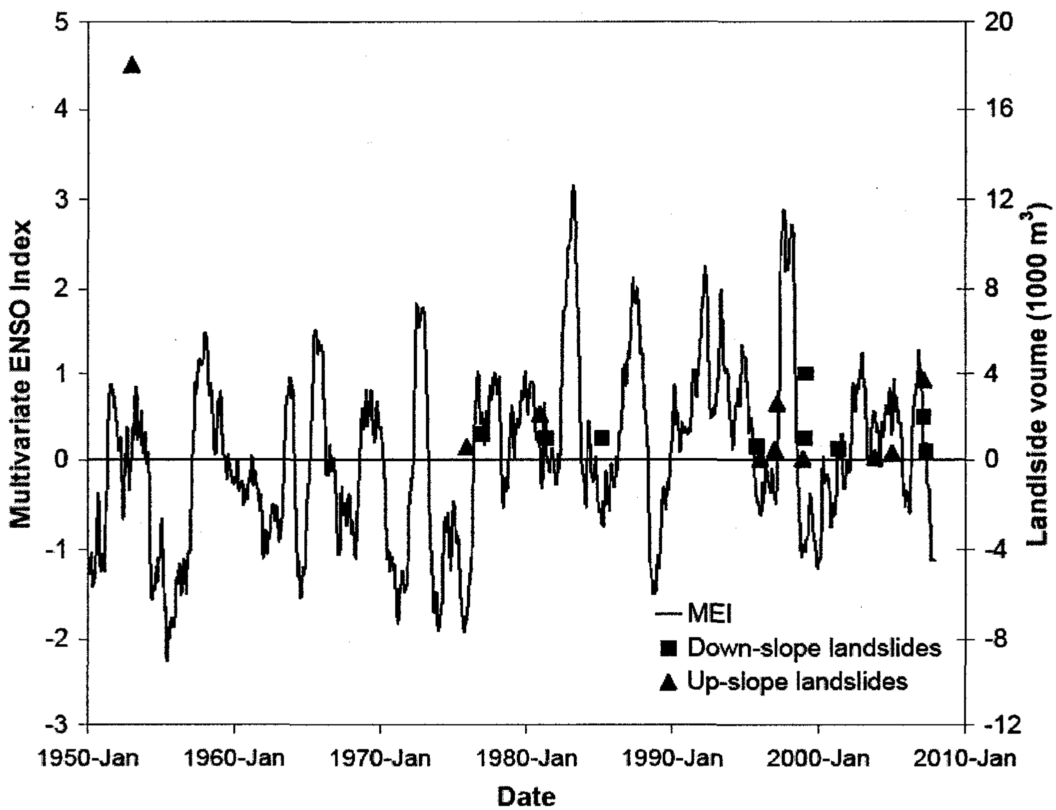

Figure 4.17 Multivariate ENSO Index from Wolter and Timlin (2008) and above and below track landslide activity at Maple Ridge, BC.

With the exception of the 1880 Haney landslide snow melt has not been correlated with any of the periods of landslide activity (Golder Associates Ltd. 1979). As shown in Figure 4.17 there is no apparent correlation of the timing or magnitude of landslides at this site and the Multivariate El Nino Southern Oscillation (ENSO) index (MEI) proposed by Wolter and Timlin (2008). This may suggest that La Nina events are worth investigating since La Nina is not correlated with El Nino.

4.5.12 Weather data

There are a number of weather stations within a few kilometres of the CASC 102.50 to 104.90 landslide area. These are listed in Table 4.4. The rank is included in the second to last column of Table 4.4. Of the nearby weather stations Haney East, Pitt Meadows CS (Campbell Scientific), Haney, Pitt Meadows Lougheed Highway, Fort Langley, and Pitt Meadows STP (Sewage Treatment Plant) rank highest and are representative of the CASC 102.50 to 104.90 landslide area, or include missing data in the highest ranked stations. The Pitt Meadows CS and Haney East form the majority of the combined data having the longest duration and being equal distance east and west of the landslides. The Pitt Meadow STP site was used to cover missing data in the Haney East record.

There are two issues that limit the use of other station data: the short duration of record, and the elevation of the station. Most of the other stations are in the second category. Stations, including Haney UBC RF Admin (University of British Columbia Research Forest Administration), Haney UBC RF Marc, and Haney Corrl Instn (Correctional Institution) were not used despite having longer records because they are higher up the slope of the mountains to the north of Maple Ridge, BC and therefore receive significantly more orographic precipitation than the lower elevation area of CASC 102.50 to 104.90. Two additional, more distant stations, Ladner and New Westminster are included in Table 4.4 because they are the only ones with data from the period of the largest landslide.

Table 4.4 Environment Canada weather stations near Cascade sub, miles 102.50 to 104.90. The stations used are shown in bold.

Weather station name	Latitude (degrees)	Longitude (degrees)	Elev-ation (m)	EC Station No.	Start or record	End of record	Length of record (years)	Distance from slide (km)	Rank (record/distance) (years/km)	Internet Station Id. No.
MAPLE RIDGE STP	49.22	-122.63	6.1	110D90K	1974-Apr-01	1974-Jun-01	0.2	1.0	0.2	674
FORT LANGLEY	**49.20**	**-122.62**	**6.1**	**1102910**	**1953-Mar-01**	**1956-Jul-01**	**3.3**	**1.5**	**2.2**	**770**
HANEY	**49.22**	**-122.60**	**25.9**	**1103322**	**1958-Feb-01**	**1962-Dec-01**	**4.8**	**1.6**	**3.0**	**771**
MAPLE RIDGE	49.23	-122.62	23.0		1973-Jan-01	1977-Dec-01	4.9	1.8	2.7	804
HANEY EAST	**49.20**	**-122.57**	**30.5**	**1103326**	**1956-Apr-01**	**2005-Feb-28**	**48.9**	**3.9**	**12.5**	**773**
HANEY 532	49.25	-122.62	3.0	1103327	1967-Mar-01	1970-Jul-01	3.4	4.0	0.8	
LANGLEY 96 AVENUE	49.18	-122.60	13.0	1104569	1987-Jun-01	1987-Oct-31	0.4	4.0	0.1	
PITT MEADOWS STP	**49.22**	**-122.68**	**4.9**	**110FAG9**	**1974-Apr-01**	**1993-Oct-31**	**19.6**	**4.4**	**4.4**	**682**
PITT MEADOWS CS	**49.20**	**-122.68**	**5.0**	**1106178**	**1994-Feb-01**	**2007-Aug-31**	**13.6**	**4.6**	**2.9**	**6830**

Table 4.4 Environment Canada weather stations near Cascade sub, miles 102.50 to 104.90. The stations used are shown in bold.

Weather station name	Latitude	Longitude	Elev-ation	EC Station No.	Start or record	End of record	Length of record	Distance from slide	Rank (record/ distance)	Internet Station Id. No.
	(degrees)	(degrees)	(m)				(years)	(km)	(years/ km)	
PITT MEADOWS LOUGHEED	**49.23**	**-122.68**	**6.1**	**1106179**	**1960-Feb-01**	**1969-Jun-01**	**9.3**	**4.7**	**1.9**	**841**
LANGLEY	49.17	-122.67	N.A.	1104551	1939-Mar-01	1940-Dec-01	1.8	6.1	0.3	
HANEY UBC RF ADMIN	49.27	-122.57	147	1103332	1961-Oct-01	2007-Sep-01	46.0	7.2	6.4	776
PITT MEADOWS A	49.22	-122.72	3.4	1106177	1959-Sep-01	1960-Aug-01	0.9	7.3	0.1	
HANEY MICROWAVE	49.20	-122.52	N.A.	1103328	1963-Nov-01	1984-Apr-30	20.5	7.4	2.8	Not avail
LANGLEY PRAIRIE	49.15	-122.65	86.9	1104560	1953-Mar-01	1964-Mar-01	11.0	7.43	1.5	
LANGLEY	49.18	-122.53		1104550	1878-Jan-01	1900-Oct-01	22.0	7.5	2.9	
HANEY UBC RF MARC	49.28	-122.58	114.3	110CCCC	1945-Aug-01	1972-Jul-01	26.9	7.9	3.4	672
LANGLEY RIVER ROAD	49.17	-122.53	N.A.	1104562	1987-Jun-01	1988-May-01	0.9	8.2	0.1	
PITT MEADOWS ALOUETTE RIVER	49.28	-122.67	6.0	110FJPP	1986-Oct-01	1992-Oct-31	6.1	8.2	0.7	

Table 4.4 Environment Canada weather stations near Cascade sub, miles 102.50 to 104.90. The stations used are shown in bold.

Weather station name	Latitude (degrees)	Longitude (degrees)	Elev-ation (m)	EC Station No.	Start or record	End of record	Length of record (years)	Distance from slide (km)	Rank (record/distance) (years/km)	Internet Station Id. No.
HANEY CORRL INSTN	49.25	-122.52	141.7	1103324	1960-May-01	1981-Apr-01	20.9	8.3	2.5	772
LADNER	49.0833	-123.0667	9.1	1104468	1878-Jan-01	1934-Dec-31	57	35.0	1.6	789
NEW WEST-MINSTER	49.2167	-122.9333	118.9	1105550	1874-Jan-01	1966-Dec-01	93	22.2	4.2	812

4.5.13 Weather data analysis

The data primarily from Haney East and Pitt Meadows CS were combined using the reciprocal distance squared formula (Equation 3.2) to calculate the estimated precipitation at the landslides. As per Appendix F and based on the average annual conditions at Haney East (Figure 4.18) the driest part of the year is August. Therefore the annual series is extracted using September 1 and August 31 and the start and end of the year.

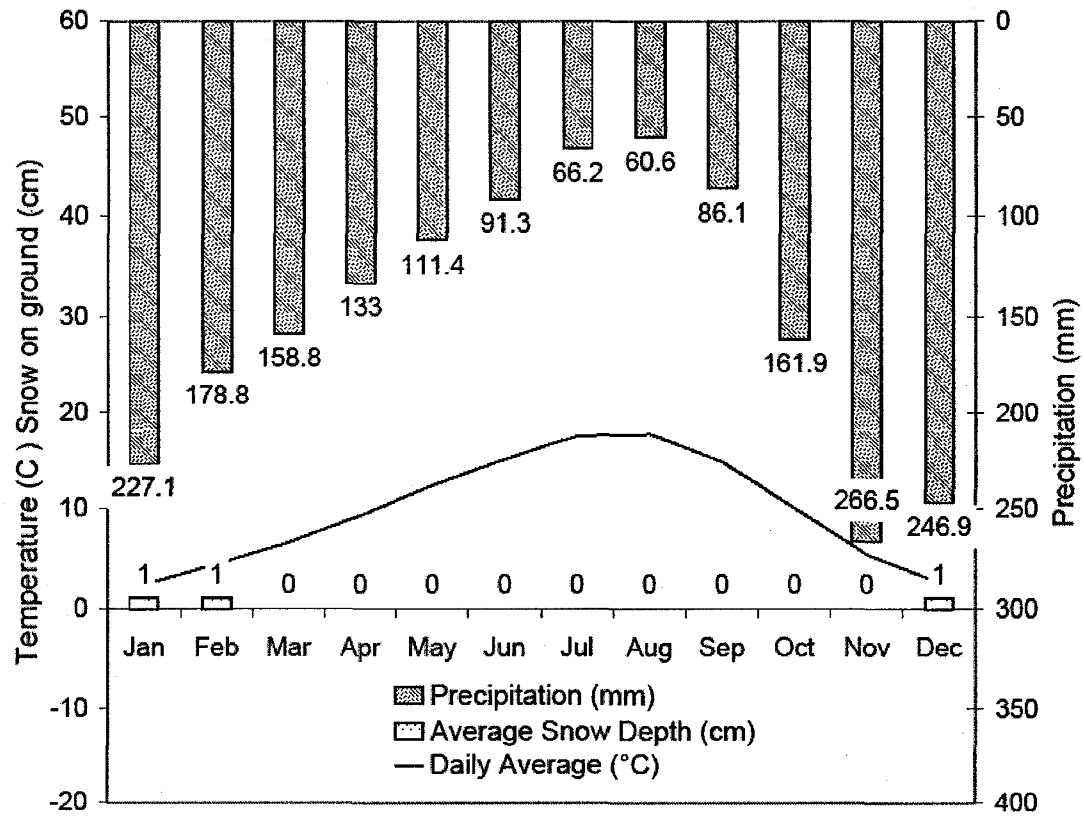

Figure 4.18 Climate for 1971-2000 for Haney East (Environment Canada 2006a)

The data were assembled, combined, and summed for 1 day and multi-day antecedent durations.

4.5.13.1 Modified Chleborad antecedent precipitation analysis

The landslides listed in Table 4.5 have been selected from the Table 4.3 for use in the Modified Chleborad analysis. Only landsides that have high confidence dates are included in Table 4.5.

Table 4.5 Landslides considered in the modified Chleborad analysis for the period of record 1975 January to 2007 September 1

Ref no.	Mileage	Date	Type	No. of L[1]	Volume (m^3)
10	102.95	1981-Apr-23 or 1981-May-3	Bank erosion - earth slide	1	1000
12	104.57	1995-Nov-29	Bank erosion - earth slide	1	600
14	103.32 to 103.80	1997-Jan-29	Debris or earth slide - above track	4	450
15	103.39 to 104.3	1997-Mar-18	Debris or earth slide - above track	5	2600
15a	103.3	1997-Mar-19	Debris or earth slide - above track	1	75
17	104.23	1999-Jan-14	Bank erosion - earth slide	1	4000
18	103.75	1999-Dec-21	Debris or earth slide - above track	1	50
21	104.5	2003-Nov-28	Debris or earth slide - above track	1	100
22	103.39 to 104.3	2005-Jan-20	Debris or earth slide - above track	6	300
23	103.41	2007-Mar-11	Debris or earth slide - above track	1	80
24	103.20 to 104.20	2007-Mar-24	Debris or earth slide - above track	15	3000
25	103.81	2007-Mar-25	Debris or earth slide - above track	1	500

[1] L = Landslides

The methodology described in Appendix H is used to determine the antecedent durations to which the Maple Ridge, BC landslides listed in Table 4.5 are most sensitive. Based on the analysis in Appendix H the Maple Ridge, BC landslides are most sensitive to the 4, 21 and 150 day antecedent precipitation. Using the data from Maple Ridge, BC the following plots can be produced consistent with the Chleborad (2000) plots. Appling the conclusion of Cannon and Ellen (1985), Keefer et al. (1987) and Wilson et al. (1993) and others the threshold in the $A_{(c\text{-}d)}$ and $A_{((d+1)\text{-}e)}$ graphs is set steeply sloping to the y at low longer-antecedent precipitations as shown in the Figures 4.19, 4.20 and 4.21.

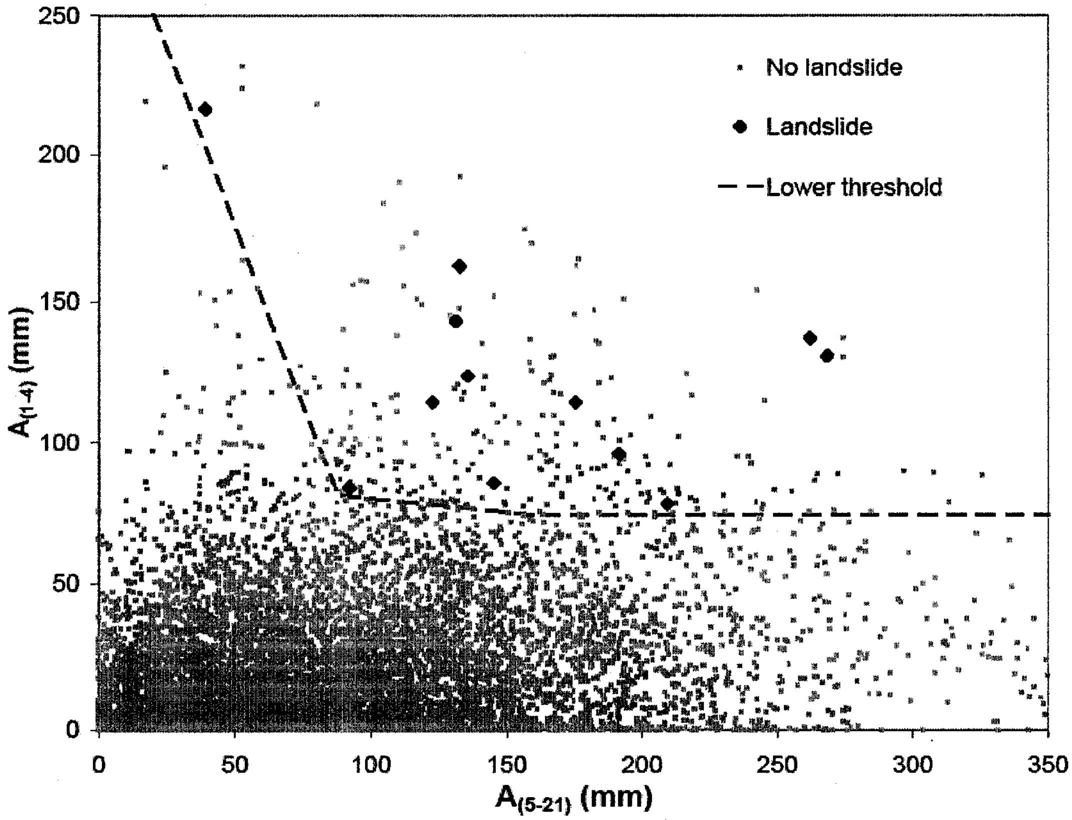

Figure 4.19 1975 January to 2007 September precipitation data for the $A_{(1\text{-}4)}$ versus $A_{(5\text{-}21)}$ for Maple Ridge, BC with lower PIL threshold added.

The plots include a tri-linear lower threshold consistent with the bi-linear threshold proposed by Chleborad. The portion sub-parallel with the y-axis is included because no landslides in the Maple Ridge have been induced by high intensity rainfall without previous elevated longer duration antecedent precipitation. The thresholds have been established such that 100% of the accurately dated landslides are above the thresholds. Consistent with the GEV Antecedent Precipitation Induced Landslide Return Period Analysis (GEV APIL RPA) method the Chleborad method provides warning of landslides 12 and 17 which are below-track earth slides.

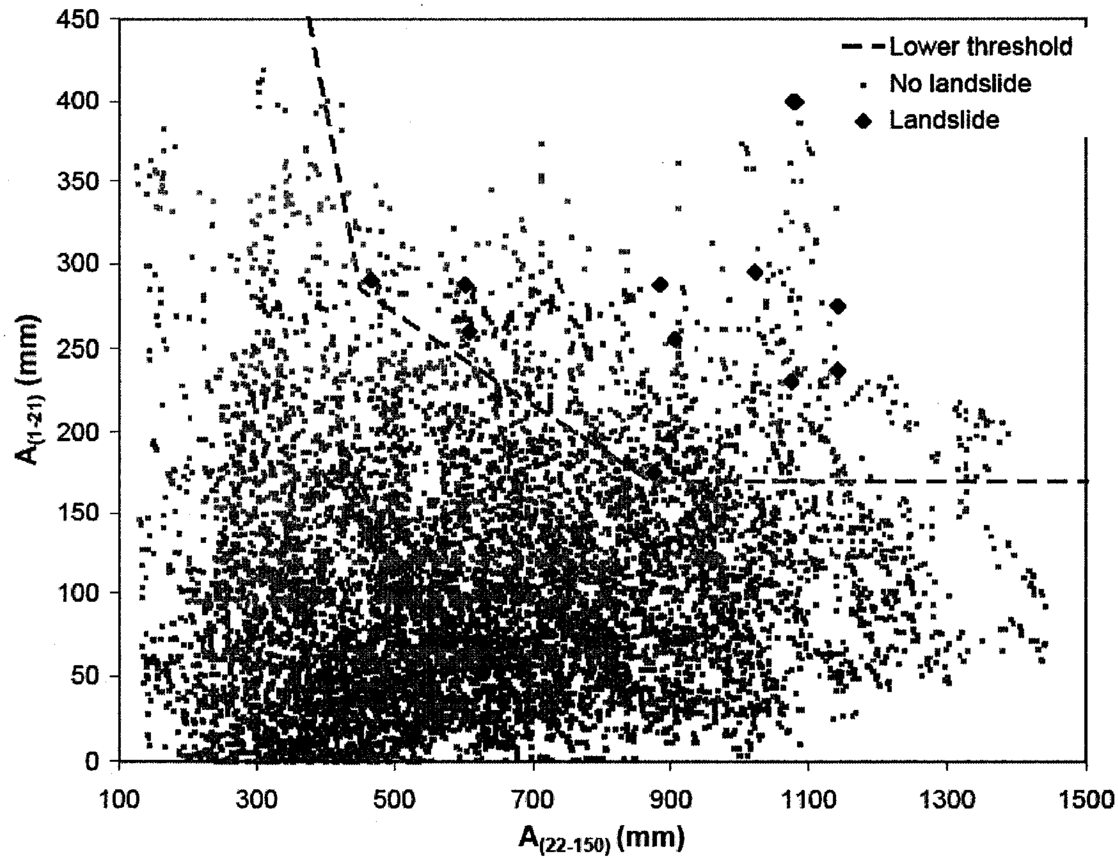

Figure 4.20 1975 January to 2007 September precipitation data for the $A_{(1\text{-}21)}$ versus $A_{(22\text{-}150)}$ for Maple Ridge, BC with lower PIL threshold added

To assess the effectiveness of the Chleborad method the number of days with antecedent precipitation above the threshold is compared to the number of days with landslides and the total of number of days in the period of record. Table 4.6 contains a summary of these comparisons. There are 11931 days between 1975 January and 2007 September 1 and there have been landslides on 12 of these days.

As can be seen the criteria that include the $A_{(1\text{-}4)}$ data result in the few number of days above the thresholds indicating a strong relationship between landsliding and short term antecedent conditions. The low number of days with rain above the combined $A_{(1\text{-}4)}$ and $A_{(5\text{-}150)}$ threshold indicates a strong dependence on longer term antecedent conditons. As will be seen in the following section this is consistent with the GEV APIL RPA. Combining all three criteria results in a 1.0% false-positive outcome or

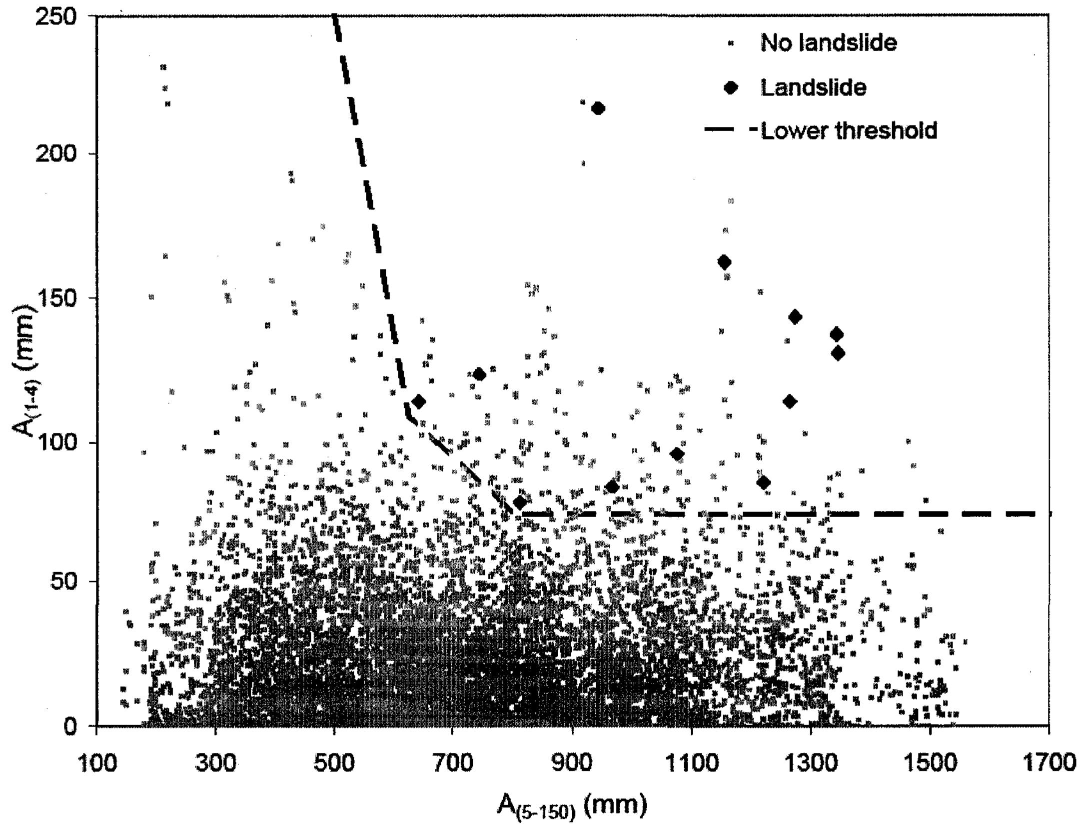

Figure 4.21 1975 January to 2007 September precipitation data for the $A_{(1-4)}$ versus $A_{(5-150)}$ for Maple Ridge, BC with lower PIL threshold added

Table 4.6 Days with precipitation above the lower PIL thresholds shown and the percent of false-positives

Figure Number	X axis	Y-axis	Days of rain above lower threshold	False-positives	
				Ratio	Percent
4.19	$A_{(5-21)}$	$A_{(1-4)}$	259	247/11,931	2.0
4.20	$A_{(22-150)}$	$A_{(1-21)}$	827	815/11,931	6.8
4.21	$A_{(5-150)}$	$A_{(1-4)}$	205	193/11,931	1.6
All			133	121/11,931	1.0
Figure 4.19, and Figure 4.21			148	136/11,931	1.1

3.7 days per year on average. Combing the $A_{(1-4)}/A_{(5-21)}$, and $A_{(1-4)}/A_{(5-150)}$ thresholds results in 1.1 false-positive result.

Table 4.7 Performance of the warnings based on the modified Chleborad method PIL thresholds for the Maple Ridge, BC 1975 to 2007 precipitation and dated landslide data

	Landslide **occurs**	Landslide does **not occur**
Landslide warning **issued**	0.1% (true-positive)	1.0% (false-positive)
Landslide warning **not issued**	0% (false-negative)	98.9% (true-negative)

In conclusion, the modified Chleborad method requires a means of identifying which antecedent precipitation durations a given set of landslides is sensitive to. This has been provided (Appendix H). However, the process of identifying which antecedent duration the landslides are induced by is dependent on having a relatively large number of landslide and date information. In addition, there are still a number of steps that require non codified judgment including the definition of thresholds. When fewer landslides are available the correlation of the maximum annual series and the antecedent precipitation on the day of the landslide used in Appendix H becomes unreliable. However, the antecedent durations identified as being the most sensitive in from the GEV APIL RPA could be used to assist the Chleborad method.

4.5.13.2 GEV antecedent precipitation induced landslide return period analysis

The generalized extreme value (GEV), Antecedent Precipitation Induced Landslide, Return Period Analysis (GEV APIL RPA) is undertaken for the Maple Ridge, BC landslides in this section.

The return period of antecedent precipitation was calculated for each antecedent duration using the method included in Appendix F and the GEV distribution procedure in Appendix I to produce the GEV location, scale and shape parameters for each antecedent duration as summarized in Table 4.5. The goodness-of-fit of the GEV distributions was checked using the methods provided in Appendix J and Section 4.2.4. The three parameters were then used to calculate the predicted antecedent conditions at various return periods. The results are plotted in Figure 4.19.

Table 4.8 GEV parameters for 1952 to 2007 Maple Ridge, BC, precipitation data

GEV parameters		**Location, $\hat{\mu}$ (mm)**	**Scale, $\hat{\sigma}$ (mm^{-1})**	**Shape, $\hat{k}$**
Antecedent duration (days)	1	60.6	14.5	-0.0984
	3	105.6	28.7	0.0370
	7	157.7	34.4	0.0403
	15	230.0	56.5	0.2820
	30	344.8	74.9	0.3157
	60	552.0	129.8	0.3082
	90	742.1	182.6	0.3801
	120	912.6	208.7	0.3371
	150	1076.8	244.8	0.4092
	180	1211.7	270.7	0.4637
	270	1552.6	293.6	0.4792

Comparison of Figures 4.1 and 4.22 again demonstrates how much better the GEV distribution fits the data than the Gumbel distribution. This is most evident for the estimates of the higher return period and higher antecedent durations.

4.5.14 Comparison of landside history and the antecedent precipitation

The comparison between the landslides with known dates and the coincident weather conditions in completed in a number of tables in this section. The next two sub-sections, 4.5.14.1 and 4.5.14.2 investigate the temporal coincidence of landslides and the return period of the various antecedent precipitation durations.

4.5.14.1 Review of severe precipitation events

Initially the most extreme conditions are assessed for each return period to see if any obvious correlations between the landslide activity and precipitation is apparent. Table 4.9 contains the first and second most extreme return periods for each antecedent duration. As described in the List of variables, $T_{(d)}$ is used as an abbreviation for the return period of the antecedent duration d days long.

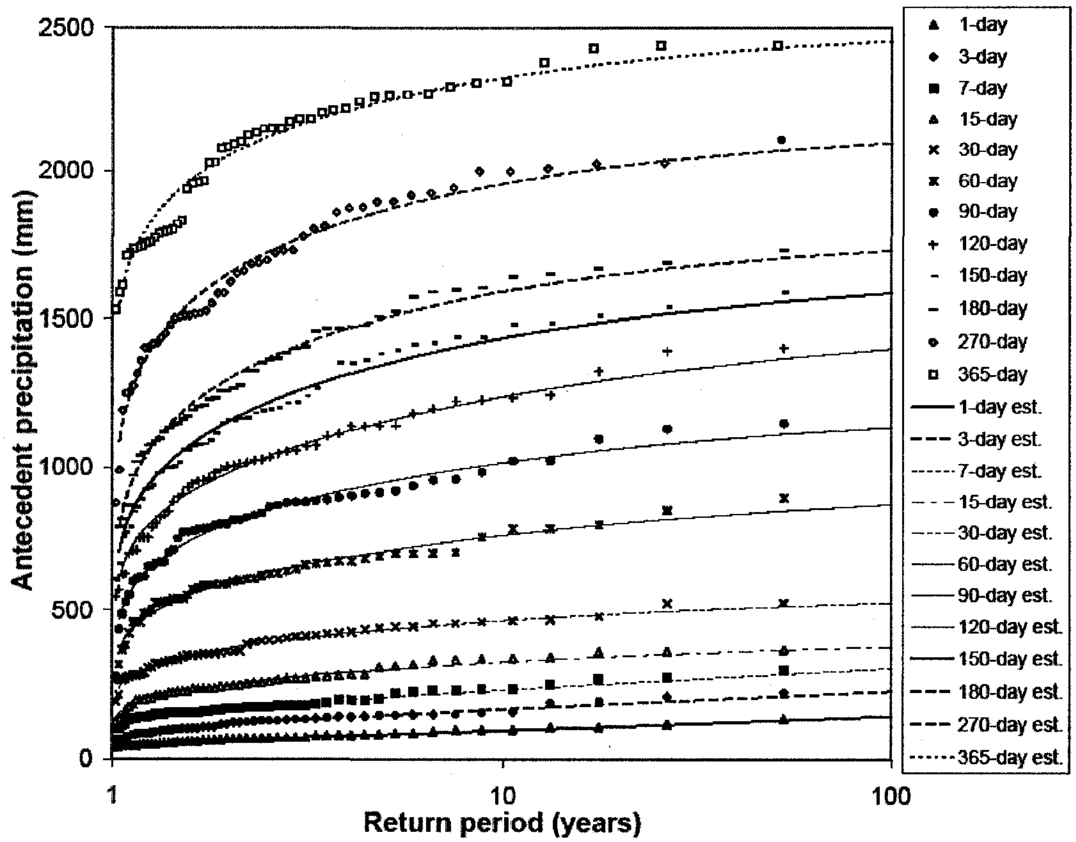

Figure 4.22 GEV distribution for Maple Ridge, BC precipitation data between 1953 and 2007. The markers are the recorded antecedent precipitations. The lines are the GEV distribution prediction of the antecedent precipitation.

For the longer antecedent duration indices the second rarest event will commonly be within a few days of the rarest event. As a result, the second rarest return period is not necessarily considered the second highest rarest antecedent precipitation. For this summary the second rarest return period must be at least one antecedent duration from the rarest return period.

Table 4.9 Highest return period antecedent precipitation events and most relevant landslide activity

Index	Date of rarest period	Preceding and subsequent landslide activity	Date of 2nd rarest period	Most relevant landslide activity
$T_{(1)}$	2003-Oct-08	No landslides until 2003-Nov-28	2007-Mar-11	80 m^3 debris flow on 2007-Mar-11. Fourteen landslides late in March 2007
$T_{(3)}$	2003-Oct-17	No landslides until 2003-Nov-28	1968-Jan-20	No landslides recorded but records incomplete
$T_{(7)}$	2003-Oct-21	No landslides recorded until 2003-Nov-28	1979-Dec-18	No landslides recorded
$T_{(15)}$	2007-Mar-24	15 (totalling 5,000 m^3) landslides on 2007-Mar-24	1979-Dec-17	No landslides recorded
$T_{(30)}$	1999-Dec-5	No landslides until 1999-Dec-15	1966-Dec-23	No landslides recorded but record incomplete
$T_{(60)}$	1967-Jan-20	No landslides recorded but records incomplete	1975-Dec-12	Two landslides in 1975-Dec to 1976-Mar
$T_{(90)}$	1967-Feb-17	No landslides recorded but records incomplete	1999-Feb-08	Two landslides in 1999 January as $A_{(90)}$ increased.
$T_{(120)}$	1999-Mar-03	2 landslides in 1999 January as $A_{(120)}$ increased.	1967-Feb-14	No landslides recorded but records incomplete
$T_{(150)}$	1999-Feb-28	2 landslides in 1999 January as $A_{(120)}$ increased.	1976-Feb-28	Two landslides between 1975-Dec and 1976-Mar
$T_{(180)}$	1998-Mar-29	No landslides	1976-Mar-30	Two landslide in 1976-Mar
$T_{(270)}$	1997-Jun-30	No landslides	1972-Jul-12	No landslides recorded but records incomplete
$T_{(365)}$	1997-Oct-09	No landslides	1982-Mar-13	No landslides

Table 4.9 indicates that the highest $T_{(1)}$, $T_{(3)}$, and $T_{(7)}$ precede landslides by 37 days or more and are therefore not good predictors of landslides. The highest value of the $T_{(15)}$ index relates directly to a major landslide incident. The highest $T_{(30)}$ precedes a minor landslide. The dates of the highest $T_{(60)}$, $T_{(90)}$ and $T_{(120)}$ are roughly coincident with landslide activity. The second highest $T_{(180)}$ is coincident with a moderate sized landslide. The highest $T_{(270)}$ and $T_{(365)}$ indices do not related to landslide activity. This suggests the 15 to 180 day antecedent precipitations are most closely related to landslide activity.

4.5.14.2 Comparison of landslide episodes and precipitation conditions

The landslides in Table 4.3 are divided into three types: larger above-track earth slides (Table 4.10), below-track bank erosion - earth slides (Table 4.11) and smaller above-track landslides (Table 4.12). Using the recorded date of each landslide the antecedent precipitation index with the highest return period (or rarest event on the day of the landslide) is considered to be the condition that induces the landslide. The results are compiled in the respective tables.

Table 4.10 Earth slides greater than 50,000 m^3 on the Cascade Subdivision between miles 102.5 and 104.90 between 1790 and 2007

Ref. No	Mileage	Date	Total volume (m^3)	Antecedent duration of maximum return period or comments
1	104.35	1790's	1.3 million	Landslide date not accurate
2	103.0	1880-Jan-30	1.5 million	Haney Landslide insufficient precipitation data
3	104.60	1904 to 1929	300,000	Landslide date not accurate
4	103.92	1904 to 1929	80,000	Landslide date not accurate

Unfortunately, the dates of three of the four larger recorded landslides in this area are not accurately documented despite the fact that 2 of the four must have resulted in significant interruptions in CP rail service. There is no record of these events in the CP NHID or Train Accident database, but both databases are incomplete during the time of these landslides. The closest weather data available during the 1880 Haney Slide is from New Westminster 22 km west of the slide. The distance of the weather station from the large earth slide compared with the closer weather data precluded detailed analysis of this New Westminster information.

Table 4.11 Below-track earth slides on the Cascade Subdivision between miles 102.50 and 104.90 between 1975 and 2007

Ref. No	Mileage	Date	Total volume (m^3)	Antecedent duration of maximum return period or comments	PIL
7	103.80	1975 Dec to 1976 Jan	7000	Maximum $T_{(d)}$ in this period and date $T_{(60)}$=55 years on 1975-Dec-12, $T_{(90)}$=15 years on 1976-Jan-23, $T_{(120)}$=27 years on 1976-Jan-29,	Y
8	104.27	1977-Jan-19	1,200	No return periods greater then 2 years	N
10	102.95	1981-May-3	1,000	$T_{(180)}$=2.5 years on 1981-May-3	N
11	102.95	1985-Mar-1	1,000	$T_{(120)}$=2.4 year on 1981-Feb-26	N
12	104.57	1995-Nov	600	$T_{(60)}$ = 3.2 years on 1995-Nov-29	N
16	102.95	1999-Jan	1,000	Maximum $T_{(60)}$=14, $T_{(90)}$=11 and $T_{(120)}$=7 years in 1999-Jan	Y
17	104.23	1999-Jan-14	4,000	$T_{(90)}$=6 years on 1999-Jan-14	Y
20	102.95	May 2001	500	No return periods greater then 2 years	N
24	103.20	March 24, 2007	2000	$T_{(15)}$=56 years and $T_{(150)}$=16 years on 2007-Mar-24	Y
26	102.95	2007-April and May	400	$T_{(180)}$ reached 10 years during 2007 April	Y

Table 4.12 Above track landslides less than 50,000 m^3 on the Cascade Subdivision between miles 102.50 and 104.90 for 1937 and 2007 with complete data for 1975 to 2007

Ref. No	Mileage	Date	Total volume (m^3)	Antecedent duration of maximum return period or comments
5	103.31 to 103.91	1937 and 1938	22,000 (eighteen landslides - largest was 5600 m^3)	Landslide dates not recorded. Possibly multiple landslide episodes
6	103.31 to 103.57	1952 and 1953	1,800 (six landslides - largest was 450 m^3)	Landslide dates not recorded. Possibly multiple episodes
7	103.5 and 103.9	1975- Dec to 1976-Mar	600 (two landslides largest was 500 m^3)	Maximum $T_{(d)}$ in this period and date $T_{(60)}$=55 years on 1975-Dec-12, $T_{(90)}$=15 years on 1976-Jan-23, $T_{(120)}$=27 years on 1976-Jan-29, $T_{(150)}$=38 years on 1976-Feb-28
9	103.51 104.25	1980-Dec to 1981-Mar	2,100 (Six landslides largest was 780 m^3)	$T_{(1)}$=12 years on 1980-Dec-25, $T_{(60)}$=9 years on 1980-Dec-30
13	104.50	1996-Jan-16	70	$T_{(120)}$=6 years and $T_{(90)}$= 4.2 years on 1996-Jan-16
14	103.32 to 103.80	1997-Jan-29	450	$T_{(120)}$=4.1 years and $T_{(150)}$=3.8 on 1997-Jan-29
15	103.39 to 104.30	1997-Mar-18 and 19	2,600 (Six landslides - largest was 1,200 m^3)	$T_{(150)}$= $T_{(180)}$=6 and 8 years on 1997-Mar-18 and 19
18	103.75	1999-Dec-21	50	$T_{(60)}$=4.7 years on 1999-Dec-21

Table 4.12 Above track landslides less than 50,000 m^3 on the Cascade Subdivision between miles 102.50 and 104.90 for 1937 and 2007 with complete data for 1975 to 2007

Ref. No	Mileage	Date	Total volume (m^3)	Antecedent duration of maximum return period or comments
19	103.80	1999-Dec after the 21st	20	Max $T_{(60)}$= 4.7 in late 1999-Dec
21	104.50	2003-Nov-28	100	$T_{(1)}$=6 and $T_{(60)}$=3.6 years on 2003-Nov 28
22	103.39 to	2005-Jan-20	300	$T_{(7)}$=14 and $T_{(60)}$=2.3 years on 2005-Jan-20
23	103.41	2007-Mar-11	80	$T_{(1)}$=28, $T_{(3)}$=7 and $T_{(150)}$=4 years on 2007-Mar-11
24	103.30 to 104.20	March 24, 2007	850 (in 15 landslides - largest was 300 m^3)	$T_{(15)}$=56 years and $T_{(150)}$=16 years on 2007-Mar-24
25	103.81	2007-Mar-25	500	$T_{(15)}$=12 years and $T_{(150)}$=15 years on 2007-Mar-25

It is apparent that five of the ten below-track landslides were precipitation induced landslides (PIL) since at least one antecedent precipitation conditions was above the 4 year return period when they occurred. The 1977 January 19, 1995 November, and 2001 May landslides do not have return period indices above 2 year. Similarly the highest return period indices for the 1981 May 3 and 1985 March 1 landslides were less than 3 years. If these 5 landslides were caused by antecedent precipitation they would be occurring more than once every three years. Since this does not occur other processes, including river erosion, as discussed in Section 4.5.1.8 must be more significant causal factors than antecedent precipitation. The below-track bank erosion - earth slides in 1975 December to 1976 January, 1999 January and 2007 March and May correlate with the elevated antecedent conditions but the lack of sensitivity for the other landslides makes precipitation an unreliable indicator of landslide hazard. Using an index and threshold that results in 50% false-positives will not provide a useful operational tool.

There have been 12 episodes of recorded smaller above-track landslides between 1975 and 2007. Therefore, on average there has been one smaller above-track landslide every 2.7 years. Figure 4.23 illustrated the coincidence of one or more high return-period antecedent precipitation conditions with each of the above track landslide episodes of the last 55 years. With the exception of the 1997 January 29 each landslide episode is coincident with a period of higher return period antecedent conditions for at least one antecedent duration approaching a 5 year return period.

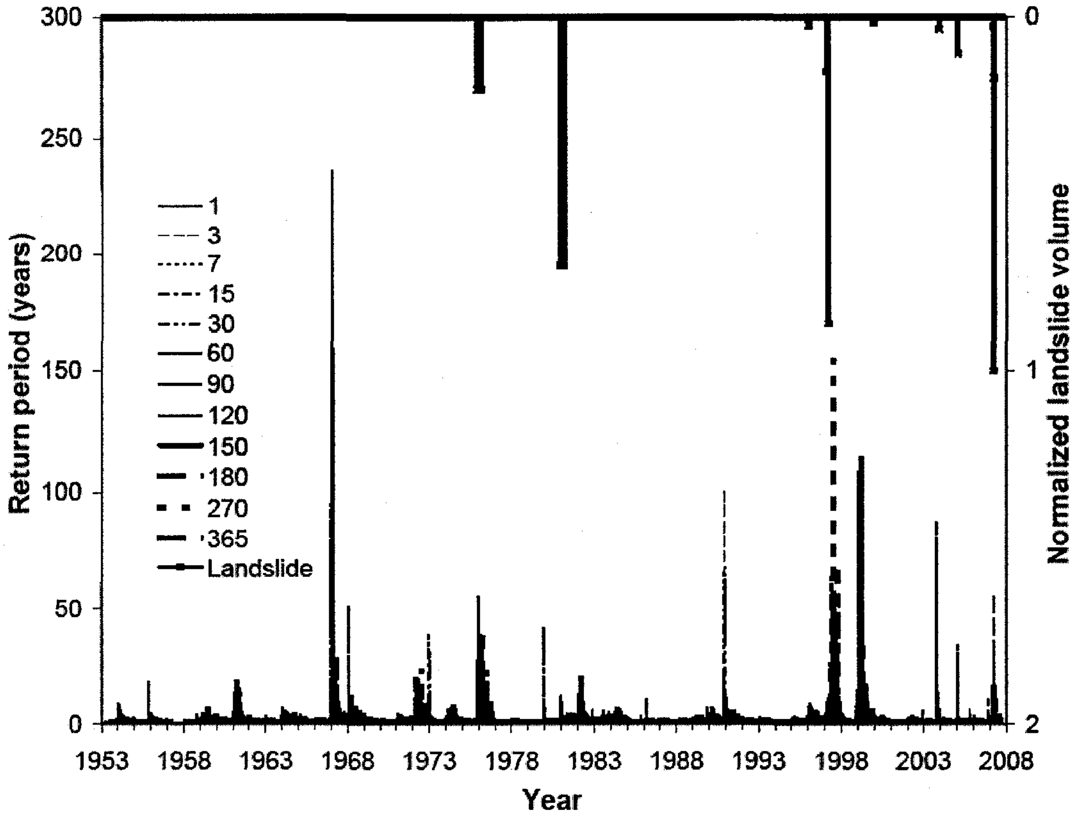

Figure 4.23 Return period for each antecedent duration considered and the landslide record, by normalized volume, for all the above track landslides between 1953 and 2007 at Maple Ridge, BC.

Table 4.13 Highest return periods for smaller above-track earth slide and debris flows between CASC 102.50 and 104.90

Ref. no.	**Date**	**Total volume (m^3)**	$T_{(1)}$	$T_{(3)}$	$T_{(7)}$	$T_{(15)}$	$T_{(30)}$	$T_{(60)}$	$T_{(90)}$	$T_{(120)}$	$T_{(150)}$	$T_{(180)}$
7	1975- Dec to 1976-Mar	2,500 m^3						55	15	27	38	
9	1980-Dec to 1981-Mar	2,100 m^3	12					9.1				
13	1996-Jan-16	70 m^3							4.2	6.2		
14	1997-Jan-29	450 m^3								4.1	3.7	
15	1997-Mar-18 and 19	2,600 m^3									6.1	6.0
18	1999-Dec-21	50 m^3						4.7				
19	1999-Dec	20 m^3						4.7				
21	2003-Nov-28	100 m^3	6.1					3.5				
22	2005-Jan-20	300 m^3			14			2.3				
23	2007-Mar-11	80 m^3	28	7							4.0	
24	2007-Mar 24	3,000 m^3				56					16	
25	2007-Mar-25	500 m^3				12					15	
Count of high $T_{(d)}$ during landslides			3	1	1	1	0	6	2	3	6	1

As discussed in Section 4.2.2.2 the highest return period events occurring on the recorded date of the landslide are assumed to be the landslide inducing antecedent precipitation conditions. These are summarized in Table 4.13 for each of the smaller above-track debris slides.

Based on Table 4.13 the following conclusions can be made:

1. Daily (1 day) precipitation is linked to three events and always in combination with at least one high return period, longer antecedent condition.
2. The $T_{(60)}$, and $T_{(150)}$ are elevated for 11 of 12 events with landslide dates and weather data.
3. Generally, the smaller volume landslides have a shorter return period for longer antecedent durations than the larger landslides. This is expected because larger landslides will take longer to saturate and longer for infiltration to reach the failure surface.
4. It can be seen that each of the landslide episodes over 1,000 m^3 occurred during an antecedent precipitation condition with return periods of 6 years or more. Episode 7 had high $T_{(60)}$, $T_{(90)}$, $T_{(120)}$ and $T_{(150)}$ conditions. Episode 9 had high $T_{(1)}$ and $T_{(60)}$ conditions. Episode 15 had high $T_{(150)}$ and $T_{(180)}$ conditions. Episodes 24 had high $T_{(15)}$ and $T_{(150)}$ conditions.

Based on the results, warning threshold can be determined as per Table 4.14.

It becomes apparent that the smaller above-track landslides in this area are sensitive to lower (3.5 to 4.7 year) $T_{(60)}$ to $T_{(120)}$ conditions and insensitive to all but the higher (6 years of more) antecedent conditions less than 60 days and greater than 150 days. In other words, in this area, an event with a return period greater than 6 to 14 years for all but the 30 day antecedent duration, would be expected to cause landslides. However, above-track landslides are susceptible to shorter return period 60 to 120 day antecedent conditions. This is illustrated in Figure 4.24 where the combined threshold dips below the 5 year return period line in the Caine (1980) type intensity duration plot.

The assessment of the volume and number of landslides and the magnitude of the associated return periods suggests a relationship exists. The rarest precipitation event was for landslide No. 24 where the $T_{(15)}$ = 56 years. In this case, the landslide consists of 14 debris flows totalling 3,000 m^3 of material resulting in an average volume of approximately 200 m^3 per debris flow. At the other extreme, the four debris flows

Table 4.14 Antecedent thresholds for smaller above-track debris slide

Antecedent duration, d (days)	Primary threshold, $T_{(d)}$ (years)	Primary antecedent threshold precipitation (mm)	Secondary threshold, $T_{(d)}$ (years)	Based on landslide episode
1	6.1	88	Combined with $T_{(3)}$ >= 7.0 years, $T_{(60)}$ >= 3.5 years or $T_{(150)}$ >= 4.0 years	9 an 21
3	See 1 day precipitation threshold			
7	14.2	243	Combined with $T_{(60)}$ >= 2.3	22
15	56	366	Could combine with $T_{(150}$ >= 16 but is likely non-conservative	24
30	None of the above track landslides were induced by 30 day antecedent precipitation			
60	4.7	702		18 and 19
90	4.2	930	$T_{(120)}$ >= 6.2	13
120	4.1	1129	$T_{(150)}$ >= 3.7	14
150	6.1	1377	$T_{(180)}$ >= 6.0	15
180	None			
270	None			
365	None			

(No. 13, 14, 18 and 19) with the lowest $T_{(d)}$ had volumes of 70 m^3, 450 m^3 in four debris slides, 50 m^3, and 20 m^3 so the average debris slide volume is about 100 m^3, which is half of the highest $T_{(d)}$ landslides. This relationship has not been pursued further because the relationship becomes poorly defined for the intermediate $T_{(d)}$ induced debris slides such as No. 22 and No. 25 which have average debris slide volumes of 50 m^3 and 500 m^3 respectively.

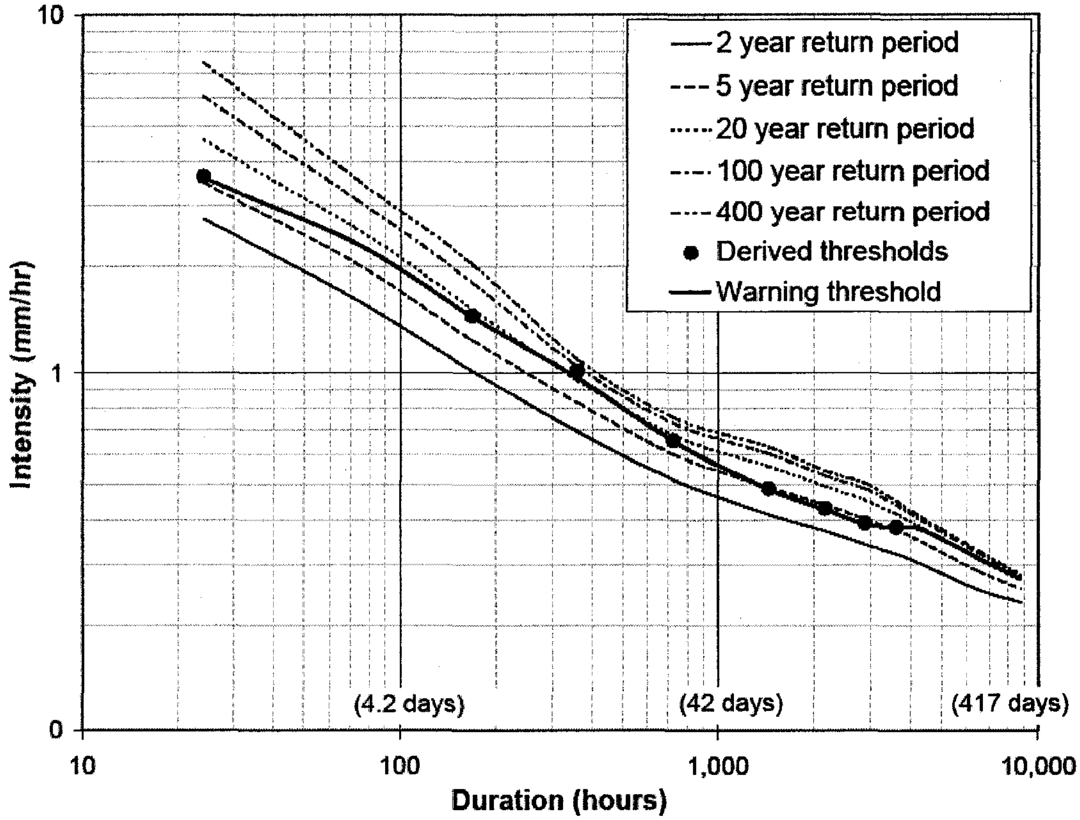

Figure 4.24 A Caine (1980) type plot for the Maple Ridge, BC 1953 to 2007 *precipitation data, 1975 to 2007 landslide data and derived PIL threshold*

Figure 4.24 should be compared to Figures 2.5 and 2.13 to see the difference and similarities in the proposed warning criteria resulting from this research. However, unlike the Caine (1980) intensity duration plot, Figure 4.24 represents the threshold for a single climatic location and specific types of landslides. As such, it is also similar to the weather station criteria use by the Japanese Railways (Rimm-Kaufman 1996).

For the $T_{(15)}$ and $T_{(30)}$ the comment in Table 4.14 regarding the secondary threshold being non-conservative indicates that the primary threshold is so limiting that the probability of the two thresholds being exceeded at the same time is very low. An estimate can be calculated using the inverse of the product of the inverse of the two return periods. Therefore $T(T_{(15)} >= 56$ and $T_{(30)} >= 16) \sim 900$ years. As a result, it is more conservative not to require the secondary conditions. Furthermore, as discussed in Section 4.5.15 it is considered prudent to set the operational warning thresholds below the thresholds suggested by the actual landslide to provide a safety margin.

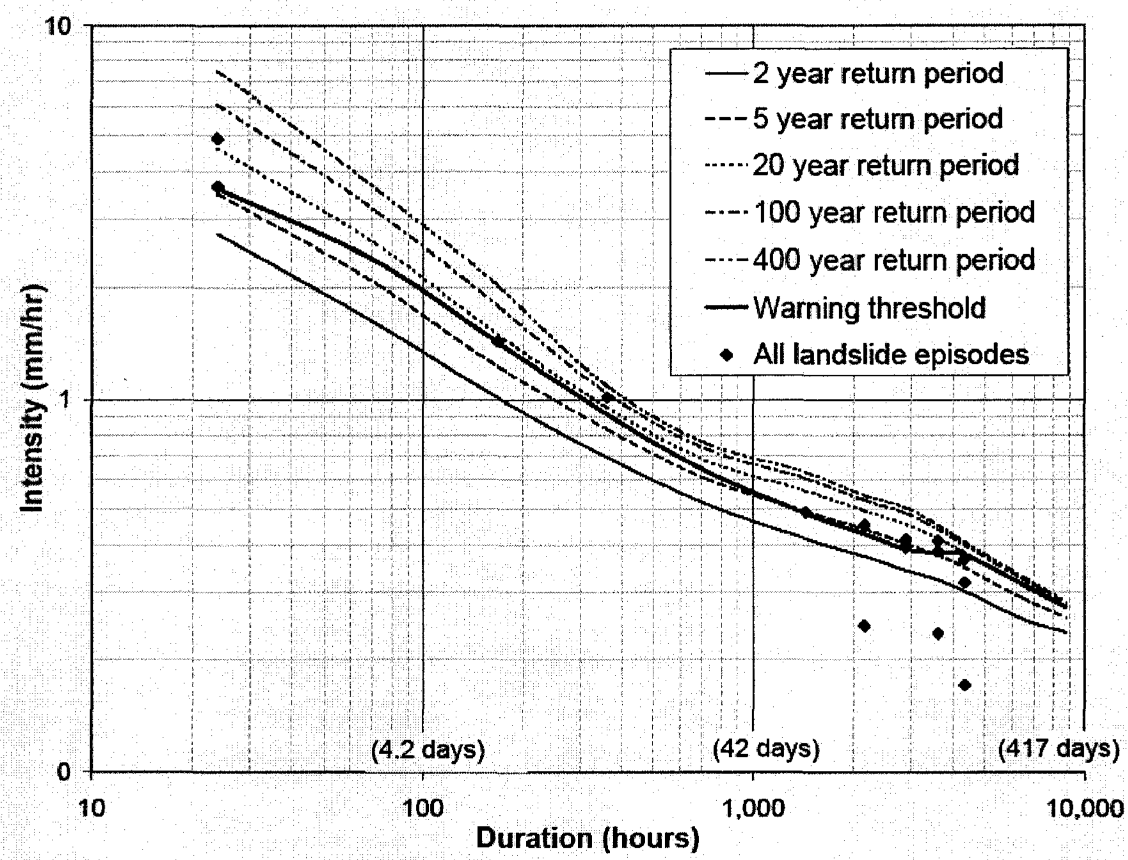

Figure 4.25 A Caine (1980) type plot for the Maple Ridge, BC 1953 to 2007 precipitation data the landslide data with reliable dates from Table 4.3. The proposed warning threshold is also shown. The five landslides below the Warning threshold are the five below-track landslide episodes in Table 4.11 that were insensitive to precipitation conditions

Figure 4.26 is compiled by building a simple logic engine with one condition for each of the thresholds or combinations of thresholds in Table 4.14. Each index is assigned a value of 1 if the threshold is exceeded. The combined index is the sum of all of the index values. Therefore, if three indices are exceeded on a given day the combined index will have a value of three. The normalized landslide episode volume is calculated by dividing each landslide episode volume by the largest landslide episode volume to derive a normalized index of 0 to 1. As shown in Figure 4.26 there does not appear to be any relationship between the total volume of landslides and the combined index. A preliminary review of the number of landslides and volume of each landslide episode does not reveal any relationship. As a result, no attempt at weighting the indices has been undertaken. However, there is a correlation between times with higher combined index and landslides and times with a lower combined index and no landslides. Therefore, during a combined index of 1 the potential of landslides would be high, for a combined index of 3 the landslide potential is very high, and extreme when the combined index reaches more than 5.

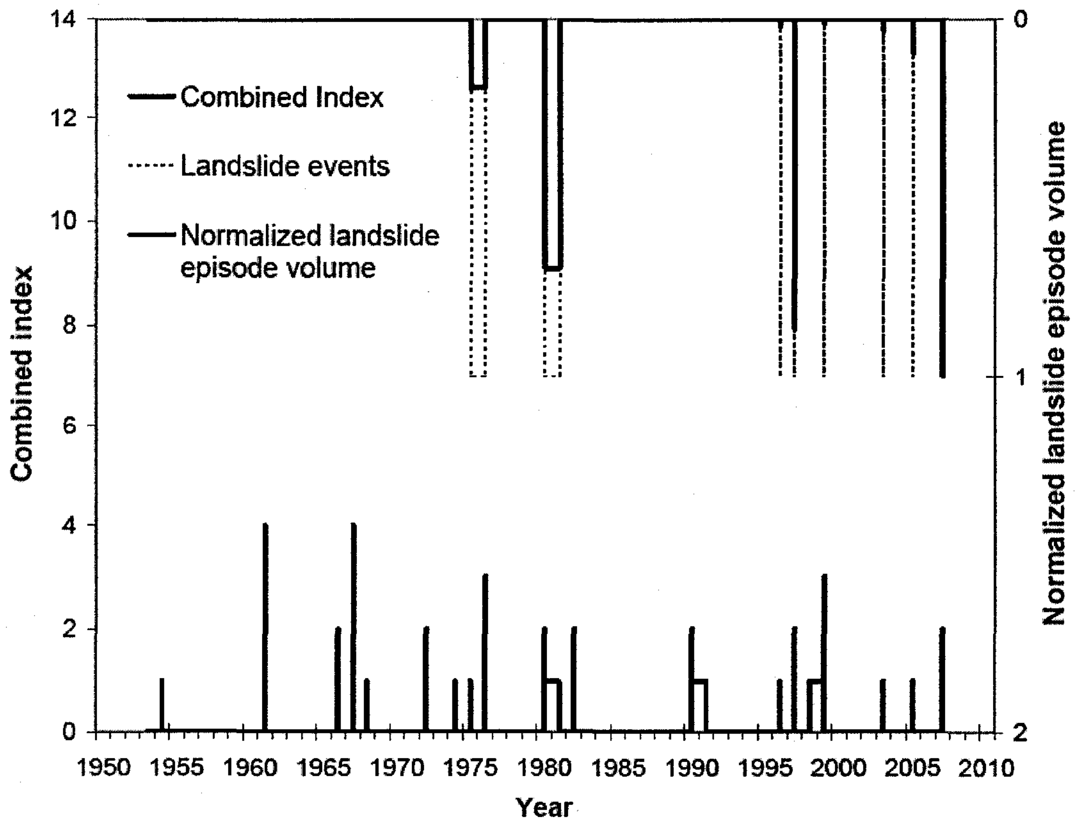

Figure 4.26 Plot of the combined index and the landside activity at Maple Ridge, BC between 1975 and 2007. The volume of landslide episodes is normalized by the 3000 m^3 2007 March 24 landslide.

A qualitative analysis of the results presented in Figure 4.26 has been completed to determine the frequency with which these conditions are met. When compared to the number of landslides recorded the potential for false alarms can be assessed.

The above thresholds result in the performance summarized in Table 4.15. This table is compiled by adding the total number of times; (a) the combined index predicted a landslide and one occurred (true-positive); (b) the combined index did not predict a landslide and one occurred (false-negative); (c) the combined index predicted a landslide and one did not occur (false-positive); and (d) the combined index did not predict a landslide and one did not occur (true-negative). Then (a), (b), (c) and (d) are divided by the number of days of record which is the sum of (a), (b), (c) and (d).

Table 4.15 Performance of the GEV APIL RPA thresholds for the Maple Ridge, BC 1953 to 2007 precipitation and landslide data

	Landslide **occurs**	Landslide does **not occur**
Landslide warning **issued**	0.5% (true-positive)	2.4% (false-positive)
Landslide warning **not issued**	0.5% (false-negative)	96.6% (true-negative)

A perfect system would produce no false alarms (no false-positives) and not miss identifying any landslides (no false-negatives) and therefore the sum of true-positives and true-negatives would be 100%. The false-negatives are of most significant concern because this implies that the system will not warn of some above-track landslides that could inundate and block the track. However, inspection of the data reveals that all the true-negatives are attributed to the landslides where the actual date of the landslide is not known. As a result, the true-negative rate jumps to 97.1% since no landslide warning was issued and in all likelihood, none occurred.

Figure 4.26 shows two landslide periods where the date of the landslide is not known just the general 2 to 3 month periods in the winters of 1975/1976 and 1980/1981 that the landslides occurred. It is worth noting that the algorithm developed identified one or more periods of high combined index during these winters.

4.5.15 Safety margin and warning thresholds

As discussed in Section 4.4.15 safety margins need to be applied to each threshold to ensure an adequately conservative warning system.

For the Maple Ridge above-track landslides a safety margin, k_{sm} = 1.05% was applied in the return period domain using Equation 4.10. Table 4.16 contains a summary of the thresholds from Table 4.14 and proposed warning thresholds. Figure 4.25 is a plot of the warning thresholds in Table 4.16.

Table 4.16 Determined and return period warning thresholds for Maple Ridge, BC smaller above-track landslides

Index duration d (days)	$T_{(d)}$ threshold (years)		Warning threshold			
			$T_{(d)}$ (years)		$A_{(d)}$ (mm)	
	Primary	Secondary	Primary	Secondary	Primary	Secondary
1	6.1	$T_{(3)}$>=7.0 $T_{(60)}$>=3.5 $T_{(150)}$>=4.0	5.8	$T_{(3)}$>=6.7 $T_{(60)}$>=3.3 $T_{(150)}$>=3.8	86.9	$A_{(3)}$>=89.6 $A_{(60)}$>=665.6 $A_{(150)}$>=1306.8
3			10.2	-	168.2	
7	14.2	$T_{(60)}$>=2.3	13.5	$T_{(60)}$>=2.2	241.5	$A_{(60)}$>=612.3
15	56	12.1	11.5		328.4	
30			8		456.4	
60	4.7		4.5		698.1	
90	4.2	$T_{(120)}$>=6.2	4.0	$T_{(120)}$>=5.9	923.3	$A_{(120)}$>=1180.7
120	4.1	$T_{(150)}$>=3.7	3.9	$T_{(150)}$>=3.5	1120.9	$A_{(150)}$>=1291.9
150	6.1	$T_{(180)}$>=6.0	5.8	$T_{(180)}$>=5.5	1372.3	$A_{(180)}$>=1518.3
180	None		15		1626.5	
270	None		25		2033.0	
365	None		25		2397.2	

As per the discussion in Section 4.4.15 thresholds for the non-sensitive indices are also recommended to provide warning of rare events and the combination of rare events such that a continuous threshold in the intensity duration domain is applied to the precipitation data. In this case $T_{(270)}$ and $T_{(365)}$ are set to 25 years to notify the railway of unusual conditions that may cause other problems including sub-grade plastic deformation, sub-grade dynamic liquefaction failure (Keegan 2007), high stream flow and other hazards exacerbated by high antecedent precipitation. The high initial primary $T_{(15)}$ threshold is reduced to 11.5 (12.1 years times k_{sm}) years consistent with the secondary threshold that contributed to the March 25, 2007 event and to avoid missing any rare events that could cause geotechnical hazards. $T_{(3)}$ and $T_{(180)}$ are set to values midway between the $T_{(1)}$ and $T_{(7)}$ and $T_{(150)}$ and $T_{(270)}$ respectively. This provides a smooth transition in the intensity duration domain and warning of unforeseen combinations of unusual events.

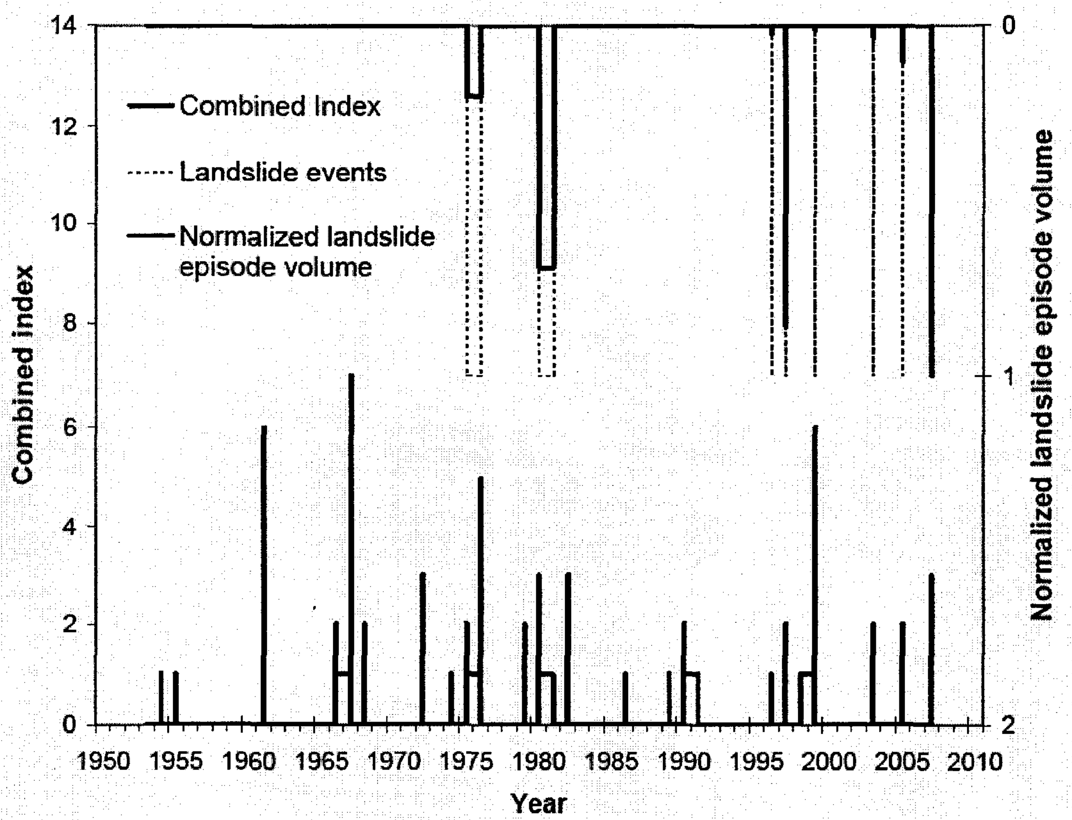

Figure 4.27 Plot of the combined warning index, the landside activity, and the normalized episode volume of smaller above track landslide at Maple Ridge, BC between 1975 and 2007

The warning thresholds and additional indices result in the alarm condition performance shown in Figure 4.27 and Table 4.17. The subtle differences between Figures 4.26 and 4.27 include a wider range of the combined index as the result of more indices and the simultaneous exceedance of multiple thresholds. If desired, the combined index could be normalized to avoid perceived variations in hazard between sites with more and fewer indices. There are also several more low-value combined index bars on the plot as demonstrated by the increase in false-positives in Table 4.17.

Table 4.17 Performance of warning thresholds based on the GEV APIL RPA thresholds for the Maple Ridge, BC 1953 to 2007 precipitation and smaller up slope landslide data

	Landslide **occurs**	Landslide does **not occur**
Landslide warning **issued**	0.6% (True-positive)	3.2% (False-positive)
Landslide warning **not issued**	0% (True-negative)	96.2% (False-negative)

Using the weather of the past 55 years this system and safety margin would result in the issuance of an average of 14 daily warnings per year. As per Section 4.5.14.2, the landslide record indicates there are only 0.4 smaller above-track debris slide episodes per year. The risk reduction in responding to this level of error in the system is investigated in the risk estimation of Section 5.

As with any index method the use of forecast precipitation data is advised to warn of predicted hazardous conditions.

It should be possible to develop indices using longer antecedent precipitation durations provided an appropriate frequency distribution can be identified that adequately models the data. It should also be possible to assess river erosion and flood conditions in a consistent manner to improve prediction of the below-track bank erosion - earth slide scenario.

Each time a landslide occurs the data should be acquired and an additional or refined threshold implemented. In this way, the system can learn from experience and continue to improve. However, as more experience is gained with precipitation induced landslides the number of conditions that are known to cause landslides will increase and the system may be become overly conservative. If the rate of false-positives becomes intolerable, inverse criteria can be developed to reduce the number of warnings based on known extreme precipitation conditions that have not caused landslides. This is beyond the scope of the current research. In addition, it should be possible to reduce the safety margin when the system adequately predicts a landslide.

4.5.16 Case study conclusions

Using the GEV APIL RPA the frequent smaller above-track landslides in Maple Ridge, BC have been shown to be induced by antecedent precipitation with durations 60 to 150 days and with a return period of about 4 years. Indices based on these conditions and additional indices for specific shorter duration antecedent precipitation have been identified. These indices have been adjusted with the application of a safety margin to produce a warning system with a 96.8% reliability and a 3.2% false-positive rate. It was not possible to build an algorithm for the large landslides in the CP NHID and several of the below-track bank erosion - earth slides were shown to be insensitive to the precipitation conditions investigated. However, the above track warning thresholds would have provided notification for 4 of the 9 below track landslide episodes. In addition, it is very likely that the due to the conservative nature of the warning thresholds the large above track earth slides would also have been predicted.

The modified Chleborad (2000) method produced consistent results showing a dependence on both short 1 to 4 day precipitation and longer 5 to 21 and 5 to 150 day antecedent durations.

The dependence on the longer term antecedent conditions in both the modified Chleborad and the GEV APIL RPA suggest that groundwater and the delay resulting from the infiltration and groundwater migration process identified by Hvorslev (1951) is relevant to the landslides induced by precipitation in this area. The magnitude of the delay is expected to be site specific due to the variation in geologic and groundwater at this site compared to other landslide sites.

4.6 Real time system

A real time WIS system would complete the following steps on a daily or more frequent basis.

1. The daily precipitation would be acquired from the two national weather services and any other weather data providers.

2. The forecast precipitation for each weather station would be acquired where it is available.
3. The antecedent precipitation indices would be calculated using the previous days antecedent precipitation information, the actual precipitation and the predicted precipitation over the subsequent 1 to 4 days.
4. The actual and predicted intensity would be calculated for each index.
5. The actual and predicted intensity and duration would be compared to the threshold either graphically or within a logic routine.
6. If the threshold is exceeded a warning would be issued to CP.
7. The process would be repeated each time updated forecast or precipitation data is available.

Either the GEV APIL RPA, the modified Chleborad or both indices and thresholds could be used.

4.7 Conclusions

The return period calculations are dependent on the ability to fit the antecedent precipitation data to a frequency distribution. If this cannot be done successfully the GEV APIL RPA system will not correctly predict which events are the most likely to induce landslides.

In summary, the frequency distribution fit of the antecedent precipitation data is used to identify the condition that induced the landslide. The landslide inducing conditions are then used to develop a logic engine in which the criteria can be used to distinguish the re-occurrence of hazardous conditions. There is always the potential for other combinations of antecedent conditions to induce landslides so the model may fail to predict all landslides. However, it will predict landslides that occur due to the reoccurrence of similar conditions to those that induced them previously.

The modified Chleborad method is well suited to the analysis of data from multiple precipitation induced landslides because it relies on the correlation of precipitation events with the maximum annual series. As a result, it averages the results of conditions that triggered several landslides to identify the specific conditions that trigger the average landslide. In contrast, the GEV APIL RPA preserves the individual landslide inducing precipitation conditions for each landslide and then provides a means of combining the data into a continuous criterion in the IDF domain. It has the added benefit of being widely accepted in other countries and locations and therefore supporting data can be relied upon where the CP NHID is incomplete or lacking an extensive landslide history.

Chapter 5 Risk estimation of geotechnical hazards within the railway industry

This chapter starts by summarizing the use of risk management for geotechnical hazards within CP and the North American rail industry in general. In Section 5.1 the current use of risk management tools and methodologies is discussed. Then the chapter follows the structure and process provided in the publication Risk Management Guideline for Decision Makers (Canadian Standards Association 1997). As such, the remainder of the chapter includes Section 5.3 on the *Initiation* of the risk management process. Section 5.4 covers *Preliminary Analysis* where the geotechnical loss-record of CP is reviewed. The CP loss-record is compared to that of CN where published literature is available. Section 5.5 on *Risk Estimation* contains the innovative component of this chapter and includes a methodology for quantitative risk estimation of various loss scenarios. This methodology is applied to the case study provided in Chapter 4. Section 5.7 includes a discussion of several risk control options available to railways. Section 5.8 includes the *Risk Evaluation* where the CP loss-record is compared to risk levels considered tolerable within other industries. Two *Risk Controls and Options* available to railways are evaluated in Sections 5.7.1 and 5.7.2. Additional *Risk Controls and Options* are discussed in Section 6.5.1 of Chapter 6. Due to the academic nature of this research, contrary to Canadian Standards Association (1997), risk communication will not be emphasized.

5.1 Risk management within geotechnical engineering for railways

As demonstrated by Fell (1994), Bunce et al. (1997), McClung (1999), Roberds (2005), Hungr (2005), Cheung (2006), Porter et al. (2007), and others, the use of risk assessment techniques for managing landslide hazards is becoming more frequent. However, at present, geotechnical risk assessment methodologies are limited to qualitative methods (Keegan 2007) within the North American railway industry.

5.1.1 Current geotechnical risk assessment within railway operations

There are numerous geotechnical hazards and associated risks within the railway industry. With the exception of hazards to Maintenance-of-Way (MOW) employees, Keegan (2007) provided an extensive and detailed classification of geotechnical railway risk scenarios. The following risk analysis and risk estimation focuses on earth slides and debris slides, although where applicable, other mechanisms are discussed. The exposure of MOW employees is also considered.

Currently, within CP, incomplete qualitative risk assessments are completed and utilized within the geotechnical hazard and stabilization assessment processes to determine which hazards present the highest safety and service interruption risks. Funding allocations for current and subsequent years are made using qualitative risk criteria. This process includes the following steps:

1. A qualitative hazard and vulnerability assessment is completed for the site of each identified hazard. This includes consideration of the following hazard and vulnerability factors:
   (a) the likelihood of the hazard influencing the safety of the track in the subsequent hours, days, months and/or years;
   (b) the frequency of the type of hazard;
   (c) the likelihood that a train(s) would be derailed, damaged or delayed by the hazard; and
   (d) the consequence of a train accident including the likelihood of a fatality.
2. The assessment is then qualitatively compared to hazard and consequence information from other known geotechnical hazards. Those hazards considered to present severe risks to the safe and efficient operation of the railway are included in the stabilization plan for the current year. Those hazards identified as being less severe are deferred until the following year. At the start of the following year, the deferred projects are reviewed and compared to the other known hazards and included in that year's stabilization plan or scheduled in the multi-year plan for stabilization in a subsequent year.

5.1.2 Deficiencies in geotechnical risk assessment within railway operations

As indicated in the previous section qualitative risk assessment of geotechnical hazards are completed. As a result, the influences of the above four factors (a to d) in step 1 of Section 5.1.1 and additional eleven bullets below are not consistently or quantitatively considered in the risk assessment. Following from factors a to d above the additional hazard and vulnerability factors below are not considered in the present assessment process:

(a) the probability of loss of life or severe injury of the train crew, the MOW personnel, or passengers;

(b) the probability for injury of the train crew, or MOW personnel;

(c) the reduction in exposure due to a hazard detection system (HDS);

(d) the influence of a track circuit on the detection of the hazard;

(e) the influence of track speed on a train accident outcome;

(f) the quantitative inclusion of train frequency;

(g) the presence of regular commuter or seasonal tourist passenger rail service on the track;

(h) the potential for dangerous cargo to be involved in a train accident;

(i) the presence and proximity of environmental receptors to dangerous cargo in the event of a train accident including the contamination of water and the influence on aquatic and terrestrial species; and

(j) the potential for and the duration of a train service delay.

The non-standardized inclusion and omission of the fourteen factors (Section 5.1.1, bullet 1 (a) to (d) and Section 5.1.2 (a) to (j)) makes it difficult to discriminate the difference in the potential loss resulting from very large but infrequent rock slides, like the Frank Slide, and a track subsidence site that reoccurs every few years but can be managed with a periodic slow order.

The 15th factor or (k) factor below, the influence of the weather, also needs to be considered as it affects the temporal variation of risk.

(k) the variation in the hazard frequency due to the weather and especially the antecedent precipitation conditions.

With the exception of item (k), the previous fourteen factors can be assumed to be temporally uniform over the course of a year. However, it is considered an over simplification to assume that the influence of weather is constant over the course of a year

A semi-quantitative risk assessment procedure using weights-of-evidence has been presented by Keegan (2007) for use by railways. A quantitative risk estimation methodology for geotechnical hazards and the influence of the above noted factors is developed as part of this thesis.

5.2 Risk management for railway geotechnical hazards

The subsequent sections follow the Canadian Standards Association (1997) risk management and assessment process.

5.3 Initiation

The initial step of the risk management process is primarily focused on the administrative details of setting up a risk management process within a large organization and should be explored more fully in that setting. A discussion of the components of the initiation of a risk management process within the geotechnical discipline of the railway industry follows.

Within CP, the engineering group has the responsibility for responding to geotechnical risks such that a uniform protocol and standards are applied across the entire rail network.

The problem is defined as the management of risks and losses associated with geotechnical hazards. As shown in Figure 5.1 there are a number of outcomes from these hazards. The two most significant outcomes are the probability of a fatality and the probability of a train accident. The most significant outcomes are fatality health losses resulting from train accidents (derailments and train damage) because they include all the potential losses identified later in Section 5.4.2. Combined with the information on the population exposed, the risk of a fatal accident can be used to determine the Probability of a Death of an Individual (PDI). PDI is widely used in the insurance industry and risk literature as a measure for comparing risks (Hambly and

Hambly 1994, Bunce et al. 1997, Leroi et al. 2005, Terbrugge et al. 2006, and others). A comparison of the PDI several activities is included in Figure D1. PDI allows for the comparison of risks from geotechnical hazards within CP to other similar and dissimilar sources of risks. The probability of a derailment and train damage is of interest to the railway because this influences the length of the delay and cost of the event. The length of the delay is significant to a railway because it influences their ability to achieve the primary goal of a railway, to realize a profit by moving freight. Given the extensive use of PDI in the risk literature and the level of interest in train accidents by the railways, these two risks, PDI and probability of a train accident, are the primary focus of this risk estimation. These two risks are correlated or dependent. Other potential risk probabilities of interest are identified, discussed, and summarized in Chapter 6 for others to explore. The risk estimation section of this thesis will also be primarily limited to earth slide and debris flow hazards with differentiation of those induced by and independent of precipitation conditions.

A risk management process for geotechnical hazards is needed within three areas of a railway: Train operations, Maintenance-of-way, and Engineering. First, a railway needs to be prepared to adjust its train operations in response to temporal changes in the operating environment. Second, the MOW group has to understand how geotechnical risks influence their work environment. In response to variable weather conditions they may need to change their work practices. Third, the engineering group within a railway needs to be able to quantify the risks and the benefits of risk reduction strategies to identify how best to allocate limited resources between competing needs.

The stake-holders in train operations, MOW, and engineering, need to be involved in providing input to the risk management process, especially considering the influence changing operations can have on the ability of the railway to generate income by moving trains. Any change in the movement of trains must be clearly justified and planned to ensure that the required traffic is achieved in a given period, especially within areas that are at, or approaching the maximum capacity of the existing infrastructure.

A risk management process for geotechnical hazards within a railway will be primarily undertaken by the engineering group and include (where available) the geotechnical group. In railways without a dedicated geotechnical group, external consultants provide this function. Once the engineering group has developed a risk management process and is ready to implement it, train operations managers, MOW managers, and financial officers will be required to join the implementation effort to ensure it is adopted across the organization.

Geotechnical hazards influence a wide group of internal and external stakeholders. The following is a list of stakeholders:

1. Engineering managers, supervisors and MOW employees responsible for responding to service disruptions caused by geotechnical hazards
2. Managers, supervisors and MOW personnel working in areas that could be influenced by geotechnical hazards
3. Managers, supervisors, and train crews responsible for the safe and efficient passage of trains and the occupants across area potentially impacted by geotechnical hazards
4. Engineering staff responsible for the design of the railway infrastructure,
5. Financial managers responsible for the expenditure of resources to reduce safety risks and minimize service disruptions
6. Train operations personnel responsible for the safe operation of the train and those most likely to be harmed in the event of a train accident.
7. The environment and the regulators empowered to protect the environment
8. Neighbouring property owners influenced by the safe operation of the railway in close proximity to their property
9. Railway operation regulators
10. Railway company shareholders whose primary interest is realizing the highest return possible while minimizing the potential for financial loss

Each of these groups will be affected (to a lesser or greater degree) by the outcome of the risk management process. Some of the stakeholders will influence how the process is utilized. Others will be influenced by how the risk management options are implemented.

Initial risk communications should focus on making the stakeholders aware that a risk management process for geotechnical hazards is being initiated, that they have been identified as stakeholders, and the identity of the other stakeholders. The stakeholders also need to be informed how long the process will take and what deliverables can be expected.

5.4 Preliminary risk analysis

The preliminary risk analysis of geotechnical hazards has been described by Keegan (2007) and will not be duplicated here. His work includes the identification of risk scenarios resulting from earth slides, debris flows, and other geotechnical and hydraulic hazards. He also considers the factors influencing how the hazards affect the track. Keegan emphasizes how the hazards influence the use and maintenance of the track. The remainder of the section below deals with several relevant and significant steps in setting up a risk management process.

5.4.1 Classes of hazards

Four classes of hazards that generate risks are identified by Canadian Standards Association (1997). However, the scope of this hazard analysis is limited to specific geotechnical hazards. As a result, only the following three hazard classes are relevant.

1. Natural hazards under consideration are geotechnical hazards including those listed by Keegan (2007) and including rock slides, debris slides, earth slides, track settlement, and ground collapse. These can all be induced by precipitation conditions but debris slides and earth slides are most commonly associated with precipitation conditions.
2. There is a potential for systems or equipment failure to play a roll in the outcome of various risk scenarios. This is especially true where various track warning systems exist to warn train traffic of exceptions to the standard operating conditions.
3. The actions of employees, and human errors in response to hazards, influence the outcome of some hazards and therefore should be considered in the risk analysis where it can be reasonably predicted.

The fourth class of hazard described by Canadian Standards Association (1997), economic hazards such as inflation and taxes, are not considered because they are beyond the scope of this discussion.

5.4.2 Types of losses from geotechnical hazards

Landslide hazards result in eight types of losses for railways. The potential losses are approximately ordered from least to most severe in the following list.

1. Cost of implementation of preventative measures due to a perceived risk.
2. Train service delays due to a perceived risk. I.e. trains are slowed because the train crew or the MOW believe the risk to be increased.
3. Train service delays due to increased risk. I.e. trains are slowed because landslide activity is increasing the risk.
4. Interruptions in train service due to a realized event including the delay caused to assess and mitigate any increased risk resulting from the event.
5. MOW accident due to a realized event.
6. Train accidents due to a realized event.
7. Health losses including death and injury due to a train accident or MOW incident.
8. Environmental losses resulting from the negative influence of one or more of the losses due to bullet 1, 4, 5, and 6 above.
9. Loss of reputation and potentially customer and shareholder confidence.

Although some losses are considered later in the chapter, only losses from bullets 4, 5, 6, and 7 above will be discussed in the remainder of Chapter 5. As reviewed in Section 5.3 losses from bullets 6 and 7 above will be the primary topic of the following risk estimation.

5.4.2.1 The influence of geotechnical hazards on train operations

There are numerous hazards to which railways are exposed. Keegan (2007) has identified these hazards and provides a means of classifying them into scenarios. He also provides a description of potential outcomes and failures of the track system.

The seven track failure modes identified by Keegan (2007) are:

1. Removing support of the track structure,
2. Blocking the track,
3. Impacting a train (moving or stationary),
4. Deflecting the track rail surface,
5. Changing the gauge of the track,
6. Damaging track components including ties, tie plates, rail clips, rails, joints and signals, and

7. Damaging track structures including bridges, retaining walls, and culverts.

Keegan (2007) provides additional details and examples of how geotechnical hazards affect these outcomes to the track. A brief description is included here to demonstrate how earth slides and/or debris flows could produce these outcomes.

The Maple Ridge, BC, Lytton, BC, and other landslides have produced several of the influences identified in the seven bullets above. For each of the seven bullets above, a corresponding example is provided below.

1. The March 12, 2007, Lytton THOM 085.20 and 086.90 overland flow - gully erosion - debris flows both resulted in what is commonly referred to as skeleton track, where the support of the track was removed and only the steel rails were spanning the void, suspending the ties in mid-air (Photo 5.1)
2. At CASC 103.39 and 103.41 several above track debris and earth slides inundated and blocked the track on March 18, 1997 such that it was impassable by rail traffic. None of the landslides caused a derailment. A train ploughed into one landslide and rail traffic was interrupted for more than 6 hours while stability of the site was assessed to ensure it was safe to work in the area, remove the train from the debris, and the clear the track of soil and debris.
3. The recent CASC 103.81 debris slide - debris flow on March 25, 2007 impacted a train moving through the area. Fortunately, a speed restriction (slow order) had been placed on the track following the landslide activity the day before. As a result, the train quickly came to a stop and was not derailed. The track was closed for several hours while the site safety was assessed, the train extracted, and the track cleared of debris.
4. Minor Port Hammond earth slide, the Fir Street earth slide and the 1981 May 3, CASC 102.95 bank erosion - earth slide extended both up and down slope of the track and deflected the track surface as they failed. The 1981 May 3 event caused the derailment of a coal train. Trains can only tolerate a few centimetres of deflection over about 20 m length of track, at normal track speeds, before they will derail.

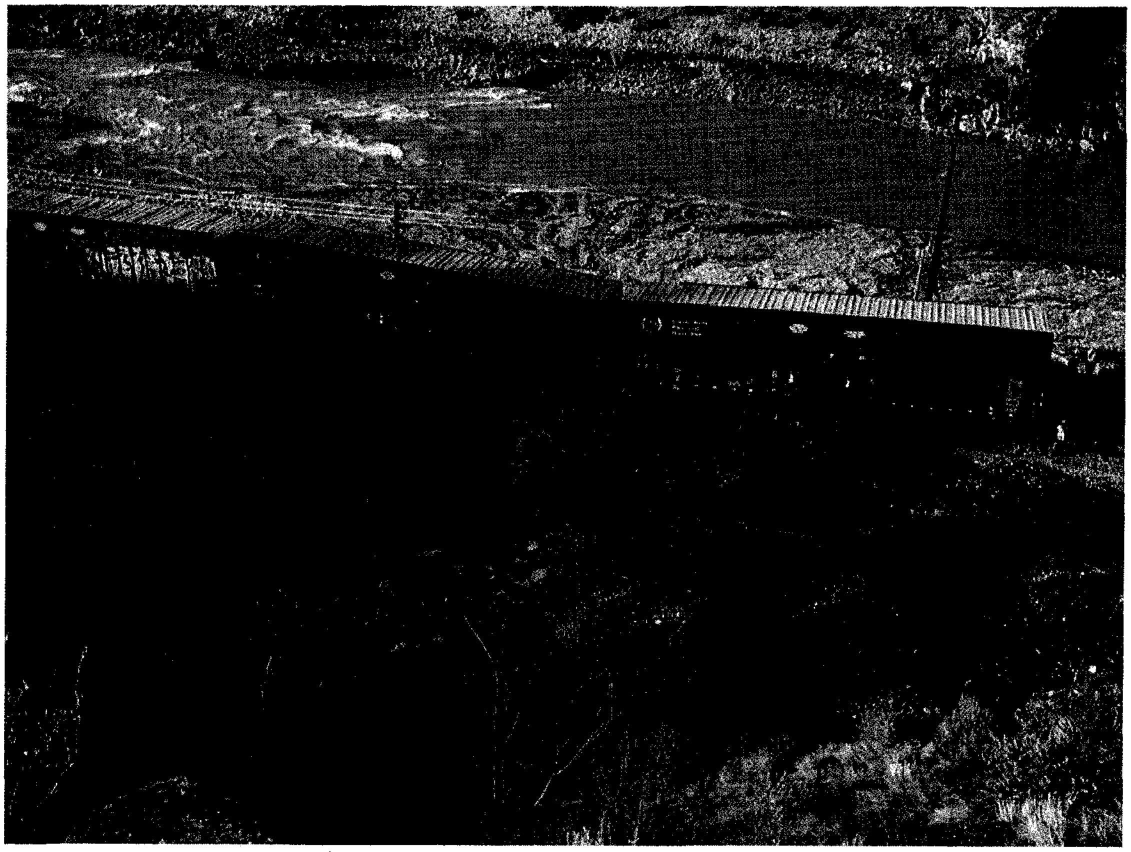

Photo 5.1 March 12, 2007, Lytton THOM 085.20 overland flow - gully erosion - debris flow event left the track skeleton over a 30 m length. A string of box-cars was stationary in the siding track at the time of the overland flow and is shown stranded over the unsupported track. The damage was caused by the bed-load and debris in the initial overland flow plugging the culvert. Subsequent gully erosion and debris flow erosion failed and eroded the track embankment spanning the gully.

5. The impact of a rock fall on the rails can reduce the gauge of the track. Track subsidence can cause failure of cross-ties, which allows widening of the track gauge in response to train loads.
6. Undetected increases in the longitudinal stress on the rail due to slow earth slide movement can overstress the track making it more susceptible to fracture.
7. Any of the hazards located coincident with a track structure including bridges retaining walls, and culverts can damage those structures. However,

bridges, landslide sheds, and tunnels are often built to avoid known landslide and debris flow hazards and therefore rarely suffer damage from them.

5.4.2.2 The influence of geotechnical hazards on maintenance-of-way operations

As demonstrated by the fatality and injury statistics summarized in Section 5.4.4.3 employees maintaining the track have a comparable loss history to those operating trains. The MOW fatalities in the CP Natural Hazard Incident Database (CP-NHID) have resulted from rapid events impacting unsuspecting workers. The size of the hazard would be expected to have a direct correlation on the number of fatalities.

An important consideration for any of the examples described above is the safety of those completing the recovery work. CP and other North American railways identify the safety of their employees as a primary goal. As a result, the return of a track to service after any one of these types of events must be undertaken with due regard for the safety of the employees and contractors doing the work. A thorough geotechnical assessment of the post landslide conditions is completed and any safety measures are implemented prior to any recovery work being done. In general, CP has been very successful in this regard having suffered a high number of fatalities during recovery from avalanches in the earlier part of the 20th century.

5.4.3 Identification of risk scenarios

Based on the CP-NHID numerous risk scenarios and outcomes are identified. The seven track failure modes identified by Keegan are combined with eight types of losses which results in a multitude of track vehicle risk scenarios. Within CP and most railways there are two groups of employees that are most exposed to geotechnical hazards: the running-trades or train crews that operate the locomotives, and the MOW personnel who maintain the track, structures, and signal systems.

Figure 5.1 depicts an event tree of the frequent scenarios affecting the first group, the running-trades.

The outcomes identified in Figure 5.1 are considered in more detail in subsequent figures and sections. A "Train derailment" occurs when the train leaves the

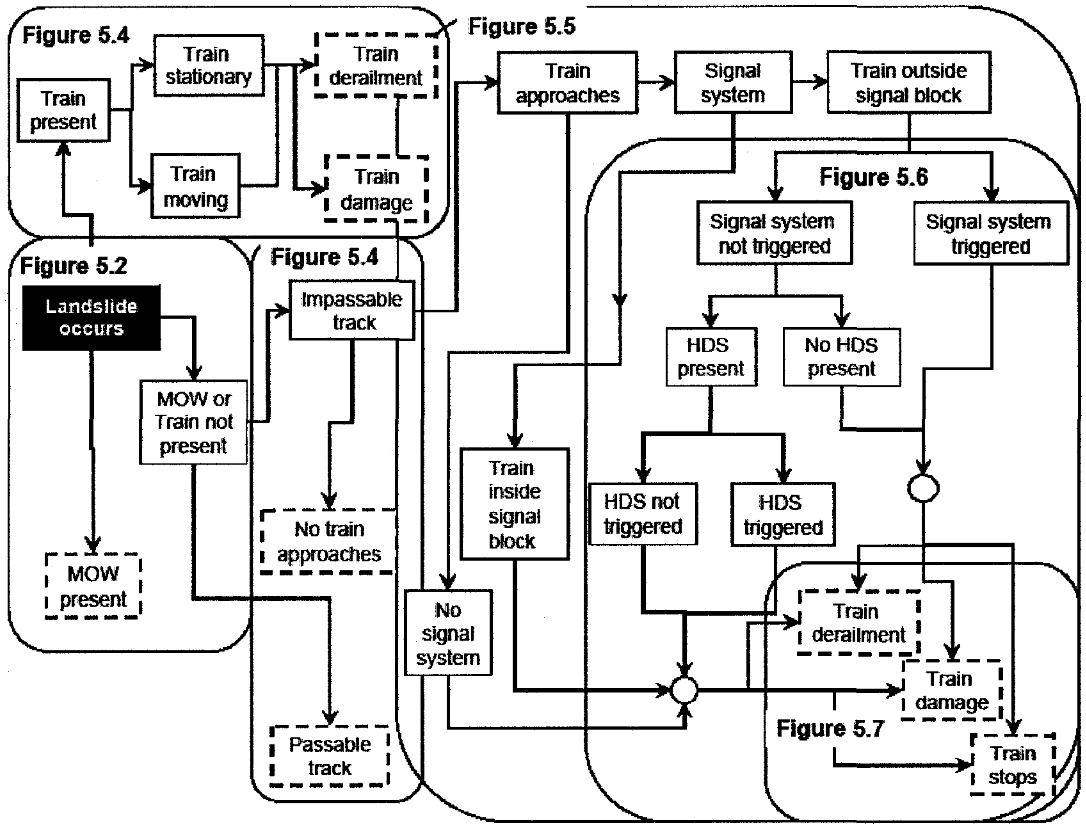

Figure 5.1 Overview of event tree for the risk of derailment, train damage, service interruption, MOW accident and less severe consequences given a landslide occurs. The black box on the left centre is the starting point. Any one of the seven dashed boxes is a possible outcome.

track. A "Train damage" incident occurs any time a train is involved in a collision with no derailment. Train accidents include both train derailments and train damage incidents. "Train stops" indicates the first train to encounter the hazard stops before impacting the obstruction of the track. An interruption of service occurs for all three situations including Trains stops, because time is needed to remove the obstruction from the track.

The following is a description of the events and various scenarios depicted in Figure 5.1. The scenarios all start with a landslide event. The frequency of the landslide size and mechanism and the probability of each branch of the tree determines the probability of each scenario. The landslide can either hit a train or influence the track. If it does neither of these, the landslide is not a hazard to the track. If the train is present, it can be either moving or stationary. The stationary train scenario is explored in Section 5.5.3 and the risks associated with moving trains are discussed in Sections 5.5.2 and 5.5.4. The scenario when a train is not present is the most common and the most complex because of the various signal and hazard detection systems and their limitations. This scenario is discussed further in Section 5.5.4.

The differentiation between passable track and impassable track following a landslide is significant. Passable track occurs in two situations:

1. When small volume debris flows, and soil and rock falls cover the track but are removed or passed over without damage by subsequent trains, and
2. When sub-grade landslides cause ground movements that deform the track, such that the track speed is reduced to afford the safe passage of trains.

Where the track is impassable, either the material is cleared from the track or the track alignment is supported or realigned before rail traffic can resume. In either case, an approaching train can knowingly or unknowingly encounter the obstructed or damaged track resulting in a broad range of outcomes and consequences depending on the site, train and operating conditions. As indicated above, Section 5.5.3 explores these outcomes in more detail. There are situations where a train encounters debris on the track and the operators decide that slowing the train as much as possible is the safest course of action. When a train impacts debris at a lower speed, less damage is likely to result. However, stopping the train as fast as possible can result in a derailment due to the change in momentum of the head-end of the train compared to the rest or back of the train. This scenario is considered a derailment caused by a landslide even though the derailment is due to the over-reaction of the operator. CP identifies this type of derailment scenario as being caused by the landslide because CP supports the train crews' prudent response to hazards that could influence their safety and the severity of a train accident.

The scenario where the track is impassable, but no train approaches, is included to represent the condition when the first encounter with the landslide, whether knowingly or unknowingly, is by MOW forces, inspecting the track or completing their regular duties. The risks associated with this scenario are considered in Figure 5.2, and described below.

The second group of employees exposed to geotechnical hazards are the maintenance-of-way employees. This includes those Track Maintenance and Structures Forces, S&C personnel and contractors that undertake component maintenance and renewal programs on track, bridges, structures, and signals and communications related to railway infrastructure. These groups work and travel along the tracks to and from their work places on a regular basis. The equipment they utilize to travel and work in is also exposed to hazards. An event tree depicting their exposure to geotechnical hazards is provided in Figure 5.2.

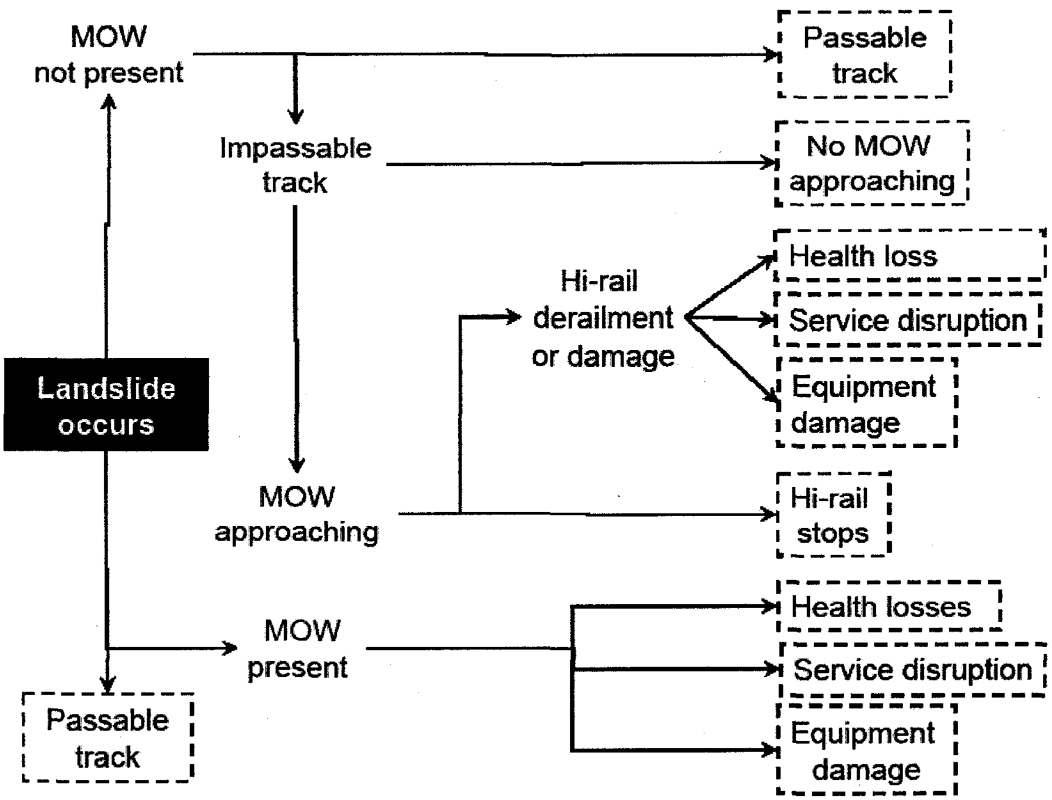

Figure 5.2 Event tree for MOW employees and damage to maintenance equipment given a landslide occurs. The black box on top left is the starting point. Any one of the nine dashed boxes is a potential outcome.

The event tree for the MOW personnel is arranged to avoid duplication of conditions covered by the event tree for a train. With one exception, trains are not considered in Figure 5.2. If there were no trains on the track at all, once the track is rendered impassable the MOW personnel would eventually come upon the impassable track. The "No MOW approaching" outcome occurs when a train is the first rail traffic to encounter the obstruction which is covered by Figure 5.1. Rail travel by MOW personnel is not governed by the signal system or existing HDS. There are three reasons for this:

1. MOW personnel can get on and off the track between signals and therefore cannot be expected to know the status of a signal behind them which may warn of a track condition ahead of them.
2. MOW can be involved with the maintenance of the signal system and therefore cannot be governed by it.
3. The vehicles they use may, or may not, trigger components of the signal system that make the system valid.

As a result, MOW personnel approaching a hazard do not realize the benefits of the signal system and therefore have a higher probability of unknowingly encountering a hazard.

Of the outcomes identified in Figure 5.1, train derailment and train damage incidents can result in health losses. In order of most to least severe, health losses, service interruptions, and equipment damage are the outcomes of greatest concern and interest to the railways. As a result, these three types of losses will be discussed in the subsequent sections of Chapter 5, with an emphasis on health losses.

5.4.3.1 Risk of health losses

As identified in Section 5.4.2.2, health losses include both fatalities and injuries. The risk or probability of a health loss includes the probability of the loss of life and the probability of an injury. Based on the safety records of CP health losses due to geotechnical hazards occur in the following conditions:

1. Running-trades personnel are hurt or killed by the impact or sudden deceleration of a train when it impacts an obstruction or stops suddenly after falling from the track. They may also be drowned if the train falls from the track into deep water.
2. MOW personnel are injured or killed when they are directly impacted or inundated by geotechnical hazards. Based on the CP NHID, the two geotechnical fatalities of MOW personnel occurred when the employees were either directly hit by a rock fall or buried by a debris flow. The most frequent

accidents occur when track vehicles stop suddenly after impacting a geotechnical hazard affecting the track. However, only MOW personnel are injured in these incidents.

These two causes of injuries and fatalities are treated separately in the following sections. A review of the health loss-record is included in Section 5.4.4.

5.4.3.2 Review of CP fatality and injury records related to geotechnical and hydraulic hazards

A review of the CP-NHID indicates that 13 CP employees have died due to geotechnical hazards between 1937 and 2007. Other fatalities have been attributed to geotechnical hazards but these were non-CP employees, primarily passengers. In one case, a trespasser riding the train was killed. These incidents date back to periods where passenger rail service was more common than at present. With the exception of commuter-transit services in urban areas, present passenger rail on CP track is infrequent compared with levels 20 to 30 years ago. Passenger service is limited to small sections of the CP network and a limited number of tourist trains on track in Alberta and BC. The risk estimation in this thesis is based on exposure of current CP personnel.

5.4.4 Information library

As discussed previously, the Railway Transport Committee (1973) directed Canadian railway operators to compile records of geotechnical hazards that influence the track. This has been done by CP for the past 32 years. This information has been supplemented with injury, fatality, and loss-records compiled by non-geotechnical groups within the railways and forms the information library needed to complete the investigation and assessment of risk. In addition, since the 1990's, CP has compiled more detailed information on geotechnical hazards and their influence on specific locations. These three data sets form the information library available for the risk management process.

The following sections review the CP fatality, injury and service disruption records within the CP-NHID.

5.4.4.1 Review of CP fatality records related to geotechnical and hydraulic hazards

The following is a summary of the CP personnel fatality records attributed to geotechnical and hydraulic hazards. There are two sources of information on fatalities caused by geotechnical and hydraulic hazards at CP: the CP NHID, and the Railway Transport Commission (1973) report. These sources have different time periods and include data from different regions. The injuries and fatalities in the CP NHID reliably cover the period between 1960 January and 2007 September (47.7 years) for the entire CP system including tracks divested in this period. The Railway Transport Commission report covers the period 1937 to 1970 (43 years) but only includes those health losses that occurred in the Canadian Cordillera.

There are 9 fatalities of CP employees recorded in 5 events with fatalities attributed to geotechnical hazards within the CP NHID. The Railway Transport Commission (1973) report includes an additional fatal geotechnical event that resulted in 4 deaths within the Canadian Cordillera prior to 1973. As a result, there are a total of 13 deaths attributed to geotechnical hazards to CP. However, because the Railway Transport Commission report is limited to the Canadian Cordillera there may have been additional CP employee deaths caused by geotechnical hazards in the rest of Canada and the US in the period 1937 to 1970. There are no reports of fatalities caused by geotechnical hazards in CP US operations in either source. Similarly, there are no fatalities attributed to hydraulic hazards.

Hydraulic hazards are less likely to cause injuries, fatalities, and train accidents because they become a hazard to the track more slowly, progressively and obviously than many geotechnical hazards. The slow progression of a hydraulic hazard is normally identified by track inspectors or passing train crews before it becomes an imminent hazard. Rail traffic is suspended before the hazard causes a train accident. In addition, hydraulic hazards are commonly coincident with extreme weather, or has significant lead time so warnings are usually provided. As a result, track inspectors and train crews are alerted to the possibility of hydraulic hazards and respond appropriately.

CP's record on hydraulic fatalities is consistent with data presented by Keegan (2007) for the period 1992 to 2002. As a result, the remainder of this section deals only with geotechnical related fatalities. However, the methodology developed could also be applied to hydraulic hazards.

Several additional fatal incidents are included in both the CP NHID and the Railway Transport Commission's report. These are discussed in the following bullets. The rationale for the omission of these incidents from the subsequent analysis is also provided:

1. There is an additional fatality in the CP NHID not included in the 9 discussed above. This event occurred in 2006 when an ice fall was triggered by a co-worker removing ice from a tunnel wall, which landed on the victim. This fatality has not been included in this discussion because ice fall is not a geotechnical hazard and this was not a natural event. The probability of a natural ice fall fatality would be calculated in the same manner as a rock fall fatality using the frequency of ice falls in place of the frequency of landslides. Ice fall frequency is not documented within the CP-NHID because once the ice has fallen it is not a hazard to the train traffic. Typically ice fall debris does not have the strength to inhibit or damage a train or the track. As a result, ice is only considered a hazard to train traffic (and therefore removed) when it interferes with the clearance envelope of a train.
2. There is an additional fatality reported in the Railway Transport Commission (1973) report attributed to CP. However, the deceased was a passenger on a passenger train and not a CP employee. This moving train rock fall accident at Mile 10.5 of the Shuswap Sub on 1968 August 26 also injured 7 passengers and 3 employees.

The 9 fatalities in the CP NHID attributed to geotechnical hazards between 1960 and 2007 indicate the annual probability of an event resulting in one or more fatalities is 0.11 or one event resulting in one or more fatalities every 9.4 years. Of the five events resulting in a health loss, three resulted in multiple fatalities (for safety reasons, CP employees work in groups of at least two). However, natural hazard accidents that are severe enough to kill one worker are usually fatal to all those involved. Of the five fatal incidents, three were caused by the derailment of a train and the subsequent destruction. The other two fatal incidents were the result of geotechnical hazards impacting MOW employees. The geotechnical incident with the highest death toll occurred at least partly as the result of an anthropogenic cause when three track maintenance employees were buried by a coal-mine waste-dump failure, while working on the track below the mine.

The four fatal geotechnical train accidents are summarized in Table 5.1.

Table 5.1 Geotechnical train accidents resulting in one or more CP employee fatalities

Location			Date (period)	Fatalities	Injuries	Ratio of train crew killed (%)
Subdivision	Mileage	Province				
Cascade[1]	11.4	British Columbia	Nov 16, 1944	4	0	100
Thompson	74.9	British Columbia	Mar 17, 1974	2	0	100
Shogomoc	82.7	New Brunswick	Apr 1, 1976	1	3	50
Nelson	111.0	British Columbia	Jan 20, 1995	2	1	100

[1] Railway Transport Commission (1973) data for the Canadian Cordillera only, from 1937 to 1970

Table 5.2 Summary of geotechnical train accidents resulting in CP employee fatalities

Area		Canadian Cordillera	Canadian Cordillera	CP Network
Dates	From	Jan-1937	Jan-1960	Jan-1960
	To	Sep-2007	Sep-2007	Sep-2007
Period (years)		70.7	47.7	47.7
Fatalities		9	4	5
Probability		0.127	0.084	0.105
Fatal train accidents		3	2	3
Probability, $P[F{:}Accident]$		0.042	0.042	0.063
Return period (years)		23.6	23.8	15.9
Average ratio of train crew killed (%)		87.5	100.0	83.3

As shown in Table 5.2, assuming that there are two operators per train, consistent with current practice, the chance of a member of the train crew, who is involved in a fatal geotechnical train accident, dying, is 87.5%.

In summary, based on the CP-NHID the expected annual probability of a train accident resulting in one or more employee fatalities (a fatal train accident) caused by a geotechnical hazard between 1960 and 2007 is 3 in 47.7 years (0.063 per year or once every 15.9 years). When only the data from the CP NHID for the Canadian cordillera are considered there are 2 fatal train accidents in 47.7 years (0.042 per year or once every 23.8 year). Using the CP NHID data and the Railway Transport commission (1973) report data, for the Canadian Cordillera the rate is 3 fatal train accidents in 70.7 years, 0.042 per year or one in 23.6 years. A summary of additional injury and hazard probabilities based on the CP NHID is included in Table 5.3.

The Railway Transportation Commission (1973), Keegan (2007), and Rossetti (2006) all include information on train accidents caused by geotechnical hazards. However, incomplete information with regard to the population exposed to the hazards does not allow the comparison of CP fatality records to other railways or railway industry groups.

5.4.4.2 Review of CP injury records related to geotechnical and hydraulic hazards

The following is a summary of employee injuries, caused by geotechnical and hydraulic hazards, extracted from the CP NHID. Considering both hazards there have been 165 injuries between 1960 January and 2007 September (47.7 years) in 58 events. Hydraulic hazards have resulted in only 11 of these events resulting in 26 (16%) individual injuries. The annual probability and return period of an event resulting in one or more injuries is summarized in Table 5.3.

Forty-seven geotechnical events resulted in an injury. Twenty-one events resulted in only one injury. One incident was responsible for the injury of 46 employees. This incident was a passenger train derailment caused by a Seepage erosion - earth (embankment) slide - earth flow (Keegan 2007) event where 107 passengers were also injured. This is also the accident mentioned in Section 5.4.3.2, where a trespasser was killed.

Given that the incident resulting in 46 employee injuries is not representative of operations in 2007 and the foreseeable future, the total number of geotechnical event related injuries is reduced by 44. Two injuries related to this event are included to account for the injuries sustained by the train crew operating the locomotive. Therefore, the number of injuries caused by geotechnical hazards is 95 in 47.7 years.

The number of injuries sustained by train crew and MOW personnel is 61 and 34, respectively. In addition, 15 of the MOW incidents and 30 of the injuries occurred while the employees were traveling along the track in hi-rails or other MOW track vehicles. This suggests that momentum of the train, hi-rail, or track motor car, contributes to the likelihood of injuries. Only 4 injuries in 4 events were sustained by CP employees working on or about the track in 47.7 years as the result of geotechnical hazards. A total of 91 injuries in 44 events involving travel by trains or rail mounted vehicles are attributed to geotechnical hazards.

5.4.4.3 Summary of CP fatality and injury records related to geotechnical and hydraulic hazards.

Table 5.3 is a summary of the statistics and information discussed in the two previous sections. Keegan (2007) and Railway Transport Committee (1973) provide several comparable statistics to those summarized in Table 5.3.

The incident rate is the sum of the fatality incidents and the injury incidents divided by the period of record. The incident rate and the fatality rate, due to geotechnical hazards of 1.3 and 0.19 per year, respectively, for 1960 to 2007 for the entire CP network compares to a much higher rate of 3.8 incidents and 0.71 fatalities per year for both CP and CN combined, for BC only, for the period 1937 to 1970. The historical data is from Keegan (2007), the Railway Transport Committee (1973) and others. It must be remembered that the 1960 to 2007 CP data are for the entire CP network compared to the combined CP and CN network. Given that the highest density of geotechnical hazards is in BC, this comparison is reasonable. However, CP operates less than half of the combined CP and CN rail network within BC. Therefore the 1973

Table 5.3 Summary of CP fatality and injury records from 1960 to 2007 (47.7 years) attributed to geotechnical and hydraulic hazards and the probability and return period of these events

Hazard type	Loss	Number of incidents	Annual probability/ frequency[1]	Return period
Fatalities				
Geotechnical[2]	Fatality	9	0.19	5.2
	Incidents resulting in fatalities	5	0.11	9.5
Geotechnical train accidents	Fatality	5	0.11	9.5
	Incidents resulting in fatalities	3	0.063	16
MOW accidents	Fatality	4	0.084	12
	Incidents resulting in fatalities	2	0.042	24
Injuries				
Geotechnical and Hydraulic	Injuries	165	3.5	0.29
	Incidents resulting in injuries	58	1.2	0.82
Geotechnical train accidents	Injuries	139	2.9	0.34
	Injuries (non passenger)	95	2.0	0.50
	Incidents resulting in injuries	47	1.0	1.0
Hydraulic train accidents	Injuries	26	0.55	1.8
	Incidents resulting in injuries	11	0.23	4.3
Geotechnical - MOW traveling on the track	Injuries	91	1.9	0.52
	Incidents resulting in injuries	44	0.92	1.08
Geotechnical - MOW working on the track	Injuries	4	0.084	12
	Incidents resulting in injuries	4	0.084	12

[1] Values in this column less than unity are the expected probability of the event. Where the value in this column is greater than unity it is the expected annual frequency of occurrence.

[2] There are no fatalities caused by hydraulic hazards so the combined geotechnical and hydraulic fatalities category and hydraulic fatalities category have been omitted.

data represent more than twice the track miles, exposed to geotechnical hazards, than CP alone. The Railway Transportation Committee (1973) identified several reasons CN has more fatalities and injuries than CP. Presently there are more trains running and therefore more trains crews working on CP trains than in 1973. However, the train crew size has been reduced from a minimum of three to a minimum of two and the size of the MOW work force has been reduced by the introduction of more mechanization. Normalizing to account for these variables has not been completed as part of this research. It is expected that, given that train traffic has increased since pre 1970, and given the above factors, the railways have achieved a net reduction in the probability of health loss incidents and fatalities, due to geotechnical hazards, since the publication of the 1973 data. As a result, it appears that CP and CN have reduced the influence of geotechnical hazards on operations over the past 35 years.

5.4.4.4 Risk of service interruption

The risk of service interruption is generally equal to the probability of the hazard, for every hazard that reaches the track. One of the most significant aspects of a service interruption from a railway perspective is the length of the delay. Generally, the length of interruption is proportional to:

1. the volume of the landslide,
2. the remaining risks that influence the removal of the debris or the repair of the track, and
3. whether a train or personnel were directly affected by the landslide.

The geotechnical hazard database is incomplete with respect to delay and landslide volume data, and the numerous factors affecting the recovery and return to normal operations. The CP-NHID has 3,910 records of geotechnical and hydraulic incidents. However only 2,295 (59%) have data on the volume of the incident. Of the records with volume data, only 419 (11% of the total and 18% of those with volume data) include information on the length of the service interruption. Figure 5.3 provides a rough correlation for the expected and upper bound length of the delay based on the volume of the landslides.

In Figure 5.3 the three incidents above the upper boundary are not considered representative for the following reasons. The 0.003 m^3 rock fall that caused the 9 hour delay (labelled 1) derailed a train by falling so that it jammed a track switch. This is the smallest rock recorded to have derailed a train in CP's database. The next smallest rock falls to cause a derailments were at least 0.1 m^3.

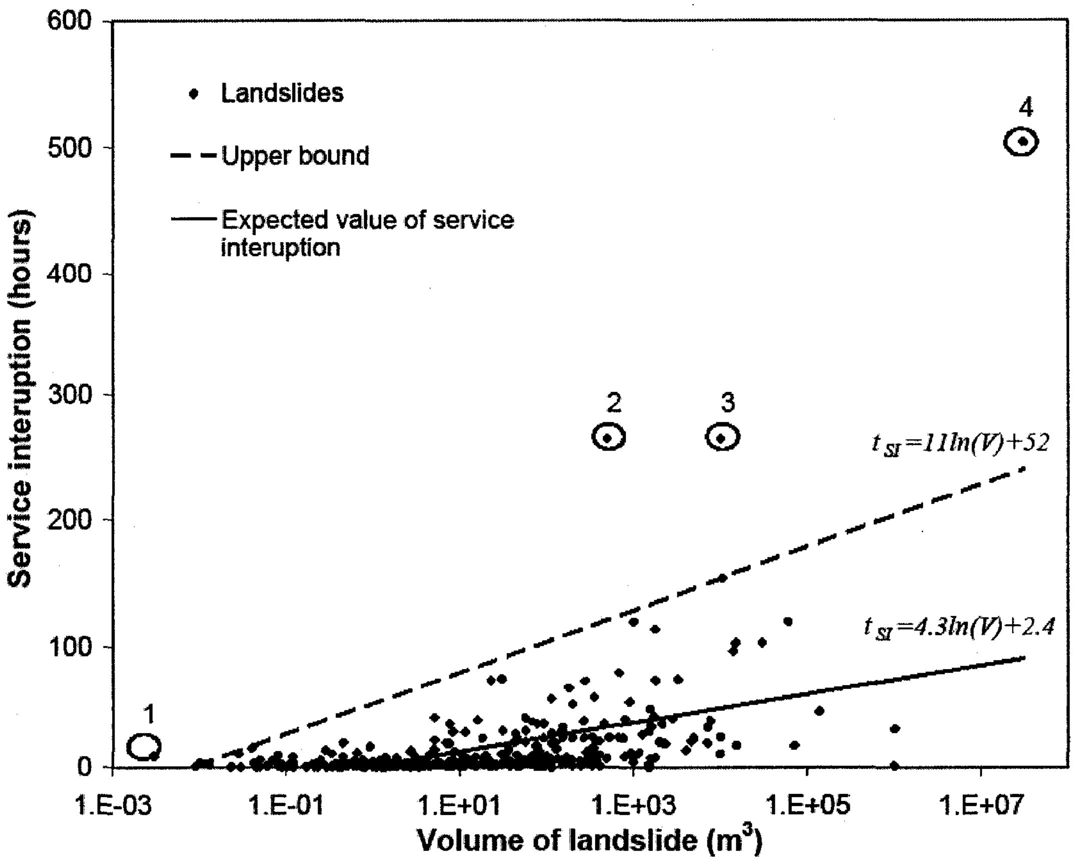

Figure 5.3 Graph shows the correlation between train delay and volume of landslide. The 4 circled and numbered landslides are discussed in the text.

Two incidents caused delays of 264 hours (11 days). The landslide labelled 2 was a derailment on the south track of the Ignace Sub at Mile 109.4 on 1997 April 4. The long service interruption was due to the low urgency to return this area of double track to service. A few years later, this area of double track was entirely removed from service due to under utilization. Both the volume and length of service interruption for the landslide labelled 3 are suspect because the data is from the CN Conrad 1997 March 26 incident (Transportation Safety Board 1997a). Also of note is the 30 million m^3, 1903 Frank Slide (labelled 4) that caused a 21 day (Kerr 1990) to 25 day (Cruden and Langenberg 2003) service interruption of the CP track. It is a testament to the railway workers of the day that they were able to return the track to service in such a short period considering the volume of rock blocking 1.95 km (1.2 miles) of track (McConnell and Brock 1904) and the equipment they were working with.

Factors that influence the lengths of delays due to landslides include:

1. access to the landslide site,
2. delays due to residual hazards that endanger personnel undertaking the recovery effort,
3. occurrence of a train accident, or not
    a. if there was a fatality, or not, and the coroner's investigation of any fatalities, if they occurred,
    b. the recovery of train equipment, and
4. the volume of the landslide.

These factors would have to be investigated to develop a reliable risk assessment hazard/service-interruption relationship. The work of Hungr et al. (1999) could be used to estimate the frequency of various landslide volume classes. Consistent with Section 5.3, the risk of service interruption is not analyzed further within this research. However, a methodology similar to that described in the remainder of Chapter 5 could be used to undertake an analysis of this relationship.

5.5 Risk Estimation

The frequency of several of the scenarios identified in Figures 5.1 and 5.2 and the probability of the possible consequences is analyzed in this section to complete the risk estimation step. The quantitative risk estimation calculation is limited to losses suffered by railways because of geotechnical hazards. It has the ability to analyze the change in risk as the result of precipitation conditions and quantify the reduction in risk achieved by specific mitigative measures. An example is provided to illustrate the risk exposure of the numerous possible scenarios and outcomes in a specific case.

Consistent with Einstein (1988), Canadian Standards Association (1991) Abbot et al. (1998a), Roberds (2005) and others the basic premise is to divide the hazard scenarios identified by Keegan (2007) into as many steps and branches as needed to allow each influencing variable to be represented. Then the product of the conditional probabilities of each branch with a consistent outcome is summed.

5.5.1 Quantitative risk estimation

An event tree analysis (Canadian Standards Association 1991) is used to deconstruct the numerous conditional probabilities so that each scenario can be adequately investigated and a realistic and defensible risk estimate derived. The event tree is developed to analyze the most likely scenarios. Each division of a branch of the tree has a probability of occurrence for each of the sub-branches such that the sum of the sub-branch probabilities is unity. In some cases, the two probabilities of a two branch division are zero and unity, where a branch is or is not relevant, given certain conditions. For example, this happens where the probability of a Hazard Detection System (HDS) providing notification of a hazard is dependent on the existence or absence of an HDS.

5.5.1.1 Types of train and landslide interactions

Four train and landslide interactions may or may not result in an accident. Consistent with Bunce et al. (1997), McClung (1999), and Roberds (2005) these are:

I Moving train / active landslide - A moving train being impacted by an active landslide is the rarest type of event since the landslide movement has to be synchronous with the passing of the train.

II Stationary train / active landslide - It is relatively rare that a stationary train is impacted by an active landslide because railways try to minimize the time that trains are stationary and the time that they are exposed to the hazards.

III Moving train / recently active landslide - This is the most common train accident scenario and results when a moving train encounters a landslide that has rendered the track impassable. The landslide has occurred since the last train or hi-rail.

IV Moving train / inactive landslide - this is the most common scenario of all and is the null event. It is included here to complete the summary of possible train and landslide interactions but not discussed further.

These scenarios are simpler than those on highways (Roberds 2005 and Bunce et al. 1997) because there is no potential for a follow-on accident and generally there is only one way train traffic in areas influenced by landslides (although provisions for two way double track can be made).

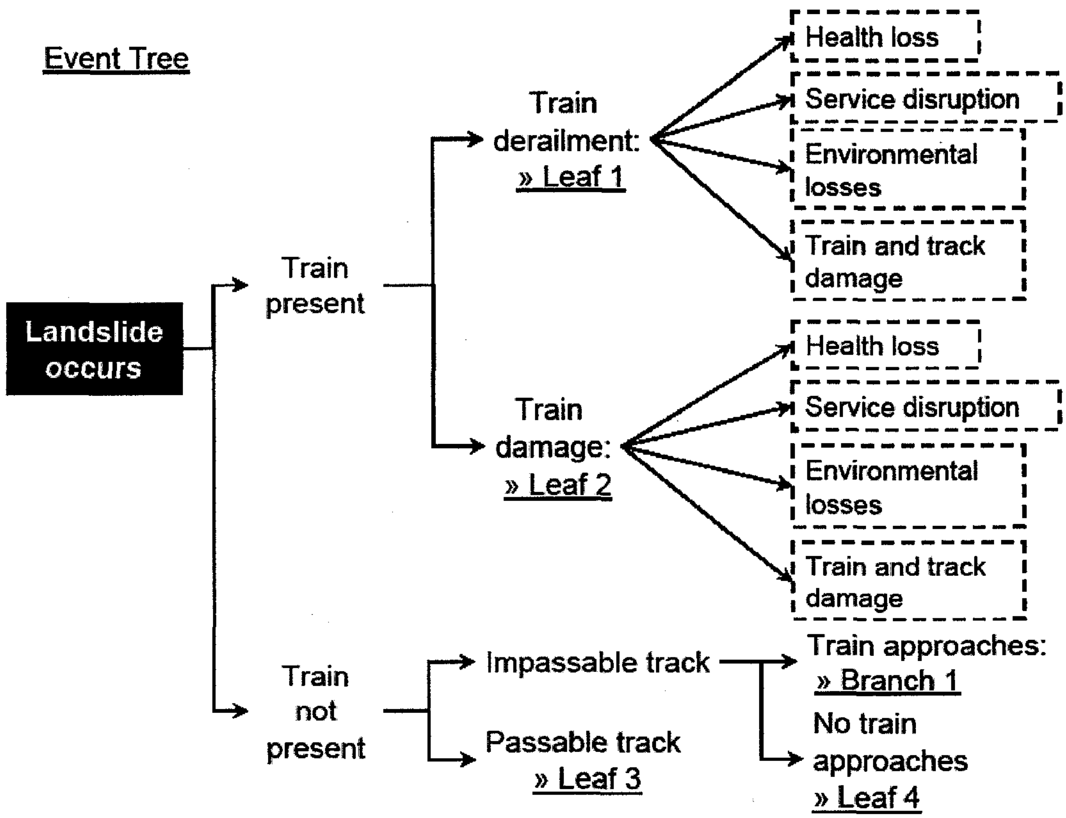

Figure 5.4 This is a more detailed depiction of Figure 5.1 but only shows the full set of possible outcomes when a train is present. The details of the train not present scenario are completed in Figure 5.5. The solid box on the left is the triggering condition. The dashed boxes on the right are the possible loss outcomes.

Figures 5.4, 5.5, 5.6 and 5.7 show the relationship between the various scenarios. These figures provide a more detailed overview of the risk scenarios presented in Figure 5.1. They are consistent with an event tree. The branches represent steps in a scenario and the leaves representing the outcomes. To reduce duplication, where components of the tree (leaves or branches) are common to more than one scenario they are labelled and the branch or leaf labels are used elsewhere. Branches and leaves are marked with the », underlined, and expanded on a subsequent figure.

Figure 5.4 is the main decision tree and illustrates the train present condition from landslide to outcome. Figure 5.5 shows additional scenarios arising from Branch 1 identified in Figure 5.4. Figure 5.6 includes branches 2 and 3 referred to in Figure 5.5. Figure 5.7 includes the outcomes or leaves 3, 4 and 5 referred to in Figures 5.4, 5.5, and 5.6.

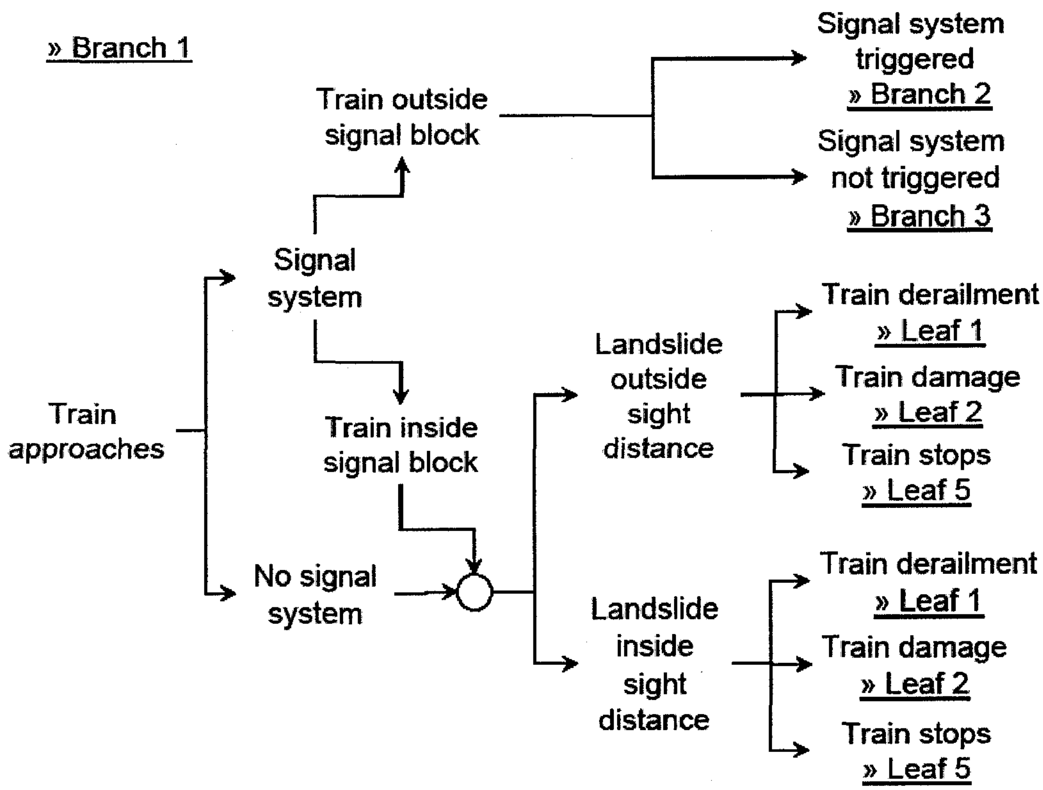

Figure 5.5 Scenarios resulting when a train approaches a landslide that has rendered the track impassable. The triggering condition is omitted, but follows from Figure 5.4. The references to branches 2 and 3 refer to the remainder of the branch in Figure 5.6. The outcomes for train derailment, train damage, and train stops incidents, where the train is within the signal block or there is no signal system are included in Figure 5.7.

The conditional probabilities of the various outcomes, depend on the preceding steps in the scenario. For example, the probability of a health loss (especially a fatality) differs for a derailment and a train damage incident.

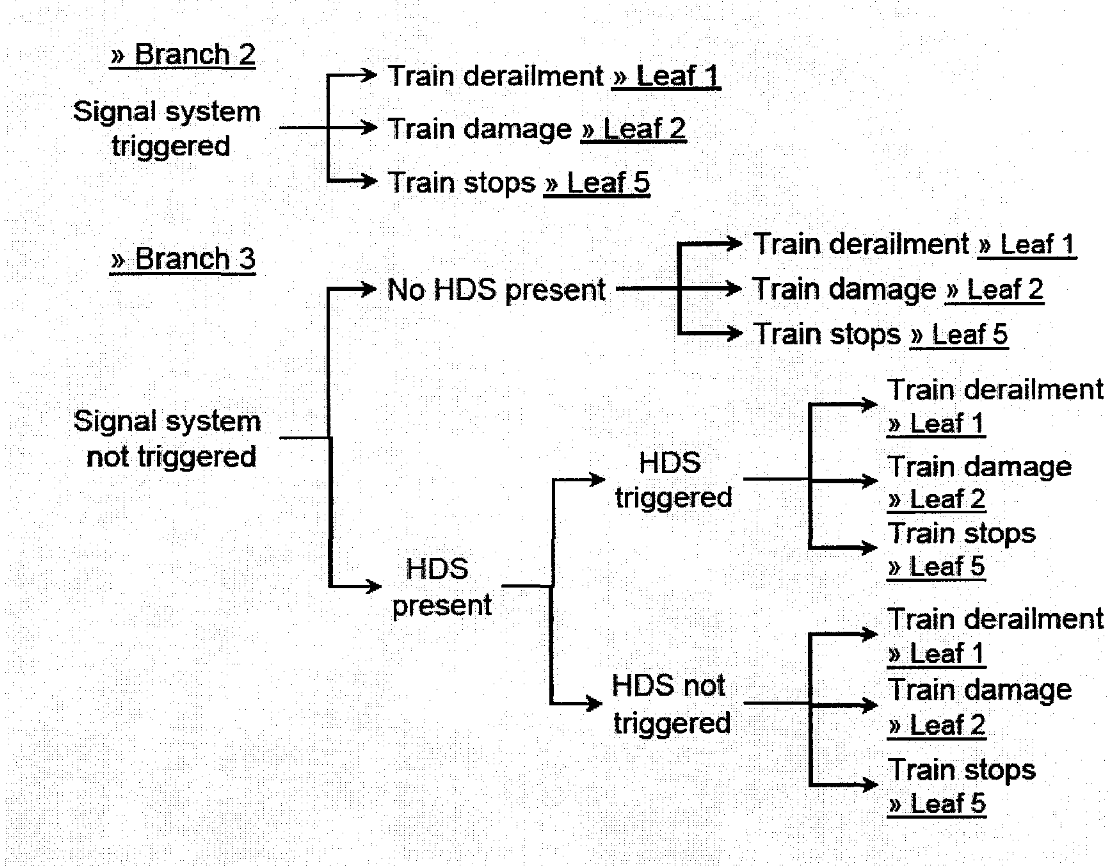

Figure 5.6 Scenarios when a train approaches a landslide that has rendered the track impassable with a signal system that is triggered or not triggered. The triggering conditions are omitted, but follow from Figure 5.5.

5.5.1.2 Nomenclature for probabilities

Consistent with many authors in Hungr et al. (2005), the following nomenclature will be used to represent the various probabilities discussed in the following sections. "P[]" will indicate the probability of the outcome expressed within the square brackets. Conditional probabilities will be expressed with the outcome first, a colon, and then any conditions limiting the outcome last. Where the condition or conditions are dependent on another variable, the variable is indicated within round brackets "()" following the condition. The types of train landslide interaction will be indicated by the subscripts I, II, III or IV following the outcome or condition depending on which it applies. If the type applies to both it is only included after the outcome.

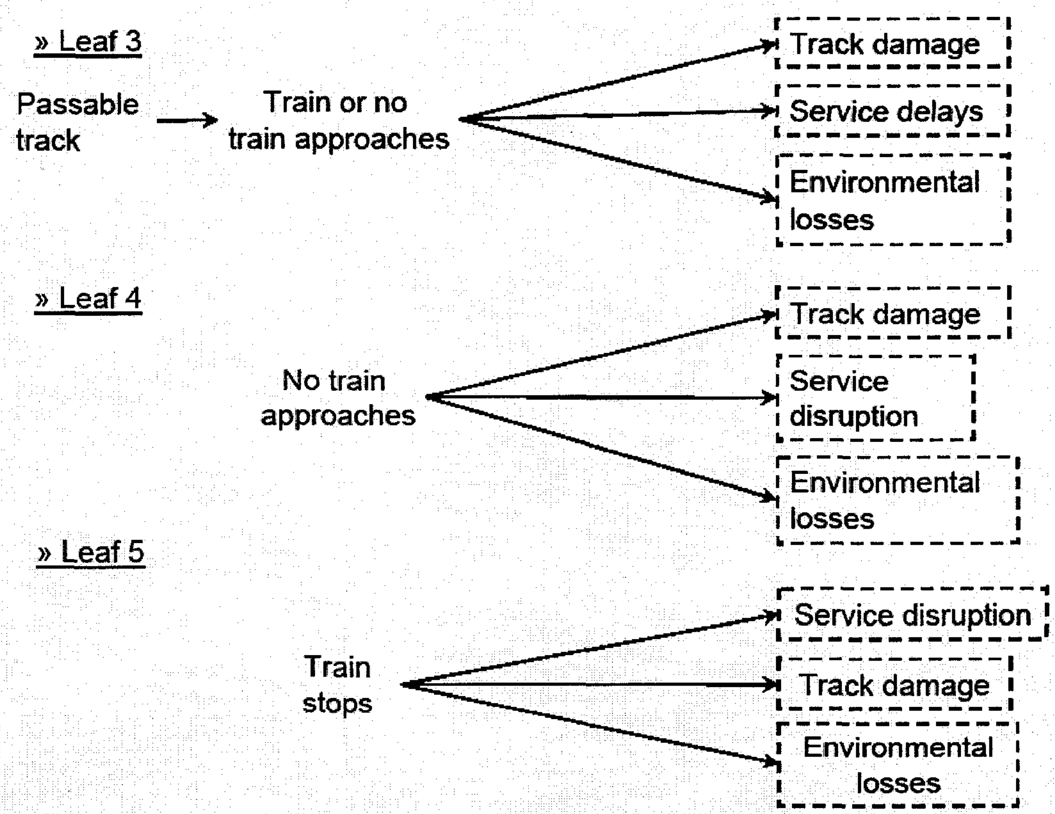

Figure 5.7 Outcomes (leaves) referred to in Figures 5.4, 5.5 and 5.6 when the track is passable, impassable track and no train approaches, and the train stops short of the landslide.

Therefore, $P[F]$ is the probability of a fatality. $P[F_{III}]$ is the probability of a fatality resulting from the Type III track unit - landslide interactions. Therefore $P[F]$ is the sum of the independent probabilities of a fatality given all three derailment types:

$$P[F] = P[F_I] + P[F_{II}] + P[F_{III}]$$

$P[F{:}Derail._{III}]$ is the probability of a fatality given a Type III derailment.

$P[Derail._{III}{:}H]$ is the probability of a Type III derailment given all hazards.

$P[Derail._{III}{:}H(V_i)]$ is the sum of the probability of a Type III derailment where the probability of each hazard volume class has been considered independently. Numerous other combinations of variables are used throughout the remainder of this chapter but all follow these rules. The abbreviations of the outcome and conditions used in this research are provided in the List of variables at the end of this chapter.

5.5.2 Type I - Train impacted by an active landslide as the train passes (Moving train / active landslide)

This is the rarest risk scenario because two events, a landslide and a train passing, have to occur at the same time. There are two subsets to this condition: Type Ia - a train being impacted by an extremely rapid to rapid landslide (Cruden and Varnes 1996); and Type Ib - a train being affected by the track which is unsupported or inundated by a moderate to extremely slow landslide. In the Type Ia case, the risk scenarios include fatalities due to the impact and the potential for a train accident. In the Type Ib case the risk scenario and potential for fatalities are limited to those resulting from derailment. Since a Type Ib hazard takes longer to occur than the passage of a train past a given location (5.0 seconds for a 175 m (574 ft) long passenger train traveling 127 kmph (79 mph) compared to 4 minutes for a 2740 m (9,000 ft) long freight train traveling 40 kmph (25 mph)), the hazard can be considered to occur prior to the passage of the train. As a result, only Type Ia cases are considered in this section. Type Ib cases are analyzed as Type III cases.

A number of assumptions are required to derive the relationships that follow. These include:

1. Trains travel at the posted track speed.
2. The average train length can be used to represent all trains.
3. The temporal distribution of trains and landslides is uniform throughout a 24 hour period. The most obvious violation of this assumption is for the commuter-transit rail service that only runs during the early morning and late afternoon. Provided there is no higher or lower probability of landslide activity within the diurnal period, this should not be significant.
4. The timing of each landslide is assumed independent of any other landslide and therefore a uniform temporal distribution of landslides can be assumed. This is contrary to the proposition that landslides are induced by precipitation conditions and will be discussed further in Section 5.7.2.
5. Rail traffic and landslide activity are independent. This may not be true for smaller Type Ib sub-grade landslides that may be triggered by the load of the train but these are considered a Type III scenario. There is no correlation

between rail traffic and above track geotechnical hazards or more trains that are moving would be impacted by falling debris.

6. The hazard is equal for trains traveling east and west. This may not be true for areas of double track depending on the size of the landslides.

The spatial probability that a train will be present at any given hazard location, $P[S_I{:}H]$ can be calculated by considering the percentage of time, t, a train will be present in the length of track, L_H, influenced by the landslide. For the purposes of this discussion, in this section, the term "train" will represent all track units. The residency time of a passing train is depicted in the schematic of Figure 5.8 provided the length of the hazard is less than the length of the train. Given the length of most freight trains is approaching 3 km (2 miles) this is usually the case.

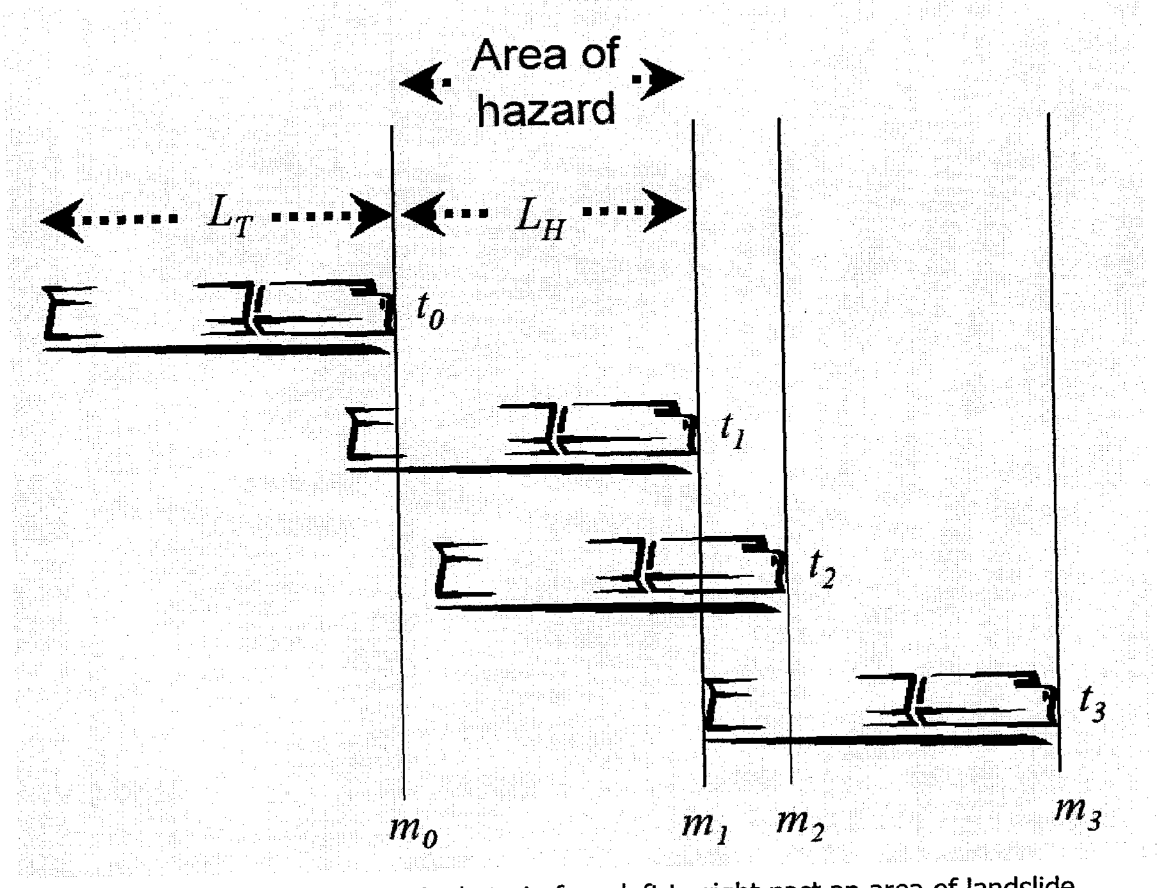

Figure 5.8 Exposure time a single train from left to right past an area of landslide hazard extending from mileage m_1 to m_2 and length, L_H, at a constant speed, v_T. At time t_0 the head-end of the train is about to be exposed to the landslide at mileage m_0. Between mileage m_0 and m_1 (t_0 and t_1), on

average a train is exposed to ½ the length of the hazard. Between mileage m_1 and m_2 (t_1 and t_2) a train is fully exposed to the length of the hazard. From mileage m_2 and m_3 (t_2 to t_3) a train is again, on average, only exposed to ½ the length of the hazard.

Setting $t_0 = 0$,

$$t_1 - t_0 = \frac{L_H}{v_T} \quad \text{Equation 5.1}$$

$$t_2 - t_1 = \frac{(L_T - L_H)}{v_T} \quad \text{Equation 5.2}$$

$$t_3 - t_2 = \frac{L_H}{v_T} \quad \text{Equation 5.3}$$

Since a train is only fully exposed to the hazard for ½ of (t_2 - t_1) and (t_3 - t_2), the total time of exposure, t, can be expressed as:

$$t = \frac{(t_1 - t_0)}{2} + (t_2 - t_1) + \frac{(t_3 - t_2)}{2} \quad \text{Equation 5.4}$$

$$t = \frac{L_H}{2v_T} + \frac{(L_T - L_H)}{v_T} + \frac{L_H}{2v_T} \quad \text{Equation 5.5}$$

$$t = \frac{L_T}{v_T} \quad \text{Equation 5.6}$$

Therefore, where the length of the hazard is less than the length of the train, the hazard length is not significant. As a result,

$$P[S_I : H] = \frac{N_T L_T}{24 v_T} \quad \text{for } L_H \le L_T \quad \text{Equation 5.7}$$

Conversely, where the hazard length is greater than the train length, Equation 5.7 changes to:

$$P[S_I : H] = \frac{N_T L_H}{24 v_T} \quad \text{for } L_T \le L_H \quad \text{Equation 5.8}$$

where N_T is the number of trains per day. This is the most commonly used unit for N_T within CP but the number of trains in any duration can be used to obtain this number. Generally, the longer the period is the more accurate the average number. Provided the train speed, v_T is in miles per hour, the denominator of 24 converts from hours to days of exposure time.

If the landslide of volume class, V_i, has a frequency of x events in y years, the probability, $P[H(V_i)]$, of the hazard, H, occurring in any given year is x/y. The risk of the landslide impacting a moving train or other track vehicle, and causing an accident is $P[Accident_I(V_i)]$ and

$$P[Accident_I(V_i)] = P[S_I : H(V_i)]\,P[H(V_i)] \qquad \text{Equation 5.9}$$

The frequency and therefore probability of the hazard, $P[H_I(V_i)]$, varies with the volume, V, of the landslide as shown by Hungr et al. (1999). If the frequency of the hazard exceeds one per year the binomial theorem as applied by Bunce et al. (1997) and Roberds (2005) should be used to calculate $P[Accident_I(V_i)]$. These higher frequencies generally are only relevant for rock fall events less than 1 m^3 or if L_H encompasses numerous hazards and is miles long.

It should be noted that $P[Accident_I(V_i)]$ is the sum of the probability of a derailment given a landslide hits a moving train, $P[Derail._I(V_i)]$, and the probability of train damage given a landslide hits a moving train, $P[Train\ damage_I(V_i)]$. There is no record of a rock fall less than 1 m^3 hitting and derailing a moving train in the CP-NHID, so this volume of landslide need not be considered in the calculation of derailment probability. CP records indicate that the smallest rock fall to derail a moving train was 1 m^3. Trains have been derailed by rock falls smaller than 1 m^3 but these incidents occurred when moving trains encountered stationary rocks on the track. This is considered a Type III interaction. The frequency of Type I interactions for each volume class needed to estimate $P[Accident_I(V_i)]$ has not been extracted from the CP-NHID. As will be shown, $P[Accident_I]$ is sufficiently low that the effort to extract $P[Derail._I]$ and $P[Train\ damage_I]$ information is not justified as part of this research.
Furthermore, information on the $P[Train\ damage_I]$ is notoriously unreliable because the damage is not attributed to any location or volume of event since the damage is not detected until train reaches the next inspection point. As a result, unless the landslide impacts the cab of the locomotive, the potential for a health loss of the train crew is exceedingly low. As a result, $P[Derail._I]$ will be the primary focus of discussion for the

remainder of the chapter. The ratio of $P[Derail._I]$ and $P[Train\ damage_I]$ determines the $P[Derail._I{:}Accident_I]$. This ratio is dependent on the volume of the hazard so this term is $P[Derail._I{:}Accident(V_i)]$.

5.5.2.1 Type I - Probability of derailment

Computation of the probability of a moving train derailed by a moving landslide at a single location requires the summation of each class of landslide volume. The probability is calculated for a representative length of hazard using Equation 5.10:

$$P[Derail._I] = \sum_{all\ V_i} P[S_I : H(V_i)] P[H_i(V_i)] P[Derail._I : Accident(V_i)] \quad \text{Equation 5.10}$$

where each volume class, V_i, will have a corresponding $P[H(V_i)]$ and $P[Derail._I{:}Accident(V_i)]$ is determined from the CP NHID.

It is possible to determine the probability and the frequency of derailments expected over a subdivision or length of track by summing the $P[Derail._I]$ for each known landslide location.

5.5.2.2 Type I - Probability of one or more fatalities

The probability of a fatality, F, is the sum of the probability of a landslide impacting the train and directly killing the operator(s), $P[F_I{:}Train\ damage]$, and the probability of the landslide derailing the train and a fatality ensuing, $P[F_I{:}Derail.]$. When considering $P[F_I{:}Accident]$ the probability of a fatality increases the closer the impact of the hazard is to the cab at the head-end of the first locomotive where the train crew resides. The probability distribution function (Roberds 2005) of a fatality given a train accident, $p[F_I{:}Accident]$, is expected to be represented by a function with a large probability of fatal events if the hazard impacts the head-end of the locomotive near the cab. It is expected to reduce rapidly to near zero a few car lengths from the head-end of the train.

A number of probability distributions could be used to represent this function including the exponential, Weibull, gamma, log-normal, or trapezoidal. A plot of these functions with appropriate factors is provided in Figure 5.9. The Weibull appears to be the most useful since it can be manipulated to provide a non-zero probability of fatality in the event that the landslide impact is at the front of the train. However, it could be argued that a landslide impacting the front of the train should be considered as a Type III interaction where the landslide has impacted the track in advance of the oncoming locomotive.

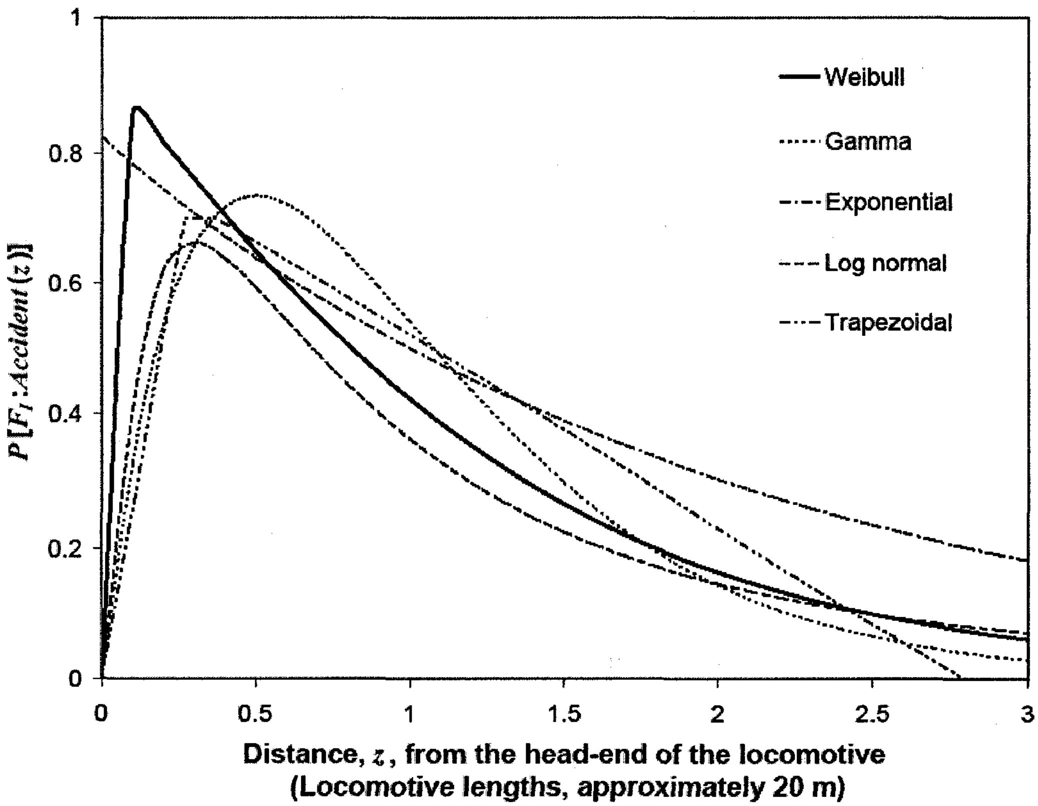

Figure 5.9 Probability of a fatality given a landslide impacts a moving train as a function of where the landslide impacts the train.

The probability of a fatality is highest if the landslide impacts the cab of the locomotive about one tenth to two tenths of the locomotive length from the head-end of the locomotive. The distributions selected can be adjusted to represent the geometry and dimensions of the locomotive. In this case, the length of the train in Equations 5.7 or 5.8 is limited to the length of the locomotives because an impact on the freight cars is very unlikely to result in a fatality of the crew riding in the cab.

Both $P[F_I{:}Train\ damage]$ and $P[F_I{:}Derail.]$ are expected to be dependent on the volume of the landslide. The larger the landslide is the higher the probability of a derailment. As a result, the larger the landslide is the higher the probability of a fatality.

To use Equations 5.7 or 5.8 the length of the locomotive impacted by the landslide, with L_H is required. L_H could be estimated in various ways but a value equal to the cube root of the volume of the landslide, suggested by Roberds (2005), appears reasonable, especially given that the area of impact is limited to that which can occur while the train passes at track speed. Therefore if the $p[F_I{:}Accident]$ is known or can be approximated using one of the distributions above then:

$$P[F_I : Accident] = \int_a^b p[F : Accident, x]dx \qquad \text{Equation 5.11}$$

where

$$a = E[F_I : Accident] - \frac{V_i^{\frac{1}{3}}}{2} \text{ and } b = E[F_I : Accident] + \frac{V_i^{\frac{1}{3}}}{2} \qquad \text{Equation 5.12}$$

and $E[F_I{:}Accident]$ is the maximum expected value of $p[F_I{:}Accident]$. This formulation calculates the probability of a fatality given the landslide impacts the locomotive centred on the location most likely to result in a fatality.

There have been no cases of a landslide impacting the locomotive of a moving train resulting in a fatality. As a result, there is no guidance with respect to this probability.

As discussed further in Section 5.5.4 a reduction in speed should reduce $P[F_I{:}Derail.]$ but it will increase $P[F_I{:}Train\ damage]$ by increasing the exposure time.

The equation to calculate the probability of a fatality becomes

$$P[F_I] = \sum_{all\ V_i} P[S_I : H(V_i)]P[H(V_i)]P[F(V_i)_I : Accident] \qquad \text{Equation 5.13}$$

The probability of a moving MOW vehicle being hit by a moving landslide is calculated in the same way using the length of the track unit occupied by the operators as the L_T. This is significantly lower than $P[F_I]$ for a train because the frequency of MOW vehicles along the track is commonly an order of magnitude less than the train frequency.

5.5.2.3 Type I - Example of Maple Ridge, BC

An example is provided using the landslide frequency and dimensions from the Maple Ridge, BC data summarized in Chapter 4. The change in risk given extreme and non-extreme antecedent precipitation conditions is analysed in Section 5.7.2.

A Risk of derailment

As reviewed in Section 4.5.9 there have been at least 50 landslides in 32 years. However, as soon as the first landslide occurs and blocks the track, no further trains can pass until the debris is removed. If there are ongoing landslides, the track will not be cleared of debris until it can be done safely (as discussed in Section 5.4.2.2). As a result, only the first landslide in each episode is considered a hazard to passing trains. Therefore, the hazard frequency is equivalent to the episode frequency of 18 episodes in 32 yeas or an annual probability of 0.56. This can be further subdivided by volume class. However, from Table 4.3, excluding the landslides greater than a million cubic metres, and using the cube root volume/width relationship (Roberds 2005), the average landslide width is 17 m (0.011 miles). This is less than L_T. Therefore, $L_H \leq L_T$ and Equation 5.7 is applicable. Combining Equations 5.7 and 5.9 and using the values in Table 5.4, the annual risk of a freight and passenger trains being impacted by a landslide while both are moving is calculated using Equation 5.14.

$$P[Accident_I] = \frac{N_T L_T}{24 v_T} P[H] \qquad \text{Equation 5.14}$$

Table 5.4 Summary of variables and resulting probability of a train being impacted by a rapid landslide

Train type	Train length, L_T			Train speed		Average train frequency	$P[Accident_I]$
	(km)	(ft)	(miles)	(mph)	(kmph)	(trains/day)	
Freight	2740	9,000	1.7	30	48	22.5	0.030
Passenger[1]	0.17	569	0.11	50	80	7.1 [2]	$3.8*10^{-4}$
						Sum	0.030

[1] - Assuming passenger trains consist of 6 cars, each 25.9 m long (Bombardier 2008) plus a 17.8 m long locomotive (West Coast Express 2008a).
[2] - Ten trains per day 5 days a week (West Coast Express 2008c)

This is consistent with the CP NHID that includes a single incident where a moving train was impacted by a debris flow in the 32 year period of record ($P[Accident_I]$ = 0.031).

For the Maple Ridge, BC landslides the $P[Derail._I:Accident(V_i)]$ is assumed to be equal to one for all landslide volumes above 10 m^3 since the landslides in this area are of a sufficient volume and viscosity to cover the track and bury it such that a moving train will ride up on the debris and derail. Equation 5.10 is used to calculate $P[Derail._I]$. Since the volume of all the recorded landslide in the CP NHID for this site are greater then 10 m^3 the $P[Derail._I:Accident(V_i)]$ equals the $P[Accident_I]$ and $P[Train\ damage_I]$ equals zero.

B Risk of fatality

The risk of a fatality is proportional to the volume of the landslide. As discussed in Section 5.5.2.2 there have been no fatalities caused by a landslide hitting a moving train. As a result, no empirical data is available to guide the selection of $P[F_I:H(V_i)]$.

The probability of a landslide impacting a freight locomotive is estimated using Equations 5.7 or 5.8 with L_T set to the length of the lead locomotive impacted by the landslide. Given that $p[F_I:Accident]$ is not known, $P[F_I:Accident]$ is set as per Table 5.5 and L_H is set to the cube root of the average landslide volume in each volume class, as per Table 5.5. Using Equation 5.8:

$$P[S_I:H] = \frac{(22.5\ \text{trains/day})(50\ \text{m}^3)^{1/3}}{(1{,}609\ \text{m/mile})(30\ \text{mph})(24\ \text{hrs/day})} \qquad \text{for } 10\ \text{m}^3 < V_i < 100\ \text{m}^3$$

$P[S_I:H] = 7.2*10^{-5}$

Similarly, for the locomotive of a passenger train:

$$P[S_I:H] = \frac{(7.1\ \text{trains/day})(50\ \text{m}^3)^{1/3}}{(1{,}609\ \text{m/mile})(50\ \text{mph})(24\ \text{hrs/day})} \qquad \text{for } 10\ \text{m}^3 < V_i < 100\ \text{m}^3$$

$P[S_I:H] = 2.1*10^{-5}$

However, when considering the probability of one or more fatalities on a passenger train, the entire length of the passenger cars has to be considered, so $L_H \leq L_T$ such that Equation 5.7 governs and:

$$P[S_I:H] = \frac{(7.1\ \text{trains/day})(155.4\ \text{m})}{(1{,}609\ \text{m/mile})(50\ \text{mph})(24\ \text{hrs/day})}$$

$P[S_I:H] = 5.7*10^{-4}$

Using Equation 5.13 for each landslide volume class, V_i:

$$P[F_I(V_i)] = P[S_I:H(V_i)]P[H(V_i)]P[F_I(V_i):Accident]$$

The risk of a fatality and the sum of all the volume cases is calculated and compiled in Table 5.5.

Table 5.5 Summary of the probability of one or more fatalities for a landslide impacting a moving freight train.

Landslide volume ($\log_{10}$ m^3)	$L_T(V_i)$ (m)	$P[H(V_i)]$[1] per year	$P[F_I(V_i)$: $Accident]$[2]	$P[F_I(V_i)]$
$1 < V_i \le 2$	3.8	5/32	1/100	$1.2*10^{-7}$
$2 < V_i \le 3$	8.2	7/32	1/10	$3.5*10^{-6}$
$3 < V_i \le 4$	18	1/55 [4]	1	$6.2*10^{-6}$
$4 < V_i \le 7$	170	4/217	[3]	
			Total	$9.8*10^{-6}$

[1] - The number of events from Tables 4.7, 4.8, and 4.9 in each volume class for the 32 year period from 1975 to 2007 is used to estimate $P[H(V_i)]$. The limited number of 10 m^3 to 100 m^3 events suggests an under reporting of this volume class but is also partially attributed to the averaging of landslide volumes per episode.
[2] - The $P[F_I(V_i):Accident]$ are estimated orders of magnitude given that no data is available.
[3] - As per the discussion at the beginning of Section 5.5.2, very large and below track landslides are considered too slow to impact a moving train and therefore not considered.
[4] - The $P[H(V_i)]$ for $3 < V_i \le 4$ is considered an upper bound based on events 5 and 6 in Table 4.9.

As can be seen in Table 5.5 the cube root of the average landslide volume provides a reasonable approximation of the length of a locomotive impacted by a landslide from above.

Similarly, the probability of one or more fatalities resulting from a landslide impacting a moving passenger locomotive is summarized in Table 5.6.

Table 5.6 Probability of one or more train crew fatalities for a landslide impacting the locomotive of a moving passenger train

Landslide volume ($\log_{10}$ m^3)	L_T (m)	$P[H(V_i)]$ per year	$P[F_I(V_i)$: *Accident*]	$P[F_I(V_i)]$
$1 < V_i \leq 2$	3.8	5/32	1/100	$2.2*10^{-8}$
$2 < V_i \leq 3$	8.2	7/32	1/10	$6.6*10^{-7}$
$3 < V_i \leq 4$	18	1/55	1	$1.2*10^{-6}$
			Total	$1.9*10^{-6}$

The probability of a passenger train crew being fatally injured is about 1/5 that of a freight train crew because of the number of trains per day and the higher speed of the passenger trains.

Table 5.7 is a summary of the probability of one or more fatalities resulting from a landslide impacting a moving passenger train. The expected number of fatalities is based on all the passengers within the portion of the train that is impacted being killed. The portion of the train impacted is based, as before, on the cubed root of the landslide volume.

On average, the West Coast Express (2008b) carries 8,402 passengers per day or 840 per train. The Port Haney and Maple Meadows Stations are east and west of the CASC 102.5 to 104.9 landslide area. The Port Haney Station is the second to last of the eight stations on the commuter-transit rail service between Vancouver and Mission. Therefore, a given commuter passenger train is about 2/7 full, or carrying 240 passengers when it passes the Maple Ridge landslide area. Given the average commuter-train car length of 6 cars times 25.9 m per car the portion of the train carrying passengers is 155.4 m long. This works out to 5.4 passengers per metre of train when it is full and 1.5 passengers per metre of train when it passes Maple Ridge. This may seem high but the trains have four seats across and two levels of seating. Therefore, one fatal train accident caused by a landslide impacting a moving train is expected to result in between 21 and 95 fatalities depending on the volume of the landslide, if the train is full. Again, depending on the volume of the landslide, 6 to 27 fatalities would be expected if the train were full proportional to the number of stations it has serviced or has yet to service. These are likely the minimum number of fatalities given that the additional passengers could die of injuries sustained in parts of the train not directly impacted by the landslide, but hurt by the ensuing derailment expected for the larger landslide volumes classes.

Table 5.7 Probability of one or more passenger fatalities for a landslide impacting a moving passenger train

Landslide volume ($\log_{10}$ m^3)	L_T[1] (m)	$P[H(V_i)]$ per year	$P[F_I(V_i)$: $Accident]$[2]	$P[F_I(V_i)]$	No. of fatalities	
					Full train	Partially full train
$1 < V_i \leq 2$	155	5/32	1/50	$1.8*10^{-6}$	21	6
$2 < V_i \leq 3$	155	7/32	1/5	$2.5*10^{-6}$	44	13
$3 < V_i \leq 4$	155	1/55	1	$1.0*10^{-5}$	95	27
			Total	$3.7*10^{-5}$		

[1] - The length of the train is the length of the six, 25.9 m long commuter cars and does not include the length of the locomotive.
[2] - The $P[F_I(V_i){:}Accident]$ are estimated orders of magnitude because no data is available. These probabilities are increased from those of the locomotive crew because the structural integrity of a passenger car is less than that of a locomotive.

Considering the complete West Coast Express Mission to Vancouver commuter-transit rail service, the risk of one or more fatalities will be about 3 to 4 times the risk levels calculated for the site at Maple Ridge because there are at least 3 other areas with comparable landslide activity to that of Maple Ridge. This is because there are at least three other areas with comparable landslide activity to that of Maple Ridge along the commuter-transit rail system. As noted previously, risks from some volume classes will be different for east and west bound passenger trains because of the double track infrastructure in this area.

5.5.2.4 Type I - Conclusion

In conclusion, for rapidly moving landslides hitting a moving train, the probability of a train being impacted by a landslide, and a train being derailed by a landslide can be calculated. Due to the low frequency of this event, there is insufficient data on fatal train accidents resulting from moving landslides impacting moving trains within the CP-NHID to assess the probability of one or more fatalities given an accident or derailment.

However, by using assumed values for some parameters, estimates of the risk of fatalities can be approximated.

For the case study in Section 4.5, the calculated and empirical probability of a train being impacted is one in 30 years. The collective risk of fatality to CP freight train crews is $9.8*10^{-6}$ per year (from Table 5.5). The collective risk to the passenger train crews is $1.9*10^{-6}$ per year (from Table 5.6). Both these values are for CP train crews. The risk of a fatality of a single trip and an individual train crew member would be lower than this value as a proportion of the number of trains and work force respectively. These values are for this single area of track. Numerous other hazard areas would have to be considered to estimate the risk for the entire subdivision or system. The risk of one or more fatalities within the passenger rail service is estimated at $3.7*10^{-5}$ or one every 27,000 years. Due to the assumed probabilities of a fatality given a train being impacted, the highest risk events are for the larger volume cases. This may not be true because generally, larger volume landslides travel slower than smaller volume landslides. However, this assessment does not directly account for landslide velocity.

As would be expected, slowing trains increases the exposure time and therefore the risk of being impacted. This is discussed further in Section 5.5.4 but is more than compensated by the reduction in risk when a train encounters a landslide in its path.

These risk levels will be compared to tolerable risk levels in Section 5.8.

5.5.3 Type II - Stationary train is impacted by a moving hazard (Moving Hazard / Stationary train)

As discussed previously, the goal of a railway company is to achieve train movement. As a result, they minimize the length of time trains are stationary. Generally, trains are only stationary for more than a few hours in a rail yards, which is typically located in large flat areas not influenced by landslide hazards. In addition, the locations of sidings or passing tracks, where one train is stationary while a second passes, have been preferentially selected (with a few exceptions) where they are the less costly to construct, which requires avoidance of areas exposed to landslide hazards. Railways have selected siding locations requiring the limited grading and affording easier construction. Easy sites are generally on flat ground away from natural landslide hazards. Where sidings were unknowingly or unavoidably coincident with landslide hazards the hazards have generally been mitigated or in some cases the sidings abandoned.

One scenario where a train is exposed to a higher risk of being impacted by a landslide is when a train is stopped due to a hazard having affected the track ahead of it. This is often referred to as "stacking trains" while the railway is waiting for the service disruption to be rectified. "Stacking trains" allows the railway to arrange high priority trains such that the most profitable sequence of trains can pass the landslide once service is resumed. Unfortunately, electrical power failures, signal failures and geotechnical failures may all be triggered by severe weather resulting in more frequent service disruptions. If additional landslides occur during these disruptions, stopped trains can be at increased risk from weather induced landslides.

The probability of a landslide affecting a stationary train is dependent on the length of time the train is stationary.

A number of assumptions are required to derive the following relationships:

1. The location of the stopped train and the location of the landslide are independent. This may not be always true especially is the railway identifies specific non-hazardous stopping locations.
2 The average train length can be used to represent all trains.
3. The spatial distribution of landslides is uniform within the identified landslide area.
4. The timing of each landslide is assumed independent and therefore a uniform temporal distribution of landslides can be assumed. This is contrary to the proposition that landslides are induced by precipitation. However, this condition is true if PIL and non-PIL conditions are treated separately.

The probability of a landslide hitting a stationary train, $P[Accident_{II}]$ is proportional to the fraction of the track occupied by the train, $P[Accident_{II}:H]$, the probability that the train is stationary when the landslide occurs, $P[t_s:H]$ and the probability of the hazard, $P[H]$.

The probability that the train is stationary is proportional to the portion of the year, t_s, that the train is stopped. Therefore:

$$P[t_s:H] = t_s \qquad \text{Equation 5.15}$$

making sure the units of t_s are years.

$$P[Accident_{II}:H] = L_T / L_R \quad \text{Equation 5.16}$$

where L_R is the length of the railway (R) with frequency of landslides $P[H]$. If $L_T \geq L_R$, $P[Accident_{II}:H] = 1$. For example all landslides falling within L_{Tr} will hit a train because L_R is fully occupied by a train.

Then the probability of a landslide hitting a stationary train, $P[Accident_{II}]$ is:

$$P[Accident_{II}] = P[t_s : H]P[Accident_{II} : H]P[H] \quad \text{Equation 5.17}$$

For cases where the L_R is long, the frequency of the hazard may result in $P[H]$ approaching unity. In these cases the binomial theorem adopted by Bunce et al. (1997) should be used where F_H is the frequency of the hazard in events per year.

$$P[Accident_{II}] = P[t_s : H]\left\{1 - \left(1 - P[Accident_{II} : H]\right)^{F_H}\right\} \quad \text{Equation 5.18}$$

As indicated, the number of stationary trains impacted by moving landslides is highly dependent on the length of time a train stops. Given this information is case specific this will not be investigated further here.

As indicated in Section 4.5.3 there is double track at Maple Ridge, BC. As a result, there is no reason for a train to stop below the hazard unless it is stuck in the debris. Where there are two tracks a train stopped by the landslide can move away from the obstruction without hindering work-trains requiring access to the landslide.

The probability of a fatality of a train crew would be calculated by reducing the length of the train to the length of the locomotive occupied by the train crew, which is less than 10 m long.

During higher PIL conditions trains and especially passenger trains should be directed to back away from obstructions and only stop once they are in a safe location. Generally passenger trains return to the nearest station that the passengers detrain and are transferred to alternate transportation modes.

5.5.4 Type III - Train approaches hazard that occurred previously (Stationary hazard / Moving train)

The occurrence of a moving train impacting landslide material on the track, or encountering unsupported track, or otherwise impassable track conditions are the most common of the Type I, II and III interactions. This is because even on the busiest corridor, the track is vacant at least 80% of the time. Events that occur when the track is vacant are only a hazard to the next train along the track. Consideration of the probability of a moving train encountering these conditions is dependent on several factors. There are multiple sub-sets of this event as shown in Figures 5.4 to 5.7.

The following conditions are relevant to the risk estimation:

1. The landslide must be a sufficient volume to result in one or more of the outcomes in Figures 5.4 and 5.7. Therefore, only landslides larger than 0.1 m^3 (an approximately 0.5 m cube) will be considered.
2. The landslide may occur within or beyond the sight distance (SD) of the train crew. If the landslide impacts the track outside the SD, the train crew should be able to reduce the severity of the impact by putting the train's brakes to "emergency" (all brake systems on). If the landslide influences the track within the sight distance of the train crew, the severity of the collision is increased because the train has less opportunity to slow down. As a result, higher train speed increases the severity of the consequences because it increases the stopping distance and the momentum at impact.
3. In areas where landslides are excessively costly to stabilize or avoid, many railways have installed hazard detection systems (HDS) as discussed in the Glossary. Most railways utilize a limited selection of track side hazard-detection-systems. These include trip wire rock fall detection signal or slide (AREMA 2003) fences, electro-level tip-over posts and other less common systems. These are connected to the rail signal system so that when a hazard detection system is tripped, the signal system directs all subsequent trains to proceed at restricted speed. If the track has been damaged or blocked, either the train will stop short of the damage, or the consequences of the derailment will be reduced because of the reduced speed of the train traveling at restricted speed. Restricted speed directs the crew to operate at a speed that allows stopping within half the sight distance. Therefore, a train traveling at restricted speed should be able to stop before encountering the impassable track. Restricted speed must not exceed 24 kmph (15 mph). The quantitative risk reduction provided by these systems will be assessed in

Section 5.7.1. In many cases train crews are provided with warnings but are still only able to slow the train before encountering the damaged or obstructed track. However, the slower train speed reduces the consequences of the train accident. It should be noted that HDS also reduce average train speeds because they trigger false alarms and cause prolonged restricted speed conditions if they are not promptly reset. The quantitative risk assessment methodology developed below should aid in the rationalization of the expenditures required to install additional or remove existing HDS systems.

The following assumptions are required to make it possible to derive the relationships that follow. These include:

1. The speed of the trains is the posted track speed, or where applicable, restricted speed of 24 kmph (15 mph).
2. The temporal distribution of trains and landslides is uniform throughout a 24 hour period.
3. The timing of each landslide is assumed independent and therefore a uniform temporal distribution of landslides can be assumed. This assumption will be discussed further with respect to precipitation conditions in Section 5.7.2.
4. Rail traffic and landslide activity are independent. Trains do not trigger landslides especially those that occur before their arrival. Smaller sub-grade landslides triggered by the previous train would be considered to have occurred prior to the on-coming train.
5. Only the first train to encounter a hazard is considered at risk.
6. The probability of derailment, train damage, and a train stopping incident before encountering the landslide is a function of the train speed.

5.5.4.1 Landslide hazard

The quantitative risk estimation is undertaken using the following method. The temporal probability of a landslide of volume class V_i is $P[H(V_i)]$. If the landslide has a frequency of x events in y years, the probability of H in any given year is x/y. Again, if the landslide frequency is such that more than one landslide is likely per year, the binomial theorem (Bunce et al. 1997, Roberds 2005) should be utilized.

5.5.4.2 Track impassable

Given the volume of the landslide, the probability that an above track landslide obstructs or a below track landslide undermines the track can be estimated. This is the conditional probability, $P[Impass.:H(V_i)]$ that the track will be impassable given the landslide occurs. This will be close to unity for most types and for larger volumes of landslides. However, $P[Impass.:H(V_i)]$ would be less than unity for a sub-grade landslide that encroaches on the shoulder of the track, but does not undermine the track. In this case, the first train over the landslide area may not be affected and subsequent trains may be able to proceed under the inspection of a watchperson, until the landslide damage can be repaired. However, there is a non-zero probability that the landslide could retrogress and derail a train.

5.5.4.3 Type of track unit

In this step the probability of a freight train, passenger train, or MOW track vehicle is evaluated. The probability of a given track unit is proportional to the number of freight trains, passenger trains, and MOW vehicles divided by the sum of all the track units. The sum of $P[Freight]$, $P[Passenger]$ and $P[MOW\text{-}TV]$ must equal unity.

$$P[Freight] = N_{Freight}/(N_{Freight}+N_{Passenger}+N_{MOW\text{-}TV}) \quad \text{Equation 5.19}$$

$$P[Passenger] = N_{Passengert}/(N_{Freight}+N_{Passenger}+N_{MOW\text{-}TV}) \quad \text{Equation 5.20}$$

$$P[Train] = P[Passenger]+ P[Freight] \quad \text{Equation 5.21}$$

$$P[MOW\text{-}TV] = N_{MOW\text{-}TV}/(N_{Freight}+N_{Passenger}+N_{MOW\text{-}TV}) \quad \text{Equation 5.22}$$

$$\Sigma P[track\ units] = 1 \quad \text{Equation 5.23}$$

Where $N_{Freight}$, $N_{passenger}$, and $N_{MOW\text{-}TV}$ are the number of each class of track units and are expressed in consistent units of track units per time period.

On high traffic rail lines there could be up to 40 to 45 trains and 1 to 2 MOW track vehicles per day, so $P[Train]$ would be 40/41.5 or 0.964. On a moderate traffic lines with 10 trains per day Transport Canada (Railway Association of Canada 2008) requires two inspections per week and MOW crews might pass over the track 1 to 2 times more per week. Therefore, $P[Train]$ would be 70/73.5 or 0.952. At the other extreme, on very low traffic rail lines, where the frequency of hazards is high and no signal system exists, there can be an inspection in front of each train plus normal MOW. In this case there are more track vehicle trips than train trips. Assuming 2 trains per day, 2 track inspections per day (one in front of each train), and 1 MOW trip per week, the resulting $P[Train]$ is 14/29 or 0.48. This is the situation on the Nelson Sub in southeast BC between Creston and Nelson where there are only two trains a day and each is preceded by an inspection vehicle.

5.5.4.4 Signal system

$P[TC]$ is the probability that a track circuit is present. A track circuit is a system used by the Signals and Communications (S&C) departments of railways whereby the rails are used as conductors to transmit electrical signals. The information is used by the Centralized Traffic Control (CTC) to locate trains and direct their movement. For a given section of track the presence or absence of a track circuit is known. Therefore, $P[TC]$ will normally be unity or zero. Where there is a potential for the track circuit to be out of service and normal train operations prevail there may be cause to assign a value of slightly less than unity to $P[TC]$. Abbott et al. 1998a introduced factors into their rock fall hazard and risk assessment methodology to account for the influence of track circuit and hazard detection systems, but they did not complete a quantitative assessment of the influence of these measures.

A Train inside or outside signal

When an HDS or track circuit is present, a train can receive warning of a landslide in its path before it encounters the landslide. However, a train receives the warning and the directions to proceed from the track-side signal system. Therefore, if the train is past the last signal (spatially before the landslide), when the landslide occurs, the train does not receive the warning. Figure 5.10 depicts various train, signal, and landslide scenarios.

Scenario 1 of Figure 5.10 shows the condition where no landslide occurs and no warning is provided to the approaching train. Scenario 2 shows the desired conditions where the train receives warning of the landslide prior to entering the signal block. In scenario 3 the train has passed the signal, in front of the landslide, prior to the hazard occurring.

In this scenario the signal system does not warn the train crew to slow to restricted speed, and the train encounters the hazard at regular track speed.

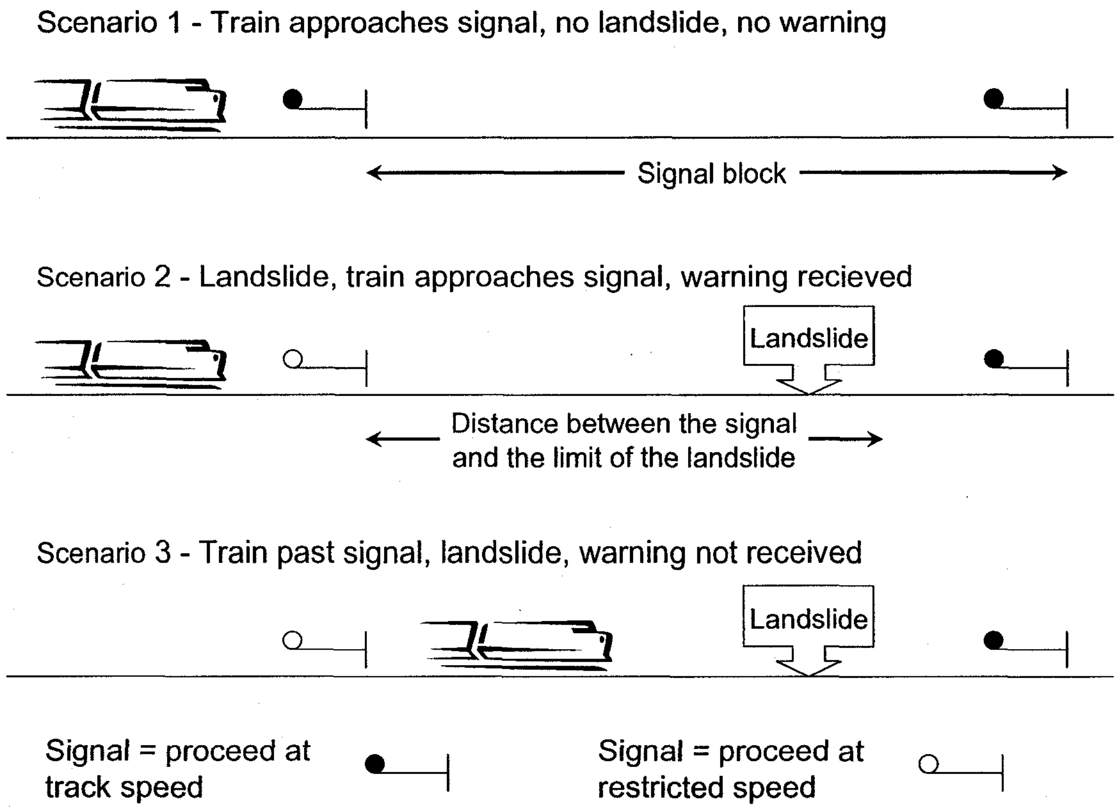

Figure 5.10 Scenarios where train does and does not receive warning of a landslide from the signal system

The calculation of the time, *t*, a train is within the nearest signal is similar to but simpler than the calculation of the time the moving train is exposed to the falling hazard in Section 5.5.2.

$$t = \frac{L_S}{v_T} \qquad \text{Equation 5.24}$$

For the period, *t*, a train is not protected by any components of the signal system. L_s is the length of the signal block and v_T is the train speed. If the hazard is limited to a specific section of track within the signal block, L_s in Equation 5.24 can be shortened such that L_s is the distance between the signal and the limit of the landslide hazard as shown in Scenario 2 of Figure 5.10.

Some railways use talker systems. A talker system consists of an HDS and radio system capable of broadcasting an automated verbal radio warning when the HDS has been triggered. However, the use of the radio for other communication precludes the HDS providing a positive notification. The use of an exception broadcast does not provide a vital signal system because no warning can occur when other radio communications are being broadcast at the same time, the system is not working, or it has not been triggered. As a result, CP avoids deploying talker type systems.

The conditional probability that trains are inside the signal system given a signal system or HDS is present or is functional is $P[\textit{Train inside signal}]$. This probability is equal to the percent of time, t, trains are within the signal block, or between the signal and the far side of the hazard (whichever is smaller). This is equal to the time the head-end of the train takes to pass through the signal block, multiplied by the number of trains per day,

$$P[\textit{Train inside signal}] = \frac{N_T L_S}{24 v_T} \qquad \text{Equation 5.25}$$

where N_t is the number of trains per day. Provided L_s is in miles and the track speed, v_T, is in miles per hour, the denominator, 24, converts from hours to days of exposure time.

The probability of the train being outside the signal block is also needed. However, since the train is either inside or outside the signal:

$P[\textit{Train outside signal}] = 1 - P[\textit{Train inside signal}]$

As shown in Figure 5.5, if the train is inside the signal block, the outcomes are the same as if there was no signal system. If the train is inside the signal block, the train speed is equal to the track speed if the train encounters an obstruction. If the train is outside the signal block, the train speed is equal to the restricted speed if it encounters an obstruction. $P[\textit{Train inside signal}]$ and $P[\textit{Train outside signal}]$ influences the train speed which is required in Sections 5.5.4.5 - A to assess the stopping distance.

B Track circuit continuity

When the track circuit is intentionally or unintentionally connected or disconnected, the nearest signal shows a track occupation. This limits the authority of the approaching train to proceed (Abbott et al. 1998a). When track circuit continuity is broken, the S&C system notifies the Network Management Centre (NMC) that some unknown condition has occurred. Depending on the situation, the NMC will dispatch track maintenance personnel to inspect the area, or the NMC may provide authority for the train to proceed, at restricted speed, to assess the situation. If the track is undermined but left skeleton (Photo 5.1), the track circuit will be intact. Conversely, if the track is impacted by a rock slide, it may be broken, severing the track circuit. As a result, there is a conditional probability, $P[TC\ trig.:H\&TC]$, that the track circuit is broken by a landslide provided a hazard and a track circuit are present.

C Hazard detection system

As discussed above, there may also be a hazard detection system (HDS) present. The probability of an HDS, $P[HDS]$, can be set to unity where one is present or set at the rate they are deployed on the sub-division or region of the rail network.

The probability, $P[HDS\ trig.:H]$, that the HDS is tripped given one exists, and that the landslide event has tripped the HDS, should be near unity if the HDS is suited to the hazard. There is also the probability, $P[\text{HDS}\ trig.:NH]$, that the HDS is tripped but No hazard (NH) occurred (a false-positive). This results in train delays but no damage or health losses.

5.5.4.5 Type III - Outcomes

There are numerous outcomes resulting from a moving train encountering an obstruction of the track as illustrated in Figures 5.3 to 5.6. The probability of a train accident, track damage, and health loss are analysed in the subsequent sub-sections.

A Probability of train accident

The likelihood of a train accident is estimated by considering the probability that the train crew has sufficient time and information to stop the train before encountering the obstruction of the track. The probability of a moving train being derailed after running into a landslide, $P[Derail._{III}]$, should include a term that considers the speed of the train and the probability of a derailment, $P[Derail._{III}:H(V,Type)]$ and train damage given the volume and type of landslide, $P[Train\ damage._{III}:H(V,Type)]$. For this investigation the $P[Derail._{III}:H]$ and $P[Train\ Damage._{III}:H]$ are assumed to be independent of landslide volume and type. Further information on $P[Derail._{III}:H(V,Type)]$ and $P[Train\ Damage._{III}:H(V,Type)]$ could be extracted from the CP-NHID.

The speed of the train is influenced by whether or not the train receives notification from the signal system that a hazard may or may not have occurred. If the train has received notification from the signal system (as per the previous three subsections), it is assumed to be proceeding at restricted speed. Provided the sight distance to the obstruction is greater than the stopping distance at restricted speed the operators should be able to stop the train safely without incident.

The sight distance is highly variable. It is dependent on weather, day and night lighting, horizontal and vertical track curvature, the direction of travel, and vegetation, among other things. Sight distance must be assessed under average conditions in both directions and an average value identified to complete the analysis. Estimates of average conditions are used for subsequent examples.

Stopping distance is a complex field. Barney et al. (2001), and Loumiet and Jungbauer (2005) have investigated and developed means of considering the following influences on stopping distance:

1. the braking force of the train brakes,
2. the wheel to rail adhesion,
3. weight and distribution of the weight of the train or track vehicle,
4. speed with which the brakes are applied by the air pressure activated train braking system,
5. the initial speed of the train,
6. the grade of the track over the length of the train and its braking distance, and
7. other factors.

Some references describe:

1. a 9,070 tonnes (10,000 ton) train moving at 97 kmph (60 mph) on level ground requires 2 km (1.25 miles) to stop (Office of the Federal Coordinator for Meteorological Service and Supporting Research (OFCMSSR) 2002);
2. an average freight train traveling 88 kmph (55 mph) has a stopping distance of a 1.6 km (1 mile) or more (Roy and Mills 2005), and
3. an 8 car passenger train traveling 127 kmph (79 mph) has a stopping distance of 1.6 km (1 mile) or more (Roy and Mills 2005).

However, these examples do not indicate if they are emergency brake stopping distances or otherwise.

Computer programs are available for computing stopping distances of specific train and track configurations (Barney et al. 2001 and Loumiet and Jungbauer 2005). Figure 5.11 shows the relationship between train speed and emergency braking or stopping distance based on a similar figure in Loumiet and Jungbauer (2005). The heavy freight train consists of four locomotives and 100 loaded cars. The passenger train is an Amtrak train consisting of two locomotives, one baggage car, and thirteen passenger cars, and is consistent with actual brake test data from the Southern Pennsylvania Transportation Authority. The data shown in Figure 5.11 is for specific trains, rail and track grade conditions, and therefore cannot be used for all trains. However, Figure 5.11 does provide an indication of the variation in braking distance between freight and passenger trains. The examples in the subsequent sections are based on the Loumiet and Jungbauer (2005) information in Figure 5.11. Other information included in Figure 5.11 shows the same tendency for lighter shorter trains to stop in a shorter distance from the same traveling speed, but suggest Loumiet and Jungbauer (2005) may be non-conservative.

Using Figure 5.11, the stopping distance is determined for the track speed, and restricted speed. The stopping distance is then used in the analysis below to determine the probabilities of the possible outcomes of the train landslide interaction.

If the sight distance, D_{Si}, is less than the stopping distance, D_{St}, the operator does not see the obstruction until it is too late for the operator to stop the train before reaching the obstruction. Therefore, there is a high likelihood of a derailment or train damage. The shorter the sight distance in comparison to the stopping distance (lower

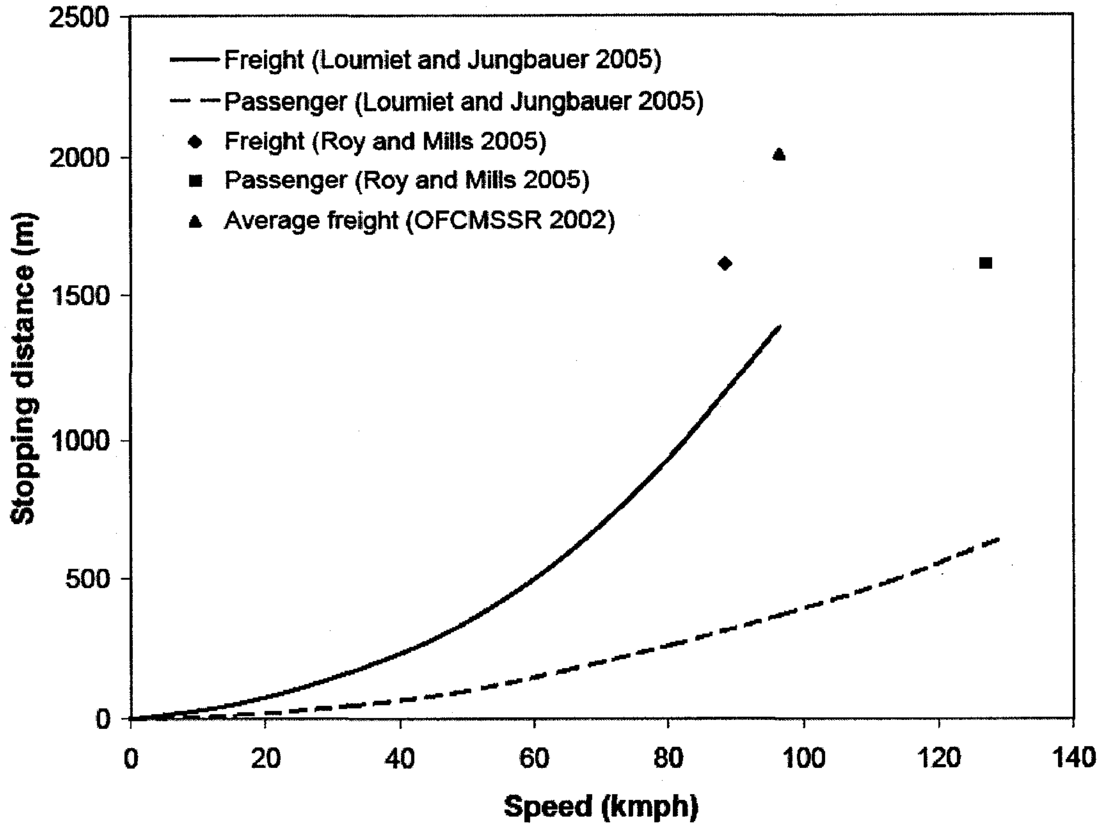

Figure 5.11 Train speed versus braking distance after Loumiet and Jungbauer (2005)

D_{Si_r}/D_{St_r}) the higher the likelihood of a derailment, and the lower the probability of train damage. As D_{Si_r}/D_{St_r} approaches zero the probability of no accident approaches some residual value. As the ratio of the sight distance to stopping distance approaches one half, the probability of a derailment decreases, and the probability of train damage and the train stopping increases, because the operator has more time to reduce the speed of the train resulting in a less severe impact with the obstruction. As the ratio of the sight distance to the stopping distance approaches one, the probability of a derailment and train damage approaches some residual value, and the probability of a train stopping approaches a value close to one. There is always a residual chance that the operator does not respond appropriately even if the sight distance is greater than the stopping distance so $P[Derail._{III}:H]$ and $P[Train\ damage_{III}:H]$ never equal zero and $P[Train\ stops_{III}:H]$ never equals unity. These conditions are summarized as:

$$P[Accident_{III}:H] = P[Derail._{III}:H] + P[Train\ damage_{III}:H] \qquad \text{Equation 5.26}$$

$P[Train\ stops_{III}{:}H] + P[Accident_{III}{:}H] = 1$ Equation 5.27

for $\frac{D_{Si}}{D_{St}} \to 0$

$P[Derail._{III}{:}H] \to 1 - \delta_D$

$\delta_{Td} < P[Train\ damage_{III}{:}H] < P[Derail._{III}{:}H]$ and

$P[Train\ stops_{III}{:}H] << 1$ Equation 5.28

for $\frac{D_{Si}}{D_{St}} \approx \frac{1}{2}$

$P[Train\ damage_{III}{:}H] \approx P[Derail._{III}{:}H]$ and,

$P[Train\ stops_{III}{:}H] << 1$ Equation 5.29

for $\frac{D_{Si}}{D_{St}} \to 1$

$P[Derail._{III}{:}H] \to \delta_D$

$P[Train\ damage_{III}{:}H] \to \delta_{Tr}$ and

$P[Train\ stops_{III}{:}H] \to 1 - \delta_D - \delta_{Tr}$ Equation 5.30

Where δ_D and δ_{Tr} are small numbers representing the residual probability that a derailment or train damage, respectively, can occur, even though the train operators are able to see the obstruction of the track within their sight distance. This would include exceeding the restricted speed such that they were unable to stop or slow the train before hitting the obstruction or not identifying the obstruction because it was indiscernible within the sight distance.

For this research the following relationships are adopted. The exponential integral (normal distribution) is used to provide smooth transition between low, medium, and high probabilities of a train accident. Other functions could be used to achieve similar results.

For $0 \le \frac{D_{Si}}{D_{St}} \le 2$, this means the sight distance is less than twice the stopping distance.

$$P[Derail._{III} : H] = \delta_D + \left(1 - \delta_D - \delta_{Td}\right)\int_{-\infty}^{b} \frac{1}{\sqrt{2\pi\sigma_D}} e^{-a}$$ Equation 5.31

Where

$$a = \left(1.5 - \frac{D_{Si}}{D_{St}} - \mu_D\right)^2 \Big/ 2\sigma_D^2$$

$b = D_{Si}/D_{St}$,

μ_D is the expected value at value of D_{Si}/D_{St} at $P[Derail._{III}] = 0.5$, and

σ_D is the standard deviation or steepness of the probability of derailment function.

Similarly, for a train stops incident,

$$P[Train\ stops_{III} : H] = (1 - \delta_D - \delta_{Td}) \int_{-\infty}^{b} \frac{1}{\sqrt{2\pi\sigma}} e^{-c} \qquad \text{Equation 5.32}$$

Where

$$c = \left(\frac{D_{Si}}{D_{St}} - \mu_{Ts}\right)^2 \Big/ 2\sigma^2$$

$b = D_{Si}/D_{St}$

μ_{Ts} is the expected value at value of D_{Si}/D_{St} at $P[Train\ stops{:}H] = 0.5$, and

σ_{Ts} is the standard deviation or steepness of the probability train stops function.

It follows that:

$$P[Accident_{III} : H] = 1 - P[Train\ stops_{III} : H] \qquad \text{Equation 5.33}$$

$$P[Train\ damage_{III} : H] = P[Accident_{III} : H] - P[Derail._{III} : H] \qquad \text{Equation 5.34}$$

The $(1 - \delta_D - \delta_{Td})$ term in Equations 5.31 and 5.32 are scaling factors to account for δ_D and δ_{Ts} .

For $\frac{D_{si}}{D_{st}} \geq 2$, i.e. the sight distance is more than twice the stopping distance.

$P[Derail._{III}{:}H] = \delta D$ Equation 5.35

$P[Train\ damage_{III}{:}H] = \delta_{Td}$, Equation 5.36

$P[Train\ stops_{III}{:}H] = (1 - \delta_D - \delta_{Td})$ Equation 5.37

The value of δ_D and δ_{Td} are set to 0.05 for this research indicating 19 out of every 20 train crews identify and respond appropriately when they encounter an obstruction of the track. The database is incomplete with regard to sight distance and therefore no data are available to support this assumption. Figure 5.12 depicts these relationships using $\mu_D = 1.5$, $\sigma_D = 0.2$, $\mu_{Ts} = 1.1$, and $\sigma_{Ts} = 0.1$.

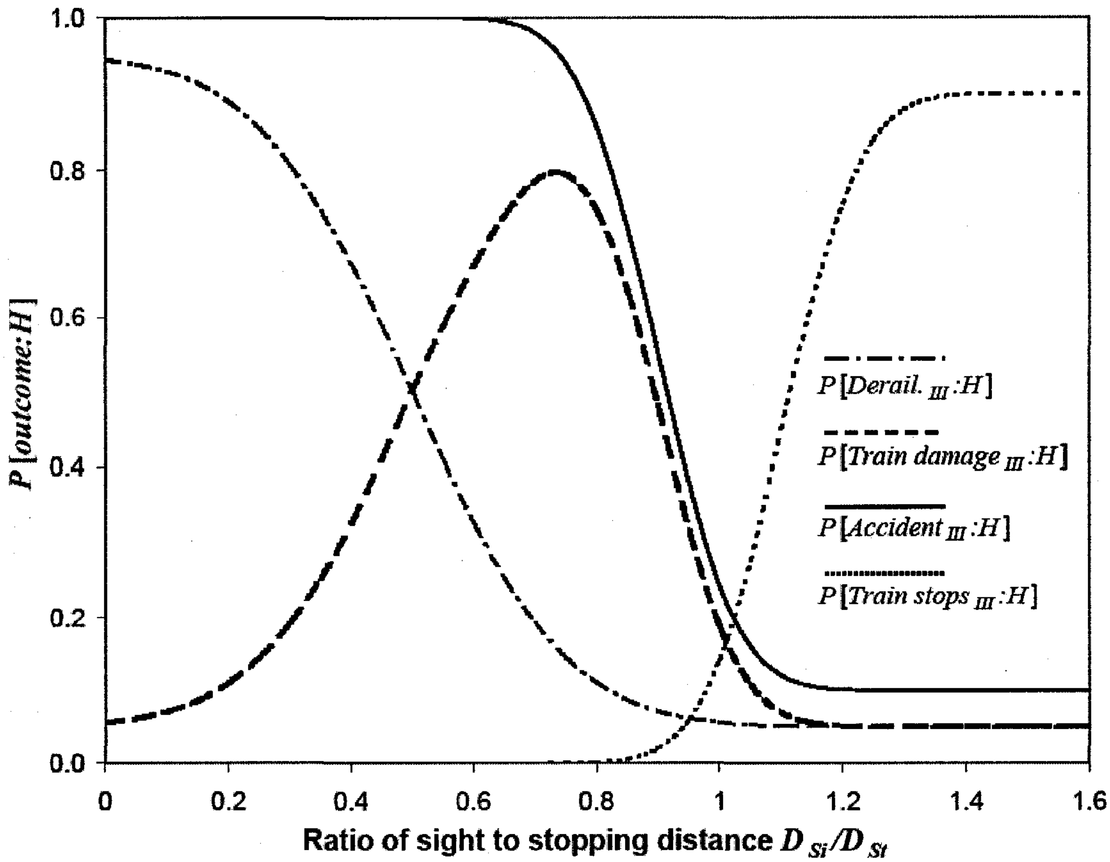

Figure 5.12 Example of the variation of probabilities of derailment, train damage, accident, and train stops before hitting the landslide obstruction versus the ratio of sight to stopping distance.

B Summary of train and track influences on Type III interaction

Due to the number of conditional probabilities and outcomes, an event tree is used to structure and complete the risk calculation. Figure 5.13 depicts this process and the combinations of outcomes. The conditional probabilities developed in Sections 5.5.4.1 to 5.5.4.5 are multiplied by each other to calculate the probability of a train encountering a landslide.

Therefore $P[Accident_{III}]$ is the product of the following variables:

1. $P[H(V_i)]$
2. $P[Impass.:H(V_i)]$

3. $P[Freight]$ or $P[Passenger]$ or $P[MOW\text{-}TV]$
4. $P[TC]$
5. $P[Train\ inside\ signal]$ or $P[Train\ outside\ signal]$
6. $P[TC\ trig.:H\&TC]$
7. $P[HDS]$
8. $P[HDS\ trig.:H(V_i)]$
9. $P[Accident_{III}:H]$,

$P[Derail._{III}(V_i)]$ is the product of terms 1 to 8 and $P[Derail._{III}:H(V_i)]$. Similarly, $P[Train\ damage_{III}(V_i)]$ is the product of terms 1 to 8 and $P[Train\ damage_{III}:H(V_i)]$, and $P[Train\ stops_{III}(V_i)]$ is the product of terms 1 to 8 and $P[Train\ stops_{III}:H(V_i)]$. A detailed set of formulas is provided in Appendix L.

C Probability of derailment for multiple hazards or the assessment of a length of track

Computation of the probability of a moving train being derailed when it encounters a landslide over a subdivision or length of track, requires the summation of each class of landslide volume using a representative length of hazard, and can be calculated using:

$$P[Outcome_{III}] = \sum_{all\ V_i\ and\ type} P[Outcome_{III} : H(V_i, Type)]P[Outcome : H(V_i)] \quad \text{Equation 5.38}$$

Equation 5.38 is generalized for each outcome (Accident, Derailment, Train damage or Train stops) where each hazard volume class, V_i, and hazard type (rock fall, debris flow, and above and below track landslide) will have a corresponding $P[H_i]$ and $P[Outcome_{III}:H]$ as determined from the CP-NHID.

D Probability of injury and fatality - freight and passenger train crew

The conditional probability of a fatality resulting from a train impacting and derailing as the result of a previous landslide is $P[F_{III}:Derail.]$. The conditional probability of a fatality resulting from a train accident caused by a train encountering a landslide without a derailment is $P[F_{III}:Train\ damage]$. The probability of a fatality $P[F_{III}]$ is therefore the sum of $P[F_{III}:Derail.]$ and $P[F_{III}:Train\ damage]$.

Given a train accident, the probability of a fatality is influenced by a number of conditions. In general, specific conditions must be present to result in death of one or more members of the train crew. Of the five deaths related to geotechnical-hazard train-accidents recorded by CP in the past 47.7 years, all have occurred after a locomotive derailed and fell into water (Transportation Safety Board 1995). The most recent CN geotechnical related fatality, the 1997 Conrad derailment, (Keegan 2007 and Transportation Safety Board 1997a) resulted when the locomotive descended 12 m into a void left by a landslide. These derailments, and others that have not resulted in fatalities, indicate that derailments into water and or a significant vertical drop, combined with train speeds in excess of restricted speed, are present when a fatality occurs. Geotechnical derailments where locomotives have not descended a steep slope or fallen into water, and have not been traveling at track speed, have not resulted in fatal accidents (Transportation Safety Board 1995 and 1997b).

The CP Freight Main line, Mile 698.90 overland flow - gully erosion - erosion event in Northern Pennsylvania on 2002 May 14, resulting in the derailment and injury of two locomotive operators is an example of the train crew being injured but not killed because the derailed locomotives dropped less than 5 m and were not submerged. As a result, it can be concluded that, for locations where a train is unlikely to drop a significant vertical distance or fall into water, the probability of a fatality is low. This demonstrates that the consequences of the derailment must be considered to assess the probability of a fatality.

CP has recorded over 230 mainline derailments due to geotechnical hazards, but only three derailments have resulted in one or more fatalities in 47.7 years. Therefore, the probability of a derailment resulting in a fatality is 3/230 or 0.013 for all topographic and water hazard conditions. This assumes the same for the period of record. Derailments that could occur at sites with minimal topography and no water hazards should have conditional probabilities of a fatality no more than half 0.013. In areas where there is a significant potential for the derailed train to descend a steep slope or to fall into water the $P[F_{III}:Derail.]$ could be expected to be an order of magnitude higher. Since no train damage incidents have resulted in a fatality it is reasonable to assume that the probability of death for this outcome would be at least a magnitude lower than that for a derailment and therefore no greater than 0.0013. Each of the three fatal incidents occurred at track speed. Since no fatalities have occurred at restricted speed, it is reasonable to assume that trains traveling at restricted speed would have a probability of death of at least one order of magnitude lower than those traveling at track speed. Table 5.8 provides a summary of these assumptions. The bold value indicates the sole data point extracted from the CP NHID.

Table 5.8 Summary of probability of a fatality given a derailment and train damaging accident

	$P[F_{III}$:*Derail.*]		$P[F_{III}$:*Train damage*]	
Consequence level	**Track speed**	**Restricted speed**	**Track speed**	**Restricted speed**
High	<0.13	<0.013	<0.013	<0.0013
Moderate	<0.06	<0.006	<0.006	<0.0006
Low	**<0.013**	<0.0013	<0.0013	<0.00013

The probability of injury is significantly higher than a fatality. For the same 230 derailments and 230 train damage incidents there have been 58 incidents that resulted in one or more injuries. Therefore, there is a 58/460 or 0.12 probability of a train accident causing an injury. Therefore, *P*[*Injury:Train accident*] is approximately an order of magnitude higher than $P[F_{III}$:*Derail.*]. The comparison of the conditional probability of injuries due to all types of train accidents and fatalities due to Type III derailments (which have caused all the recorded fatalities) is not strictly appropriate. The subtle differences in these two conditional probabilities should be further investigated in the accident record, but will be assumed inconsequential for the purposes of this study.

As discussed in Section 5.4.4.1 there are generally two fatalities or injuries per train accident.

5.5.4.6 Type III - Example of Maple Ridge, BC

An example is provided using the landslide frequency and railway parameters from the Maple Ridge, BC data. The change in risk given precipitation induced landslide (PIL) and non-PIL antecedent precipitation conditions identified in Chapter 4 is considered in Section 5.7.2. To illustrate the variation in risk for different conditions six cases are reviewed. A description of these cases is provided in Table 5.9 along with the location of the results and the section in which they are discussed.

Table 5.9 Maple Ridge, BC cases considered

Case	Description	Results in Table	Discussed in section
1	All landslides, without an HDS	5.14	5.5.4.6 - A
2	All landslides, with an HDS	5.16	5.7.1
3	Only PIL with slow order applied	5.17	5.7.2
4	PIL at track speed	5.18	5.7.2
5	Non PIL at track speed	5.19	5.7.2
6	Sum of Cases 3 and 5. All landslides (PIL at restricted speed plus non PIL at track speed)	5.20	5.7.2

A Probability of train accident and derailment

As previously discussed, there have been at least 50 landslides in 32 years. However, as soon as the first landslide occurs and blocks the track no further trains can pass until the debris is removed from the track. As a result, only the first landslide in each episode is considered a hazard to approaching trains. For landslide that affect the track the landslide frequency for this site is compiled in Table 5.9 for large earth slides, below track earth slides, and smaller above track landslides for both precipitation and non precipitation induced landslide episodes from Tables 4.7, 4.8 and 4.9. The episode frequency and therefore $P[H(V_i)]$ are not the same as in Table 5.5 because the Type I risk assessment did not consider the very large landslides or the below track landslides.

Table 5.10 Landslide magnitude frequency data for PIL, and

Risk estimation parameter	Landslide cause	Landslide volume ($\log_{10} m^3$	$1<V_i\leq2$	$2<V_i\leq3$	$3<V_i\leq4$	$4<V_i\leq7$	Total
$P[H(V_i)]^1$ per year	PIL	Large				4/217 = 0.018	0.018
		Below track	0	1/32 = 0.031	4/32 = 0.13		0.15
		Above	5/32 = 0.16	5/32 = 0.16	1/32 = 0.031		0.36
		All [2]	5/32 = 0.16	5/32 = 0.16	4/32 = 0.13	4/217 = 0.018	0.46
	Non PIL	Large					0
		Below track		2/32 = 0.063	3/32 = 0.094		0.13
		Above		1/32 = 0.031			0.031
		All	0	3/32 = 0.094	3/32 = 0.094		0.19
	All		5/32 = 0.16	8/32 = 0.25	7/32 = 0.22	4/217 = 0.018	0.64
LT(Vi) (m)			3.8	8.2	18	170	
$P[Impass.:H(V_i)]^3$			1/2	19/20	1	1	
$P[TC\ trig.:H\&TC]$			0.001	0.01	0.1	1	

1 Assume all larger landslides and those without specified dates are PIL unless there is precipitation data to suggest they are not PIL
2 This value is adjusted to reflect the double counting of two episodes, which had both an above and below track PIL
3 This value is estimated. Additional statistics could be extracted from CP_NHID

The overall landslide frequency is one every 1.6 years, or a combined probability of $\sum_{all\ V_i} P[H(V_i)] = 0.64$

For the upper bound of the conditional probability of the track circuit being broken by the landslide, *P*[*TC trig.:H&TC*], at Maple Ridge, BC is provided in Table 5.10. No landslides since 1975 in this area are recorded to have broken the track. *P*[*TC trig.:H&TC*] is set to unity for the landslides greater than 10^4 m^3. It is set to 1/1,000 for all landslides less than 100 m^3. *P*[*TC trig.:H&TC*] is set to incremental values as per Table 5.10 for landslides with volumes between 100 m^3 and 10,000 m^3 to provide a transition between the two end conditions.

The probability that the HDS system will be triggered by the various sizes of events should be near unity for all events above 100 m^3 and 0.95 for landslides smaller than 100 m^3. The reduced *P*[*HDS trig.:H*] for smaller landslide volumes is to account for the possibility that a small volume, liquid debris flow could pass under the proposed HDS system undetected. These values are summarized in Table 5.13.

The probability of freight and passenger trains and MOW Track Vehicle (TV) is evaluated using Equations 5.19, 5.21, and 5.22.

$$P[Freight] = \frac{22.5\ Freight/day}{(22.5\ Freight/day + 7.1\ Passenger/day + 1\ MOW - TV/day)}$$

= 0.735

$$P[Passenger] = \frac{7.1\ Passenger/day}{(22.5\ Freight/day + 7.1\ Passenger/day + 1\ MOW - TV/day)}$$

= 0.232

$$P[MOW\ TV] = \frac{1\ MOW\ track\ vehicle/day}{(22.5\ Freight/day + 7.1\ Passenger/day + 1\ MOW - TV/day)}$$

= 0.033

$\Sigma P[Train] = P[Freight] + P[Passenger] + P[MOW\text{-}TV] = 1$

At Maple Ridge a track circuit is present. However, allowing for 1 day per year out of service time *P*[*TC*] is set to 364/365 which equals 0.997.

For westbound trains approaching the area of the Maple Ridge landslides there are signals at miles 101.24, 103.40, 104.60 and 106.173. For eastbound trains there are signals at miles 106.38, 104.65, 103.45 and 101.41. The westbound signal at

103.40 and the eastbound signal at 104.65 are within the landslide zone. As a result, they are not considered, because they cannot warn trains of landslides at lower and higher mileages, respectively. The eastern and western limit of the landslide hazard is 102.80 and 104.90. Therefore, for westbound rail traffic:

$L_{S\text{-}West}$ = 104.90 - 101.24 = 3.46 miles (5.57 km)

For eastbound rail traffic:

$L_{S\text{-}East}$ = 106.38 -102.80 = 3.58 miles (5.76 km)

In some cases effective $L_{S\text{-}East}$ and $L_{S\text{-}West}$ can vary more drastically. Using Equation 5.25 the *P*[*Train inside signal*] is calculated and included in Table 5.11.

Table 5.11 Train frequency and operations parameters

Train type	***P*[*rail traffic*]**	**Train speed**		**Average train frequency**	***P*[*Train inside signal*]**	
		(kmph)	(mph)	(trains/day)	Westbound	Eastbound
Freight	0.735	48	30	22.5	0.114	0.112
Passenger[1]	0.232	80	50	7.1	$2.2*10^{-3}$	$2.1*10^{-3}$
MOW vehicle	0.033	48	30	1	$5.1*10^{-3}$	$4.9*10^{-3}$

The Maple Ridge, BC site is characterized by relatively gentle track curves separated by 0.3 to 0.6 km (0.2 to 0.4 mile) long tangents, combined with visibility-impairing, lush temperate rain-forest vegetation. As a result, the sight distance (SD) for this site is set to an average of 0.32 km (0.20 miles or 1056 ft).

Table 5.12 Train sight and stopping distance ratio parameters used for Maple Ridge, BC to develop Figure 5.12 and to utilize Equations 5.31 to 5.34

Outcome (subscript)	Average, μ D_{Si}/D_{St} for *P*[outcome] =0.5	Standard deviation σ	Residual risk δ
Derailment (*D*)	1.5	0.2	0.05
Train stops (*Ts*)	1.1	0.1	0.05

The operation parameters are summarized in Table 5.11, the sight and stopping distance ratio parameters are included in Table 5.12. The *P*[F_{III}:*Derail.*] and

$P[F_{III}:Train\ damage]$ values are specified in Table 5.13. These parameters are used to calculate the probabilities in the Summary of Case Tables 5.14, 5.15, and 5.17 to 5.20. Figure 5.13 illustrates a portion of the event tree used to develop the Summary of Case tables. In Figure 5.13 the grey boxes indicate the fields calculated by the formulas provided in Section 5.5.4. Open boxes are input parameters included in Tables 5.8, 5.10, 5.11, 5.12 and 5.13. This major branch of the event tree is repeated for each volume class of landslide that is known to occur. As a result, there are three additional similar branches to the one shown in Figure 5.13, one for each volume class. The volume classes should be grouped by their impact on the track and rail traffic. If the duration of the service interruption is of primary interest, the landslide classes may be different as suggested by the data in Figure 5.3.

Table 5.13 Probabilities of input parameters for four landslide volumes and two cases

Case	**Landslide volume ($\log_{10}$ m^3)**	$P[H]$[1] **(per year)**	$P[HDS]$	$P[HDS\ trig.:H]$
1a	$1<Vi\leq2$	0.16	0	0.95
1b	$2<Vi\leq3$	0.25	0	0.999
1c	$3<Vi\leq4$	0.22	0	0.999
1d	$4<Vi\leq7$	0.018	0	1
2a	$1<Vi\leq2$	0.16	1	0.95
2b	$2<Vi\leq3$	0.25	1	0.999
2c	$3<Vi\leq4$	0.22	1	0.999
2d	$4<Vi\leq7$	0.018	1	1

[1] From Table 5.10

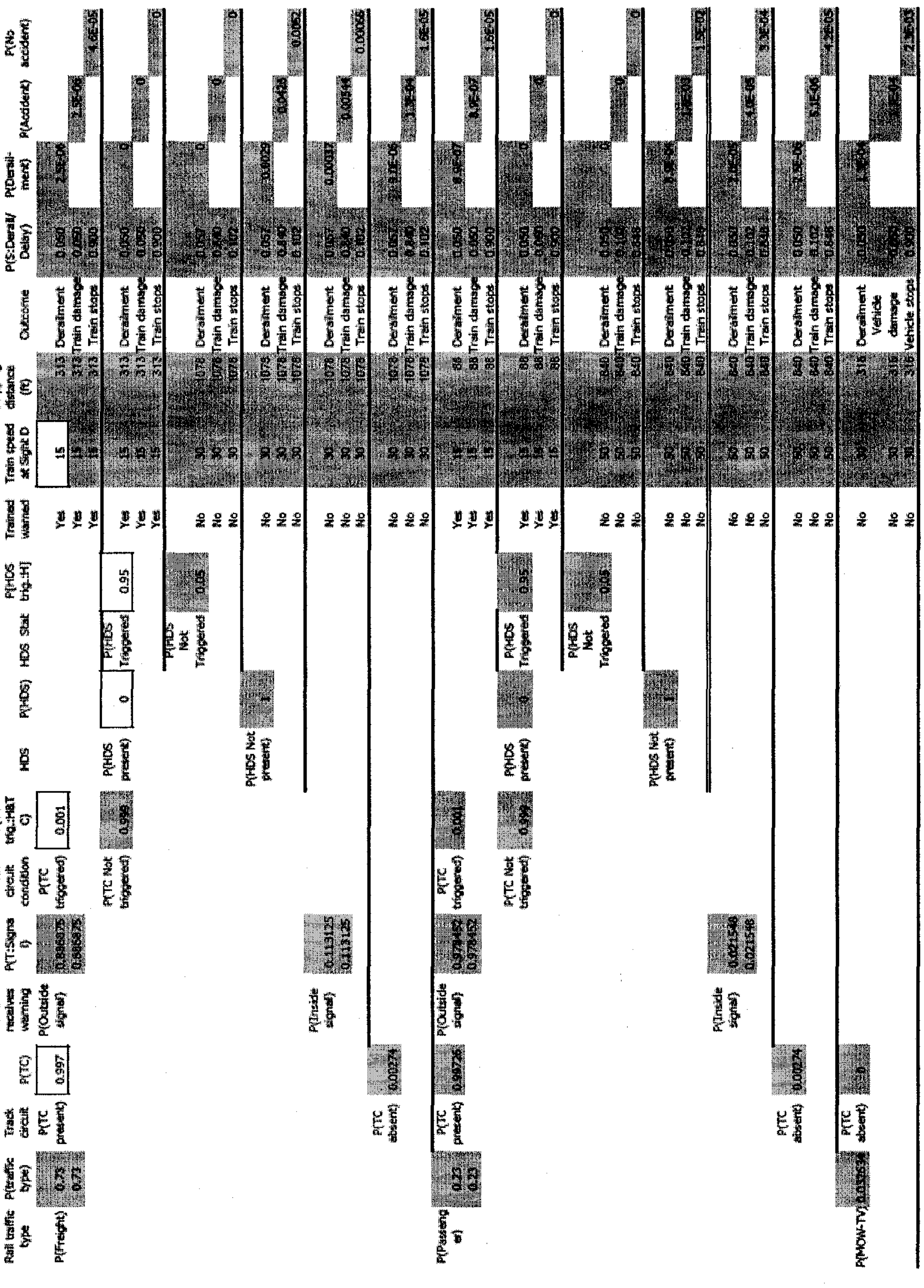

Figure 5.13 One branch of the event tree used to calculate the probabilities included in the Summary of Case Tables

Table 5.14 Summary of Maple Ridge, BC Case 1 with no signal fence

Case 1a - Small landslide - 5 episodes in 32 years

Type of track vehicle	$P[F_{III}]$	$P[Injury_{III}]$	$P[Service\ disruption]$	$P[Track\ vehicle\ damage_{III}]$	$P[Track\ damage]$
Freight	5.3E-04	5.3E-03	5.7E-02	5.1E-02	5.7E-02
Passenger	1.1E-05	1.1E-04	1.8E-02	2.8E-03	1.8E-02
MOW vehicle	9.1E-07	9.1E-06	2.5E-03	2.5E-04	2.5E-03
No Track Vehicle damage		7.8E-05	7.8E-02	3.9E-02	3.9E-02
Total	5.4E-04	5.5E-03	0.16	9.4E-02	0.12

Case 1b - Medium landslide - 8 episodes in 32 years

Freight	1.6E-03	1.6E-02	0.17	0.16	0.17
Passenger	3.3E-05	3.3E-04	5.5E-02	8.4E-03	5.5E-02
MOW vehicle	2.8E-06	2.8E-05	7.8E-03	7.8E-04	7.8E-03
No Track Vehicle damage		1.3E-05	1.3E-02	6.3E-03	6.3E-03
Total	1.6E-03	1.6E-02	0.25	0.17	0.24

Case 1c - Large landslide - 7 episodes in 32 years

Freight	1.4E-03	1.4E-02	0.16	0.13	0.16
Passenger	2.9E-05	2.9E-04	5.1E-02	7.5E-03	5.1E-02
MOW vehicle	2.6E-06	2.6E-05	7.1E-03	7.1E-04	7.1E-03
No Track Vehicle damage		0.0E+00	0.0E+00	0.0E+00	0.0E+00
Total	1.4E-03	1.4E-02	0.22	0.14	0.22

Case 1d - Very large landslide - 4 episodes in 217 years

Freight	1.9E-05	1.9E-04	1.4E-02	2.6E-03	1.4E-02
Passenger	1.6E-06	1.6E-05	4.3E-03	4.4E-04	4.3E-03
MOW vehicle	2.2E-07	2.2E-06	6.0E-04	6.0E-05	6.0E-04
No Track Vehicle damage		0.0E+00	0.0E+00	0.0E+00	0.0E+00
Total	2.0E-05	2.0E-04	1.8E-02	3.1E-03	1.8E-02

Case 1 - All landslides

Freight	3.5E-03	3.5E-02	0.41	0.34	0.41
Passenger	7.5E-05	7.5E-04	0.13	1.9E-02	0.13
MOW vehicle	6.4E-06	6.4E-05	1.8E-02	1.8E-03	1.8E-02
No Track Vehicle damage		9.1E-05	9.1E-02	4.5E-02	4.5E-02
Total	3.6E-03	3.6E-02	0.64	0.41	0.60

As shown in Table 5.14 without an HDS, for all track vehicles, the risk of damage at CASC 102.50 to 104.90 is calculated to be about 0.4 per year or once every 2.5 years. This exceeds the recorded train accident rate of about one event every 10 years by a factor of four. Four conditions influence the actual train accident record, which are not accounted for in the predicted frequency:

1. The train crew may elect to slow a specific train or the TMS may elect to temporarily slow all trains in response to severe weather or other indication of landslide activity (such as debris flows in the immediate or local area). The third example in Section 5.4.2.1 is an illustration of this situation. Discretional speed reductions are not recorded and have not been modeled. However, providing standardized PIL notifications should reduce the number of train accidents further and make the safety of the train crews and passengers less dependent on the Train crews experience and that of the TMS.
2. The probability of a train accident is also dependent on the sight and stopping distances. The probability of a train accident is sensitive to this ratio as illustrated by the steepness of the curves in Figure 5.11. An underestimation of the site distance or an overestimation of the stopping distance will have an influence on the $P[Accident_{III}:H]$.
3. The analysis completed did not account for the double track conditions at this site. However, the influence of double track can only reduce the $P[Accident_{III}:H]$ by less than a factor of two since trains on the down-slope (south) track are less exposed to debris slides than the up-slope (north) track but are more exposed to down-slope landslides.
4. Another condition is that the train accident record is the integration of the probability function derived over the past 32 years compared to the $P[Accident_{III}:H]$ calculated for the current conditions. Train frequency, including the addition of the commuter-transit rail service in the early 1990's, has increased significantly during this period.

The sum or total of the probabilities of a service disruption is 0.64, which is equal to the probability of a landslide. This demonstrates that all the branches of the event-tree calculation sum correctly to the landslide frequency since each landslide episode will cause a service disruption.

B Probability of injury and fatality - freight and passenger train crews

Using data and the formulas provided throughout Section 5.5.4, the probability of one or more fatalities or injuries can be calculated. The results for the base case are summarized in Table 5.14. The sum of the freight and passenger train crews $P[F_{III}]$ is 0.0036 or one fatality every 280 years at current train operation levels for this location.

C Risk of injury and fatality - passenger

The probability of one or more fatalities resulting when a passenger train encounters a landslide is more difficult to assess because there is little information on passenger train fatalities within the CP-NHID. There has also been a significant variation in the number of passengers traveling on trains over the last 70.7 years especially in hazardous areas of BC and Alberta. It may be possible to obtain information on the probability of passenger train fatalities from the Federal Railway Authority (FRA) and European railway databases where passenger rail traffic is more common. However, the speed of the train on impact is expected to be a significant variable influencing the number of deaths. It seems reasonable to assume that the probability of at least one fatality on a passenger train is higher than the probability of fatality of a freight train crew member involved in the same accident because there are more lives exposed. This may be high because although passenger trains travel faster than freight trains, they should be traveling slower at the time of impact, because they have braking distances of less than a freight train, even at the higher track speeds as depicted in Figure 5.11.

As indicated, the average West Coast Express (2008b) commuter-transit service carries 840 passengers per train. I have assumed that there will be 10 to 100 passenger deaths for every train crew death.

5.5.4.7 Type III - Conclusion

A methodology for quantitatively determining the risk of a moving train encountering a stationary landslide obstructing the track has been demonstrated in Section 5.5.4. This methodology has been applied to a case study with appropriate results in Section 5.5.4.6.

Although there are a number of subjective parameters used to compute the risk of fatalities, injuries, service interruptions, train damage and track damage the methodology can be used to compare the risk of different hazards and different locations and is therefore of benefit in deciding where best to allocate limited resources to reduce risks. In the example above, the risk estimation process can be used to demonstrate the benefits of measures such as an HDS (signal fence) or other measures such as slope stabilization of one or more of the potential future landslide sites.

Using the assumptions summarized below it is possible to estimate the number of sites of similar risk to Maple Ridge, BC within the CP rail system.

1. Assuming all sites have an equal level of risk to that of Maple Ride, BC.
2. Assuming the probability of a train crew fatality at Maple Ridge, BC of $3.6*10^{-3}$ from Table 5.14
3. Assuming the probability of a geotechnical hazard resulting in one or more fatalities in BC and Alberta is 3 in 70.7 years (from Section 5.4.4.1).

There would be approximately 12 sites within the BC and Alberta CP network with an equivalent level of risk of fatality to that of Maple Ridge, BC. However, the Maple Ridge, BC site was selected because it is one of the highest risk locations in the CP network due to the frequency of the hazard, the number of trains, and the commuter passenger traffic, among other things. As a result, it is unlikely that more than a few other sites would approximate the risk of this site. The majority would have a level of risk lower than this site but there are several hundred of them.

5.6 Conclusions of risk estimation

In conclusion, a methodology for calculating the probability of a train crew fatality caused by a moving train being impacting by a landslide, a stationary train being impacted by a landslide, and a moving train impacting a landslide that has rendered the track impassable, has been developed. By assuming values for a limited number of parameters, the risk of fatalities can be approximated at specific sites.

For the case study in Section 4.5 the calculated and empirical probability of a train being impacted by a landslide is 1 in 30 years. The risk of death to a freight and passenger train crew for several of the scenarios discussed in Sections 5.4.3 and 5.5.1.1 are summarised in Table 5.15.

Table 5.15 Summary of risks at Maple Ridge, BC

Scenario	**Annual probability of fatality of train crew**		
	Freight train	**Passenger train**	**Freight and Passenger**
Type I - Landslide hits moving train	$9.8*10^{-6}$	$1.9*10^{-6}$	$1.2*10^{-5}$
Type III - Moving train hits a stationary hazard	$3.5*10^{-3}$	$7.5*10^{-5}$	$3.6*10^{-3}$
Combined	$3.5*10^{-3}$	$7.7*10^{-5}$	$3.6*10^{-3}$

It can be seen from Table 5.15 that the probability of a fatality, $P[F_I]$, for a train being hit by a landslide is several magnitudes lower than the $P[F_{III}]$ of a fatality that results when a train runs into a landslide. As a result, the reduction of $P[F]$ achieved by increasing the speed of a train (due to the reduced exposure of the train being hit by a landslide) has less influence on the combined $P[F]$ realized by slowing a train such that its stopping distance is reduced and its speed at impact is reduced. Slowing trains decreases the consequences when a landslide is encountered more than increasing the speed reduces the exposure time and related consequences because of the significant difference in overall risk from the two scenarios. It has therefore been demonstrated that the risk reduction achieved by slowing trains is greater than the risk reduction of increasing train speed for landslide hazards.

The risk of fatality of MOW employees is only considered for the case where their vehicle impacts a landslide, but has not been fully evaluated.

The probability of a fatality for a single train crew employee is calculated and compared to tolerable risk level in Section 5.8.

5.7 Risk Control

This section assesses two risk control options available to railways. The first risk control system is a hazard detection system. The second is a precipitation induced landslide warning system based on the research included in Chapter 4. Several other risk control options are discussed in Chapter 6. The effectiveness of both options is evaluated using the risk estimation methodology developed in the pervious section.

5.7.1 Change in risk with a hazard detection system

As of 2007 August there was no HDS between CASC 102.50 and 104.90 but CP planned to install one in the spring of 2008. As a result, both $P[HDS]$ of 0 and 1 are evaluated and summarized in Tables 5.14 and 5.16 respectively. The HDS reduces the probability of a train accident to about a third of its original value.

As can be seen from Tables 5.14 and 5.16 the risk of fatalities and injuries decreases to approximately one sixth of its original value when a hazard detection system (slide fence) is present. Using the $P[F_{III}]$ in Tables 5.14 and 5.16 and assuming the cost (all values in 2008 Canadian dollars) of two fatalities (since they most frequently occur in pairs) is $4 million (assuming $2 million per fatality Tatone (2007)) the annual expected loss due to fatalities at this location would be $33,600 per year (the product of $P[F_{III}]$ and the assumed value of a life). With an HDS this could be reduced to $4,800, a saving of $28,800 annually. The cost of an HDS is about $200,000. Therefore, not including the cost of capital, it would take 6.5 years to realize a return on the capital investment of the signal fence. When the potential for multiple fatalities due to a passenger train derailment, the value of any damaged equipment, and recovery costs are included the time to realize a return on the investment in a signal fence is less than 6.5 years and may be justified.

There is also a loss of confidence among passengers, employees, customers and regulators unless the railway makes a reasonable investment to improve safety in response to an incident.

Table 5.16 Summary of Maple Ridge, BC Case 2 with a signal fence

Case 2a - Small landslide - 5 episodes in 32 years

Type of track vehicle	$P[F_{III}]$	$P[Injury_{III}]$	$P[Service\ disruption]$	$P[Track\ vehicle\ damage_{III}]$	$P[Track\ damage]$
Freight	1.0E-04	1.0E-03	5.7E-02	1.3E-02	5.7E-02
Passenger	9.8E-06	1.0E-04	1.8E-02	1.9E-03	1.8E-02
MOW vehicle	9.1E-07	9.1E-06	2.5E-03	2.5E-04	2.5E-03
No Track Vehicle damage		7.8E-05	7.8E-02	3.9E-02	3.9E-02
Total	1.1E-04	1.2E-03	0.16	5.4E-02	0.12

Case 2b - Medium landslide - 8 episodes in 32 years

Freight	2.4E-04	2.4E-03	0.17	3.4E-02	0.17
Passenger	2.0E-05	3.0E-04	5.5E-02	5.6E-03	5.5E-02
MOW vehicle	2.8E-06	2.8E-05	7.8E-03	7.8E-04	7.8E-03
No Track Vehicle damage		1.3E-05	1.3E-02	6.3E-03	6.3E-03
Total	2.6E-04	2.8E-03	0.25	4.6E-02	0.24

Case 2c - Large landslide - 7 episodes in 32 years

Freight	2.2E-04	2.2E-03	0.16	3.1E-02	0.16
Passenger	1.9E-05	2.7E-04	5.1E-02	5.2E-03	5.1E-02
MOW vehicle	2.6E-06	2.6E-05	7.1E-03	7.1E-04	7.1E-03
No Track Vehicle damage		0.0E+00	0.0E+00	0.0E+00	0.0E+00
Total	2.4E-04	2.5E-03	0.22	3.7E-02	0.22

Case 2d - Very large landslide - 4 episodes in 217 years

Freight	1.9E-05	1.9E-04	1.4E-02	2.6E-03	1.4E-02
Passenger	1.6E-06	1.6E-05	4.3E-03	4.4E-04	4.3E-03
MOW vehicle	2.2E-07	2.2E-06	6.0E-04	6.0E-05	6.0E-04
No Track Vehicle damage		0.0E+00	0.0E+00	0.0E+00	0.0E+00
Total	2.0E-05	2.0E-04	1.8E-02	3.1E-03	1.8E-02

Case 2 - All landslides

Freight	5.8E-04	5.8E-03	0.41	8.0E-02	0.41
Passenger	5.0E-05	6.9E-04	0.13	1.3E-02	0.13
MOW vehicle	6.4E-06	6.4E-05	1.8E-02	1.8E-03	1.8E-02
No Track Vehicle damage		9.1E-05	9.1E-02	4.5E-02	4.5E-02
Total	6.4E-04	6.7E-03	0.64	0.14	0.60

5.7.2 Change in risk due to precipitation conditions

The change in the probability of a derailment as a result of climatic conditions is significant if the hazards are sensitive to climatic conditions. As demonstrated in Section 2.3.1 and Chapter 4, some landslide hazard scenarios are induced by climatic conditions and indices and thresholds can be identified to warn of these periods of increased hazards.

As shown in Chapter 4, during severe precipitation conditions landslides are more likely. For days when the precipitation conditions exceed the specified thresholds, the probability of a landslide episode at Maple Ridge, BC is increased. One means of estimating the probability distribution resulting from multiple thresholds being exceeded is to subdivide the severe precipitation into multiple levels. Figure 5.14 provides an example of this technique. Analysis of the data used to develop Figure 5.14 indicates that there were 11,931 days (32.7 years) days of precipitation records between the start of the CP's landslide "period of record" in 1975 January to 2007 September 1. In this period, there were 14 days with episodes of precipitation induced landslides as described in Chapter 4 and summarized in Table 5.10. Only 12 episodes have reliable dates. As a result, the nominal probability of a landslide episode is 0.001 per day (0.37 per year). However, for days below the Lower threshold there was only one PIL landside episode, so the probability of a landslide episode on days that do not exceed the lower threshold is 0.0001 per day (0.031 per year). Within the period of record there were 135 days that exceeded the lower threshold and there were 11 landslide episodes on these days. Therefore, provided the lower threshold is exceeded, the probability of a landslide episode is 11/135 or 0.081, more than 800 times or almost three orders of magnitude greater than the probability below the lower threshold.

It might be expected that the probability of a landslide would increase at higher thresholds and this is partly true in this example. For instance, within the period of record, there are 88 days that exceeded the lower threshold but not the moderate threshold. As a result, the probability of a landslide episode, given the antecedent precipitation conditions are between the lower and moderate thresholds, is 4/88 or 0.045. Similarly, if the precipitation conditions are between the moderate and upper thresholds the probability of a landslide episode increases to 5/31 or 0.16 per day. However, if the upper threshold is exceeded, the probability of a landslide drops to 2/16 or 0.125 per day. Of course, due to the limited landslide record, the predicted probabilities are dependent on the selection of the lower, moderate, and upper threshold values. These values are arbitrary and a slight shift in the threshold would alter the probability of each condition.

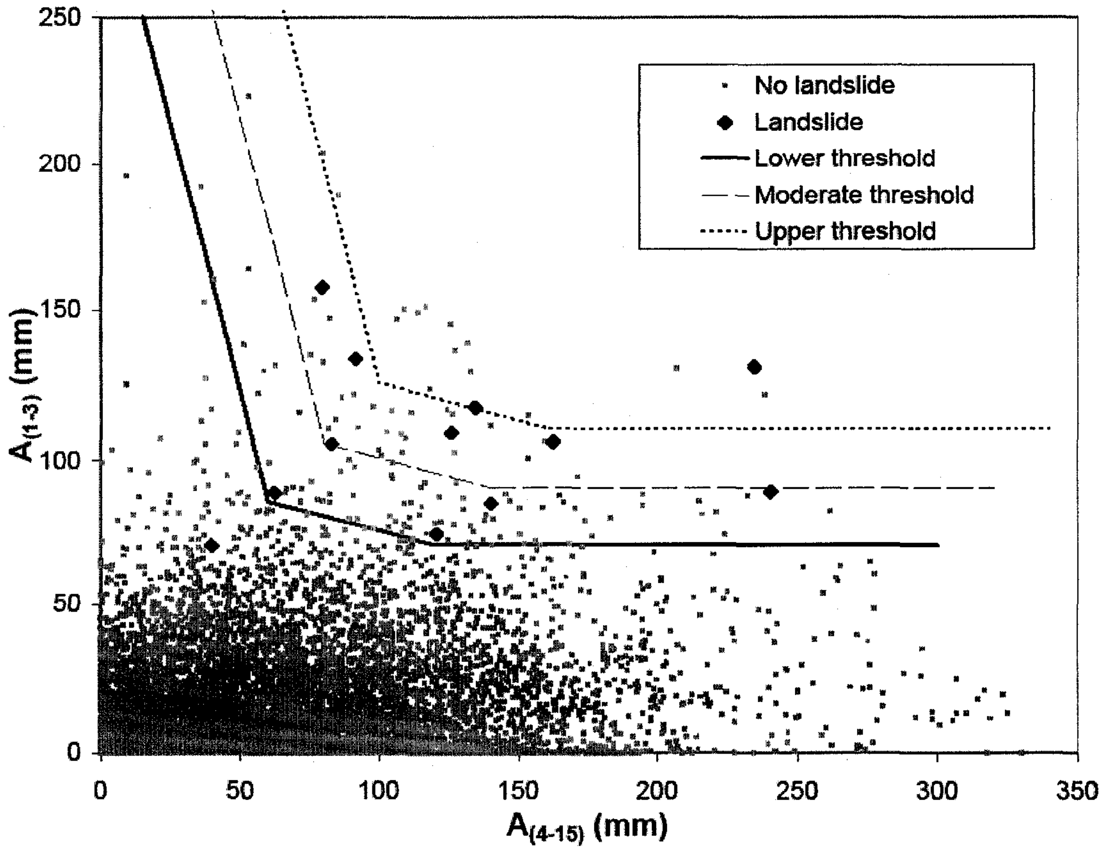

Figure 5.14 Example of modified Chleborad method analysis with multiple precipitation thresholds

The most significant conclusion that can be drawn from this discussion is that the probability of a landslide can increase by almost three orders of magnitude when the lower threshold is exceeded.

Similarly, the PIL thresholds developed using the GEV antecedent precipitation induced landslide return period assessment (GEV APIL RPA) method, to determine the index with the highest return period at the time of the landslide, can also be used to assess the change in risk with antecedent precipitation conditions. Using the results summarized in Table 4.13 the PIL thresholds will be exceeded 3.8% of the time (3.2% false-positive + 0.6% true-positive). Therefore, the probability of a PIL on a day when the PIL thresholds are exceeded is 0.6/3.8 or 0.16. This is two orders of magnitude higher than the probability of 0.0015 (one landslide per 649 days) when no precipitation indices are applied. Conversely, the probability of a PIL should approach zero when no thresholds are exceeded. However, non PIL will result in a probability of landslides when the thresholds are not exceeded.

As introduced in Section 4.5.15 a safety margin was included to account for the uncertainty between 0% and 100% probability of a landslide. However, a probability function could be introduced in place of the safety margin approach. In this way Figure 4.21 could be modified to include all landslide, PIL and non PIL. Lower, Moderate and upper thresholds could then be established consistent with the warning threshold and the precipitation return periods that would provide a variable probability of landslides depending on the threshold exceeded.

Based on the preceding discussion, for Maple Ridge, BC it is therefore reasonable to assume that the annual probability of a landslide impacting a train or being hit by a train on a day when the precipitation inducing index thresholds are exceeded is at least two orders of magnitude higher than on a day when the thresholds are not exceeded. In summary, based on the history of the site landslides are likely to occur on only a few days of the year when PIL thresholds are exceeded. Conversely, very few landslides are likely to occur on the much more common days when PIL thresholds are not exceeded.

To provide a means of assessing the benefits of a precipitation induced landslide warning system, the probability of a fatality, $P[F_{III}]$, is assessed for the non PIL frequencies, plus the $P[F_{III}]$ for the PIL frequencies identified in Table 5.10. The trains are assumed to operate at track speed for the non PIL frequencies and at restricted speed for the PIL frequencies, as would be the case if a PIL warning system was operational. This is compared to the $P[F_{III}]$ calculated for Case 1 when no landslide warning system is active. The change in $P[F_I]$ when a PIL warning system is operational has not been computed because the change in $P[F_I]$ would be insignificant compared to the change in $P[F_{III}]$ as per Table 5.14.

As can be seen in Table 5.17 compared to Table 5.18 the running of trains at restricted speed when the PIL threshold is exceeded reduces the $P[F_{III}]$ by 2.5 times. As shown in Table 5.20 when combined with the six additional non-PIL recorded at

Table 5.17 Summary of Maple Ridge, BC Case 3 - PIL only with slow order applied

Case 3a - Small landslide - 5 PIL episodes in 32 years

Type of track vehicle	$P[F_{III}]$	$P[Injury_{III}]$	*P*[*Service disrupt-ion*]	*P*[*Track vehicle* $damage_{III}$]	*P*[*Track damage*]
Freight	2.0E-04	2.0E-03	5.7E-02	5.7E-03	5.7E-02
Passenger	1.0E-05	1.0E-04	1.8E-02	1.8E-03	1.8E-02
MOW vehicle	9.1E-07	9.1E-06	2.5E-03	2.5E-04	2.5E-03
No Track Vehicle damage		7.8E-05	7.8E-02	3.9E-02	3.9E-02
Total	2.2E-04	2.2E-03	0.16	4.7E-02	0.12

Case 3b - Medium landslide - 5 PIL episodes in 32 years

Freight	3.9E-04	3.9E-03	0.11	1.1E-02	0.11
Passenger	1.9E-05	1.9E-04	3.5E-02	3.5E-03	3.5E-02
MOW vehicle	1.7E-06	1.7E-05	4.8E-03	4.8E-04	4.8E-03
No Track Vehicle damage		7.8E-06	7.8E-03	3.9E-03	3.9E-03
Total	4.1E-04	4.1E-03	0.16	1.9E-02	0.15

Case 3c - Large landslide - 4 PIL episodes in 32 years

Freight	3.1E-04	3.1E-03	9.2E-02	9.2E-03	9.2E-02
Passenger	1.6E-05	1.6E-04	2.9E-02	2.9E-03	2.9E-02
MOW vehicle	1.5E-06	1.5E-05	4.1E-03	4.1E-04	4.1E-03
No Track Vehicle damage		0.0E+00	0.0E+00	0.0E+00	0.0E+00
Total	3.2E-04	3.2E-03	0.13	1.3E-02	0.13

Case 3d - Very large landslide - 4 PIL episodes in 217 years

Freight	1.5E-05	1.5E-04	1.4E-02	1.4E-03	1.4E-02
Passenger	1.6E-06	1.6E-05	4.3E-03	4.3E-04	4.3E-03
MOW vehicle	2.2E-07	2.2E-06	6.0E-04	6.0E-05	6.0E-04
No Track Vehicle damage		0.0E+00	0.0E+00	0.0E+00	0.0E+00
Total	1.7E-05	1.7E-04	1.8E-02	1.8E-03	1.8E-02

Case 3 - All PIL episodes

Freight	9.1E-04	9.1E-03	0.27	2.7E-02	0.27
Passenger	4.6E-05	4.6E-04	8.6E-02	8.6E-03	8.6E-02
MOW vehicle	4.3E-06	4.3E-05	1.2E-02	1.2E-03	1.2E-02
No Track Vehicle damage		8.6E-05	8.6E-02	4.3E-02	4.3E-02
Total	9.6E-04	9.7E-03	0.46	8.0E-02	0.41

Table 5.18 Summary of Maple Ridge, BC Case 4 - PIL at track speed

Case 4a - Small landslide - 5 episodes in 32 years

Type of track vehicle	$P[F_{III}]$	$P[Injury_{III}]$	*P*[*Service disrupt-ion*]	*P*[*Track vehicle* $damage_{III}$]	*P*[*Track damage*]
Freight	5.3E-04	5.3E-03	5.7E-02	5.1E-02	5.7E-02
Passenger	1.1E-05	1.1E-04	1.8E-02	2.8E-03	1.8E-02
MOW vehicle	9.1E-07	9.1E-06	2.5E-03	2.5E-04	2.5E-03
No Track Vehicle damage		7.8E-05	7.8E-02	3.9E-02	3.9E-02
Total	5.4E-04	5.5E-03	0.16	9.4E-02	0.12

Case 4b - Medium landslide - 5 episodes in 32 years

Freight	9.9E-04	9.9E-03	0.11	9.7E-02	0.11
Passenger	2.1E-05	2.1E-04	3.5E-02	5.2E-03	3.5E-02
MOW vehicle	1.7E-06	1.7E-05	4.8E-03	4.8E-04	4.8E-03
No Track Vehicle damage		7.8E-06	7.8E-03	3.9E-03	3.9E-03
Total	1.0E-03	1.0E-02	0.16	0.11	0.15

Case 4c - Large landslide - 4 episodes in 32 years

Freight	7.7E-04	7.7E-03	9.2E-02	7.6E-02	9.2E-02
Passenger	1.7E-05	1.7E-04	2.9E-02	4.3E-03	2.9E-02
MOW vehicle	1.5E-06	1.5E-05	4.1E-03	4.1E-04	4.1E-03
No Track Vehicle damage		0.0E+00	0.0E+00	0.0E+00	0.0E+00
Total	7.9E-04	7.9E-03	0.13	8.1E-02	0.13

Case 4d - Very large landslide - 4 episodes in 217 years

Freight	1.9E-05	1.9E-04	1.4E-02	2.6E-03	1.4E-02
Passenger	1.6E-06	1.6E-05	4.3E-03	4.4E-04	4.3E-03
MOW vehicle	2.2E-07	2.2E-06	6.0E-04	6.0E-05	6.0E-04
No Track Vehicle damage		0.0E+00	0.0E+00	0.0E+00	0.0E+00
Total	2.0E-05	2.0E-04	1.8E-02	3.1E-03	1.8E-02

Case 4 - All landslides

Freight	2.3E-03	2.3E-02	0.27	0.23	0.27
Passenger	5.0E-05	5.0E-04	8.6E-02	1.3E-02	8.6E-02
MOW vehicle	4.3E-06	4.3E-05	1.2E-02	1.2E-03	1.2E-02
No Track Vehicle damage		8.6E-05	8.6E-02	4.3E-02	4.3E-02
Total	2.4E-03	2.4E-02	0.46	0.28	0.41

Table 5.19 Summary of Maple Ridge, BC Case 5 - Non PIL at track speed

Case 5a - Small landslide - 0 episodes in 32 years

Type of track vehicle	$P[F_{III}]$	$P[Injury_{III}]$	$P[Service\ disruption]$	$P[Track\ vehicle\ damage_{III}]$	$P[Track\ damage]$
Freight	0.0E+00	0.0E+00	0.0E+00	0.0E+00	0.0E+00
Passenger	0.0E+00	0.0E+00	0.0E+00	0.0E+00	0.0E+00
MOW vehicle	0.0E+00	0.0E+00	0.0E+00	0.0E+00	0.0E+00
No Track Vehicle damage		0.0E+00	0.0E+00	0.0E+00	0.0E+00
Total	0.0E+00	0.0E+00	0.0E+00	0.0E+00	0.0E+00
Case 5b - Medium landslide - 3 episodes in 32 years					
Freight	6.0E-04	6.0E-03	6.5E-02	5.8E-02	6.5E-02
Passenger	1.2E-05	1.2E-04	2.1E-02	3.1E-03	2.1E-02
MOW vehicle	1.0E-06	1.0E-05	2.9E-03	2.9E-04	2.9E-03
No Track Vehicle damage		4.7E-06	4.7E-03	2.3E-03	2.3E-03
Total	6.1E-04	6.1E-03	9.4E-02	6.4E-02	9.1E-02
Case 5c - Large landslide - 3 episodes in 32 years					
Freight	5.8E-04	5.8E-03	6.9E-02	5.7E-02	6.9E-02
Passenger	1.3E-05	1.3E-04	2.2E-02	3.2E-03	2.2E-02
MOW vehicle	1.1E-06	1.1E-05	3.1E-03	3.1E-04	3.1E-03
No Track Vehicle damage		0.0E+00	0.0E+00	0.0E+00	0.0E+00
Total	5.9E-04	5.9E-03	9.4E-02	6.0E-02	9.4E-02
Case 5d - Very large landslide - 0 episodes in 217 years					
Freight	0.0E+00	0.0E+00	0.0E+00	0.0E+00	0.0E+00
Passenger	0.0E+00	0.0E+00	0.0E+00	0.0E+00	0.0E+00
MOW vehicle	0.0E+00	0.0E+00	0.0E+00	0.0E+00	0.0E+00
No Track Vehicle damage		0.0E+00	0.0E+00	0.0E+00	0.0E+00
Total	0.0E+00	0.0E+00	0.0E+00	0.0E+00	0.0E+00
Case 5 - All landslides					
Freight	1.2E-03	1.2E-02	0.13	0.12	0.13
Passenger	2.5E-05	2.5E-04	4.3E-02	6.3E-03	4.3E-02
MOW vehicle	2.1E-06	2.1E-05	6.0E-03	6.0E-04	6.0E-03
No Track Vehicle damage		4.7E-06	4.7E-03	2.3E-03	2.3E-03
Total	1.2E-03	1.2E-02	0.19	0.12	0.19

Table 5.20 Summary of Maple Ridge Case 6 - Sum of PIL at restricted speed and Non PIL at track speed

Type of track vehicle	$P[F_{III}]$	$P[Injury_{III}]$	$P[Service\ disruption]$	$P[Track\ vehicle\ damage_{III}]$	$P[Track\ damage]$
Case 6a - Small landslide - 5 PIL and 0 Non PIL episodes in 32 years					
Freight	2.0E-04	2.0E-03	5.7E-02	5.7E-03	5.7E-02
Passenger	1.0E-05	1.0E-04	1.8E-02	1.8E-03	1.8E-02
MOW vehicle	9.1E-07	9.1E-06	2.5E-03	2.5E-04	2.5E-03
No Track Vehicle damage		7.8E-05	7.8E-02	3.9E-02	3.9E-02
Total	2.2E-04	2.2E-03	0.16	4.7E-02	0.12
Case 6b - Medium landslide - 5 PIL and 3 Non PIL episodes in 32 years					
Freight	9.8E-04	9.8E-03	0.17	6.9E-02	0.17
Passenger	3.1E-05	3.1E-04	5.5E-02	6.6E-03	5.5E-02
MOW vehicle	2.8E-06	2.8E-05	7.8E-03	7.8E-04	7.8E-03
No Track Vehicle damage		1.3E-05	1.3E-02	6.3E-03	6.3E-03
Total	1.0E-03	1.0E-02	0.25	8.3E-02	0.24
Case 6c - Large landslide - 4 PIL and 3 Non PIL episodes in 32 years					
Freight	8.8E-04	8.8E-03	0.16	6.6E-02	0.16
Passenger	2.8E-05	2.8E-04	5.1E-02	6.1E-03	5.1E-02
MOW vehicle	2.6E-06	2.6E-05	7.1E-03	7.1E-04	7.1E-03
No Track Vehicle damage		0.0E+00	0.0E+00	0.0E+00	0.0E+00
Total	9.2E-04	9.2E-03	0.22	7.3E-02	0.22
Case 6d - Very large landslide - 4 PIL and 0 Non PIL episodes in 217 years					
Freight	1.5E-05	1.5E-04	1.4E-02	1.4E-03	1.4E-02
Passenger	1.6E-06	1.6E-05	4.3E-03	4.3E-04	4.3E-03
MOW vehicle	2.2E-07	2.2E-06	6.0E-04	6.0E-05	6.0E-04
No Track Vehicle damage		0.0E+00	0.0E+00	0.0E+00	0.0E+00
Total	1.7E-05	1.7E-04	1.8E-02	1.8E-03	1.8E-02
Case 6 - All landslides					
Freight	2.1E-03	2.1E-02	0.41	0.14	0.41
Passenger	7.1E-05	7.1E-04	0.13	1.5E-02	0.13
MOW vehicle	6.4E-06	6.4E-05	1.8E-02	1.8E-03	1.8E-02
No Track Vehicle damage		9.1E-05	9.1E-02	4.5E-02	4.5E-02
Total	2.2E-03	2.2E-02	0.64	0.20	0.60

Maple Ridge, BC there would only be a $0.2*10^{-3}$ or 10% reduction in the risk of a fatality even though more than half the landslides were predicted. However, when Table 5.16 and 5.20 are compared the PIL warning system is shown to reduce the $P[F_{III}]$ by 39%. It should be noted that more restrictive train speeds when PIL thresholds are exceeded could further reduce the risk of PIL fatalities by another order of magnitude. Other steps discussed in Chapter 6 could also be considered.

5.8 Risk evaluation

The risks previously estimated need to be compared to the needs of the stakeholders. As in previous sections this section focuses on the risk of train crew and passenger fatalities. To assess acceptability of the risks, thresholds need to be identified to which the calculated risks can be compared. As indicated by Canadian Standards Association (1997) the risk will fall into one of three categories:

1. Acceptable at its current level,
2. Unacceptable at its current level, and
3. The risk might be acceptable but risk control measures should be evaluated.

This third category is often referred to as the region where risk should be reduced to As Low As Reasonably Achievable (ALARA). The subsequent section will compare the results of Section 5.5 to broadly acceptable risk levels, and evaluate the benefits of the two measures, HDS, and PIL notifications, discussed previously in the context of the ALARA ideal.

5.8.1 Identify potential railway policy consistent with societal risk tolerance

Numerous authors (including Fell 1994, Walker et al. 2000, Leroi et al. 2005, Terbrugge et al. 2006 and others) have written on the acceptable levels of risk in geotechnical engineering and landslide hazards. It is generally accepted that the involuntary probability of death of an individuals (PDI) most exposed to the hazard should not exceed $1*10^{-4}$ (Terbrugge et al. 2006, Porter et al. 2007, and others). Hambly and Hambly (1994), Bunce et al. (1997), Leroi et al. (2005) and Terbrugge et al. (2006), discuss the distinction between voluntary and involuntary risk. Hambly and Hambly (1994), and Terbrugge et al. (2005) suggest that employment risk is voluntary because each employee accepts that benefits (income) are at least partial compensation for the perceived risk, provided the risk is adequately understood. As a result, they suggest that the tolerable upper limit for voluntary risk at work is 10^{-3}.

Although, CP does not have an explicitly stated risk tolerance level, the 10^{-4} level achieved and considered acceptable by most industries is a reasonable target consistent with present operations and hazard avoidance efforts.

5.8.2 Comparison of railway risk performance and tolerance

Previously, in Chapter 5, the annual probability of an event or fatality has been considered. In order to compare these risks to those of other hazards and industries the risks need to be expressed as the annual Probability of Death of an Individual (*PDI*) exposed to the hazard. To transform the previously calculated probabilities of fatality, $P[F]$ for the entire CP system, into *PDI,* the populations exposed must be considered. The same transformation is done for the Canadian Cordillera and a specific location by

Table 5.21 Numbers of CP employees exposed to landslide hazards and the corresponding $P[F_{III}]$ and *PDI*

<table>
<tr><th>Region</th><th>Population exposed</th><th>$P[F]$ within CP</th><th>PDI</th></tr>
<tr><td>Maple Ridge, BC</td><td>460</td><td>$3.6*10^{-3}$</td><td>$1.4*10^{-5}$</td></tr>
<tr><td>Vancouver Service Area</td><td>460</td><td rowspan="4">$4.3*10^{-2}$</td><td rowspan="4">$7.2*10^{-5}$</td></tr>
<tr><td>BC Interior Service Area</td><td>530</td></tr>
<tr><td>Alberta Service Area[1]</td><td>60 (880)</td></tr>
<tr><td>Canadian Cordillera</td><td>1,050</td></tr>
<tr><td>CP network</td><td>5,540</td><td>$5.7*10^{-2}$</td><td>$1.8*10^{-5}$</td></tr>
</table>

[1] The number of running-trades employees in Alberta operating trains in the Canadian Cordillera is estimated by the proportion of mainline track in the mountains within this service area and the total length of mainline track in the service area. Only 100 km (60 miles) of the Laggan sub, from Canmore, Alberta to Field, BC, and 20 miles of the Crowsnest Sub, from Burmis, Alberta to Crowsnest, BC are in the mountains. As a result, 130 to 1900 km (80 of 1,200 miles) of main line track in the Alberta Service Area (7%) are in the mountains.

considering the appropriate exposed population. Table 5.21 includes the numbers of CP personnel exposed to the different types of hazards for the Maple Ridge, BC case, the Canadian Cordillera, and the whole CP network. As in Section 5.6, the risks of fatality from a Type III scenario is at least two orders of magnitude greater than the Type I risks for any group.

The individual risk of fatality or injury of a CP train crew member is the ratio of the number of fatalities or injuries and the number of running-trades employees operating the trains times the *P[Individual fatality:Crew fatality]*.

$$PDI = \frac{(P[F])(P[Individual\ fataility : Crew\ fatality])}{(population)} \qquad \text{Equation 5.39}$$

The Vancouver Service Area employs approximately 460 running-trades employees who work in 230 two person crews and operate the trains over the Maple Ridge, BC section of track. The probability of being one of the fatalities given a fatal accident occurs, *P[Individual fatality:Crew fatality]*, is 0.875 (from Table 5.2). Therefore, the probability of death of an individual (*PDI*) for running-trades employee at the Maple Ridge, BC landslide site is $1.4*10^{-5}$. However, this is just one site of many in the Vancouver Service Area. Other sites would likely have lower risk values due to more infrequent events. However, the sum of the risks at all the sites across the Vancouver Service Area would be expected to raise this value. Based on the proportion of track in the Vancouver Service Area compared to the Canadian Cordillera it could approach half the value of the risk level for the Canadian Cordillera calculated below. A complete assessment of the known hazards within a Service Area would be beneficial to identify the locations exposing the running-trades employees to the highest risk of fatality and injury.

The whole CP network employs approximately 5,500 running-trades personnel operating trains. In the Canadian Cordillera this number is about 1,050 or 525 two-person train crews. As indicated in Section 5.4.4.1, three geotechnical hazard events in the Canadian Cordillera have resulted in fatalities over the 70.7 years between 1937 and 2007. This means locomotive engineers and conductors working in BC and Alberta have an annual risk of being involved in a fatal geotechnical accident of about $8.2*10^{-5}$ for a crew of two. Using the *P[Individual fatality:Crew fatality]* of 0.875 from Table 5.2, BC and Alberta locomotive engineers and conductors working in the mountainous region have a PDI of $7.2*10^{-5}$ from a geotechnical train accident. Outside the Canadian Cordillera there has been one train crew fatality due to a geotechnical hazard in the past 47.7 years. Considering the 4,500 running-trades personnel outside of the Canadian Cordillera, the annual probability of death for an individual running-trades employee is $5.6*10^{-6}$.

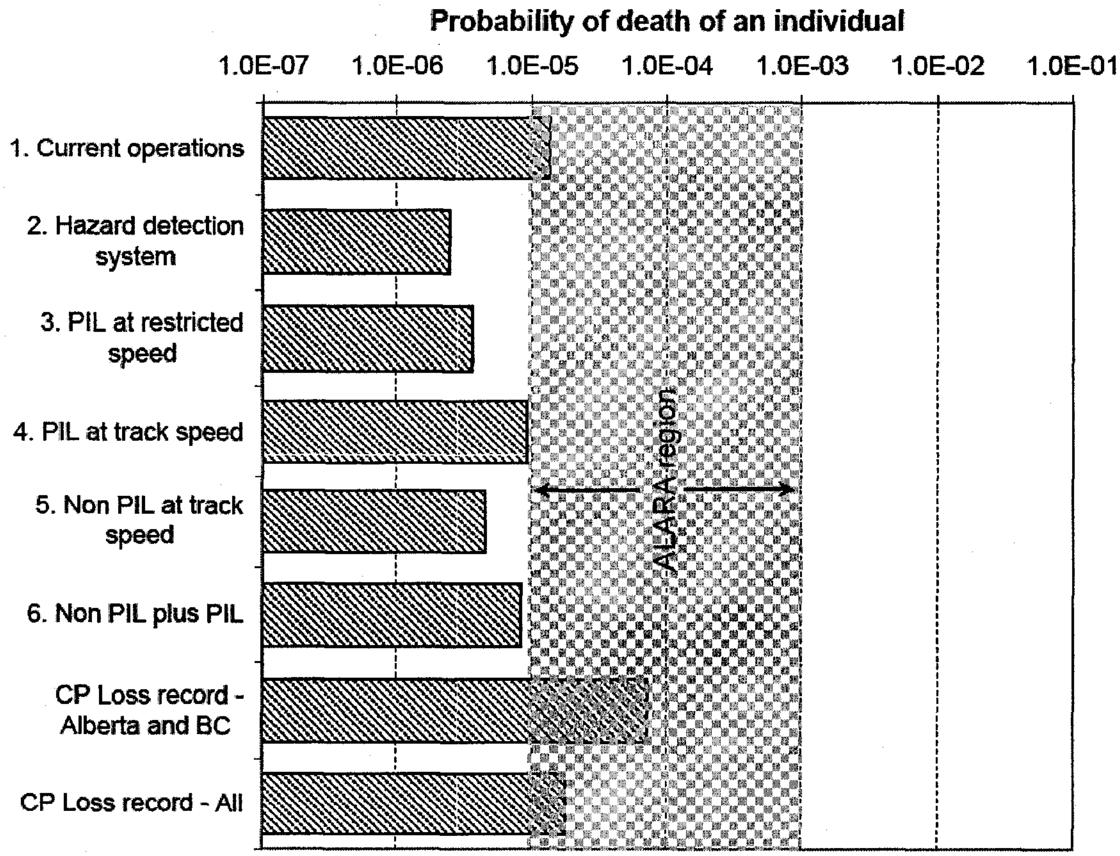

Figure 5.15 Probability of death of an individual for several operating conditions reviewed in Cases 1 to 6 from Section 5.5.4.6 and the CP loss-record from Table 5.3 as summarized in Table 5.21. Plot is presented consistent with Figure D1 after Terbrugge et al. 2006.

For comparison, Figure 5.15 illustrates the probability of a fatality between the different cases. These probabilities are computed by dividing the probability of one or more fatalities calculated in Cases 1 to 6 (Tables 5.14, and 5.16 to 5.20) by the number of crews exposed to the hazard and multiplying by the *P[Individual fatality:Crew fatality]*. These values are comparable with those summarized by Terbrugge et al.

(2006) and are presented in a similar format for ease of comparison. However, the values numbered 1 to 6 are for a single site and not the sum of the probability of death for an individual (PDI) exposed to the landslide hazards along the track on which they work. The seventh value is for a larger area and the eighth is for the entire CP network.

To complete the risk assessment for an individual passenger a number of assumption regarding trips per day, occupancy at Maple Ridge, BC and other factors would have to be considered. This is more appropriately undertaken by the commuter-transit rail service provider using the CP NHID information.

Service interruptions influence the profitability of the company and have to be assessed from a corporate financial risk perspective. Consideration of this risk is beyond the scope of this research.

5.8.3 Declaring a "level of safety"

Given that the risk of fatality can be quantified to a reasonable level of accuracy, consistent with the railway performance over the last 30 to 35 years, the railways could consider the adoption of a declared level of safety. The railway could then identify specific locations that contribute to the overall risk level and the location where risk reduction strategies would reduce the overall risk measurably. Tolerable geotechnical risk thresholds could be established for individual sites, complete subdivisions, and Service Areas to ensure an appropriate distribution of resources to mitigate the highest risks. This would allow for the effective communication and rationalization of the expenditure of limited resources.

5.9 Conclusions

The analysis completed in this chapter shows that the risk of a train encountering a landslide is the most likely geotechnical railway scenario to result in a train accident or health loss. This is consistent with the loss-record. The analysis indicates that, at present, CP is within industrial PDI standards but above those considered as a lower threshold for ALARA. As a result, CP should continue to undertake measures that will reduce the probability of geotechnical train accidents. The assessment of measures such as an HDS, which only reduce the probability of a train accident and fatality, and measures that reduce the frequency of the hazard, can now be compared on an equal benefit scale. A consistent analysis for the probability of service interruptions and duration could be completed to provide a second means of measuring the benefit of a specific mitigation strategy. However, the non-linear evaluation of the cost of various lengths of service interruptions would be required to complete this analysis.

It has been shown for the Maple Ridge, BC site that, given the ability to identify periods of higher landslide frequency based on the antecedent precipitation conditions, a significant reduction in the risk associated with landslides can be realized. Section 5.7.2 demonstrated that the probability of a landslide, given one or more thresholds is exceeded, can be used to identify periods of increased landslide frequency. It was also shown that, when precipitation induced landslide thresholds are exceeded, slowing trains reduces the probability of train accidents, derailments, and health losses. Chapter 6 discusses other risk reduction strategies.

Chapter 6.0 Conclusions and recommendations

6.1 Introduction

This chapter summarizes the conclusions of the research completed in this thesis. It also provides several recommendations for additional research and suggestions for application of the research results to the management of railway geotechnical risks. Following the introduction, the chapter is divided into six parts. Section 6.2 reviews the justification for the research. Section 6.3 summarizes each chapter of the thesis. Section 6.4 identifies the major conclusions. Section 6.5 discusses the potential application of the research. Section 6.6 suggests the integration of the findings into the operating environment of a railway and includes recommendations for additional research. Section 6.7 provides closing remarks.

6.2 Justification for this research

When railways assess their options for managing the risks from geotechnical hazards two options, consistent with the National Research Council (2004), are commonly identified: reduce the hazard and avoid the hazard. Although railway tracks and the supporting infrastructure are exposed to geotechnical hazards all the time, unlike other industries and agencies, the most vulnerable component of the railway, the trains and railway personnel, are only exposed to hazards when they are near the hazard. Since trains and personnel occupy any given section of track less than 20% of the time, railways have the additional option of avoiding the hazard when it is most likely to occur. As a result, railways have three options when it comes to reducing the influence of geotechnical hazards.

1. **Reduce the hazard** by stabilizing the landslide or process causing the hazard. This is a costly option and requires adequate knowledge of the hazard to be completed effectively and within budget. This option is only applicable to site specific hazards that have been identified.
2. **Avoid the spatial hazard** by moving the track away from the influence of the hazard. Generally, avoiding the hazard is costly because moving the track is difficult in locations influenced by geotechnical hazards. Realignment is costly primarily because of two factors:

a) Railways are limited to track grades of less than 2%.

b) Areas of significant geotechnical hazards may be located on steep slopes with lakes, rivers or seas at the toe of the slope.

As a result, tunnels, bridges or protective sheds costing several tens of thousands of dollars per metre are required to protect the track or to avoid the hazard.

3. **Avoid the temporal hazard** by managing the exposure of trains to the hazard. This requires identification of the periods of greatest hazard and the reduction of the frequency and/or speed of trains exposed during these times.

Option 3 is the preferred choice as it is achievable at the least cost to benefit ratio provided the rail traffic can be rescheduled or re-routed. This is usually practical provided the frequency of any delay is not excessive or prolonged. However, requirements for freight rail traffic are such that even this may be impractical on some routes. Railways would select option 3 and avoid the capital expenditures required in options 1 and 2 if the following conditions were met:

a. Rail traffic requirements are manageable.

b. The occurrence of each geotechnical hazard is predictable.

c. The frequency of hazards is consistent with or lower than historical levels.

d. No trains are unnecessarily delayed when no hazard occurs (no false-positives).

However, it is not yet possible for railways to economically collect sufficient data, to adequately model and predict landslides, and to communicate the warning to trains because of at least five major factors:

1. The number of known and unknown landslide hazards that pose or could pose a hazard to the railway is in the hundreds within CP at any given time based on past records. These hazards are concentrated in the Canadian Cordillera but others are broadly distributed across the CP network.

2. The cost to instrument each known landslide is not considered an economic option. Landslide investigation and monitoring is currently estimated to cost $100,000 to $400,000 per landslide.

3. The engineering effort required to determine which parameters need to be monitored to provide prior notice of the hazard, would have to be determined and the appropriate thresholds identified. This would require additional time, effort, and cost.
4. The cost and infrastructure required to communicate the appropriate warnings to the trains would also be significant. The limitations of the existing track-side signal warning systems would only protect between 80 and 90% of trains (see Section 5.5.4.4 - A). A landslide warning system capable of providing closer to 100% temporal coverage would require the development of a warning communication system that provides immediate vital communication with the train crews.
5. Not all the landslide hazards have been identified.

Without these components, the reliable prediction and communication of all increased landslide hazards in response to changing stability conditions can not be provided to the train crews.

However, it has been demonstrated by this research and by others, that climatic indices indicative of higher landslide potential can be identified. The cost of developing these indices would be a fraction of the cost of reducing or avoiding the hazard (options 1 and 2) capable of providing the same risk reduction. The indices also reduce the exposure to as yet unidentified hazards, sensitive to the same precipitation conditions. Furthermore, the frequency and time sensitivity of the warnings based on these climatic indices is such that they can be communicated using existing technology to engineering and operation personnel who are responsible for the protection of trains and personnel working on the track. The investment would be on the order of hundreds of thousands of dollars for the entire CP system, can be implemented incrementally, and would cover multiple hazard sites per weather station.

Unfortunately, as demonstrated in Chapter 4, the condition b above cannot be achieved such that every hazard is predicted. Therefore, some level of hazard exposure remains. Furthermore, some low level of false alarms (condition d above) occur and must be tolerated with a hazard prediction system. However, the prediction of a significant percentage of geotechnical hazards make avoidance of the temporal hazard (Option 3) viable and worthy of evaluation. To evaluate the three options a detailed quantitative measure of the effectiveness of each option and cost is required. Risk estimation can be used to provide this measure and resolve the predicted and capital cost of each option so that the costs and benefits of each option can be compared. To address this need, a quantitative risk estimation methodology was developed in Chapter 5.

This research is of value to railways, weather information service providers and others as it demonstrates a means of determining the temporal variation in landslide hazards and associated risks due to severe weather and other hazard mitigation measures.

6.3 Summary of thesis chapters

Chapter 1 of this thesis reviewed the need for weather information within CP. It also described how weather information is used within the railway industry and specifically how it is currently used at CP to assess geotechnical conditions and the influences they may have on the safety and reliability of railway operations.

In Chapter 2, the physical processes linking climatic conditions and landslide activity were reviewed. A literature review of the current state of research of precipitation induced landslides (PIL) and the state of practice used to assess and predict PIL was summarized. A review of the application of risk management techniques in geotechnical engineering was also provided.

Chapter 3 investigated the numerous types of data that are needed to be able to complete the assessment of climatic influences on landslide activity.

Chapter 4 documented how the relationship between precipitation and landslides can be assessed, appropriate indices selected, and thresholds set. It also demonstrated the use of two methods to determine the indices and thresholds to which specific landslides are sensitive. The identification of a frequency distribution capable of representing the antecedent precipitation conditions for periods in excess of those previously modeled was identified and tested. This is a key finding of this research. The concept that landslides do not occur during normal conditions but do occur as a result of unusual climatic conditions was applied. The most unusual antecedent precipitation conditions at the time of the landslide are identified as having induced the landslide. The combination of unusual climatic conditions that have induced landslides within the area for which the precipitation data are representative, are then used to form a set of criteria above which future landslides are assumed to be more likely. A means of identifying the rarity (or highest return period) of antecedent precipitation events on the day of the landslide is adopted using the generalized extreme value frequency distribution to determine the frequency of the event.

In Chapter 5, the probabilities of train accident and fatalities were calculated for several scenarios including with and without a theoretical PIL warning system. These risks were also compared to generally acceptable risks from other hazards.

6.4 Conclusions

The major conclusions for each chapter are summarized below.

6.4.1 Chapter 1

Chapter 1 concluded that available weather information should be investigated and any guidance regarding the timing of landslides be extracted and made available to those responsible for the day to day safety of the track and operation of trains.

It also concluded that a means of assessing the risk exposure of railways to these hazards would be required to assess the benefits of any warning system.

6.4.2 Chapter 2

Chapter 2 concluded that a relationship between precipitation, infiltration, groundwater conditions, and other factors; and the mechanisms controlling landslide hazards exists and is generally understood. It also concluded that numerous investigators have identified means of predicting landslides using precipitation data. Based on the literature reviewed it is concluded that the application of risk estimation within geotechnical engineering is a viable means of assessing the effectiveness of a PIL warning system.

The identification of the need to document the influences of geotechnical hazards on the railway by Peckover (1972) and the Railway Transportation Committee (1973) was critical to the development of the CP Natural Hazard Incident Database (CP NHID). Without this database this research would have been unachievable.

6.4.3 Chapter 3

Chapter 3 concludes that precipitation data and PIL indices are available from several sources. It also concluded that numerous techniques are available for predicting landslides based on precipitation but that few provide guidance on how to select the index that is most appropriate for the landslide being assessed.

The concepts of Chleborad (2000), Floris et al. (2007), Walker (2007) and others, were identified as the most effective and promising means of developing a methodology for identifying the PIL indices and thresholds capable of predicting landslide activity. The use of weather station specific indices and thresholds is adopted from the Japanese railway industry (Muraishi et al. 1992, Okada, 1994, Rimm-Kaufman 1996 and others).

6.4.4 Chapter 4

Chapter 4 concluded that the three parameter Generalized Extreme Value (GEV) frequency distribution can be used to predict the return period of antecedent precipitation conditions from 1 day to at least 270 days for several data sets from across Canada. Provided the precipitation data is from a single weather station, the ability of the GEV to fit extreme value data including antecedent precipitation is better than any other frequency distribution and adequate for the proposed application.

The chapter also concluded that, given the available weather and landslide information, it is possible to develop a means of predicting the occurrence of a sub-set of landslides using precipitation data.

6.4.5 Chapter 5

It was demonstrated in this research that geotechnical hazards have not exposed individual CP train crews or MOW employees to an intolerable risk of fatality. However, the loss records over the past 35 years are such that reductions in the risk are desirable. The risk estimation process developed in Chapter 5 allows the estimation of the risk of a fatality at a specific site based on the current operating conditions. However, geotechnical hazards are but one of the risks to which these populations are exposed. All of the risks need to be assessed to determine if the levels for any geographic group or category of employee is exposed to an intolerable level of risk.

The inclusion of all the relevant hazard and operating parameters in the risk estimation process allows the assessment of future risk levels given that various measures or operational changes are implemented. The risk reduction provided by installing additional hazard detection systems (HDS) including weather stations, can now be quantified. This will aid in the rationalization of the expenditure required to add a PIL notification system to the existing weather information system and install other HDS systems.

It was demonstrated, for a specific site, that the inclusion of an HDS in the train warning system and a PIL warning system could significantly reduce the risks. The risk analysis also indicated that the risks associated with a moving train being impacted by an active landslide are significantly less than the risks associated with a moving train impacting a landslide that has obstructed the track.

6.5 Application of research

The potential applications of this research are discussed in the following subsections.

6.5.1 Risk reduction strategies

There are numerous hazards, including rock falls and large landslides, for which the railways have developed monitoring systems that notify approaching trains that hazards may exist ahead of the train. Rock fall hazard detection systems (signal or slide fences) are the most widespread example. Signal fences are used by Class 1 railway in North America that is exposed to rock fall hazards. In most cases where rock fall hazards exist, rock falls are so numerous and dispersed that reducing the hazard at all locations is not considered cost effective. Instead, at many sites, railways have elected to employ means of notifying approaching trains of the potential of obstructions of the track ahead of the trains. With large landslides moving at rates of less than 50 mm per year, movements of the landslides can be accommodated by periodic realignments of the tracks without exposing the trains to undue risks. These landslides are so large that multi-million dollar stabilization efforts would be required to achieve even a modest increase in the factor of safety. To address the potential for more rapid landslide movement, railways commonly employ "tip-over-post" systems to warn oncoming trains that landslides may have moved and that the tracks may not be passable.

Similarly, weather warning systems could be used to lower the frequency and severity of train accidents resulting from geotechnical hazards by warning trains of their potential occurrence without having to stabilize all the hazards. Given that railways can slow, suspend, and schedule rail traffic, these warning systems could be integrated into operations. The following sections include a discussion of several mitigative operational and engineering measures that could be implemented before and when PIL thresholds are exceeded or predicted to be exceeded.

6.5.2 Mitigative operational actions

The railway industry has control of the temporal operation of the highest consequence components (trains and personnel) on its right-of-way. Other linear transportation corridors, including the public roadway system, utilities (pipelines, electrical transmission systems, and fibre optics transmission systems), and others, do not have this option. As a result, during higher hazard periods that could reduce either the safety, reliability, or the serviceability of the railway track, numerous actions can be taken to reduce the consequences in the event a hazard occurs. These actions are focused on preventing or reducing the consequences of a train accident caused by a hazard rather than preventing the occurrence of the hazard. They do not address or reduce the potential for service interruptions although they should reduce the duration of a service interruption by reducing the recovery time.

Potentially mitigative measures in response to periods of higher hazard in order of their impact on operations are presented and discussed in the subsequent numbered bullets.

1. **Increase the number of track inspections**

   Federal regulations dictate how frequently a track must be inspected based primarily on the track speed, and gross annual tonnage of the track. The required frequency of track inspection ranges from once every two days to once per month (Railway Association of Canada 2008). Once an elevated risk has been identified due to a climatic event or other condition, more frequent inspections are undertaken at the discretion of the Track

Maintenance Supervisor (TMS). As the frequency of inspections increases, the level of inspection, described later in bullet 3 below, will occur.

As shown in the risk assessment, as the proportion of track inspections increases, the probability of a train derailment and a fatality decreases. This is partially because a hi-rail vehicle can stop quicker than a train resulting in a lower probability of a fatality. Furthermore, the recovery time from a hi-rail accident is less than that of a train accident.

2. **Temporarily reduced train speed**

   The lower the train speed the shorter the stopping distance of the train. Therefore the chance of a derailment and the severity of its consequences, are reduced. Train speed can be reduced progressively, depending on the severity of the risk, or the consequence reduction desired. High vulnerability (dangerous cargo and passenger) trains could be slowed more than low vulnerability (inter-modal and bulk cargo freight) trains to achieve an equivalent risk reduction. An example where all trains were slowed in response to severe precipitation has been quantified in Section 5.7.2 and showed a 39% reduction in the probability of fatalities and a 51% reduction in the probability of train accidents.

3. **Track inspection in front of each train**

   During severe climatic conditions it is possible to complete an inspection of the track before each train. There are limitations to the benefit of this type of inspection. Due to track-safety operational requirements, an inspection vehicle cannot be within the same track limits as a train. Given the length of most track limits, this can be between 1.6 and 16 kilometres (1 and 10 miles). This means that the inspection vehicle will be 1 to 24 minutes ahead of the train given track speeds of 40 to 95 kmph (25 to 60 mph). As a result, this type of patrol may not significantly decrease the risk since the previous train over the track might only be an hour ahead of any given train. The benefit of this type of inspection diminishes the higher the train frequency.

   It has been suggested that robotic track inspection vehicles (RTIV) be deployed in front of each train (T. DeMarco, CP, personal communications 2003). A robot would travel some lead distance in front of a train to confirm the continuity of the track. The lead distance would be defined as a multiple of the stopping distance of the train. If the RTIV encountered an obstruction, the train would be notified and stop within its stopping distance before encountering the obstruction. To be reliable, the robot would have to impose a load equivalent to the heaviest train car within the train. Mid train, load induced, pore pressure triggered, sub-grade dynamic liquefaction earth slides (Keegan 2007) would not be protected against because the single car RTIV would not induce the repetitive cyclic loading commonly cited as causing this type of failure. Due to the lead distance between the RTIV and the train, there will always be some percentage of time that the RTIV does not provide protection. Given the technology required to develop an RTIV, the benefit of this would have to be compared to operating the locomotive remotely, without an onboard operator. However, the use of remotely operated trains only reduces the probability of a fatality and not a derailment. An RTIV reduces the probability of fatalities and train accidents.

4. **Delay lower priority, passenger, or dangerous cargo trains**

CP and other railways prioritize trains to meet the demands of their customers, often charging higher rates for faster delivery. It should be possible to delay lower priority trains without influencing net train throughput. Using the risk analysis procedure, it is possible to quantify the benefit of reducing the train frequency when PIL thresholds are exceeded, combined with higher train frequencies when PIL thresholds are not exceeded. This would further reduce the combined risk of all trains compared to the risk reduction analyzed in Section 5.2.4. These measures can be quantified and compared to the annual cost of delaying the lower priority trains. The same approach could be used to test the risks and benefits of running higher priority trains, passenger trains, and trains transporting dangerous cargo.

5. **Temporarily interrupt rail service**

The most severe measure would be to implement an artificial service interruption rather than take the chance that a train might be influenced by a landslide. It is likely that this would only be justified in extreme conditions, when all the antecedent precipitation thresholds were exceeded or forecast to be exceeded. This has happened in the recent past. In 1997 February, and between 2007 December 3 to 5, CP shut down rail operations in response to several days of heavy snowfall and subsequent melting in the Fraser Canyon of BC between North Bend and Hope. CP was unable to get train crews to trains because the highways were impassable. The BC Hydro electric power distribution system was also out of service and CP signal systems were not functioning. Before train operations could be restored, it took about 24 hours to clear the track of debris and snow avalanches that would have delayed and presented a hazard to trains had they been able to keep running despite the road closure and power failure.

As was discussed in Section 5.5.3 any trains stopped due to severe weather conditions should be located where there are no known weather sensitive hazards.

It should be recognized that, because rail traffic is approaching capacity on several rail lines, especially in the Canadian Cordillera of the CP rail network, maintenance and grading projects requiring long periods with no train traffic are preferably completed during service interruptions. These projects include bridge maintenance or replacement that might temporarily influence the capacity of the bridge, or open excavations for culvert replacements. If this work is to be completed during a severe weather service interruption it should be demonstrated that the work can be completed without placing the MOW employees at an increased risk due to the weather conditions.

6. **Risk based train scheduling**

It should be possible to develop an automated computer algorithm that optimizes the train schedule to minimize the risk of derailment or fatality. The system would use forecast weather data, train schedule requirements, and the PIL warnings within the four day, and possibly longer forecast period, to optimize the train schedule and track speed to minimize the collective risk to CP within the forecast period. Remembering that PIL warnings will only be issued for a low percentage of the days of the year for any one weather station, this may prove to be beneficial without being onerous. The program would only be utilized when a PIL warning was forecast.

6.5.3 Mitigative engineering actions

There are at least two ways this research can be applied to mitigation within the engineering discipline of a railway. Both pertain to the evaluation of mitigative solutions.

6.5.3.1 Install more hazard detection systems

Railways use several types of track-side hazard detection systems (HDS) as discussed in Section 5.5.4 and the Glossary. By deploying more of these systems, a railway can further reduce the risk to rail traffic as demonstrated in Chapter 5.

Several issues should be considered before additional HDS are deployed because of the following factors:

1. HDS only reduce the vulnerability and therefore the PDI of the railway. HDS do not reduce the hazard, therefore they do not directly improve the service or reliability of a railway. HDS should reduce the number and severity of train accidents and thereby reduce the recovery time following a landslide.
2. HDS introduce additional delays if they produce false-positive indications. The excessive use of HDS that produce false-positive results reduces the efficiency of the railway to move rail traffic, which can become critical in capacity constrained rail corridors.
3. HDS only provide notification to trains between 80 and 90% of the time, depending on rail traffic density, signal spacing, and train speed. However, this short-coming is incorporated into the risk reduction evaluation techniques present in Chapter 5.
4. HDS do not influence or reduce the risk to MOW personnel because MOW personnel track movements are not governed by the track signal system to which the HDS are connected.
5. The deployment of HDS that have to be manually reset, as do the traditional trip-wire signal fences, increases the risk of fatality to Signals & Communications (S&C) personnel. The more HDS deployed requiring manual

reset, the more time S&C personnel are required to be on the track to reset them. Therefore, more HDS results in more S&C exposure to hazards.

These factors must be considered during the process of evaluating the deployment of additional HDS. All factors can be modeled in the risk estimation process.

6.5.3.2 Increase the number of sources of precipitation data

As discussed in Chapters 3 and 4, there are numerous sources of climatic, and more specifically, precipitation information. The railways and their weather information service providers should undertake to gather as much information as possible to provide the most site specific guidance to the TMS and Operations personnel. Initiatives such as Clarus (Pisano et al. 2005) and MADIS (National Oceanic and Atmospheric Administration 2007c) have demonstrated that there are additional data available beyond that of the two national weather services of Canada and the United States.

Ultimately, each railway track-side signal could be equipped with a precipitation gauge similar to that proposed by Chien-Yuan et al. (2005). When PIL index thresholds specific to that location are exceeded, the signal would indicate restricted speed. The logistics and resources needed to implement this scale of weather warning system would take considerable effort to justify and time to implement. It would also require the development of thresholds calibrated and based on the next nearest weather station since there would be a deficit of historical data for the first 20 to 30 years for the exact location of each signal. Grid precipitation forecast data from ensemble climate models (Environment Canada 2008) could be integrated with the precipitation data from each signal to provide predictive warnings.

6.5.4 Influence of hazard reduction strategies on risks

It has been demonstrated that the introduction of precipitation indices can reduce the risk of train accidents and loss of life by a significant proportion of the total risk. For instance, given the identification of a period of increased landslide potential due to one or more PIL thresholds being exceeded, one or more of the operational mitigative strategies identified in Section 6.5.2 could be applied. For instance, if the

Maple Ridge, BC thresholds identified in Table 4.13 of Section 4.5.15 were exceeded, a slow order over this section of track could be issued by the NMC or TMS. If this were undertaken for each period the thresholds were exceeded for the entire year, the risk of a fatality at this site would be reduced by 39% of current risk levels, as demonstrated in Section 5.7.2. However, rail traffic would be slowed 3.8% of the time as it travels through the Maple Ridge, BC landslide area.

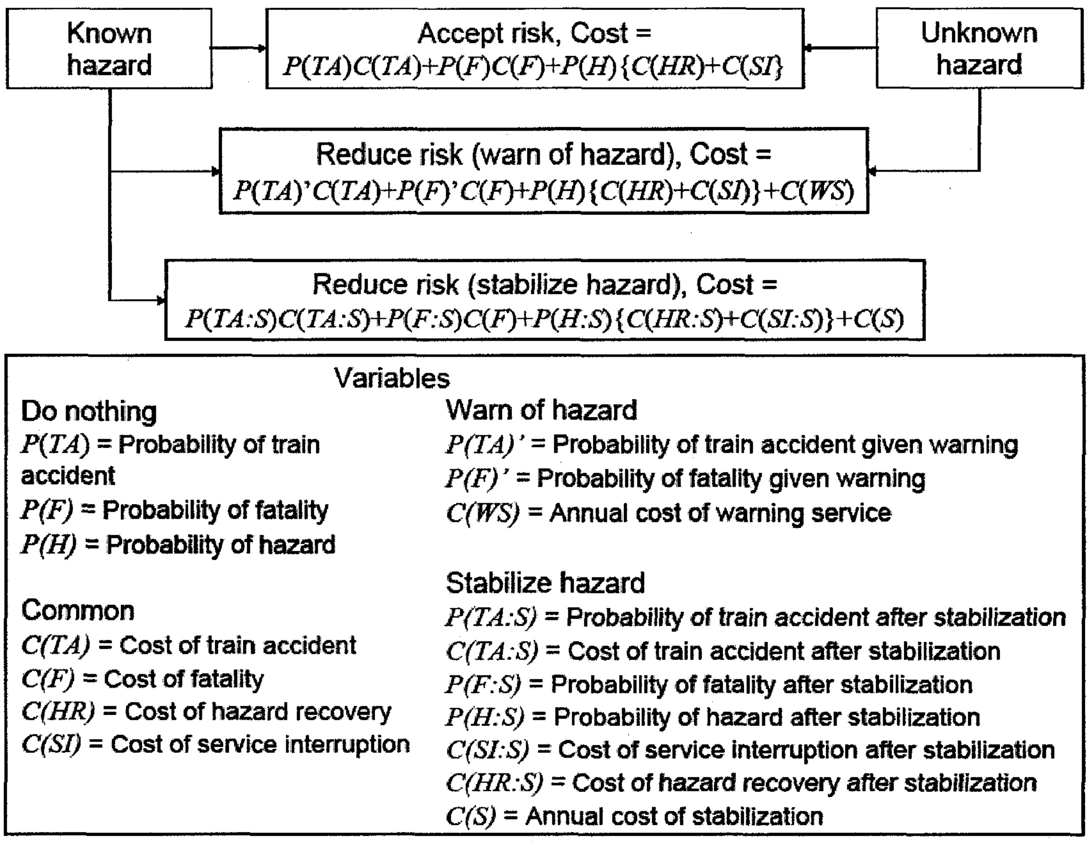

Figure 6.1 Analysis of costs and benefits of three risk control options. Each formula provides the annual cost of the hazard.

Consistent with Leroi et al. (2005) the overall cost benefit analysis would have to assess the cost of accepting the risk (do nothing), reducing the risk by implementing a weather information system analysis, or reducing the risk by stabilizing the hazard. This assumes that the cost to avoid the hazard is presently prohibitive. The risks associated with unidentified hazards would also have to be quantified in this analysis. The CP-NHID could be used to assess the proportion of known and unknown hazards but the ratio is expected to be high in favour of unknown hazards. Figure 6.1 provides an overview of a basic cost comparison framework and the variables that would have to be quantified for each hazard. Although it may be possible to reduce the number of unknown hazards by completing more extensive hazard investigations, this will increase the number of known hazards and increase the cost of stabilization more significantly than the cost of a warning system. Aggregating the results of each known hazard and an appropriate proportion of unknown hazards could be used to provide justification for a hazard notification system based on antecedent precipitation indices.

The option resulting in the lowest annual cost would be selected. Clearly this evaluation would take a significant effort if it was completed on each individual hazard and the results aggregated into a system-wide total. However, it should be possible to determine or estimate the system-wide costs and assess the cost benefit of a warning service on a system-wide basis.

6.6 Recommendations

6.6.1 Recommendations for future research

There are opportunities for numerous additional areas of research in geotechnical hazards, climatic influences on geotechnical hazards, and the risks associated with hazards from a railway perspective. Some of these are identified below.

6.6.1.1 Geotechnical

1. Additional research is required into the climatic influence of geotechnical hazards. Additional PIL sites should be assessed and the site specific indices and thresholds derived. Warnings based on these can be implemented as they become available within current weather information systems.
2. Further investigation of the size of the landslide and the severity (rarity) of the antecedent event can be established now that a frequency distribution has been identified that adequately fits the antecedent data. It is expected that the larger the landslide the more unusual the climatic inducing conditions given that more common climatic conditions have already triggered the smaller events. This theory was tested in Section 4.5.14.2 but

the results were inconclusive. A larger data set should be considered to further investigate this logical relationship.

3. Each new precipitation induced geotechnical incident can be used to directly increase the effectiveness of a PIL system. This incremental increase in knowledge can be used to improve the accuracy of the PIL warning system. This will either:

   a) Provide fewer warnings by making the precipitation threshold higher and therefore resulting in fewer false-positives and the related delays these introduce, or

   b) Produce a more conservative warning system by lowering the precipitation thresholds and providing a more accurate prediction of PIL (true-positives). Since the current thresholds are excessively low or non-existent for most antecedent durations the outcomes in Section 6.5.3.1 bullet 2 above will be more common until a mature system is developed.

As a result, each time a landslide occurs, the data should be assessed and an additional or refined threshold implemented. In this way, a PIL weather warning system can be incrementally improved over time. If the rate of false-positives becomes intolerable, inverse criteria can be developed to reduce the number of warnings based on known extreme precipitation conditions that have not caused landslides.

6.6.1.2 Climate data

1. The availability of hourly rain gauge precipitation data should be investigated. Currently, this information is not readily available. If and when it becomes available, this information could be used to complete analysis and define additional PIL indices. To move beyond the analysis of daily data completed in this research would require an order of magnitude more data analysis. Real time hourly precipitation data and accurate documentation of the time, location, and characteristics of the hazards would be required. Generally, this is not available for geotechnical hazards that do not result in a train accident, because no one was present to observe and document them.

2. Investigate use of radar data. A further 2 orders of magnitude (temporal 15 minute data and spatially 2 km grid in areas covered by weather radar) of data would have to be considered if weather radar data were to be utilized.
3. Further analysis of antecedent precipitation data longer than 365 days is recommended. This would allow the investigation of landslides that are sensitive to antecedent precipitation of longer than 1 year to be analyzed.
4. Assess available climatic data sources to investigate if there is sufficient information to model the influence of evaporation and transpiration on infiltration. If information is available, the influence of evaporation and transpiration should be incorporated into the antecedent precipitation index to form a new index with a potentially better correlation with landslide activity than the indices defined in this research, especially in arid areas.

6.6.1.3 Risk estimation

1. More information can be extracted from the CP NHID on the percentages and probabilities of specific events. For example, the probability of a derailment, given the impact of a train, for different volumes and types of landslides, could be extracted from the CP NHID.
2. A number of cases within the CP NHID are incomplete. Additional investigation of geotechnical incidents would provide additional information on numerous hazards and would assist in the understanding of the landslides and railway hazard interaction.
3. The volume delay relationship should be analyzed for various volume classes. This could also include an assessment of the volume/delay relationship for those events resulting in a train accident but not resulting in a derailment.
4. Additional geotechnical hazard train accident data could be collected. If the North American railway industry wants to move beyond the work completed by Peckover (1972) the industry needs to collect more data on the interaction of trains and landslides. This would allow a more detailed understanding and more reliable estimation of several of the parameters and probabilities utilized and identified in Chapter 5 to evaluate the risk of a train accident and

health loss. In addition to the list provided by Peckover (1972) the additional items in Table 6.1 should be documented.

Table 6.1 Recommendation for the collection of additional data for geotechnical hazards

Category from Peckover (1972) list	Additional items
Weather	- Return period of several standard antecedent precipitation conditions
Train delays [and accidents][1]	- Information on when and if the train crew received warning of the hazard and how they responded - Train speed at impact using train event recorder data - Exact time of landslides (not just the dates)
Rocks on track	- Failure mode as per Keegan (2007)
Removal of fallen debris not reaching the track	- Failure mode as per Keegan (2007)
Repairs to warning installations [HDS]	- Time to repair - Delay in time to repair because the conditions were unsafe or the weather indicated it would be unsafe to enter the hazard zone

[1] [] indicates text added to Peckover category for clarity

6.6.2 Recommendation for implementation

6.6.2.1 Precipitation induced warnings

Implementation of precipitation indices and thresholds should be considered by the railway industry for several reasons. The data is available and the means to utilize the data for the prediction of increased landslide hazards has been demonstrated. Railways have an obligation to their employees and shareholders to utilize the available data and knowledge to increase employee safety and reduce shareholder risk. It is expected, that as this research and that of others is disseminated, railways will require their Weather Information Service providers to incorporate more PIL warning criteria for specific PIL hazards into the notification system. CP has begun this process with its weather service provider and similar efforts are being undertaken at CN (T. Edwards, CN, personal communications, 2007).

6.6.2.2 Risk Assessment

The risk assessment techniques and methodologies developed in Chapter 5 allow for the comparison of a variety of risk mitigation strategies including those listed in Section 6.5.1. This should provide the engineering groups within railways the means to evaluate the cost benefit of numerous options and to be able to select the most cost effective options.

This research demonstrates that it would be possible to develop a real time risk weather hazard management system. The systems would have the following components and processes described below:

1. The weather service information provider would notify the railway NMC as forecasts come available (at least daily) when a PIL threshold is exceeded, or forecasted to be exceeded within a defined period, possibly as long as four days.

2. The NMC would then review which trains are scheduled to leave before, during, and after the PIL is forecasted to be exceeded.

3. The NMC would then enter the various acceptable combinations of train densities into a risk estimation algorithm. This would calculate the risk of each combination and identify which combination of train schedules and forecast PIL warnings result in the lowest overall risk within the forecast period. The option of implementing train or hazard location specific slow orders and additional track inspections would also be assessed.

4. The NMC would select the lowest risk option that achieved the minimum operating requirements and direct the trains, TMS, and or MOW personnel to execute the plan.

6.7 Closing remarks

This research has provided significant progress in the analysis of precipitation induced landslides and risk estimation. The application of this research on precipitation induced landslides is not limited to the railway industry and could be applied to the investigation of landslides that are suspected of being induced by antecedent precipitation conditions. This research would not have been possible without the compilation of the CP NHID initiated in response to the original work of Peckover (1972). The continued compilation of landslide data will provide critical information for future investigations of geotechnical railway hazards.

It has demonstrated a means of analyzing the return period of antecedent precipitation conditions of 1 to 365 days using the generalized extreme values frequency distribution. It has also developed a method of determining the risk of a fatality and train accident for an individual location within the existing railway operating environment. Risk estimation provides a measuring stick by which numerous hazards and potential mitigation options can be evaluated and compared.

Bibliography

Abbott, B., Bruce, I., Savigny, W., Keegan, T., and Oboni, F. 1998a. A methodology for the assessment of rockfall hazard and risk along linear transportation corridors. Proceedings, 8th International Congress, International Association for Engineering Geology and the Environment, *Edited by* D.P. Moore, and O. Hungr, Vol. 2: 1195 - 1200

Abbott, B., Bruce, I., Savigny, W., Keegan, T., and Oboni, F. 1998b. Application of a new methodology for the management of rockfall risk along a railway. Proceedings, 8th International Congress, International Association for Engineering Geology and the Environment, *Edited by* D.P. Moore and O. Hungr, Vol. 2: 1201 - 1208.

Aleotti, P. 2004. A warning system for rainfall-induced shallow failures. Engineering Geology, **73**(3-4): 247 - 265.

Aleotti, P. and Chowdhury, R. 1999. Landslide hazard assessment: summary review and new perspective. Bulletin of Engineering Geology and the Environment, **58**: 21 - 41.

American Society of Civil Engineers (ASCE). 1996. Hydrology Handbook. Task Committee on Hydrology Handbook, New York. 784 p.

American Railway Engineering & Maintenance of Way Association (AREMA). 2003. Practical Guide to Railway Engineering. *Developed by* Committee 24 Education and Training.

Armstrong, J. E. 1980. Surficial Geology, New Westminster, West of Sixth Meridian, British Columbia, Geological Survey of Canada. Ottawa. Map No. 1484A

Association of American Railroads (AAR). 2006. Class 1 Railroad Statistics. Policy & Economics Department. Available from http://www.aar.org/PubCommon/Documents/AboutTheIndustry/Statistics.pdf [cited 24 October 2007].

Gerath, R., Jakob, M., Mitchell, P. and VanDine D., 2006. Guidelines for Legislated Landslide Assessments for Proposed Residential Development in British Columbia. Association of Professional Engineers and Geoscientists of British Columbia (APEGBC). Available from http://www.apeg.bc.ca/ppractice/documents/ppguidelines/guidelineslegislatedlandslide.pdf [cited 10 November 2006].

Barney, D., Haley, D., and Nikandros G. 2001. Calculating Train Braking Distance. Proceedings of the 6th Australian workshop on Safety critical systems and software, Brisbane, Australia. Australian Computer Society. **3**: 23 - 29. Available from http://crpit.com/confpapers/CRPITV3Barney.pdf [cited 3 February 2002]

Baum, R.L., Chleborad, A.F., and Schuster, R.L. 1998. Landslides triggered by the Winter 1996-97 Storms in the Puget Sound Lowland, Washington. U.S. Geological Survey Open-file Report 98-239. 16 p.

Baum, R.L., Godt, J.W., Harp, J.W., and McKenna, J.P. 2005. Early warning of landslides for rail traffic between Seattle and Everett, Washington. *In* Proceedings, International Conference on Landslide Risk Management, Vancouver, B.C., 31 May - 3 June. *Edited by* O. Hungr, R. Fell, R. Couture, and E. Eberhardt, A.A. Balkema, London, U.K. pp. 731 – 740.

Baum, R.L., Savage, W.Z., and Godt, J.W. 2002. TRIGRS — A Fortran Program for Transient Rainfall Infiltration and Grid-Based Regional Slope-Stability Analysis. USGS Open-file Report 02-424 Available from http://pubs.usgs.gov/of/2002/ofr-02-424/ofr-02-424-508.pdf [cited 4 June 2004].

Bell, R. and Glade, T. 2004 Quantitative risk analysis for landslides - Example from Bildudalur, NW-Iceland. Natural Hazards and Earth Systems Sciences. **4**: 117 - 131.

Bertrand, J. and Falls L.C. 2006. An Investigation of the Effects of Weather on Rail Heating. Presented at Grad Conference at U of C, Calgary, Alberta, 1 May 2006. 21 p.

Bombardier 2008. Technical Data, BiLevel Coaches - Vancouver Canada. Bombardier Available from http://www.bombardier.com/index.jsp?id=1_0&lang=en&file=/en/1_0/1_1/1_1_3_1_5_3.jsp [cited 10 January 2008].

Boundary County 2007. Section 6 Hazard Profiles - Landslides, All Hazards Mitigation Plan. Boundary County Idaho, Local Emergency Planning Committee. Available from http://www.boundarycountyid.org/emermgmt/mitigationdraft/sec04.htm [cited 5 July 2007.

Brand, E.W., Premchitt, J., and Phillipson, H.B. 1984. Relationship between rainfall and landslides in Hong Kong. Proceedings of the 4th International Symposium on Landslides, 1984 - Toronto, Canada: BiTech Publishers, Vancouver. pp 377 to 384.

Brawner, C.O. 1994. Rockfall hazard mitigation Methods, Participant Workbook, Course No. 13219, National Highways Institute, US Department of Transportation.

Bromhead, E.H. 1992. The Stability of Slopes, Second edition, Blackie Academic & Professional, Glasgow. 411 p.

Bruce, J.P. 1961. Frequency of heavy rainfall in the lower Fraser Valley. Metrological Branch – Department of Transport – Canada. CIR. -3468. TEC.-354.

Bunce, C.M. 1994. Risk analysis for rock fall on a highway. M.Sc. thesis, Department of Civil Engineering, University of Alberta, Edmonton, Alberta. 130 p.

Bunce, C.M., Cruden, D.M., and Morgenstern N.R. 1997. Assessment of the hazard of rock fall on a highway. Canadian Geotechnical Journal **34**: 344 - 356.

Bunce, C.M., MacKay, C.H., and Martin C.D. 2003. Severe Weather Warning Levels for Geotechnical Railway Hazards. Proceedings, 3rd Canadian Conference on Géotechnique and Natural Hazards. Edmonton, Alberta, June 9 - 10, 2003. pp. 335 - 342.

Bunce, C.M., Martin, C.D., Keegan, T., Hutchinson, D.J., Ruel, M., and Lemay, P. 2006. An overview of the Canadian Railway Ground Hazard Research Program. 7th World Congress on Railway Research. 4 - 8 June 2006, Montreal, Canada. 14 p.

British Columbia Ministry of Environment 2006. River Forecast Centre. Available from http://www.env.gov.bc.ca/rfc/ [cited 12 October 2007].

Browning, S. 2003. Using GIS and Digital Data to Calculate Local Watershed Areas for Conservation Planning. Ohio Geospatial Technologies Conference for Agriculture and Natural Resources 24 - 26 March 2003, Columbus, Ohio. Available from http://geospatial.osu.edu/conference/proceedings/workshops/browning_2.pdf [cited 10 June 2004].

Canadian Pacific. 2007a. A Brief History. Available from http://www8.cpr.ca/cms/English/General+Public/Heritage/A+Brief+History.htm [cited 25 October 2007].

Canadian Pacific. 2007b. Slopes & Embankments, Standard Practice Circular 30. . Engineering Services. Calgary, Alberta. 23 pp.

Canadian Pacific Railway. 2000. Right of Way Maintenance, Standard Practice Circular 1. Engineering Services. Calgary, Alberta. 9 pp.

Canadian Pacific Railway. 2005. General Board Orders (GBO) 5th edition. General Code of Operating Rules Committee. Operations Department, Calgary

Canadian Transportation Agency. 2003. Uniform Classification of Accounts. Available from http://www.cta-otc.gc.ca/rail-ferro/finance/uca/1100_e.html [cited 24 October 2007]

Canadian Standards Association. 1991. Q634-91-CAN/CSA – Risk analysis requirements and Guidelines, Quality management. A National Standard of Canada. Canadian Standard Association, Etobicoke, Ontario, Canada.

Canadian Standards Association. 1997. Q850-97-CAN/CSA - Risk Management: Guideline for Decision-Makers, Canadian Standard Association, Etobicoke, Ontario, Canada.

Caine, N. 1980. The rainfall intensity-duration control of shallow landslides and debris flows. Geografiska Annaler **62**: 23-27.

Cannon, S.H. and Ellen, S.D. 1985. Rainfall conditions for abundant debris avalanches, San Francisco Bay region, California. California Geology. **38**: 267–272.

Chan, R.K.S. and Pun, W.K. 2004. Landslip Warning System in Hong Kong. Geotechnical News **22**:4 33 - 35.

Changnon, S. A. 2006. Railroads and Weather. American Metrological Society. Boston, Mass. 125 p.

Chen, H., Crosta, G.B., and Lee C.F. 2006. Erosional effects on runout of fast landslides, debris flows and avalanches: a numerical investigation. Géotechnique **56**(5): 305 - 322.

Cheung, S.P.Y. 2006. The application of information technology in managing landslide risk. Geotechnical Engineering Office, Civil Engineering and Development Department. In Symposium on 'Science in Public Services', Hong Kong. Available from www.science.gov.hk%e3%80%82/ paper/CEDD_SammyCheung.pdf. [cited 10 June 2007].

Chien-Yuan, C., Tien-Chien, C., Fan-Chieh, Y., Wen-Hui, Y., and Chun-Chieh, T. 2005. Rainfall duration and debris flow initiated studies or real-time monitoring. Environmental Geology **47**: 715 - 724.

Chleborad, A.F. 1997. Temperature, Snowmelt and the Onset of Spring Season Landslides in the Central Rock Mountains, Washington. USGS Open file Report 1997-027.

Chleborad, A.F. 2000. Preliminary method for anticipating the occurrence of precipitation-induced landslides in Seattle, Washington. USGS Open file Report 00-479.

Chleborad, A.F., Baum R,L., and Godt, J.W. 2006. Rainfall Thresholds for Forecasting Landslides in the Seattle, Washington, Area - Exceedance and Probability. USGS Open file Report 2006-1064.

Chow, V.T., Maidment, D.R., Mays, L.W., 1988. Applied hydrology, New York McGraw-Hill, 572 p.

Chowdhury, R.N. and Flentje, P. 1998. Effective Urban Landslide Hazard Assessment. Proceedings, 8th International Congress, International Association of Engineering Geology and the Environment, *Edited by* D.P. Moore and O. Hungr, Vol. **2,**: 871 – 877

Chowdhury, R.N. and Flentje P. 2002. Uncertainties in rainfall-induced landslide hazard. Quarterly Journal of Engineering Geology **35**: 61 - 70.

Clarus Initiative 2007. A National Surface Transportation Weather Observing and Forecasting System. Available from http://www.clarusinitiative.org/background.htm [cited 10 June 2007].

Collier, C. and Hardaker, P. 2004. Using Radar in Hydrometeorology. *In* Weather Radar, Principles and Advanced Applications, *Edited by* Peter Meischner, Springer-Verlag, 337 pp.

Couture, R. and Evans, S. G. 2000, Five-Mile Creek debris flow, Banff National Park, near Banff, Alberta, August 4, 1999, Geological Survey of Canada, Open File 3876.

Crozier, M.J. and Elyes, R.J. 1980. Assessing the Probability of Rapid Mass Movement. *In* Proceedings, Third Australia-New Zealand Conference on Geomechanics, Wellington, New Zealand, New Zealand Institution of Engineers, pp 2-47 - 2-51.

Crozier, M.J. 1999. Prediction of rainfall-triggered landslides: a test of the antecedent water status model. Earth surface Process and Landforms. **24**: 825-833

Cruden, D.M. and Varnes, D.J. 1996. Landslides: Investigation and Mitigation. Chapter 3 – Landslide types and processes, Special Report No. 247. *Edited by* A.K. Turner and R.L. Schuster. Transportation Research Board, Washington, USA.

Cruden, D.M., and Langenberg, W., 2003. McConnell and Brock's report on the great landslide at Frank, District of Alberta, Northwest Territory. Proceedings, 3rd Canadian Conference on Géotechnique and Natural Hazards. Edmonton, Alberta, June 9 - 10, 2003. pp. 235 - 241.

Dai, F.C. and Lee, C.F. 2001. Frequency – volume relation and prediction of rainfall-induced landslides. Engineering Geology, **59**: 253 - 266.

Dai, F.C. and Lee, C.F. 2003. A spatiotemporal probabilistic modeling of storm-induced shallow landsliding using aerial photographs and logistic regression. Earth Surface Process and Landforms **28**: 527 - 545.

Dean, J.D. and Snyder, W.M. 1977. Temporally and Areally Distributed Rainfall. Journal of the Irrigation and Drainage Division, ASCE, **103**(IR2): 221 - 229.

DM&E. 2007. Overview. Available from http://www.dmerail.com/OVERVIEW.htm [cited 25 October 2007].

Einstein, H.H. 1988. Landslide risk assessment procedure. Proceedings of the 5th International Symposium on Landslides, Lausanne. 10 - 15 July 1988. Vol. 2, pp 1075 - 1090.

Environment Canada. 2004. Automated Weather Observation System - AWOS. Available from http://www.msc.ec.gc.ca/msb/manuals/awos/awosovrv_e.html [cited 2 November 2007].

Environment Canada. 2005. Welcome to the National Climate Data and Information Archive. Available from http://www.climate.weatheroffice.ec.gc.ca/Welcome_e.html [cited 12 November 2005].

Environment Canada. 2006a. Climate normal 1971 to 2000 Haney East, BC. Available from http://climate.weatheroffice.ec.gc.ca/climate_normals/results_e.html?Province=ALL&StationName=haney&SearchType=BeginsWith&LocateBy=Province&Proximity=25&ProximityFrom=City&StationNumber=&IDType=MSC&CityName=&ParkName=&LatitudeDegrees=&LatitudeMinutes=&LongitudeDegrees=&LongitudeMinutes=&NormalsClass=A&SelNormals=&StnId=773& [cited 6 February 2007].

Environment Canada. 2006b. Canadian Weather Alerts. Available from http://www.msc-smc.ec.gc.ca/cd/brochures/warning_e.cfm [cited 5 January 2005].

Environment Canada. 2007. Public Weather Warnings for Canada. Available from http://www.weatheroffice.gc.ca/warnings/warnings_e.html [cited 9 January 2007].

Environment Canada. 2008. Canadian ensemble forecasts. Available from http://www.weatheroffice.gc.ca/ ensemble/index_e.html [cited 20 January 2008].

Eshraghian, A., Martin, C.D., and Cruden, D.M. 2005. Landslides in the Thompson River Valley between Ashcroft and Spences Bridge, British Columbia. *In* Proceedings, International Conference on Landslide Risk Management, Vancouver, B.C., 31 May - 3 June. *Edited by* O. Hungr, R. Fell, R. Couture, and E. Eberhardt, A.A. Balkema, London, U.K. pp. 437 – 446.

Eshraghian, A., Martin, C.D., and Cruden, D.M. 2007. Complex earth slides in the Thompson River Valley, Ashcroft, British Columbia. Environmental and Engineering Geoscience. **13**(2): 161 - 181.

Fannin, R.J. and Jaakkola, J. 1999. Hydrological response of hillslope soils above a debris-slide headscarp. Canadian Geotechnical Journal **36**(6): 1111 - 1122.l

Fannin, R.J., Moore, G.D., Schwab, J.W., and VanDine, D.F. 2005. Landslide risk management in forest practices. *In* Proceedings, International Conference on Landslide Risk Management, Vancouver, B.C., 31 May - 3 June. *Edited by* O. Hungr, R. Fell, R. Couture, and E. Eberhardt, A.A. Balkema, London, U.K. pp. 299 - 320.

Federal Geographic Data Committee. 2005. Common Alerting Protocol. available from http://www.fgdc.gov/international/common-alerting-protocol [cited 10 November 2006].

Federal Railway Authority. 1997. Notice of Safety Advisory 97-1 - Damage to tracks, roadbed, and bridges resulting from uncontrolled flows of water and similar weather-related phenomena. Available from www.fra.dot.gov/downloads/safety/advisories/sa97_1.pdf [cited 2 September 2005].

Federal Railway Authority. 2007. About the FRA. Available from http://www.fra.dot.gov/us/content/2 [cited 10 September 2007].

Fell, R. 1994. Landslide risk assessment and acceptable risk. Canadian Geotechnical Journal. **31**(2): 261 - 272.

Findlay, P.J., Fell, R., Maguire, P.K. 1997. The relationship between the probability of landslide occurrence and rainfall. Canadian Geotechnical Journal. **34**: 811 - 824.

Fiorillo, F., Guadagno, F.M., Aquino, S., and De Blasio, A. 2001. The December 1999 Cervinara landslides: further debris flows in pyroclastic deposits of Campania (Southern Italy). Bulletin of Engineering Geology and the Environment, **60**: 171 - 184.

Flentje, P.N. and Chowdhury, R.N. 2001. Aspects of Risk Management for Rainfall - Triggered Landsliding. *In* Proceedings of the Engineering and Development in Hazardous Terrain Symposium. New Zealand Geotechnical Society Inc, University of Canterbury, Christchurch, New Zealand, The Institution of Professional Engineers New Zealand, 24 to 25 August 2001, pp. 143-150.

Flentje, P.N. and Chowdhury, R.N. 2002. Frequency of landsliding as part of risk assessment. Australian Geomechanics News, Australian Geomechanics Society, Institution of Engineers. 37(2): 157 - 167

Flentje, P.N., Chowdhury, R.N., Tobin, P., and Brizga, V. 2005. Towards real-time landslide risk management in an urban area. *In* Proceedings, International Conference on Landslide Risk Management, Vancouver, B.C., 31 May - 3 June. *Edited by* O. Hungr, R. Fell, R. Couture, and E. Eberhardt, A.A. Balkema, New York, pp. 741 – 751.

Floris, M. and Bozzano, F. 2007. Evaluation of landslide reactivation: A modified rainfall threshold model based on historical records of rainfall and landslides. Geomorphology doi:10.1016/j.geomoph.2007.04.009.

Floris, M., Mari, M., Romeo, R.W., and Gori, U. 2004. Modelling of Landslide-Triggering Factors - A Case Study in the Northern Apennines, Italy. In Engineering Geology for Infrastructure Planning in Europe, Lecture Notes in Earth Sciences, **104**: 745 - 753.

Franks, C.A. 1999. Characteristics of some rainfall-induced landslides on natural slopes, Lantau Island, Hong Kong. Quarterly Journal of Engineering Geology **32**: 247 - 259.

Froehlich, D.C, 1995. Long-Duration–Rainfall Intensity Equations. Journal Irrigation and Drainage Engineering. **121**(2): 248 - 252.

Gabella, M., Joss, J., Perona, G., and Galli G. 2001: Accuracy of rainfall estimates by two radars in the same Alpine environment using gauge adjustment. Journal of Geophysical Research, 106-D6, pp. 5139 - 5150.

Gasmo, J.M., Rahardjo, H., and Leong, E.C. 2000. Infiltration effects on stability of a residual soil slope. Computers and Geotechnics **26**: 145 - 165.

Geertsema, M., Egginton, V.N., Schwab, J.W., and Clague, J.J. 2007. Landslide and historic climate in northern British Columbia. *In* Proceedings, International Conference on Landslides and Climate Change, Ventnor, Isle of Wight, U.K., 21 to 24 May 2007, *Edited by* R. McInnes, J. Jakeways, H. Fairbank, and E. Mathie. Taylor & Francis, London, U.K.

Gekat, F., Meischner, P., Friedrich, K., Hagen, M., Koistinen, J., Michelson, D.B., and Huuskonen, A. 2004. The state of Weather Radar Operations, Networks and Products. *In* Weather Radar: Principles and Advanced Applications. *Edited by* P. Meischner. Springer monograph series Physics of Earth and Space Environment, 337 p.

Germann, U. and Joss, J. 2004. Operational measurement of precipitation in mountainous terrain. *In* Weather Radar: Principles and Advanced Applications. *Edited by* P. Meischner. Springer monograph series Physics of Earth and Space Environment, 337 p.

Gitirana Jr., G.F.N. 2005. Weather-Related Geo-Hazard Assessment Model for Railway Embankment Stability. Ph.D. Thesis. University of Saskatchewan, Saskatoon, SK, Canada, 411 p.

Gitirana Jr., G.F.N., Fredlund, M.D., and Fredlund, D.G. 2005. Infiltration-runoff boundary conditions in seepage analysis. In Proceedings of the 58th Canadian Conference, Saskatoon, SK, Canada, 6 pp.

Glade, T. 1998. Establishing frequency and magnitude of landslide-triggering rainstorm event in New Zealand. Environmental Geology **35**: 160 - 174

Glade, T., Crozier, M., and Smith, P. 2000. Applying Probability Determination to refine Landslide-triggering Rainfall Thresholds Using an Empirical "Antecedent Daily Rainfall Model" Pure and Applied Geophysics **157**(6-8): 1059 - 1079

Golder Associates Limited. 1979. Report to Ministry of Environment, Water Investigations Branch, on Stability Study, Fraser River North River Bank, Haney to Port Hammond, British Columbia. August 1979. Doc No. 782-1179.

Golder Associates Limited. 2004. Geotechnical Seismic Vulnerability Assessment of Fraser River Escarpment, Maple Ridge, BC. Report to the District of Maple Ridge, 2004 March 23. Doc No. 03-1411-018.

Godt, J.W., Baum, R.L., and Chleborad, A.F. 2006 Rainfall characteristics for shallow landsliding in Seattle, Washington, USA. Earth Surface Processes and Landforms. **31**(1),: 97-110.

Google 2007. Google Earth Pro. Internet geographic information system. Available from https://registration.keyhole.com/choice_kh_initial.html [cited 20 September 2007].i

Gray D.M., Toth, B., Zhao, L., Pomeroy, J.W., and Granger, R.J. 2001. Estimating areal snowmelt infiltration into frozen soil. Hydrological Processes, **15**: 3095 - 3111.

Grivas, D.A., Schultz, B.C., O'Neil, G.D., and Simmonds, G.R. 1996. Phenomenological models to predict rainfall-induced ground movement. In Proceedings of the 15th International Conference on Offshore Mechanics and Artic Engineering, Florence, Italy. 16-20 June 1996. American Society of Mechanical Engineers.

Grivas, D.A., Schultz, B.C., and O'Neil, G.D. 1998. Ground movement hazards to pipeline integrity: Quantifying the effect of snowmelt. In Proceedings of the 17th

International Conference on Offshore Mechanics and Artic Engineering, Lisbon, Portugal. 5 - 9 July 1998. American Society of Mechanical Engineers.

Guidicini, G. and Iwasa, O.Y. 1977. Tentative correlation between rainfall and landslides in a humid tropical environment. Bulletin of the International Association of Engineering Geology **16**: 13 - 20.

Guzzetti, F., Peruccacci, S., and Rossi, M. 2005. RISK AWARE, Risk-Advanced Weather forecast system to Advise on Risk Events and management. IRPI, Perugia, Italy. 38 p. Available from http://www.smr.arpa.emr.it/riskaware/?page=download [cited 20 May 2007].

Guzzetti, F., Peruccacci, S., Rossi, M., and Stark, C.P. 2007. Rainfall thresholds for the initiation of landslides in central and southern Europe. Meteorology and Atmospheric Physics. DOI 10.1007/s00703-007-0262-7.

Guzzetti, F., Peruccacci, S., Rossi, M., and Stark, C.P. 2008. The rainfall intensity-duration control of shallow landslides and debris flows. Landslides **5**: 3 - 16. DOI 10.1007/s10346-007-0112-1.

Hambly, E.C. and Hambly, E.A. 1994. Risk evaluation and realism. Proceedings of the Institute of Civil Engineers and Civil Engineering, **102**: 64 - 71.

Harry, K.F. and Wright, J.B. 1957. The Climate of Vancouver. CIR-2985, TEC-258. Department of Transport - Metrological Branch, Government of Canada. 43 pp.

Hoblit. B., Vieux, B., Holder, A., and Bedient P. 1999. Predicting with Precision, Real time rainfall tracking uses advanced radar, GIS and the web to improve the lead times and geographic accuracy of flood warnings. Civil Engineering, ASCE, **69**:11, 40 - 43

Hogg, W.D. and Carr, D.A. 1985. Rainfall Frequency Atlas for Canada. Ministry of Supply and Services Canada, Canadian Government Publishing Centre, Ottawa.

Hong, Y., Adler, R.F. 2007. Towards an early-warning system for global landslides triggered by rainfall and earthquake. International Journal of Remote Sensing. **28**(16): 3713-3719.

Hong, Y., Adler, R.F., Huffman, G. 2007a. An Experimental Global Prediction System for Rainfall-Triggered Landslides Using Satellite Remote Sensing and Geospatial Datasets. IEEE Transactions on Geoscience and Remote Sensing. **45**(6): 1671-1680.

Hong, Y., Adler, R.F., Hossain, F., Curtis, S., and Huffman, G.J. 2007b. A first approach to global runoff simulation using satellite rainfall estimation. Water Resources Research, 43, 8 p., doi:10.1029/2006WR005739.

Hong Kong Observatory 2005. Landslip Warning System. The Government of Hong Kong Special Administrative Region. Available from http://www.weather.gov.hk/wservice/warning/landslip.htm [cited 14 November 2007].

Horiuchi, M. 1998. Development of Risk Assessment Method for Railway System. Japanese Railway Engineering. No. 141: 9 - 11

Hosking, J.R.M., Wallis, J.R., and Wood, E.F. 1984. Estimation of the generalized extreme value distribution by method of probability weighted moments. Institute of Hydrology, Report 89, Wallingford, England, 27 p.

Hungr, O., Evans, S.G., and Hazzard, J. 1999. Magnitude and frequency of rock falls and rock slides along main transportation corridors of southwestern British Columbia. Canadian Geotechnical Journal **36**: 224 - 238.

Hungr, O., Fell, R., Couture, R., and Eberhardt, E. 2005. Landslide Risk Management - Proceedings, International Conference on Landslide Risk Management, Vancouver, Canada, 31 May - 3 June 2005, Balkema, London, U.K. 765 pp. and CD ROM.

Hvorslev, M.J. 1951. Time lag and soil permeability in ground-water observations. Waterways Experiment Station, United States Army Corps of Engineers, Vicksburg, Mississippi. Bulletin No. 36. 50 p.

Ibsen, M.L. and Casagli, N. 2004. Rainfall patterns and related landslide incidence in the Porretta-Vergato region, Italy. Landslides **1**: 143–150. DOI 10.1007/s10346-004-0018-0.

Inagaki, K. and Sadohara, S. 2005. Real Time Landslide Disaster System in Yokohama, Japan. ERSI international User Conference. Available from http://gis.esri.com/library/userconf/proc07/papers/abstracts/a1331.html [cited 12 October 2007]

Islam, A. and Kumar, A. 2003. Hydro : A program for Frequency Analysis of Rainfall Data. Agricultural Engineering Journal Institution of Engineers (India) **84**: 1 - 5

Available from http://www.ieindia.org/publish/ag/0603/june03ag1.pdf [cited 11 November 2007].

Istituto di Ricersa per la Protezione Idrogeologica (IRPI) 2007. Research Institute for Hydrogeological and Geological Hazard Prevention. Available from http://www.pd.cnr.it/ist/geo/geo.html [cited 2 June 2007].

International Landslide Centre. 2006. The International Landslide Centre landslide fatality database. Available from http://www.landslidecentre.org/database.htm [cited 12 December 2007].

Iverson, R.M. 2000. Landslide triggering by rain infiltration. Water Resources Research, **36:**(7) 1897 - 1910.

Jakob, M., Holm, K., and Lange, O. 2005. Hydro-meteorological threshold for landslide initiation and forest operations shutdown in the Kalum and North Coast Forest Districts. BGC Engineering Inc. for the British Columbia Ministry of Forests. Available from http://www.for.gov.bc.ca/hfd/library/fia/html/FIA2005MR120.htm [cited 12 February 2007].

Jakob, M., Holm, K., Lange, O., and Schwab, J.W. 2006. Hydrometeorological thresholds for landslide initiation and forest operation shutdowns on the north coast of British Columbia. Landslides, **3**(3): 228 - 238.

Jakob, M., McKendry, I., and Lee, R. 2003. Long term Changes in Rainfall Intensity in Vancouver, British Columbia. Canadian Water Resources Journal **28**(4): 587 - 604.

Jakob, M. and Weatherly, H. 2003. A hydroclimatic threshold for landslide initiation on the North Shore Mountains of Vancouver, British Columbia. Geomorphology, **54**: 137 - 156.

Jenkinson, A.F. 1955. The frequency distribution of the annual maximum (or minimum) values of metrological elements. Quarterly Journal of the Royal Meteorological Society. **81**: 158-171

Kanji, M.A. Massad, F., and Cruz, P.T. 2003. Debris flows in areas of residual soils: occurrence and characteristics. International Workshop on the occurrence and mechanisms of flows in natural slopes and earthfills: Sorrento, 14 - 16 May 2003 Available from http://www.unina2.it/flows2003/flows2003/articoli/kanji.pdf [cited 8 November 2007].

Kawamoto, K., Oda, M., and Suzuki, K. 2000. Hydro-Geological Study of Landslides caused by Heavy Rainfall on August 1998 in Fukushima, Japan. Journal of Natural Disaster Science, **22**(1): 13 - 22.

Katayose, N. 1987. Disasters Suffered (during the Past Twenty Years) and Measures against Them. Japanese Railway Engineering. No 103: 21 - 24.

Keefer, D.K., Wilson, R.C., Mark, R.K., Brabb, E.E., Brown III, W.M., Ellen, S.D., Harp, E.L., Wieczorek, G.F., Alger, C.S., and Zatkin, R.S. 1987. Real-Time Landslide Warning During Heavy Rainfall. Science. **238**(4829): 921 - 925. DOI: 10.1126/science.238.4829.921.

Keegan, T.R. 2007. Risk Management methodology for Railway Ground hazards. Ph.D. thesis, Department of Civil and Environmental Engineering, University of Alberta, Edmonton. 452 pp.

Keegan, T.R., Cruden D, Martin, D., Morgenstern, N., Ruel, M., and Pritchard, M. 2007. A railway ground hazard risk analysis overview. 60th Canadian Geotechnical Conference & 8th Joint CGS/IAH-CNC Groundwater Conference, Ottawa, Canada. 21 to 24 October, 2007. pp 2278 to 2286.

Kerr, J.W. 1990. Frank Slide. Barker Publishing, Calgary, Alberta. 23 p.

Klemes, V. 2000. Common Sense and other heresies, Selected papers on Hydrology and Water Resource Engineering, Waterloo Printing Co. Ltd. Cambridge, Ontario, Canada, 378 p.

Ko Ko, C., Flentje, P., and Chowdhury, R. 2003. Quantitative Landslide Hazard and Risk Assessment: a case study. Quarterly Journal of Engineering Geology **36**: 261 - 272.

Ko Ko, C., Flentje, P., and Chowdhury, R. 2004. Interpretation of probability of landsliding triggered by rainfall. Landslides **1**: 263 - 275.

Ko Ko, C., R. Chowdhury, R., and Flentje, P. 2005. Hazard and Risk assessment of rainfall - induced landsliding along a railway line. Quarterly Journal of engineering Geology and Hydrogeology **38**: 197 - 213.

Lavallée, O. 1974. Van Horne's road: an illustrated account of the construction and first years of operation of the Canadian Pacific Transcontinental Railway. Railfair Enterprises. Montreal Quebec.

Lee, E.M. and Jones, D.K.C. 2004. Landslide Risk Assessment. Thomas Telford. London, U.K.

Lee, D.T.T., Rahardjo, H., and Leong, E.C. 2001. Runoff Measurements on Residual Hillslopes from Simulated and Natural Rainfall Events. *In* Proceedings of the International Conference on In Situ Measurements of Soil Properties and Case Histories, Bali, Indonesia, 21-24 May 2001. *Edited by* P. P. Rahardjo and Tom Lunne. Parahyangan Catholic University, Bandung, Indonesia.

Leeper, J. and Smith, M. 1998. Weather warnings and protection of track and structures. Part I: The Railroad perspective on weather. Part II: How Weatherdata Tracks the weather. 1998 AREMA Track and Structures Conference, Chicago, Illinois, American Railway Engineering and Maintenance-of-Way Association. 13 pp.

Leroi, E., Bonnard, Ch., Fell, R., and McInnes, R. 2005. Risk assessment and management. *In* Proceedings, International Conference on Landslide Risk Management, Vancouver, B.C., 31 May - 3 June. *Edited by* O. Hungr, R. Fell, R. Couture, and E. Eberhardt, A.A. Balkema, London, U.K. pp. 159 - 198.

Leventhal, A.R., Stone, P.C., and Christie, D. 2000. Landsliding of the South Coast Railway - the Coalcliff Slide. *In* GeoEng 2000, An International Conference on Geotechnical & Geological Engineering. 19 - 24 November 2000, Melbourne, Australia. Available from http://lib.hpu.edu.cn/comp_meeting/ [cited 2 November 2007].

Li, L., Schmid, W., and Joss, J. 1995. Nowcasting of motion and growth of precipitation with radar over a complex orography. Journal of Applied Meteorology, **34**(6): 1286 - 1300.

Lan, H., Martin, C.D., and Lim C.H. 2007. RockFall analyst: A GIS extension for three-dimensional and spatially distributed rockfall hazard modeling. Computers & Geosciences 33, Issue 2, February 2007, pp. 262-279.

Lloyd, D.M., Anderson, M.G., Hussein, A.N., Jamaludin, A., and Wilkinson, P.L. 2001. Preventing landslides on roads and railways: A new risk-based approach. Proceedings of the Institution of Civil Engineers: Civil Engineering, **144(**3): 129 - 134.

Loucks, E.D., Kimberly, A.O., and Heineman, M.C. 2005. Frequency Characteristics of Long Duration Rainfall Events. *In* Proceedings of the 2005 World Water and Environmental Resources Congress, May 15-19, 2005, Anchorage, Alaska; Environmental and Water Resources Institute (EWRI) of the American Society of Civil Engineers, *Edited by* Raymond Walton.

Loumiet, J.R. and Jungbauer, W.G. 2005. Train Accident Reconstruction and FELA and Railroad Litigation. Lawyers ad Judges Publishing Company, Tucson, Arizona. pp. 576.

MacKay, C.H. 1997. Management of rock slopes on the Canadian Pacific Railway. In Landslide Risk Assessment. *Edited by* D. Cruden and R. Fell. Balkema, Rotterdam, pp. 271 - 275.

Maertens Jr., T.B. (1990) The relationships of climate and terrain to maintenance of way on the Norfolk Southern Railroad between Norfolk, Virginia, and Portsmouth, Ohio. Ph.D. dissertation, The University of Tennessee, Knoxville, Tennessee, 228 p.

Matsushi, Y. and Matsukura, Y. 2007. Rainfall thresholds for shallow landsliding derived from pressure-head monitoring: cases with permeable and impermeable bedrock in Boso Peninsula, Japan. Earth Surface Process and Landforms. **32**: 1308 - 1322 DOI: 10.1002/esp1491.

Matsuura, S., Asano, S., Okamoto, T., and Takeuchi, Y. 2003. Characteristics of the displacement of a landslide with shallow sliding surface in a heavy snow district of Japan. Engineering Geology. **69**(1-2): 12 - 35.

McClung, D.M. 1999. The encounter probability for mountain slope hazards. Canadian Geotechnical Journal **36**(6): 1195–1196

McConnell, R.G. and Brock R.W. 1904. Report on the great landslide at Frank, Alberta. Annual report for 1903, Part 8. Department of the Interior, Ottawa, Ontario.

Melloh, R.A. 1999. A Synopsis and Comparison of Selected Snowmelt Algorithms Cold Regions Research and Engineering Laboratory (CRREL) Report 99-8. US Corp of Engineers. 24 p.

Merriam-Webster 2005. Merriam-Webster Online Dictionary. Merriam-Webster Incorporated. Available from http://www.merriam-webster.com/ [cited 10 January 2008]

Miller, J.F. 1964. Technical Paper No. 49. Two to Ten Day Precipitation for return periods of 2 to 100 years in the Contiguous United States. US Department of Commerce, Weather Bureau. Technical Paper No. 49. Washington, DC. 29 pp.

Miles, M. 2001. Effects of climate change on the frequency of slope instabilities in the Georgia Basin, BC - Phase 1. Canadian Climate Action Fund Project Number A160. Canadian Climate Action Fund, Natural Resources Canada. 31 p.

Misumi, R. Masayuki, M., Iwanami, K., Maruyama, K., and Park, S. 2005. Realtime forecasting of shallow landslides using radar-derived rainfall. World Weatehr Research Program Symposium on Nowcasting and Very Short Range Forecasting. 5 to 9 September 2005, Toulouse France. Available at http://www.meteo.fr/cic/wsn05/resumes_longs/5.20-91.pdf [cited 3 March 2006]

Morgenstern, N.R. 2000. Performance in Geotechnical Practice. The Inaugural Lumb Lecture,May 10, 2000, Department of Civil Engineering, The University of Hong Kong Available at http://www.hku.hk/civil/lumb_lecture/morgenstern-paper.pdf [cited 3 March 2006].

Moser, M. and Hohensinn, F. 1983. Geotechnical aspects of soil slips in alpine regions. Engineering Geology **19**: 185 - 211.

Muraishi, H. and Okada, K. 1988. A Method of Rainfall Depth Estimation at Slope Failure Point along Railway. Quarterly Report of Railway Technical Research Institute, Japan, **29**(4): 190 - 196.

Muraishi, H., Sugiyama, T., and Samizo, M. 1992. Proposals about Slope Risk Evaluation and Subsequent Operation Control during Rainfall. Japanese Railway Engineering. **118**: 12 - 16.

Nagarajan, R., Roy, A., Kumar, R.V., Mukherjee, A., Khire M.V. 2000. Landslide hazard susceptibility mapping based on terrain and climatic factors for tropical monsoon. Bulletin of Engineering Geology and the Environment, **58**(4): 275 - 287.

National Aeronautics and Space Administration 2008a. Global Precipitation Measurement. Available at http://gpm.gsfc.nasa.gov/ [cited 5 February 2008]

National Aeronautics and Space Administration 2008b. MODIS web. Available at http://modis.gsfc.nasa.gov/about/ [cited 10 March 2008]

National Center for Atmospheric Research (NCAR). 2004. Enhancing Rail Car Blow-over Prediction and Mitigation. Boulder, CO.

National Climate Data Center (NCDC) 2007. National Oceanic and Atmospheric Administration (NOAA) Satellite and Information Service. Available at http://www.ncdc.noaa.gov/oa/ncdc.html [cited 2 December 2007]

National Oceanic and Atmospheric Administration 2006. Precipitation Monitoring. Climate Predication Center, National Weather Service. Available at http://www.cpc.ncep.noaa.gov/cgi-bin/US_anom_realtime.sh [cited 2 April 2007].

National Oceanic and Atmospheric Administration 2007a. Advanced Hydrologic Prediction Service. National Weather Service. http://water.weather.gov/ Available at [cited 10 October 2007]

National Oceanic and Atmospheric Administration 2007b. Expert Assessment. Climate Prediction Center. National Weather Service. Available at http://www.cpc.ncep.noaa.gov/products/expert_assessment/ [cited 10 November 2007]

National Oceanic and Atmospheric Administration 2007c. Meteorological Assimilation Data Ingest System (MADIS). http://madis.noaa.gov/ Available at [cited 10 April 2007]

National Research Council. 2004. Partnerships for reducing landslide risk, Assessment of the National Landslide Hazards Mitigation Strategy. Committee on the Review of the National Landslide Hazards Mitigation Strategy, Board of the Earth Sciences and Resources, Division on Earth and Life Studies. National Academies Press, Washington DC. 131 p.

Natural Resources Canada. 2007. Landslide - Be informed. Reducing Risks from Natural Hazards Program, Geologic Survey of Canada, Earth Sciences Sector. Available at http://gsc.nrcan.gc.ca/landslides/index_e.php [cited 12 December 2007]

Noguchi, T. and Fujii, T. 2000. Minimizing the Effect of Natural Disasters. Japan Railway & Transport Review **23**: 52 - 59.

Noguchi, T. Muraishi, H., and Sugiyama, T. 1997. Slope disasters along railways and countermeasures. World Congress on Railway Research, Florence Italy. Available at http://www.rtri.or.jp/infoce/wcrr97/B616/B616.html [cited 5 March 2004]

Office of the Federal Coordinator for Meteorological Service and Supporting Research. 2002. Weather Information for Surface Transportation, National Needs Assessment Report. FCM-R18-2002. U.S. Department of Commerce/National Oceanic and Atmospheric Administration, Washington D.C. pp. 302.

Okada, K. and Sugiyama, T. 1994. A risk estimation method of railway embankment collapse due to heavy rainfall. Structural Safety, **14**: 131 - 150.

Okada, K., Sugiyama, T., Muraishi, H., Noguchi, T., and Samizo, M. 1994. Statistical risk estimating method for rainfall on surface collapse of a cut slope. Soils and Foundations, **34**(3): 49 - 58.

Oke, T.R. 1987. Boundary Layer Climates, Second edition. Routledge. 435 p.

Ortigao, J.A.R., Justi, M.G., D'Orsi, R., and Brito, H. 2001. The Rio de Janeiro landslide alarm system. *In* Proceeding of the 14th Southeast Asian Geotechnical Conference, *edited by* Ho & Li, Hong Kong, Balkema Vol. 3, pp. 237 - 241.

Ortigao, B. and Justi, M.G. 2004. Rio-Watch: the Rio de Janeiro Landslide Alarm System. Geotechnical News, September 2004, pp. 28 - 31.

Palynchuk, B., Sather, S, and Bunce, C. 2007. Approaches to mitigating decayed buried timber within railway embankments. 60th Canadian Geotechnical Conference & 8th Joint CGS/IAH-CNC Groundwater Conference, Ottawa, Canada. 21 to 24 October, 2007. pp 2255 - 2262

Pasuto, A. and Silvano, S. 1997. Rainfall as a trigger of shallow mass movements. A case study in the Dolomites, Italy. Environmental Geology **35**(2-3): 184 - 189.

Peckover, F.L. 1972. Treatment of Rock falls on Railway Line, A Study for the CN Main Line, Jasper - Vancouver, Part A - Policy and Planning, Office of the Chief Engineer, Canadian National Railways, Montreal, Quebec, 24 January 1972.

Pedrozzi, G. 2004. Triggering of landslides in Canton Ticino (Switzerland) and prediction by rainfall intensity and duration method. Bulletin of Engineering Geology and the Environment **63**: 281 - 291

Petrucci, O. and Polemio, M. 2003, The use of historical data for the characterization of multiple damaging hydrogeological events. European Geosciences Union, Natural Hazards and Earth System Sciences, **3**: 17 - 30.

Picarelli, L., Urciuoli, G., and Russo, C. 2004. Effect of groundwater regime on the behaviour of clayey slopes. Canadian Geotechnical Journal. **41**: 467 - 484.

Pisano, P.A., Pol, J.S., Stern, A.D., and Goodwin, L.C. 2005. Clarus - The nationwide surface transportation weather observing and forecasting system. Presented at the 2005 Annual Meeting of the Transportation Research Board, January 2005. Available from http://clarusinitiative.org/documents/Clarus_TRB2005.pdf [cited 10 July 2007].

Plotkin, D. 2003. Department of Transportation-Federal Railroad Administration. *In* National Landslide Hazards, Mitigation Strategy - A Framework for Loss reductions Circular 1244. *by* E.C. Spiker and P.L. Gori. United States Geological Survey. Reston Virginia. 56 pp.

Porter, M.J., Savigny, K.W. Keegan, T.R., Bunce, C.M., and Mackay, C. 2002. Controls of the stability of the Thompson River Landslides. *In* Proceedings of the 55th Canadian Geotechnical and 3rd Joint IAH-CNC and CGS Groundwater Speciality Conference, Niagara Falls, Ontario, October 20 to 23, 2002. pp. 1393 - 1400

Porter, M., Jakob, M., Savigny, K.W., Fougere, S., and Morgenstern, N. 2007. Risk management for urban flow slides in North Vancouver, Canada. 60th Canadian Geotechnical Conference & 8th Joint CGS/IAH-CNC Groundwater Conference, Ottawa, Canada. 21 to 24 October, 2007. pp 690 - 698

Potter, J.R. and Savonis, M.J. 2003. Transportation in an age of Climate change. TR News, No. 227, p 26.

RadHyPS Inc. 2007. RadHyPS Introduction. Gatineau Quebec. Available from http://www.radhyps.com/RADHYPSe.htm [cited 20 July 2007].

Rahardjo, H. and Fredlund, D.G. 1995. Procedure for slope stability analyses involving unsaturated soils. In Developments in Deep Foundations and Ground Improvement Schemes, *Edited by* A.S. Balasubramaniam, D.T. Bergado, N. Phien-wej, S.W. Hong, S. Ashford, and P. Nutulaya, Balkema, Rotterdam, pp. 33 - 56.

Rahardjo, H., Lee, T.T., Leong, E.C., and Rezaur, R.B. 2005. Response of a Residual Soil Slope to Rainfall. Canadian Geotechnical Journal, **42**(2): 340 – 351.

Rahardjo, H., Leong, E.C., Deutscher, M.S., Gasmo, J.M., and Tang, S.K. 2000. Rainfall-Induced Slope Failures: Geotechnical Engineering Monograph 3. NTU-PWD Geotechnical Research Centre, Nanyang Tevhnological University, Singapore. 86 pp.

Rahardjo, H., Leong, E.C., Rezaur, R.B., Tang, S.K., and Qua, C.N. 2001a. Rainfall-Induced Slope Failures: Mechanism and Assessment. CSE Research Bulletin No. 14.

Rahardjo, H., Li, X.W., Toll, D.G., and Leong, E.C. 2001b. The effect of antecedent rainfall on slope stability. Geotechnical and Geological Engineering, **19**: 371 - 399.

Railway Association of Canada 2008. Rules Respecting Track Safety, 17 March 2008, TC E-30, Transport Canada, Ottawa, Ontario. Available from http://www.railcan.ca/documents/rules/1686/2008_03_20_TC_E_30_TSR_en.pdf [cited 2 Jan 2007.

Railway Transportation Committee, 1973. Report on inquiry into safety of operation in the mountain territory of Canadian National and Canadian Pacific. *Prepared by the* Director of Engineering, 23 February 1973, Canadian Transport Commission, Ottawa, Ontario. pp. 39.

Redding, T.E. and Devito, K.J. 2005. Snowmelt Infiltration and Runoff from Forested Hillslopes, Boreal Plain, Alberta. 62nd Eastern Snow Conference. Waterloo, Ontario, Canada, pp. 105 - 108.

Reliability Analysis Center. 2003. Anderson-Darling; A Goodness of Fit Test for Small Samples Assumptions. Start Selected Topic in assurance related technologies. Department of Defense Information, **10**(5) 6 pp. Available from http://src.alionscience.com/src/listing.do?root=2036 [cited 23 December 2007].

RISK AWARE 2005. Risk Advanced Weather forecast system to Advise on Risk Events and Management. Available from http://www.smr.arpa.emr.it/riskaware/ [cited 20 August 2006].

Rimm-Kaufman, A.P. 1996. Risk Mitigation Models for a Japanese railroad. Ph.D. thesis. Department of Electrical Engineering and Computer Science. Massachusetts Institute of Technology, Massachusetts. 222 pp.

Roberds, W.J. 2005. Landslide State of the Art Paper 5 - Estimating temporal variability and vulnerability. *In* Proceedings, International Conference on Landslide Risk Management, Vancouver, B.C., 31 May - 3 June. *Edited by* O. Hungr, R. Fell, R. Couture, and E. Eberhardt, A.A. Balkema, London, U.K. pp. 129 - 157.

Rossetti, M.A. 2006. Analysis of weather events on U.S. railroads. 23rd Conference on International Interactive Information and Processing System (IIPS) for Meteorology, Oceanography and Hydrology. 14 - 18 January 2007 San Antonio, Texas. Available from http://ams.confex.com/ams/87ANNUAL/techprogram/paper_118791.htm [cited 20 July 2007].

Roy, R. and Mills, S. 2005. Highway-Rail Grade Crossing Safety Sept. 30, 2005. Available at http://www.aar.org/newsroom/bnsf_ppts/hiway_grade_xing/4_gcs_9.05.ppt [cited 29 February 2008].

Ryerson, C.C. 1998. Advanced Weather Systems for Railroad Winter Operational Needs. 1998 AREMA Track and Structures Conference, Chicago, Illinois, American Railway Engineering and Maintenance-of-Way Association. 17 pp.

Schaefer, D.G. 1973. A record breaking summer rainstorm over the lower Fraser Valley. Canadian Atmospheric Environment Service Technical Memoranda; 787. Canada - Atmospheric Environment, Downsview, Ontario.

Scheiner, J.I., Cheng, Y., Engle, B., and Roberts, B.C. 1997. US rainfall intensity trends for IDF curve revisions. Bentec Associates and the National Corrugated Steel Pipe Association. 12 pp.

Scire, J.S, Robe, F.R., Fernau, M.E., and Yamartino, R.J. 2000. A User's Guide for the CALMET Meteorological Model (Version 5), Earth Tech Inc. Concord Massachusetts .

Selig, E.T. and Waters, J.M. 2002. Track Geotechnology and Substructure Management. Thomas Telford Publications, London.

Sevruk, B. and Geiger, H. 1981. Selection of distribution types for extremes of precipitation. Operational Hydrology Report 15. World Meteorological Organization. Geneva. Switzerland. WMO - No. 560.

Shi, R. 2006. A Methodology for Evaluating Rainfall-induced railway ground hazards encountered at Port Douglas, June 1998. M.Sc. thesis. Department of Civil and Environmental Engineering, University of Alberta. Edmonton, Alberta. 163 p.

Shimamura, M. and Suzuki, H. 1995. Development of a rational rule for train service restriction under the rainfall risk. Japanese Railway Engineering, **134**: 7 - 10

Sidle, R.C. 2006a. Using Weather and Climate Information for Landslide Prevention and Mitigation. International Workshop on Climate and Land Degradation, Arusha, Tanzania 11-12 December 2006. Available from http://www.wamis.org/agm/meetings/wocald06/S4-Sidle.pdf [cited 12 July 2007]

Sidle, R.C. 2006b. Using Weather and Climate Information for Landslide Prevention and Mitigation. In Climate and Land Degradation. Springer, Berlin, pp. 285-307.

Sirangelo, B., Versace, P., and Capparelli, G. 2003. Forewarning model for landslides triggered by rainfall based on the analysis of historical data file. Hydrology of Mediterranean and Semiarid Regions. International Association of Hydrological Sciences, Publication, IAHS Publication No. 278. pp. 298-304.

Spiker, E.C. and Gori, P.L. 2003. National Landslide Hazards, Mitigation Strategy - A Framework for Loss reductions, Circular 1244. United States Geological Survey. Reston Virginia. 56 p.

Stull, R.B. 2000. Meteorology for Scientists and Engineers. Brooks/Cole Thomson Learning, Pacific Grove, California. 502 p.

Sugiyama, T., Okada, K., and Muraishi, H. 1995. Development of a New Method of Embankment Risk Estimation by Critical Rainfall. Japanese Railway Engineering, **134**: 11 - 14.

Tatone, B. 2007. The analysis of rock slope stability and stabilization alternatives for a rail corridor in Southeastern British Columbia using a risk-based approach. 2006 Canadian Geotechnical Society Student Competition. 90 p.

Terbrugge, P.J., Wesseloo, J., Venter, J., and Steffen, O.K.H. 2006. A risk consequence approach to open pit slope design. Journal - South African Institute of Mining and Metallurgy. **106**(7) 503 - 511.

Terlien, M.T.J. 1998. The determination of statistical and deterministic hydrological landslide triggering thresholds. Environmental Geology. 35(2-3): 124 - 130.

Thornes, J. E. and Davies, B.W. 2002. Mitigating the impact of weather and climate on railway operation in the U.K. In Proceedings of the 2002 ASME/IEE Joint Rail Conference. 23 - 25 April 2002. Washington DC. pp. 29 - 38.

Toews, D.A.A. 1991. Climatic and hydrologic circumstances antecedent to mass wasting events in southeastern British Columbia. 59th Annual Proceedings of the Western Snow Conference. Juneau, Alaska 12 15 April 1991. pp. 91 - 102.

Toews, D.A.A. and Gluns, D.R. 1986. Snow accumulation and ablation on adjacent forested and clear-cut sites in south-eastern British Columbia. 54th Annual Proceeding of the Western Snow Conference, Phoenix, Arizona; 15 - 17 April 1986. pp. 101 - 111.

Toll, D.G. 2001. Rainfall-induced landslides in Singapore. Geotechnical Engineering. **149**(4): 211 - 216.

Toll, D.G. Tsaparas, I., and Rahardjo, H. 2001. The influence of rainfall sequences on negative pore-water pressures within slopes. *In* Proceeding of the 15th International Conference on Soil Mechanics and Geotechnical Engineering, Istanbul, Turkey, A A Balkema. pp. 1269 - 1272

Tommasi, P., Pellegrini, P., Boldini, D., and Ribacchi, R. 2006. Influence of rainfall regime on hydraulic conditions and movement rates in the overconsolidated clayey slope of the Orvieto hill (Central Italy). Canadian Geotechnical Journal, **43**(1), 70-86.

Toth, V.T. 2006. Calculators and the Gamma Function. RSKey.org. Available from http://www.rskey.org.gamma.htm [cited 23 December 2007]

Towhata, I., Uchimura, T., and Gallage, C. 2005. On Early Detection and Warning against Rainfall-Induced Landslides (M129). In Landslides - Risk Analysis and Sustainable Disaster Management, *Edited by* K. Sassa, H. Fukuoka, F. Wang and G, Wang. Springer, Berlin. pp. 133 - 139.

Transport Canada 2001. Railway Safety Act - Railway Safety Management System. Transport Canada, Ottawa. Canada. Available from http://www.tc.gc.ca/acts-regulations/GENERAL/r/rsa/act/rsa.html [cited 28 February 2007]. Government of Canada, Ottawa

Transport Canada 2006. Railway Safety Program Strategic Overview. Government of Canada, Ottawa. Available from http://www.tc.gc.ca/tdc/projects/rail/h/8242.htm [cited 10 September 2007].

Transport Canada 2007. Railway Safety Ground Hazard Program. Government of Canada, Ottawa. Available from http://www.tc.gc.ca/railway/RSSO/RSSO_e.htm [cited 4 January 2007].

Transportation Safety Board 1973. Report of inquiry into safety of Canadian National and Canadian Pacific. Government of Canada, Ottawa

Transportation Safety Board 1995. Railway Occurrence Report, Derailment, Canadian Pacific Limited, Mile 111.0, Nelson subdivision, near Procter, British Columbia, 20 January 1995, Report Number R95V0017. Government of Canada, Ottawa.

Transportation Safety Board 1997a. Railway Occurrence Report, Derailment, Canadian National, Train No. Q-102-51-26, Mile 106.15, Ashcroft Subdivision, Conrad, British Columbia, 26 March 1997, Report Number R97V0063. Government of Canada, Ottawa.

Transportation Safety Board 1997b. Railway Occurrence Report, Subgrade Failure, Canadian Pacific Railway, Train No. 935-06, Mile 44.8, Parry Sound Subdivision, Pointe au Baril, Ontario, 07 April 1997, Report Number R97T0097. Government of Canada, Ottawa.

Trewartha, G.T. 1981. The Earth's Problem Climates, 2nd Edition - Map of North America. Available from http://fp.arizona.edu/kkh/dendro/climate_links.htm [cited 28 November 2007]

Tse, C.M., Chu, T., Lee, K., Wu, R., Hungr, O., and Li, F.H. 1999. A risk-based approach to landslide hazard mitigation measure design. Proceedings of the Seminar on Geotechnical Risk Management, Geotechnical Division, Hong Kong Institution of Engineers, pp. 35-42.

Turner, A.K. 1996. Colluvium and Talus. *Edited by* A.K. Turner and R.L. Schuster. Transportation Research Board. National Research Council. Special report 247. Washington, DC, pp. 525 - 554.

United States Army Corp of Engineers. 1998. Engineering and Design - Runoff from Snowmelt. Engineering Manual 1110-2-1406. 142 p.

United States Geological Survey. 2007. Advisors, Landslide Hazard Program. Available from http://landslides.usgs.gov/advisories/ [cited 11 November 2007].

VanDine, D.F. and Bovis, M. 2002. History and Goals of Canadian Debris Flow Research, A Review. Natural Hazards. **26**(1): 67 - 80.

VanDine, D.F. 1985. Debris flows and debris torrents in the Southern Canadian Cordillera. Canadian Geotechnical Journal. **22**: 44 - 68.

Vu, H.Q., Kelly, A.J., Clifton, A.W., Bunce, C.M., and Choi, E.S. 2005. Numerical investigation of the derailment caused by prolonged rainfall snowmelt event. In

Proceedings of the 58th Canadian Conference, Saskatoon, Saskatchewan, Canada, 9 p.

Walker, B., Baynes, F., Braybrooke, J., Davies, W., Fell, R., Leventhal, A., Moon, A., and Volk, P. 2000. Landslide Risk Management Concepts and Guidelines, Australian Geomechanics Society Sub-Committee on Landslide Risk Management in Landslides, Australian Geomechanics, 35: 51 - 93. Available from www.australiangeomechanics.org/LRM.pdf [cited 12 January 2006].

Walker, B.F. 2007. Rainfall data analysis at Newport. Australian Geomechanics. **42**(1): 1 - 17

Watanabe, S., Sugiyama, T., Nunokawa, O., Fujii, T., and Okada, K. 2006. A study of debris flow disasters along Japanese railways and it critical rainfall. Monitoring, Simulation, Prevention and Remediation of Dense and Debris Flows. Vol. 1, pp. 343-352.

West Coast Express 2008a. About us. Available from http://www.westcoastexpress.com/AboutWCE.htm, [cited 9 January 2008]

West Coast Express 2008b. Fact and Figures. Available from http://www.westcoastexpress.com/Facts.htm#Ridership [cited 9 January 2008]

West Coast Express 2008c. Schedules. Available from http://www.westcoastexpress.com/Schedules.htm [cited 9 January 2008]

Wieczorek, G.F. 1996. Landslide triggering mechanisms. In Landslides: investigation and mitigation. *Edited by* A.K. Turner and R.L. Schuster, Transportation Research Board, National Research Council, Special report 247. Washington, DC, pp. 76 -90.

Wieczorek, G.F. and Glade, T. 2004. Climatic Factors of Debris Flows. *In* Debris-flow hazards and related phenomena. *Edited by* M. Jacob and O. Hungr. Springer, Berlin pp 325 - 362.

Wilson, R.C., Mark, R.K., and Barbato, G. 1993. Operation of a Real-Time Warning System for Debris Flows in the San Francisco Bay Area, California. In Hydraulic Engineering. Proceedings of the Conference. San Francisco, California, 25-30 July 1993. *Edited by* H. W. Shen, S. T. Su, and F. Wen. American Society of Civil Engineers, New York, pp. 1908 - 1913.

Wilson, R.C. 1997. Normalizing rainfall/debris flow thresholds along the U.S. Pacific Coast for Long-Term Variations in Precipitation Climate. In Proceedings of the First International Conference on Debris-Flow Hazards Mitigation: Mechanics, Prediction, and Assessment. 7-9 August 1997. San Francisco California. *Edited by* C-L Chen. Hydraulics Division, American Society of Civil Engineers, pp. 32 - 43.

Wise, M., Moore, G., and VanDine, D.F. 2004. Landslide risk case studies in forest development planning and operation, B.C. Ministry of Forest Research Branch, Victoria, B.C. land management Handbook No 56. Available from http://www.for.gov.bc.ca/hfd/pubs/docs/lmh/lmh56.htm [cited 16 May 2005].

Wolter, K. and Timlin, M.S. 2008. Multivariate ENSO Index (MSI). Earth System Research Laboratory, Physical Sciences Division, NOAA Research, National Oceanic & Atmospheric Administration, U.S. Department of Commerce. Available at http://www.cdc.noaa.gov/people/klaus.wolter/MEI/#ref_wt1 [cited January 15 2008]

Wooten, R.M., Latham, R.S.; Witt, A.C., Reid, J.C., and Fuemmeler, S. 2006. Landslide hazards and landslide hazard mapping in North Carolina. Abstracts with Programs - Geological Society of America, 38(3), pp. 28.

World Meteorological Organization. 1973. Manual for estimation of probable maximum precipitation. Operation Hydrology Report No. 1. Secretariat of the World Metrological Organization, Geneva, Switzerland. WMO-No. 332.

World Meteorological Organization. 1983. Guide to Hydrological Practices. Volume II - Analysis, Forecasting and other Applications. 4th edition. Secretariat of the World Metrological Organization, Geneva, Switzerland. WMO-No. 168.

Wu, T.H. 1996. Soil strength properties and their measurement. In Landslides: investigation and mitigation. *Edited by* A.K. Turner and R.L. Schuster . Transportation Research Board. National Research Council. Special report 247. Washington, DC, pp. 319 - 336.

Wu, T.H. 2003. Assessment of landslide hazard under combined loading. Canadian Geotechnical Journal. **40**: 821 - 829.

Zézere, J.L., Ferreira, A.D., and Rodrigues, M.L. 1999. The role of conditioning and triggering factors in the occurrence pf landslides: a case study in the area north of Lisbon (Portugal), Geomorphology **30**(1-2): 133 - 146.

Zhang, X., Hogg, W.D., and Mekis, E. 2001, Spatial and temporal characteristics of heavy precipitation events over Canada", Journal of Climate, **14**(9):1923-1936.

Appendix A Canadian Pacific railway operations

A 1.0 History of the Canadian Pacific

The Canadian Pacific railway was built between 1881 and 1885 (Canadian Pacific 2007a). Initially it was a single mainline track built to unite the country of Canada and to ensure that the United States of America did not annex British Columbia (BC). During its history, the rail network grew to service customers across northern North America. A northern route across the Canadian Prairies was added in the 1920's. CP has owned a majority of the Soo Line from the US/Manitoba border to Chicago since the 1890s but it did not take full control of this track until the 1990's. Prior to being fully integrated with CP, the Soo Line had absorbed the Milwaukee Road in 1985 and the Minneapolis, Northfield and Southern (MNS) in 1982. CP also acquired the Delaware and Hudson Railway (D&H) in 1991, which provides access to the U.S. Northeast.

In 2001 Canadian Pacific Limited was dissolved and Canadian Pacific Railway (now Canadian Pacific) became a fully independent, public company separate from its sister companies: Fording Coal, CP Ships, Fairmont (previously CP) Hotels and PanCanadian Energy.

The book Van Horne's Road by CP's corporate historian Lavallée (1974) provides a description of the construction of the CP network. Peckover (1972) observed that CP, being the first railway through the mountains and especially along the Thompson and Fraser River Valleys, selected a route that avoided more geotechnical hazards than the CN route.

CP now operates a 22,400 km (14,000 mile) rail network from Vancouver in the west to Montreal in the east of Canada. The Soo Line forms an important link from the Canadian east/west corridor into Chicago and the US Mid-West. Tracks also extend from Montreal south into New York and Pennsylvania. CP has major lines from Toronto into Detroit and Buffalo. The forthcoming acquisition of the Dakota, Minnesota & Eastern Railroad (DM&E) will add another 4,000 km (2,500 miles) of track in Illinois, Iowa, Minnesota, Missouri, Nebraska, South Dakota, Wisconsin and Wyoming (DM&E 2007). With the planned construction of 320 km (200 miles) of new track, the DM&E acquisition provides CP with an opportunity to be the third rail carrier to service the Powder River Basin in Wyoming.

A 2.0 Comments on railway operating practice

A 2.1 Warning conditions and reliability

To discuss the assessment of the reliability of warning systems, the following terminology is adopted. A positive prediction is when an alarm is issued predicting a landslide will occur. If a landslide occurs and the prediction is correct, the prediction is referred to as a "true-positive". Alternately, if a landslide is predicted and no landslide occurs, the prediction is incorrect and this is called a "false-positive". Similarly, if no landslide is predicted and one occurs the outcome is a "false-negative". If no landslide is predicted and non occurs the warning system has produced a "true-negative". Table A1 provides an overview of the four cases.

Table A1 Potential outcomes of warning system

		Actual condition	
		Landslide	No Landslide
Test result	Warning issued	Indices exceeded AND landslide occurs (True-positive)	Indices exceeded BUT no landslide occurs (False-positive)
	Warning not issued	Indices not exceeded BUT a landslide does occur (False-negative)	Indices not exceeded AND no landslide occurs (True-negative)

Due to the generic nature of the current weather indices and thresholds, CP receives an excessive number of false-positive warnings. Currently the rainfall indices and thresholds result in several warnings per day across the CP system, yet no landslides occur. This is because the thresholds are set too low and/or the indices are not appropriate for the locations for which they are issued. This is not surprising because the indices and thresholds were set based on Environment Canada rainfall warning criteria, not for railway or geotechnical hazards.

Based on the current warning levels, CP and other railways receive an excessive number of false-alarms (false-positives) and an inadequate number of true-positive warnings. During the more than 10 years that CP has subscribed to a weather service provider, there are only a few times where true-positive heavy rainfall warning have been received concurrently with a landslide. One goal of this research is to reduce the current number of false-positives without introducing false-negative outcomes. This can be achieved by modifying the type, number, and combination of indices and thresholds used to determine if warnings should be issued or not. Given that the existing indices have produced only a few true-positive warnings, improvement should be possible.

A 2.2 Track and railway direction terminology

CP uses the following hierarchy to describe and divide its railway network such that it can be described with a minimum of effort. The entire CP rail network is divided into 10 Service Areas. Within each Service Area there are numerous subdivisions. A subdivision is a unit of track going from one point to another. A subdivision is typically no longer that 240 km (150 miles) but can be any length. A spur may branch off a subdivision but generally only serve a few customers and terminate at some point without connecting to another track.

CP has adopted conventions for describing the physical environment of the railway right-of-way. These conventions are adhered to in this research. A description of the conventions used within CP, consistent with those used in the other Class 1 railway in North America is provided below.

1. Track locations are identified by distance in miles from a specific location. The metric system is not used.
2. Each track is assigned a unique subdivision name.
3. Each track is designated to travel east to west, west to east, north to south, or south to north.
4. Directions are specified relative to the track based on its designated direction of travel. For an east to west designated track, (the most common in Canada since the track was built from the east to the west) track miles increase from east to west. When facing towards the increasing track mile the right hand side of the track is track north and the left is track south as if the track followed a straight path from east to west. If the geographic direction of an east-west track is oriented north - south for a short section, a location to the right of the track is still track north regardless of the fact that

at this specific location it is geographically east of the track. This system avoids the use of directions like northeast and southwest because there is always a mileage track south or track north of a track location.

5. Cross-sections are always projected looking towards the higher mileage. This is consistent with hydrology where cross-sections and chainage increases towards the destination, assuming one is traveling downstream. The term cross-section refers to a vertical section perpendicular to the direction of travel. The track centreline is used as the zero offset chainage in all cross-sections with positive to the right (usually north) and negative to the left.
6. The term track-profile refers to a vertical section parallel with the direction of rail travel. The higher mile is always to the left so the section looks towards the track north for an east to west track.

The use of these conventions provides for the rapid and consistent interpretation of railway information.

A 3.0 Previous means of protection against weather induced hazards

Within CP this is the responsibility of engineering services personnel and specifically the Track Maintenance Supervisor (TMS). This responsibility is documented in the railway's Standard Practice Circulars (SPC) (Canadian Pacific 2000 and 2007b). The railway relies upon the knowledge of each TMS of the track and of the geotechnical hazards prevalent in their area of responsibility to determine what conditions could be detrimental to the safety of the track. In the past, a new TMS worked with the previous TMS in the same region before taking on the responsibility of the TMS role. Thereby the new TMS gained practical knowledge and experience from their predecessor on the influence of extreme weather conditions on the safe operation of the railway.

However, in the last several decades, railways have utilized a more mobile work force, that is responsible for larger territories, often with limited experience in their current region of responsibility. As a result, the following conditions can arise:

1. Individuals at one location may not be aware of the severe weather conditions occurring in other regions of their area of responsibility.

2. Individuals may not be familiar with the range and effect of local weather conditions due to relatively short experience in a region.
3. The high level of rail traffic in some corridors results in limited time for track inspections.

These conditions reduce the ability of track maintenance personnel to assess the track and assess changes in the exposure of the track to weather sensitive geotechnical hazards.

A 3.1 Existing CP weather information system

Simultaneous with the reduced reliance on the TMS to be aware of weather conditions within their area of responsibly, various information technologies have become more available and less costly. This has allowed the proliferation of weather sensors, reduced sensor and data transmission costs, and provided the means to access, filter, process, and disseminate weather information to the TMS and others.

To address the requirements of FRA Safety Advisory 97-1 and to compensate for the current dispersed work force, most Class 1 railways in North America have increased the accessibility of weather data to their employees via information and communications systems. To reduce the amount of weather information being provided to the railways to only that which is relevant to their employees, the railways utilize weather information systems.

For example, CP has developed a purpose-built internet-based railway weather information system (RailWIS) with RadHyPS Inc., a third party weather information supplier. The other class 1 railways employ similar systems supported by third party information suppliers and forecasters. These systems take advantage of communication and data processing technology to offset the reduced knowledge of the Track Maintenance personnel discussed in Appendix A, Section 3.0. RailWIS type systems have the ability to make relevant weather information from several sources directly accessible to those responsible for the ongoing safety of the track structure. They allow the engineering personnel to see the weather data geographically referenced to the railway network so they can determine which sections of the track are at greatest risk. In addition, these information systems have the ability to send electronic messages describing severe conditions, area of influence, and the timing of the expected events to the specific individuals likely to be affected.

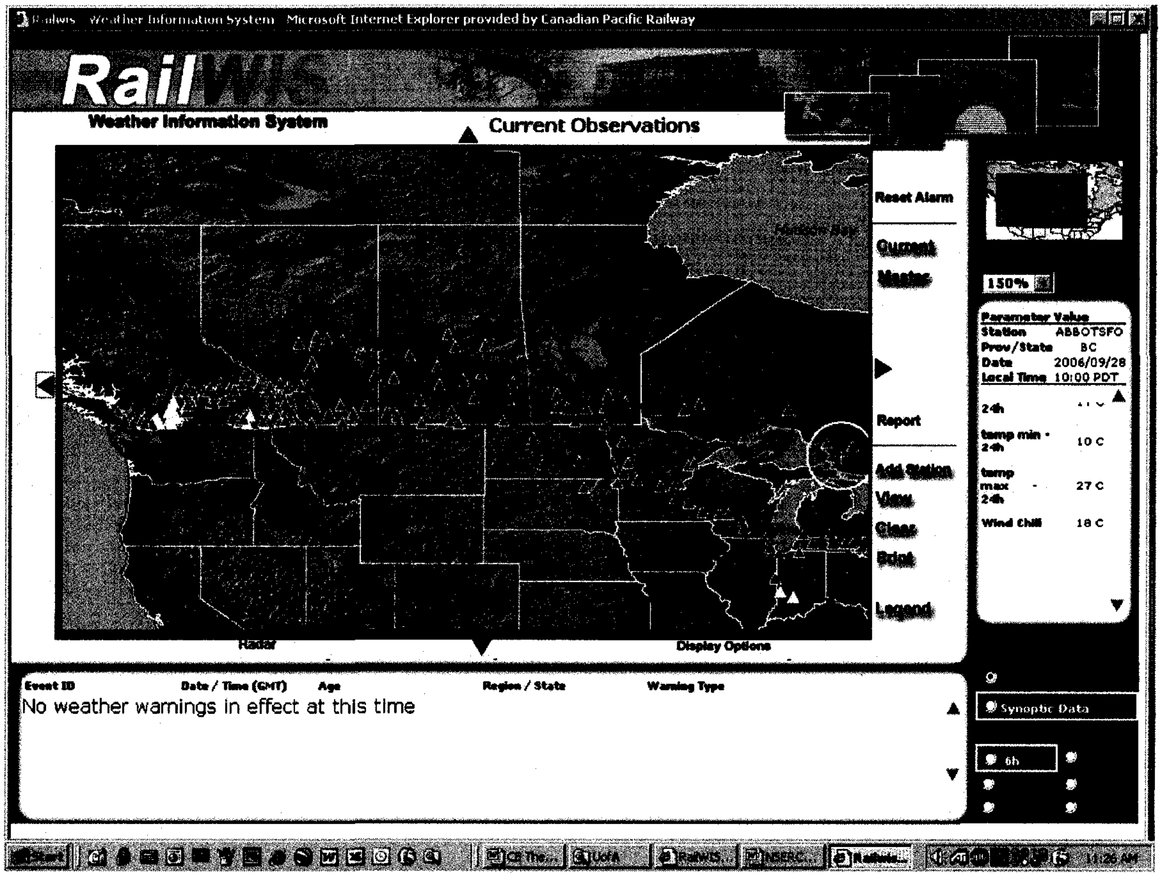

Figure A1 The RailWIS main display provides access to weather information across the CP via the internet. Information at specific locations in graphic and text form is provided.

However, due to the limitation of the TMS (discussed in Appendix A, Section 3.0) they may not be able to assess what is a severe condition and what response is warranted. At present, severe weather warnings of interest to the general public are provided by the national weather agencies. These agencies and service providers do not have the ability to identify which weather conditions are hazardous to the railways. Specific geographic hazard warning criteria for geotechnical hazards would improve the utility of WIS systems. Warnings for temperature conditions are discussed in Appendix A, Section 3.2.

A 3.2 Other weather warning criteria

Identification of warning criteria is relatively simple for some weather conditions like the low temperature index that is used to reduce the increased frequency of broken rails when the temperature a certain temperature. Although there are some regional variations in the low temperature threshold at which slow orders are imposed, the index, thresholds, and response are uniform within large regions within railways and generally between railways. The weather information service provider notifies the railway when the temperature is predicted to be below the low temperature threshold in the appropriate General Bulletin Order (GBO) and the trains are directed to operate at a reduced speed.

Appendix B Weather and landslide hazards

Climate is the summary of the cyclic meteorological variation of the weather at a given location over a number of years. Weather is a description of the atmospheric conditions at a particular time and or place (Oke 1987). This research will investigate the climatic data for a specific location to assess how the current or forecast weather may influence the stability of landslides and ultimately the exposure of railway to these hazards.

In Sections B 1.1 to 1.6 the mechanisms by which water enters the soil and migrates to the groundwater system are discussed. Next, our understanding of how the infiltrated surface water interacts and affects the stability of slopes and embankment is reviewed in Sections B 1.7 and 1.8.

B 1.0 Hydrologic cycle and landslides

The interaction of the weather and the climate on the Earth's surface and potentially unstable slopes and existing landslides is caused by the dependence of slope stability on the pore pressure of the soil and the fact that the atmosphere is such a significant component of the water cycle.

A depiction of the interaction of the atmosphere and particularly the moisture cycle between the atmosphere and soil is shown in Figure B1. The soil and aquifers are shown as individual entities in Figure B1 to differentiate between the unsaturated and saturated (aquifer) soil conditions. Water flows into and out of the soil by means of:

1. infiltration from, exfiltration to, and vapour diffusion to the land surface;
2. interflow to and from streams, lakes, rivers and oceans;
3. percolation from and capillary rise to aquifers; and
4. groundwater flow to and from the streams, lakes, rivers, and oceans.

The primary energy source of the hydrologic cycle is solar energy whereby radiation, convection, conduction increase the potential energy of water causing it to evaporate into the atmosphere. To complete the cycle water to loses potential energy due to gravity. The primary means by which the atmosphere loses water is by precipitation. Precipitation results in water on the land surface. Once the rain or snowmelt reaches the land surface, the partitioning of the water between surface runoff, evaporation and infiltration determines the amount of water available for infiltration. As a result, soil moisture is highly influenced by the precipitation and runoff conditions. In contrast to the atmosphere, the flow of water within the soil is dominated by gravitational flow downward. Although vapour diffusion, exfiltration, and capillary rise result in the upward flow of water out of soils and aquifers, the volume and flow rate is small compared to the rate caused by gravity.

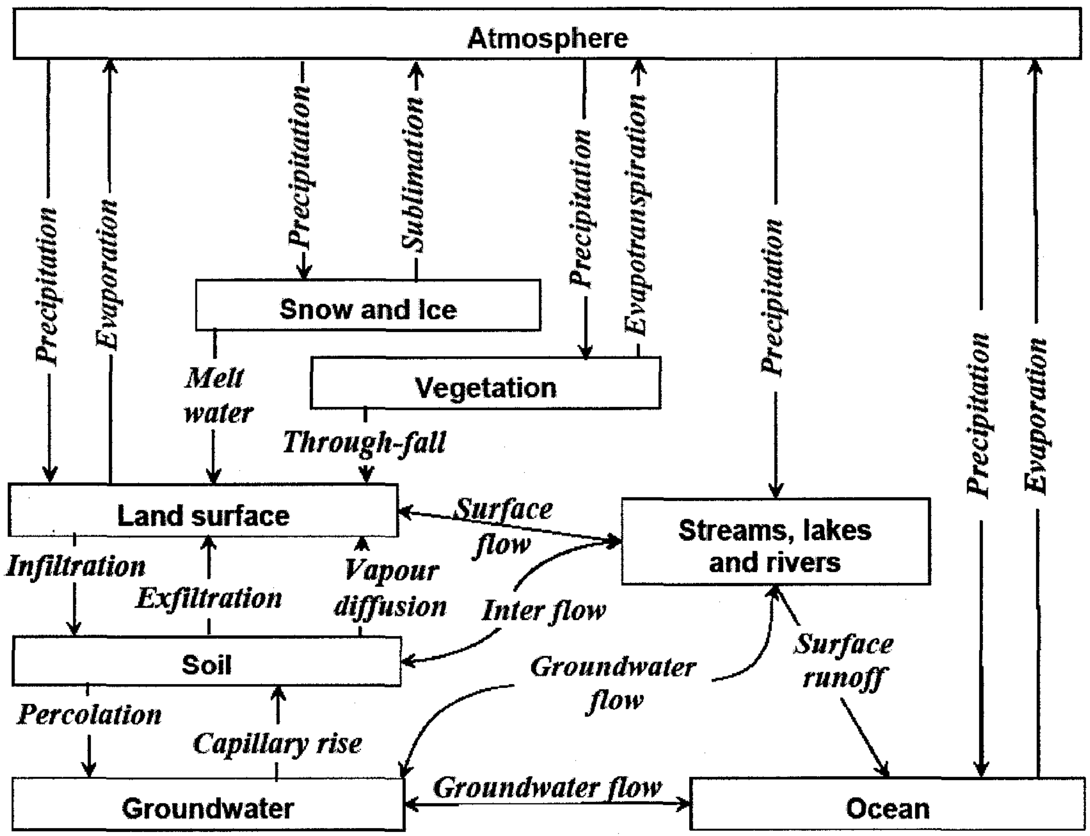

Figure B1 The hydrologic cycle (after Gitirana 2005)

As will be demonstrated, since stability of the soil is dependent on soil moisture and the groundwater level within the saturated soil, it is desirable to be able to model each of the inflow and outflow processes and the partitioning of water at the land surface. The following subsections will briefly describe the physical process, ability, and required information needed to model them.

As illustrated in Figure B1 there are several interactions between the soil and the hydrologic cycle influencing the soil moisture and groundwater conditions. These include

1. Land surface water partitioning
2. Infiltration into the soil
3. Snow and ice melt that then infiltrates into the soil
4. Evapotranspiration of the soil moisture

Depending on the climatic conditions, these may or may not be significant. Each interaction is discussed in the following sections.

B 1.1 Land surface water partitioning

Land surface water is commonly partitioned into four components 1) evaporation, 2) interception and depression storage, 3) infiltration and 4) rainfall excess. Evaporation is the component of precipitation that returns to the atmosphere. Interception is the component that is retained and taken up by vegetation and later expelled by the vegetation as evapotranspiration. This portion of precipitation never has the opportunity to infiltrate into the soil/groundwater system. Depression storage is the water stored in puddles, lakes and oceans that may or may not reach the soil/groundwater system before it evaporates or flows away. Infiltration is the component that enters the soil/groundwater system. Rainfall excess is the portion directly available for runoff and is of primary interest to the field of hydrology.

B 1.2 Infiltration

Infiltration is the process of water entry from the land surface into the soil. The rate of infiltration is governed by the Richards equation, which represents the movement of water into unsaturated soil (Chow, Maidment and Mays 1988 and ASCE 1996).

$$\frac{\partial \theta}{\partial t} = \frac{\partial}{\partial z}\left(K(\psi)\left(\frac{\partial \psi}{\partial z} + 1\right)\right) \quad \text{Equation B1}$$

Where θ is the water content of the soil, and $K(\psi)$ is the hydraulic conductivity of the soil. The Richards equation states that the rate of infiltration or change of water content, $\partial\theta / \partial t$ of the soil is dependent on the hydraulic conductivity and the change in suction head over elevation, z. However, the hydraulic conductivity is also dependent on the suction head, ψ. Since hydraulic conductivity is a function of the suction head and varies with depth, the Richards equation does not have a closed form solution but solutions have been developed using finite difference and finite element methods.

Generally, the initial soil moisture varies with depth, z, below the land surface and suction head and hydraulic conductivity vary inversely, as the suction head decreases the hydraulic conductivity increases (Chow, Maidment and Mays 1988). The higher the moisture content, the lower the suction head and the higher the hydraulic permeability.

Assuming a negligible depth of water is ponded at the surface Horton's equation provides a means of predicting the infiltration rate, f based on the fact that infiltration starts at an initial rate f_o and exponentially decreases until it reaches a constant rate, f_c.

$$f(t) = f_c + (f - f_c)e^{-kt} \qquad \text{Equation B2}$$

where t is time and k is a decay constant with units of [T^{-1}].

Alternately, the Green-Ampt method is consistent with Darcy's law of saturated flow during ponding of a nominal depth on the surface. It assumes a wetting front resulting in saturated flow above some depth and progressive saturation of the soil below the wetting front. The Green-Ampt formula is commonly written:

$$f = K_{sat}\left(\frac{\psi\Delta\theta}{F} + 1\right) \qquad \text{Equation B3}$$

Where F is the cumulative depth of infiltrated water. Equation B4 is solved for F by iteratively solving the equation starting with an initial seed value for F. Once F has stabilized it is used in Equation B3 to solve for f.

$$F(t) = K_{sat}t + \psi\Delta\theta\left(\frac{F(t)}{\psi\Delta\theta}\right) \qquad \text{Equation B4}$$

Where $\Delta\theta$ is the change in moisture content from initial moisture content, θ_i, to fully saturated, which is equal to the soil porosity, η, and t is time. The Green-Ampt formula is used to calculate the rate of infiltration, f; when the initial saturation, θ_i; porosity, η; soil suction head, ψ; and saturated hydraulic conductivity, K_{sat} are known.

As indicated by Horton's equation and the Green-Ampt method the rate of infiltration, f, decreases to the hydraulic conductivity for large t. As a result, for long duration precipitation events the infiltration rate will approach the hydraulic conductivity of the soil. Numerous additional land surface factors affect the rate of infiltration including: soil type, surface conditions, soil-conservation management practices, and vegetation and crop types and their maturity. The two methods above only consider the soil water interaction.

The surface of the land cover strongly influences the infiltration rate and considerable work with hydrology and agricultural has been undertaken to quantify the effect of varied land-surface cover conditions. Surface cover such as bare soil, organic cover, and shrub canopy have all been found to influence infiltration rates. Generally, some type of surface cover inhibits the development of a soil crust and thereby enhances infiltration. The configuration or amount of tillage of the surface influences the infiltration. The more tillage the higher the infiltration, which then generally declines with exposure to rain (ASCE 1996).

Several excess rainfall models have been developed for use in the study of hydrology. These include the phi index, initial and constant loss rate, constant proportional loss rate, and the US Soil Conservation Service (SCS) Runoff Curve Number. The phi index is based on separating the base flow runoff from the total runoff and then determining the phi value to equal the total runoff. The SCS Runoff Curve Number method was developed by the Soil Conservation Service (ASCE 1996) and has been widely accepted in North America. However, the excess rainfall models lump the non-surface runoff losses rather than calculating the infiltration.

The physical and mineral/water properties of a soil influence the hydraulic conductivity of the soil. The texture or grain size distribution, morphology (density, clay and organic content) of the soil influences its hydraulic conductivity. The coarser the soil grain size the higher the hydraulic conductivity. With the exception of clay soils the more uniform the grain size distribution the higher the hydraulic conductivity. The lower the density and organic content, the higher the hydraulic conductivity. In clay rich soils the mineralogy of the clay influences the soil suction and hydraulic conductivity of soils due to the propensity of some clay minerals to attract and retain water within their crystal structures. The ability of the clay minerals to retain water strongly influences the suction head and the hydraulic conductivity.

Several investigations have been undertaken to determine characteristics of infiltration with soil conditions and slope geometries typical of landslides. The results of a few of these are briefly summarized. Gitirana et al. (2005) demonstrate the ability of computer algorithm for runoff, infiltration and vapour flow equations to model the relationship established by Horton. They modelled precipitation rates at multiples of the saturated hydraulic conductivity over a 7 day period.

Rahardjo et al. (2001a) instrumented a slope consisting of residual soil exposed to natural rainfall for a period of 2 ½ months in Singapore to investigate the influence of rainfall infiltration on slope stability. They found that infiltration reduced the suction head from its initial level to a depth of up to 5 m within 4 hours of the initiation of the rainfall and caused the pore water pressure to reach hydrostatic conditions to a depth of about 3 m in the same time. Lee et al. (2001) undertook similar work applying artificial rainfall to a natural slope. They found that the initial runoff is delayed by the time it takes to fill the initial storage capacity of the soil and that the duration of the delay is proportional to the rate of infiltration and the soil properties. As per Horton, infiltration rate decreases to a minimum constant value with increasing time, provided the rain continues.

Gasmo et al. (2000) undertook numerical studies of infiltration effects on the stability of a residual soil slope. They demonstrated that for the steady state rainfall the infiltration would be the same for rainfall intensities that are less than one or more orders of magnitude of k_s. They showed that the crest of the slope is the area of highest infiltration for rainfall rates within one order of magnitude of k_s. For rainfall below and above k_s the infiltration rate starts below and above k_s respectively and then increases or reduces towards k_s respectively as time proceeds. Baum et al. (2002) use a linearized solution of the Richards equation to model the transient rainfall infiltration for the analysis of slope stability.

B 1.3 Snow and ice melt

Snowmelt, runoff, and infiltration are more complex than precipitation runoff and infiltration due to the dependence on temperature, and solar radiation and the temperature history of the ground and air, over the life of the snow. Whether precipitation reaches the ground as snow or rain is determined by the melting level. Above and below the melting level snow and rain hits the ground respectively. The melting level varies between 0 and 4° C. The accumulation of snow is dependent on the air and ground temperature when it falls. During the life of the snow, it undergoes metamorphosis depending on the humidity temperature and movement of the air and solar radiation it receives. The albedo or fraction of light reflected by the snow also has an influence on the energy absorption of snow (Oke 1987). The relative importance of each snowmelt process is dependent on the atmospheric, vegetation, aspect, location, wind, season, snow-albedo and other factors (ASCE 1996). The US Army Corp of Engineers (1998) summarizes the energy balance to melt snow as:

$$Q_m = Q_{sn} + Q_{\ln} + Q_h + Q_e + Q_g + Q_p + \Delta Q_i \qquad \text{Equation B5}$$

where

Q_m is the energy total energy available for snowmelt,

Q_{sn} is the short-wave net radiation,

Q_{ln} is the long-wave net radiation

Q_h is the convection from the air (sensible energy),

Q_e is the vapor condensation (latent energy),

Q_g is the heat conducted from the ground,

Q_p is the energy contained in rainfall, and

ΔQ_i is the change in the internal energy stored in the snow per unit area of snow-pack.

The 8 energy fluxes are in units of energy per time per unit area of snow. The last term includes the energy to melt the snow (from its ice form), freeze liquid within the snow, and the variation of the snow temperature. During warming ΔQ_i is positive and during cooling negative. Due to the proximity to the energy sources and the insulation provided by snow, melting occurs at the air and ground and within the snow at different rates. The phase transformation of snow into water is governed by the relationship:

$$M = \frac{Q_m}{334.9 \rho B} \qquad \text{Equation B6}$$

Where M is the snowmelt in mm of water, Q_m is the sum of all heat components in kJ/m2, B is the ratio of heat required to melt a unit weight of the snow to that of ice at 0° C, 334.9 is the latent heat of fusion of ice in kJ/kg, and ρ is the density of water, kg/m.

Due to the lack of information on several of the forms of energy exchange involved in melting snow, and the resulting inability to model them, accurate snowmelt predictions for all conditions are not available. Despite this limitation, simplified snowmelt modeling systems have been developed for relatively specific conditions.

One of the simplest and most widely used snowmelt approaches is the Temperature index degree-day method (Melloh 1999 and US Army Corp of Engineers 1998) because it uses only temperature data. It is expressed:

$$M = C_d(T_a - T_b) \qquad \text{Equation B7}$$

where M is the snowmelt in one day with units of mm/day, C_d is the degree-day melt coefficient, T_a is the air temperature, and T_b is the base temperature at which melting occurs. The value of Cd is derived empirically and varies between 1.8 to 3.7 mm/° C/day. US Army Corp of Engineers (1998) provides a discussion of using various value of C_d under a number of different conditions. They also provide similar equations with more terms integrating wind velocity and precipitation rates. For example, one of the equations is applicable to open or partly forested areas when rain is falling, and therefore short wave radiation is absent due to the cloud cover producing the precipitation.

Under sub-zero temperature conditions snowmelt is a relatively slow process resulting equivalent to a few mm/day of water reaching the land surface. As a result, investigators have developed snowmelt models specifically for conditions when isothermal (a uniform temperature throughout) or "ripe" snow conditions are present and the highest rates of melting are possible. During these conditions water delivery rates can reach tens of mm/hr and continue for several weeks, depending on the depletion of the snow pack.

Although glaciers influence peak and base flow runoff in water courses and groundwater conditions throughout the year (United States Army Corp of Engineers 1998), they have minimal influence on infiltration. Furthermore, their influence on groundwater conditions will vary annually, and in the event of climate change, but not related to daily weather.

Matsuura et al. (2003) measured the rain and snowmelt water reaching the ground with a lysimeter to assess the influence of snowmelt on a shallow landslide in Japan. They found that snowmelt had strong influence on the pore pressure, within a few decimeters of the failure surface, which was at a depth of 4.3 m. The highest pore pressures of the year were concurrent with the highest snow melt condition.

Vu et al. (2005) analyzed the precipitation and snowmelt in Southern Alberta prior to and during a sub-grade plastic deformation (Keegan 2007) failure. Due to the warm temperatures, the ripe nature of the snow pack, and availability of representative snow-on-the-ground measurements, they were able to sum the daily precipitation and the water equivalent reduction in snow-on-the-ground to arrive at a daily estimate of the surface water available for infiltration. Although not from the same region, this is consistent with work by Redding and Devito (2005) that found that near surface snowmelt runoff is not common in Northern Alberta and that the infiltration capacity into frozen soil far exceeded the snowmelt water supply rate, resulting in a high proportion of snowmelt infiltrating into the soil.

To summarise Sections B 1.2 and B 1.3, the estimates of infiltration rate can be compared to the precipitation rate and the time to saturate the soil can be determined. As will be shown in Section B 1.6 and B 1.7 respectively, the influence of infiltration on the change in the suction and groundwater conditions within the slope can then be approximated.

B 1.4 Evaporation and transpiration

Evaporation and transpiration are the two most significant processes by which moisture can return to the atmosphere and exit the terrestrial water cycle. As discussed previously this is the process whereby potential energy is supplied to the hydrologic cycle and is dependent on the sun for that energy. Transpiration is a special case of evaporation whereby moisture on the surface of plants is lost by the plant to the atmosphere. Air and ground temperature, humidity, solar radiation and wind speed all have an influence on evaporation and transpiration. The Penman-Monteith equation provides the most basic and practical means of assessing the potential influence on evaporation and transpiration on the hydrologic cycle. However, the complexity of its formulation and the number of adaptations and modifications to account for various ground conditions, crop type, and climate factors preclude a more complete discussion. ASCE (1996) provides a detailed review of the application of the Penman-Monteith equation.

B 1.5 Groundwater

Once infiltrated water has reached the saturated zone or groundwater table Darcy's law governs waters movement. The law states that the rate of flow of water, v_s in a soil in direction s is directly proportional to the gradient of the potential head, $\frac{\partial \Phi}{\partial s}$. To equate the two variables Darcy introduced the concept of hydraulic conductivity of the soil, K, or K_s, in direction s such that,

$$v_s = -K_s \frac{\partial \Phi}{\partial s}$$ Equation B8 (Bromhead 1992)

The potential head, Φ is equal to the sum of the elevation, z of the point and the pressure head, h at that point.

Hydraulic conductivity, K is the flow of a unit volume under a unit hydraulic-gradient through a unit cross-sectional area at constant temperature and is expressed in units of distance per unit time. Permeability is only dependent on the properties of the soil and unlike hydraulic conductivity is not influenced by the properties of the fluid including the density of the fluid, ρ the influence of gravity, g or the viscosity of the fluid, μ. As a result,

$$K = \frac{k\rho g}{\mu}$$ Equation B9

and k therefore has units of distance squared.

As indicated by Darcy's law the velocity of flow, permeability of the soil and the gradient, are dependent on direction. As a result, when modeling flow, all three potential directions of flow must be considered. To account for the change in permeability of the soil with suction head, k is replaced with k_w and Equation B7 is rewritten following Rahardjo and Fredlund (1995) as

$$v_w = -k_w(u_a - u_w)\frac{\partial h}{\partial s}$$ Equation B10

In a saturated soil k_w equals the saturated coefficient of permeability, k_s when the soil is unsaturated k_w is less than k_s and varies as a function of the matrix suction or water content depending on the formulation selected. u_a and u_w are the pore air pressure and the pore water pressure respectively. The difference of u_a and u_w is the matrix suction.

Numerous commercial computer programs are available for modeling saturated and unsaturated groundwater flow and the pore pressure distribution in the soil.

Where groundwater influences the stability of a landslide there will be a time lag between the period of precipitation, the response of the groundwater table and the influence on the landslide. This time lag is introduced by the physical process of infiltration, saturation and migration of water in unsaturated and saturated soils. The time dependence of the infiltration process is illustrated by Equation B2 or B4. The migration of groundwater from a source area to a landslide can be assessed using the rate of flow. Hvorslev (1951) discusses the further time lag introduced by pore water pressure measurements instruments. Determination of the actual delay time in all but the simplest flow regimes requires 2 and 3 dimensional modeling of transient head conditions in response to infiltration and groundwater flow. Iverson (2000) considered an idealized geologic model and derived a relationship for the response (or lag) time of a landslide and a rainfall event. The relationship is dependent on the rainfall duration, the diffusivity of the soil, the depth of the failure surface and the ratio of the rainfall intensity to the hydraulic conductivity.

B 1.6 Landslide stability analysis

The stability analysis of soil and rock slopes can be divided into two basic methods. 1) Limit equilibrium analysis can be used to determine the static equilibrium of the soil but does not provide any indication of the stress/stain behaviour of the soil. 2) The Finite Element method is used to model the stress/strain behaviour but does not provide a direct measure of the factor of safety of the soil (Duncan 1996).

By defining the Factor of Safety as the ratio of the shear strength to shear stress required for equilibrium, limit equilibrium analysis is completed by considering the strength/stress ratio at equilibrium on an element of soil or more commonly a number of elements of soil. The basic equation for any element is

$$FOS = \frac{c + \sigma \tan \phi}{\tau_{eq}} \qquad \text{Equation B11}$$

where FOS is the factor of safety, c is the cohesion of the soil, ϕ is the angle of internal friction of the soil, σ is the normal stress on the failure surface and τ_{eq} is the shear stress required for equilibrium. If FOS is less than unity landslide movement is predicted.

To account for the reduction in normal stress due to the pore pressure of saturated soil, μ, the concept of effective stress, σ' is used whereby:

$$\sigma' = \sigma - \mu \qquad \text{Equation B12}$$

As a result, an increase in pore pressure will decrease the factor of safety.

The stability of a slope is often the result of suction in the unsaturated zone. However as saturation by infiltration occurs the suction is reduced and the factor of safety is reduced. To account for the suction head within the soil the numerator in Equation B11 is expanded (Rahardjo and Fredlund 1995) to:

$$\tau_{ff} = c' + (\sigma_f - u_a)_f \tan \phi' + (u_a - u_w) \tan \phi^b \qquad \text{Equation B13}$$

where τ_{ff} is the shear stress on the failure surface at failure, c' is the effective cohesion, σ_f is the normal stress on the failure surface, ϕ' is the angle of internal friction of the soil at the effective stress, and ϕ^b is the angle representing the rate of increase of the shear strength with change in soil suction. As described by Gitirana (2005) and others the matrix suction of the soil decreases rapidly below the air entry value of the soil even for small increases in the saturation of the soil.

Methods for subdividing the soil mass into elements, and for satisfying and computing one or both of the force and moment equilibrium conditions for each element, have been developed by researchers including Bishop, Janbu, Morgenstern and Price, Sarma and others. A discussion of the merits and limitations of the methods is provided by Duncan (1996) and Bromhead (1992) and others.

Infinite slope stability analysis is often cited in high intensity precipitation triggered landslides because of several factors. The depth of the failure surface of an infinite slope failure is usually small compared to the width or length of the landslide. Similarly, the depth of many precipitation-induced landslides is low compared to the width and length of the landslide due to the limited depth of infiltration of precipitation. Within the shallow depth the infiltrated water has a significant influence on the suction head, the density of the soil and the pore pressure on the failure surface. The general FOS for uniform slope failure is commonly written (Bromhead 1992) as:

$$FOS = \frac{\frac{c'}{\gamma z} + (1 - r_u)\cos^2\alpha \tan\phi'}{\sin\alpha\cos\alpha} \qquad \text{Equation B14}$$

where the r_u is the pore pressure ratio of the density of water and soil, times the ratio of the height of the groundwater above the failure surface, h_w and the depth to the failure surface z such that:

$$r_u = \frac{\gamma_w h_w}{\gamma z} \qquad \text{Equation B15}$$

Numerous commercial slope-stability computer-programs have been developed to model slope stability and many have been combined with groundwater modeling programs to assess the influence of infiltration and groundwater on the pore pressure and therefore the slope stability. Keefer et al. (1987) utilized Equation B14 to calculate the stability of an infinite-slope and infiltration models to analyze the process of increasing pore pressure (or r_u) at the failure surface, and the reduction in FOS due to rain. Gasmo et al. (2000) modeled the stability of a residual soil slope exposed to rainfall and found that during a dry period evaporation increased the slope stability by about 30%. A rainfall of 80 mm/day or 9.2 x 10^{-7} m/s, which is equivalent to the permeability of the soil, resulted in a 25% reduction in FOS in about 12 hours. They also noted that as the soil properties and layering in the field became more variable, it became more difficult to model the stability of the slope. Iverson (2000) and Picarelli et al. (2004) both used formulations of the infinite slope stability equation to assess the influence of precipitation on the groundwater regime and its affect on the slope stability of clay rich soil.

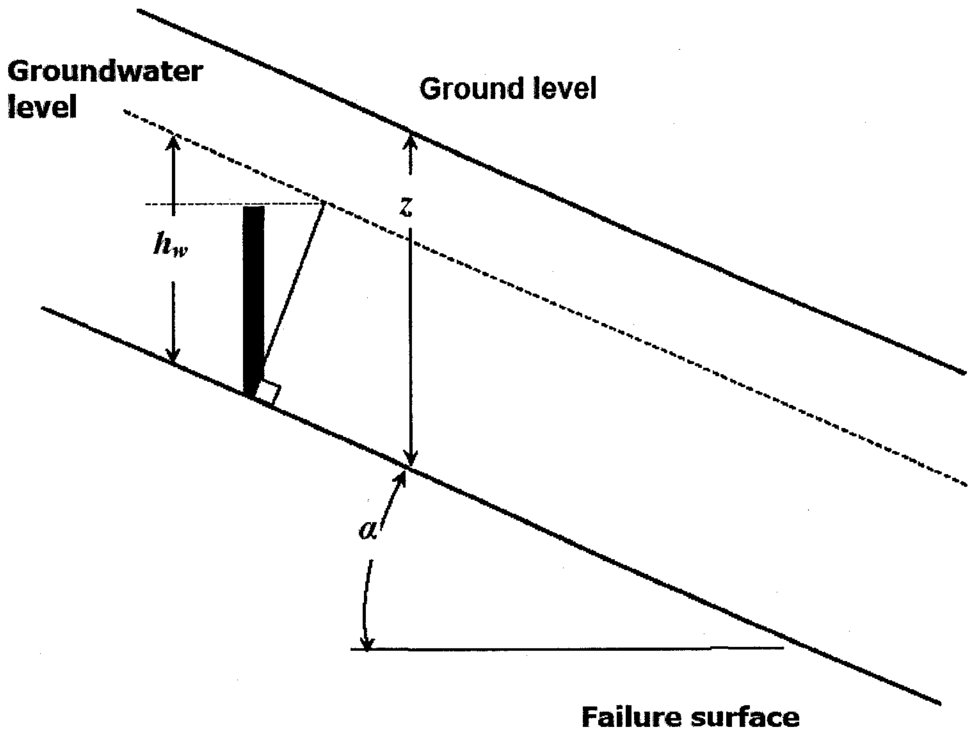

Figure B2 The geometry of infinite slope stability analysis (after Bromhead 1992)

Wu (2003) reviews the influence of combined loads including the pore pressure from infiltration of rainfall and snowmelt and the loss of root reinforcement as the result of logging or forest fires.

B 1.7 Debris flow

Debris flows are the movement of material with the behaviour of a viscous liquid (Cruden and Varnes 1996). Debris flows can be triggered by two scenarios:

1. A landslide impedes the flow of a water course such that the water course is either dammed or entrains the landslide material and becomes a dense viscous flow. The mechanisms of triggering the landslide and resulting debris flow can be governed by the infiltration, ground, and slope stability processes previously discussed (Keegan 2007, VanDine 1985).
2. Overland flow causes severe erosion or multiple small landslides <10m^3 which results in an increase of the density of the overland fluid flow (Couture and Evans 2000 and Chen et al. 2006, VanDine 1985). The dense fluid has greater

erosive characteristics and thereby entrains more bed-load thereby further increasing the fluid density. The result is high stream flow with a high bed-load which when the gradient of the stream reduces becomes a debris flow deposit. This process is dominant in post forest-fire debris flows where the infiltration is reduced by the post fire ash being more hydrophobic than the native soil and the preponderance of fine, loose, light, highly erodible ash to act as the initiating solid that increases the density of the fluid.

Numerous authors have investigated the triggers of debris flows. The VanDine and Bovis (2002) review of debris flow research in Canada highlighted both a dependency on precipitation and or rapid snowmelt and a need for sufficient available debris within the drainage. However, they emphasized that "a hydro-climatic event (rainfall, rain-on-snow, snowmelt or jökulhlaup) is a necessary, but not a sufficient, condition for debris flow occurrence". Fiorillo et al. (2001) identified the statistical characteristics of a storm that caused numerous debris flows in Southern Italy using Generalized Extreme Value statistics. They looked at antecedent durations up to from 1 hour to 90 days. They concluded that the flow were caused by artificial cuts made for track ways across the slope, because a similar storm several decades prior to the construction of the track ways had not caused debris flows.

B 1.8 Conclusions on landslides and precipitation

The stability of the a slope is influenced by several conditions that are affected by precipitation. OF the parameters that change in time, almost all are controlled by soil moisture and therefore precipitation has an influence.

These include:

1. Saturation of the near surface and the corresponding loss of suction.
2. The increase in the density of the near surface soils. (This is often identified as the most significant factor of rainfall from those that do not appreciate the physical process at work below the soil surface). But as can be seen in Equation B14 an increase in density only decreases one of the three terms in the numerator of the FOS equation.
3. The increase in the shallow groundwater condition in the slope leading to uniform slope type failure.

4. The infiltration of the water from the unsaturated zone to the groundwater table during long episodes of precipitation. The time frame of the influence on the groundwater table is controlled by the hydraulic conductivity of the soil.

The factors that change that are unrelated to precipitation include:

1. The change in the shear strength over time. This is most significant in organic soils due to decay (Keegan 2007). This also includes changes in the effect of root mat strength and the change in strength over time due to vegetation growth or decay (Turner 1996). Sidle (2006a) suggests that following harvesting the roots strength of the deforested vegetation deteriorates over time. Concurrently the root strength of the regenerating forest increases with time. There is some period where the sum of the decaying roots and the regenerating roots is at a minimum. If the land use is changed from large vegetation with large root system to an agricultural use with smaller plants with limited root systems, the effective root strength and depth of the root strength will be reduced until larger vegetation re-grows.
2. Progressive failure whereby strength of the soil or rock on the failure surface decreases due to localized stress exceeding the peak shear strength. As a result the shear strength of the material at the failure surface is progressively reduced to its residual shear strength leading to eventual catastrophic landslide movement of the slope. This is most common in brittle material with a high peak and low residual strength such as clay shale (Wu 1996).
3. External loading such as train loads, erosion, deposition and earthquakes (Wieczorek 1996).
4. Changes in groundwater not related to precipitation or lack of precipitation including rapid draw down and inundation (Wieczorek 1996).

Despite the brevity of this list, there is a large group of trigger types, especially those described by bullet 3 (above), which are not considered in this research.

The contribution of each mechanism to the destabilization of the soil is difficult to assess without detailed knowledge of the soil moisture at numerous points in time at numerous positions within the slope. Investigators (Fannin and Jaakkola 1999, Rahardjo et al. 2001a, and others) have investigated the relative importance of these processes. Some investigators have undertaken this research by artificially causing rainfall on natural and artificial slopes and others have instrumented natural slopes and waited for natural precipitation events.

The time scale and sensitivity to high intensity versus long duration precipitation is dependent on several factors. For short duration precipitation the change in stability of the slope is dominated by permeability of the soil, the soil suction, the antecedent soil moisture in the unsaturated zone, density changes of the soil during infiltration, initial pore pressure at the potential failure surface, and the depth to the saturated zone. During long duration precipitation conditions the stability of the slope is dominated by the permeability of the slope and the change in pore pressure over time.

Appendix C Weather indices for the prediction of geotechnical hazards

C 1.0 Development of weather indices for the prediction of landslide hazards

C 1.1 Rainfall

Numerous researchers have demonstrated the link between the triggering of earth and debris slides and long and short duration precipitation. Of the 194 deadly landslides in 2003 listed in the International Landslide Centre (2006) website, 79% were attributed to heavy rain alone and a further 2% were attributed to heavy rain in combination with other factors. Wieczorek (1996) identified intense rainfall as one of the five triggers that can cause a near immediate response resulting in both increasing stresses due to increased loading and reduced shear strength. Aleotti (2004) opens his paper on a warning system for rainfall-induced shallow landslides by stating, "... it is widely recognized that soil slips and debris flows are triggered by short intense storms". Ibsen and Casagli (2004) begin their discussion of rainfall patterns and related landslide incidents in Italy with a quote from Corominas stating "... rainfall is the most frequent landslide triggering factor in many regions of the world". Nagarajan et al. (2000) indicate that rainfall is the most common trigger of landslides of colluvium. They suggest that understanding the relationship between rainfall and landslides provides a basis for predicting widespread slope landslides by identifying a relationship between the short term (less than 24 hours) and longer term rainfall. Chowdhury and Flentje (1998 and 2002) demonstrate the correlation between landslide movement based on slope inclinometer monitoring data and low percent-exceedance time antecedent-rainfall events. Guzzetti et al. (2007) published an extensive review of previous research of 124 rainfall landslide thresholds and summarized their own research on the topic. They provide a useful classification of the types of landslide rainfall indices and thresholds. The 5 types are:

1. Process-based models that include decay type antecedent precipitation indices,
2. Empirically based models,

3. Event thresholds,
4. Thresholds that consider antecedent conditions, and
5. Other types of thresholds.

The following is a review of some of the findings and research undertaken by others, presented chronologically.

The nomenclature used in Guzzetti et al. (2007) is used within this document wherever possible. A modified list of rainfall and weather variables from Guzzetti et al. (2007) is included in the List of variables.

Guidicini and Iwasa (1977) analyzed the precipitation records for 40 landslides in nine different regions of Brazil. They introduced the concept of the ratio of yearly antecedent rainfall, $A_{(y)}$ to Mean Annual Precipitation, MAP or $A_{(y)MAP}$. They found that by using a variable threshold for $A_{(y)MAP}$ throughout the year, as defined by previous landslide activity, they could identify zones on the annual plot where landslides were very likely, moderately likely, possible, and unlikely. They defined the year as starting at the driest time of the year rather than the calendar year.

Caine (1980) compiled the rainfall intensity and duration data for 73 debris flows from published data from around the world. He plotted them on the log/log rainfall intensity versus rainfall duration (ID) plot, normally used by hydrologists and meteorologists (Figure C1). Caine used the critical duration period identified by other researchers but provides no methodology or consistent criteria for determining the duration. Given the range of intensities Caine appears to be combining the maximum hourly rainfall intensity, I_{max}, the critical hourly rainfall intensity I_c and the average rainfall intensity over the duration of the rainfall, D. The range of duration extends from 0.02 hours (1.2 minutes) to 2208 hours (92 days) for a sites in the Himalaya and Scandinavia respectively. This suggests that Caine is also mixing data that is based on the duration of a period (with discontinuous rain), D and the duration of the critical continuous rainfall event, D_c. For example, there are two data points with intensities of 138 and 60 mm/hr and durations of 0.02 hours (1.2 minutes) that define the lower threshold for precipitation-induced-landslides at low durations. This suggests that a rainfall of 2.76 and 1.2 mm in 1.2 minutes, induced landslides independent of previous rain. Although these are intense rains, intensities at least an order of magnitude higher have been recorded (WMO 1984). It is therefore unlikely that a 1.2 minute rain triggered a landslide without some prior rain. It is suggested that if the definition of I and D were defined and adhered to these two landslide inducing precipitation events would likely plot at lower intensities and greater durations, and the I versus D threshold would be reconfigured. Having plotted the ID data Caine fit a lower bound threshold at which most of the landslides occurred above and found the relationship:

$$I=14.82D^{-0.39}$$ Equation C1

The plot and relationship developed by Caine (1980) has become the most commonly used relationship for precipitation-induced landslides (Guzzetti et al. 2007). Caine comments that, although not part of his research, the minimum recurrence interval for each location could be determined by comparison with the precipitation Intensity-Duration-Frequency (IDF) curve for the site of the landslide. In this first application of the IDF plot for precipitation-induced landslides Caine extended the plot out to 90 days in recognition of the influence of antecedent precipitation on debris flows.

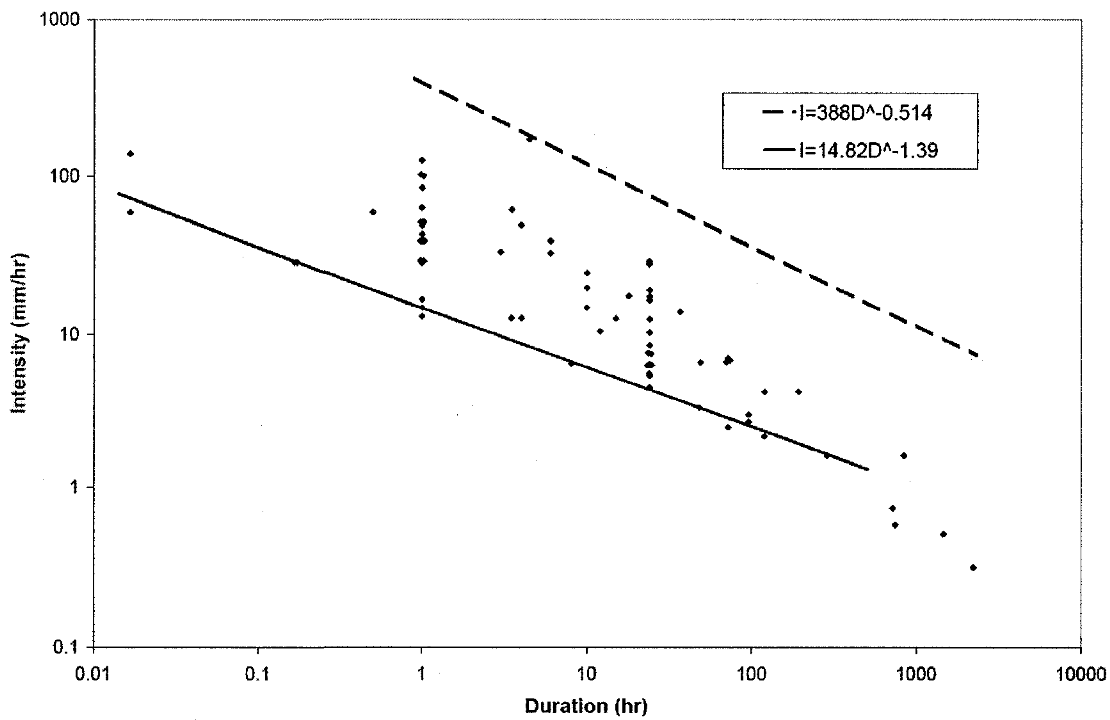

Figure C1 Rainfall intensity versus duration with rainfall induced landslide threshold after Caine (1980)

Moser and Hohensinn (1983) related the duration and intensity of rainfall conditions triggering 140 landslides in the Alpine regions of Austria using an infinite slope model to represent the landslides. They found that the landslides all fell into specific regions of the rainfall intensity-duration plot extending to periods as long as 10 days.

Cannon and Ellen (1985) demonstrated a link between rainfall and debris-flow and earth-slide activity once the seasonal rainfall had reached a general threshold. They used the MAP to delineate regions within an area of about 7500 km^3 in the San Francisco Bay area (SFB) with similar rainfall characteristics. They then plotted the rainfall intensity for the duration of the storm, I versus the duration (up to 45 hours) of storm events for each MAP area that did, and did not have concurrent landslide events. Based on the distribution of the landslide inducing storms they identified a threshold for storms causing landslides and compared their threshold to those of previous authors working in areas in and near SFB.

Muraishi and Okada (1988) discuss the use of continuous versus hourly precipitation to differentiate between rainfalls that could and those that are unlikely to cause landslides in Japan. They identified 5 typical rainfall patterns which caused landslides. These rainfall-induced landslide patterns can are summarized by the following:

1. Landslides during a rainfall after a period of no rain
2. Landslides during repeated periodic rainfalls
3. Landslides during a continuous heavy rainfall
4. Landslides a few days after a moderate rainfall
5. Landslides during a continuous moderate rainfall

Okada et al. (1994), Okada and Sugiyama (1994) and Sugiyama et al. (1995) assessing landslides in Japan, proposed that a slope has a rainfall resistance, S that is a function of the slope angle, height, cohesion, internal friction angle, density, pore pressure, permeability, and a factor to account for the groundwater leakage, weathering and other factors. They then equate the S to the product of the hourly rainfall intensity, I and the cumulative storm rainfall, $E_{(h)}$, using the equation:

$$S = E_{(h)}^{m} I^{n} \qquad \text{Equation C2}$$

Where m and n are exponents determined by maximizing the multiple correlation coefficient of the dependents of S. In this application I is the hourly intensity. The Okada et al. (1994) definition of $E_{(h)}$ is such that it is reset to zero every time the rainfall is interrupted for 12 hours or more. For a specific set of conditions, S is a constant and Equation C2 forms a hyperbola in the $I\text{-}E_{(s)}$ plot (Figures 10 and 11 of Okada et al. 1994) above which landslides are likely. However, Okada and Sugiyama (1994) indicate that the formulation requires "some experience and engineering considerations" to shift the "critical rain curve" to an appropriate location on the hourly intensity and cumulative rainfall plot, based on landslide and none landslide events.

Grivas et al. (1996) demonstrated that ground movement was delayed by approximately 1 month from the rainfall event for an earth slide in central Alberta, Canada. They provided several potential relationships between ground movement and rainfall such that:

$$M(r,t)=a*f(r/t,t-\lambda) \qquad \text{Equation C3}$$

Where $M(r,t)$ is the movement of the slope, a is a constant scaling factor, $f(r/t, t-\lambda)$ is an exponential function, r/t is the ratio of rainfall, r, and time, t, and $t\text{-}\lambda$ is the time lag of rainfall and landslide movement.

To allow the application of rainfall/debris flow indices over a wider region Wilson (1997) used the concept of using both MAP and the frequency of precipitation or number of days in a year with measurable rain or the rainy day normal (RDN). Wilson demonstrated that when plotting the RDN and 24 hr triggering rainfall, R_c the critical lower bound threshold was $R_c = 14(RDN)$.

Terlien (1998) studied 11 landslides in Manizales, Columbia. He used a trial and error technique of plotting normalized daily rainfall, R_n, versus normalized accumulated rainfall not including R, or $A^{n}_{(1\text{-}d)}$ for several d. He demonstrated that one d provided a significantly better distinction between rainfall conditions that did and did not induce landslides than the other d 's he tried. He appears to have normalized R and $A_{(1\text{-}d)}$ by dividing them by the maximum R and $A_{(1\text{-}d)}$ because the range of R and $A_{(1\text{-}d)}$ is from 0 to 1. Most other investigators have normalized by MAP. He stressed the importance of selecting an index with the correct antecedent duration before setting a threshold. He also suggests that the index duration is related to the depth of landslide such that the deeper the failure surface the longer the duration of the most significant antecedent index. This is consistent with the mechanics of infiltration and landslides discussed in Appendix B.

Based on a study of 65 landslides in the Rio de Janeiro area, Ortigao et al. (2001) found that the relationship between 24 hr rainfall, R, and the antecedent rainfall over the previous 4 days, $A_{(4)}$ were the most useful indices for precipitation-induced landslides. As shown in Figure C2 if the intersection of the R and $A_{(4)}$ intersect above the "New criteria", landslides are likely to occur. In this plot R and $A_{(4)}$ are not independent because $A_{(4)} = R + A_{(3)}$ so the plot has the tendency to take on the one to one relationship for low R *and* $A_{(4)}$.

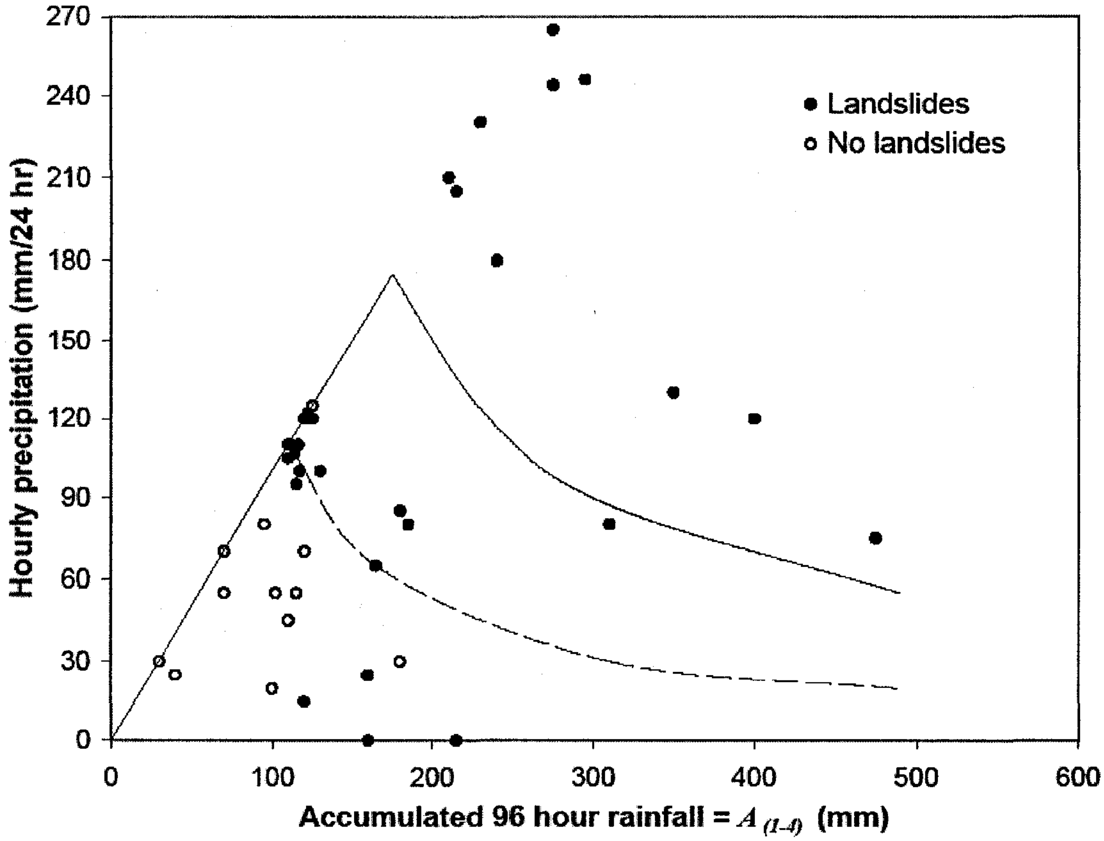

Figure C2 Precipitation induced landslide criteria used by the Rio-Watch system (after Ortigao et al. 2001). The y axis may be miss labelled in the original figure. The original axis title, figure title and axis units are inconsistent. The dashed line is the "New criteria".

Aleotti and Chowdhury (1999) indicate that the cause and effect relationship between rainfall and landslides is identifiable when analysis of the rainfall data provides definition of the triggering threshold and the recurrence interval of the critical rainfall.

They also present an intensity duration plot of rainfall from 1 to 1000 hours (0.04 to 42 day) overlaying soil permeability (as an indicator of potential lower bound of infiltration) and the soil depth at which landslide activity occurs.

Crozier (1999) and Crozier and Elyes (1980) proposed the use of an antecedent soil water status model (Equation C5) that uses a concept somewhat consistent with the antecedent precipitation index (API) (Equation C4) used in hydrology (D. Jobin, RadHyPS Inc., personal communications 2002).

$$API_0 = P_0 + KR_1 + K^2P_2 + K^3P_3 \ldots = P_0 + KAPI_1 \qquad \text{Equation C4}$$

$$\begin{aligned} EPa_0 &= KEP_1 + K^2EP_2 + \ldots + K^nEP_n \\ &= K(EP_1 + EPa_1) \quad where \quad n = \infty \end{aligned} \qquad \text{Equation C5}$$

where API_0 is the antecedent precipitation index on current day, API_1 is the antecedent precipitation index on the previous day. Similarly P_i is the precipitation on the ith day. EPa_0 is the excess precipitation index on the current day, EP_i is the excess precipitation index on the ith day, and n is the length of the antecedent duration of interest. K is a constant usually between 0.8 and 0.999 depending on the soil type, runoff and the evapotranspiration conditions and the formulation used. The difference between these two formulations is subtle, but significant. Crozier (1999) uses a fixed antecedent duration and is independent of the day zero rainfall. Equation C4 of D. Jobin (personal communications 2002) is dependent on P_i and places no limit of the period of antecedent precipitation considered.

Although K is assumed to be a constant in this formulation, it does vary. K is actually dependent on temperature, runoff conditions such as frozen ground, and whether growing or dormant vegetation is present. If considered these variations introduce discontinuities into the API and EPa_0 functions such that the analysis or comparison of index values to one another is not appropriate due to variation in K.

Crozier and Elyes (1980) and Crozier (1999) plotted the daily rainfall and soil moisture (which is their equivalent to API) and defined an area with and without slides on the plot. Inagaki and Sadohara (2005) provide an alternate antecedent precipitation index using a variable K dependent on factors related to the sensitivity of landslides to antecedent rainfalls and the time between the landslide and the contributing rainfall.

Glade et al. (2000) introduce the Antecedent Daily Rainfall Model and related indices. This improves upon the earlier work of Crozier by providing a methodology for replacing K with a constant determined by assessing surface runoff data. The method uses a maximum antecedent duration of 10 days. Based on the likelihood of a landslide occurring for a given antecedent daily rainfall and daily rainfall, they introduce a means of calculating the probability of landsliding. In this formulation antecedent precipitation does not include the daily rainfall and therefore the two indices are independent.

Chleborad (2000) proposed a means of identifying precipitation-induced landslides by relating the 3 day antecedent rainfall and the 15 day antecedent rainfalls prior to the 3 days triggering precipitation. As per Appendix F this is the $A_{(3)}$ and $A_{(3-18)}$. In this way Chleborad developed two independent indices where Ortigao et al. (2001), Muraishi et al. (1992) and others have worked with dependent indices which renders a portion of their plots void of data. During periods when the two specified thresholds shown in Figure C3 were exceeded he found that there was a greater likelihood of precipitation-induced landslides. Chleborad also found a correlation of landslides and warming trends. This is likely the result of low-pressure rainfall inducing cyclonic weather systems being associated with warmer air masses in comparison to drier colder continental outflow during the winter months in the Seattle area.

Nagarajan et al. (2000) found that rainfall intensities exceeding 200 mm/day initiated catastrophic landslides in the Konkan coast area of India and that, due to the high permeability of the soil, antecedent conditions were also relevant. Furthermore, they suggest that isohyetal maps (a contour map of equal rainfall in a set period which is usually annual) could be used to identify areas of potential landslides in the absence of rain gauge information. The use of isohyetal maps will be discussed in Chapter 3.

In their monograph on rainfall-induced landslides in Singapore, Rahardjo et al. (2000) concluded that antecedent rainfall was of greater importance in areas with lower permeability soils. They explain that lower permeability soils are unable to redistribute higher pore pressures resulting from precipitation-induced infiltration. Therefore, if continued rainfall occurs when pore pressures are elevated by previous rainfall, they will continue to rise due to the most recent rains. There is however, a limiting condition when permeability of the soil reaches its minimum (its saturated permeability) and the influence of further precipitation is reduced. Soils with higher permeability can more rapidly drain infiltrated water and thereby return to pre-rainfall conditions quicker.

However, less permeable groundwater boundary conditions can increase the influence of antecedent precipitation despite the permeability of the soil.

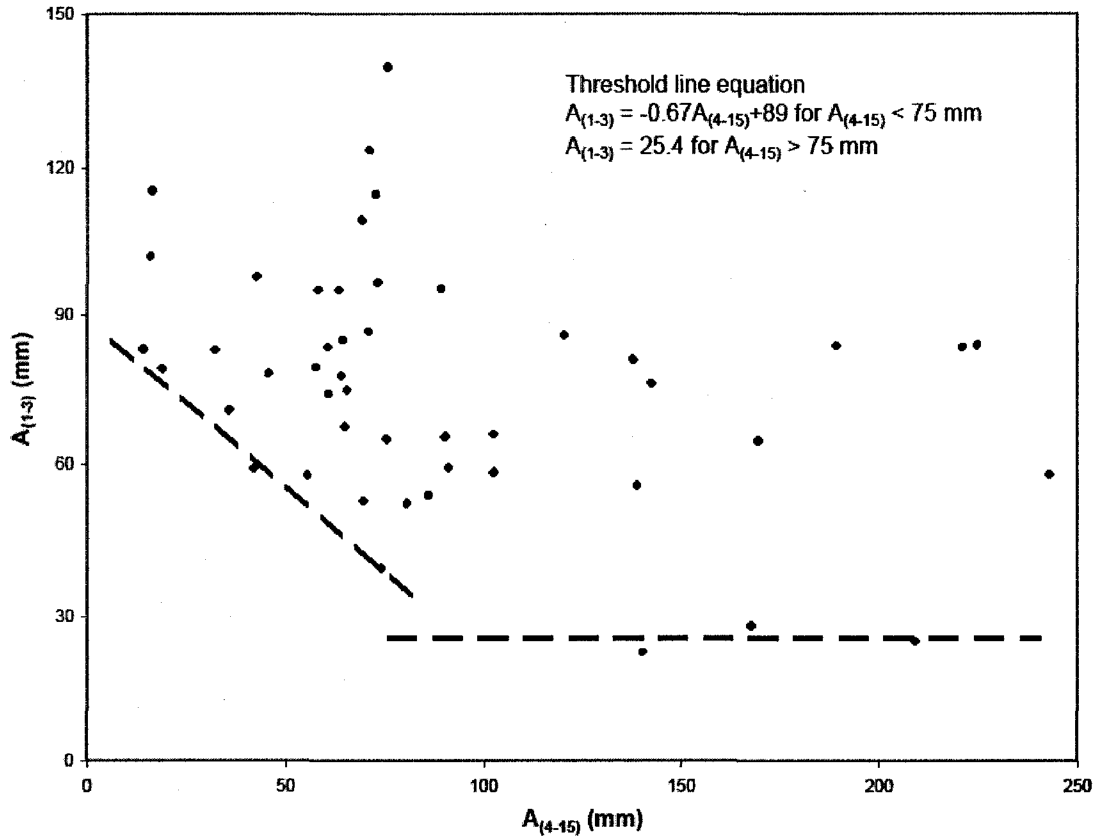

Figure C3 Antecedent precipitation $A_{(1-3)}$ versus $A_{(1-15)}$ conditions above solid lines are likely to induce landslide after Chleborad (2000)

Kawamoto et al. (2000) investigated the hydrologic triggering of two landslides in August of 1998 in Fukushima Japan. They plotted the cumulative rainfall for a storm versus the rainfall intensity at any given time. This plot is typical of Okada et al. (1994) and other Japanese studies. They compared the rainfall of the two storm-induced landslides to thresholds developed earlier. The plots provided indicate that the cumulative/intensity rainfall thresholds were exceeded several times in the hours prior to the landslide suggesting that the thresholds are set such that warning of the landslides will be provided.

The large number of rainfall-induced landslides in Hong Kong motivated Dai and Lee (2001) and many others to investigate the relationship between rainfall intensity and the frequency and volume of landslides. They found that for the highly unstable residual soil slopes of areas the amount of rainfall in 12 and 24 hour periods provided the best correlation with the number of landslides. Dai and Lee clearly demonstrate that more rain causes more landslides and larger landslides.

Miles (2001) assessed the effect of climate change on the frequency of landslides in the Georgia Basin of southwest BC. He applied the PIL thresholds identified by Caine (1980) to his study area and as a result derived thresholds that were independent of the geotechnical conditions of the area. He then predicted that a 20% change in the annual precipitation conditions would increase the rate of landslides by up to 278% in areas of 2,000 to 3,000 mm average annual precipitation for the 6 hour rainfall duration. Areas with 300 to 1,000 mm of average annual precipitation were predicted to have percentage increases in landslide activity of 119% for the 6 hour rainfall duration. Although a relationship between the change in annual rainfall and change in landslide frequency as function of average annual rainfall and rainfall duration is not well supported, Miles shows how the relationships developed by Caine could be applied. It also demonstrates that site specific PIL thresholds are needed provide defensible predictions.

Toll (2001) and Rahardjo et al. (2001b) assessed rainfall-induced landslides in Singapore and found that precipitation-induced landslide thresholds could be identified when the combination of R and $A_{(2-5)}$ and R and $A_{(2-15)}$ were related to minor and major landslides respectively. The relationship between larger landslides and longer antecedent indices is consistent with Terlien (1998). Although not explicitly stated it appears that Toll uses the Guzzetti et al. (2007) definition of antecedent rainfall such that the R and $A(c\text{-}d)$ are independent. Toll demonstrated that the slope stability FOS for shallow residual soils in Singapore is reduced by the infiltration of short and longer term (5 day) antecedent precipitation. By reviewing rainfall events that were more severe than the rainfall conditions that induced landslides, Toll determined that the 5 day antecedent and daily rainfall must both be severe to induce landslides.

Flentje and Chowdhury (2001) and Chowdhury and Flentje (1998 and 2002) introduced the concept of computing the rolling 7, 30, 60 90 and 120 day cumulative rainfall for the complete rainfall history of a rain gauge representative of a landslide. These are equivalent to the Guzzetti et al. (2007) (from Govi and Sorzana) definition of antecedent rainfall, $A_{(d)}$ with the period over which the rainfall is summed starting on the day of the landslide. Therefore, the period of $A_{(d)}$ is relative to the landslide, not the start of the landside triggering rainfall. As a result $A_{(e)}$ is not independent of $A_{(f)}$ where e is less than f. Chowdhury and Flentje compared the $A_{(d)}$ to the slope inclinometer records and subjectively select the $A_{(d)}$ index that best correlated with the ground movement record. Once the $A_{(d)}$ index is identified they determine the threshold at which ground movement is expected. To establish the frequency of the threshold they calculated the Antecedent Rainfall Percent Exceedance Time or $ARPET$ for each $A_{(d)}$. The $ARPET$ is calculated by determining the percent of time the threshold of any value is exceeded using the following equation.

$$ARPET = 100\frac{n_i}{N} \qquad \text{Equation C6}$$

Where n_i is the number of days that each rainfall value is equalled or exceeded and N is the number of days of record. The $ARPET$ method does not provide a means to assess the severity of a current rainfall because there is no means to compute the severity or rarity of the rainfall without comparing it to every rainfall in the period of record. In their 2001 paper they also relate the $ARPET$ thresholds to the ID plot used by Caine (1980).

Ko Ko et al. (2003) studied landslides along the Unanderra to Moss Vale railway line about 95 km southwest of Sydney, Australia. They identified a means of identifying which of the potential antecedent precipitation periods was the most critical by determining which were the rarest events that most commonly resulted in landslide activity. Ko Ko et al. (2003) presented this analysis in Figure C4. They use the same method of calculating $A_{(d)}$ as Chowdhury and Flentje (1998) and therefore each $A_{(d)}$ was not independent of any other $A_{(d)}$.

Ko Ko et al. concluded that because landslides occurred in 1991 and 1998 and Figure C4 showed that each $A_{(d)}$ in 1991 was the rarest $A_{(d)}$ recorded and second rarest for $A_{(15)}$ and $A_{(30)}$ in 1998 that the $A_{(15)}$ and $A_{(30)}$ were the $A_{(d)}$ to which the landslides are most sensitive. Based on the paper it is assumed that the landslides were inactive during the second highest R, $A_{(3)}$, $A_{(5)}$, and $A_{(7)}$ in 1986, and the second highest $A_{(60)}$, $A_{(90)}$, and $A_{(120)}$ in 1988. This method provided a means of identifying which $A_{(d)}$ a landslide is likely to be most sensitive, based on historical data from which rainfall indices can then be set. Apparently assessing the year with the highest index rather than some shorter period worked because the period of landslide activity was several months long and the movement data were only obtained periodically during that period. Ko Ko et al. (2003) identified the $A_{(15)}$ as the best indices of landslide movement at the sites they studied and that 788 mm ± 10% in 15 days was a logical threshold to use.

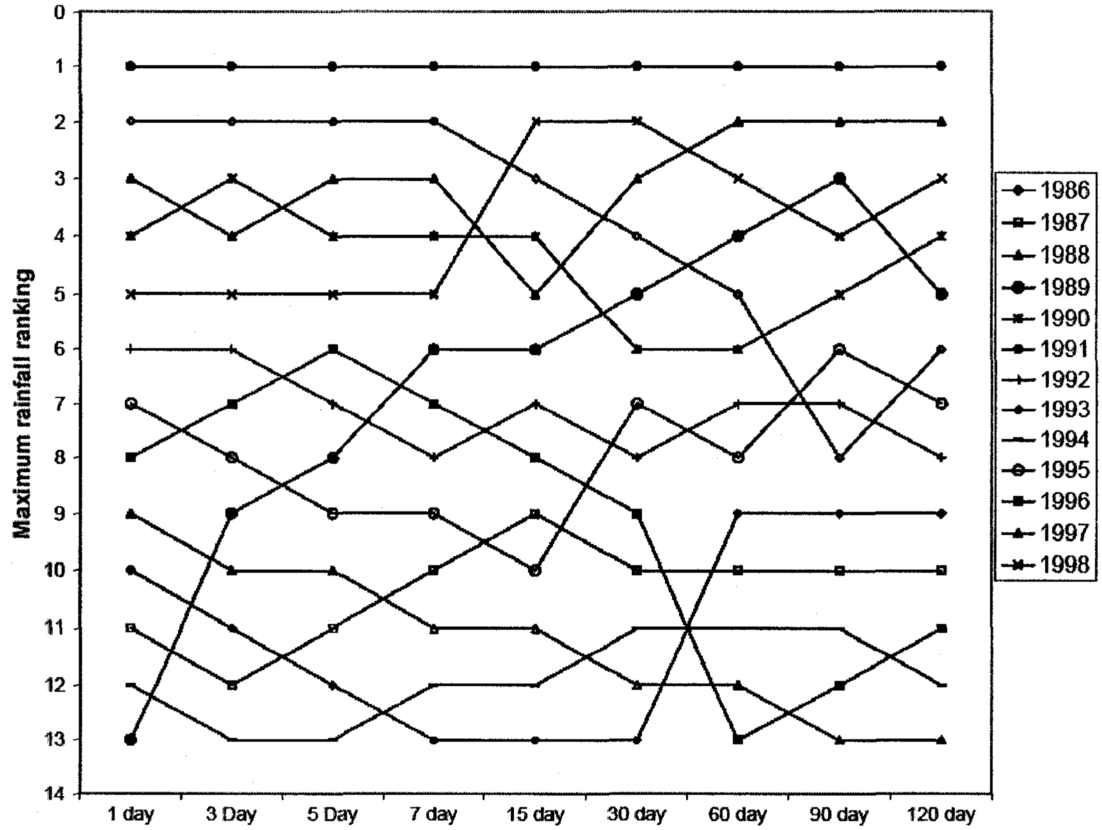

Figure C4 1986 to 1998 rainfall ranking for R, $A_{(3)}$, $A_{(7)}$, $A_{(15)}$, $A_{(30)}$, $A_{(60)}$, $A_{(90)}$, $A_{(120)}$ at Robertson, NSW Australia after Ko Ko et al. (2003)

Dai and Lee (2003) summarize the work of others in Hong Kong dating back to the early 1980's which initially focused on the failure of anthropogenic slopes but later included natural slopes as well. For natural slopes a threshold of 200 mm in 24 hours causes landslides on the order of 1 per km^2. As the 24 hour rainfall increases to 400 mm the density is found to increase to 10 per km^2. Dai and Lee found that antecedent rainfall is not an important factor due to the high permeability of the soil and the shallow depth of the landslides. As a result, Dai and Lee and others use rolling 24 hr rainfall or daily rainfall as the most common rainfall indices in Hong Kong.

Jakob and Weatherly (2003) developed two discriminant functions, CS_L and CS_{NL}, to identify when landslide triggering and stable conditions were present for the North Shore Mountains near Vancouver, BC. They started by considering precipitation intensity data from 1 to 48 hours, stream-flow data and antecedent rainfall from $A_{(1)}$ to $A_{(28)}$. The stream-flow data were assumed to model the snowmelt influence. The stepwise discriminant function analysis identifies which input parameters have the highest correlation and by what factor they should be multiplied to achieve the highest CS_L or CS_{NL} corresponding to the landslide, no landslide condition respectively. Jakob and Weatherly found that the flow rate in a nearby stream, the $A_{(28)}$, and the I_{6h}, combined with weighting factors produced the most effective CS_L and CS_{NL}. Provided the 1 hour rainfall intensity was 4 mm/hr or higher and the difference of CS_L or CS_{NL} was greater than a landslide warning threshold, landslides were possible. This level of detailed analysis appears to be beneficial where multiple data types are available and a single index is desirable. Where only daily and antecedent precipitation data are available, the additional effort may not be justified.

Kanji et al. (2003) presented an accumulated rainfall versus time plot. They defined the starting time of the accumulated rainfall as the time rainfall starts following a dry period. If the rain stops the accumulated rainfall is reset to zero. This limitation is not imposed on most other intensity duration plots. Kanji et al. do not specify how long the rain should stop for, but suggest that even if it stops for a few days the accumulated rainfall and time should be reset to zero. They found that the debris flows did not occur when the accumulated precipitation was less than P in time t where

$$P = 22.4t^{0.41} \qquad \text{Equation C7}$$

Their expression of P versus t can be restated in the more conventional intensity duration type equation of Caine (1980) by replacing P with the relationship $I = P / D$. This transforms Equation C7 into

$$I = 22.4D^{-0.59} \qquad \text{Equation C8}$$

The constant and the exponent are within the range of other intensity duration relationships summarised by Guzzetti et al. (2007).

By modeling generic, 5 and 15 m high railway embankments Gitirana (2005) demonstrated that typical clay railway embankments have a high sensitivity to the soil suction air entry value (discussed in Appendix B, Section 1.6), the saturated hydraulic conductivity, the cohesion, and the friction angle when exposed to wetting events of 40 mm/day for 8 days. Clay railway embankments are common in area of predominantly clay soil and especially throughout the prairie states and provinces. He also confirmed that the initial pore water pressure has a significant influence on the factor of safety. The wetter the soil was at the onset of the rainfall the lower initial soil suction and the lower the Factor of Safety at the end of the rainfall.

Adding to the work of Chleborad (2000), Baum et al. (2005) measured the soil moisture, rainfall and landslide conditions and demonstrated that increased soil moisture resulting from antecedent precipitation combined with frequent or prolonged rainfall caused landslides near Seattle, Washington.

Chien-Yuan et al. (2005) initiated studies for the development of a real-time monitoring system to warn of rainfall-induced debris flows in Taiwan. They analyzed 61 events and adopted the widely used intensity duration type equation consistent with Equation C1 first introduced by Caine (1980) however, they only consider durations up to 4 days.

Rahardjo et al. (2005) correlated short-term rainfall, infiltration, and landslides using hourly and shorter duration rainfall data. They also demonstrated that, depending on the soil type, 40 to 100% of the rainfall may contribute to infiltration and that the larger the total rainfall the smaller the proportion of the rainfall that will infiltrate the soil.

Jakob et al. (2006) propose the use of a decision tree with three levels of 24 hour, and 4 week antecedent precipitation ($A_{(28)}$) thresholds with consideration of the storm-class where storm class is based on wind direction and speed, storm moisture and other factor. The use of a storm classification is similar with Chleborad use of temperature. The storm class is such that severe cyclonic storms are identified. The choice of 24 hour and $A_{(28)}$ indices were based on earlier work by Jakob and Weatherly (2003).

Godt et al. (2006) reintroduced the concept of antecedent soil moisture (AWI) from Crozier with a new formulation from others. They use the equation:

$$AWI_i = AWI_{i-1}e^{-k_d\Delta t} + \frac{I_i}{k_d}(1 - e^{-k_d\Delta t})$$ Equation C9

where k_d is an empirical drainage constant and Δt is the time increment, i count of the time step, and I_i is the rainfall intensity at time i. They note that the formulation is an index not a true measure or model of the physical process or infiltration, evaporation, or surface water partitioning. They compare the change in AWI to the change in measured soil moisture at a site near Edmonds, Washington with favourable results, although they point out that initialization of the AWI is critical to reflect the initial moisture content of the soil. As with the soil moisture index of Crozier, k_d is dependent on various factors and is expected to vary with time of the year due to the variable influence of vegetation and temperature on infiltration and evapotranspiration. The means of determining and the temporal variation k_d make this formulation awkward to apply.

Shi (2006) used unsaturated and saturated soil mechanics, consistent with that described in Section 2.3, to model a number of railway embankments and precipitation conditions. Shi modeled an extreme rainfall event in 1998 June in North-eastern New York State along the western limit of Lake Champlain, when CP experienced earth-slides, debris flow, debris flow - gully erosion and seepage erosion events at 28 different sites. Shi demonstrated for the earth-slide failure mechanism that the embankment stability decreased continuously during the periods of rainfall. Shi also shows that the depth of the lowest factor of safety failure-surface in the soil reduces as the rainfall continues. Consistent with the findings of others Shi showed that the initial pore pressure distribution in the embankment and therefore the antecedent rainfall conditions had a significant influence on the stability of the embankment. Shi documented the two railway ground hazard scenarios (Keegan 2007): 1) debris flow - avulsion - erosion, earth slide or earth flow and 2) earth slide. In the first scenario Shi identifies the erodibility of the soil as being a contributing factor to the initial debris flow.

Tommasi et al. (2006) demonstrated that the 60 to 180 day antecedent rainfall for the Porta Cassia Slide area of central Italy reactivated a large 3 million m^3 landslide and triggered shallow smaller slides. The authors used the Gumbel analysis to assess the frequency of the antecedent rainfalls but failed to identify the inability of the Gumbel distribution to reliably model longer antecedent duration rainfalls. This is illustrated by the maximum return period (~19 years) calculated for the 120 day antecedent precipitation compared to the period of record (45 years). Thus when the return period of the 120 day antecedent precipitation is compared to other longer or shorter antecedent precipitation return periods the relative rarity of the two events may not be indicated.

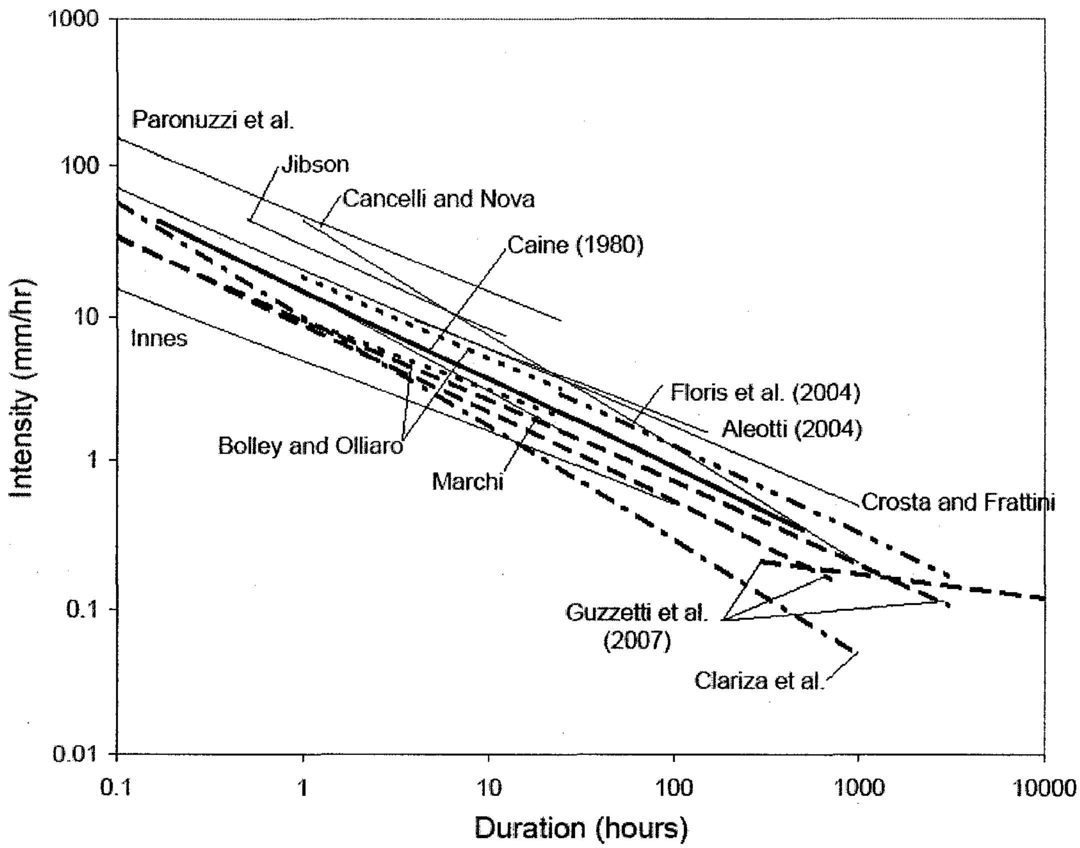

Figure C5 Intensity-duration plot showing the results of CADSES study by Guzzetti et al. (2007) compared to global threshold proposed by others referenced in Guzzetti et al. (2007)

Empirical landslide rainfall thresholds have been developed for the Central European Adriatic Danubian South-Eastern Space (CADSES) area by Guzzetti et al. (2005) and Guzzetti et al. (2007). They also summarize 125 different precipitation indices and thresholds. Of the indices identified 48% are based on intensity (or normalized intensity) duration relationships. Thirteen percent are based on event-precipitation duration relationships. The remaining indices are based on numerous relationships between event rainfall, antecedent rainfall over a specific period, daily rainfall, hourly rainfall, and normalized versions of these. Only a few of these indices consider the influence of drainage basin areas on the rainfall indices or the size of the landslide.

Guzzetti et al. (2007) also assessed over 663 rainfall events that resulted in one or more landslides in the CADSES region. They defined intensity-duration thresholds and normalized thresholds for the entire set of intensity-duration data with duration data out to 4,000 hrs (170 days) as shown in Figure C5.

Guzzetti et al. (2007) divides the various precipitation indices into the following 5 general categories;

1. Intensity duration indices that can be expressed in the form:

   $$I = c + \alpha D^{\beta} \qquad \text{Equation C10}$$

   where $c \geq 0$, and α and β are constants for a given location and range between 4 to 176.4 and -0.19 to -2.0 respectively. D varies from 1 to 3360 hours (140 days) but is more commonly limited to 100 hours. The constant, c is most commonly zero. This reduces Equation C10 to power law relationship of Caine (1980).

2. Normalized rainfall intensity duration indices of the form in Equation C7.

   $$I_{MAP} = c + \alpha D^{\beta} \qquad \text{Equation C11}$$

   These thresholds are more applicable for exportation to new regions because they account for regional differences in rainfall intensity. In this formula c is commonly zero, and α and β range between 0.02 to 4.62 and -0.21 to -0.79 respectively. Normally D varies from 1 to 200 hours (8 days).

3. Cumulative rainfall thresholds for a storm event. Expressed as $A(n)$, E, $EMAP$ or R greater than some threshold. Some indices are only applicable when multiple conditions are required for precipitation.

4. Cumulative rainfall event duration indices and normalized versions of same. These most commonly take the form:

   $$E = c + \alpha D^{\beta} \qquad \text{Equation C12}$$

Durations, D are typically in the 25 hour range but one notable exception (Kanji et al. 2003) extends the range of D to 10,000 hours (416 days). In this relationship, c ranges from 0 to 375, α from to 1 to 55, and β from 0.41 to 1.

5. Rainfall event intensity versus event rainfall and normalized versions of same. These generally take the form

$$I = c + \alpha E^{\beta} \qquad \text{Equation C13}$$

Where I and E may or may not be normalized and in some case the natural log or exponent of I and E are used in place of I and E.

Based on the combined review of previous research and their own work Guzzetti et al. (2007) also concluded the following:

1. High intensity short duration rainfall is more likely to trigger landslides in soil with a relatively high permeability. Low intensity long duration precipitation is more likely to trigger landslides in impermeable soils. These two conclusion are consistent with the hydrology and landslide stability models since:
    a. higher permeability soils allow the infiltration of precipitation during high intensity rainfall while lower permeability soils will result in more surface runoff or surface storage of the rainfall, and
    b. in most cases permeable soils will allow low intensity rainfalls to drain without resulting in a continued increase in soil moisture or pore pressure over the duration of the rainfall.
2. Rainfall duration of ~4 to ~21 days are most important for the initiation of larger volume landslides particularly in low permeability clay rich soils.
3. During long periods of low intensity precipitation evapotranspiration can have a significant influence on the volume of water affecting the potentially unstable volume of soil. This is more significant at low and mid latitudes where higher average temperatures result in higher evaporation rates despite the rain inducing cloudy atmosphere blocking direct solar radiation.
4. With increased rainfall duration the minimum intensity likely to trigger slope failure decreases linearly in the log-log intensity duration plot and this

behaviour is consistent for three orders of magnitude from 0.3 hrs (20 minutes) to 300 hrs (12 days).

5. Normalization of the rainfall intensity by RDN was better than normalization by the MAP when comparing data from different regions and rainfall patterns.
6. When they grouped the data by climatic region they found that the threshold line was steeper ($-0.70 < \beta < -0.81$) for mild mid-latitude Mediterranean climates compared to the threshold line for mountainous and colder climates typical of northern Italy ($-0.48 < \beta < -0.64$). This suggests that a lower intensity long duration rainfall is required to induce landslides in mild mid-latitude locations compared to mountainous ones. Alternately, rainfall duration is more critical in a mild mid-latitude location than a mountainous one.
7. Of significance to this study Guzzetti et al. (2007) noted that the thresholds for B.C. (Jakob and Weatherly 2003) were one of two thresholds that predicted lower values of average rainfall intensities which could trigger landslides compared to world wide threshold for rainfalls durations of 0.3 to 5 hours.

Guzzetti et al. (2007) and the associated Istituto di Ricersa per la Protezione Idrogeologica (2007), and RISK AWARE (2005) programs and websites are providing a means of collecting and exchanging the growing experience with precipitation-induced landslide-indices and threshold information.

Walker (2007) studied 195 landslides between 1970 and 2004 near Newport, New South Wales, 27 km north-northwest of Sydney in Australia. He compiled the rainfall data for 7 weather stations and then computed the rolling cumulative rainfall totals for 2, 5, 10, 20, 30, 60 and 90 day periods. He then plots the rainfall data against the Gumbel distribution return period plotting position. Walker notes that there are large steps in the longer period antecedent rainfall return-period graph and suggests that these steps may be introduced by rainfall conditions that represent an event with a longer return period than the period of record.

Walker showed that the 1 to 5 day rainfall computed using the Gumbel distribution were consistent with the Australian rainfall and runoff guide for flood estimation. Based on this correlation he assumes that the longer antecedent rainfall durations also fit the Gumbel distribution. This assumption may not be well founded and is undermined by his comments regarding the large steps in the longer antecedent duration rainfalls. Despite this assumption, he calculates the return period of each of the seven antecedent durations at the time of each landslide. Using the logic that each landslide was induced by the rarest antecedent precipitation condition at the time of failure he assumes that the antecedent duration with the highest return period is the antecedent rainfall condition that triggered the landslide. His results indicate that most of the landslides were influenced by rainfalls with relatively short return periods of 1 to 5 years but that more than half the landslides were most sensitive to cumulative rainfall over the 30 days prior to the landslide event. As discussed in Chapter 4 the application of the Gumbel distribution to non-Gumbel distributed data can cause an underestimation of the return period of the longer antecedent precipitation indices. This could discount the significance of longer antecedent durations and underestimate the return period of the landslide inducing antecedent events.

Zézere et al. (1999), Floris et al. (2004), Ibsen and Casagli (2004), and Pedrozzi (2004) use a similar approach to Walker using the Gumbel distribution. Floris and Bozzano (2007), and Petrucci and Polemio (2003), utilize the generalized extreme value GEV distribution of Jenkinson (1955) and Hosking et al.(1984) to provide a better fit to the longer antecedent duration rainfalls and therefore more reliable estimates of return period and the therefore better resolution of the most significant antecedent duration.

C 1.2 Snowmelt and landslides

Several researchers have studied the relationship between landslides and snowmelt and suggested correlations for snowmelt-induced landslides (SIL). Even the earliest papers on precipitation-induced landslides (Caine 1980) suggest snowmelt of 4 mm per hour likely influenced the stability of a landslide.

Toews (1991) states, "The two important snowmelt processes are rain-on-snow and radiation or warm weather melt". Based on his review of 11 debris flows in South Eastern B.C. he states that the "Guidelines and warning systems for mass wasting occurrences based on rainfall intensity alone are therefore inappropriate." He claims that summertime convective storms contributing to mass wasting are highly localized such that they have and will not be recorded by nearby weather stations. Slides occur either during or immediately after snowmelt. Toews and Gluns (1986) found that snow accumulation was 37% greater on clear-cut sites than on forested sites and that snow ablation rates are increased by 38% in areas where the forest cover is removed. These two factors increase the infiltration and runoff of logged areas from snowmelt compared to areas covered by mature forest.

Chleborad (1997) found that the snowmelt-induced landslides in the Central Rocky Mountains of Wyoming and Colorado occurred coincident with the first yearly occurrence of the 6 day moving average temperature exceeding 58° F. He based his study on 20 landslides.

Grivas et al. (1998) used stream flow data as a surrogate measurement of snowmelt (prior to the onset of spring rains) to predict ground movement. They concluded that snowmelt resulted in infiltration because the period of snow dissipation did not cause a significant change in stream flow levels. However, there was a relationship between cumulative stream flow discharge between February and May and ground movement one month later in the period between February and June.

Matsuura et al. (2003) found that there was no observable relationship between the amount of rain and snowmelt water, MR reaching the ground and the rate of landslide movement over the course of four winters. They found that landslide movement occurred before the snow accumulated and several months after the highest MR. They also used an antecedent snowmelt index, EMR analogous to Equations 2.19 but with MR substituted for precipitation, to assess the influence of antecedent rain and melt water on the landslide. The comparison of EMR to landslide was no more successful but they used a low decay factor of 0.84 appropriate for high runoff or rapidly draining soils despite the geology being influenced by interbedded sands and bentonite clay with a high water retention.

As discussed previously, Vu et al. (2005) include a consideration of snowmelt into clay soil in southeast Alberta, Canada. They showed that infiltration of snowmelt was consistent with other surface water infiltration at reducing the suction head in the unsaturated zone until bearing capacity or sub-grade plastic deformation (Keegan 2007) occurred and resulted in track settlement sufficient to cause a derailment. They used stress deformation analysis to model the reduction in elastic modulus that, under train loading, allowed track settlement and caused a derailment.

C 1.3 Other factors

Wind has not been identified as directly causing landslides but because of its influence on vegetation, it can influence small volumes of earth and fractured rock (Brawner 1994) especially during periods of high soil moisture. Wind can cause trees to sway and the force of the wind is transferred to the root system. The swaying tree trunk and roots act as a lever on soil and rock the tree is rooted in and can cause small landslides and rock falls. The CP Natural Hazard Incident Database (CP NHID) includes a number of events which cite wind loading on trees as the trigger of the soil and/or rock fall.

C 1.4 Limitations

Sidle (2006a) points out that the proposition of using one or more precipitation indices to predict the stability of numerous slopes is unreasonable due to the multi-factored control of infiltration and the slope stability. At best, any precipitation index is going to identify periods of high landslide potential. Furthermore, due to the incomplete record of precipitation-induced landslides, the conditions that induced some can not been identified and therefore landslides triggered by similar conditions will not be predicted.

In many of the studies cited by others the timing of the failure is usually not reliable unless a significant loss was recorded. In the absence of documented information on the timing of landslides in Hong Kong, Frank (1999) identified the highest return period events as the triggering events for natural landslides identified from air-photos. Even when the date of the landslide is known, the time of the event may not be available or accurate. As a result, in most cases the daily temporal resolution of most landslides events is the best that can be expected and therefore daily rainfall data are often sufficient. Aleotti (2004) recognises that rainfall does not directly cause landslides but does cause a reduction in matrix suction and may the increase of pore pressure in the slope, as governed by the processes of infiltration of surface water and migration of groundwater. As such, precipitation is an index of increased landslide activity, not a predictive tool for landslide occurrence.

C 2.0 Use of weather indices for warning of landslide hazards

Weather information systems in Hong Kong (Dai and Lee 2001, Hong Kong Observatory 2005, and others), Rio de Janeiro (Ortigao and Justi, 2004) and San Francisco (Cannon and Ellen 1985 and others).

The following section provides citations and a description of various existing and proposed precipitation-induced landslide-warning systems. The section is ordered geographically from north to south, starting in the Americas and progressing westward around the world to Europe. Systems specific to railways are reserved for discussion in Appendix C, Section 2.3.

C 2.1 British Columbia, Canada

A number of precipitation shutdown guidelines have been developed for the forest industry in B.C. Table C1 from Jakob et al. (2005) summarizes a number of the guidelines.

Initial guidelines were based on water balance whereby the snowmelt and soil drainage and rainfall are considered. More recent indices have been based primarily on rainfall intensity. Due to the orographic influence on rainfall these thresholds are applied over wide ranges of elevation and annual rainfall conditions. Jakob et al. (2006) suggest further improvements to the BC Forest service. These suggestions involve combining barometric data indicative of severe low-pressure cyclonic weather systems approaching the B.C. north coast with 28 day and one-day rainfall indices. With the exception of the Jakob et al. (2006) method, none of the other systems considers the antecedent condition.

Using the discriminant functions developed by Jakob and Weatherly (2003) the Greater Vancouver Regional district is equipped to issue landslide warnings, and notices when the conditional landslide threshold is exceeded. A rational for removal of the warnings is also provided. At the time the 2003 paper was written the thresholds had not been implemented.

Jakob et al. (2006) and others have demonstrated and recommended the potential to use increasingly sophisticated empirical thresholds to influence activity within the logging industry in B.C.

Table C1 Shutdown guidelines developed in the British Columbia forest industry from Jakob et al. (2005)

Author	Type	Location of original study	Shutdown threshold
Chatterton	Water balance	Vancouver, Vancouver Island (applied to N. Coast)	Water balance > 55 mm (dry zone); > 100 mm (wet zone)
Interfor	Rainfall intensity	North Coast, Kalum Forest Districts	24 mm/12 hrs; 100 mm/24hrs; 150 mm/48 hrs; 200 mm/72 hours
AGRA	Rainfall intensity	Prince Rupert Forest Region	2-year return period rainfall
Madrone	Water balance	North Coast, Kalum Forest Districts	Level 1 Shutdown, Level 2 Shutdown: Eastern Zone: Water balance > 60 mm, >75 mm Western Zone: Water balance > 40 mm, >55 mm
Price	Rainfall intensity	North Coast Forest District	100 mm/48 hrs
Interpac Resources Inc.	Rainfall Intensity	Not specified	75 mm/12 hrs; 100 mm/48 hrs; 200 mm/72 hrs.

C 2.2 USA

The United States Geologic Survey (2007) operates an experimental landslide warning program in cooperation with National Oceanic and Atmospheric Administration (NOAA) and other federal, state, and local agencies. The USGS experimental systems currently provide warnings for debris flow for burned areas in southern California, precipitation-induced landslides in the Seattle, Washington area and landslides induced by hurricane rainfall on the U.S. East and Gulf Coasts. These warnings are broadcast via the Common Alerting Protocol (CAP) (Federal Geographic Data Committee, 2005).

C 2.2.1 Seattle, Washington

Baum et al. (2005) and Chleborad et al. (2006) review the development of the precipitation-induced landslide warning system used in the Seattle region of North-western Washington. They note the potential to supplement the trip-wire landslide detection system used by Burlington Northern Santa Fe (BNSF) railway in this and other areas.

Godt et al. (2006) propose a decision tree for the issuance of precipitation-induced landslide warnings that includes an antecedent soil moisture index, AWI and previously identified criteria for intensity and duration. It is proposed that the AWI provides a means of predicting the development of elevated soil moisture conditions over the course of the wet season.

C 2.2.2 San Francisco, California

Using criteria from Cannon and Ellen (1985) and others, Wilson et al. (1993) document the operation of a real-time warning system for debris flows in the SFB area. The system issues warning based on three indices and related thresholds, and uses quantitative precipitation forecasts produced by the NWS. As of 1993 the system was in operation for at least 7 years and issued at least four warnings. They also discuss the adaptation of the warning system for special conditions such as the prediction of debris flows following a firestorm in 1991 in the Oakland area. Keefer et al. (1987) document the effect of the issuance of landslide warnings in the SFB area prior to and during the storm of Feb 12 to 21, 1986. The weather conditions resulted in more than 100 landslides.

C 2.2.3 Rio de Janeiro, Brazil

Ortigao and Justi (2004) and Ortigao et al. (2001) document the Rio-Watch system, which provides early warning of landslides. The system uses both weather radar and conventional rain gauge information. When the Rio-Watch's meteorologists identify a forecast rainfall condition that will exceed the thresholds set out in Figure C2 they contact GeoRio who in turn consult the Civil Defense Division of the Rio Government to assess whether an alarm is warranted. Alarms are then sent by fax to the media for dissemination to the public. The warnings include notification about the current situation, and the identification of areas and roads that should be avoided. Emergency response agencies are also placed on alert.

C 2.2.4 Hong Kong

Cheung (2006), Chan and Pun (2004) and others describe the landslide warning system developed by the Geotechnical Engineering Office (GEO) of the Civil Engineering and Development Department and the Hong Kong Observatory (2007). Due to the monsoon climate 80% of the annual rainfall occurs between May and September. This causes precipitation-induced landslides every year. The system monitors 110 rain gauges over an area of 1100 km^2 or more than one per 10 km^2 and issues radio and television warnings to the public when specified rainfall thresholds are exceeded. Numerous GEO researchers and others (Findley et al. 1997) have investigated the correlation between climate, rainfall, the landslide hazards, and events within Hong Kong.

C 2.2.5 Others

Aleotti (2004) proposes that the development of a real-time landslide warning system in the northwest region of Italy be undertaken. He identifies a number of rainfall normalization schemes to allow the wider spatial application of the criteria and an operating procedure for the application of the system. He also discusses landslide-warning systems in New Zealand and South Africa in addition to the ones discussed above.

Towhata et al. (2005) proposes the development of a micro precipitation-induced landslide-monitoring system for deployment in rural areas including their study area of central and East coast Japan. They provide some examples of how to develop warning criteria based on soil moisture and landslide data. The scale of the approach is novel but not well suited to a large system like a rail network.

New technologies are also being proposed for predicting precipitation induced landslides. Hong et al. (2007a), Hong et al (2007b) and Hong and Alder (2007) have proposed conceptual real-time global landslide prediction system (Figure C6) for rainfall triggered landslides and runoff using satellite remote sensing data. They propose the superposition of landslide susceptibility maps and precipitation information from multiple satellites including the US National Aeronautics and Space Administration (NASA) Tropical Rainfall Measuring Mission (TRMM).

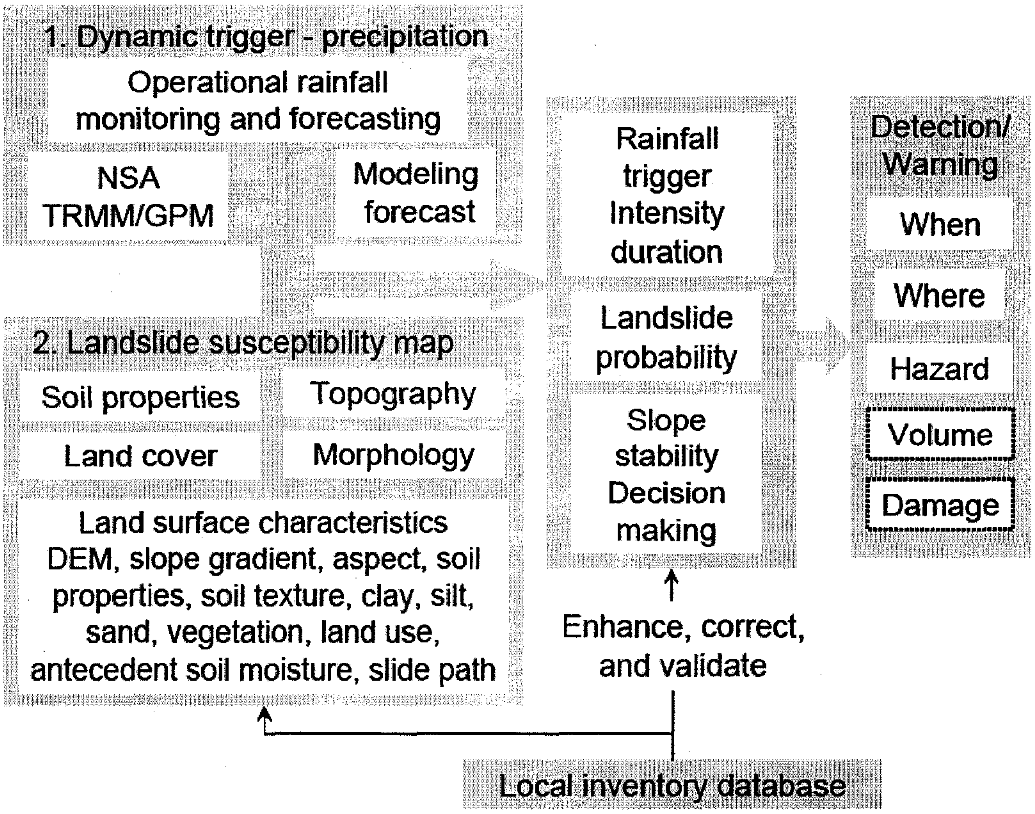

Figure C6 Conceptual real-time warning systems for precipitation induced landslides after Hong et al. (2007a)

However, several components of this type of system are not readily available without significant investment of time and resources. Hong et al. (2007a) propose to use worldwide rainfall landslide relationships. To develop reliable landslide susceptibility maps for the Earth or a railway network of thousands of kilometres would require a concerted effort by dozens of researchers working several years. This is not to suggest that the development of landslide susceptibility maps is not a worthwhile and needed undertaking. However, a real time landslide monitoring system need not be dependent upon nor wait for the completion of this component.

In the interim, provided sufficient empirical data is available, a warning system can be developed utilizing known landslide occurrences and their temporal relationship to precipitation conditions. However, this system still needs to have a set of precipitation induced landslide (PIL) indices and thresholds with the minimum of false-positive warnings. The threshold for each index needs to be set to minimize the number of false-positive warnings and maximize the number of landslides predicted (true-positives). The research completed as part of this thesis will develop a methodology for: identifying precipitation induced landslide indices and setting warning thresholds.

C 2.3 Use of weather information for natural hazard prediction in the railway industry

As discussed in Section (1.2.1) weather information has been used to assess the likelihood of geotechnical hazards but few have made the effort to document their findings and develop useful indices for use by others. There is a story within CP that the railway building and staff accommodation in Revelstoke, B.C. are built with corrugated steel roofs at a particular slope such that when the snow slides off the roof it is an indication that the avalanche hazard in Rogers Pass is high. However, even something as practical as this, unless proven and documented, cannot be used as a codified index.

Based on available documentation in English, the use of weather information for natural hazard prediction within the railway industry is relatively limited. There are two primary reasons for this. Firstly, most railways do not publish information regarding their risk management practices because of the need to maintain a competitive advantage amongst their rivals. Secondly, railways seldom discuss vulnerabilities of their rail system because of concerns regarding shareholder valuation of their stock. The information on the European rail network is limited by the publication of this type of information in the language of the country. Despite these limitations, the available information has been reviewed and presented below.

C 2.3.1 Wollongong, Australia

Ko Ko et al. (2003) and Flentje et al. (2005) and Walker et al. (2000) discuss the progress towards the development of a real-time landslide risk tool used in Wollongong south of Sydney Australia. A rail line passes through the area covered by the landslide warning system and the rail operators have access to the warnings issued by the system.

Leventhal et al. (2000) discuss the influence of the rainfall on the Coal Cliff landside and its affect on the South Coast Railway of Australia. They identify correlations between antecedent rainfall and deep-seated landslides that affect the South Coast Railway. They identify that the 650,000 m^3 Coal Cliff landslide is most sensitive to the 3 month antecedent rainfall and that accumulations above 600 mm (or antecedent intensities of 6.7 mm/day) accelerate ground movement.

C 2.3.2 Japan

The earliest documented application of rainfall indices for the prediction of rainfall-induced landslides in the railway industry are those of the Japanese National Railway system dating back to the 1980's. It appears that the Japanese National Railway has been a leader in this technique. However, documentation of this early system in English is limited. Katayose (1987) describes how in response to "abnormal weather" such as heavy rainfall, train speeds are reduced or train operations are suspended. He further explains that watches and imposed controls are undertaken based on predetermined standards, although he does not elaborate on the derivation or nature of the standards.

Several Japanese researchers have published their findings relating rainfall and geotechnical hazards along railways. Muraishi et al. (1992) review the Japanese Railways (JR) Group evaluation of slope hazards and operational control during rainfall. They introduce an empirical precipitation threshold which, when exceeded, either invokes train speed restrictions or suspends rail operations. The standard technique is a combination of hourly precipitation and continuous precipitation as per Figures 10 and 11 of Okada et al. (1994). Unfortunately, no background on how the standard is selected is provided. The authors discuss the issue of frequent issuance of rainfall warnings that invoke operational controls when no hazard occurs (false-positive in Table A1). They also discuss rainfall induced geotechnical hazards occurring prior to the issuance of a warning (true-negative). To increase the reliability of the precipitation warning system they propose using the product of the hourly precipitation and the continuous precipitation both raised to an optimum exponent to derive a "critical precipitation". They conclude that "critical precipitation" values produce a hyperbolic curve of equal landslide hazard above which the hazard would be high and below which the hazard would be low (see Figure C7).

Consistent with Muraishi et al. (1992), Okada et al. (1994) provides the mathematical definition of the critical rainfall as discussed in Appendix C, Section 1.1. Okada et al. (1994) comments that the existing Japanese railway system is based on the combination of the cumulative rainfall after 12 hours with no rain, and the hourly rainfall intensity. Muraishi and Okada (1988) identify that the continuous precipitation being used is inconsistent with the hydrologic hyetograph (Chow, Maidment and Mayes 1988) definition of a storm where the cumulative rainfall is limited to a single continuous period of rainfall.

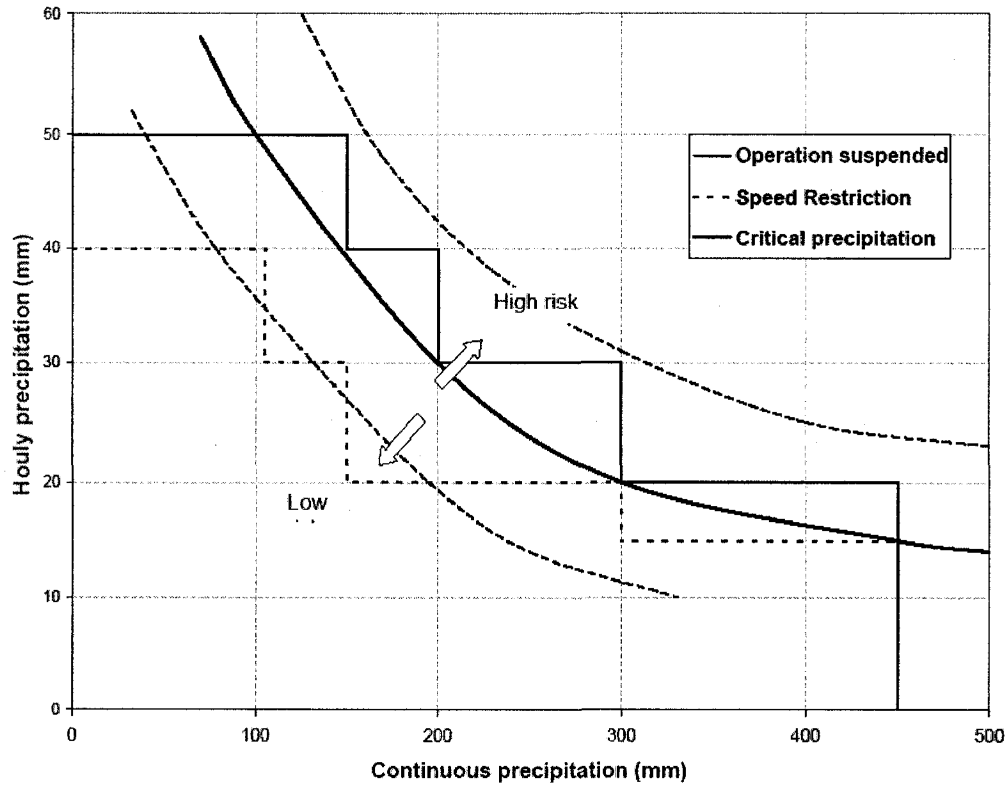

Figure C7 Conceptual critical precipitation curve proposed by Muraishi et al. (1992) overlain on representation of the system in use in 1992

Okada et al. (1994) mentions the Japanese National Railway (that has now been disbanded) practice of 'marking tables' (as shown in Figure C8) being used for the 'macro-estimation method'. Rimm-Kaufman (1996) reviews the influence of the Japanese Railway rainfall warning system on the operational of rail traffic, but not being a geotechnical engineer, provides no further insight into the derivation of the indices. His work does identify that the Japanese system is based on specific rainfall criteria for each group of weather stations. Rimm-Kaufman goes on to propose the use of a decay type antecedent precipitation index where the decay is dependent on the exponent of the inverse of the time since the rainfall. He computes this index for average rainfall indices for 1 to 90 hours (0.4 to 3.75 days).

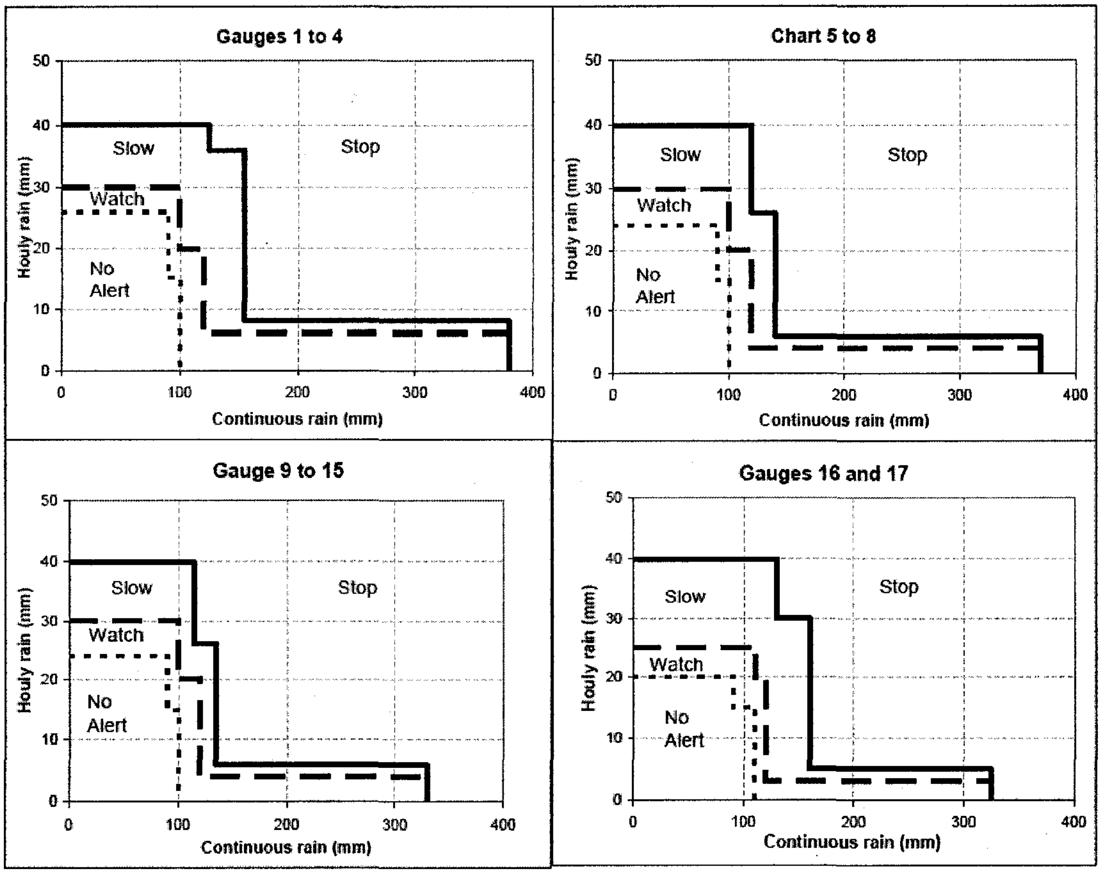

Figure C8 Rainfall gauge thresholds for the Suigun Line of the Japanese Railway East (from Rimm-Kaufman 1996). Each group of rainfall gauges has its own unique set of No Alert, Watch Slow and Stop continuous versus hourly precipitation thresholds.

A shortcoming of basing an index on the relationship of I and E is that it does not account for the antecedent condition greater than 12 hours before the start of a period of continuous rain. Based on the available literature (Noguchi et al. 1997, Noguchi and Fujii 2000) it appears that the Japanese Railway system has migrated from a stepwise function of the marking tables to a continuous function consistent with Okada et al. (1994). Noguchi and Fujii (2000) provide an overview of Japanese measures to minimize the effects of natural disasters including safe guarding trains from heavy rains and the associated precipitation induced landslides. Shimamura and Suzuki (1995) discuss the high false-positive rate of the then current Japanese Railway rainfall index and threshold system. They propose a antecedent precipitation index based on the integration of the rainfall intensity multiplied by a decay function related to the time of the rainfall before the time or interest. Watanabe et al. (2006) indicates that Japanese railways continue to utilize plots of hourly versus continuous rainfall with "critical (threshold) rainfall". Events that result in a combination of high hourly and high continuous rainfall that exceed the critical rainfall are identified as being likely to induce landslides.

C 2.3.3 Britain

Thornes and Davis (2002) write about the influence of the weather on railway operations in the U.K. They describe how the cold influences the mechanical performance of the cars; how track becomes brittle at cold temperatures and can buckle or kink at high temperatures; how snow blowers at switches are required to keep the switch points free to move when required; how high winds can affect overhead power-supply catenary systems for electric railways; and how flooding can undermine bridges. They suggest indices for each weather variable such that maintenance can be undertaken or train operation measures implemented when a predetermined threshold is exceeded. They describe the U.K. Meteorology office provision of a service called OpenRail that provides notification of weather events to the railway. However, they note that it was 30 years out of date in 2002 when compared to the system provided for the U.K. highway network. They state that heavy rain can cause landslides and that thresholds should depend on antecedent precipitation conditions that influence groundwater conditions. With the exception of a threshold for the level of water over the rail, they do not provide any indication of what, if any, rainfall indices are used nor do they provide any guidance in setting the thresholds for this hazard.

C 2.3.4 North America

This section provides an overview of information published, or known to the author, about weather information systems at other railways in North America.

The North America rail industry has and continues to integrate an increasing number of real-time systems for monitoring the mechanical condition of the trains. This has reduced the resistance to, and simplified the integration of other real-time information into the railway dispatch and control systems. For example, existing monitoring includes hot box detectors that sense the temperature of each axles of each car as it passes a sensor. If there is excessive friction on the axle the axle temperature will be elevated. An axle that is determined to be hotter than a threshold is identified. Hot axels are indicative of a ceased or resistant bearing that could cause the axle to break and derail the train. Similarly, wheel-impact load-detectors (WILD) sites sense the impact each wheel make on the track to assess if the wheel has a flat or tangent on its circumference. Wheels causing high impact loads can crack or break a rail resulting in derailment of the cars following the one causing the high impacts. The information from these sensors is issued to both the train crew and dispatch and control centre who then take steps to remove the car, with non-compliant components, from the train so that the rest of the train can maintain its schedule. The removed car is then designated out-of-service and repaired. Neither of these systems are weather related but they have set a precedent within the railway industry that is making it easier to integrate other warning systems into the railway operation and control systems.

Within the railway industry, weather hazard-notification has been successfully implemented for high and low temperatures that cause an increased frequency of broken rails and rail kinks (Bertrand and Falls 2006). Typically, a weather-information service-provider notifies railways when the temperature is predicted to be below the low temperature threshold or above the high temperature threshold specified in railway operating rules. At CP, this document is called the General Bulletin Order (GBO) (CPR Operations 2005). When these thresholds are exceeded trains are operated at reduced speeds. The threshold temperatures vary depending on the temperature at which the rail is laid (the layering temperature). However, but due to the relatively uniform properties of steel used in rails the high and low temperature threshold at which slow orders are imposed is uniform over large regions. Research by Bertrand and Falls (2006) indicates that additional indices should be considered to account for the influence of solar radiation on the temperature of rails. In many case false-positive and false-negative slow orders are being imposed due to overly cautious or non-conservative assumptions about the relationship between ambient air temperature and rail temperature. Despite this unresolved difficulty, the interaction of weather and geotechnical hazards is significantly more complex than the influences of the weather on the steel with both uniform and predictable properties.

Consistent with the approach for monitoring real-time mechanical train conditions all the major class 1 railways in North America subscribe to one or more weather information services. Leeper and Smith (1998) document the process and benefits within the BNSF. Union Pacific uses a similar system and have also been a leader in the development and application of wind warnings to avoid wind related derailments of cars carrying empty double-stack inter-modal containers (National Center for Atmospheric Research 2004). Ryerson (1998) suggested that railways were well positioned to take advantage of advances in weather information technology and communications and participate in existing weather hazard systems developed for the air and road transportation systems in the US. Changnon (2006) reviews the growing trend in the use of weather sensors and communication of the data collected. None of these authors discuss how to establish weather indices or thresholds.

The existence of weather information services and the parallel development of real-time train control systems, based on the combination of multiple sources of information, have provided an opportunity to integrate precipitation-induced landslide indices, thresholds, and response protocols into the management of derailment risk within a railway.

The next section reviews the currently available warnings for precipitation conditions provided by the weather information suppliers and demonstrates why they are of limited applicability to geotechnical hazards.

C 2.3.5 CP practices

The historical processes for monitoring and responding to weather were discussed in Appendix A, Section 3.0 and in Bunce et al. (2003). This section describes the Weather Information System (WIS) that CP subscribes to known as RailWIS. The system has numerous components all directed at providing weather information to numerous users within CP, all with different goals and responsibilities. As a result, RailWIS has to meet a number of demands. It has three basic components: a data ingestion module; an email notification generator; and a website that allows CP employees to access all the data on demand. The website is maintained in a secure environment and password protected for use by CP employees only.

As described in Appendix C, Section 2.3.5.2, RailWIS provides warnings and notifications for a number of different weather conditions that influence the railway operation. These include the health and safety of personnel working outside and weather conditions that influence the ability of personnel to travel by road to railway facilities. The only indices that relate to geotechnical hazards being considered in this research are those regarding rainfall. As indicated, the existing precipitation thresholds are based on the predicted return period of rare rainfall events, without regard for landslide activity or consideration of antecedent conditions.

It is expected that once the finding of this research are fully implemented, an expanded set of precipitation-induced landslide indices and thresholds for each relevant weather station would be established. When these thresholds are exceeded email or pager notifications would be sent to the appropriate TMS and RTC and posted to the website. The TMS would then follow railway protocol to protect rail traffic and personnel.

C 2.3.5.1 Available weather warnings

The national weather agencies of both Canada (Environment Canada (EC)) and the USA (National Weather Service (NWS) branch of the NOAA) collect and provide access to climatic data in North America. These agencies are the two primary sources of information posted on the weather information systems. These agencies also provide interpretations and forecasts of the data by climatologists. Based on the assessment of these experts various watches and warning criteria have been established for a number of weather hazards. There are three limitations with these criteria and warnings within the context of geotechnical hazards and railway operations.

1. **Not relevant** – Firstly, the two national weather agencies issue general warnings for weather conditions that do not pose a hazard for the railway. For example: 1) Numerous high wind and rough sea warnings might be issued for a single coastal storm that would have little or no influence on CPR's operation. 2) The railway is not vulnerable to hail damage. 3) The EC and NWS issue severe thunderstorm watches and warnings to notify the

public when lightning may occur. In general, only railway signals and communication (S&C) infrastructure is vulnerable to lightning. Other than grounding the S&C equipment little can be done to prevent lightning damage. A railway is aware of a damaging lightning strike as soon as it occurs because the affected signals stop working. To protect against this rare but inevitable event, train-operating rules are in place to assure safe train operation when a signal is not functioning. As a result, a high percentage of the warnings sent by the national weather services are not a hazard to railways and there would be no significant benefit to a railway if it slowed or stopped trains in the vicinity of each watch or warning issued.

2. **Area of warning** – Secondly, in Canada, and to a lesser extent in the US, the area of a warning area is large (several thousand sq km). Maps of Environment Canada (2007) warning regions are available at http://www.weatheroffice.gc.ca/warnings/warnings_e.html. Commonly only a small portion of each warning area is occupied by a railway. The weather warning does not always pertain to the entire warning area. As a result, only a small portion or none of the railway is exposed to the weather conditions that warrant a warning.

3. **Large number** – Thirdly, in both the US and Canada the weather services issue a "watch" notifying the public that the probability of a given weather event is elevated. Once the event is expected to occur imminently or has been reported occurring NWS and EC issue a "Warning" or "Alert" respectively. These watches, warnings and alerts may occur in rapid succession or be spread over a few hours or days (Environment Canada 2006b).

It is common for EC to issue warnings that are only relevant to the railway under certain conditions. For instance, a warning for the Greater Vancouver area predicting "... winds of 50 to 70 km/h with gusts up to 90 km/h..." was issued by Environment Canada (Nov 3, 2005). The influence of this type of wind is usually limited to dropping tree branches across the track which is not a significant hazard to trains. However, in some instances combined weather information can provide a useful warning that would benefit the railways. With the exception of high winds perpendicular to bridges or track across large flat areas, wind by itself is not a significant hazard to trains, except when a train includes with cars with empty inter-modal containers stacked two high. However, if high winds are concurrent with saturated ground conditions, the potential for large trees to blow over is increased. High winds combined with saturated ground conditions are documented to have caused trees to sway imposing lateral forces on the tree roots which then trigger rock falls (Brawner 1994). It should be possible to derive a combined wind and rainfall index that tree fall and or rock fall is more likely when high winds and saturated ground conditions are both present or expected. This type of warning is typically responded to by undertaking an inspection of the track to assess the influence of the wind related hazards on track safety.

Due to the large number of notifications and the high proportion that are irrelevant, engineering personnel pay limited attention to the warnings and the warnings lose their effectiveness. Despite efforts by the service providers to devise automated filters and thresholds to intercept the irrelevant information, the TMS still receives numerous false-positive warnings on a near daily basis. Filtering to reduce the number of warnings is also reviewed in Appendix C, Section 2.3.5.2

C 2.3.5.2 CP existing weather indices and thresholds

The indices and thresholds currently in use by CP are included in Tables C2, C3 and C4. There are a number of weather indices used by CP Operations Department related primarily to the ability of employees working outdoors in exposed environments. These indices and thresholds were not developed with the intention of predicting or warning of landslide activity.

The indices most relevant to geotechnical hazards are those regarding rainfall and are plotted on the ID type graph in Figure C9. As can be seen CP rainfall threshold for the issuance of a warning are above the Guzzetti et al. (2007) threshold but only provide a single point along the continuum of possible antecedent indices. The development of a methodology for the identification of additional weather station specific precipitation-induced landslide thresholds is one of the two goals of this research.

Table C2 CP weather warning indices and location matrix for western Service Areas

Weather condition	Modifier	Service Area					Hazard
		Vancouver			B.C. Interior		
		Vancouver to Yale	Yale to Chase	Lytton to Chase	Chase to Lake Louise and Trail to Elko	Alberta plus Elko to Sparwood	
Rainfall (including thunder storms	**Heavy Rain**	50 mm (2") in 24 hrs	25 mm (1") in 24 hrs			30 mm (1.2") in one hr or less of 75 mm (3")	Heavy rainfall
	10 yr for 1 day[1]	90 mm (3.5")	47 mm (1.9")	32 mm (1.3")	52 mm (2")	64 mm (2.5")	Ground saturation and flash flooding
	50 yr for 1 day[1]	112 mm (4.4")	62 mm (2.4")	44 mm (1.7")	67 mm (2.6")	86 mm (3.4")	
	100 yr for 1 day[1]	122 mm (4.8")	68 mm (2.7")	49 mm (1.9")	73 mm (2.9")	96 mm (3.8")	
Snowfall	**Minimal wind**	15 cm (6") in 12 hrs	10 cm (4") in 24 hrs	15 cm (6") in 24 hrs	20 cm (8") in 24 hrs	10 cm (4") or more in 12 hrs of less 15 cm (6") or more in 24 hrs or less	Snow accumulation
Freezing precipitation	**Freezing rain or hail**	All events of hail of 20 mm or larger	2 hrs or more of freezing rain or ice accretion of 1 mm (0.04"			All occurrences of hail of 20 mm (0.75") or larger	Hazardous working, damage to overhead wires

[1] - 10 , 50 or 100 yr for 1 day is the 1 in 10, 50 or 100 year return period rainfall in 1 day

Table C3 CP weather warning indices and location matrix for eastern Service Areas

Weather condition	Modifier	Service Area								Hazard
		Saskat-chewan	Man-itoba	Northern Ontario	Southern Ontario & Montreal	New York	Penn-sylvania	St Paul	Chicago	
Rainfall (including thunder storms	**Heavy Rain**	50 mm (2″) in one hr or less 75 mm (3″) in 3 hrs or less 50 mm (2″) or more in 12 hrs			50 mm (2″) in 12 hrs					Heavy rainfall
	10 yr for 1 day[1]	61 mm (2.4″)	74 mm (2.9″)		73 mm (2.9″)	91 mm (3.6″)	108 mm (4.3″)	80 mm (3.1″)	102 mm (4″)	Ground saturation and flash flooding
	50 yr for 1 day[1]	81 mm (3.2″)	964 mm (3.8″)		95 mm (3.7″)	118 mm (4.6″)	142 mm (5.6″)	108 mm (4.3″)	133 mm (5.2″)	
	100 yr for 1 day[1]	89 mm (3.5″)	106 mm (4.2″)		104 mm (4.1″)	132 mm (5.2″)	159 mm (6.3″)	121 mm (4.8″)	149 mm (5.9″)	
Snowfall	**Minimal wind**	10 cm (4″) or more in 12 hours or less, or 15 cm (6″) or more in 24 hrs or less			15 cm (6″) in 12 hrs					Snow accumulation
Freezing precipitation	**Freezing rain or hail**	All occurrences of hail of 20 mm (0.75″) or larger								Hazardous working, damage to overhead wires

[1] - 10 , 50 or 100 yr for 1 day is the 1 in 10, 50 or 100 year return period rainfall in 1 day

Table C4 CP weather warning indices used across the rail system

Weather condition	Modifier	All CP Service areas	Hazard
Wind	High	90 km/h (55 mph) consistent with UP, also see blizzard	Double stack blow over
Temperature	High	More than 32° C (90° F)	Sun kinks
	Low	Less than –25° C (–13° F)	Mechanical operating limits
Snowfall	First snowfall of season	All occurrences	Unprepared for snow
	Blizzard	Visibility less than 1 km (0.6 miles) in snow or blowing snow and wind chill greater than 1600 watts/sq. m OR Wind greater than 40 km/h (25 mph) and conditions expected to last more than 4 hrs	Low visibility and working conditions
	Drifting snow	Drifts greater than 30 cm (1 foot)	Localized snow accumulation
Tornado	Wind	Watch warning	Damage due to extreme winds
Severe thunderstorm	Rainfall	10 mm (3/8″) hail, > 25 mm (1″) rainfall More than 500 lighting strikes per hour	Working conditions
Cold wave warning	Cold	Large change in temperature in 24 hours to a least –20° C (-4° F)	Stranded workers and working conditions,
Wind-chill	Cold	Wind chill index of -35° C	Working conditions
Flooding	Damage to sub-grade and structures	Report all flood warnings in the US and Canada	Erosion of embankment and track and flooding of yards

Abbreviations: C - Celsius, cm - centimeters, F - Fahrenheit, hrs - hours, ″ - inches, km/h - kilometres per hour, m - metres, mm - millimeters, mph - miles per hour, sq. - square, UP - Union Pacific Railway, yr. - year.

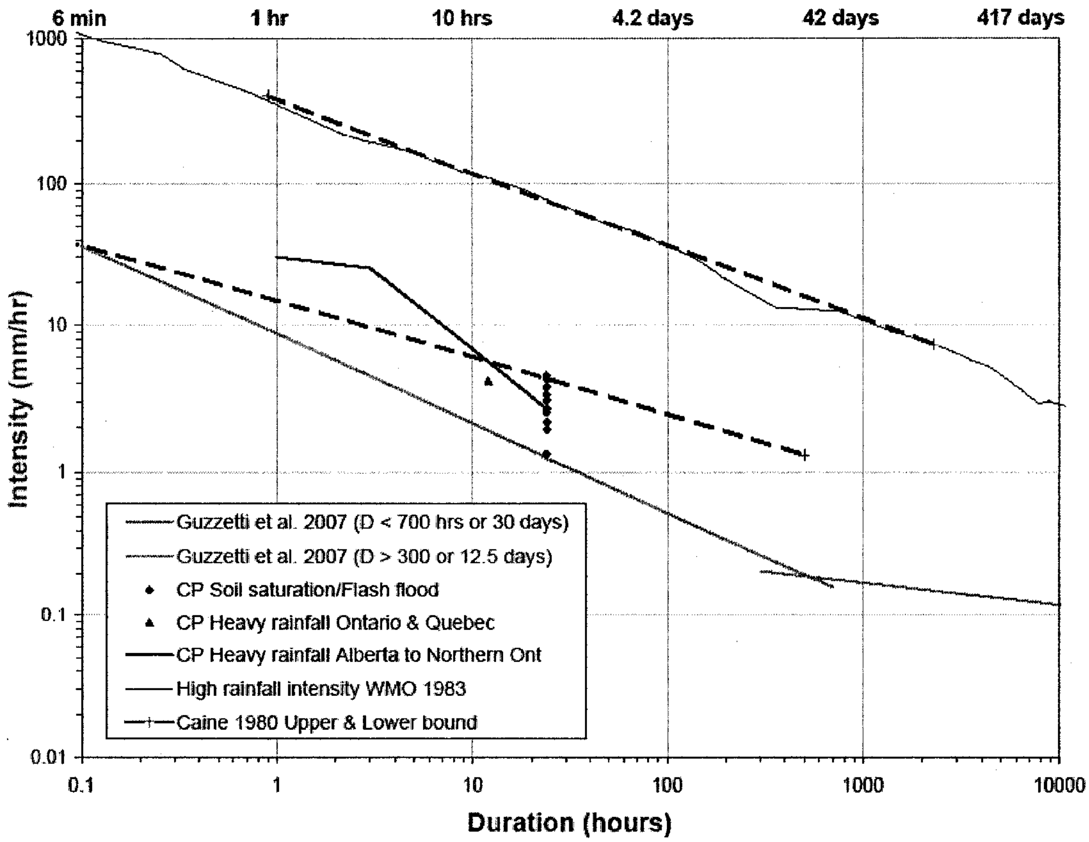

Figure C9 Intensity duration plot of CP's current precipitation thresholds compared to Guzzetti et al. (2007). The upper and lower limit from Caine (1980) for rainfall-induced landslides is also shown. The upper limit is consistent with the World Metrological Organization (1983) compilation of high rainfall intensities events. Therefore rainfall above the upper limit are very unlikely.

To assess the CP RailWIS system's ability to filter out messages not relevant to CP, an audit of its performance in 2007 May was completed. The audit determined that 869 EC and NWS messages that met the geographic and warning type filters were received by the RailWIS service provider. Of these, 45 (5.2%) were Tornado or Flash Flood warnings and as per FRA 97-1 (Federal Railway Authority 1997) were sent directly to the CP. Another 16 (1.8% of the total) messages were automatically sent to CP because the WIS provider was unable or unavailable to filter them within the 15 minute time limit specified in FRA 97-1. If they cannot be screened for any reason they are automatically forwarded to CP in case they are Tornado of Flash flood warnings. Of the remaining 824 only 385 (44% of the total) were relevant or not repeats and therefore were sent to CP. Figure C10 shows the distribution by type of warning. The audit was completed for the month of May. There were no snow, cold or hot temperature warnings reported.

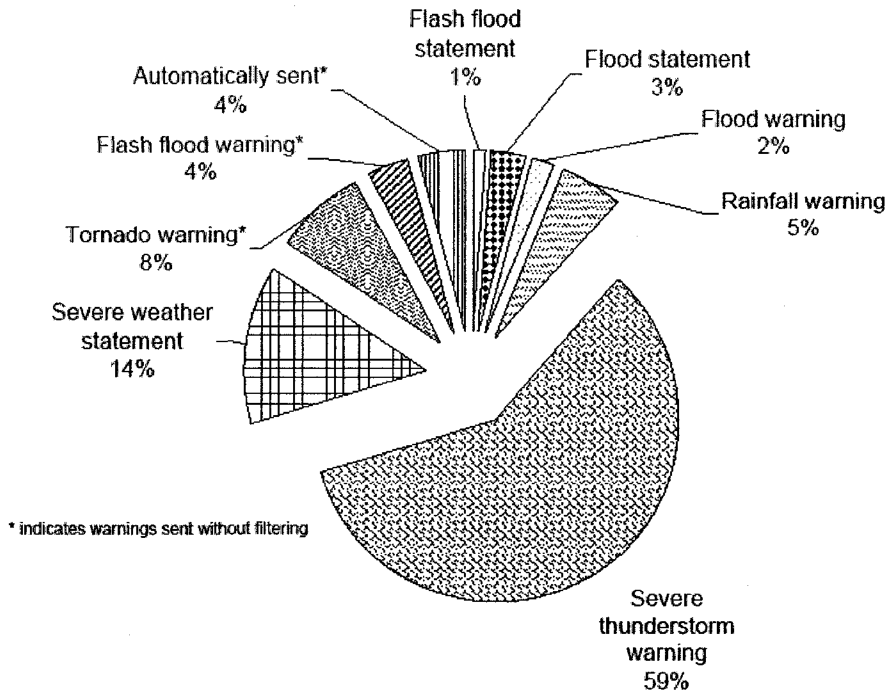

Figure C10 RailWIS message types determined from audit of 2007 May

In May severe thunderstorms were by far the biggest single group of messages accounting for almost 3 of every 5 messages. However, the influence of severe thunderstorms on landslide activity is limited and likely to be dependent on antecedent conditions. As a result the forecast of a severe thunderstorm should not be used alone to warrant a response by operations or engineering to modify their awareness of landslide hazards.

C 2.4 Deficiencies with previous and current practices

With the exception of Seattle and San Francisco in the U.S.A., neither of the national weather services have the ability to issue weather indices that purport to warn of geotechnical hazards or hazards within the rail industry. Due to the specialized nature of the railways, the sensitivity of their infrastructure and the risk tolerance exercised by each railway to satisfy both their shareholders and regulatory bodies, it is not reasonable to expect the national weather services to develop warnings suitable for the railways. Fundamentally, weather service warnings are not intended to provide warnings for geotechnical hazards within the railway-operating environment.

In the earlier part of this Appendix it was demonstrated that throughout the world precipitation can be used as an indicator of landslide activity and landslide hazard. As a result, railways have an opportunity to utilize the available precipitation information to reduce safety risks, reduce delays due to inappropriate warnings and maximize rail traffic. The reason railways are not able to utilize this information in a quantitative means is because of two missing components:

1. There is no means to identify which precipitation index is most applicable to a given area and geotechnical hazard and
2. There is minimal guidance on how to set the threshold of the index once the index is established.

Chapter 3 will describe how and why the process adopted for this research has been developed.

Appendix D Risk management

To use risk management and understand it meaning a point or reference on the risk continuum is needed. Hambly and Hambly (1994), Terbrugge et al. 2006 discuss and provide a summary of tolerated, intolerable, voluntary, and involuntary risks. When the potential for a fatality is being considered, risk is commonly expressed as the probability of death of an individual (PDI). Figure D1 illustrates the PDI of common and unusual activities and occupations. This suggests the tolerable limit at work is 10^{-3} fatalities/year or one per thousand employees per year, however 10^{-4} is more consistent with CP goals.

The following subsections focus on the literature specifically on risk analysis techniques for landslides and risk analysis within the railway industry

D 1.1 Risk analysis of geotechnical hazards

Several methodologies have been developed within the geotechnical and non-geotechnical literature for assessing risk. However, Canadian Standards Association (1997) provides a consistent structure utilized by several authors writing on geotechnical risk (Keegan 2007, Potter et al. 2007, Wise et al. 2004, and others), and is adopted for this research.

Numerous authors have included risk consideration in their research. Einstein (1988), the Canadian Standards Association (1991) publication, and others provide direction on the risk estimation step. They recommend the dissection of the risk such that the variables influencing each conditional probability can be quantified and integrated into the final formulation.

Fell (1994) provides a means of completing a quantitative risk evaluation using the formulation that risk is the product of the probability of the hazard and the probability of a specific loss. He also identified that the risk of failure can be dependent on the probability of the landslides being caused by several different causes including landslides induced by precipitation conditions. Walker et al. (2000) expands and generalizes the scope of his 1994 paper. Gerath et al. (2006) identifies the potential use of quantitative and qualitative risk analysis of landslide hazards in its guidelines for legislated landslide assessment for new residential developments. Tse et al. (1999)

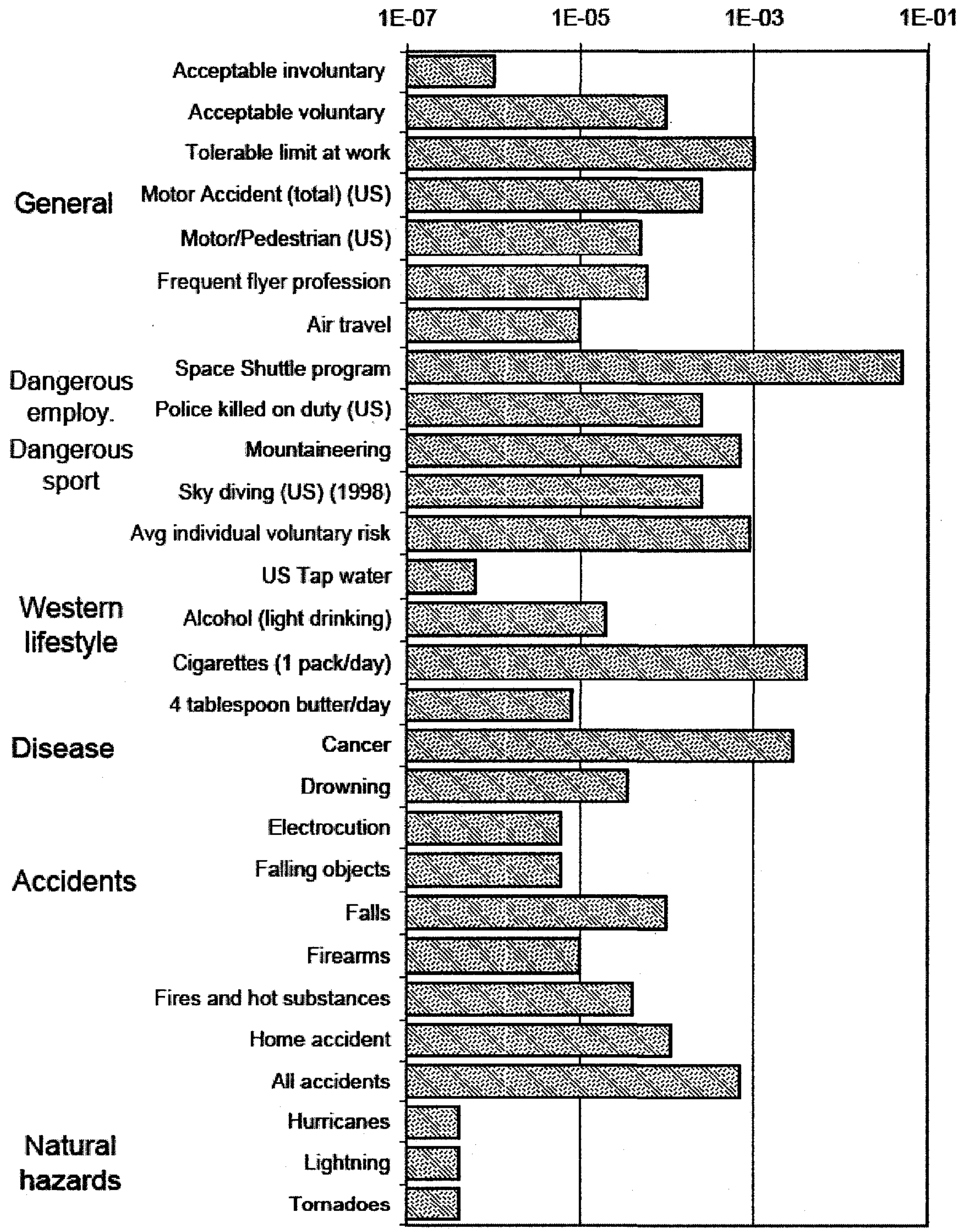

Figure D1 Comparative probability-of-death statistics (after Terbrugge et al 2006)

quantify the probability of the capacity of a debris flow defense being exceeded. Morgenstern (2000) reviews the appropriate application of risk management and identifies the benefits and pitfalls of its application. Wise et al. (2004) provide a summary of types of qualitative and quantitative risk estimation techniques used for landslide risk analysis. Roberds (2005) focuses on estimating the temporal and spatial variation in hazards and vulnerability. Fannin et al. (2005) provide an overview of qualitative risk management practices of the Forest industry within British Columbia. Flentje and Chowdhury (2001) discuss the aspects of risk management for rainfall induced landslides using a preliminary qualitative matrix based hazard consequence model. They suggest that continued research will enable the development of near real time systems capable of providing early warning of landslides. Aleotti and Chowdhury (1999), and Flentje and Chowdhury (2002) progress the 2001 work into quantitative risk assessment. Bell and Glade (2004) complete a quantitative risk analysis for debris flow and rock fall hazards in Iceland in response to Icelandic regulation requirement for the same.

Lloyd et al. (2001) document the application of a risk based approach for the prevention of landslides on a highway in Malaysia. They indicate that the risk-based approach resulted in a 50% reduction in the amount spent on remedial works. Consistent with CP experience they also indicate that the expenditure for repairing a slope after it has failed costs up to five times that of pre-failure slope stabilization work. Potter et al. (2007) demonstrate the use of quantitative risk estimation in the consideration of landslides within a residential development.

Bunce et al. (1997), McClung (1999), and Roberds (2005) demonstrate the application of the binomial theorem for quantitative risk calculation of frequent hazards impacting moving elements. Bunce et al. (1997) and Walker et al. (2000) provide a method for calculating the probability of a rock falling onto a moving vehicle. Roberds (2005) includes a detailed quantitative risk analysis for a vehicle traveling a highway. There are several similarities between a vehicle traveling on a highway and a train traveling on a track that will be explored in Chapter 5. Lee and Jones (2004) provide a comprehensive overview of Landslide Risk Assessment theory and processes. Their text includes a number of applications of quantitative risk assessment for specific examples.

D 1.2 The use of risk assessment of geotechnical hazards within the railway industry

Several authors have presented ways of assessing the risk associated with geotechnical hazards within the Railway industry. Keegan (2007) focuses on the dissection of the hazard scenarios resulting in a loss to the railway industry as a result of geotechnical hazards. Ko Ko et al. (2003 and 2005) consider the risk to railway operations as a result of a precipitation induced landslide in Australia.

MacKay (1997) describes the rock slope hazard assessment utilized by CP and suggests a quantitative risk assessment process be developed.

Abbott et al. (1998a and 1998b) provide a methodology and example of its application to the assessment of rock fall hazards along linear facilities in their two complementary papers. They use the term "Avoidance Factor" (AF) to represent the influence of train speed and hazard detection systems. They propose that:

$$AF = TSF * SDF \qquad \text{Equation D1}$$

Where TSF = Train Speed Factor and is between 0 and 1. They state that because TSF is proportional to the kinetic energy of the train it is proportional to the square of the train speed. Given that TSF is proportional to the kinetic energy, it must also be proportional to the mass of the train. The mass of a train varies widely, especially passenger compared to freight, and empty compared to full freight trains. As a result, the mass of the train should also be considered. However, Abbott et al. (1998a) consider the mass of the train to be constant in their example because the information is not readily available except in a real-time rail operation control setting. The SDF factor accounts for the influence of the Slide Detector Fence, a hazard detection system.

Abbott et al. (1998a) also incorporate the presence or absence of the Centralized Traffic Control (CTC) into the hazard assessment. The glossary includes a description of the CTC.

Horiuchi (1998) provides an overview of railway risks due to geotechnical hazards. He summarises passenger deaths per 0.1 trillion passenger miles for several jurisdictions in the industrialized world. He outlines a risk assessment process consistent in many way to that of Canadian Standards Association (1997). He identifies train speed as a factor influencing the outcome of a train accident hitting or stopping short of a geotechnical hazard. Rimm-Kaufman (1996) investigated and proposed methods for assessing the risk associated with train collisions, earthquakes, and rainfall induced landslides for Japanese railway line. He uses his rainfall index to determine how many false-positive train delays will occur compared to true-positive events. He uses this to assess the probability of the rainfall warnings providing warning of a landslide compared to the number of unnecessary delays. He limits his detailed investigation to the risk of delays. He does not extend his discussion into the risk of derailment and the potential for fatalities based on the loss record of a specific Japanese Railway.

Keegan (2007) provides a description of the risk scenarios leading to derailments and a quantitative risk assessment methodology suitable for the comparison of one hazard site or type to others. The risk assessment process results in a collection of loss severity ratings which are combined into a total severity rating. This process is configured to identify high risk locations based on annual inspection results and prioritize locations for stabilization work. The risk scenario descriptions developed by Keegan are used throughout this work and are recommended for adoption within the railway industry.

Tatone (2007) completed a risk assessment of the 1995 fatal rock fall derailment on the CP Nelson subdivision in Southeastern BC (Transportation Safety Board 1995). He showed that by combining the probability of failure and the value of the elements exposed to the hazard using a risk methodology, he could justify various levels of expenditure to stabilize the slope. He did not consider the likelihood that the hazard was identified prior to the failure.

D 1.3 Regulatory requirements for railway risk management systems for geotechnical hazards

The Transport Canada (2001) Railway Safety Act requires each railway to develop and implement a Safety Management System (SMS). The adequacy of the SMS is periodically verified by Transport Canada through independent audits. A number of performance indicators are identified which are monitored by Transport Canada.

A Safety Management System is defined to be "a formal framework for integrating safety into day-to-day railway operations and includes safety goals and performance targets, risk assessments, responsibilities and authorities, rules and procedures and monitoring and evaluation processes" (Transport Canada 2006). The regulation is intended to ensure that safety is given priority equivalent to that of corporate, financial and operational targets.

The current CP geotechnical safety management system is described in Section 5.1.1. This system is linked to the multi-year capital improvement plan such that geotechnical safety issues are identified and then resolved with the appropriate resources being allocated based on an annual review. Chapter 6 includes a discussion on the improvements to the CP geotechnical SMS that can be achieved using quantitative risk analysis.

Appendix E Excerpt of the CP Natural Hazard Incident Database

Data for Cascade Subdivision between Mile 102.5 and 104.9.

Mileage	Category (Level I)	Process (Level II)	Process (Level III)	State	Rate	Relation to the track	Rail bed	Date	Time	Failure Mechanism	File Number / Source	Description of hazard	Influence of hazard on railway	Train & MOW encounter	Size of slide	Size m3	Equipment affected	Track Closure (HRS)	Latitude	Longitude	Height (m)
104.6	GEOTECHNICAL	LANDSLIDE	EARTH SLIDE	ACTIVE		ABOVE & BELOW		1929-Jan-01	1904 to 1929	Minor Port Hammond Slide	RBA-CASC-103.00	Golder August 1979 report to the BC Ministry of Environment			600 ft wide, 400 ft long assume 80 ft deep	300,000	No		49.20814	-122.64211	
103.31	GEOTECHNICAL	LANDSLIDE	EARTH SLIDE	ACTIVE	RAPID	ABOVE	CUT & FILL	1938-Jan-01	No exact date	UNKNOWN	RBA CASC 103.40 Vol. 2	Maple Ridge Bluff Instability. Thurber Engineering Ltd. March 25, 1997	Earth slide from natural slope observed from 1938 airphotos		Area of 22 by 55 m. Assume 2 m thick	2,420	No		49.213235	-122.61458	25
103.33	GEOTECHNICAL	LANDSLIDE	EARTH SLIDE	ACTIVE	RAPID	ABOVE	CUT & FILL	1938-Jan-01	No exact date	UNKNOWN	RBA CASC 103.40 Vol. 2	Maple Ridge Bluff Instability. Thurber Engineering Ltd. March 25, 1997	Earth slide from natural slope observed from 1938 airphotos		Area of 38 by 45 m. Assume 2 m thick	3,420	No		49.213217	-122.615211	25
103.36	GEOTECHNICAL	LANDSLIDE	EARTH SLIDE	INACTIVE	RAPID	ABOVE	CUT & FILL	1938-Jan-01	No exact date	UNKNOWN	RBA CASC 103.40 Vol. 2	Maple Ridge Bluff Instability. Thurber Engineering Ltd. March 25, 1997. 20 different slide areas identified	Earth slide from natural slope observed from 1938 airphotos		Area of 40 by 10 m. Assume 1 m thick	400	No		49.213186	-122.616052	25
103.38	GEOTECHNICAL	LANDSLIDE	EARTH SLIDE	INACTIVE	RAPID	ABOVE	CUT & FILL	1938-Jan-01	No exact date	UNKNOWN	RBA CASC 103.40 Vol. 2	Maple Ridge Bluff Instability. Thurber Engineering Ltd. March 25, 1997	Earth slide from natural slope observed from 1938 airphotos		Area of 70 by 40 m. Assume 2 m thick	5,600	No		49.213165	-122.616052	25
103.43	GEOTECHNICAL	LANDSLIDE	EARTH SLIDE	INACTIVE	RAPID	ABOVE	CUT & FILL	1938-Jan-01	No exact date	UNKNOWN	RBA CASC 103.40 Vol. 2	Maple Ridge Bluff Instability. Thurber Engineering Ltd. March 25, 1997	Earth slide from natural slope observed from 1938 airphotos		Area of 45 by 10 m. Assume 1 m thick	450	No		49.213113	-122.617104	25
103.47	GEOTECHNICAL	LANDSLIDE	EARTH SLIDE	INACTIVE	RAPID	ABOVE	CUT & FILL	1938-Jan-01	No exact date	UNKNOWN	RBA CASC 103.40 Vol. 2	Maple Ridge Bluff Instability. Thurber Engineering Ltd. March 25, 1997	Earth slide from natural slope observed from 1938 airphotos		Area of 55 by 10 m. Assume 1 m thick	550	No		49.213075	-122.618157	25

103.73	103.72	103.68	103.65	103.63	103.59	103.52	103.49	103.48	**Mileage**
GEOTECHNICAL	GEOTECHNICAL	GEOTECHNICAL	GEOTECHNICAL	GEOTECHNICAL	GEOTECHNICAL	GEOTECHNICAL	GEOTECHNICAL	GEOTECHNICAL	**Category (Level I)**
LANDSLIDE	LANDSLIDE	LANDSLIDE	LANDSLIDE	LANDSLIDE	LANDSLIDE	LANDSLIDE	LANDSLIDE	LANDSLIDE	**Process (Level II)**
EARTH SLIDE	EARTH SLIDE	EARTH SLIDE	EARTH SLIDE	EARTH SLIDE	EARTH SLIDE	EARTH SLIDE	EARTH SLIDE	EARTH SLIDE	**Process (Level III)**
INACTIVE	INACTIVE	INACTIVE	INACTIVE	INACTIVE	INACTIVE	INACTIVE	INACTIVE	INACTIVE	**State**
RAPID	RAPID	RAPID	RAPID	RAPID	RAPID	RAPID	RAPID	RAPID	**Rate**
ABOVE	ABOVE	ABOVE	ABOVE	ABOVE	ABOVE	ABOVE	ABOVE	ABOVE	**Relation to the track**
CUT & FILL	CUT & FILL	CUT & FILL	CUT & FILL	CUT & FILL	CUT & FILL	CUT & FILL	CUT & FILL	CUT & FILL	**Rail bed**
1938-Jan-01	1938-Jan-01	1938-Jan-01	1938-Jan-01	1938-Jan-01	1938-Jan-01	1938-Jan-01	1938-Jan-01	1938-Jan-01	**Date**
No exact date	No exact date	No exact date	No exact date	No exact date	No exact date	No exact date	No exact date	No exact date	**Time**
UNKNOWN	UNKNOWN	UNKNOWN	UNKNOWN	UNKNOWN	UNKNOWN	UNKNOWN	UNKNOWN	UNKNOWN	**Failure Mechanism**
RBA CASC 103.40 Vol. 2	RBA CASC 103.40 Vol. 2	RBA CASC 103.40 Vol. 2	RBA CASC 103.40 Vol. 2	RBA CASC 103.40 Vol. 2	RBA CASC 103.40 Vol. 2	RBA CASC 103.40 Vol. 2	RBA CASC 103.40 Vol. 2	RBA CASC 103.40 Vol. 2	**File Number / Source**
Maple Ridge Bluff Instability. Thurber Engineering Ltd. March 25, 1997	Maple Ridge Bluff Instability. Thurber Engineering Ltd. March 25, 1997	Maple Ridge Bluff Instability. Thurber Engineering Ltd. March 25, 1997	Maple Ridge Bluff Instability. Thurber Engineering Ltd. March 25, 1997	Maple Ridge Bluff Instability. Thurber Engineering Ltd. March 25, 1997	Maple Ridge Bluff Instability. Thurber Engineering Ltd. March 25, 1997	Maple Ridge Bluff Instability. Thurber Engineering Ltd. March 25, 1997	Maple Ridge Bluff Instability. Thurber Engineering Ltd. March 25, 1997	Maple Ridge Bluff Instability. Thurber Engineering Ltd. March 25, 1997	**Description of hazard**
Earth slide from natural slope observed from 1938 airphotos	Earth slide from natural slope observed from 1938 airphotos	Earth slide from natural slope observed from 1938 airphotos	Earth slide from natural slope observed from 1938 airphotos	Earth slide from natural slope observed from 1938 airphotos	Earth slide from natural slope observed from 1938 airphotos	Earth slide from natural slope observed from 1938 airphotos	Earth slide from natural slope observed from 1938 airphotos	Earth slide from natural slope observed from 1938 airphotos	**Influence of hazard on railway**
									Train & MOW encounter
Area of 30 by 10 m. Assume 1 m thick	Area of 45 by 10 m. Assume 1 m thick	Area of 40 by 10 m. Assume 1 m thick	Area of 40 by 40 m. Assume 2 m thick	Area of 50 by 15 m. Assume 1 m thick	Area of 40 by 40 m. Assume 2 m thick	Area of 45 by 15 m. Assume 1 m thick	Area of 45 by 15 m. Assume 1 m thick	Area of 45 by 10 m. Assume 1 m thick	**Size of slide**
300	450	400	3,200	750	3,200	675	675	450	**Size m3**
No	No	No	No	No	No	No	No	No	**Equipment affected**
									Track Closure (HRS)
49.212385	49.212414	49.212553	49.212661	49.212733	49.212867	49.213035	49.213059	49.213067	**Latitude**
-122.624831	-122.623372	-122.622332	-122.622332	-122.62171	-122.621294	-122.619628	-122.618578	-122.618367	**Longitude**
25	25	25	25	25	25	25	25	25	**Height (m)**

103.55	103.51	103.38	103.34	103.31	103.91	103.88	103.86	103.82	**Mileage**
GEOTECHNICAL	GEOTECHNICAL	GEOTECHNICAL	GEOTECHNICAL	GEOTECHNICAL	GEOTECHNICAL	GEOTECHNICAL	GEOTECHNICAL	GEOTECHNICAL	**Category (Level I)**
LANDSLIDE	LANDSLIDE	LANDSLIDE	LANDSLIDE	LANDSLIDE	LANDSLIDE	LANDSLIDE	LANDSLIDE	LANDSLIDE	**Process (Level II)**
EARTH SLIDE	EARTH SLIDE	EARTH SLIDE	EARTH SLIDE	EARTH SLIDE	EARTH SLIDE	EARTH SLIDE	EARTH SLIDE	EARTH SLIDE	**Process (Level III)**
INACTIVE	INACTIVE	INACTIVE	INACTIVE	ACTIVE	INACTIVE	INACTIVE	INACTIVE	INACTIVE	**State**
RAPID	RAPID	RAPID	RAPID	RAPID	RAPID	RAPID	RAPID	RAPID	**Rate**
ABOVE	ABOVE	ABOVE	ABOVE	ABOVE	ABOVE & BELOW	ABOVE	ABOVE	ABOVE	**Relation to the track**
CUT & FILL	CUT & FILL	CUT & FILL	CUT & FILL	CUT & FILL	CUT & FILL	CUT & FILL	CUT & FILL	CUT & FILL	**Rail bed**
1954-Jan-01	1954-Jan-01	1954-Jan-01	1954-Jan-01	1953-Jan-01	1929-Jan-01	1938-Jan-01	1938-Jan-01	1938-Jan-01	**Date**
Spring or fall of 1953	Spring or fall of 1953	Spring or fall of 1953	Spring or fall of 1953	Spring or fall of 1953	No exact date (dated 1923 to 1938 by Thurber and 1904 to 1929 by Golder)	No exact date	No exact date	No exact date	**Time**
UNKNOWN	UNKNOWN	UNKNOWN	UNKNOWN	UNKNOWN	Fir Street Slide (dated 1923 to 1938)	UNKNOWN	UNKNOWN	UNKNOWN	**Failure Mechanism**
RBA CASC 103.40 Vol. 2	RBA CASC 103.40 Vol. 2	RBA CASC 103.40 Vol. 2	RBA CASC 103.40 Vol. 2	RBA CASC 103.40 Vol. 2	RBA CASC 103.40 Vol. 2	RBA CASC 103.40 Vol. 2	RBA CASC 103.40 Vol. 2	RBA CASC 103.40 Vol. 2	**File Number / Source**
Maple Ridge Bluff Instability. Thurber Engineering Ltd. March 25, 1997	Maple Ridge Bluff Instability. Thurber Engineering Ltd. March 25, 1997	Maple Ridge Bluff Instability. Thurber Engineering Ltd. March 25, 1997	Maple Ridge Bluff Instability. Thurber Engineering Ltd. March 25, 1997	Maple Ridge Bluff Instability. Thurber Engineering Ltd. March 25, 1997	Maple Ridge Bluff Instability. Thurber Engineering Ltd. March 25, 1997	Maple Ridge Bluff Instability. Thurber Engineering Ltd. March 25, 1997	Maple Ridge Bluff Instability. Thurber Engineering Ltd. March 25, 1997	Maple Ridge Bluff Instability. Thurber Engineering Ltd. March 25, 1997	**Description of hazard**
Earth slide from natural slope observed from 1953 airphotos	Earth slide from natural slope observed from 1953 airphotos	Earth slide from natural slope observed from 1953 airphotos	Earth slide from natural slope observed from 1953 airphotos	Earth slide from natural slope observed from 1953 airphotos	Earth slide from natural slope observed from 1938 airphotos	Earth slide from natural slope observed from 1938 airphotos	Earth slide from natural slope observed from 1938 airphotos	Earth slide from natural slope observed from 1938 airphotos	**Influence of hazard on railway**
									Train & MOW encounter
Area of 30 by 10 m. Assume 1 m thick	Area of 45 by 10 m. Assume 1 m thick	Area of 30 by 10 m. Assume 1 m thick	Area of 20 by 10 m. Assume 1 m thick	Area of 28 by 8 m. Assume 1 m thick	Area of 150 by 100 m. Assume 10 m thick	Area of 40 by 10 m. Assume 1 m thick	Area of 50 by 10 m. Assume 1 m thick	Area of 35 by 20 m. Assume 3 m thick	**Size of slide**
300	450	300	200	224	80,000	400	500	1,400	**Size m3**
No	No	No	No	No	No	No	No	No	**Equipment affected**
									Track Closure (HRS)
49.212983	49.213046	49.213165	49.213207	49.213235	49.211671	49.211822	49.211918	49.212099	**Latitude**
-122.620046	-122.618998	-122.616473	-122.615632	-122.61479	-122.628932	-122.626888	-122.626479	-122.626068	**Longitude**
25	25	25	20	15	25	25	25	25	**Height (m)**

103.8	103.9	103.8	103.5	103.57	Mileage
GEOTECHNICAL	GEOTECHNICAL	HYDRAULIC EROSION	GEOTECHNICAL	GEOTECHNICAL	Category (Level I)
SUBSIDENCE	LANDSLIDE	SUB AQUEOUS	LANDSLIDE	LANDSLIDE	Process (Level II)
SUB-GRADE DYNAMIC LIQUEFACTION	EARTH SLIDE	CHANNELIZED FLOW EROSION	EARTH SLIDE	EARTH SLIDE	Process (Level III)
ACTIVE	REACTIVATED	NA	INACTIVE	INACTIVE	State
VERY SLOW	SLOW	SLOW	EXTREMELY SLOW	RAPID	Rate
BELOW	ABOVE	BELOW	ABOVE	ABOVE	Relation to the track
CUT	CUT & FILL	CUT & FILL	CUT & FILL	CUT & FILL	Rail bed
1976-Oct-01	1976-Mar-01	1976-Jan-01	1976-Jan-01	1954-Jan-01	Date
Not exact date (likely spring 1976)	No exact date could be 1975	No exact date. May have occurred Dec 1975	No exact date. May have occurred Dec 1975	Spring or fall of 1953	Time
	Slide caused by seepage in sand layers at base of slope were it erodes sand by piping, and causing collapse of overlying material (GAL 1975?, page 44)	Undermining of slope by Fraser River along 107 m length. Scarp faces visible at high water mark.	Erosion from groundwater seepage is principal cause of soil movement on the slope (GAL 1976, p37). Erosion gullies (cutting ancient slides / scarp faces) drain into swampy area upslope of track with possible seepage into track bed.	UNKNOWN	Failure Mechanism
RBA CASC 86.9	RBA CASC 94.1	RBA CASC 94.1	RBA CASC 94.1	RBA CASC 103.40 Vol. 2	File Number / Source
Letter report to CPR on Preliminary Tests for clay mineralogy Mission City to Pitt River, BC, Golder, Aug. 1976 and Report o CPR on laboratory tests on Possible filters for mud pumping areas, Mission to Coquitlam, BC, April 1977	Inter-layered silty clay and silty sand.		Slide on slope above tracks (Golder, Aug. 1976). Fill (gravel, ho	Maple Ridge Bluff Instability. Thurber Engineering Ltd. March 25, 1997	Description of hazard
Contamination of ballast by native fines in sub-grade			Possible old slide material accumulated adjacent to track. Slope materials: laminated clays, silts and sands. Fraser River flows adjacent to slope.	Earth slide from natural slope observed from 1953 airphotos	Influence of hazard on railway
					Train & MOW encounter
0.6 m deep by 4 m wide by at least 3 m along the track	60 ft wide, 60 ft long by 10 ft thick	Assume 110 m wide 20 m long and 5 m deep	Assume at least 100 m3	Area of 35 by 10 m. Assume 1 m thick	Size of slide
7.2	530	7000	100	350	Size m3
No	No	No	No	No	Equipment affected
					Track Closure (HRS)
49.212172	49.211721	49.212172	49.213053	49.212928	Latitude
-122.624831	-122.627092	-122.624831	-122.618788	-122.620463	Longitude
				25	Height (m)

103.74	104.27	**Mileage**
GEOTECHNICAL	GEOTECHNICAL	**Category (Level I)**
LANDSLIDE	LANDSLIDE	**Process (Level II)**
EARTH SLIDE	EARTH SLIDE	**Process (Level III)**
ACTIVE	ACTIVE	**State**
		Rate
BELOW	BELOW	**Relation to the track**
		Rail bed
1978-Jan-01	1977-Jan-19	**Date**
No exact date but prior to Jan 13, 1979, Likely Winter 1975/1976 landslide	10:00	**Time**
As per Northwest Hydraulics March 23, 1979 report. Rip rap was placed during 1978 at 103.74 (Section 14, 630 ft East of Golder BH-103 and 104.27 (Section 21, 40 ft East of Golder BH 105) in 1978	Earth slide below the track caused by high groundwater conditions following heavy rains. Northwest Hydraulics March 23, 1979 report indicates rip-rap was placed during 1978 at 103.74 (Section 14, 630 ft East of Golder BH-103 and 104.27 (Section 21, 40 ft East of Golder BH 105) in 1978 and was likely as a result of this incident.	**Failure Mechanism**
RBA CASC 103.00	RBA CASC 103.00 and RBA-CASC-104.3	**File Number / Source**
Sub-grade earth slide into river	Sub-grade earth slide into river. Golder report Jan 31, 1977 and March 1977	**Description of hazard**
	Slow order. Scarp 18 " from the end of tie. Rip-rap placed on slope and geotechnical investigation by Golder	**Influence of hazard on railway**
		Train & MOW encounter
	200 ft wide, 40 ft long, 10 ft deep	**Size of slide**
	1200	**Size m3**
No	No	**Equipment affected**
		Track Closure (HRS)
49.208441	49.208441	**Latitude**
-122.596352	-122.596352	**Longitude**
		Height (m)

Mileage	103.67	103.65	103.46
Category (Level I)	GEOTECHNICAL	GEOTECHNICAL	GEOTECHNICAL
Process (Level II)	LANDSLIDE	LANDSLIDE	LANDSLIDE
Process (Level III)	EARTH SLIDE	EARTH SLIDE	EARTH SLIDE
State	ACTIVE	ACTIVE	ACTIVE
Rate			
Relation to the track	ABOVE	ABOVE	ABOVE
Rail bed			
Date	1979-Jan-01	1979-Jan-01	1979-Jan-01
Time	No exact date These are likely the four Winter 1975/1976 landslides	No exact date These are likely the four Winter 1975/1976 landslides	No exact date These are likely the four Winter 1975/1976 landslides
Failure Mechanism	Report (figure 3) identifies several "active" scarp areas at 103.46, 103.65, 103.67, and 103.87. These must have been active prior to the winter of 1979.	Report (figure 3) identifies several "active" scarp areas at 103.46, 103.65, 103.67, and 103.87. These must have been active prior to the winter of 1979.	Report (figure 3) identifies several "active" scarp areas at 103.46, 103.65, 103.67, and 103.87. These must have been prior to the winter of 1979.
File Number / Source	RBA CASC 103.40	RBA CASC 103.40	RBA CASC 103.40
Description of hazard	Golder July 1979 report proposes to carry out slope stabilization and drainage works on CPR mainline at both Mile 102.3 and between Mile 103.4 and 103.9. Proposed work involves excavation and construction of drainage systems to control surface and subsurface	Golder July 1979 report proposes to carry out slope stabilization and drainage works on CPR mainline at both Mile 102.3 and between Mile 103.4 and 103.9. Proposed work involves excavation and construction of drainage systems to control surface and subsurface	Golder July 1979 report proposes to carry out slope stabilization and drainage works on CPR mainline at both Mile 102.3 and between Mile 103.4 and 103.9. Proposed work involves excavation and construction of drainage systems to control surface and subsurface
Influence of hazard on railway			
Train & MOW encounter			
Size of slide			
Size m3			
Equipment affected	No	No	No
Track Closure (HRS)			
Latitude	49.208441	49.208441	49.208441
Longitude	-122.596352	-122.596352	-122.596352
Height (m)			

103.71	103.51	103.87	Mileage
GEOTECHNICAL	GEOTECHNICAL	GEOTECHNICAL	Category (Level I)
LANDSLIDE	LANDSLIDE	LANDSLIDE	Process (Level II)
EARTH SLIDE	EARTH SLIDE	EARTH SLIDE	Process (Level III)
ACTIVE	ACTIVE	ACTIVE	State
			Rate
ABOVE	ABOVE	ABOVE	Relation to the track
			Rail bed
1981-Mar-01	1981-Mar-01	1979-Jan-01	Date
No exact date Spring 1981	No exact date Spring 1981	No exact date but prior to Jan 13, 1979 as per Northwest Hydraulics March 23, 1979	Time
Golder report June 10, 1981 indicates 103.45 (actually 103.51), 103.65 (actually 103.71), 103.70 (actually 103.74), 103.71 (actually 103.75), 104.05 (actually 104.09) and 104.20 (actually 104.25) landslides were active in the spring of 1981	Golder report June 10, 1981 indicates 103.45 (actually 103.51), 103.65 (actually 103.71), 103.70 (actually 103.74), 103.71 (actually 103.75), 104.05 (actually 104.09) and 104.20 (actually 104.25) landslides were active in the spring of 1981	Report (figure 3) identifies several "active" scarp areas at 103.46, 103.65, 103.67, and 103.87. These must have been active prior to the winter of 1979. Golder August 1979 includes a photo of 103.9 (103.87) showing recent scarp	Failure Mechanism
RBA-CASC 103.45	RBA-CASC 103.45	RBA CASC 103.40 and 103.00	File Number / Source
Located below 21610 River Road	Located below 21760 and 21778 River Road	Golder July 1979 report proposes to carry out slope stabilization and drainage works on CPR mainline at both Mile 102.3 and between Mile 103.4 and 103.9. Proposed work involves excavation and construction of drainage systems to control surface and subsurface	Description of hazard
None provided	None provided		Influence of hazard on railway
			Train & MOW encounter
75 ft wide Assume 50 ft long and 5 ft deep	75 ft wide Assume 50 ft long and 5 ft deep		Size of slide
270	270		Size m3
No	No	No	Equipment affected
			Track Closure (HRS)
49.212931	49.21336	49.208441	Latitude
-122.62252	-122.618489	-122.596352	Longitude
			Height (m)

104.09	103.75	103.74	**Mileage**
GEOTECHNICAL	GEOTECHNICAL	GEOTECHNICAL	**Category (Level I)**
LANDSLIDE	LANDSLIDE	LANDSLIDE	**Process (Level II)**
EARTH SLIDE	EARTH SLIDE	EARTH SLIDE	**Process (Level III)**
ACTIVE	ACTIVE	ACTIVE	**State**
			Rate
ABOVE	ABOVE	ABOVE	**Relation to the track**
			Rail bed
1981-Mar-01	1981-Mar-01	1981-Mar-01	**Date**
No exact date Spring 1981	No exact date Spring 1981	No exact date Spring 1981	**Time**
Golder report June 10, 1981 indicates 103.45 (actually 103.51), 103.65 (actually 103.71), 103.70 (actually 103.74), 103.71 (actually 103.75), 104.05 (actually 104.09) and 104.20 (actually 104.25) landslides were active in the spring of 1981	Golder report June 10, 1981 indicates 103.45 (actually 103.51), 103.65 (actually 103.71), 103.70 (actually 103.74), 103.71 (actually 103.75), 104.05 (actually 104.09) and 104.20 (actually 104.25) landslides were active in the spring of 1981.	Golder report June 10, 1981 indicates 103.45 (actually 103.51), 103.65 (actually 103.71), 103.70 (actually 103.74), 103.71 (actually 103.75), 104.05 (actually 104.09) and 104.20 (actually 104.25) landslides were active in the spring of 1981	**Failure Mechanism**
RBA-CASC 103.45	RBA-CASC 103.45	RBA-CASC 103.45	**File Number / Source**
Located below 11540 Anderson Road	Located below 21536/Public ROW and 21564 River Road	Located below 21564 River Road	**Description of hazard**
None provided	None provided	None provided	**Influence of hazard on railway**
			Train & MOW encounter
75 ft wide Assume 50 ft long and 5 ft deep	75 ft wide Assume 50 ft long and 5 ft deep	100 ft wide Assume 75 ft long and 7 ft deep	**Size of slide**
270	270	780	**Size m3**
No	No	No	**Equipment affected**
			Track Closure (HRS)
49.211038	49.212745	49.212893	**Latitude**
-122.6206	-122.623653	-122.623427	**Longitude**
			Height (m)

102.98	102.95	102.95	104.25	**Mileage**
GEOTECHNICAL	GEOTECHNICAL	GEOTECHNICAL	GEOTECHNICAL	**Category (Level I)**
LANDSLIDE	LANDSLIDE	LANDSLIDE	LANDSLIDE	**Process (Level II)**
EARTH SLIDE	EARTH SLIDE	EARTH SLIDE	EARTH SLIDE	**Process (Level III)**
ACTIVE	ACTIVE	ACTIVE	ACTIVE	**State**
VERY RAPID	VERY SLOW	VERY SLOW		**Rate**
ABOVE & BELOW	BELOW	BELOW	ABOVE	**Relation to the track**
FILL	FILL	FILL		**Rail bed**
1880-Jan-30	1985-Mar-03	1981-May-03	1981-Mar-01	**Date**
			No exact date Spring 1981	**Time**
Haney Side - Triggered by high groundwater, or river erosion. Slide originates 125 m north of the track, extends 100 m south of the track and 225 m along the track	Present instability is likely local in nature and associated with embankment and immediate sub-grade only and local seepage and drainage conditions. Likely that track settlement occurred in the days prior to the letter date	Cause of derailment not attributed to track settlement or conditions	Golder report June 10, 1981 indicates 103.45 (actually 103.51), 103.65 (actually 103.71), 103.70 (actually 103.74), 103.71 (actually 103.75), 104.05 (actually 104.09) and 104.20 (actually 104.25) landslides were active in the spring of 1981	**Failure Mechanism**
RBA CASC 103.40 Vol. 2	RBA CASC 102.9	RBA CASC 102.9	RBA-CASC 103.45	**File Number / Source**
Memo from P.J. Woods of the BC Ministry of Environment dated Jan 3, 1995. Evans and Savigny, 1994. Fraser River North River Bank monitoring and stabilization study in Maple Ridge, BC concluded that slopes in critical zone have adequate safety factor against	Inspection of rail embankment distress at mile 102.9, located at east end of the 1880 Haney Slide. Present movement involves eastbound track about 50 m in length and 25 mm settlement and 15 mm of horizontal displacement to south. (letter from Golder, March 4th 1985)	Derailment recorded cause unknown track settlement suspected	Located below 11446 River Wynd	**Description of hazard**
Haney river slide in January 30, 1880	Derailment May 03, 1981; possible track settlement due significant antecedent rainfall. Site is 100 m east of 1880 Haney slide, in same soil type	Derailment May 03, 1981; possible track settlement due significant antecedent rainfall. Site is 100 m east of 1880 Haney slide, in same soil type	None provided	**Influence of hazard on railway**
	LANDSLIDE UNDER MOVING TRAIN	LANDSLIDE UNDER MOVING TRAIN		**Train & MOW encounter**
Estimated 250 m by 200 and 30 m deep.	Assume at least 1,000 m3	Assume at least 1,000 m3	75 ft wide Assume 50 ft long and 5 ft deep	**Size of slide**
1,500,000	1000	1000	270	**Size m3**
No	Derailment	Derailment	No	**Equipment affected**
				Track Closure (HRS)
49.212461	49.212212	49.212212	49.210041	**Latitude**
-122.614369	-122.605368	-122.605368	-122.634336	**Longitude**
				Height (m)

103.41	103.39	103.8	103.68	103.43	103.32	104.5	104.57	**Mileage**
GEOTECHNICAL	GEOTECHNICAL	GEOTECHNICAL	GEOTECHNICAL	GEOTECHNICAL	GEOTECHNICAL	GEOTECHNICAL	GEOTECHNICAL	**Category (Level I)**
LANDSLIDE	LANDSLIDE	LANDSLIDE	LANDSLIDE	LANDSLIDE	LANDSLIDE	LANDSLIDE	LANDSLIDE	**Process (Level II)**
EARTH SLIDE	EARTH SLIDE	EARTH SLIDE	EARTH SLIDE	EARTH SLIDE	EARTH SLIDE	EARTH SLIDE	EARTH SLIDE	**Process (Level III)**
ACTIVE	ACTIVE	ACTIVE	ACTIVE	ACTIVE	ACTIVE	ACTIVE	ACTIVE	**State**
RAPID	RAPID	RAPID	RAPID	RAPID	RAPID	UNKNOWN		**Rate**
ABOVE	ABOVE	ABOVE	ABOVE	ABOVE	ABOVE	ABOVE	BELOW	**Relation to the track**
CUT & FILL	CUT & FILL	CUT & FILL	CUT & FILL	CUT & FILL	CUT & FILL	CUT & FILL		**Rail bed**
1997-Mar-18	1997-Mar-18	1997-Jan-29	1997-Jan-29	1997-Jan-29	1997-Jan-29	1996-Jan-16	1995-Nov-01	**Date**
23:00	21:37					2:10	No exact date in Nov 1995	**Time**
Saturation of colluvium	This debris slide was observed. OTHER WAY AND STRUCTURE DEFECT	Saturation of colluvium	Saturation of colluvium	Saturation of colluvium	Saturation of colluvium	Debris slide from above the track	Earth slide below the south track	**Failure Mechanism**
RBA CASC 103.40 Vol. 2	SAL Vol. 1989-95 report 98TA0469 119564	RBA CASC 103.40 Vol. 2	RBA CASC 103.40 Vol. 2	RBA CASC 103.40 Vol. 2	RBA CASC 103.40 Vol. 2	3200 CASC 121.6 Shell Slide file	RBA-CASC-104.60	**File Number / Source**
Maple Ridge Bluff Instability. Thurber Engineering Ltd. March 25, 1997	TRAIN ACCIDENT; M101; While traveling at 30 mph crew encountered mud slide. Locomotive engineer placed train into emergency and train stopped with 7th, 8th, and 9th cars in slide. No derailment, all cars remained upright. Damage to signals 103.4 N - 103.5 N. South track clear at 0200 North track clear at 0400	Maple Ridge Bluff Instability. Thurber Engineering Ltd. March 25, 1997	Maple Ridge Bluff Instability. Thurber Engineering Ltd. March 25, 1997	Maple Ridge Bluff Instability. Thurber Engineering Ltd. March 25, 1997	Maple Ridge Bluff Instability. Thurber Engineering Ltd. March 25, 1997	Recorded as a mud slide at Mile 105.40 however there is no slope above 105.40	Golder (March 16, 1996) indicates failure occurred in November 1995 during heavy rains.	**Description of hazard**
Signal towers. Fallen signal was hit by train. Soil crossed both tracks and contaminated	A train moving at 30 mph encountered mud slide and the signals that were foul of the track. The signals, locomotives and cars were damaged by the collision. South track closed 4.4 hr.	Occurred in late January 1997			Occurred in late January 1997			**Influence of hazard on railway**
SIGNAL SYSTEM	MOVING TRAIN HIT DEBRIS							**Train & MOW encounter**
100 m3		20 m long by 1 m thick with a total volume of 100 m3	27 m long by 9 m wide with a volume of 250 m3	35 m long with a total volume of 25 m3	15 m long by 1 m thick with a total volume of 50 m3		25 m wide, by 15 by 3 m deep	**Size of slide**
100	100	100	250	25	50	71	600	**Size m3**
Damage	Damage	No	No	No	No	No	No	**Equipment affected**
YES	4.4	0			0			**Track Closure (HRS)**
49.213144	49.21316667	49.212172	49.212553	49.213113	49.213227	49.209201	49.207732	**Latitude**
-122.616684	-122.6162667	-122.625246	-122.623163	-122.617946	-122.615001		-122.604599	**Longitude**
25		25	25	25	25			**Height (m)**

102.95	104	103.3	104.3	103.43	103.42	**Mileage**
GEOTECHNICAL	GEOTECHNICAL	GEOTECHNICAL	GEOTECHNICAL	GEOTECHNICAL	GEOTECHNICAL	**Category (Level I)**
LANDSLIDE	LANDSLIDE	LANDSLIDE	LANDSLIDE	LANDSLIDE	LANDSLIDE	**Process (Level II)**
EARTH SLIDE	EARTH SLIDE	DEBRIS SLIDE	EARTH SLIDE	EARTH SLIDE	EARTH SLIDE	**Process (Level III)**
ACTIVE		ACTIVE	ACTIVE	ACTIVE	ACTIVE	**State**
VERY SLOW		RAPID	RAPID	RAPID	RAPID	**Rate**
BELOW	ABOVE	ABOVE	BELOW	ABOVE	ABOVE	**Relation to the track**
FILL		CUT & FILL	CUT & FILL	CUT & FILL	CUT & FILL	**Rail bed**
1999-Jan-21	1997-Jan-01	1997-Mar-19	1997-Mar-18	1997-Mar-18	1997-Mar-18	**Date**
No exact date prior to Jan 21, 1999	Not exact date (assume Jan and March 1997 failures)	16:00				**Time**
Same slide as earlier reports. Ongoing frequent track maintenance.	Development and down-slope creep of sensitive clayey colluvium and build-up of pore water pressure.	Saturation of colluvium. Slide is 75 m north of the track	Saturation of colluvium	Saturation of colluvium	Saturation of colluvium	**Failure Mechanism**
RBA CASC 104.3 vol. 2 and RBA drive CASC 102.90	RBA CASC 103	RBA CASC 103.40 Volume 2	RBA CASC 103.40 Vol. 2	RBA CASC 103.40 Vol. 2	RBA CASC 103.40 Vol. 2	**File Number / Source**
Inspection of rail embankment distress at mile 102.9, located at east end of the 1880 Haney Slide. Present movement involves eastbound track about 15 m in length and (Golder summary, Jan 29, 1999)	Maple Ridge Slope Instability report, Mile 103 to 104.7, describes suspected areas of landslide activity and recommends investigation and mitigative measures. Provides relative probability for landslide occurrence. (Thurber, March 11, 1998)	Maple Ridge Bluff Instability. Thurber Engineering Ltd. March 25, 1997	Maple Ridge Bluff Instability. Thurber Engineering Ltd. March 25, 1997	Maple Ridge Bluff Instability. Thurber Engineering Ltd. March 25, 1997	Maple Ridge Bluff Instability. Thurber Engineering Ltd. March 25, 1997	**Description of hazard**
		Observed by track maintenance forces at the end of the day on March 19, 1976	Earth slide from the shoulder of the track to within 1 m of the end-of-tie	Soil crossed both tracks, contaminated the ballast and required clean up	Soil crossed both tracks, contaminated the ballast and required clean up	**Influence of hazard on railway**
				NONE		**Train & MOW encounter**
Assume 15 m by 20 m by 5 m		18 m long by 1.5 m deep with a volume of 75 m3	20 m wide Assumed to by at least 3 m thick and 20 m long	2 m thick, 1000 m3	150 m3	**Size of slide**
800		75	1,200	1,000	150	**Size m3**
No	No	No	No	No	No	**Equipment affected**
		0		YES	YES	**Track Closure (HRS)**
49.212212	49.211215	49.213242	49.209609	49.213123	49.213134	**Latitude**
-122.60639	-122.631994	-122.61458	-122.635043	-122.617104	-122.616894	**Longitude**
		25	25	25	25	**Height (m)**

102.95	103.8	103.75	104.23	**Mileage**
GEOTECHNICAL	GEOTECHNICAL	GEOTECHNICAL	GEOTECHNICAL	**Category (Level I)**
LANDSLIDE	LANDSLIDE	LANDSLIDE	LANDSLIDE	**Process (Level II)**
EARTH SLIDE	DEBRIS SLIDE	DEBRIS SLIDE	EARTH SLIDE	**Process (Level III)**
ACTIVE	ACTIVE	ACTIVE	ACTIVE	**State**
VERY SLOW			VERY SLOW	**Rate**
BELOW	ABOVE	ABOVE	BELOW	**Relation to the track**
FILL	CUT & FILL	CUT & FILL	CUT & FILL	**Rail bed**
2001-May-03	1999-Dec-31	1999-Dec-21	1999-Jan-14	**Date**
	Between Dec 21, 1999 and Feb 2, 2000			**Time**
This slide has been regularly moving for at least the past 10 years coinciding with heavy rain. Suspected contributing factors include river scour, culvert erosion from outfall, precipitation infiltration. Track lifted 3 to 4 times per year. Track settlement occurred in April 23 to 30, 2001		Grogan indicates the slide took place on Dec 23, 1999 but this is not supported elsewhere.	1220 ft west of Mile 104.00. Golder report Feb 1, 1999	**Failure Mechanism**
RBA CASC 102.9	RBA CASC 103.75	RBA CASC 103.75	RBA CASC 124.8 and RBA CASC 104.30	**File Number / Source**
Inspection of rail embankment distress at mile 102.9, located at east end of the 1880 Haney Slide. Present movement involves eastbound track about 15 m in length and (Memo from Golder, May 7, 2001)	Message from Jan Kubik 2000/02/02 describes failure(s) and there is a follow up by Alistair Grogan in 2000/02/9. Message from Kubik was not sent until 10 days after he reported it occurring.	Message from Jan Kubik 2000/02/02 describes failure(s) and there is a follow up by Alistair Grogan in 2000/02/9. Message from Kubik was not sent until 10 days after he reported it occurring.	Slump of the river side embankment, 2 ft. drop, about 50 ft. long, also 8 inch tension crack in the devil strip about 20 ft. long. Rock fill which was added 2 yrs ago at the east end of the ground movement may have caused slump. Rip-rap placed on toe to stabilize the situation. Shoulder repaired.	**Description of hazard**
Also refer to earlier description below	None documented some ditch cleaning	None documented some ditch cleaning. Location 21536 River Road - Bruce McLaren, phone 467-6360	South track was closed for several days. Golder observations Jan 29, 1999	**Influence of hazard on railway**
				Train & MOW encounter
15 m along track, 10 m long and assume 5 m deep			20 m wide, Modeling indicates 40 m long and 10 m deep	**Size of slide**
400	20	40	4000	**Size m3**
No	No	No	No	**Equipment affected**
				Track Closure (HRS)
49.212212	49.212172		49.209718	**Latitude**
-122.60639	-122.624831		-122.634083	**Longitude**
				Height (m)

103.52	103.39	103	104.5	**Mileage**
GEOTECHNICAL	GEOTECHNICAL	TREE	GEOTECHNICAL	**Category (Level I)**
LANDSLIDE	LANDSLIDE	FAILURE	LANDSLIDE	**Process (Level II)**
DEBRIS SLIDE	DEBRIS SLIDE	TREE	EARTH SLIDE	**Process (Level III)**
ACTIVE	ACTIVE		ACTIVE	**State**
				Rate
ABOVE	ABOVE	ABOVE	ABOVE	**Relation to the track**
CUT & FILL				**Rail bed**
2005-Jan-20	2005-Jan-20	2004-Jun-18	2003-Nov-28	**Date**
				Time
	This small failure occurred at the slope crest above PAD2. Some private fence debris is strewn on the slope and		Mud slide foul of North track, approx 3 ft deep and 30 ft long.	**Failure Mechanism**
RBA CASC 103.4	RBA CASC 103.4	186,272	RBA-CASC-094.39	**File Number / Source**
A localized slope failure is shown in the photo below. No slumped material is visible at the toe of the slope. The failed mass appears to be sitting on a bench at about 1/3 of the slope height measured from the toe. (Thurber 2005 report)	The failed mass or run-out damaged the east collectorpipe and the volume of material at the toe is approximately equal to 5to 10 m3. There appears to be an old slump that may predate thisfailure about half way up the slope. A swimming pool is present abovethe slope crest. (Thurber 2005 report)	CP Freight train struck five trees that had fallen on the right of way during freak wind storm. Locomotive DE 9713 sustained the following damage: Left hand rail bent, cow catcher dented, right ditch light broken, left fuel cut-off switch smashed. Estimate of damage $500. Train speed was 45 mph.	Excavator arriving on site now and should have North Track open approx 2200. Watchman will be on site tonight. Special patrols continue on the Cascade Subdivision this evening as far east as Ruby Creek.	**Description of hazard**
	No additional information provided.		delay, open by 2200, watchman onsite	**Influence of hazard on railway**
		MOVING TRAIN HIT DEBRIS		**Train & MOW encounter**
Assume 100 m3			30 ft wide, 30 ft long, 3 ft deep	**Size of slide**
50	10	10	75	**Size m3**
No	No	Damage	No	**Equipment affected**
				Track Closure (HRS)
49.21303	49.2132		49.20814	**Latitude**
-122.618676	-122.6158		-122.64211	**Longitude**
				Height (m)

Mileage	104.2	103.78	103.68
Category (Level I)	GEOTECHNICAL	GEOTECHNICAL	GEOTECHNICAL
Process (Level II)	LANDSLIDE	LANDSLIDE	LANDSLIDE
Process (Level III)	DEBRIS SLIDE	DEBRIS SLIDE	DEBRIS SLIDE
State	INACTIVE	ACTIVE	ACTIVE
Rate			
Relation to the track	ABOVE	ABOVE	ABOVE
Rail bed	CUT & FILL	CUT & FILL	CUT & FILL
Date	2005-Jan-20	2005-Jan-20	2005-Jan-20
Time			
Failure Mechanism	Same location as the March 27, 2007 observations. Shifted location from 104.23 to 104.20 to correspond to Thurber and Golder observations in 2007		There are photos of a recent failure on the slope above the forth of five manholes of the seepage/storm water collector conduits that are presumably connected with a collector pipe. Little flow was observed in the west culvert inlet.
File Number / Source	RBA CASC 103.4	RBA CASC 103.4	RBA-CASC 103.4
Description of hazard	A backyard fill failure located above the culvert designated as 900 mm CMP is shown in the oblique aerial photo below. Several boulders were observed near the crest of the slope. There also appears to be a drainage pipe on the slope face. The failure run-out is confined by the gully and no run-out was observed at the toe of the slope or in the ditch (Thurber 2005 report)	The oblique aerial photo below shows a recent event on a slope where most of the trees have been cut down. Oil filters and other man-made debris were observed in slide debris which is encroaching on the track. (Thurber 2005 report)	Slide debris including brush at the toe covers the manhole inlet. The oblique photo shows the two brown, failure surfaces near the crest of the slope. The longer one to the east appears to be undercutting the one to the west and is continuous from the slope crest to toe. (Thurber 2005 report)
Influence of hazard on railway	No additional information provided.		
Train & MOW encounter			
Size of slide	Assume 50 m3	Assume 50 m3	Assume 100 m3
Size m3	50	50	100
Equipment affected	No	No	No
Track Closure (HRS)			
Latitude	49.210415	49.212409	49.212906
Longitude	-122.633369	-122.624276	-122.622297
Height (m)			

103.39	103.35	103.32	103.2	103.41	104.3	Mileage
GEOTECHNICAL	GEOTECHNICAL	GEOTECHNICAL	GEOTECHNICAL	GEOTECHNICAL	GEOTECHNICAL	Category (Level I)
LANDSLIDE	LANDSLIDE	LANDSLIDE	LANDSLIDE	LANDSLIDE	LANDSLIDE	Process (Level II)
DEBRIS SLIDE	DEBRIS SLIDE	EARTH SLIDE	DEBRIS SLIDE	DEBRIS FALL	DEBRIS SLIDE	Process (Level III)
ACTIVE	ACTIVE	ACTIVE	ACTIVE	ACTIVE	ACTIVE	State
						Rate
ABOVE	ABOVE	ABOVE	BELOW	ABOVE	ABOVE	Relation to the track
					CUT & FILL	Rail bed
2007-Mar-24	2007-Mar-24	2007-Mar-24	2007-Mar-24	2007-Mar-11	2005-Jan-20	Date
						Time
Remnants of fencing tilt over the slope crest. No significant seepage. 4 of 15 landslide on March 24, between Mile 103.2 and 104.12	3 of 15 landslide on March 24, between Mile 103.2 and 104.12	2 of 15 landslide on March 24, between Mile 103.2 and 104.12	Triggered by high rainfall and river erosion. 1 of 15 landslide on March 24, between Mile 103.2 and 104.12			Failure Mechanism
RBA-CASC-103.60 - 104.7 20070324 debris slides	RBA-CASC-103.60 - 104.7 20070324 debris slides	RBA-CASC-103.60 - 104.7 20070324 debris slides	RBA-CASC-103.60 - 104.7 20070324 debris slides	Incident report 2002- June 2007	RBA CASC 103.4	File Number / Source
Failure that originated possibly in fill materials at crest of slope above tracks. (est. volume 5 cubic metre.) Debris flowed along side horizontal drain discharge pipe.	Failure originated mid-slope above tracks and failure mass crossed the north track. (est. volume 300 cubic metre.)	At crest of slope above tracks. (est. vol. 50 cubic metre.)	Toe of historic Haney Slide – three separate failures below the tracks along the edge of the Fraser River. (est. volume 2,000 cubic metre.)	Mud Slide over both north and south tracks. Slide hit 103.50N Signal bending. Same location as previous slide. Slow order of 10 MPH placed - both tracks. Excavator used to clear tracks for 3 hours.	The photos below show the retaining wall, cut brush, recent slide scarp and run-out at the track at Mile 104.3. There is a possible irrigation pipe on slope face with what appears to be a vertical perforated drain just right of the fence-line. Only minor seepage is visible on the failure scarp. (THURBER 2005 REPORT)	Description of hazard
Minimal hazard to trains		No additional information provided.	These three slides are about 70 to 100 m south of the track and pose no threat to the railway at present.	Debris on track	No additional information provided.	Influence of hazard on railway
			However, they may influence the stability of the Haney Slide mass.			Train & MOW encounter
			2000 cubic metres		Assume 50 m3	Size of slide
5	300	50	2,000	75	50	Size m3
No	No	No	No	No	No	Equipment affected
						Track Closure (HRS)
49.21316667	49.212375	49.213429	49.212375	49.213144	49.209787	Latitude
-122.6162667	-122.6114972	-122614982	-122.6114972	-122.616684	-122.635469	Longitude
				9.14		Height (m)

103.79	103.78	103.72	103.7	103.69	103.47	103.42	**Mileage**
GEOTECHNICAL	GEOTECHNICAL	GEOTECHNICAL	GEOTECHNICAL	GEOTECHNICAL	GEOTECHNICAL	GEOTECHNICAL	**Category (Level I)**
LANDSLIDE	LANDSLIDE	LANDSLIDE	LANDSLIDE	LANDSLIDE	LANDSLIDE	LANDSLIDE	**Process (Level II)**
DEBRIS SLIDE	DEBRIS SLIDE	DEBRIS SLIDE	DEBRIS SLIDE	DEBRIS SLIDE	DEBRIS SLIDE	DEBRIS SLIDE	**Process (Level III)**
ACTIVE	ACTIVE	ACTIVE	ACTIVE		ACTIVE	ACTIVE	**State**
							Rate
ABOVE	ABOVE	ABOVE	ABOVE	ABOVE	ABOVE	ABOVE	**Relation to the track**
							Rail bed
2007-Mar-24	2007-Mar-24	2007-Mar-24	2007-Mar-24	2007-Mar-24	2007-Mar-24	2007-Mar-24	**Date**
							Time
11 of 15 landslide on March 24, between Mile 103.2 and 104.12	10 of 15 landslide on March 24, between Mile 103.2 and 104.12	9 of 15 landslide on March 24, between Mile 103.2 and 104.12	8 of 15 landslide on March 24, between Mile 103.2 and 104.12	Incorrectly identified as 103.67 in Golder notes. Based on House numbers this is 103.69. 7 of 15 landslide on March 24, between Mile 103.2 and 104.12	6 of 15 landslide on March 24, between Mile 103.2 and 104.12	5 of 15 landslide on March 24, between Mile 103.2 and 104.12	**Failure Mechanism**
RBA-CASC-103.60 - 104.7 20070324 debris slides	RBA-CASC-103.60 - 104.7 20070324 debris slides	RBA-CASC-103.60 - 104.7 20070324 debris slides	RBA-CASC-103.60 - 104.7 20070324 debris slides	RBA-CASC-103.60 - 104.7 20070324 debris slides	RBA-CASC-103.60 - 104.7 20070324 debris slides	RBA-CASC-103.60 - 104.7 20070324 debris slides	**File Number / Source**
Failure that originated at crest of slope, failure mass did not reach ditch or tracks. (est. volume 10 cubic metre.)	Failure that originated mid-slope above tracks and covered tracks. (est. volume 40 cubic metre.)	Failure that originated at crest of slope. Failure mass has accumulated about 10 m above tracks. (est. vol. 250 cubic metre)	Failure and sloughing that originated at crest of slope. Failure mass did not reach ditch or tracks. (est. volume 30 cubic metre.)	Failure that originated at crest of slope in fill materials placed along crest of slope. Refuse observed along entire failure track. Failure mass reach the ditch.	Failure that originated about 5 m below crest of slope above tracks, slide did not reach tracks. (est. volume 10 cubic metre.)	Above Signals, originated near the crest of the slope above the tracks, failure mass likely covered north track. (est. volume 100 cubic metre.)	**Description of hazard**
No additional information provided.	No additional information provided.	No additional information provided.	No additional information provided.	No additional information provided.	No additional information provided.		**Influence of hazard on railway**
							Train & MOW encounter
							Size of slide
10	40	250	30	30	10	100	**Size m3**
No	No	No	No	No	No	No	**Equipment affected**
							Track Closure (HRS)
49.212598	49.212409	49.212836	49.212865	49.212913	49.213516	49.213436	**Latitude**
-122.625538	-122.624276	-122.62299	-122.622743	-122.622596	-122.616827	-122.616612	**Longitude**
							Height (m)

Mileage	104.2	104.15	103.98	103.93
Category (Level I)	GEOTECHNICAL	GEOTECHNICAL	GEOTECHNICAL	GEOTECHNICAL
Process (Level II)	LANDSLIDE	LANDSLIDE	LANDSLIDE	LANDSLIDE
Process (Level III)	DEBRIS SLIDE	DEBRIS SLIDE	DEBRIS SLIDE	DEBRIS SLIDE
State	ACTIVE	ACTIVE	ACTIVE	ACTIVE
Rate				
Relation to the track	ABOVE	ABOVE	ABOVE	ABOVE
Rail bed				
Date	2007-Mar-24	2007-Mar-24	2007-Mar-24	2007-Mar-24
Time				
Failure Mechanism	Failure and sloughing that originated at crest of slope, possibly in fill materials, about 50 m horizontal distance away from tracks. Same location as the Thurber 2005 observations. 15 of 15 landslide on March 24, between Mile 103.2 and 104.12	Large tension, about 30 m in length at crest of slope near existing house. Movements have impacted the deck. Separate ground movements are likely affected the existing garage. 14 of 15 landslide on March 24, between Mile 103.2 and 104.12	Shifted to 104.00 from 103.98 based on photos and address. 1 3 of 15 landslide on March 24, between Mile 103.2 and 104.12	Shifted to 103.92 from 103.95 based on photos and address. 1 2 of 15 landslide on March 24, between Mile 103.2 and 104.12
File Number / Source	RBA-CASC-103.60 - 104.7 20070324 debris slides	RBA-CASC-103.60 - 104.7 20070324 debris slides	RBA-CASC-103.60 - 104.7 20070324 debris slides	RBA-CASC-103.60 - 104.7 20070324 debris slides
Description of hazard	Failure mass did not reach ditch or tracks. Boulders situated along crest of slope. (est. volume 10 cubic metre.)	The failure mass does not yet appear to be impacting the tracks, ditch invert is higher in area below observed movement. (est. volume 500 cubic metre.)	Sloughing that originated near the crest of the slope, about 10 m above the tracks. (est. volume 10 cubic metre.)	Sloughing and slips observed along slope about 7 to 8 m above the tracks. (est. volume 5 cubic metre.)
Influence of hazard on railway	No additional information provided.		No additional information provided.	No additional information provided.
Train & MOW encounter				
Size of slide		30 m wide by 30 m long, assume 5 m deep		
Size m3	10	2,000	10	5
Equipment affected	No	No	No	No
Track Closure (HRS)				
Latitude	49.210415	49.210142	49.211353	49.211873
Longitude	-122.633369	-122.63074	-122.628791	-122.627439
Height (m)				

104.35	102.92	103.81	**Mileage**
GEOTECHNICAL	GEOTECHNICAL	GEOTECHNICAL	**Category (Level I)**
LANDSLIDE	LANDSLIDE	LANDSLIDE	**Process (Level II)**
EARTH SLIDE	EARTH SLIDE	DEBRIS SLIDE	**Process (Level III)**
ACTIVE	REACTIVATED	ACTIVE	**State**
UNKNOWN	SLOW		**Rate**
ABOVE & BELOW	BELOW	ABOVE	**Relation to the track**
CUT & FILL	FILL		**Rail bed**
1790-Jan-01	2007-May-08	2007-Mar-25	**Date**
No exact date			**Time**
Port Hammond Slide occurred in approximately 1790's. Thurber report March 25, 1997 Maple Ridge Bluff Instability.	Inspection of rail embankment on May 8, 2007. Distress at mile 102.9, located at east end of the 1880 Haney Slide. Present movement involves eastbound track about 50 m in length and 25 mm settlement and 15 mm of horizontal displacement to south. (letter from Golder, Ma	Shifted to 103.81 from 103.82 based on photos and address	**Failure Mechanism**
RBA CASC 103.40 Vol. 2	RBA 102.8, RBA CASC 102.90 BGC report 20070508	RBA-CASC-103.60 - 104.7 20070324 debris slides	**File Number / Source**
	Same site as the May 3, 1981 derailment site. The site is covered in wood waste. Toe was excavated and replaced with rip-rap 2007/05/01	Failure that originated at crest of slope, heavy seepage and flowing drain pipes observed in failure head scarp. (est. volume 400 cubic metre.)	**Description of hazard**
Large million cubic metre earth slide in fluvial and lacustrine clays and silts	Erosion, a crack in the wood waste and the potential for flooding predicated the inspection and protection of the slope with rip-rap. A slow order and track lift have been required periodically	Failure mass hit train on March 25, 2007.	**Influence of hazard on railway**
		FALLING DEBRIS HIT MOVING TRAIN	**Train & MOW encounter**
400 m wide, 300 m long and 20 m deep	10 m along the slope, slope distance 10 m depth 3 m		**Size of slide**
1,300,000	160	400	**Size m3**
No	NO	Derailment	**Equipment affected**
	NA		**Track Closure (HRS)**
49.210435	49.212212	49.212554	**Latitude**
-122.635043	-122.605368	-122.624994	**Longitude**
			Height (m)

Appendix F Precipitation data analysis

The following procedure is used to determining the most significant antecedent precipitation index for landslide activity based on recorded events.

1. Plot the geographic distribution of the landslide events on a map and the location of the available climatic data.
2. Select the most relevant climatic data and download the data from Environment Canada or NOAA. Google Earth Pro was used for this purpose during this research.
3. Compile and combine data from the nearest weather station in single file. The number of stations selected will depend on the proximity of the weather stations each other and the landslide location. Some guidance is provided in Section (data sources) regarding the selection of weather station data with respect to proximity, elevation and orographic influences on precipitation. Test the individual weather station data by using the analysis of the Gumbel maximum annual one day precipitation. If the data are similar proceed otherwise discard the data that are expected to be least representative of the area of the landslide and proceed with two data sets of replace the discarded data set with a set of data expected to be more representative (yet more distant) than the discarded one if one is available.
4. Select the antecedent precipitation durations, d to be analyzed. This is arbitrary but an approximate base 2 power sequence (Jakob and Weatherly 2003) is often adopted of 1, 2, 4, 7, 15, 30, 60, 90, 120, (150), 180, 365, 730, 1460 days to match anthropogenic and terrestrial climatic durations of a day, week, month, season (quarter of a year), third of a year, half year, year and multi-year. Given limitless computational resources it would be desirable to analyses all antecedent durations such that d = 1, 2, 3, ...
5. Using the one day precipitation data, p_i where p is the precipitation on day i for a specific weather station and i ranges from 1 at the start of the record to n and the end of the record. To ensure reliable analysis n should not be less than about 7,300 (20 years of data (Miller 1964))

6. To assess the seasonal variation in the precipitation data, p_i calculate the mean daily precipitation, $\overline{p}_j$ where j = 1, 2, 3, ..., 366 and j represents the days of the year including those years that are leap years for the period of record. The period of record, m is the number of full years represented in the data, p_i such that $m = \text{int}(n/365)$. Then use the mean daily precipitation data, $\overline{p}_j$ to compile the mean antecedent precipitation, $\overline{A}_{(d)j}$ where $\overline{A}_{(d)j} = \sum_{i=0}^{d} \overline{p}_{j-i}$

   for each antecedent duration, d where d= 1, 2, 3, 5, 7, 10, 15, 30, 60, 120, 150, 180, 270, 365. To calculate $\overline{A}_{(d)j}$ for j less than d use the $\overline{p}_j$ from the 365 - j. Note $\overline{A}_{(1)1} = \overline{p}_1$.

7. Select the start of the annual analytical cycle based on the lowest mean antecedent precipitation for the daily, 2, 3 or 5 day antecedent durations. This is consistent with the approach used by Guidicini and Iwasa (1977) and Walker (2007). In many parts of North America the wettest season of the year is the winter or spring. As a result the wettest season can be bisected by the calendar year. If the January 1st is used as the start of the analytical year two high precipitation events can be selected for a given wet season, one before and one after January 31. Then the next or previous wet season is not sampled. Using the annual dry cycle to define the start of the year maintains the maximum annual series and avoids resorting to a partial duration series which in the case or the longer antecedent durations may not be independent. Thereby the annual highest antecedent precipitation is selected from the data with the analytical year starting during the driest part of the year. In much of North America the beginning of August is the driest part of the year and as a result August 1, and July 30 will be used as the start and end of the analytical year in the remainder of this example.

8. Again starting with the daily precipitation data, p_i where i = 1, 2, 3 ... n and n is the number of days of the precipitation record compiled, calculate

the antecedent precipitation, $A_{(d)i}$ where $A_{(d)i} = \sum_{j=0}^{d-1} p_{i-j}$ for each i where d= 1, 2, 3, 5, 7, 10, 15, 30, 60, 90, 120, 180, 365, 730 and 1460, the antecedent duration. $A_{(d)i}$ for i less than d are not defined. Note as with the mean antecedent precipitation $A_{(1),1} = p_1$.

9. To avoid introducing artificially low antecedent precipitation values the data should be screened for missing data. In this study if more than 1/3 of the data in a given antecedent duration was missing the antecedent precipitation was set to null and not included in the return period calculations for $d < 30$. For $d > 30$ the threshold for missing data was set to 1/10 of the antecedent duration. Data from nearby stations can be used to fill in large data gaps as per step 3.

10. To assess the frequency distribution of the $A_{(d)i}$ data, the data are divided into 10 or more increments and the frequency of data in each increment compiled. Commonly the $A_{(d)i}$ for $d > 10$ days is dominated by frequent low precipitation with rare extremes, which are of most interest.

11. The Gumbel frequency distribution analysis return period of the daily and antecedent precipitation is then calculated following the procedure in Appendix B.

12. As is discussed in Section 4.2.2, Figure 4.1 the calculated Gumbel return period for antecedent durations longer than a month are not representative of the expected return period of the antecedent precipitation because the antecedent precipitation longer than one month are not well matched by the Gumbel distribution. The Anderson-Darling statistic can be used to test the goodness of fit of the Gumbel Distribution. It has been shown that for $d < 10$ the Gumbel is usually the distribution of choice. It has also been shown that antecedent precipitation longer than a few weeks to 12 months and beyond are best fit by the Generalized Extreme Value (GEV) frequency distribution.

13. The Generalized Extreme Value (GEV) frequency distribution is calculated following the procedure in Appendix D. As is discussed in Section 4.2.2 the

GEV has been found to represent calculated antecedent precipitation data well for all antecedent durations up to 1 year. As indicated by Chen (2007) there is no means of quantifying the goodness of fit other than the visual inspection of the Q-Q plots.

14. Extract the dates i_L of the landslides from the CP landslide database

15. The dates of the landslides, i_L are then correlated with the daily and antecedent precipitation $A_{(d)i}$ where the dates i are equal.

16. Using the results of the Gumbel and GEV analysis the return period, $T_{(d)i}$ of the various antecedent precipitation durations is computed for each day, i.

17. Interrogate the return periods, $T_{(d)}$ to determine which are the highest and most applicable as the threshold for landslide activity on the day, i of the landslide. The highest return period, $T^*_{(d)}$ for each landslide from a given location are then compared. The lowest of $T^*_{(d)}$ is then selected as the threshold $T'_{(d)}$ for which the landslides could occur. If the $T^*_{(d)}$ shorter than the observed return period for landslides it may be dismissed. In this case the landslides would not be considered to be induced by antecedent precipitation. In cases where the value of two $T^*_{(d)}$ are close a primary, $T'_{(d)}$ and secondary, $T''_{(d)}$ may be used.

18. The antecedent thresholds, $A'_{(d)}$ and $A''_{(d)}$ are then calculated for each $T'_{(d)}$ and $T''_{(d)}$ for the landslide(s) of interest.

Appendix G Gumbel moment estimates analysis

G 1.0 Analysis steps

The Gumbel analysis is complete by undertaking the following steps modified slightly from Hogg and Carr 1985.

1. Using the antecedent precipitation, $A_{(d)i}$ for each antecedent duration, d; select the highest value from annual analytical cycle as discussed in Appendix A, step 7. This can be done for all $A_{(d)i}$ for $k = 1$ to m and m is the number of years of record or $n/365$ rounded to the nearest integer. The selected $A_{(d)i}$ become the maximum annual series of the antecedent precipitation, $A_{(d)mas,k}$

2. Sort the $A_{(d)mas,k}$ for k equals 1 to m by size and assign the rank, r to each $A_{(d)mas,r}$. For the remainder of the analysis the $A_{(d)mas,k}$ series are independent of the year they occurred so the designation k can be dropped.

3. Calculate the plotting position τ of the $A_{(d)mas,r}$ using $\tau = \frac{(m+1)}{r}$. Adopting the nomenclature of Section 5.5.1.2 the probability of antecedent precipitation greater than $A_{(d)r}$, $P(A_{(d)} > A_{(d)r}) = 1/T$ where T is the return period of $A_{(d)} > A_{(d)r}$. Therefore the probability $P(A_{(d)} > A_{(d)r}) = r/(m+1)$. Therefore $P(A_{(d)}) < 1$ since $m \geq r$. Other alternative plotting positions include $\tau = \frac{m}{(r-1)}$, $\frac{m}{\left(r - \frac{1}{2}\right)}$ (favoured by some engineers), $\frac{m}{r}$, $\frac{m+0.4}{(r-0.3)}$. Chow et al (1988) reviews why $\frac{(m+1)}{r}$ is preferred. The expression $\tau = \frac{(m+1)}{r}$ is used exclusively in this research.

4. Calculate the mean, $x_{(d)}$ and standard deviation, $s_{(d)}$ of $A_{(d)mas}$ for all r and each antecedent duration, d.

5. To calculate the return period, $T_{(d)}$ of any $A_{(d)}$ use

$$T_{(d)} = \frac{1}{1-\exp\left(-\exp\left(-\gamma - \frac{\pi K_T}{\sqrt{6}}\right)\right)}$$

where $K_T = \frac{A_{(d)} - x_{(d)}}{s_{(d)}}$ for d = 1, 2, 3, ... 1460 or as selected in Step 8 of Appendix A.

γ = the Euler constant = 0.57721566

Then plot $A_{(d)mas,r}$ versus τ and calculate $A_{(d)}$ for several T within and beyond the range of τ using

$$A_{(d)}(T) = x_{(d)} + K_T s_{(d)} = \text{where } K_T = -\frac{\sqrt{6}}{\pi}\left(0.57721566 + \ln\left(\ln\left(\frac{T}{T-1}\right)\right)\right)$$

Then compare the ability of the Gumbel distribution to model the data.

G 2.0 Example

An example is provided of a Gumbel distribution frequency analysis for the 180 day antecedent precipitation from the Maple Ridge, BC data. Some sample data is from Pitt Meadows CS provided.

Table G1 Precipitation data for Pitt Meadows CS near Maple Ridge, BC

Date, i	Precip p_i (mm)	Date, i	Precip p_i (mm)	Date, i	Precip. p_i (mm)	j	Average precip. $\overline{p}_j$ (mm)
1954-Jan-01	13.7	1955-Jan-01	1.0	2007-Jan-01	25.0	1	6.4
1954-Jan-02	12.7	1955-Jan-02	0.0	2007-Jan-02	65.4	2	5.3
1954-Jan-03	4.6	1955-Jan-03	0.0	2007-Jan-03	9.0	3	4.8
1954-Jan-04	25.7	1955-Jan-04	11.7	2007-Jan-04	0.0	4	7.8
1954-Jan-05	20.3	1955-Jan-05	6.1	2007-Jan-05	26.8	5	6.5
1954-Jan-06	35.1	1955-Jan-06	1.8	2007-Jan-06	3.2	6	7.0
1954-Jan-07	10.2	1955-Jan-07	0.0	2007-Jan-07	23.2	7	7.9
1954-Jan-08	22.9	1955-Jan-08	0.0	2007-Jan-08	3.6	8	8.8
1954-Jan-09	0.0	1955-Jan-09	0.0	2007-Jan-09	8.2	9	5.8
1954-Jan-10	0.0	1955-Jan-10	0.0	2007-Jan-10	0.0	10	8.2
1954-Dec-28	19.6	1955-Dec-28	0.0	2006-Dec-28	0.0	362	9.9

1954-Dec-29	18.0	1955-Dec-29	0.0	2006-Dec-29	1.0	363	6.8
1954-Dec-30	27.2	1955-Dec-30	0.0	2006-Dec-30	0.0	364	8.2
1954-Dec-31	7.1	1955-Dec-30	2.0	2006-Dec-30	0.0	365	4.3

Leap years with a February 29th were treated by assuming the year had no December 31st. Therefore j does not exceed 365.

The mean daily precipitation, $\overline{p}_j$ is calculated by summing the daily precipitation for the same day each year for the Pitt Meadows CS record for the period of record. The sum for each day of the year is then divided by the number of years of record as per Table G1. Then the average antecedent precipitation, $\overline{A}_{(d)j}$ is calculated for each day of the year and each antecedent duration, d. For example $\overline{A}_{(30)j}$ for j = Dec 28 is the sum of the $\overline{p}_j$ for Nov 28 to Dec 28 and equals 267.3 mm in the example in Table G2. When d is greater than j the data from the end of the year is used. Therefore for d = 7, and j = 1 (Jan 1), $\overline{A}_{(7)1}$ is the sum of $\overline{p}_{360}, \overline{p}_{361}, \overline{p}_{362}, \overline{p}_{363}, \overline{p}_{364}, \overline{p}_{365}$, and $\overline{p}_1$ ($\overline{p}_j$ for Dec 26, 27, 28, 29, 30, 31 and Jan 1).

Table G2 Average antecedent precipitation for selected antecedent durations

j	Day of the year, j	Average daily precip. $\overline{p}_j$ (mm)	$\overline{A}_{(7)j}$	$\overline{A}_{(30)j}$	$\overline{A}_{(150)j}$	$\overline{A}_{(180)j}$
1	Jan-01	6.4	52.2	256.9	792.5	852.7
2	Jan-02	5.3	49.6	254.2	795.6	856.8
3	Jan-03	4.8	45.6	251.1	799.2	859.0
4	Jan-04	7.8	43.6	252.6	806.3	863.4
5	Jan-05	6.5	43.3	251.6	811.7	867.3
6	Jan-06	7.0	42.1	250.6	816.5	871.3
7	Jan-07	7.9	45.7	248.0	823.2	876.5
8	Jan-08	8.8	48.1	245.6	831.2	882.6
9	Jan-09	5.8	48.7	243.2	836.2	886.0
10	Jan-10	8.2	52.0	242.6	843.8	892.8
362	Dec-28	9.9	60.6	267.3	770.8	835.4
363	Dec-29	6.8	59.8	265.1	776.2	839.7
364	Dec-30	8.2	59.8	264.4	783.6	845.6
365	Dec-31	4.3	53.8	257.6	787.2	848.1

For ease of analysis the $\overline{A}_{(d)j}$ are plotted versus the day of the year as in Figure G1. As can be seen the lowest $\overline{A}_{(d)j}$ occur later and later in the year the longer the antecedent duration. It is computationally preferable to have common cycle for all duration, however, a different start and end for each antecedent duration is strictly correct. Unless the seasonal variation in precipitation is small, the start and end of the cycle should have no influence on the subsequent computations provided the start and end is close to a minimum in most of the antecedent durations. This research used a start and end close to the minimum of an intermediate antecedent duration such as the 30 or 60 day durations. As shown on Figure G1 the lowest antecedent condition is in early August for $\overline{A}_{(7)}$, but not until mid September for $\overline{A}_{(60)}$ and $\overline{A}_{(120)}$.

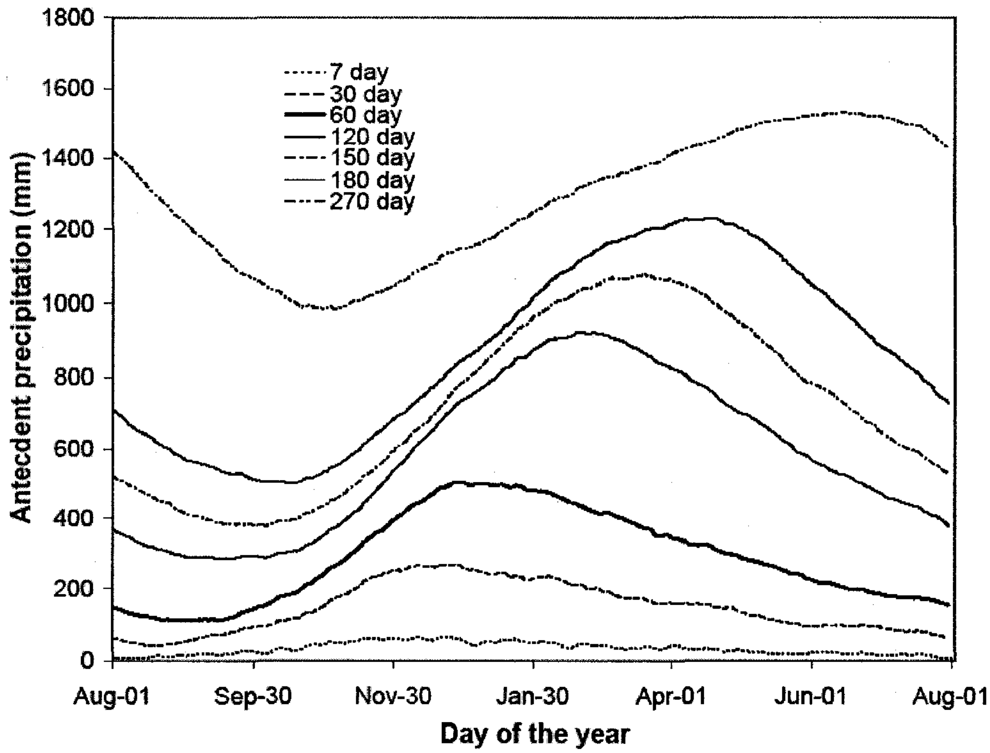

Figure G1 Average 7, 30, 60 and 120 day average antecedent precipitation

The antecedent precipitation $A_{(d)i}$ for each duration are then calculated for each day in the period of record. A sample for the Pitt Meadows CS weather station is provided in Table G3. The shaded dates and antecedent precipitations are the dates of landslides discussed in Section 4.5.9.

Table G3 Antecedent precipitation data for a sample of the Pitt Meadows CS data

Date, i	$A_{(1)}$	$A_{(2)}$	$A_{(7)}$	$A_{(15)}$	$A_{(90)}$	$A_{(150)}$	$A_{(365)}$
2007-Mar-10	35.8	39.6	69.4	127.8	697.8	1199.2	1591.4
2007-Mar-11	117.8	153.6	187.2	236.8	795.6	1317	1709.2
2007-Mar-12	0	117.8	173.8	230	780.4	1317	1709.2
2007-Mar-13	3.2	3.2	177	207.4	770.6	1317.2	1712.4
2007-Mar-14	0	3.2	165.2	207.2	752.6	1288.6	1704.8
2007-Mar-15	4.2	4.2	164.8	209.6	748.2	1291.4	1709
2007-Mar-16	20.8	25	181.8	230.4	767.8	1311.6	1728.6
2007-Mar-17	34.4	55.2	180.4	260.6	802.2	1343	1762.8
2007-Mar-18	0.4	34.8	63	250.2	801.2	1341.2	1763.2
2007-Mar-19	11.4	11.8	74.4	261.6	806	1352.6	1774.6
2007-Mar-20	0.4	11.8	71.6	248.6	802.6	1353	1775
2007-Mar-21	6.2	6.6	77.8	254.8	800.2	1359.2	1778.8
2007-Mar-22	41.6	47.8	115.2	284.6	841.8	1400.8	1795
2007-Mar-23	40.4	82	134.8	320.4	868	1433.8	1835
2007-Mar-24	49.2	89.6	149.6	365.8	895	1480.8	1876.6
2007-Mar-25	0	49.2	149.2	330	892.2	1476.6	1876.4
2007-Mar-26	0	0	137.8	212.2	892	1474.4	1872.4
2007-Mar-27	0	0	137.4	212.2	884.8	1472	1872.4
2007-Mar-28	0	0	131.2	209	884.8	1471.6	1871.6
2007-Mar-29	0	0	89.6	209	883.8	1469.6	1871.6
2007-Mar-30	1.6	1.6	50.8	206.4	885.4	1471.2	1867.2
2007-Mar-31	1.2	2.8	2.8	186.8	886.4	1472.4	1863

1. The maximum of the $A_{(d)i}$ within the 365 days defined by the start and end of the annual precipitation cycle are then selected to form the maximum annual series $A_{(d)mas}$. The maximum annual series for Pitt Meadows CS weather station using start and end of September 1 and August 31st respectively are included in Table G4.

Table G4 Sample of the maximum annual series of antecedent precipitations for Pitt Meadows CS weather station for various antecedent durations

Start date	$A_{(1)mas}$	$A_{(2)mas}$	$A_{(7)mas}$	$A_{(15)mas}$	$A_{(90)mas}$	$A_{(150)mas}$	$A_{(365)mas}$
1990-Sep-01	73	135	222	268	886	1385	2136
1991-Sep-01	92	144	251	311	1027	1362	2184
1992-Sep-01	50	83	157	247	878	1075	2182
1993-Sep-01	72	83	135	175	651	860	1720
1994-Sep-01	43	82	149	203	652	939	1709
1995-Sep-01	53	71	152	234	815	1221	1790
1996-Sep-01	58	105	163	225	958	1397	2125
1997-Sep-01	64	101	154	243	869	1417	2432
1998-Sep-01	44	66	105	182	664	1003	2441
1999-Sep-01	53	85	181	315	1134	1587	2217
2000-Sep-01	54	100	172	253	883	1204	2269
2001-Sep-01	48	58	75	126	434	664	1960
2002-Sep-01	70	103	154	221	782	1198	1956
2003-Sep-01	84	149	175	268	610	921	1816
2004-Sep-01	136	196	295	341	800	1152	1771
2005-Sep-01	98	169	271	279	831	1160	1826
2006-Sep-01	88	97	153	234	710	1094	1785
2007-Sep-01	118	154	187	366	895	1481	1946

2. The maximum annual series are then ordered by size as shown in Table G5. The rank r is assigned as per the order.

Table G5 *Ordered maximum annual series of the 150 day antecedent precipitation for Maple Ridge, BC*

Rank (r)	Max annual $A_{(150)mas}$	Plotting position τ		Rank (r)	Max annual $A_{(150)mas}$	Plotting position τ
1	1587	52.0		27	1152	1.9
2	1539	26.0		28	1116	1.9
3	1511	17.3		29	1094	1.8
4	1486	13.0		30	1082	1.7
5	1481	10.4		31	1078	1.7
6	1439	8.7		32	1075	1.6
7	1438	7.4		33	1061	1.6
8	1419	6.5		34	1060	1.5
9	1417	5.8		35	1019	1.5
10	1397	5.2		36	1003	1.4
11	1385	4.7		37	999	1.4
12	1362	4.3		38	998	1.4
13	1354	4.0		39	986	1.3

14	1353	3.7		40	982	1.3
15	1295	3.5		41	939	1.3
16	1269	3.3		42	927	1.2
17	1243	3.1		43	921	1.2
18	1221	2.9		44	891	1.2
19	1204	2.7		45	860	1.2
20	1198	2.6		46	845	1.1
21	1193	2.5		47	790	1.1
22	1186	2.4		48	772	1.1
23	1171	2.3		49	756	1.1
24	1167	2.2		50	664	1.0
25	1160	2.1		51	606	1.0
26	1159	2.0				

3. The plotting position, τ of the $A_{(150)mas}$ is calculated using $\tau = \frac{(m+1)}{r}$ and is included in Table G5.
4. The mean, $x_{(150)}$ and standard deviation, $s_{(150)}$ of $A_{(150)mas}$ for all r are 1,143.3 mm and 238.0 mm, respectively.
5. To calculate the return period, $T_{(d)}$ of any $A_{(d)}$ use

where $K_T = \frac{A_{(d)} - x_{(d)}}{s_{(d)}}$ for d = 1, 2, 3, ... 1,460 or as selected in Step 8 of Appendix A. For $A_{(150)}$ = 1400 mm

$$K_T = \frac{1{,}400 - 1{,}143.3}{238.0} = 1.08$$

$$T_{(150)} = \frac{1}{1 - \exp\left(-\exp\left(-\gamma - \frac{\pi(1.08)}{\sqrt{6}}\right)\right)} = 7.6 \text{ years}$$

Then plot $A_{(d)mas,r}$ versus τ and calculate $A_{(d)}$ for several T within and beyond the range of τ using for T = 10 years

$$K_{10} = -\frac{\sqrt{6}}{\pi}\left(0.57721566 + \ln\left(\ln\left(\frac{10}{10-1}\right)\right)\right) = 1.305$$

$$A_{(150)}(10) = 1143.3 + (1.305)(238.0) = 1453.8$$

Table G6 Calculated Gumbel K factor and estimated $A_{(150)}$ for selected return periods for Maple Ridge, BC

Return period, T (years)	K	$A_{(150)}$ estimated (mm)
1.58	-0.452	1035.8
2	-0.164	1104.2
5	0.719	1314.5
10	1.305	1453.8
25	2.044	1629.7
50	2.592	1760.2
100	3.137	1889.8
200	3.679	2018.8

Then compare the ability of the Gumbel distribution to model the data in a plot of return period, T and τ to antecedent precipitation, $A_{(d)}$ (Figure 4.1) or a Q-Q plot (Figure 4.13).

Appendix H Modified Chleborad method

H 1.0 Modified Chleborad steps

The modified Chleborad (2000) method has 12 steps.

1 Representative climatic data for a set of landslides is extracted as per Chapter 4 and Appendix A.

2. The running sum of the precipitation data is calculated for a number of antecedent durations to form $A_{(d)i}$.

3. The maximum annual series for each antecedent duration is extracted, $A_{(d)mas,k}$ where k is equal to the number of landslides recorded.

4. The antecedent conditions during each of the recorded landslides are selected determined, $A_{(d)L,k}$.

5. The two data sets are ordered from highest to lowest.

6. The difference, $\Delta A_{(d),k}$ of the two ordered sets is calculated.

   $\Delta A_{(d),k} = A_{(d)mas,k} - A_{(d)L,k}$

7. The average, $x_{\Delta A}$ and standard deviation, $s_{\Delta A}$ of $\Delta A_{(d),k}$ is determined for each durations.

8. The $x_{\Delta A}$, $s_{\Delta A}$ are normalized using the largest value in the maximum annual series.

9. The trend of $x_{\Delta A}$ to decrease with increasing durations, d is modeled for a wide range of d. Using curve fitting this relationship was found to be a power relationship of the form

   $x_{\Delta A\text{-}trend} = -\text{A} \ln(d) + \text{B}$

10. The $x_{\Delta A}$ values are subtracted from the $x_{\Delta A\text{-}trend}$ values for each d. This identifies the d which produces the least difference between the $x_{\Delta A}$ and the trend. The smaller (more negative) the difference the more consistent the $A_{(d)L,k}$ and the $A_{(d)mas,k}$ and the more sensitive the landslide is to that duration of the antecedent precipitation, d.

11. This process is completed for multiple d. Figures H1 and H2 show the results of this analysis for both a long and short range of. The d selected are local minimums on the Trend - average plot.

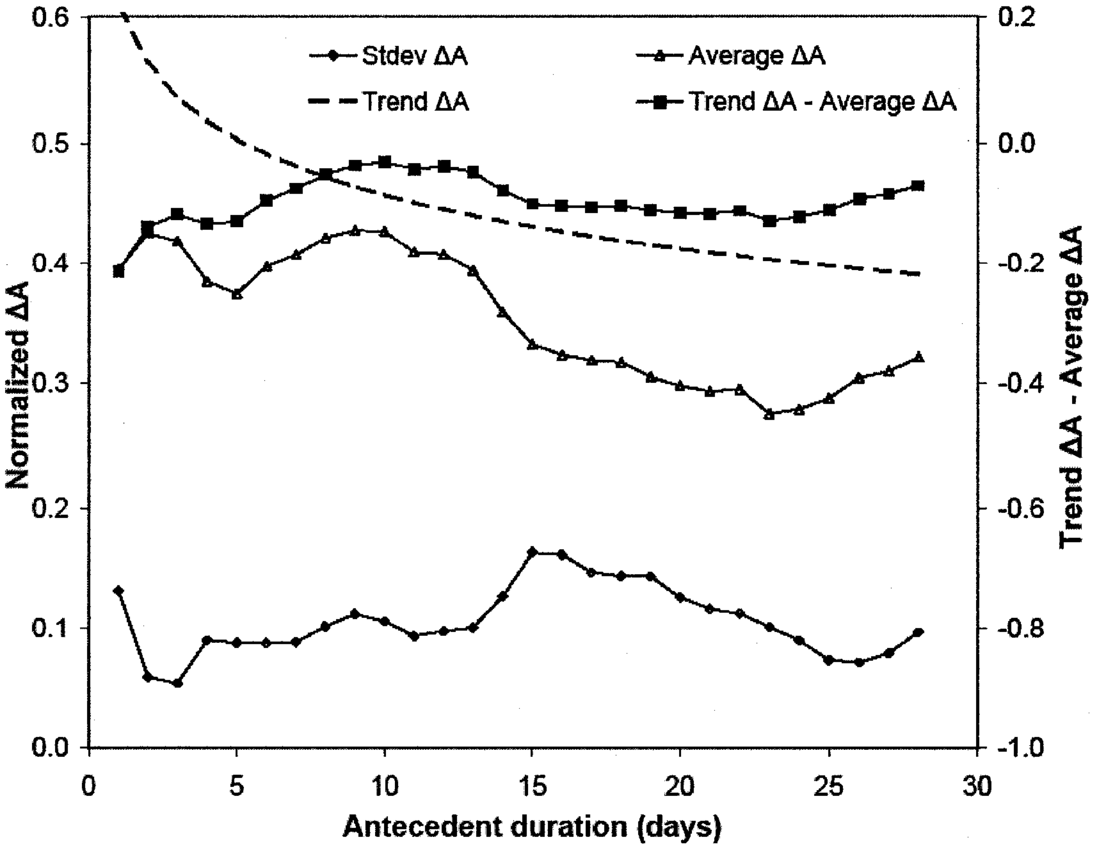

Figure H1 Identification of the antecedent duration between 1 and 30 days to which landslides are most sensitive

This correlation process identifies the landslide antecedent durations with the most similarity with the maximum annual series. The duration identified by this process is selected as the index used to determine the antecedent duration thresholds above which landsides are more likely to occur. It can be seen from Figure H1 that the difference is a maximum for d = 5 days and d = 23 days. Similarly, Figure H2 indicates a maximum difference for d = 21 days (d = 23 days was not calculated for Figure H2) and d = 150 days.

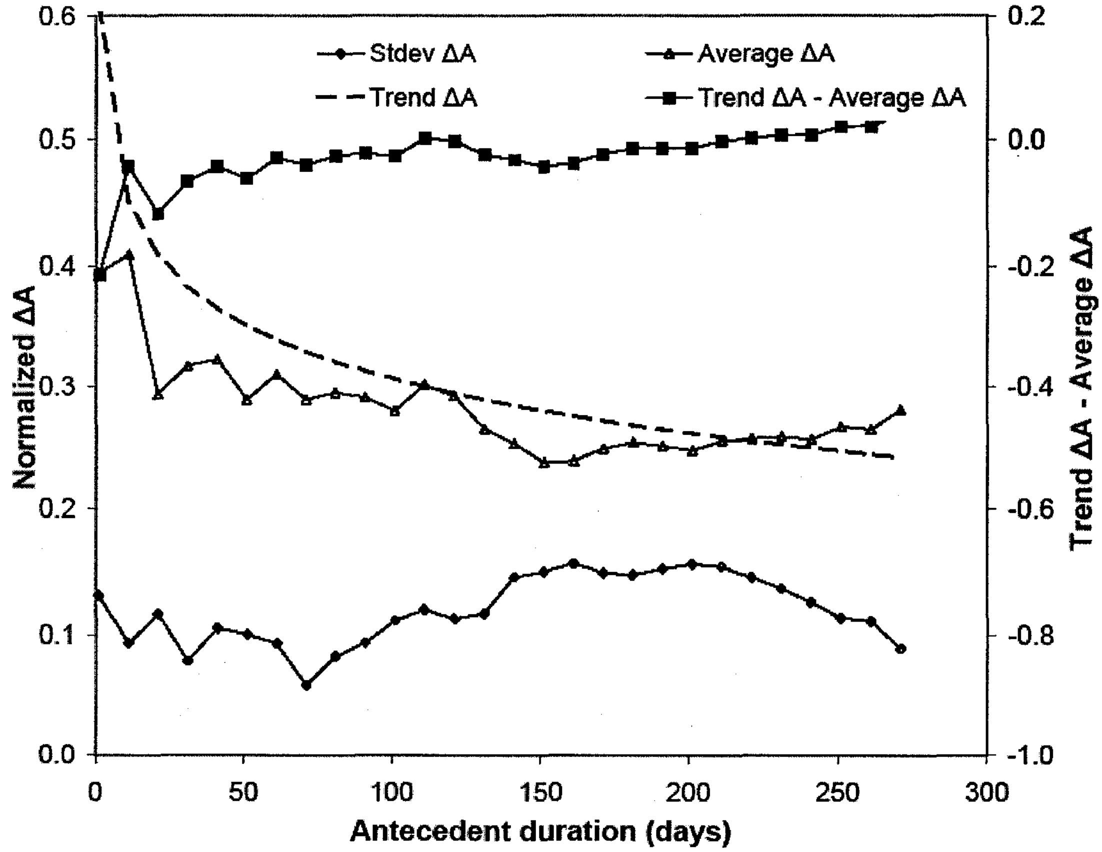

Figure H2 Identification of the antecedent duration between 1 and 300 days to which landslides are most sensitive

12. From this step onward the procedures of Chleborad (2000) are followed.

Appendix I Generalized Extreme Value distribution

I 1.0 GEV Steps

Using the Generalized Extreme Value (GEV) distribution (after Chen 2007) function the probability (P) of Z equalling or exceeding z can be calculated. The GEV distribution can be expressed as:

$$P(Z \leq z) = F(z;\mu,\sigma,k) = \exp\left\{-\left(1-\frac{k(z-\mu)}{\sigma}\right)^{1/k}\right\} \qquad \text{Equation I.1}$$

Where μ, σ, k are the location, scale and shape parameter respectively but are not equal to the moment estimates used in the Gumbel distribution. To find the best fit of the GEV to the data the best combination of location, scale and shape parameters is determined using an iterative method for each series of maximum annual antecedent precipitation values z_i.

The location, scale, and shape parameters can be determined by initially assuming they are equal to Gumbel of μ, σ, k and then solving the following system of equations and iterating the Maximum Likelihood Estimates $\hat{\mu}, \hat{\sigma}, \hat{k}$ or $\hat{\theta}$ for solution. The steps are as follows:

1. Find the average of the population, z, $\bar{z}$ and the standard deviation, s.
2. Use the Gumbel estimate of the first moment

   $$\mu = \bar{z} - \frac{\gamma s\sqrt{6}}{\pi} \quad and \quad \sigma = \frac{s\sqrt{6}}{\pi} \quad and\ assume \quad k = 0.1 \text{ initially}$$

   Set $\theta^{(0)} = (\mu, \sigma, k)$

3. Calculate the gradient vector $G(\theta) = \left(\frac{\partial l}{\partial u}, \frac{\partial l}{\partial \sigma}, \frac{\partial l}{\partial k}\right)$

Where

$$\frac{\partial l}{\partial u}=\frac{(1-k)}{\sigma}\sum_{i=1}^{n}\left[\frac{1}{\alpha_i}\right]-\frac{1}{\sigma}\sum_{i=1}^{n}\left[\frac{1}{\alpha_i}\exp\left(\frac{\ln\alpha_i}{k}\right)\right]$$

$$\frac{\partial l}{\partial \sigma}=-\frac{n}{\sigma}+\frac{(1-k)}{\sigma^2}\sum_{i=1}^{n}\left[\frac{z_i-\mu}{\alpha_i}\right]-\frac{1}{\sigma^2}\sum_{i=1}^{n}\left[\frac{(z_i-\mu)}{\alpha_i}\exp\left(\frac{\ln\alpha_i}{k}\right)\right]$$

$$\frac{\partial l}{\partial k}=-\sum_{i=1}^{n}\left[\frac{\ln\alpha_i}{k}\right]-\frac{(1-k)}{k^2}\sum_{i=1}^{n}\left[\frac{k(z_i-\mu)}{\alpha_i\sigma}+\ln\alpha_i\right]+\frac{1}{k^2}\sum_{i=1}^{n}\left[\left\{\frac{k(z_i-\mu)}{\alpha_i\sigma}+\ln\alpha_i\right\}\left\{\exp\left(\frac{\ln\alpha_i}{k}\right)\right\}\right]$$

And $\alpha_i=1-\frac{k(z_i-u)}{\sigma}$

4. Calculate the $I(\theta)=I_{ij}$ $where\ I_{ij}(\theta)=I_{ji}(\theta)$

$$I_{11}(\theta)=\frac{nu}{\sigma^2}$$

$$I_{12}(\theta)=\frac{n}{\sigma^2 k}\left(u-\Gamma(2-k)\right)$$

$$I_{13}(\theta)=-\frac{n}{\sigma k}\left(v+\frac{u}{k}\right)$$

$$I_{22}(\theta)=\frac{n}{\sigma^2 k^2}\left(1-2\Gamma(2-k)+u\right)$$

$$I_{23}(\theta)=\frac{n}{\sigma k^2}\left(1-\gamma-\frac{1-\Gamma(2-k)}{k}-v-\frac{u}{k}\right)$$

$$I_{33}(\theta)=\frac{n}{k^2}\left(\frac{\pi^2}{6}+(1-\gamma-\frac{1}{k})^2+\frac{2v}{k}+\frac{u}{k^2}\right)$$

Where

$$u=(1-k)^2\Gamma(1-2k)$$

$$v=\Gamma(2-k)\left\{\psi(1-k)-\frac{1-k}{k}\right\}$$

$$\gamma=0.57721566$$

$$\psi(\varepsilon)=\frac{d\ln\left(\Gamma(\varepsilon)\right)}{d\varepsilon}$$

And $\Gamma(\varepsilon)$ is the Gamma function. The Gamma function and its derivative can be calculated using the Lanczos approximation (Toth 2006).

$$\Gamma(\varepsilon)=\frac{\sqrt{2\pi}}{\varepsilon}\left(p_0+\sum_{n=1}^{6}\frac{p_n}{\varepsilon+n}\right)(\varepsilon+5.5)^{(\varepsilon+\frac{1}{2})}e^{-(\varepsilon+\frac{11}{2})}$$

Where:

p_0 = 1.00000000019001

p_1 = 76.18009172947140

p_2 = -86.50532032941670

p_3 = 24.01409824083090

p_4 = -1.23173957245015

p_5 = 0.00120865097387

p_6 = -0.00000539523938

To compute the derivative of the Gamma Function, $d\log\Gamma(\varepsilon)/d\varepsilon$ (also known as the poly-gamma function or digamma function) numerically at value ε, take a very small increment, say, a = 0.00005 and compute (Chen 2007)

$$\frac{\log(\Gamma(\varepsilon + a)) - \log(\Gamma(\varepsilon))}{a}$$

For example, let ε = 4.5, then

$$\frac{\log(\Gamma(4.5 + 0.00005)) - \log(\Gamma(4.5))}{0.00005} = 1.388877$$

5. Use $\theta^{(j)} = \theta^{(j-1)} + I^{-1}(\theta^{(j-1)})G(\theta^{(j-1)})$ Equation I2

For j=1,2.... At each j check if $\max\left(\left|\theta^{(j)} - \theta^{(j-1)}\right|\right) \leq \delta$

Where $\max\left(\left|\theta^{(j)} - \theta^{(j-1)}\right|\right) = \max\left(\left| \mu^{(j)} - \mu^{(j-1)}\right|, \ \left|\sigma^{(j)} - \sigma^{(j-1)}\right|, \ \left|k^{(j)} - k^{(j-1)}\right|\right)$.

That is find $|\mu^{(j)} - \mu^{(j-1)}|$, $|\sigma^{(j)} - \sigma^{(j-1)}|$, $|k^{(j)} - k^{(j-1)}|$ separately and then take the maximum of the three terms and compare it to δ, where δ is equal to some small number like 0.00005. If $\max\left(\left|\theta^{(j)} - \theta^{(j-1)}\right|\right) \leq \delta$ stop and use $\hat{\theta} = \theta^{(j)}$ to approximate the final $\hat{\mu}$, $\hat{\sigma}$ and $\hat{k}$. If $\max\left(\left|\theta^{(j)} - \theta^{(j-1)}\right|\right) > \delta$ use the Equation I2 to further refine the maximum likelihood estimates.

The return period, T_i, of each value antecedent precipitation, z_i is provided by the plotting position relationship discussed in Appendix B.

$$T_i = \tau = \frac{(m+1)}{r_i}$$

Where m is the number of years of record in the maximum annual series and r_i is the rank of the i^{th} value in the annual series.

The estimated antecedent precipitation, $\hat{z}_i$ can be calculated by solving using $\hat{\mu}$, $\hat{\sigma}$ and $\hat{k}$ the solving Equation I1 for z_i and using the relationship $T_i = 1/P_i$.

$$\hat{z}_i = \mu + \frac{\sigma}{k}\left\{1 - \left[-\ln\left(1 - \frac{1}{T}\right)\right]^k\right\}$$

Plotting z_i and $\hat{z}_i$ against each other forms the Q-Q plot from which .

I 2.0 Example

1. Using the 180 day antecedent precipitation data from 1952 to 2007 from Maple Ridge, BC contained in Table I1 below.

   Rank 180 day antecedent

   $\bar{z}$ = 1278.1827, s = 255.13897.

2. Use the Gumbel estimate of the first moment

$$\mu = 1278.1827 - \frac{(0.57721566)(255.13897)\sqrt{6}}{\pi}$$

and

$$\sigma = \frac{255.13897\sqrt{6}}{\pi}$$

So

μ = 1163.3566 and

σ = 198.93104

Therefore $\theta^{(o)} = \begin{pmatrix} 1163.3566 \\ 198.93104 \\ 0.1 \end{pmatrix}$

3. Calculate $G(\theta^{(0)})$

$$\frac{\partial l}{\partial u} = \frac{(1-k)}{\sigma}\sum_{i=1}^{n}\left[\frac{1}{\alpha_i}\right] - \frac{1}{\sigma}\sum_{i=1}^{n}\left[\frac{1}{\alpha_i}\exp\left(\frac{\ln\alpha_i}{k}\right)\right]$$

Using $\alpha_i = 1 - \frac{k(z_i - u)}{\sigma}$ from Table I1 below for α_i and $\frac{1}{\alpha_i}\exp\left(\frac{\ln\alpha_i}{0.1}\right)$

$$\frac{\partial l}{\partial u} = \frac{(1-0.1)}{198.93104}(56.191897) - \frac{1}{198.93104}(56.316197)$$

$$\frac{\partial l}{\partial u} = -0.02887163$$

$$\frac{\partial l}{\partial \sigma} = -\frac{n}{\sigma} + \frac{(1-k)}{\sigma^2}\sum_{i=1}^{n}\left[\frac{z_i-\mu}{\alpha_i}\right] - \frac{1}{\sigma^2}\sum_{i=1}^{n}\left[\frac{(z_i-\mu)}{\alpha_i}\exp\left(\frac{\ln\alpha_i}{k}\right)\right]$$

Using $\frac{z_i-\mu}{\alpha_i}$ and $\frac{(z_i-\mu)}{\alpha_i}\exp\left(\frac{\ln\alpha_i}{k}\right)$ from Table I1

$$\frac{\partial l}{\partial \sigma} = -\frac{52}{198.93104} + \frac{(1-0.1)}{(198.93104)^2}(8338.9840) - \frac{1}{(198.9104)^2}(-10061.246)$$

$$\frac{\partial l}{\partial \sigma} = -\frac{52}{198.9} + \frac{(1-0.1)}{(198.9)^2}(8338.98) - \frac{1}{(198.9)^2}(-10061.2)$$

$$\frac{\partial l}{\partial \sigma} = 0.18249351$$

$$\frac{\partial l}{\partial k} = -\sum_{i=1}^{n}\left[\frac{\ln\alpha_i}{k}\right] - \frac{(1-k)}{k^2}\sum_{i=1}^{n}\left[\frac{k(z_i-\mu)}{\alpha_i\sigma} + \ln\alpha_i\right] + \frac{1}{k^2}\sum_{i=1}^{n}\left[\left\{\frac{k(z_i-\mu)}{\alpha_i\sigma} + \ln\alpha_i\right\}\left\{\exp\left(\frac{\ln\alpha_i}{k}\right)\right\}\right]$$

$$\frac{\partial l}{\partial k} = -\sum_{i=1}^{n}\left[\frac{\ln\alpha_i}{k}\right] - \frac{(1-0.1)}{(0.1)^2}\sum_{i=1}^{n}M_i + \frac{1}{k^2}\sum_{i=1}^{n}N_i$$

$$where\ M_i = \frac{k(z_i-\mu)}{\alpha_i\sigma} + \ln\alpha_i$$

$$and\ N_i = \left\{\frac{k(z_i-\mu)}{\alpha_i\sigma} + \ln\alpha_i\right\}\left\{\exp\left(\frac{\ln\alpha_i}{k}\right)\right\}$$

Using $\left[\frac{\ln\alpha_i}{k}\right]$, M_i and N_i from Table I1

$$\frac{\partial l}{\partial k} = -(-35.617826) - \frac{(1-0.1)}{(0.1)^2}(0.63011437) + \frac{1}{k^2}(0.62650294)$$

$$\frac{\partial l}{\partial k} = 41.557826$$

$$G(\theta^{(0)}) = \begin{pmatrix} -0.02887167 \\ 0.18249345 \\ 41.557826 \end{pmatrix}$$

4. Calculate the $I(\theta) = I_{ij}$ $where\ I_{ij}(\theta) = I_{ji}(\theta)$

$$u = (1-k)^2\Gamma(1-2k)$$

$$u = (1-0.1)^2\Gamma(1-2(0.1))$$

$u = (0.81)\Gamma(0.8) = 0.81)(1.1642297)$

u = 0.94302607

And

$$v = \Gamma(2-k)\left\{\psi(1-k) - \frac{1-k}{k}\right\}$$

$$v = \Gamma(2-0.1)\left\{\psi(1-0.1) - \frac{(1-0.1)}{0.1}\right\}$$

$$v = \Gamma(1.9)\{\psi(0.9) - 9\} = 0.96176583)(-0.75492698 - 9)$$

v = -9.3819555

And

$$I_{11}(\theta) = \frac{nu}{\sigma^2}$$

$$I_{11}(\theta) = \frac{52(0.94302607)}{(198.93104)^2}$$

$$I_{11}(\theta) = 0.0012391445$$

And

$$I_{12}(\theta) = \frac{n}{\sigma^2 k}(u - \Gamma(2-k))$$

$$I_{12}(\theta) = \frac{52}{(198.93104^2)(0.1)}(0.94302607 - \Gamma(2-0.1)))$$

$$I_{12}(\theta) = 0.01314022(0.94302607 - 0.96176583)$$

$$I_{12}(\theta) = -0.00024624213$$

And

$$I_{13}(\theta) = -\frac{n}{\sigma k}\left(v + \frac{u}{k}\right)$$

$$I_{13}(\theta) = -\frac{52}{(198.93104)(0.1)}\left(-9.3819555 + \frac{0.94302607}{0.1}\right)$$

$$I_{13}(\theta) = -0.12626846$$

$$I_{22}(\theta) = \frac{n}{\sigma^2 k^2}\left(1 - 2\Gamma(2-k) + u\right)$$

$$I_{22}(\theta) = \frac{52}{(198.93104)^2(0.1)^2}\left(1 - 2(\Gamma(2-0.1) + 0.94302607\right)$$

$$I_{22}(\theta) = 0.13140087(1 - 2(0.96176583) + 0.94302607)$$

$$I_{22}(\theta) = -0.0025615817$$

And

$$I_{23}(\theta) = \frac{n}{\sigma k^2}\left(1 - \gamma - \frac{1-\Gamma(2-k)}{k} - v - \frac{u}{k}\right)$$

$$I_{23}(\theta) = \frac{52}{(198.93104)(0.1)^2}\left(1 - 0.57721567 - \frac{\left(1-\Gamma(2-0.1)\right)}{0.1} - (-9.3819555) - \frac{0.94302607}{0.1}\right)$$

$$I_{23}(\theta) = 26.139712\left(0.42278433 - \frac{(1-\Gamma(1.9))}{0.1} + 9.3818555 - 9.4302607\right)$$

$$I_{23}(\theta) = 26.139712\left(0.37447911 - \frac{(1-0.96176583)}{0.1}\right)$$

$$I_{23}(\theta) = -0.20552523$$

Finally

$$I_{33}(\theta) = \frac{n}{k^2}\left(\frac{\pi^2}{6} + (1-\gamma-\frac{1}{k})^2 + \frac{2v}{k} + \frac{u}{k^2}\right)$$

$$I_{33}(\theta) = \frac{52}{(0.1)^2}\left(\frac{\pi^2}{6} + \left(1 - 0.57721567 - \frac{1}{0.1}\right)^2 + \frac{2(-9.3819555)}{0.1} + \frac{0.94302607}{(0.1)^2}\right)$$

$$I_{33}(\theta) = 5200\left(1.6449341 + 91.72306 - 187.63911 + 94.302607\right)$$

$$I_{33}(\theta) = 163.75616$$

So

$$I_{ij}(\theta^0) = \begin{pmatrix} 0.0012391445 & -0.00024624213 & -0.12626846 \\ -0.00024624213 & 0.00256158 & -0.20552523 \\ -0.12626846 & -0.20552523 & 163.75616 \end{pmatrix}$$

$$I_{ij}^{-1}(\theta^0) = \begin{pmatrix} 933.98729 & 164.08913 & 0.92611838 \\ 164.08913 & 462.92511 & 0.70752803 \\ 0.92611838 & 0.70752803 & 0.00770874 \end{pmatrix}$$

5. Use $\theta^{(j)} = \theta^{(j-1)} + I^{-1}(\theta^{(j-1)})G(\theta^{(j-1)})$ Equation I2

For j=1

$$\theta^1 = \begin{pmatrix} 1163.3590 \\ 198.9310 \\ 0.1 \end{pmatrix} + \begin{pmatrix} 933.98729 & 164.08913 & 0.92611838 \\ 164.08913 & 462.92511 & 0.70752803 \\ 0.92611838 & 0.70752803 & 0.00770874 \end{pmatrix} \begin{pmatrix} -0.02887167 \\ 0.18249345 \\ 41.557826 \end{pmatrix}$$

And therefore

$$\theta^1 = \begin{pmatrix} 1204.8234 \\ 308.07765 \\ 0.52273927 \end{pmatrix}$$

And $\max\left(\left|\theta^{(j)} - \theta^{(j-1)}\right|\right) = 109.14661$ which is larger than 0.00005 so repeat steps 1 to 5 until $\max\left(\left|\theta^{(j)} - \theta^{(j-1)}\right|\right) \leq \delta$. For this example this takes 22 iterations and

$$\hat{\theta} = \theta^{(22)} = \begin{pmatrix} 1211.7510 \\ 270.7373 \\ 0.46398622 \end{pmatrix}$$

So the final maximum likelihood estimates are $\hat{\mu} = 1211.8$, $\hat{\sigma} = 270.7$ and $\hat{k} =$ 0.4640.

Table I1 Maximum annual series of the 180 day antecedent precipitation for Maple Ridge, BC

Rank (i)	Max annual $A_{(180)mas}$	$1/\alpha_i$	$\frac{1}{\alpha_i}\exp\left(\frac{\ln\alpha_i}{k}\right)$	$\frac{z_i-\mu}{\alpha_i}$	$\exp\left(\frac{\ln\alpha_i}{k}\right)$	M_i	N_i
52	608.8	0.7820	9.1438	-433.7	2.4590	0.02790	0.3262
51	791.5	0.8425	4.6754	-313.3	1.7137	0.01388	0.0770
50	820	0.8528	4.1913	-292.8	1.5922	0.01203	0.0591
49	865.8	0.8699	3.5063	-258.8	1.3939	0.00928	0.0374
48	867.2	0.8704	3.4870	-257.8	1.3878	0.00920	0.0369
47	972.6	0.9125	2.2798	-174.1	0.9157	0.00407	0.0102
46	1020.1	0.9328	1.8698	-133.6	0.6954	0.00236	0.0047
45	1039.4	0.9413	1.7229	-116.7	0.6045	0.00179	0.0033
44	1051.8	0.9469	1.6340	-105.6	0.5456	0.00146	0.0025
43	1077.2	0.9585	1.4646	-82.6	0.4240	0.00089	0.0014
42	1079.1	0.9594	1.4526	-80.8	0.4148	0.00085	0.0013
41	1090.9	0.9649	1.3799	-69.9	0.3578	0.00063	0.0009
40	1099.1	0.9687	1.3312	-62.2	0.3179	0.00050	0.0007
39	1122.6	0.9799	1.2002	-39.9	0.2028	0.00020	0.0003
38	1134.9	0.9859	1.1364	-28.1	0.1420	0.00010	0.0001
37	1144.4	0.9906	1.0891	-18.8	0.0948	0.00004	0.0000
36	1150.9	0.9938	1.0578	-12.4	0.0624	0.00002	0.0000
35	1162.8	0.9997	1.0025	-0.6	0.0028	0.00000	0.0000
34	1175.4	1.0061	0.9468	12.1	-0.0607	0.00002	0.0000
33	1195.3	1.0163	0.8644	32.5	-0.1619	0.00013	0.0001
32	1207.3	1.0226	0.8179	44.9	-0.2234	0.00025	0.0002
31	1210	1.0240	0.8077	47.8	-0.2373	0.00028	0.0002
30	1230.5	1.0349	0.7342	69.5	-0.3433	0.00060	0.0004
29	1235.9	1.0378	0.7158	75.3	-0.3715	0.00070	0.0005
28	1259.3	1.0507	0.6409	100.8	-0.4943	0.00124	0.0008
27	1261.2	1.0517	0.6351	102.9	-0.5044	0.00129	0.0008
26	1267	1.0550	0.6178	109.3	-0.5351	0.00146	0.0009
25	1277.7	1.0610	0.5870	121.3	-0.5920	0.00179	0.0010
24	1326.2	1.0892	0.4636	177.4	-0.8540	0.00375	0.0016
23	1327.2	1.0898	0.4614	178.5	-0.8595	0.00380	0.0016
22	1354.8	1.1065	0.4022	211.8	-1.0119	0.00530	0.0019
21	1363.9	1.1121	0.3843	223.0	-1.0626	0.00585	0.0020
20	1367.2	1.1142	0.3780	227.1	-1.0811	0.00606	0.0021
19	1386.6	1.1264	0.3426	251.5	-1.1903	0.00737	0.0022
18	1402.9	1.1369	0.3151	272.3	-1.2831	0.00859	0.0024
17	1404.2	1.1377	0.3130	274.0	-1.2905	0.00870	0.0024
16	1457.2	1.1733	0.2373	344.8	-1.5983	0.01348	0.0027
15	1467.5	1.1805	0.2246	359.0	-1.6592	0.01456	0.0028
14	1469.2	1.1817	0.2226	361.4	-1.6693	0.01474	0.0028
13	1475.1	1.1858	0.2157	369.7	-1.7044	0.01539	0.0028
12	1479.8	1.1892	0.2103	376.3	-1.7325	0.01591	0.0028
11	1507.9	1.2095	0.1806	416.7	-1.9019	0.01929	0.0029
10	1523.7	1.2212	0.1655	440.1	-1.9984	0.02137	0.0029
9	1572.7	1.2591	0.1258	515.4	-2.3038	0.02870	0.0029
8	1588.8	1.2720	0.1147	541.2	-2.4063	0.03142	0.0028
7	1595.2	1.2773	0.1105	551.6	-2.4473	0.03255	0.0028
6	1603.1	1.2838	0.1056	564.5	-2.4981	0.03397	0.0028
5	1640.6	1.3156	0.0847	627.9	-2.7431	0.04131	0.0027
4	1647.7	1.3218	0.0812	640.2	-2.7902	0.04281	0.0026
3	1669	1.3408	0.0714	678.0	-2.9327	0.04754	0.0025
2	1685.9	1.3563	0.0644	708.7	-3.0473	0.05153	0.0024
1	1730.4	1.3987	0.0488	793.1	-3.3554	0.06315	0.0022
Sum		56.191897	56.316197	8338.984	-35.617826	0.63011437	0.62650294

The standard deviation, s = 255.1; the average, $\bar{x}$ = 1278.1

Appendix J Goodness of fit tests

J 1.0 Sample Correlation test

The sample correlation coefficient (Devore 1982) test compares the recorded and predicted maximum annual series to see how much they differ from each other. The correlation coefficient, r is calculated using:

$$r = \frac{n\left(\sum_{i=1}^{n} u_i v_i\right) - \left(\sum_{i=1}^{n} u_i\right)\left(\sum_{i=1}^{n} v_i\right)}{\sqrt{n\left(\sum_{i=1}^{n} u_i^2\right) - \left(\sum_{i=1}^{n} u_i\right)^2}\sqrt{\left(\sum_{i=1}^{n} v_i^2\right) - \left(\sum_{i=1}^{n} v_i\right)^2}} \qquad \text{Equation J1}$$

Where u_i is the antecedent precipitation maximum annual series, z_i and v_i is the predicted antecedent precipitation, $\hat{z}_i$ with the same probability of occurrence, P_i (or return period $T_i=1/P_i$) as the maximum annual series based on the rank of each value, z_i in the series.

$$P_i = \frac{i}{(n+1)}$$

Where i is the rank of z_i in the maximum annual series and n is the number of values in the maximum annual series or the number of years of record.

$$\hat{z}_i = \mu + \frac{\sigma}{k}\left\{1 - \left[-\ln(1 - P_i)\right]^k\right\}$$

J 2.0 Example

The results of the calculations for the sample correlation test are included in Table J1 using the same data as in the previous example but omitting some values in the middle of the series to conserve space.

Using $\hat{\mu} = 1211.8$, $\hat{\sigma} = 270.7$ and $\hat{k} = 0.4640$ and $n = 52$.

Table J1 Part of the maximum annual series of the 180 day antecedent precipitation for Maple Ridge, BC

Rank, i	Max annual $A_{(180)mas}$, z_i	P_i	T_i	Predicted annual series, $\hat{z}_i$
52	608.8	0.019	1.019	689.1
51	791.5	0.038	1.039	783.3
50	820	0.057	1.060	843.4
49	865.8	0.075	1.082	888.9
3	1669	0.943	17.7	1639.3
2	1685.9	0.962	26.5	1666.6
1	1730.4	0.981	53.0	1702.5

r = 0.9946

Appendix K Additional GEV analysis of precipitation data

K 1.0 Lytton, BC

Precipitation data for the Lytton, BC area was analyzed using the GEV and Gumbel frequency distributions. Data was combined for the EC weather stations ID 961, 962, 963 and 966 (Lytton 2) in the Lytton, BC area for the years 1917 to 2007. Data was edited to account for missing data resulting in low antecedent precipitation. With the exception of the $A_{(0\text{-}60)}$ the GEV fits the data better than the Gumbel. Neither fits the $A_{(0\text{-}60)}$ very well. The shape parameter, k is close to zero indicating the Lytton antecedent precipitation is neither strongly upper or lower bound limited.

Table K1 GEV analysis of the Lytton, BC maximum annual series for the years 1917 to 2007 excluding those years with insufficient data

Rank	1-day	3-day	7-day	15-day	30-day	60-day	90-day	120-day	150-day	180-day	270-day	365-day
μ	31.3	48.1	62.6	79.1	107.3	158.1	204.6	244.6	279.8	317.4	398.1	510.7
σ	10.7	17.5	23.1	30.8	42.8	63.4	79.6	96.8	104.0	103.1	110.6	123.9
k	-0.1370	-0.0444	-0.0495	-0.0534	-0.1058	-0.0267	0.0057	0.0524	0.0527	0.0424	0.0352	-0.0605
n	87	87	87	87	86	86	86	84	83	82	83	83
r	0.9952	0.9845	0.9910	0.9948	0.9800	0.9786	0.9927	0.9911	0.9959	0.9957	0.9949	0.9939
1	103.5	157.3	161.3	222.95	296	422.4	557.1	682.2	742.4	758.3	856.5	1140.0
2	93	121.6	155.6	209.9	288.5	361.05	492.4	553.75	651	711.4	813.2	1076.3
3	76.7	109.5	151.7	202.4	277.5	359.9	458.1	548.35	613.25	632.15	797.5	960.5
4	69.9	97.9	147.45	182.3	276.9	353.95	456.9	494.3	593.25	631.1	748.6	941.5
5	68.7	94.8	146	176.9	251.7	353.2	455.35	490.9	557.7	602.3	723.1	936.3
6	66	93.4	140.4	172.05	249	351.5	416.1	485.1	526.3	545.1	660.5	928.1
7	61	89.7	124.2	167.1	242.4	348.5	407.7	478.7	515.25	544.6	655.6	905.5
8	60.5	87.6	121.5	166.6	237.7	346.7	392.1	461.8	511.3	534.9	646.6	866.8
9	58.6	87	120.4	160.3	237.1	342.6	386.15	452.6	507.2	534.3	634.1	830.4
10	58.4	86.3	115	157.05	219.2	342.4	383.35	443.25	490.05	529.4	633.8	769.6
11	57.4	85.4	111.7	150.7	213.75	342.1	381	442.8	481.2	519.45	630.8	765.5
12	57	84.1	110.5	143.6	212.95	318.55	376	435.7	473.6	513.4	629.2	761.6
13	56.4	83.8	109.2	142.6	211.85	314.15	369.6	417.05	469.4	513.3	616.2	756.4
14	52.6	81.4	107.7	140.05	210.8	290.2	360.35	413.9	466.2	507	608.8	745.7
15	51.8	80.1	106.7	140	206.1	280.7	343.1	407.1	465.95	506.9	603.4	744.3
16	51.8	78.7	102.9	139	201.3	266.15	329.5	406.9	436.2	492.85	593.4	741.9
17	51.6	77.7	102.7	136.4	197.3	257.3	327.1	399.6	427.8	491.4	591.8	739.1
18	51.1	77.5	100.4	134.85	190.3	256.8	326.2	389.05	423.8	475.6	570.7	721.5
19	50.2	77.5	100.4	129.35	187.8	254.7	315.4	388.25	421.4	463.75	561.1	718.4

Rank	1-day	3-day	7-day	15-day	30-day	60-day	90-day	120-day	150-day	180-day	270-day	365-day
20	50	77	99.8	124.5	187	254.45	314.55	385.8	416.9	462.1	552.7	700.4
21	48.8	76.2	98.5	124.2	184.4	248.4	312.95	373.75	414.15	448.15	524.5	696.7
22	46.8	74	98	121.8	174.1	245.7	312.7	371.9	407	446.4	522.7	681.4
23	46.2	72.4	97.35	118.75	170.75	238.25	310.55	371.25	406.5	446.2	520.9	678.4
24	46	72.4	93.6	113.7	166.8	235.5	307.55	369.4	396.9	434.4	504.7	648.6
25	45.7	72.2	91.8	113.45	163.5	230	305.15	363.1	395.9	430.05	499.0	648.5
26	44	71.5	90	113.4	157.55	229.95	303.25	352.1	391.45	427.7	496.8	646.5
27	43.2	71.4	89.9	113	150.6	226.8	297.8	351.7	386.45	422.3	487.2	635.4
28	42.2	70.4	89.2	112.7	145.85	214.05	297.4	350.7	380.25	413.05	482.0	620.6
29	42.2	68.7	87	112.7	142.5	211.8	290.7	345.25	376.5	405.55	480.6	616.1
30	42.2	65.3	86.6	110.7	142.2	210.8	289.4	342.95	373.5	398	475.3	601.7
31	41.9	64.8	86.4	109.1	141.45	209.1	287.4	336.2	365.8	395	475.2	585.3
32	41.5	63.5	83.6	104.8	141	208.6	281.6	328.4	360.95	394.5	474.5	583.0
33	40.9	62.8	82.9	104.6	139.15	204.6	279.55	326.6	357.15	391.8	464.7	579.8
34	40.8	62.6	82.7	103.6	138.9	204	274.8	324.95	356.9	384.95	460.3	576.0
35	38.6	62.2	81.45	101.9	129.7	201.65	270.35	317.85	352.1	384.05	449.3	565.6
36	38.1	62	80.6	98.8	128.7	194.85	259.75	316.9	348.75	368.65	446.9	563.6
37	38.1	61.5	77.3	98.6	127.25	192	256.85	316	347.5	367.5	446.0	559.8
38	38.1	61.4	76.1	98.15	125.6	189.35	253.45	313.7	336.35	366.65	442.7	554.7
39	38.1	60.2	74.7	94.55	123.65	188.05	253.15	310.85	325.9	365.1	442.3	553.4
40	37.6	60.2	73.75	94.05	122.6	183.45	250.75	305.9	320.65	362.95	440.7	551.2
41	37.3	60	72.9	93.25	119.4	181.95	241.4	296.3	318.05	358.35	439.8	550.7
42	35.6	59.4	72.8	93	119.25	179.85	235	286.55	316.25	351.25	438.3	545.7
43	35.6	54.3	72	89.1	118.7	175.85	231.35	280.2	309.15	346.85	432.4	543.6
44	35.6	53.8	71.8	88.7	117.4	171.4	230.6	274.8	308.35	345.2	430.5	542.1
45	35.5	52.1	69.9	88.2	115.5	170.1	226.3	274	305.45	341.75	426.6	539.6
46	35	51.7	69.3	87.95	115	170	222.2	270.25	294.8	341.05	415.3	537.8
47	34.5	51.4	68	86.4	113.2	169.45	211.15	267	293.8	325.35	415.2	530.2
48	34.5	50.6	68	83.8	112.25	167.25	211.1	253.95	290.7	321.2	414.2	528.7
49	34.3	50.5	67.8	83.8	111	163.5	208.4	252.05	288.75	319.3	412.0	526.6
50	34.3	50.1	66.55	82.2	109.35	162.1	207.25	243.8	287.55	317.05	410.4	524.9
51	33.8	49.5	66.4	81.4	108.95	161.45	206.9	243.35	285.25	310.15	404.8	509.6
52	33	49.2	66.3	81.15	108.85	160.45	203.55	242.5	276.3	309.5	403.7	509.1
53	31.2	48.1	65.6	80	108.7	159.4	203.1	241.4	273.7	309.2	401.7	507.4
54	31	48.05	62.75	79.55	106.45	158.9	197	241.3	272.95	307.15	398.9	505.5
55	31	47.8	62.7	78.75	104.9	156.25	196.35	234.95	268.05	306.8	398.6	497.6
56	30.5	45.8	58.4	78.6	103.3	155.6	195.5	231.75	267.65	305.25	398.5	494.4
57	30.2	45.6	57.65	77.5	102.4	155.05	195.45	224.5	265.7	304.65	396.2	490.9
58	30	44.2	57.3	76.2	102.2	151.75	192.9	219.1	263.85	303.5	393.7	489.6
59	29.5	43.7	55.9	74.9	99.4	150.85	192.2	213.8	261.85	302	393.2	489.5
60	29.5	43.45	54.9	73.5	99.1	149.55	191.85	210.45	259	300.4	393.1	476.9
61	29.2	43.2	54.25	72.6	98.6	147.5	182.7	207.8	254.95	296	371.4	473.2
62	29	43.2	54.1	71	97.75	143.75	179.35	206.55	251.55	279.6	365.6	470.3
63	27.9	42.7	53.9	69.95	95.6	143.4	177.85	206.2	236.8	277.25	364.9	469.9
64	27.9	42.6	53.8	69.4	95.3	139.9	175.7	205.9	231.75	273.4	362.8	469.7
65	27.8	41.9	53.8	68.35	94.75	139.25	175.15	200.95	227.8	272.75	352.6	469.4
66	27.4	41.4	53.45	67.7	93.3	138.9	174.95	199.9	226.75	270.15	348.9	468.1

Rank	1-day	3-day	7-day	15-day	30-day	60-day	90-day	120-day	150-day	180-day	270-day	365-day
67	26.4	41.4	53.45	66.7	90.5	135.8	172.2	197.35	221.95	263	347.3	463.5
68	26.1	41.1	51.85	66.6	90.25	135.2	169.8	193.3	219.3	258.05	336.8	461.0
69	26	41.1	51.8	66.6	89.05	133.1	167.9	192.9	212.2	241.4	334.9	460.1
70	25.4	40.8	51.6	66.45	88.1	126.6	167.9	188.9	209.7	240.75	321.0	455.7
71	25	40.45	51.3	65.2	86.35	126.55	167.6	188.7	202.3	239.35	319.9	451.4
72	24.9	39.65	51.15	64.2	85.15	123.6	164.85	183.15	195.2	238.4	314.0	449.2
73	24.6	38.4	48.25	63.6	85.05	118.5	150.2	175.1	193.85	234.6	313.1	428.7
74	24.3	38	47.4	58.5	83.8	115.65	145.4	167.45	190.45	228.8	309.0	412.9
75	23.9	35.65	45.6	58.5	81.95	110.4	141.85	167.2	188.1	216.9	304.0	410.2
76	23.9	34.6	44.7	58.3	80.1	105.75	140.65	160.95	173.85	210.8	300.2	400.2
77	23.6	34	44.3	56.5	80.05	105.05	129.35	160.1	170.8	203.45	291.9	395.2
78	22.8	33	43.85	52.4	77.3	102.3	128.9	156.4	164.4	195.8	289.2	391.7
79	22.8	32.5	43.2	52	75.45	97.35	127.05	146.65	160.85	186.55	273.8	382.8
80	22.1	31.55	43.1	51.3	65.9	94.65	120	142.7	152.2	184.65	258.7	360.9
81	21.6	30.2	42.6	50.95	65.15	92.95	116.85	130.1	150.55	178.5	252.4	349.7
82	21.6	29.7	42.45	45.55	58.9	89.2	115.4	127.25	131.75	173.65	232.7	345.1
83	21	27.7	38.7	43.2	57.35	88.9	113.45	120.15	128.95		226.2	318.1
84	20.3	27.65	36.8	40.1	51.5	74.05	103.65	117.35				
85	19.4	27.5	33.6	39.75	50.75	74.05	103.15					
86	17.3	27.5	32.05	39.7	48.55	66.65	100.7					
87	16.2	23.4	29.2	39.6								
88												

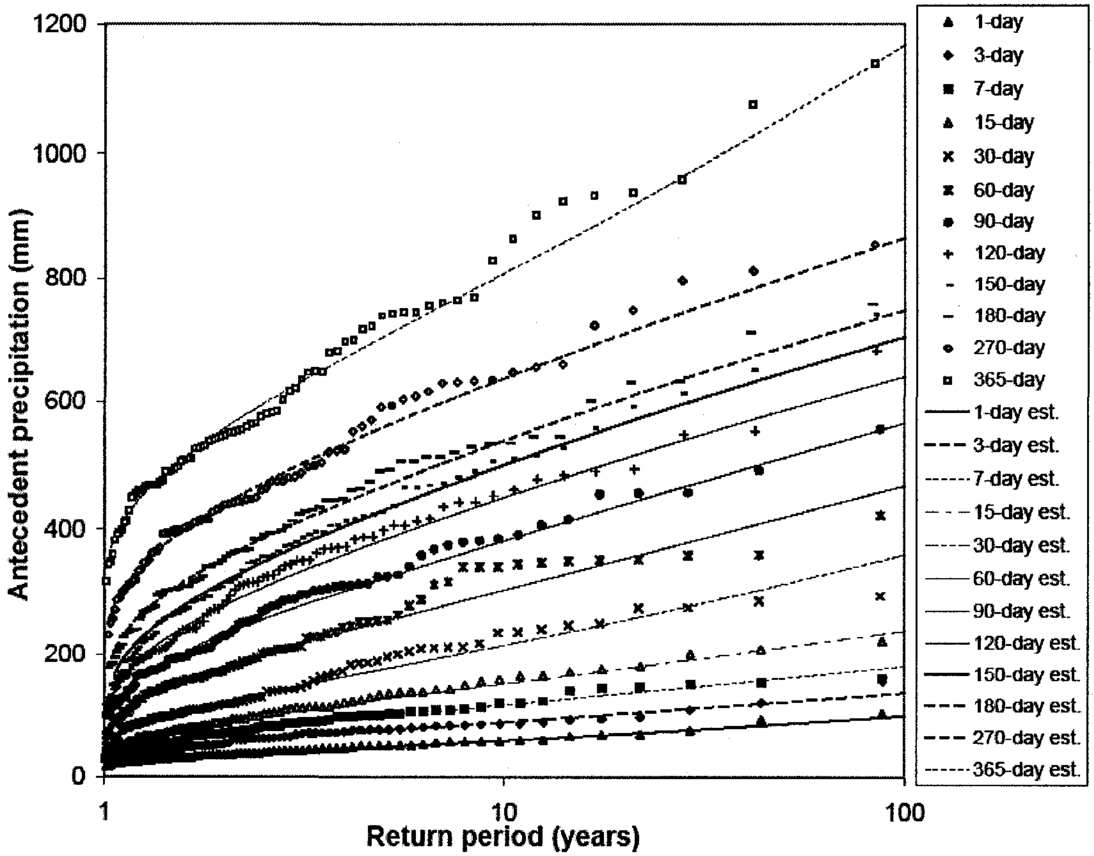

Figure K1 GEV antecedent precipitation return period analysis for Lytton, BC for data from 1917 to 2007

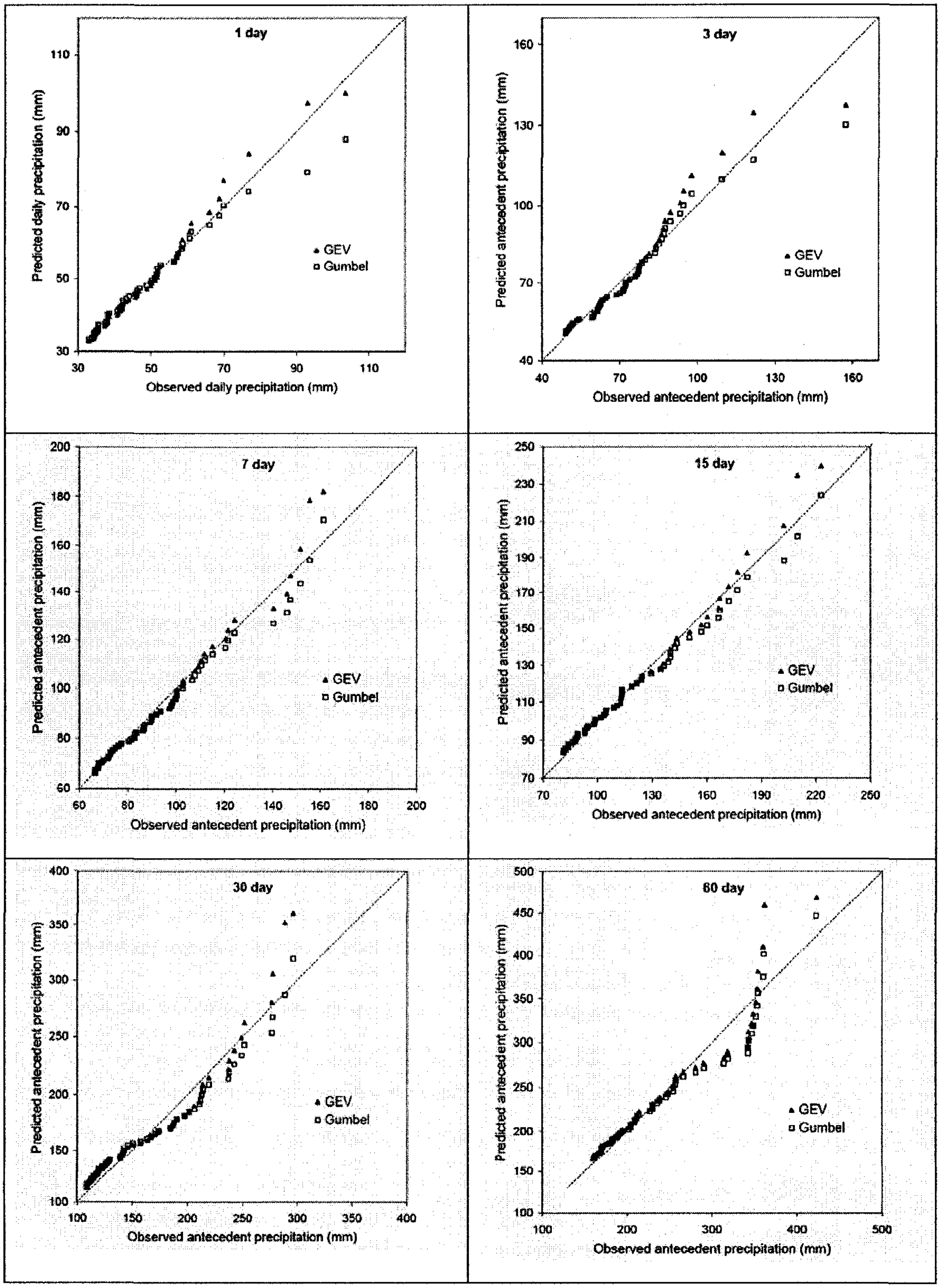

Figure K2 Q-Q plot of the 1, 3, 7, 15, 30 and 60 day antecedent precipitation for Lytton, BC for data from 1917 to 2007

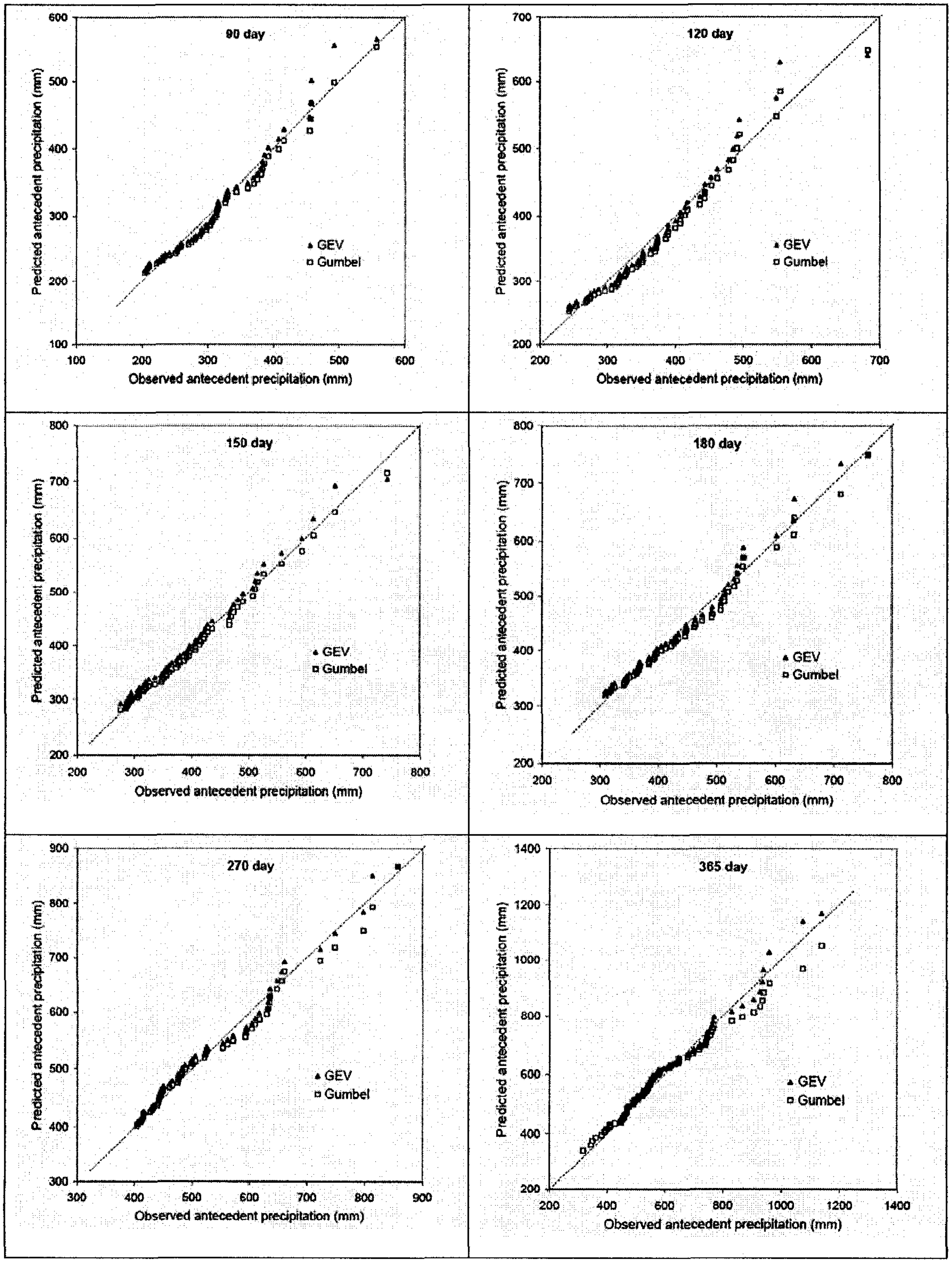

Figure K3 Q-Q plot of the 90, 120, 150, 180, 270, and 365 day antecedent precipitation for Lytton, BC for data from 1917 to 2007

K 2.0 Kenora, Ontario

Precipitation data for the Kenora, Ontario area was analyzed using the GEV and Gumbel frequency distributions. Data was combined for the Kenora and Kenora Airport EC weather stations. Data was edited to account for missing data resulting in low antecedent precipitation. The shape parameter, k is moderately negative for the shorter antecedent durations and moderately positive for longer antecedent durations indicating the Kenora antecedent precipitation is moderately lower bound limited for short antecedent durations and moderately upper bound limited for long antecedent durations.

Table K2 GEV analysis of the Kenora, Ontario maximum annual series for the years 1883 to 2007 excluding those years with insufficient data

Rank	1-day	2-day	5-day	7-day	15-day	30-day	60-day	90-day	150-day	180-day	270-day	365-day
μ	39.1	48.4	63.7	72.0	98.5	141.3	208.7	274.3	384.3	426.1	576.2	697.6
σ	14.4	16.6	20.1	23.4	29.5	38.8	57.1	71.3	93.6	97.1	104.9	117.4
k	-0.1854	-0.1517	-0.0667	0.0331	0.0987	0.0346	0.0953	0.12730	0.1124	0.1062	0.1713	0.1726
n	105	105	105	105	105	105	105	104	104	104	103	103
r	0.9951	0.9912	0.9925	0.9965	0.9963	0.9931	0.9961	0.9970	0.9955	0.9962	0.9947	0.9917
1	137.8	139.2	172.4	172.6	216.4	285.8	408.7	535.3	730.5	779.7	914.1	1041.6
2	128.3	137.8	157.2	157.5	200.1	283.8	396	508.3	686.9	760.5	903.3	1031.3
3	116.8	128.3	139.2	150.4	186.1	272.6	388.1	467.2	683.5	743.5	879.3	1028.7
4	109.2	118.1	128.3	150.1	185.4	271.8	385.6	466.2	662.8	727	864.3	1016.8
5	108	116.6	127.2	142.8	183.4	255.9	374.6	460.7	662.8	704.9	846.6	1012.0
6	92.5	108.5	126.3	140.6	178.6	253.6	370.6	458.1	638.1	704.7	844.9	989.0
7	91.6	108.2	125	135.9	173.4	253.4	352.6	454	621.9	675.9	837.4	988.9
8	90.8	108	123.9	129.8	165.1	252.6	347.3	440.4	580.1	656.8	820	981.8
9	90.2	100.8	123.6	126.2	164.4	245.2	345.9	433.1	562.9	613.3	816.1	965.6
10	87.1	99	118.1	125	158.5	242.9	341.6	424.7	560.5	604.3	811.4	965.0
11	83.8	92.5	115	123.6	157.7	232.7	337.2	415.2	559.6	601.9	768.4	960.2
12	81.5	92.4	110.4	123.1	155.7	231.6	328.7	410.5	559	597.7	762.8	950.1
13	78.2	91	109.2	122.8	152.2	230.9	320.5	405.3	556.8	592.8	762.2	919.0
14	78	88	107.5	119.4	150.4	226.5	317.4	400.7	554.1	588.2	745.7	890.7
15	77.4	87.6	104.5	116.2	150	220.6	314.4	399	549.7	587.5	734.7	890.2
16	71.9	87.2	103.4	114.5	149.6	220.5	312.4	398.9	542.3	581.2	733	885.5
17	69.8	87.1	101.6	113.6	149.2	218.9	301.3	395.7	534	571.5	726.2	880.0
18	67.4	83.6	101.3	113.1	148.6	210.8	300.1	395.6	533.6	571.4	720.1	878.7
19	67.3	80.2	100.6	112.8	148.6	204	290.2	394.8	525.6	570.8	718.8	875.7
20	67.1	79.6	100.1	111.2	147.6	202.9	283.8	389.5	523.4	570.5	707.1	873.3
21	65.3	79.2	99.5	111.1	147.3	199.4	283.5	379.3	516.5	570	704.2	859.7
22	65	78.7	99	108.5	146.4	197.3	282.6	368.9	511.7	568.4	701.8	837.6

Rank	1-day	2-day	5-day	7-day	15-day	30-day	60-day	90-day	150-day	180-day	270-day	365-day
23	61	77.6	95.7	107.5	141.9	197.2	282.4	364.2	507.6	568.1	699	831.6
24	61	77.5	94.2	106.5	139	193.3	281.5	358.2	497	555	697.7	830.7
25	60.7	76.6	92.9	106.4	137	188.7	277.7	358.1	492.3	549.3	689.9	828.3
26	59.7	76.4	92.8	104.6	135.9	187.9	277.2	357.3	492	538.5	689.5	825.2
27	58.4	75.8	92.5	104.5	133.7	187.8	276.2	356.6	489.2	536.5	688.7	824.3
28	57.2	73.4	92.5	101.4	132.8	187.6	275	351.5	483.3	534.6	687.3	821.2
29	55.9	72.9	91.4	101.4	130.2	179.4	274.8	351.4	481.2	529.6	685.1	809.8
30	55	71.9	90.9	99.8	127	178	270.6	350.6	477.6	528.4	682.6	807.5
31	54.1	71.3	89.7	99.2	126.9	178	268.3	350.6	474.9	522.2	668	806.0
32	53.3	68.9	88.8	98.2	125	174.6	266.2	344.9	474.5	521.8	666.9	803.8
33	52.3	67.3	87.2	95.7	124.7	172.8	265	341.4	473.6	517.2	665.6	795.8
34	52.1	66.5	86.7	94.5	123	172.7	264.5	337.2	473.3	514.3	665	788.1
35	51.8	65.3	83.6	93.5	122.6	172.5	261	336.5	470.1	509.7	660.3	782.0
36	51.8	65.2	83.4	93.2	122.5	170	257.1	336.4	467.5	508.4	655.9	765.8
37	51.6	63.8	82.8	92.5	122.3	168.1	256.5	334.3	464.4	508	649.8	762.4
38	51.1	63.2	82.5	91.4	122.3	168.1	255.9	332.1	462.9	507.9	647.1	759.8
39	51.1	63	82	89.2	121.8	165.6	255.4	322.3	461.3	503.6	637.9	757.4
40	50.8	62	81.8	88.9	120.5	165.5	255	321.8	458.5	502	636.6	754.3
41	50.4	62	81.7	88.8	119.3	165.5	251.9	319.2	457.3	501.6	632.8	748.1
42	50	60.8	80.2	88.6	116.1	164.9	249.1	318.6	455.2	501.3	630.7	746.1
43	49.5	60.4	80	87.1	113.3	164.6	247.7	318.3	455.1	499.1	624.2	745.8
44	49.5	58.4	79.3	86.9	113.3	164.2	247.3	315.8	453.9	498.6	623	745.1
45	49.3	58.4	79	86.4	112.3	162.2	243	315.4	450	497.4	623	740.7
46	48.8	56.9	77.4	85	112	162.1	242.1	315.1	447.6	494.9	622.7	738.9
47	47.5	55.9	76	83.8	111.6	162.1	239.5	313.2	446	491.6	620.8	737.9
48	47	54.9	76	82.5	111	161.4	237.7	305.8	439.8	489	617.6	737.8
49	46.5	54.6	76	82.3	110.7	160.9	234.7	302	435.6	480.3	613.3	737.7
50	46.2	54.6	75.2	82	109.6	160.6	234.6	301	433.9	476.8	612.6	737.7
51	45.7	54.1	73.7	81.7	109.2	159.9	233.9	299.2	431.2	475.7	612.2	736.8
52	45	53.9	73.6	81.3	108.1	159.1	230.1	299.1	429.2	464.2	612	732.4
53	44.5	53.8	72.4	81.2	107.1	158.2	228.1	297.6	425.7	462.9	610.4	722.2
54	44.5	53.3	72.4	79.7	106.1	158.2	228.1	296.3	423.4	460.1	608.4	721.5
55	43.9	53.1	70.9	79.5	105.9	157.6	227.2	295.1	423.4	457.8	602.1	720.7
56	43.7	52.8	70.6	79.3	105.4	155.1	227.1	294.1	419.7	455.4	599.1	720.6
57	43.2	52.1	68.1	78.9	105.1	153.7	226.6	293.6	416.7	454.8	596.7	718.4
58	42.9	52.1	67.9	78.6	104.4	153.4	223.4	288.1	415.8	453.8	595.6	716.5
59	42.8	52.1	66.8	78.3	104.2	153.2	223.3	287.6	412.7	448.7	590.6	713.5
60	42.7	51.8	66.8	77.6	103.9	151.7	221.4	287.3	404.6	444.9	586.6	712.3
61	42.4	50.9	66.6	76.4	103.4	151.4	220.9	285.6	402	443.8	586.2	710.6
62	41.9	50.4	66.3	76.2	102.8	151.3	218.9	284.3	401.8	443	581.8	705.5
63	41.4	50.4	65.6	74.7	102.8	150.1	215	283.1	400.5	438.1	581.7	705.0
64	40.9	50.1	64.9	73.8	99.5	147.9	214.6	282.5	395.3	428.7	580.8	704.1
65	40.6	49.2	64.4	72.9	98.6	145.4	214.1	280.3	369.6	427.5	580.3	700.5
66	40.5	49	64.4	72.1	98.3	145.1	213.9	278.7	369.4	423	575.4	696.1
67	39.9	48.8	63	71.1	98.1	143.2	213.8	278.4	367.3	420.5	574.4	693.9
68	38.9	47.5	61.9	70.3	98	143.2	213.3	271.9	366	410.7	573.4	690.9
69	37.6	46.5	60.7	69.6	97.9	141.9	210.6	271.8	364.9	407.4	570.7	685.5

Rank	1-day	2-day	5-day	7-day	15-day	30-day	60-day	90-day	150-day	180-day	270-day	365-day
70	37.6	46.2	59.7	68.9	97.8	141.7	210.3	270.4	363.8	406.5	569	681.9
71	37.3	46	59.3	68.6	97.8	141	207.4	269.2	362.1	399.6	567.2	679.2
72	37.1	45	59.2	66.8	97.7	138.2	200.9	266.2	361	398	561.8	678.4
73	37.1	44.5	59.2	66.4	96.5	133.3	200.1	261.7	358.4	395.2	556.7	677.1
74	36.3	44.3	58.9	66.2	96.4	132.3	193.1	259.5	357.7	394.6	555.6	675.6
75	36.1	43.9	57.7	65.6	96	131.2	192.7	257.8	355.4	393.8	555.5	674.6
76	35.8	43.5	56.7	65.2	94	131	191.4	254	350.5	393.8	545.2	674.5
77	35.1	43.4	56.4	65.1	92.3	130.1	187.8	253.6	349.1	390.9	541.3	668.4
78	34.8	43.2	55.9	64	91.9	129.9	187.2	253.3	348.7	389.3	539.5	666.5
79	34.7	42.4	55.4	63.7	90.2	129.6	187.1	251.4	346.1	387.7	532.5	665.5
80	33	42.4	55.1	61.8	89.6	128.9	185	246.9	343.6	384	530.8	665.4
81	32.8	42.4	54.6	61.7	89.5	127	183.8	241.1	337.4	382.2	529.6	661.8
82	32.4	42.4	53.5	61.6	88.4	126.1	181	238.6	335.9	378.6	529.2	661.7
83	32.1	42.2	53.2	60.7	87.2	122.8	180.5	237	332.6	376.6	517.8	657.9
84	32	41.8	53.1	60.4	84.6	119.4	180.3	235.9	332.3	376	515.6	646.4
85	31.8	40.9	52.1	60.2	83.7	116.1	179.8	229	330.2	374.4	514.7	646.2
86	31.5	40.4	51.9	59	81.2	115.1	174.2	228.3	328.6	372.6	514	644.5
87	31.5	39.9	50.7	58.5	80.8	114.7	172.9	222.1	324.7	369.2	509.1	643.8
88	31.3	38.9	50.5	58.4	80.8	114.4	170.8	220.6	321	363.2	508.5	639.8
89	30.5	38.8	49.2	57.7	80.7	113.8	162	219.9	320.3	361.3	505.5	620.4
90	30.5	38.3	48.8	56.8	80.4	111.6	161.7	218.4	317.4	356.4	504.2	615.6
91	29.7	38.1	48.8	55.4	75.2	110.8	158.4	215.3	310.4	355.4	499.1	615.1
92	29.7	37.6	48.6	54.1	73.7	108.7	157.2	206.4	305.3	344.6	498.1	604.2
93	29.5	36.6	48.5	50.7	73.5	108.4	152	203.7	299.4	337.2	497.5	599.5
94	29.2	34.1	48.3	50.6	72.1	107.1	151.1	201.6	294.3	334.1	490.9	587.9
95	29	34	47.3	48.5	72.1	104.6	149.9	199.8	294	330.4	483.3	587.8
96	27.2	33	44.7	48.3	71.4	104.2	148.4	196.9	290.7	327.9	482.3	581.3
97	27	33	44.2	48	70.4	101.5	145.9	195.3	289.4	321.5	477.5	551.2
98	26.6	33.0	43.2	47.7	64.0	101.2	144.8	194.7	283.2	319.6	469.7	546.4
99	26.2	32.5	43.1	47.0	59.8	101.1	143.2	193.2	266.8	313.1	460.2	545.9
100	24.4	30.2	42.9	44.7	59.1	100.4	143.0	190.9	259.4	309.7	453	539.0
101	24.0	30.0	42.2	44.5	58.9	95.3	142.5	188.5	259.2	292.9	404.4	523.2
102	21.3	28.4	41.6	44.5	58.3	89.6	140.2	177.7	257.9	286.5	400.2	491.3
103	21.1	28.2	41.4	42.4	58.2	89.0	136.5	174.6	248.7	285.3	335.1	457.3
104	20.6	27.9	37.6	41.8	55.2	88.6	130.9	156.4	246.9	273.9		
105	20.3	27.7	36.5	37.1	55.0	87.3	129.3					

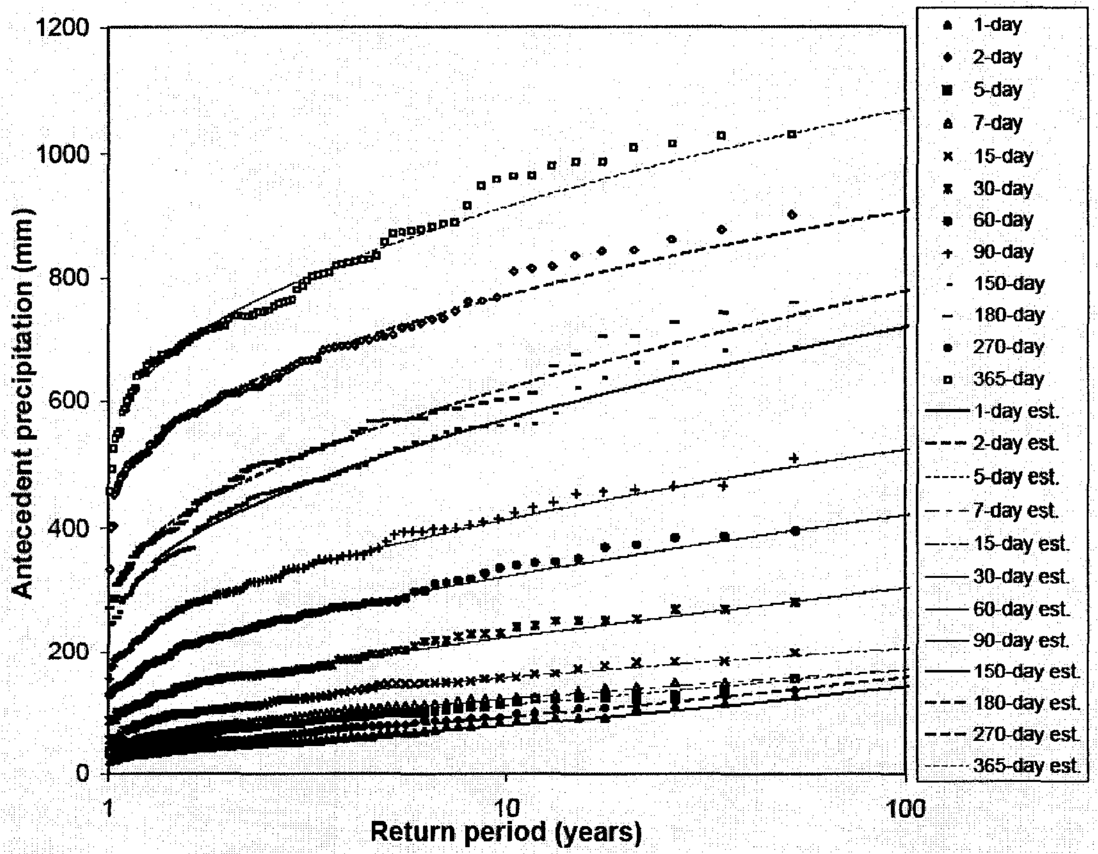

Figure K4 GEV antecedent precipitation - return period analysis for Kenora, Ontario for data from 1883 to 2007

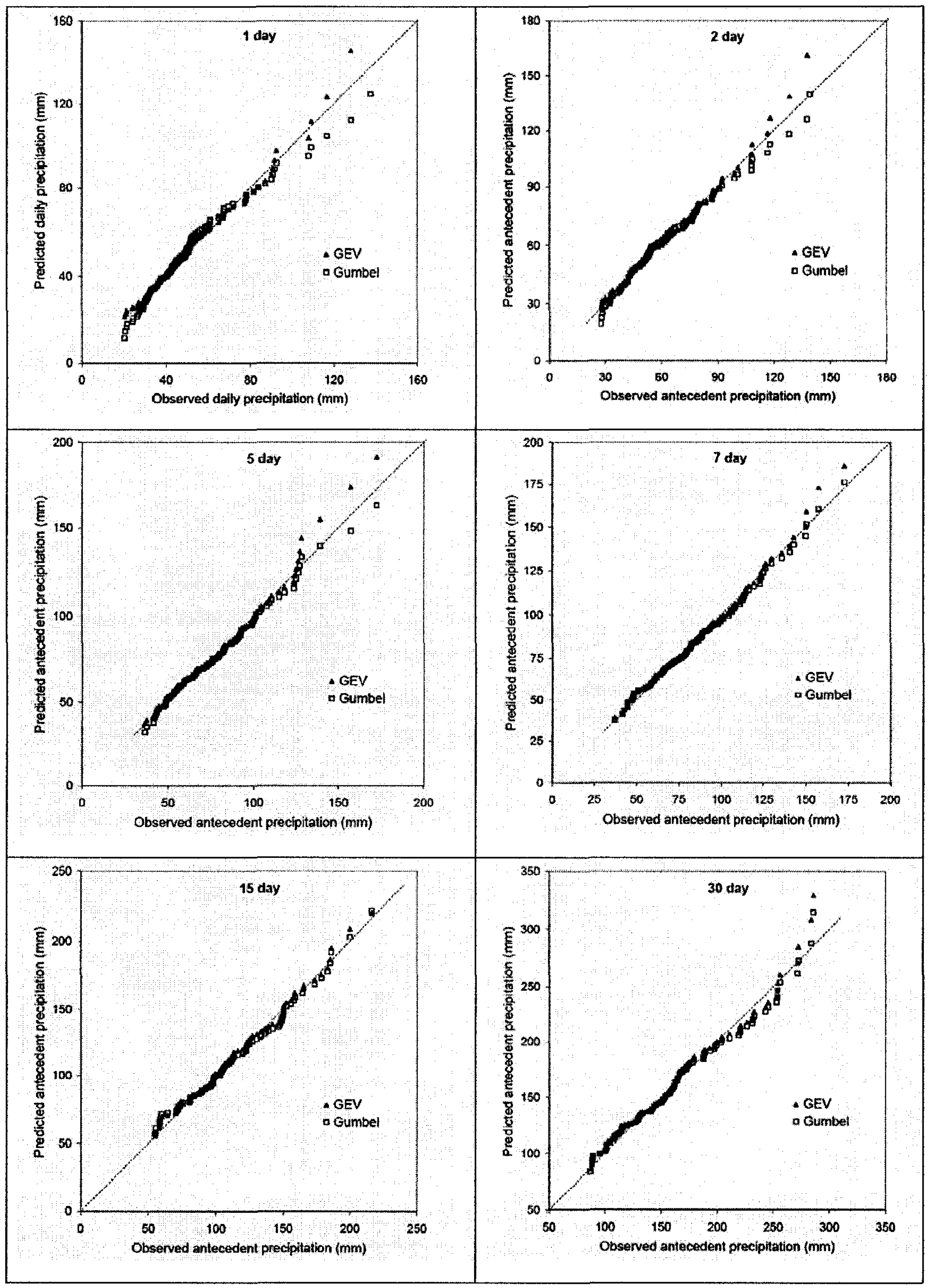

Figure K5 Q-Q plot of the 1, 2, 5, 7, 15 and 30 day antecedent precipitation for Kenora, Ontario for data from 1883 to 2007

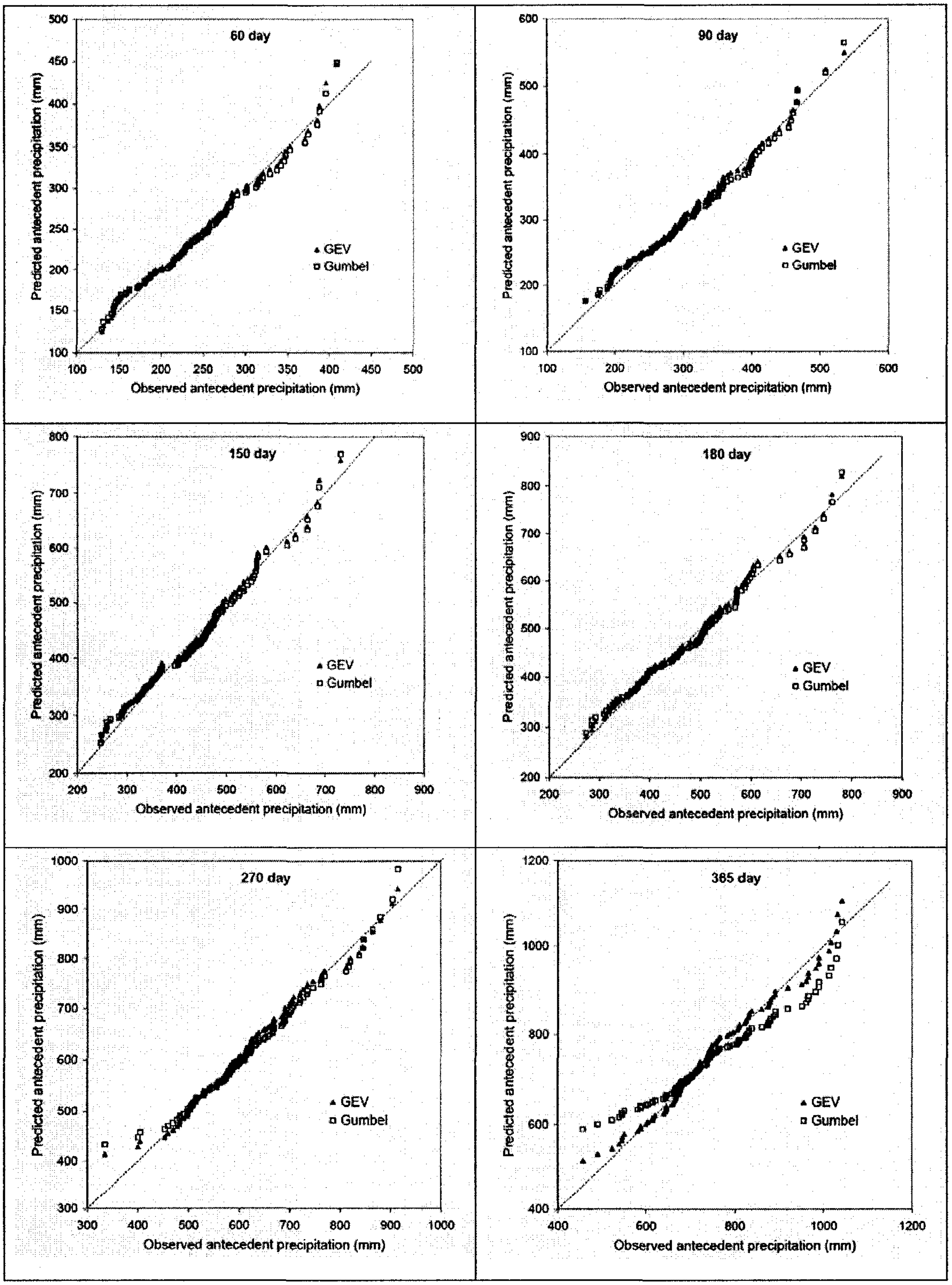

Figure K6 Q-Q plot of the 60, 90, 150, 180, 270, and 365 day antecedent precipitation for Kenora, Ontario for data from 1883 to 2007

Appendix L Risk Analysis

$P[Accident_{III}]$ is calculated as follows using the product of the conditional probabilities A to S

$A(i) = P[H(V_i)] * P[Impass.:H(V_i)]$ for each volume class i

$B(i,j) = P[Rail\ traffic\ of\ j] * A(i)$ for j = *Freight*, *Passenger*, or *MOW-TV*

$C(i,j,k) = P[TC\ k] * B(i,j)$ k = *present* or *absent*

$D(i,j,k,l) = P[Train\ l] * C(i,j)$ for l = *inside signal* or *outside signal*

$E(i,j,k,l,m) = P[TC\ m{:}H\&TC] * D(i,j,k)$ for m = *triggered* or *not triggered*

$H(i,j,k,l,m,n) = P[HDS\ n] * E(i,j,k,l,m)$ for n = *present* or *absent*

$S(i,j,k,l,m,n,o) = P[HDS\ o.{:}H(V_i)] * H(i,j,k,l,m,n)$ for o = *triggered* or *not triggered*

For m = *triggered* and o = *triggered* the train speed equals restricted speed.

For m = *not triggered* and o = *not triggered* the train speed equals track speed.

The stopping distance is obtained from Figure 5.11 or least squares quadratic curve fit to the data in Figure 5.11. Empirical relationships for the Loumiet and Jungbauer 2005 data are provided in Equations G.1 and G.2.

$D_{st} = 0.1534 V_T^2 - 0.5559 V_T$ for freight trains — Equation L1

$D_{st} = 0.0369 V_T^2 + 0.2166 V_T$ for passenger trains — Equation L2

The $P[Derail._{III}{:}H]$, $P[Train\ damage_{III}{:}H]$, and $P[Train\ stops_{III}{:}H]$ are derived from equations 5.31, 5.32, and 5.34 and respectively for $0 \le \frac{D_{si}}{D_{st}} \le 2$.

The $P[Derail._{III}{:}H]$, $P[Train\ damage_{III}{:}H]$, and $P[Train\ stops_{III}{:}H]$ are derived from equations 5.35, 5.36, and 5.37 and respectively for $\frac{D_{si}}{D_{st}} \ge 2$.

$T(i,j,k,l,m,n,o,q) = P[q{:}H)] * S(i,j,k,l,m,n,q)$ for q = *Derail.*, *Train damage*, and *Train stops*

$$P[q_{III}(V_i), j] = \sum_{for\ all\ k,l,m,n,o} T(i,j,k,l,m,n,o,q)$$

$$P[q_{III}, j] = \sum_{for\ all\ i} P[q_{III}(V_i), j]$$ for j = *Freight*, *Passenger*, or *MOW-TV*